PL-TR-92-2092

HITRAN DATABASE CONFERENCE
8-9 JUNE 1989

Editor:

Laurence S. Rothman

April 1992

PHILLIPS LABORATORY
AIR FORCE SYSTEMS COMMAND
HANSCOM AIR FORCE BASE, MASSACHUSETTS 01731-5000

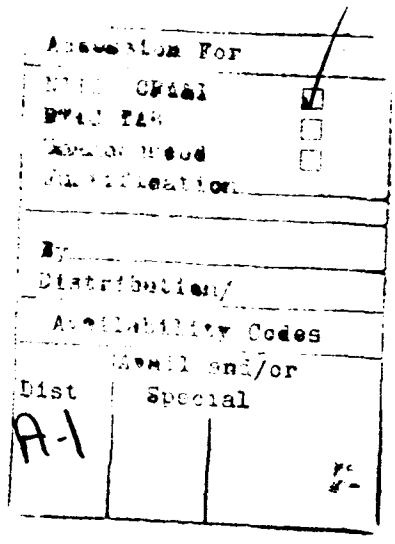

Contents

INTRODUCTION

The history of the program for the development of the molecular absorption database, now known under the acronym HITRAN, is a long and fruitful one. With the advancement of infrared sensors and calculational ability, the US Air Force recognized in the late '50s that a database of fundamental parameters for the calculation of the atmosphere's radiation environment was required. Early support of many theoretical and experimental studies of the infrared spectra of atmospheric gases was initiated by the AF Cambridge Research Center (which has evolved into the present Geophysics Laboratory). This anticipation of the need to characterize the background and intervening atmosphere in the infrared led to the creation of a team of molecular spectroscopists (known as GOAT – Group on Atmospheric Transmission) which held several meetings in the late 1960s, establishing the content, structure, and media for the molecular database. The first edition appeared in 1973 on magnetic tape and contained information for the seven infrared active atmospheric gases (water vapor, carbon dioxide, ozone, nitrous oxide, carbon monoxide, methane, and oxygen). The spectral range at that time was limited to the region of about 1 to 100 microns. Since then, HITRAN has been periodically updated, increasing in spectral coverage from the microwave through the visible, incorporating more molecular species and bands, and adding more transition parameters. HITRAN has gone from about 100,000 transitions in the first edition to well over a third of a million in the last edition of November 1986.

HITRAN has been used for a very broad range of applications (laser propagation, detection of hot sources, background characterization, remote sensing of atmospheric constituents, development of LOWTRAN band models, pollution studies, climate mechanisms, greenhouse effect, to name a few) and has a major impact as the foundation for many systems codes. As witnessed by the attendees at this meeting, it has a wide user constituency throughout the United States and internationally. The desirability of having such a database as an open reference has often promoted the free flow of data and calculations throughout the world to enhance the usefulness of this project to the world community.

Over the years since the initial GOATS meeting, numerous *ad hoc* as well as specific meetings have been held that focused on the issue of the molecular spectroscopic database. Among these have been meetings sponsored by NASA at the Langley Research Center, a session organized by John Shaw at one of the Ohio State Molecular Spectroscopy Symposia, a meeting sponsored by the Chemical Manufacturers Association at the Bureau of Standards, meetings held under the Atmospheric Spectroscopy Applications (ASA) working group of the International Radiation Commission (Greece, 1984; Rutherford Appleton Lab, UK, 1987), and a recent meeting of the database managers at JPL in 1988. The time for a conference addressing the databases is very appropriate now since much new data of very high quality is available for a significant new edition, not only of HITRAN, but of a companion high temperature atlas (HITEMP). The goal of the meeting and discussions of the next two days is to review the status of relevant new data, establish priorities for inclusion of data, and to discuss issues involving the archiving of the burgeoning amount of data to take advantage of new technology and also to provide users with the optimum ease in their applications.

We at AFGL extend a welcome to all of you and wish you a pleasant stay in the Boston area. We hope that this conference will be a fruitful one, not only because of the papers presented

and following panel discussions, but because of the informal opportunity that we will have to exchange ideas and preliminary results from our recent efforts in spectroscopy. I would also like to express my appreciation for the assistance of Dr. John Hummel and SPARTA, Inc. for their help in planning the meeting and in the preparation of these Proceedings. I would also like to extend my thanks to Lt Scott Shannon and Ms. Nancy Lott-Schlicker of AFGL for their help during the conference.

Laurence S. Rothman


EXIT
HITRAN
DATABASE
CONFERENCE
8 9 JUNE 1989

BLANK

NEW CARBON DIOXIDE LINE PARAMETERS FOR ATMOSPHERIC AND HIGH TEMPERATURE APPLICATIONS

Laurence S. Rothman
GL/OPI
Hanscom AFB, MA 01731-5000

Richard B. Wattson
Visidyne, Inc.
10 Corporate Place
Burlington, MA 01803

Robert L. Hawkins
GL/OPI
Hanscom AFB, MA 01731-5000

New Carbon Dioxide Line Parameters for Atmospheric and High Temperature Applications

Laurence S. Rothman
Optical Physics Division, Geophysics Lab, Hanscom AFB, MA 01731

Richard B. Wattson
Visidyne, Inc., 10 Corporate Place, Burlington, MA 01803

and

Robert L. Hawkins
Optical Physics Division, Geophysics Lab, Hanscom AFB, MA 01731

A continuing effort has been conducted at the Geophysics Laboratory to develop self-consistent line positions and intensities for carbon dioxide for both atmospheric and high temperature applications. In this talk we will discuss the status of carbon dioxide including recent laboratory and theoretical improvements to the CO_2 absorption parameters, problems that must be addressed as the quantity of information expands, some examples of the improvements that have been achieved, and future research.

I. Recent Contributions

Since the last update of the carbon dioxide parameters for HITRAN (Rothman, 1986), there have been significant new efforts in high resolution observations of line positions, intensities, half-widths, and also advancements in calculation of both energy levels and intensities. We will be concerned in this paper with the work involved with line positions and intensities, since several papers in this meeting will address the specific issue of line-broadening and its dependence on temperature.

To generate CO_2 line parameters for the database, two driving tables have been established. The first table contains (for the eight isotopic variants considered) the spectroscopic constants, G, B, D, and H for the vibrational energy levels, where the constants are the coefficients of a power series in J(J + 1), J being the total angular momentum. For HITRAN, over 100 levels have been given just for the principal isotope; for HITEMP, around 1500! There had been a flurry of activity in the observation of high resolution line positions, and hence spectroscopic constants, leading up to the last edition of the database. Since that edition, we have only added the data from Benner *et al.*, 1988 and Esplin, 1987. We have also improved the term value of higher levels of the bending mode (Esplin *et al.*, 1989). More of

the improvement has gone into the second table, a tabulation of all bands premeditated for the database. This table contains information on the vibrational quanta of the band, the integrated band intensity, and Herman-Wallis coefficients (if they are available to describe deviations from rigid-rotor behavior). Examples of these tables are shown in Fig. 1. The extensive bibliography used in updating these tables will be provided with the proceedings. The most recent contributions are shown in Table I.

Line parameters are generated by using the intensity table as a driver, searching for the appropriate energy level constants, and calculating the positions and intensities of individual lines and subsequently applying the cutoff criterion for inclusion into the database.

II. Direct Numerical Diagonalization

The application of Direct Numerical Diagonalization (DND) (Wattson and Rothman, 1986) has been substantially extended since the last edition of HITRAN to now include: (1) the perpendicular band intensities; (2) rotational constants for the symmetric species; and (3) band centers and intensities for the asymmetric species.

For this work we used a 35-parameter potential function based on all the observed 626 band centers. This redetermination of the potential function in normal mode coordinates has not substantially changed since 1986. Figure 2 shows the distribution of the percentage residuals (Observed band intensity - Calculated band intensity)/(Observed band intensity) for the main isotope. Forty-one intensities out of the 76 observed 626 intensities have been used to determine the dipole moment function; this is highlighted in the figure. Figures 3-4 indicate the residuals for the 636 and 628 isotopes (recall that these calculations are based only on 626 positional and intensity data).

Insofar as developing rotational constants for the levels, the original intention of the DND effort was to be able to calculate intensities for unobserved bands, especially bands necessary for the hot gas compilation, HITEMP. However, for that latter compilation, it was expected that the rotational constants of DND would be used as well. We have, as will be shown later, discovered that the energy level predictions of DND can indeed be of value even in HITRAN and we have used them for all 626 and 636 levels that have not been observed. In the case of 626, this mainly applies to some high levels above 4500 wavenumbers. One might consider, at least for HITRAN, to join the least-squares determined constants at the maximum J smoothly to the DND constants beyond that rotational level.

Figures 5-7 show the residuals of the band centers for the three most abundant isotopes and give some indication of the accuracy that can be expected from DND. Again, in the isotopic plots, only the data from the main isotope have been used in determining the potential function, yet all of the calculated band centers lie within 0.05 cm^{-1}. The residual errors are primarily due to the truncation of the potential function to 35 terms.

III. Least-squares Fitting to Observations

A new least-squares fit has been applied to the high resolution line position observations that have been collected at AFGL over the years (see references herein). These measurements are for the most part high resolution observations made with Fourier Transform Spectrometers throughout the world and comprise over 20,000 individual line positions (occasionally the same band represented by different laboratories). In the new procedure implemented by Hawkins, all levels of an isotope are simultaneously fit, rather than the "bootstrapping" method that was used in the past. In addition (Linda Brown will be happy to note), greater attention has been given to recalibrating the data. This latter effect applies mostly to the measurements of Guelachvili and of Esplin, and amounts to a correction on the order of 4-tenths of a milliKaiser. The recalibration has made a small improvement in the overall fit. We have also kept track, not only of the number of other levels each vibrational level connects to, but maximum J-value of both e- and f-levels.

IV. Theory Prevails

Recently the 2-meter path interferometer at AFGL has been modified to obtain measurements in the 15-μm region. Esplin has made a series of observations of $^{12}C^{16}O_2$ at temperatures up to 800 K. Included in these observations has been the observation for the first time at high resolution of the Fermi singlet bands (05501 <- 04401), (06601 <- 05501), and (07701 <- 06601). In an interesting marriage of theory and experiment, Esplin was able to readily identify these new levels by initiating his Loomis-Woods diagrams with the results of DND. This is shown in Fig. 8. Note that on the HITRAN database, the $7\nu_2$ level was not included due to the cutoff criterion. However, these levels will be necessary for HITEMP, and are also significant for further improvement of the potential function for DND itself.

V. Humongous Files

An issue that must be addressed in the near future is how to deal with the quantity of data that is to be made accessible to the user. For CO_2 the original number of transitions (which were also only 80 characters per transition) on the first database was about

60,000. The size of the CO_2 file for HITEMP, based on a 1000 K standard is from 100 to 200 MegaBytes! Figure 9 illustrates that the number of transitions of CO_2 is increasing almost as the fourth power of temperature. Various schemes have been suggested for dealing with this amount of data, some of which will be discussed in subsequent papers. We have attempted to archive all significant transitions in order to preserve as much of the fundamental physics as possible; codes to which these data are transitioned must make decisions whether to create intermediary files or reject insignificant transitions for their applications. Nevertheless, it seems inevitable that new storage and media, such as CD-Rom, must be pursued as the primary standard for the archived database in the near future.

VI. Improvement for Applications

The improvements that are now available to the CO_2 absorption parameters since the last edition of HITRAN should be significant to a number of applications. We cite some that affect remote sensing. The band at 720.805 cm^{-1} has had its total band intensity altered several times throughout the history of HITRAN. Recent measurements by Johns, 1989b, which have been corroborated by others (Dana, Huet *et al*, Varanasi), have increased the intensity of this band by 6 percent from the previous value. The band is one of the key channels for remote sensing experiments proposed for satellite monitoring. The nearby band at 721.584 cm^{-1} for the carbon-13 isotope has changed even more. Previously it was based simply on the isotopic ratio related to the same transition of the principal isotope (the 1973 calculated value). We calculated a 40% reduction via DND and which was later confirmed by the observations of Johns, 1989b. In addition, Clough has shown that the new value resolves some of the problems that were previously seen in both the High resolution Interferometer Sounding experiment (HIS) data taken by Smith with the University of Wisconsin airborne FTS and with the AFGL Stratospheric CRyogenic Interferometer Balloon Experiment (SCRIBE) flown by the University of Denver.

Another band in the long wavelength region used for remote sensing is at 791.447 cm^{-1}. New measurements show a 15 percent decrease from the previous band intensity in HITRAN and also, as with the bands discussed above, yield values for the Herman-Wallis factors.

The improvement of line positional accuracy is of interest to applications such as the NASA ATMOS (Atmospheric Trace Gas experiment aboard the shuttle). Figure 10 shows the result of co-added spectra on the ATMOS mission.

VII. Summary and Conclusions

Future efforts that are in progress towards the improvement of the transition frequencies and line intensities of CO_2 include the calculation of the Herman-Wallis coefficients in DND. Rotational constants for the asymmetric species will be calculated. Methods to improve the efficiency of DND are also being investigated. Measurements of intensities of more bands in the 12 to 15 micron region are being pursued. For line positions, especially significant to HITEMP, will be the reduction of Esplin's 15 micron observations.

VIII. References for Driving Tables

M.S. Abubakar and J.H. Shaw, Appl.Opt. **23**, 3310 (1984).

M.S. Abubakar and J.H. Shaw, Appl.Opt. **25**, 1196 (1986).

Ph. Arcas, E. Arie', M. Cuisenier, and J.P. Maillard, Can.J.Phys. **61**, 857 (1983).

Ph. Arcas, private communication (1985).

D. Bailly, R. Farrenq, G. Guelachvili, and C. Rossetti, J.Mol.Spectrosc. **90**, 74 (1981).

D. Bailly, Thesis, Universite' de Paris-Sud, France (1983).

D. Bailly and C. Rossetti, J.Mol.Spectrosc. **102**, 392 (1983).

D. Bailly and C. Rossetti, J.Mol.Spectrosc. **105**, 331 (1984).

A. Baldacci, C.P. Rinsland, M.A.H. Smith, and K. Narahari Rao, J.Mol.Spectrosc. **94**, 351 (1982).

D.C. Benner and C.P. Rinsland, J.Mol.Spectrosc. **112**, 18 (1985).

D.C. Benner, V.Malathy Devi, C.P. Rinsland, and P.S. Ferry-Leeper, Appl.Opt. **27**, 1588 (1988).

G. Blanquet, J. Walrand, and J.L. Teffo, Appl.Opt. **27**, 2098 (1988).

L.R. Brown, private communication (1985).

D.E. Burch, D.A. Gryvnak, and R.R. Patty, J.Opt.Soc.Am. **58**, 335 (1968).

A. Chedin and J.-L. Teffo, J.Mol.Spectrosc. **107**, 333 (1984).

V. Dana, A. Valentin, A. Hamdouni, and L.S. Rothman, to appear in Appl.Opt. (1989).

V. Malathy Devi, P. Das, and K.N. Rao, Appl.Opt. **18**, 2918 (1979).

V.Malathy Devi, B. Fridovich, G.D. Jones, and D.G.S. Snyder, J.Mol.Spectrosc. **105**, 61 (1984).

V. Malathy Devi, C.P. Rinsland, and D.C. Benner, Appl.Opt. **23**, 4067 (1984).

H.D. Dowling, L.R. Brown, and R.H. Hunt, J.Quant.Spectrosc.Radiat.Transfer **15**, 205 (1975).

J. Dupre-Maquaire and P. Pinson, J.Mol.Spectrosc. **62**, 181 (1976).

M.P. Esplin, R.J. Huppi, and G.A. Vanasse, Appl.Opt. **21**, 1681 (1982).

M.P. Esplin and L.S. Rothman, J.Mol.Spectrosc. **100**, 193 (1983).

M.P. Esplin, H. Sakai, L.S. Rothman, G.A. Vanasse, W. Barowy, and R. Huppi, Tech.Report AFGL-TR-0046 (1986).

M.P. Esplin and L.S. Rothman, J.Mol.Spectrosc. **116**, 351 (1986).

M.P. Esplin, private communication (1987).

M.P. Esplin, R.B. Wattson, M.L. Hoke, R.L. Hawkins, and L.S. Rothman, Appl.Opt. **28**, 409 (1989).

C. Freed, L.C. Bradley, and R.G. O'Donnell, IEEE J.Q.Electronics, **16**, 1195 (1980).
G. Guelachvili, J.Mol.Spectrosc. **79**, 72 (1980).
T. Huet, N. Lacome, and A. Levy, J.Mol.Spectrosc. **128**, 206 (1988).
M.L. Hoke and J.H. Shaw, Appl.Opt. **22**, 328 (1983).
J.W.C. Johns, J.Mol.Spectrosc. **134**, 433 (1989).
J.W.C. Johns, private communication (1989).
K. Jolma, J. Kauppinen, and V.-M. Horneman, J.Mol.Spectrosc. **101**, 300 (1983).
K. Jolma, J.Mol.Spectrosc. **111**, 211 (1985).
J. Kauppinen, K. Jolma, and V.-M. Horneman, Appl.Opt. **21**, 3332 (1982).
J.P. Maillard, J. Cuisenier, Ph. Arcas, E. Arie', and C. Amiot, Can.J.Phys. **58**, 1560 (1980).
J.-Y. Mandin, J.Mol.Spectrosc. **67**, 304 (1977).
J.-P. Monchalin, M.J. Kelly, J.E. Thomas, N.A. Kurnit, and A. Javan, J.Mol.Spectrosc. **64**, 491 (1977).
Y. Ouazzany and J.P. Boquillon, Europhys. Lett. **4**, 421 (1987).
N. Papineau and M. Pealat, Appl.Opt. **24**, 3002 (1985).
R. Paso, J. Kauppinen, and R. Anttila, J.Mol.Spectrosc. **79**, 236 (1980).
R. Paso, U.Oulu Finland, Private Communication (1980).
F.R. Petersen, J.S. Wells, A.G. Maki, and K.J. Siemsen, Appl.Opt. **20**, 3635 (1981).
F.R. Petersen, J.S. Wells, K.J. Siemsen, A.M. Robinson, and A.G. Maki, J.Mol.Spectrosc. **105**, 324 (1984).
A.S. Pine and G. Guelachvili, J. Mol. Spectrosc. **79**, 84 (1980).
C.P. Rinsland, D.C. Benner, D.J. Richardson, and R.A. Toth, Appl.Opt. **22**, 3805 (1983).
C.P. Rinsland and D.C. Benner, Appl.Opt. **23**, 4523 (1984).
C.P. Rinsland, D.C. Benner, and V. Malathy Devi, Appl.Opt. **24**, 1644 (1985).
C.P. Rinsland, private communication (1985).
C.P. Rinsland, D.C. Benner, and V. Malathy Devi, Appl.Opt. **25**, 1204 (1986).
L.S. Rothman, Appl.Opt. **25**, 1795 (1986).
H. Sakai, Paper ME7, 38th Molecular Spectroscopy Symposium, Ohio State University (1983).
K.J. Siemsen and B.G. Whitford, Opt.Comm. **22**, 11 (1977).
K.J. Siemsen, Opt.Comm. **34**, 447 (1980).
K.J. Siemsen, Opt.Lett. **6**, 114 (1981).
C.B. Suarez and F.P.J. Valero, J.Quant.Spectrosc.Radiat.Transfer **19**, 569 (1978).
C.B. Suarez and F.P.J. Valero, J.Mol.Spectrosc. **71**, 46 (1978).
R.A. Toth, R.H. Hunt, and E.K. Plyler, J.Mol.Spectrosc. **38**, 107 (1975).
R.A. Toth, Appl.Opt. **24**, 261 (1985).
F.P.J. Valero, J.Mol.Spectrosc. **68**, 269 (1977).
F.P.J. Valero and R.W. Boese, J.Quant.Spectrosc.Radiat.Transfer **18**, 391 (1977).
F.P.J. Valero and C.B. Suarez, J.Quant.Spectrosc.Radiat.Transfer **19**, 579 (1978).

F.P.J. Valero C.B. Suarez, and R.W. Boese,
J.Quant.Spectrosc.Radiat.Transfer **22**, 93 (1979).
F.P.J. Valero C.B. Suarez, and R.W. Boese,
J.Quant.Spectrosc.Radiat.Transfer **23**, 337 (1979).
K.P. Vasilevskii, L.E. Danilochkina, and V.A. Kazbanov,
Opt.Spektrosk. **38**, 871 ((1975).
R.B. Wattson and L.S. Rothman, J.Mol.Spectrosc. **119**, 83 (1986)
R.B. Wattson, L.S. Rothman, A. Newburgh, and R. Pavelle, Paper TE9,
43rd Molecular Spectroscopy Symposium, Ohio State University (1988).

Table I

D.C. Benner, V.Malathy Devi, C.P. Rinsland,
and P.S. Ferry-Leeper, Appl.Opt. **27**, 1588 (1988).
Intensities and line positions of bands at 3.1 μm

G. Blanquet, J. Walrand, and J.L. Teffo,
Appl.Opt. **27**, 2098 (1988).
Line positions of Q-branch of band at 865 cm^{-1}

V. Dana, A. Valentin, A. Hamdouni, and L.S. Rothman,
to appear in Appl.Opt. (1989).
Intensity of band at 791 cm^{-1}

M.P. Esplin, private communication (1987).
Line positions of oxygen-18 enriched species at 4.3 μm

M.P. Esplin, R.B. Wattson, M.L. Hoke, R.L. Hawkins,
and L.S. Rothman, Appl.Opt. **28**, 409 (1989).
Band centers of hot band sequence of bending fundamental

M.P. Esplin and M.L. Hoke, OSU Symposium (1989).
Line positions of bands near 15 μm

J.W.C. Johns, J.Mol.Spectrosc. **134**, 433 (1989).
Band intensities of parallel bands around 4.3 and 2.7 μm

J.W.C. Johns, private communication (1989).
Band intensities of perpendicular bands in 15 μm region

R.B. Wattson, L.S. Rothman, A. Newburgh, and R. Pavelle,
Paper TE9, 43rd Molecular Spectroscopy Symposium,
Ohio State University (1988).
Calculated parallel and perpendicular band intensities;
calculated line positions for unobserved symmetric species.

New Contributions to Line Positions and Intensities since 1986 HITRAN

					626	********** Table I **********				Jmax	#connections	Comments
0	0	0	0	1	' '	0.	0.39021889	1.33333	0.055	140	18	
0	1	1	0	1	'e'	667.37992	0.39063898	1.35278	0.061	115	22	
0	1	1	0	1	'f'	,,	0.39125468	1.36072	0.041	,,		
1	0	0	0	2	' '	1285.40827	0.39048224	1.57116	2.228	106	12	'Seen in Raman,
0	2	2	0	1	'e'	1335.13149	0.39166694	1.37576	-3.215	107	12	
0	2	2	0	1	'f'	,,	0.39166694	1.38080	0.061	,,		
1	0	0	0	1	' '	1388.18425	0.39018887	1.14917	1.835	108	9	
1	1	1	0	2	'e'	1932.47039	0.39074371	1.48633	-0.187	98	8	
1	1	1	0	2	'f'	,,	0.39168925	1.55575	-0.045	,,		
0	3	3	0	1	'e'	2003.24518	0.39238160	1.41511	-0.939	90	6	
0	3	3	0	1	'f'	,,	0.39238160	1.41511	-0.882	,,		
1	1	1	0	1	'e'	2076.85587	0.39040960	1.25826	0.848	96	10	
1	1	1	0	1	'f'	,,	0.39133397	1.21141	0.521	,,		
0	0	0	1	1	' '	2349.14284	0.38714134	1.32992	0.074	140	4	
2	0	0	0	3	' '	2548.36662	0.39110980	1.81556	5.429	86	4	
1	2	2	0	2	'e'	2585.02215	0.39194289	1.39665	-7.247	66	1	
1	2	2	0	2	'f'	,,	0.39194289	1.53060	0.783	,,		
2	0	0	0	2	' '	2671.14313	0.38956162	1.34648	4.910	76	4	
0	4	4	0	1	'e'	2671.71523	0.39308327	1.43293	0.	89	2	
0	4	4	0	1	'f'	..	0.39308327	1.43293	0.	..		

	********** Table II **********										1=positions ;=intensities
471.5100	2 0 0 0 3	1 1 1 0 1 626	0.01169	0.	0.	0.	0.	0.	,' ',';X'
479.8979	1 3 3 0 2	1 2 2 0 1 626	0.00147	0.	0.	0.	0.	0.	,'0',';X'
494.5853	1 2 2 0 2	1 1 1 0 1 636	0.00079	0.	0.	0.	0.	0.	,'0',' '
508.1663	1 2 2 0 2	1 1 1 0 1 626	0.06159	0.	0.	0.	0.	0.	,' ',';X'
510.3210	2 1 1 0 3	2 0 0 0 2 626	0.00476	0.	0.	0.	0.	0.	,' ',';X'
526.4760	1 1 1 0 2	1 0 0 0 1 636	0.0139	0.	0.	0.	0.	0.	,' ',';X'
535.8923	1 1 1 0 2	1 0 0 0 1 628	0.0110	0.	0.	0.	0.	0.	,' ',' '
542.2202	2 1 1 0 2	2 0 0 0 1 626	0.00818	0.	0.	0.	0.	0.	,' ',';X'
546.2861	1 1 1 0 2	1 0 0 0 1 626	3.252	0.	0.	0.	0.	0.	,' ',';AP'
557.799	1 4 4 0 2	0 5 5 0 1 626	0.00297	0.	0.	0.	0.	0.	,' ',';X'
561.1210	1 2 2 0 2	0 3 3 0 1 628	0.00580	0.	0.	0.	0.	0.	,' ',' '
564.9094	2 0 0 0 2	1 1 1 0 1 628	0.00430	0.	0.	0.	0.	0.	,' ',' '
565.6983	2 2 2 0 2	1 3 3 0 1 626	0.00159	0.	0.	0.	0.	0.	,' ',';X'
568.9074	1 3 3 0 2	0 4 4 0 1 626	0.08146	0.	0.	0.	0.	0.	,' ',';X'

Figure 1. Example of the Tables of Bands Premeditated for the Database.

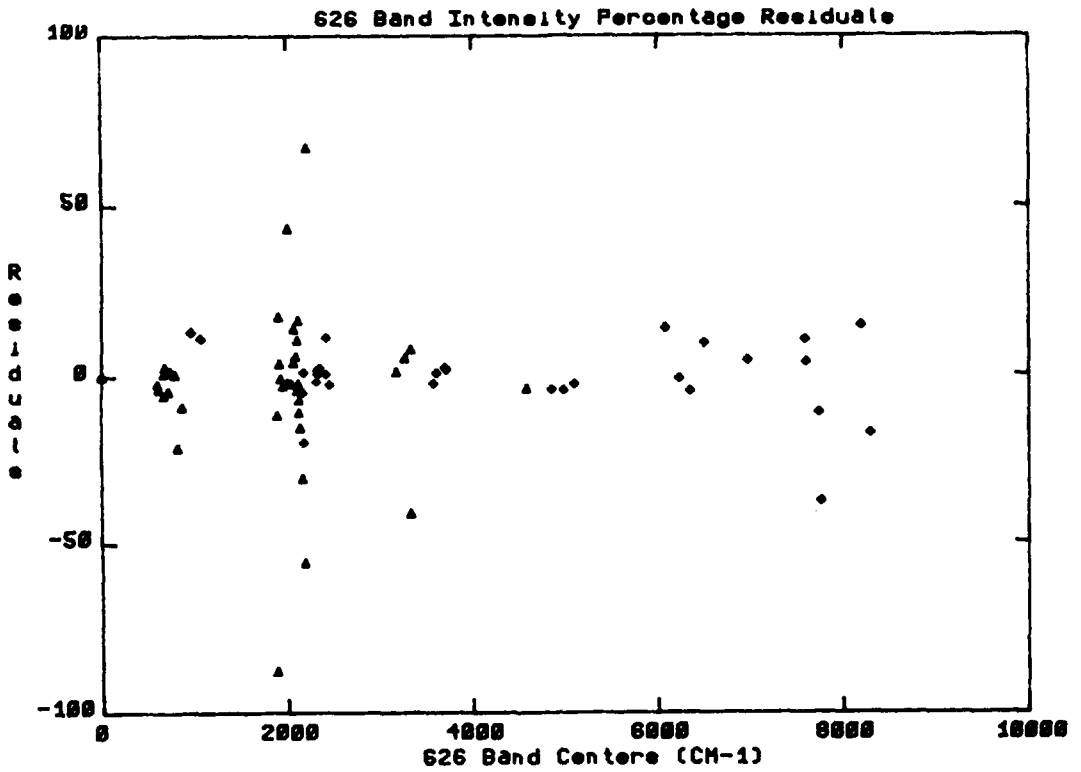

Figure 2. Distribution of the Percentage Residuals for the Band Intensities for the Main Isotope 626.

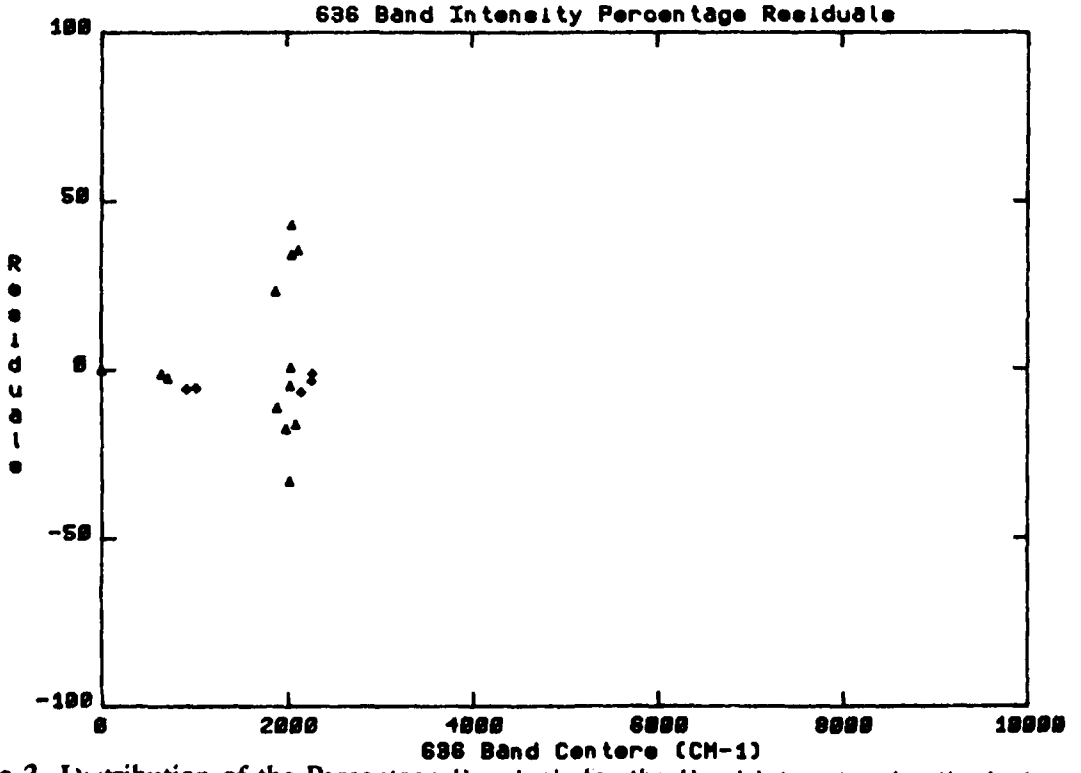

Figure 3. Distribution of the Percentage Residuals for the Band Intensities for the Isotope 636.

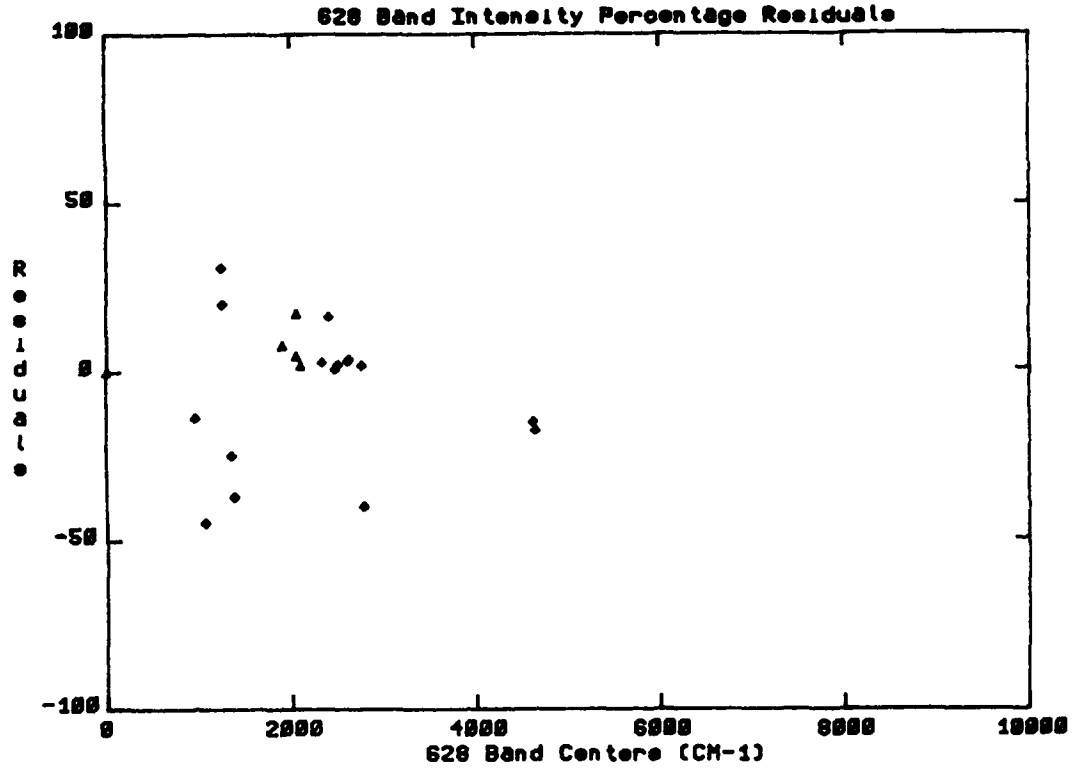

Figure 4. Distribution of the Percentage Residuals for the Band Intensities for the Isotope 628.

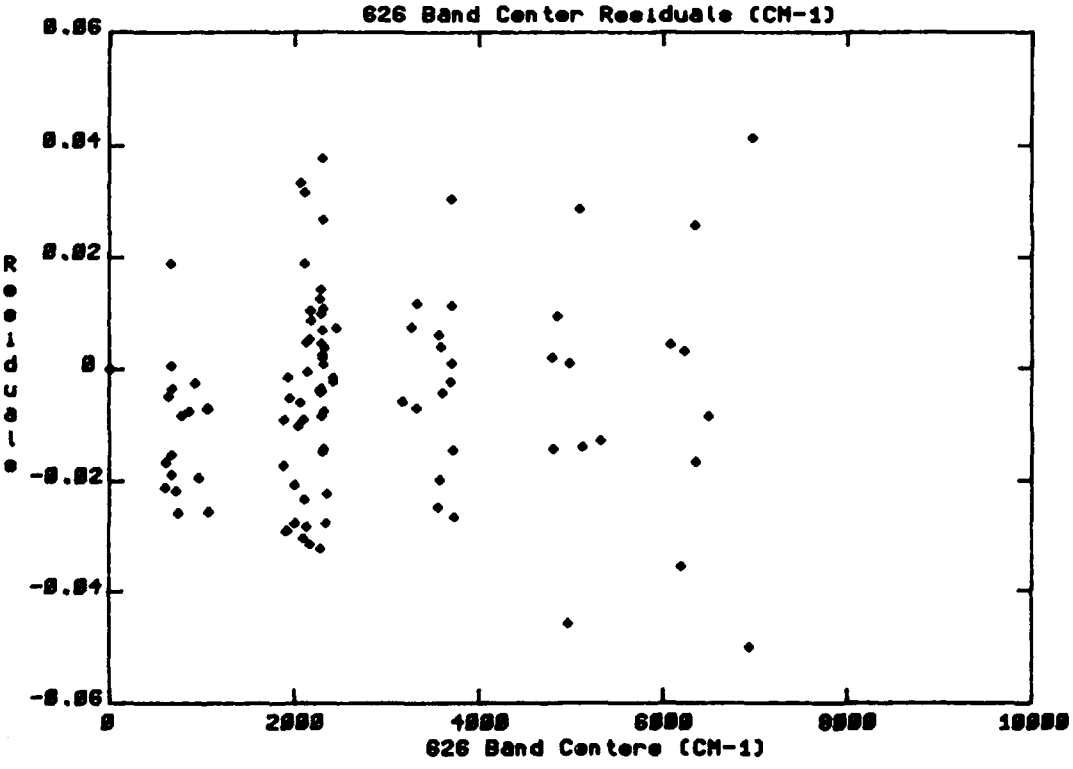

Figure 5. Distribution of the Percentage Residuals for the Band Centers for the Isotope 626.

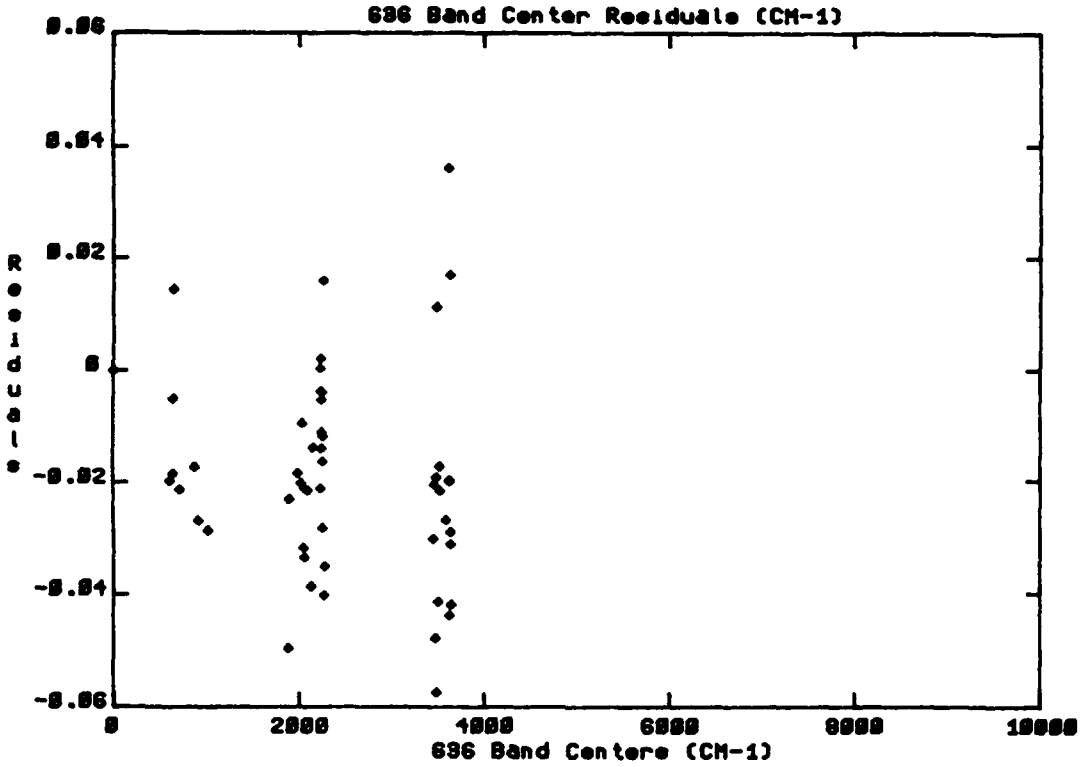

Figure 6. Distribution of the Percentage Residuals for the Band Center for the Isotope 636.

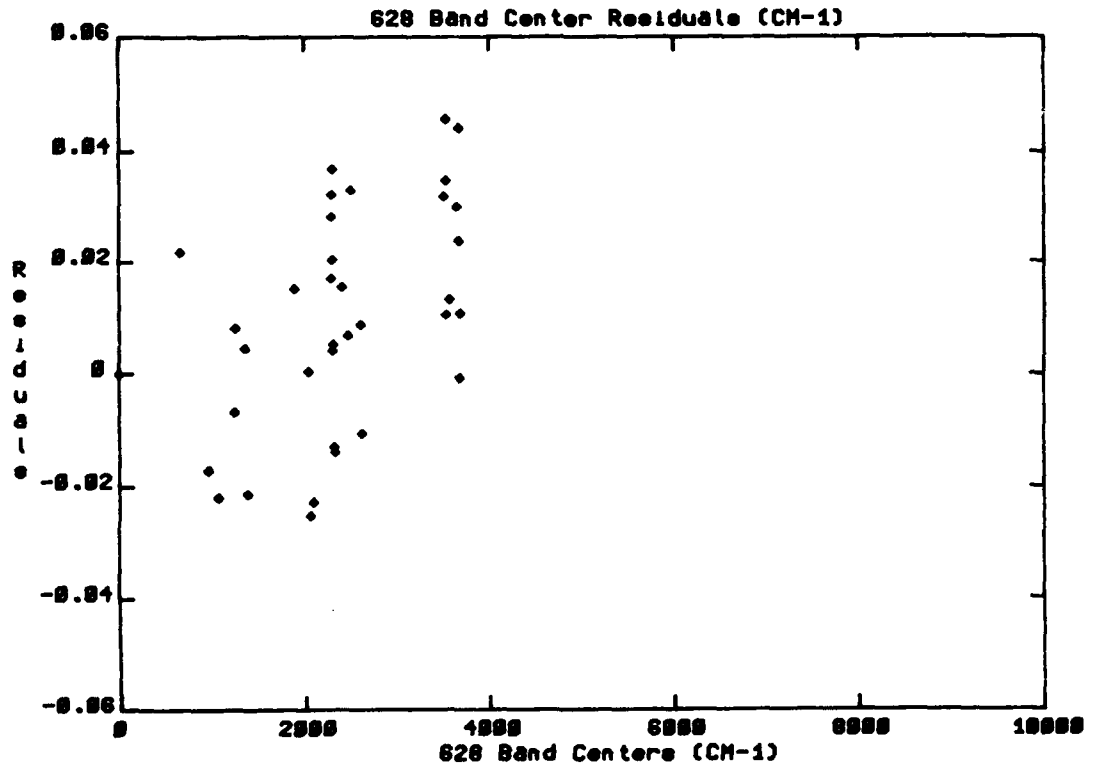

Figure 7. Distribution of the Percentage Residuals for the Band Center for the Isotope 628.

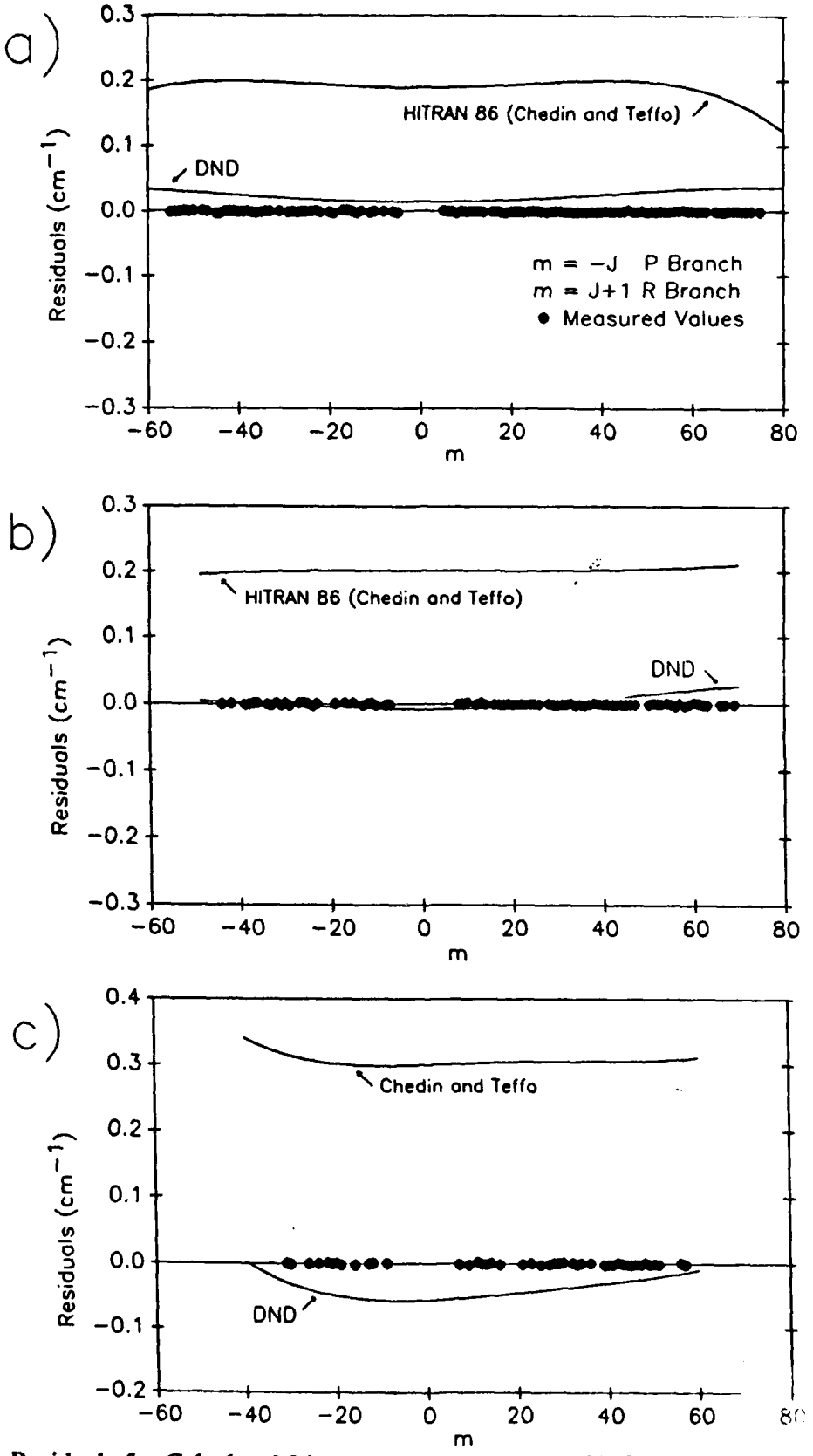

Figure 8. Residuals for Calculated Line Positions for the (a) 05501 ← 04401 Band, (b) 06601 ← 05501 Band, and (c) 07701 ← 06601 Band.

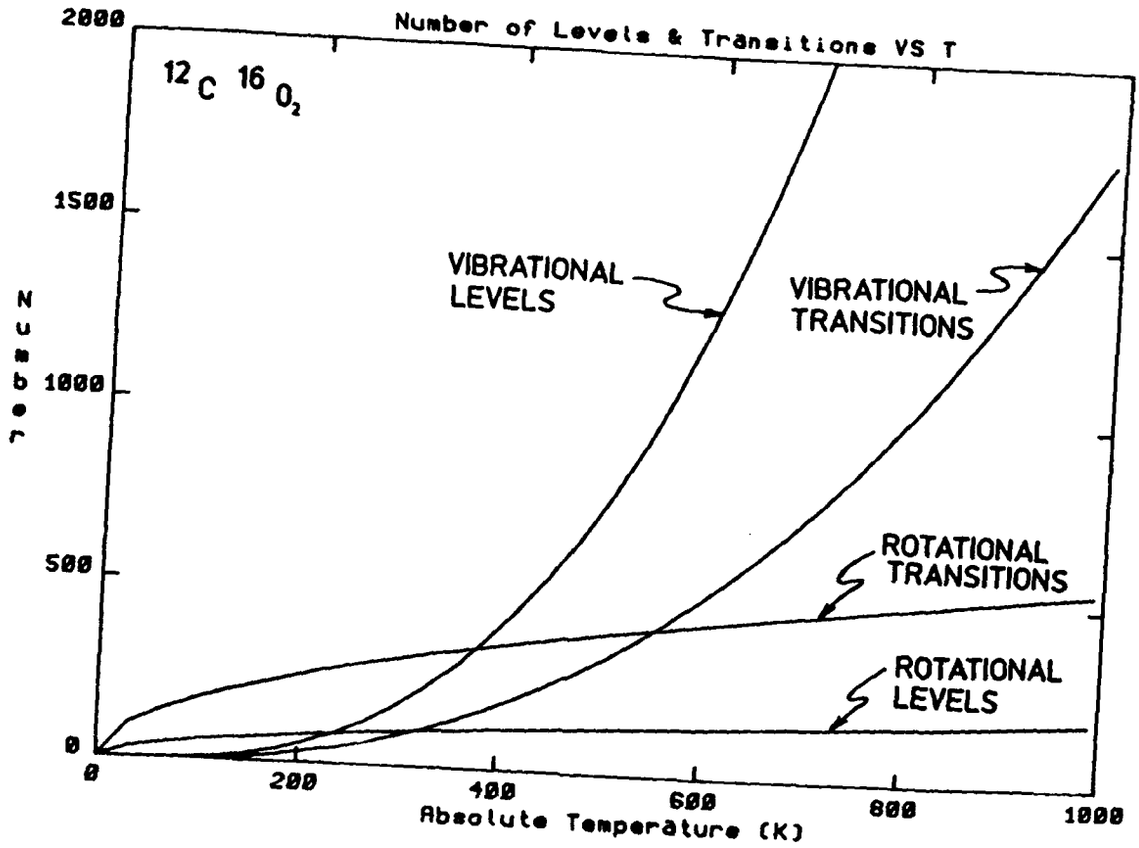

Figure 9. Number of Transitions of CO_2 in the HITEMP Database as a Function of Temperature

CO_2 LINE POSITIONS

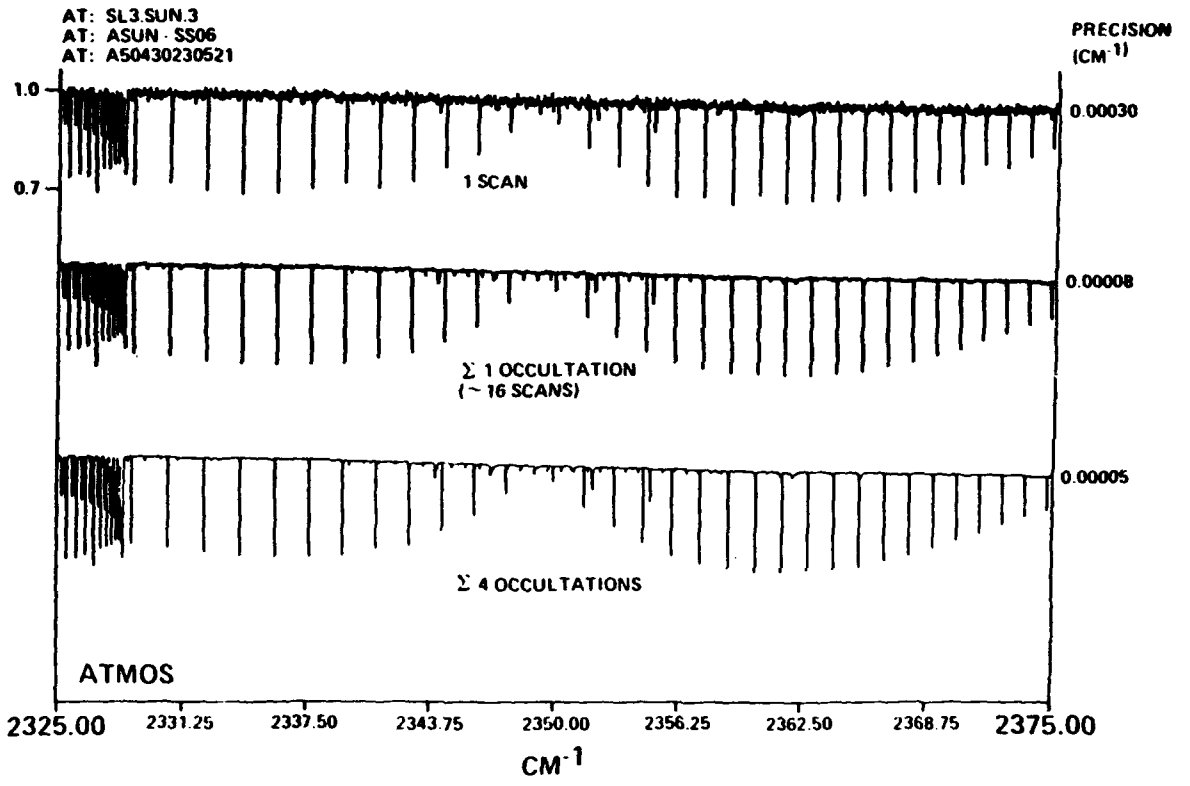

Figure 10. Bands Observed by the NASA Atmospheric Trace Gas Experiment.

INFRARED OZONE LINE POSITIONS AND INTENSITIES: IMPROVEMENTS FOR THE 1989 HITRAN DATABASE

Curtis P. Rinsland
NASA Langley Research Center
Mail Stop 401A
Hampton, VA 23665

Jean-Marie Flaud
Laboratoire de Physique Moléculaire et Atmosphérique
Université Pierre et Marie Curie
Tour 13, 4 Place Jussieu
75252 Paris Cedex 05
France

COLLABORATORS ON OZONE STUDIES

NASA LANGLEY RESEARCH CENTER
- C. P. RINSLAND
- M. A. H. SMITH

COLLEGE OF WILLIAM AND MARY
- V. MALATHY DEVI

LABORATOIRE DE PHYSIQUE MOLÉCULAIRE ET ATMOSPHÉRIQUE, PARIS
- J.-M. FLAUD
- C. CAMY-PEYRET
- A. N'GOM
- A. PERRIN

UNIVERSITY OF DENVER
- A. GOLDMAN

JET PROPULSION LABORATORY
- H. M. PICKETT
- E. A. COHEN
- L. R. BROWN

LABORATOIRE DE SPECTROMÉTRIE MOLÉCULAIRE ET ATMOSPHÉRIQUE, REIMS
- A. BARBE

ISTITUTO DI RICERCA SULLE ONDE ELETTROMAGNETICHE CNR-IROE, FLORENCE
- B. CARLI

ISTITUTO DI CHIMICA FISICA E SPETTROSCOPIA, BOLOGNA
- M. CARLOTTI

INFRARED SPECTRUM OF OZONE

(McCAA & SHAW, J.M.S. 25, 374, 1968)

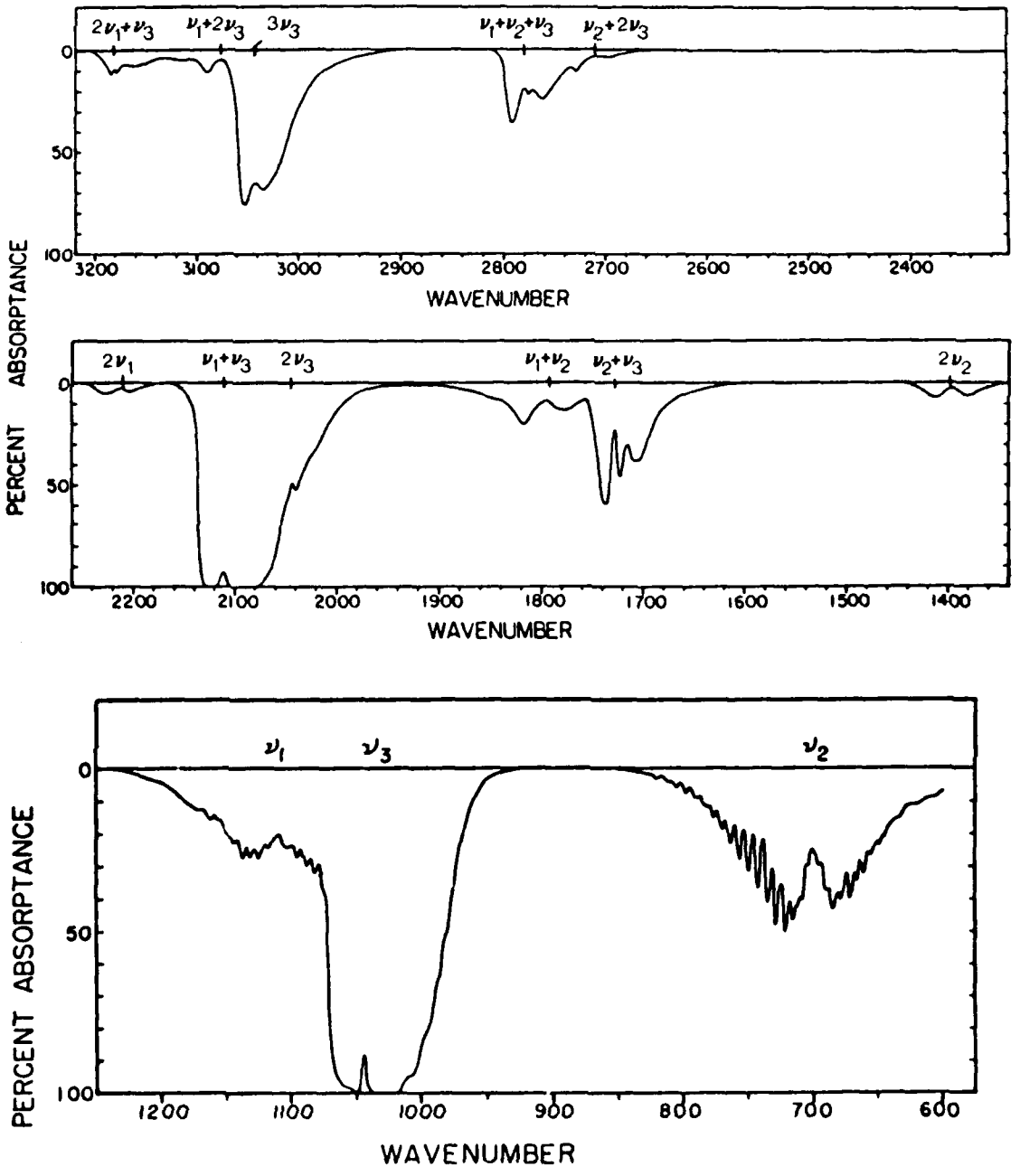

OVERVIEW OF EXPERIMENTAL CONDITIONS AND CHARACTERISTICS OF THE ABSORPTION SPECTRA

INSTRUMENT	MCMATH FTS
RECORDED SPECTRAL REGION	550-5000 cm^{-1}
STUDIED SPECTRAL REGION	550-3500 cm^{-1}
UNAPODIZED RESOLUTION	0.005 cm^{-1} (4 to 16 μm) 0.010 cm^{-1} (2 to 4 μm)
SIGNAL TO RMS NOISE RATIO	~500
CELL TEMPERATURE	~296 K
CELL LENGTHS	50, 239 cm
OXYGEN SAMPLES	NATURAL, PURE $^{16}O_2$, ^{18}O –ENRICHED
METHOD FOR GENERATING OZONE	SILENT ELECTRIC DISCHARGE

ν_2 AND $2\nu_2$-ν_2 BANDS OF $^{16}O_3$ (14.2 μm REGION)

PARAMETER	1986 HITRAN DATA[a]	1989 HITRAN DATA[b]
SPECTRAL RESOLUTION	0.02 cm^{-1}	0.0053 cm^{-1} IR 0.0033 cm^{-1} FAR IR
MAXIMUM QUANTUM NUMBERS		
ν_2 BAND	J≤52, K≤20	J≤65, K≤21
$2\nu_2$-ν_2 BAND	J≤41, K≤12	J≤54, K≤18
STANDARD DEVIATION OF FIT		
ν_2 BAND	0.00230 cm^{-1}	0.0006 cm^{-1} IR & FAR IR
$2\nu_2$-ν_2 BAND	0.00217 cm^{-1}	0.05 MhZ MICROWAVE
INTENSITY ACCURACY		±10%
INTEGRATED INTENSITY (# LINES)		
ν_2 BAND	6.283×10^{-19} (6340)	5.952×10^{-19} (7323)
$2\nu_2$-ν_2 BAND	4.164×10^{-20} (4591)	3.912×10^{-20} (4762)

[a]GOLDMAN, A., J. R. GILLIS, D. G. MURCRAY, A. BARBE, AND C. SECROUN, "ANALYSIS OF THE ν_2 AND $2\nu_2$-ν_2 OZONE BANDS FROM HIGH RESOLUTION INFRARED ATMOSPHERIC SPECTRA," J. MOL. SPECTROSC., 96, 279-287 (1982).

[b]PICKETT, H. M., E. A. COHEN, L. R. BROWN, C. P. RINSLAND, M. A. H. SMITH, V. MALATHY DEVI, A. GOLDMAN, A. BARBE, B. CARLI, AND M. CARLOTTI, "THE VIBRATIONAL AND ROTATIONAL SPECTRA OF OZONE FOR THE (0,1,0) AND (0,2,0) STATES," J. MOL. SPECTROSC., 128, 151-171 (1988).

Intensity Perturbation Effects

ν_2 Band of $^{16}O_3$

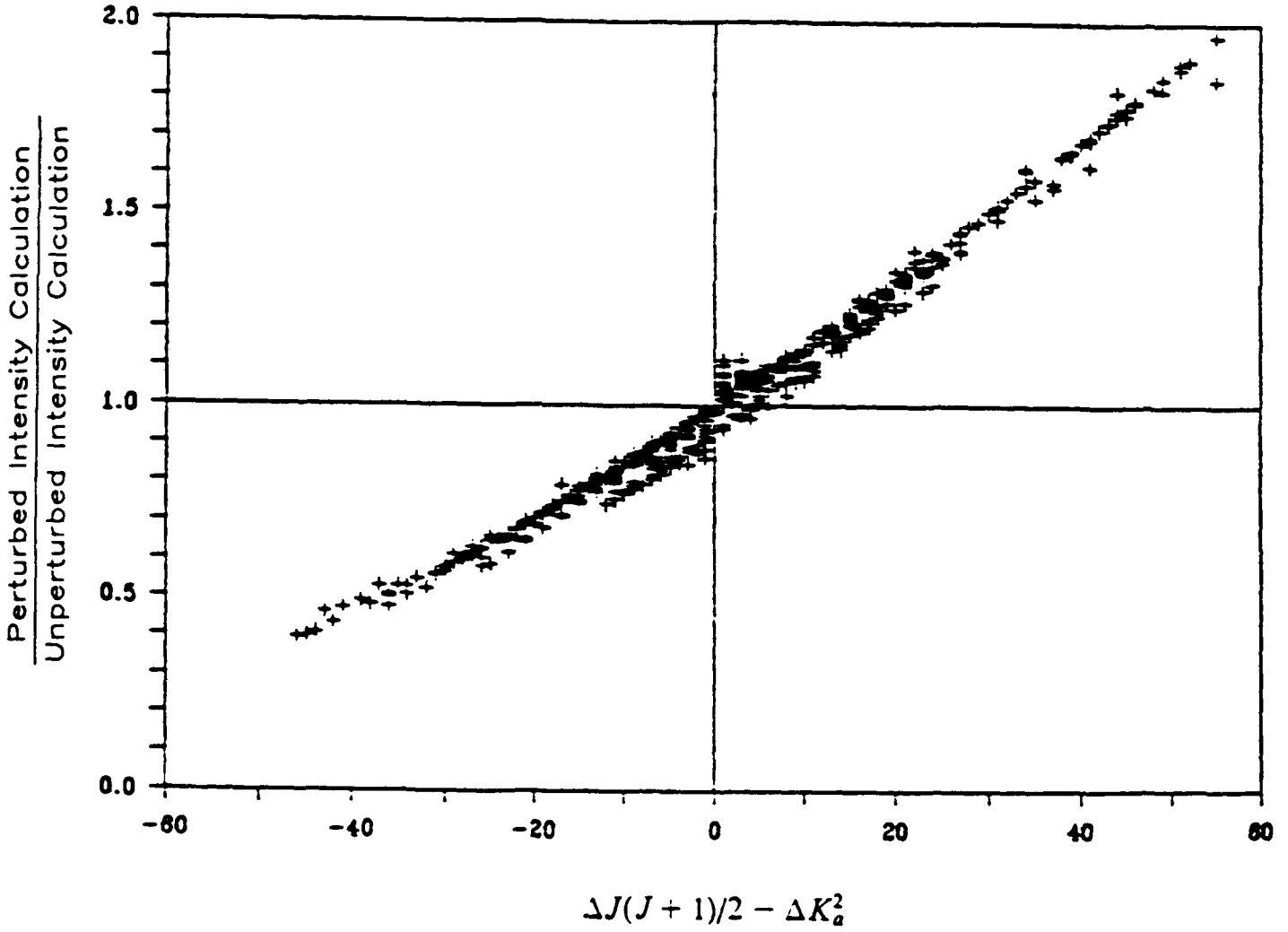

Ozone ν_2 Region: Measurement vs. Calculation

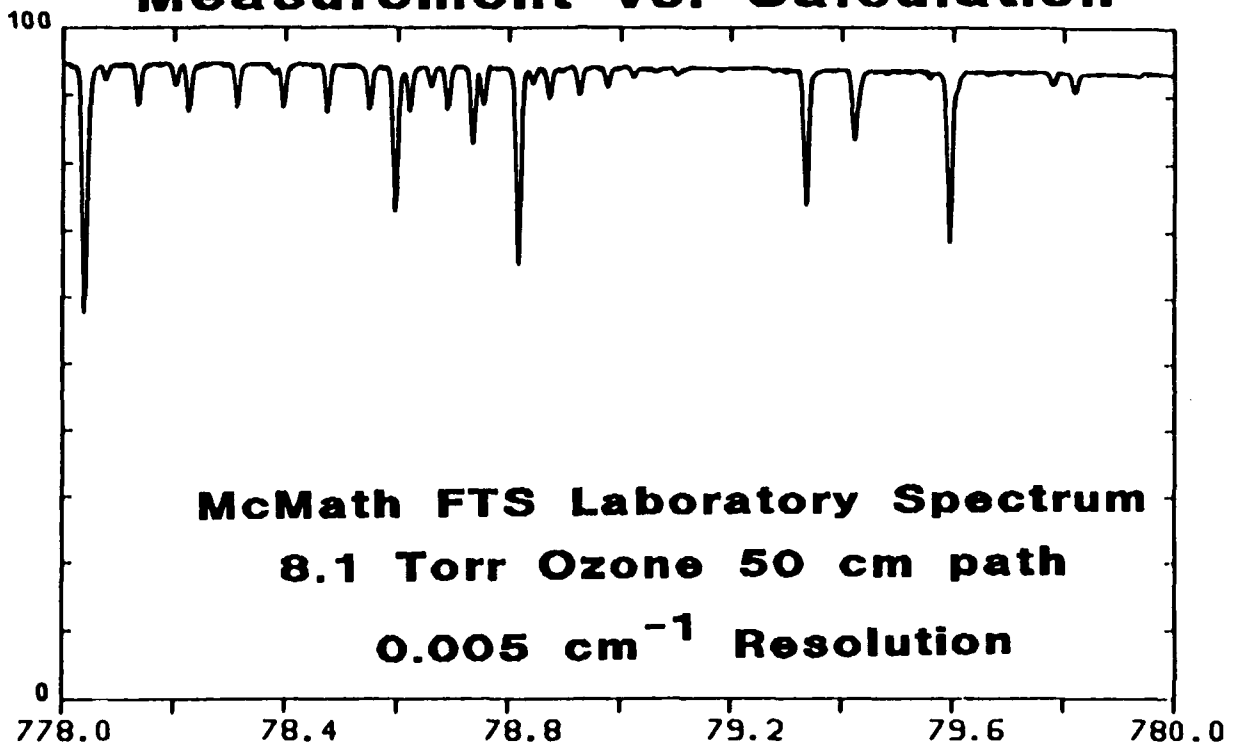

Measured Minus 1986 HITRAN

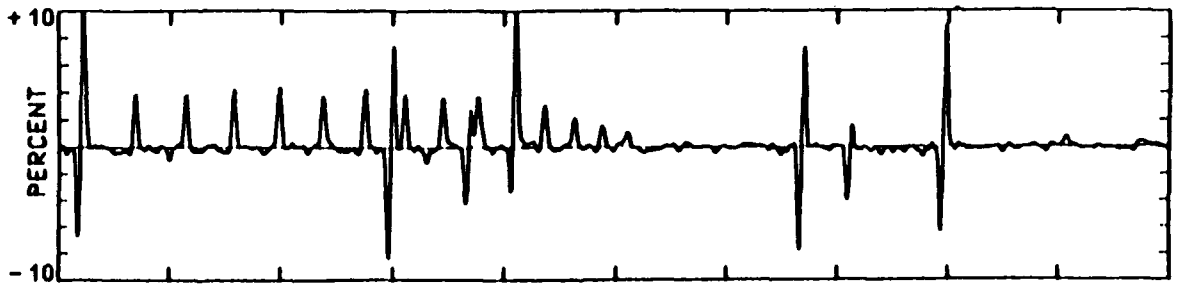

Measured Minus 1989 HITRAN

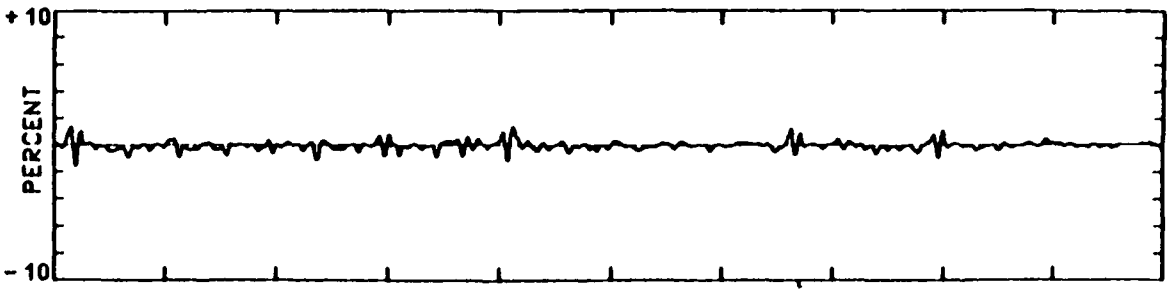

ISOTOPIC BANDS OF OZONE AT 14.3 μm[a]

VIBRATIONAL STATE UPPER	VIBRATIONAL STATE LOWER	ISOTOPE CODE[b]	BAND CENTER (cm^{-1})	SUM OF CALCULATED INTENSITIES AT 296K[c]	TOTAL NUMBER OF LINES
010	000	668	684.6134	2.596×10^{-21} [d]	-
010	000	686	693.3057	1.290×10^{-21}	-

[a]FLAUD, J.-M., C. CAMY-PEYRET, A. N'GOM, V. MALATHY DEVI, C. P. RINSLAND, AND M. A. H. SMITH, "THE v_2 BANDS OF $^{16}O^{18}O^{16}O$ AND $^{16}O\ ^{16}O\ ^{18}O$: LINE POSITIONS AND INTENSITIES," J. MOL. SPECTROSC., 133, 217-223 (1989).

[b]668 = $^{16}O^{16}O^{18}O$; 686 = $^{16}O^{18}O^{16}O$.

[c]CALCULATED WITH MOLECULAR ISOTOPIC ABUNDANCES OF 0.004 FOR $^{16}O^{16}O^{18}O$ AND 0.002 FOR $^{16}O^{18}O^{16}O$.

[d]B-TYPE COMPONENT ONLY. THE MUCH WEAKER A-TYPE COMPONENT WAS NOT OBSERVED.

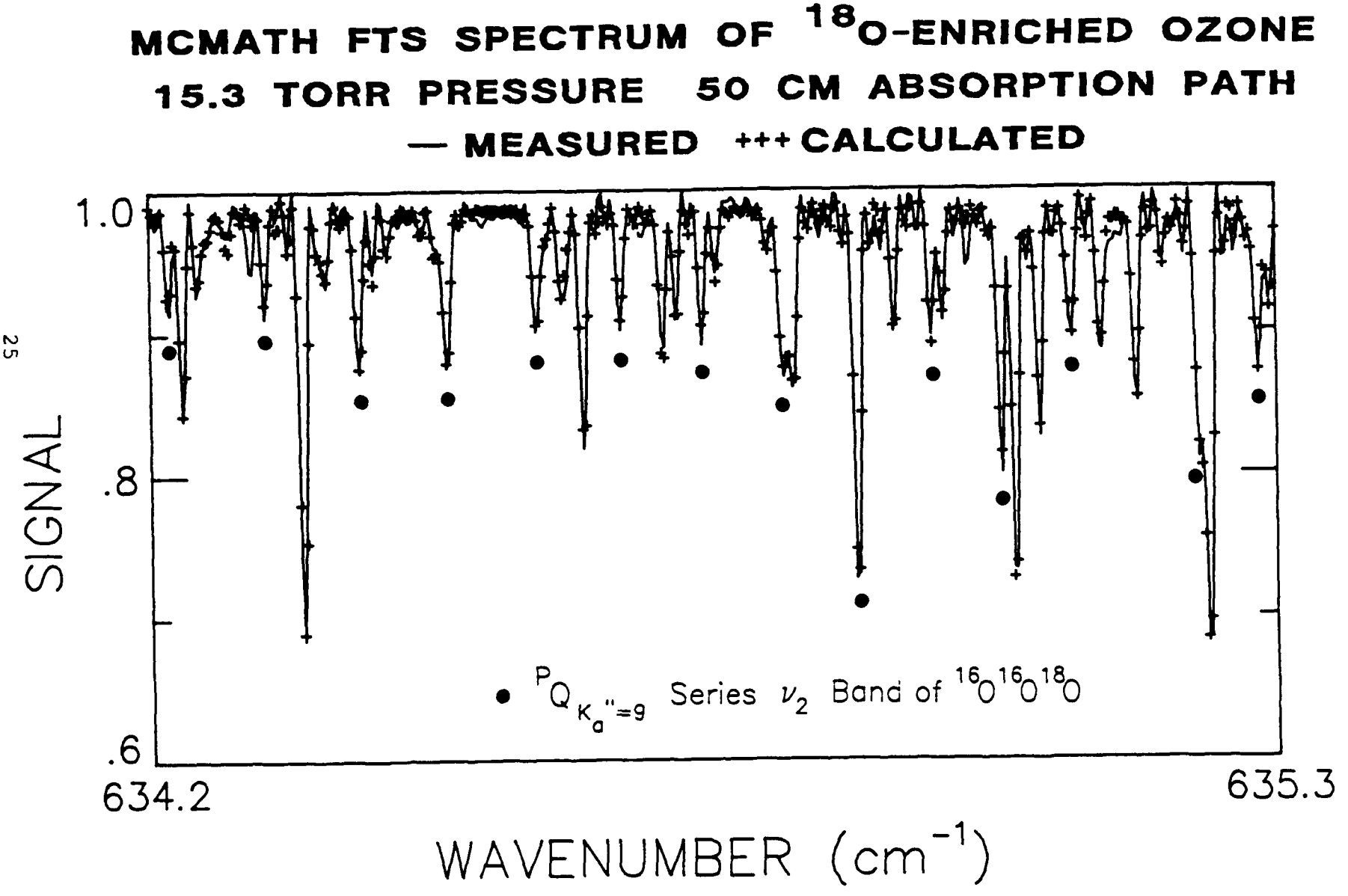
MCMATH FTS SPECTRUM OF ^{18}O-ENRICHED OZONE
15.3 TORR PRESSURE 50 CM ABSORPTION PATH
— MEASURED +++ CALCULATED
1.0
.8
.6
SIGNAL
634.2
635.3
WAVENUMBER (cm^{-1})
$^{P}Q_{K_a''=9}$ Series ν_2 Band of $^{16}O^{16}O^{18}O$

ATMOSPHERIC IMPORTANCE OF 10 MICRON OZONE BANDS

- **FREQUENCY USED FOR REMOTE SOUNDING OF OZONE**
  - LIMS EXPERIMENT ON NIMBUS 7
    REF: REMSBERG ET AL., J. GEOPHYS. RES. 89, 5161, 1984.
  - MEASUREMENT OF TOTAL OZONE IN ANTARCTIC OZONE HOLE
    REF: FARMER ET AL., NATURE 329, 126, 1987.
  - MEASUREMENT OF OZONE ISOTOPE RATIOS
    REF: RINSLAND ET AL., J. GEOPHYS. RES. 90, 10719, 1985.

- **10 MICRON BAND ABSORPTION IMPORTANT IN CLIMATE MODELS**
  REF: RAMANATHAN ET AL., J. GEOPHYS. RES. 90, 5547, 1985.

TOTAL NUMBER OF OZONE LINES AT 10 MICRONS

HITRAN LIST	NUMBER OF LINES
1980	14,266
1982	18,322
1986	20,969
1989	53,699

INTENSITY CUTOFF FOR 1989 HITRAN CALCULATIONS

ISOTOPIC SPECIES	CUTOFF
666	1.0E-25
668	5.0E-23 (2.0E-25)*
686	5.0E-23 (1.0E-25)*

* VALUE INCLUDING HITRAN ISOTOPIC ABUNDANCE FACTOR

TOTAL NUMBER OF OZONE BANDS AT 10 MICRONS

HITRAN LIST	666	668	686
1980	6	1	1
1982	6	1	1
1986	6	1	1
1989	18	2	2

Band Systems of $^{16}O_3$ at 10 μm

- [(001),(100)]←(000)
- [(011),(110)]←(010)
- [(002),(101),(200)]←[(100),(001)]
- [(021),(120)]←(020)
- [(210),(111),(012)]←[(011),(110)]

Summary of 10 μm O_3 Bands Included in the Calculations

Vibrational States					
Upper	Lower	Isotope[a]	Band Center (cm^{-1})	Sum of Calculated Intensities at 296 K[b]	Number of Lines
012	110	666	929.8447	c	c
002	100	666	954.3831	3.266×10^{-21}	951
111	110	666	988.9772	c	c
012	011	666	999.5841	c	c
101	100	666	1007.6470	6.246×10^{-20}	2646
001	000	686	1008.4528	2.649×10^{-20}	2095
021	020	666	1008.6618	1.480×10^{-20}	1431
002	001	666	1015.4364	1.680×10^{-19}	3137
011	010	666	1025.5914	4.635×10^{-19}	3883
001	000	668	1028.1120	5.121×10^{-20}	3827
001	000	666	1042.0840	1.413×10^{-17}	7224
111	011	666	1058.7166	c	c
101	001	666	1068.7003	5.238×10^{-21}	2558
100	000	686	1074.3076	4.543×10^{-22}	888
120	020	666	1087.3041	2.265×10^{-22}	864
210	110	666	1089.9162	c	c
100	000	668	1090.3541	4.071×10^{-21}	4425
110	010	666	1095.3308	1.273×10^{-20}	3885
200	100	666	1098.3883	3.299×10^{-21}	2931
100	000	666	1103.1373	5.403×10^{-19}	6766
200	001	666	1159.4416	8.340×10^{-21}	2057
210	011	666	1159.6556	c	c

Notes: a. 666= $^{16}O_3$, 686 = $^{16}O^{18}O^{16}O$, 668 = $^{16}O^{16}O^{18}O$.

b. Intensities are in cm^{-1}/molecule cm^{-2} units. Values are scaled to include the assumed molecular isotopic abundance of each species.

c. Calculations not available yet.

CALIBRATION OF THE LINE INTENSITIES

- PARTIAL PRESSURE OF OZONE NOT MEASURED DURING THE EXPERIMENT
- INTENSITIES CALCULATED ASSUMING $\left(\partial q_z/\partial q_3\right)_e = -0.2662\ D$.
- INTENSITY CALIBRATION TRANSFERRED FROM 10 MICRON REGION TO OTHER REGIONS USING RELATIVE INTENSITY MEASUREMENTS

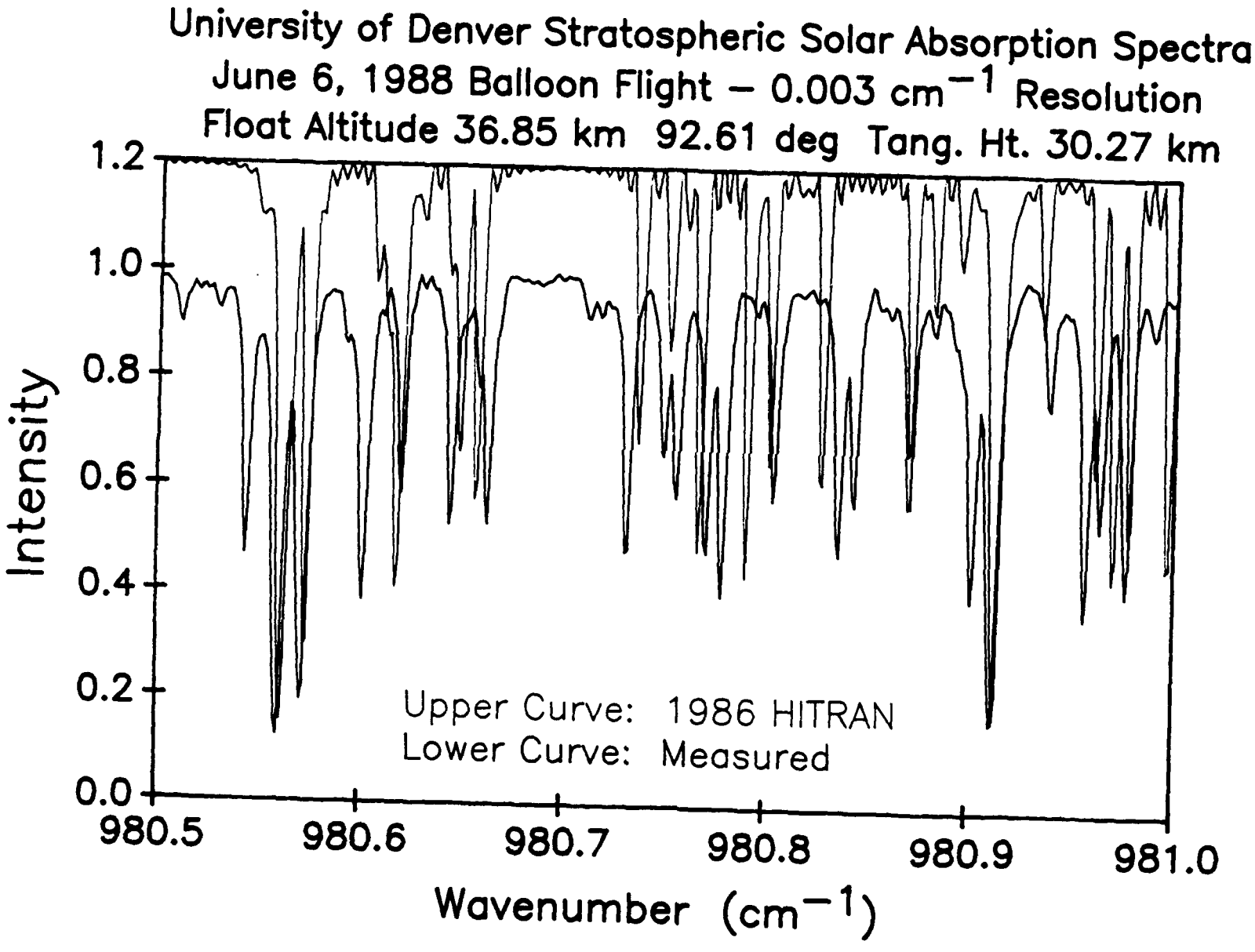
University of Denver Stratospheric Solar Absorption Spectra
June 6, 1988 Balloon Flight – 0.003 cm^{-1} Resolution
Float Altitude 36.85 km 92.61 deg Tang. Ht. 30.27 km
Intensity
1.2
1.0
0.8
0.6
0.4
0.2
0.0
Upper Curve: 1986 HITRAN
Lower Curve: Measured
980.5
980.6
980.7
980.8
980.9
981.0
Wavenumber (cm^{-1})

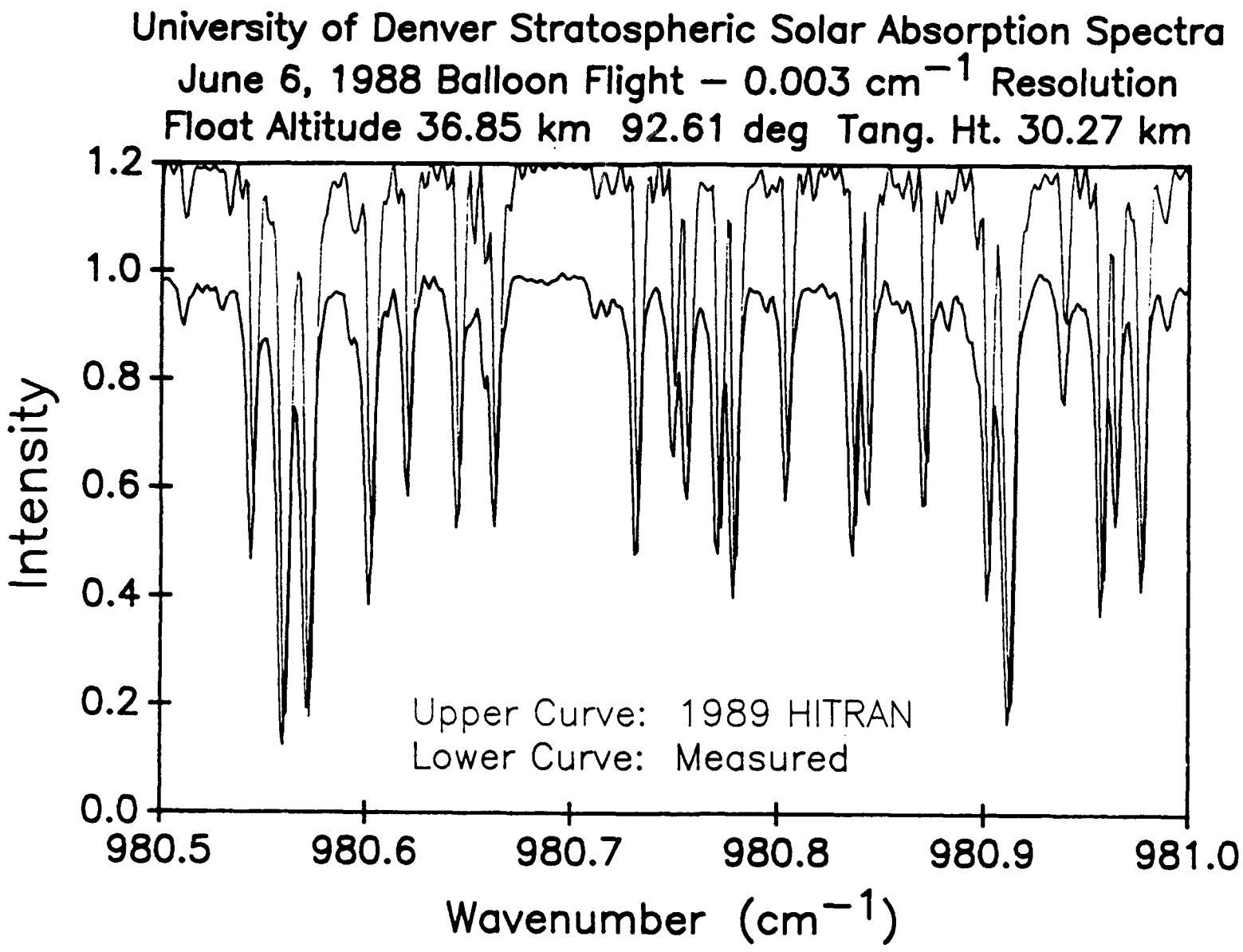
University of Denver Stratospheric Solar Absorption Spectra
June 6, 1988 Balloon Flight – 0.003 cm^{-1} Resolution
Float Altitude 36.85 km 92.61 deg Tang. Ht. 30.27 km
Intensity
1.2
1.0
0.8
0.6
0.4
0.2
0.0
Upper Curve: 1989 HITRAN
Lower Curve: Measured
980.5
980.6
980.7
980.8
980.9
981.0
Wavenumber (cm^{-1})

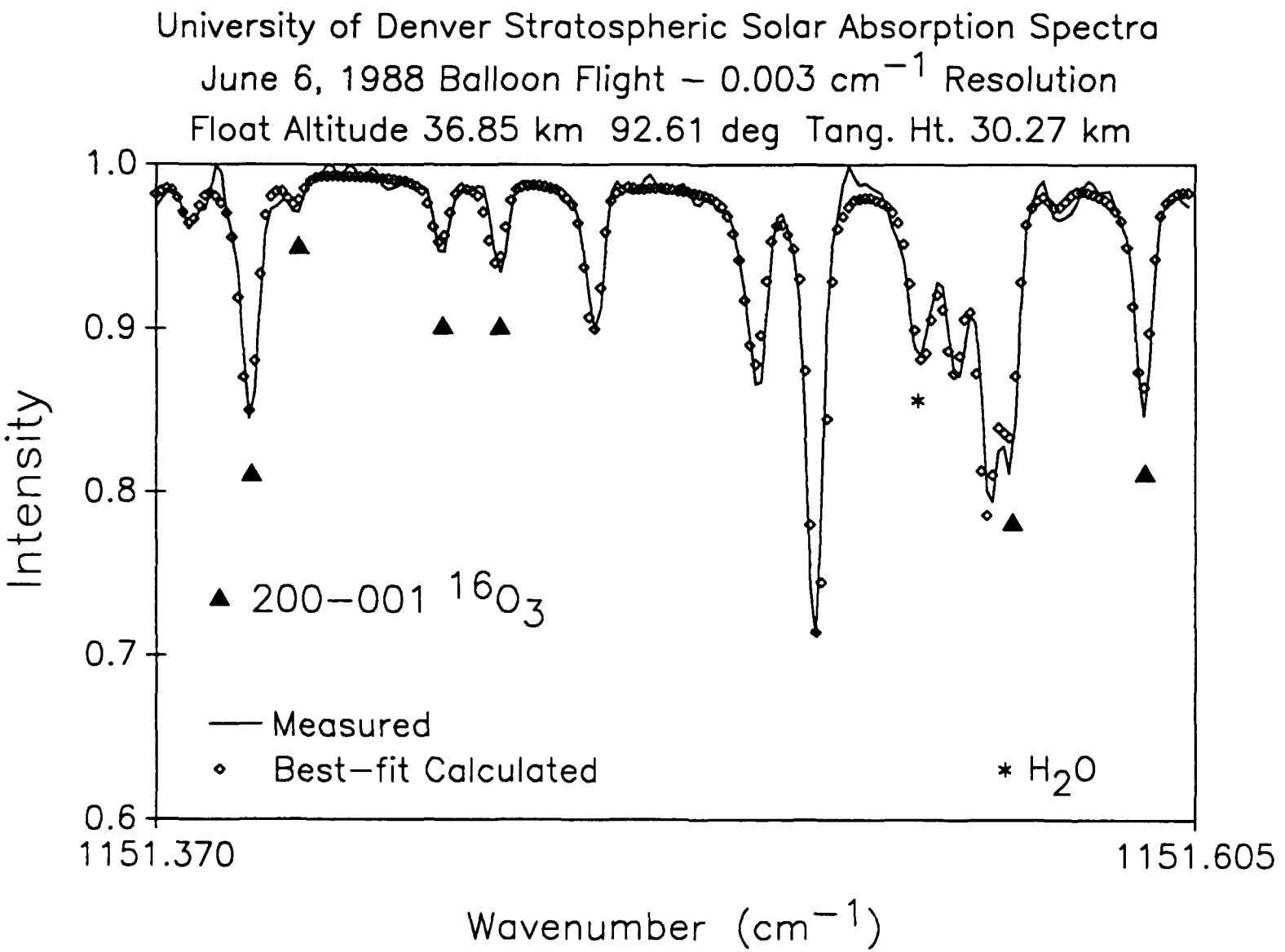
University of Denver Stratospheric Solar Absorption Spectra
June 6, 1988 Balloon Flight – 0.003 cm^{-1} Resolution
Float Altitude 36.85 km 92.61 deg Tang. Ht. 30.27 km
1.0
0.9
0.8
0.7
0.6
Intensity
▲ 200–001 $^{16}O_3$
Measured
Best–fit Calculated
* H_2O
1151.370
1151.605
Wavenumber (cm^{-1})

1989 HITRAN OZONE PARAMETERS
SAMPLE "STICK" PLOTS
(AARON GOLDMAN, PRIV. COMM.)

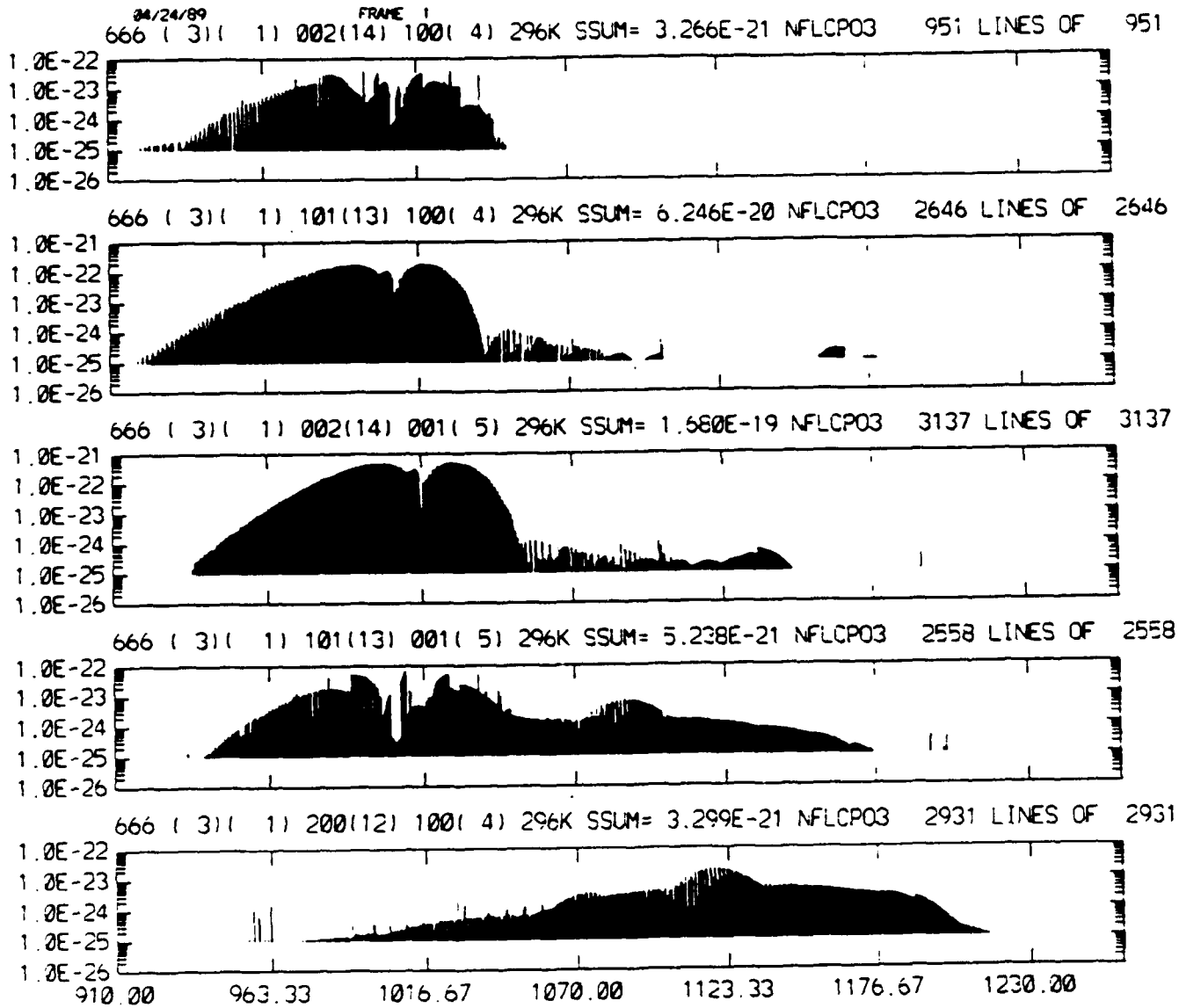

ATMOS OZONE PROFILES NEAR 30° N LATITUDE (GUNSON ET AL., J. GEOPHYS. RES., SUBMITTED)

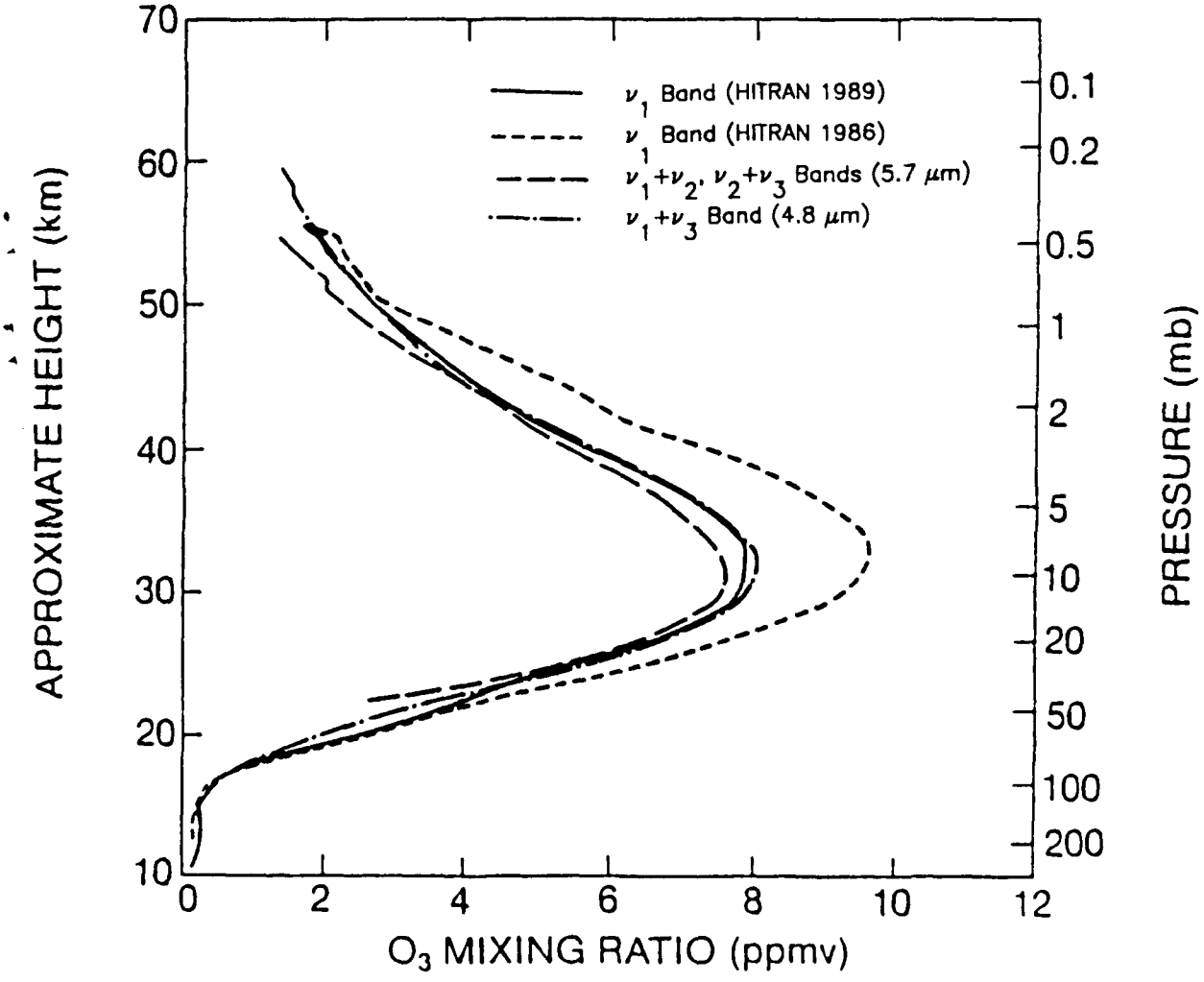

A. GOLDMAN ET AL., APPL. OPT. 9, 565-580, 1970.

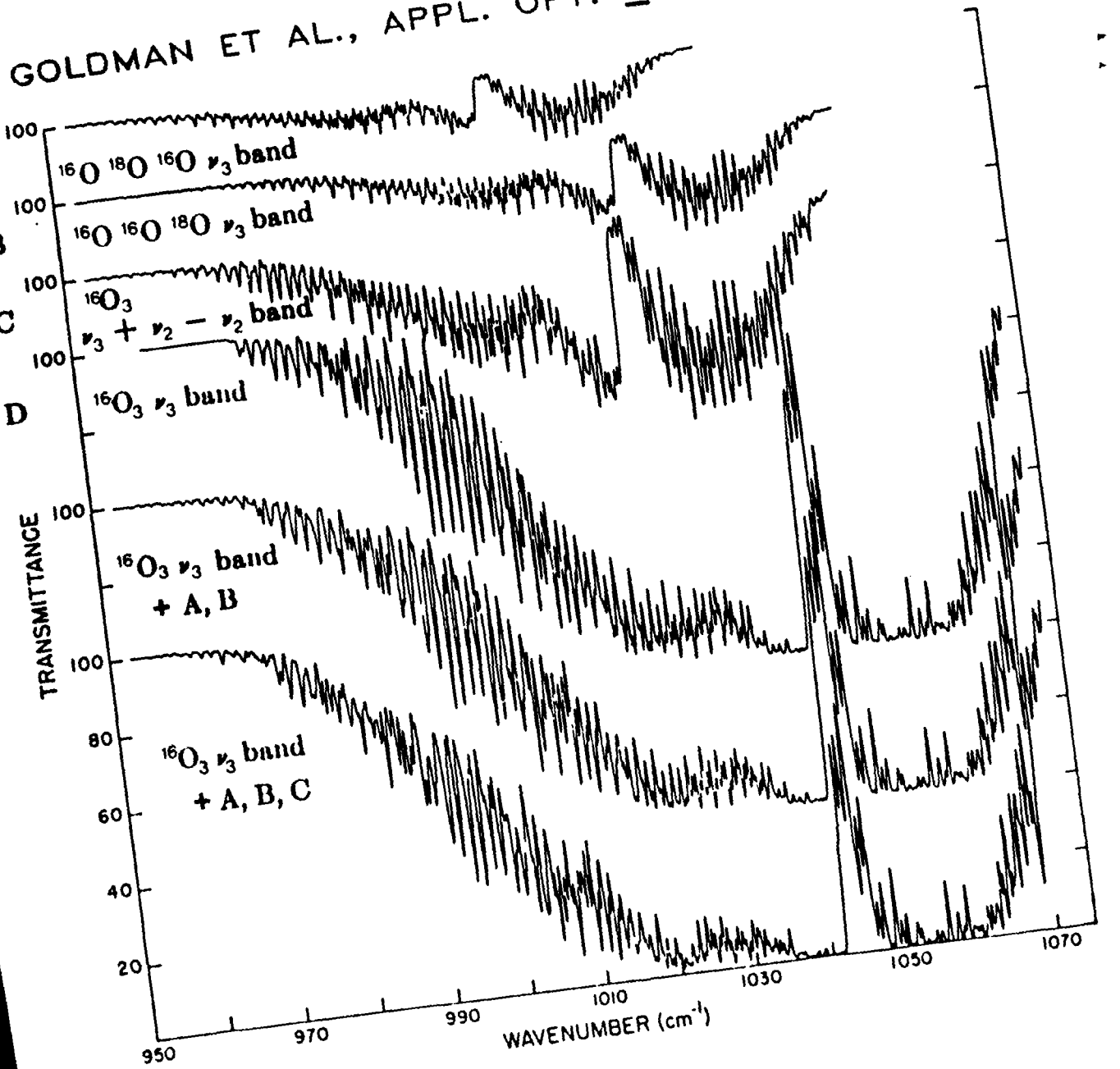

UNIVERSITY OF DENVER
STRATOSPHERIC SOLAR SPECTRA

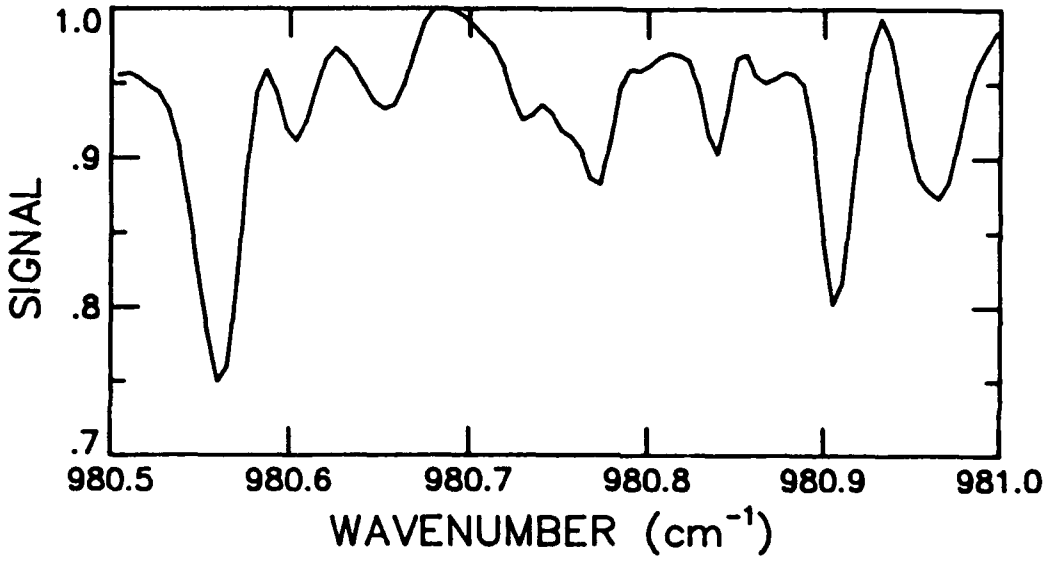

0.02 cm^{-1} Resolution

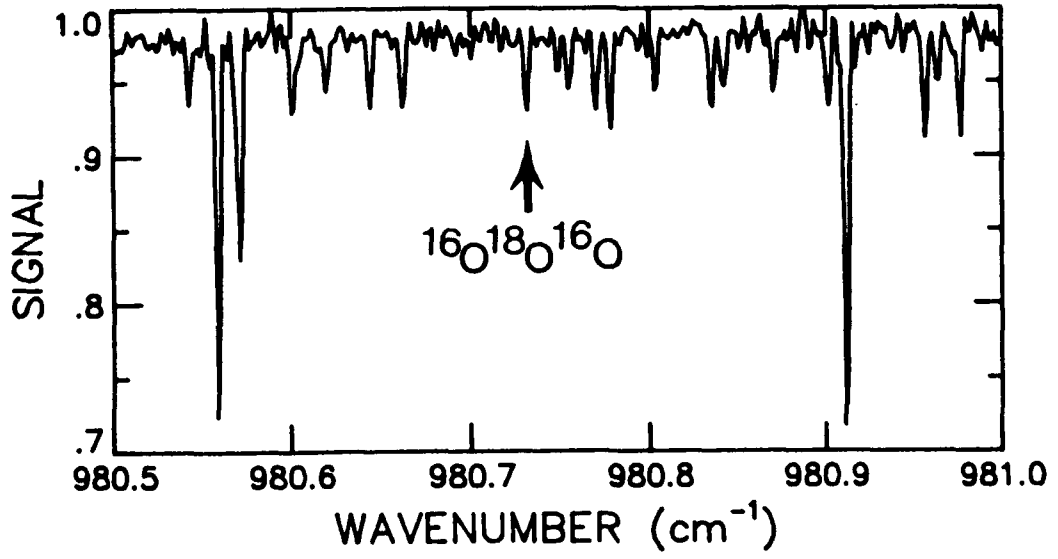

0.002 cm^{-1} Resolution

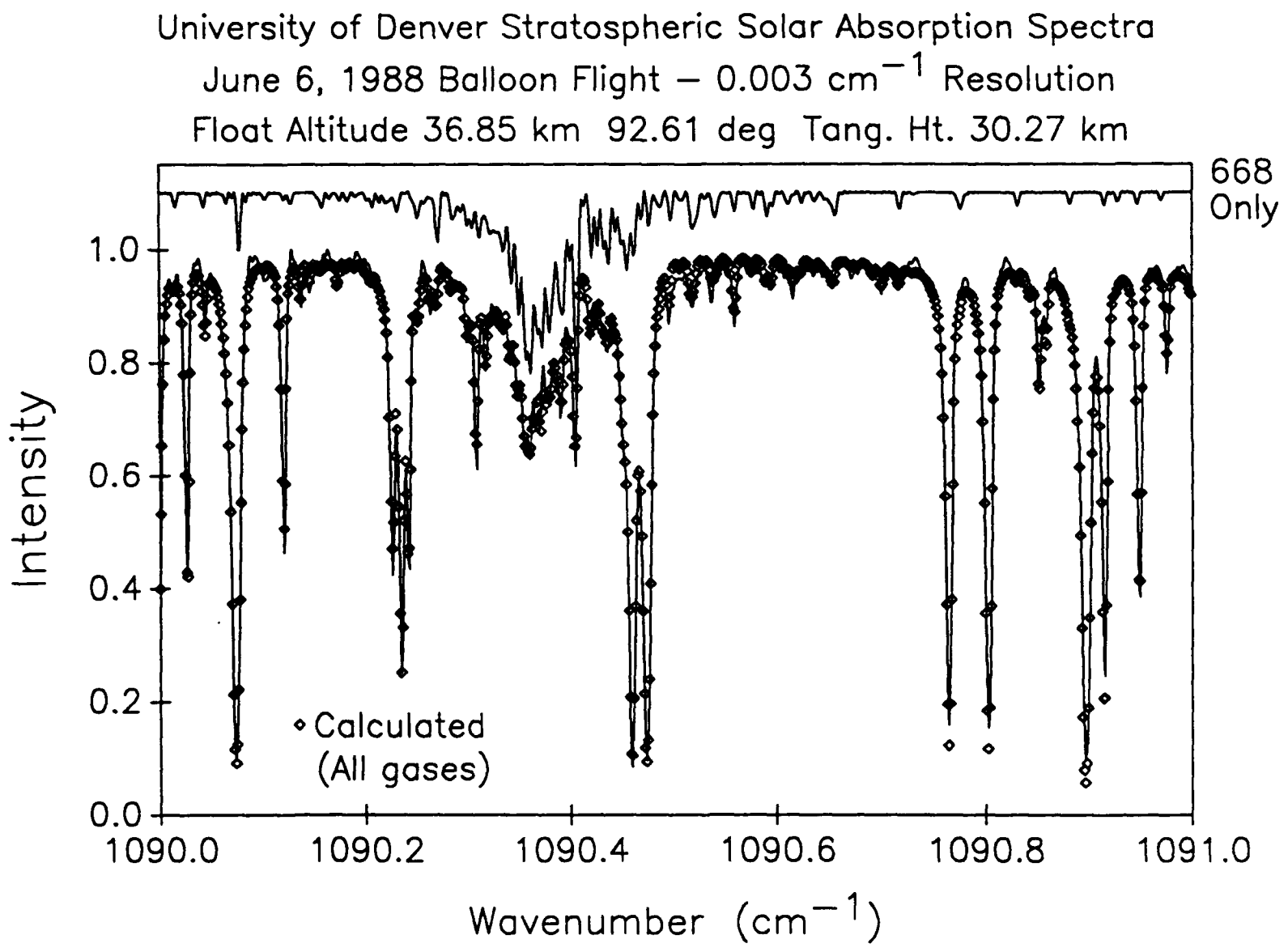
University of Denver Stratospheric Solar Absorption Spectra
June 6, 1988 Balloon Flight – 0.003 cm^{-1} Resolution
Float Altitude 36.85 km 92.61 deg Tang. Ht. 30.27 km
668 Only
Intensity
1.0
0.8
0.6
0.4
0.2
0.0
◇ Calculated (All gases)
1090.0
1090.2
1090.4
1090.6
1090.8
1091.0
Wavenumber (cm^{-1})

$^{16}O_3$ BANDS AT 7 μm: $\nu_1 + \nu_3 - \nu_2$, $2\nu_2$, AND $2\nu_3 - \nu_2$ BANDS[a]

VIBRATIONAL STATES		BAND CENTER	SUM OF CALCULATED	TOTAL NUMBER
UPPER	LOWER	(cm^{-1})	INTENSITIES AT 296 K[b]	OF LINES
002	010	1356.5893	2.064×10^{-23}	107
020	000	1399.2726	4.499×10^{-22}	1127
101	010	1409.8532	9.927×10^{-22}	1043

[a]FLAUD, J.-M., C. CAMY-PEYRET, C. P. RINSLAND, M. A. H. SMITH, AND V. MALATHY DEVI, "LINE PARAMETERS FOR $^{16}O_3$ BANDS IN THE 7-μm REGION," J. MOL. SPECTROSC., 134, 106-112 (1989).

[b]UNITS OF cm^{-1}/molecule cm^{-2}.

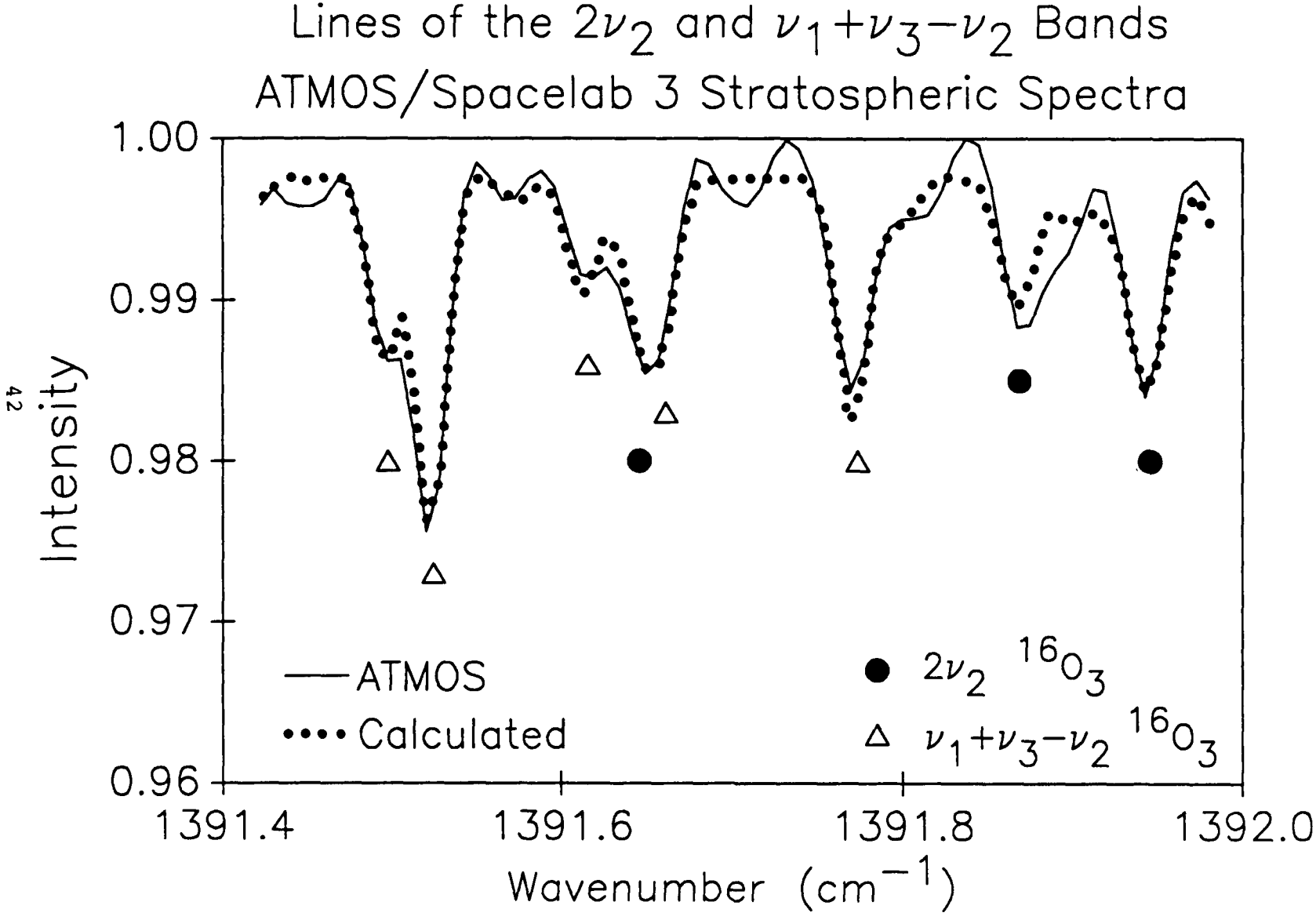
Lines of the $2\nu_2$ and $\nu_1+\nu_3-\nu_2$ Bands
ATMOS/Spacelab 3 Stratospheric Spectra
1.00
0.99
0.98
0.97
0.96
Intensity
1391.4
1391.6
1391.8
1392.0
Wavenumber (cm^{-1})
ATMOS
Calculated
$2\nu_2$ $^{16}O_3$
$\nu_1+\nu_3-\nu_2$ $^{16}O_3$

$\nu_1+\nu_2$ AND $\nu_2+\nu_3$ BANDS OF $^{16}O_3$ (5.8 μm REGION)

PARAMETER	1986 HITRAN DATA[a]	1989 HITRAN DATA[b]
SPECTRAL RESOLUTION	0.019 cm^{-1}	0.005 cm^{-1}
MAXIMUM QUANTUM NUMBERS		
$\nu_1+\nu_2$ BAND	$J<45$, $K_a\leq11$	$J\leq57$, $K_a\leq16$
$\nu_2+\nu_3$ BAND	$J\leq36$, $K_a\leq10$	$J\leq55$, $K_a\leq15$
STANDARD DEVIATION OF FIT	0.0035 cm^{-1}	0.00043 cm^{-1}
INTENSITY ACCURACY	±10-100%	±5-10%
INTEGRATED INTENSITY (#LINES)		
$\nu_1+\nu_2$ BAND	2.266×10^{-20}(2137)	2.374×10^{-20}(3695)
$\nu_2+\nu_3$ BAND	5.373×10^{-20}(1709)	5.357×10^{-20}(3415)

[a]BARBE, A., C. SECROUN, P. JOUVE, C. CAMY-PEYRET, AND J.-M. FLAUD, "HIGH RESOLUTION INFRARED SPECTRUM OF THE $\nu_2+\nu_3$ AND $\nu_1+\nu_2$ BANDS OF OZONE," J. MOL. SPECTROSC., 75, 103-110 (1979).

[b]MALATHY DEVI., V., J.-M. FLAUD, C. CAMY-PEYRET, C. P. RINSLAND, AND M. A. H. SMITH, "LINE POSITIONS AND INTENSITIES FOR THE $\nu_1+\nu_2$ AND $\nu_2+\nu_3$ BANDS OF $^{16}O_3$," J. MOL. SPECTROSC., 125, 174-183 (1987).

LEAST-SQUARES FIT
KITT PEAK OZONE SPECTRUM

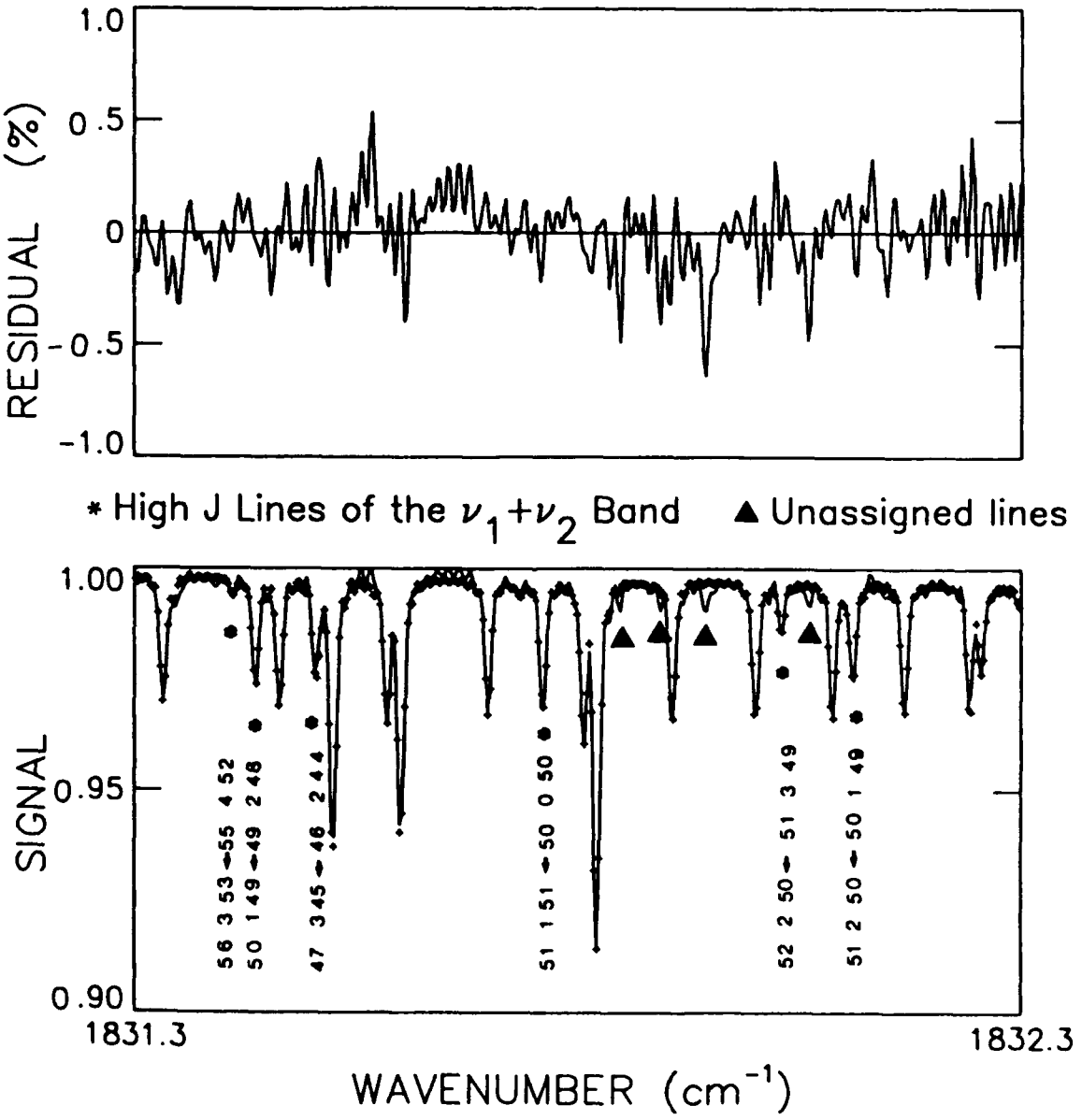

TOTAL NUMBER OF OZONE LINES AT 4.8 MICRONS

HITRAN LIST	NUMBER OF LINES
1980	5,859
1982	5,859
1986	7,328
1989	22,887

Band Systems of $^{16}O_3$ at 4.8 μm

- [(002),(101),(200)]←(000)
- [(012),(111),(210)]←(010)
- [(003),(102),(201),(300)] ← [(100),(001)]

OVERTONE AND COMBINATION BANDS OF $^{16}O_3$ AT 4.8 μm: $2\nu_3$, $\nu_1+\nu_3$, AND $2\nu_1$ BANDS

PARAMETER	1986 HITRAN DATA[a]	1989 HITRAN DATA[b]
SPECTRAL RESOLUTION	0.020 cm^{-1}	0.005 cm^{-1}
MAXIMUM QUANTUM NUMBERS		
$2\nu_3$	$J \leq 45$, $K_a \leq 10$	$J \leq 55$, $K_a \leq 17$
$\nu_1+\nu_3$ BAND	$J \leq 55$, $K_a \leq 16$	$J \leq 64$, $K_a \leq 17$
$2\nu_1$ BAND	$J \leq 50$, $K_a \leq 10$	$J \leq 55$, $K_a \leq 14$
STANDARD DEVIATION OF FIT	0.0032 cm^{-1}	0.00047 cm^{-1}
INTENSITY ACCURACY		±5-10%
INTEGRATED INTENSITY (# LINES)		
$2\nu_3$ BAND	1.11×10^{-19} (2164)	1.120×10^{-19} (5339)
$\nu_1+\nu_3$ BAND	1.13×10^{-18} (2165)	1.263×10^{-18} (5865)
$2\nu_1$ BAND	3.00×10^{-20} (1530)	3.371×10^{-20} (5024)

[a]FLAUD, J.-M. , C. CAMY-PEYRET, A. BARBE, C. SECROUN, AND P. JOUVE, "LINE POSITIONS AND INTENSITIES FOR THE $2\nu_3$, $\nu_1+\nu_3$, AND $2\nu_1$ BANDS OF OZONE," J. MOL. SPECTROSC., 80, 185-199 (1980); FLAUD, J.-M., C. CAMY-PEYRET, AND L. S. ROTHMAN, "IMPROVED OZONE LINE PARAMETERS IN THE 10- AND 4.8 μm REGIONS," APPL. OPT., 19, 655 (1980).

[b]RINSLAND, C. P., M. A. H. SMITH, J.-M. FLAUD, C. CAMY-PEYRET, AND V. MALATHY DEVI, "LINE POSITIONS AND INTENSITIES OF THE $2\nu_3$, $\nu_1+\nu_3$, AND $2\nu_1$ BANDS OF $^{16}O_3$," J. MOL. SPECTROSC. 130, 204-212 (1988).

[(012), (110), (210)]—[(010)] HOT BAND SYSTEM AT 4.8 μm

PARAMETER	1986 HITRAN DATA[a]	1989 HITRAN DATA[b]
INTEGRATED INTENSITY (# OF LINES)		
$\nu_2 + 2\nu_3 - \nu_2$		3.156×10^{-21} (2506)
$\nu_1 + \nu_2 + \nu_3 - \nu_2$	3.74×10^{-20} (1469)	4.083×10^{-20} (2514)
$2\nu_1 + \nu_2 - \nu_2$		7.663×10^{-22} (1639)

[a]CALCULATED BY GOLDMAN AND BARBE FOR THE HITRAN DATABASE.

[b]FLAUD, J.-M., C. CAMY-PEYRET, C. P. RINSLAND, M. A. H. SMITH, AND V. MALATHY DEVI, "LINE PARAMETERS FOR OZONE HOT BANDS IN THE 4.8 μm SPECTRAL REGION," IN PREPARATION FOR J. MOL. SPECTROSC.

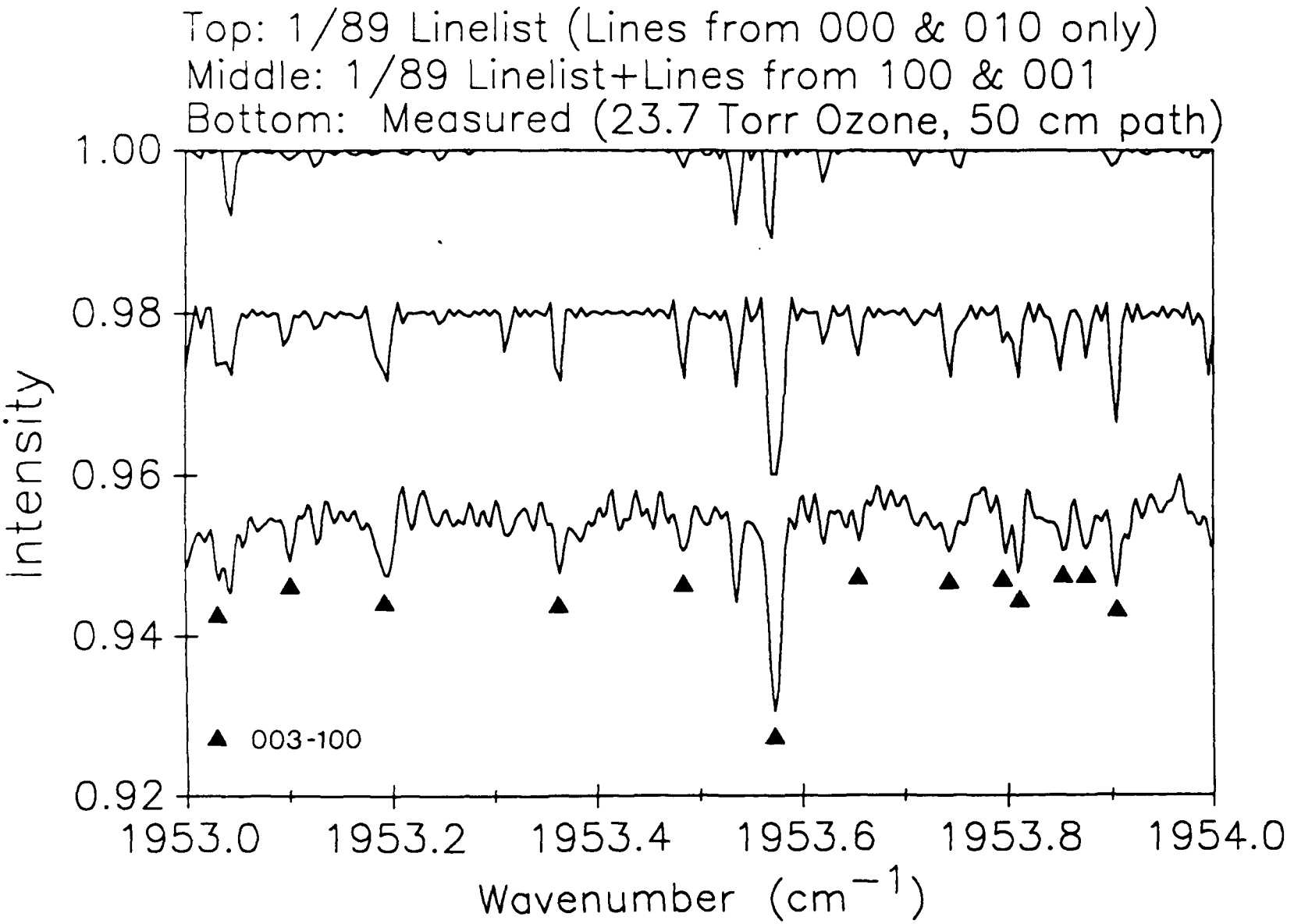
Top: 1/89 Linelist (Lines from 000 & 010 only)
Middle: 1/89 Linelist+Lines from 100 & 001
Bottom: Measured (23.7 Torr Ozone, 50 cm path)
1.00
0.98
0.96
0.94
0.92
Intensity
003-100
1953.0
1953.2
1953.4
1953.6
1953.8
1954.0
Wavenumber (cm^{-1})

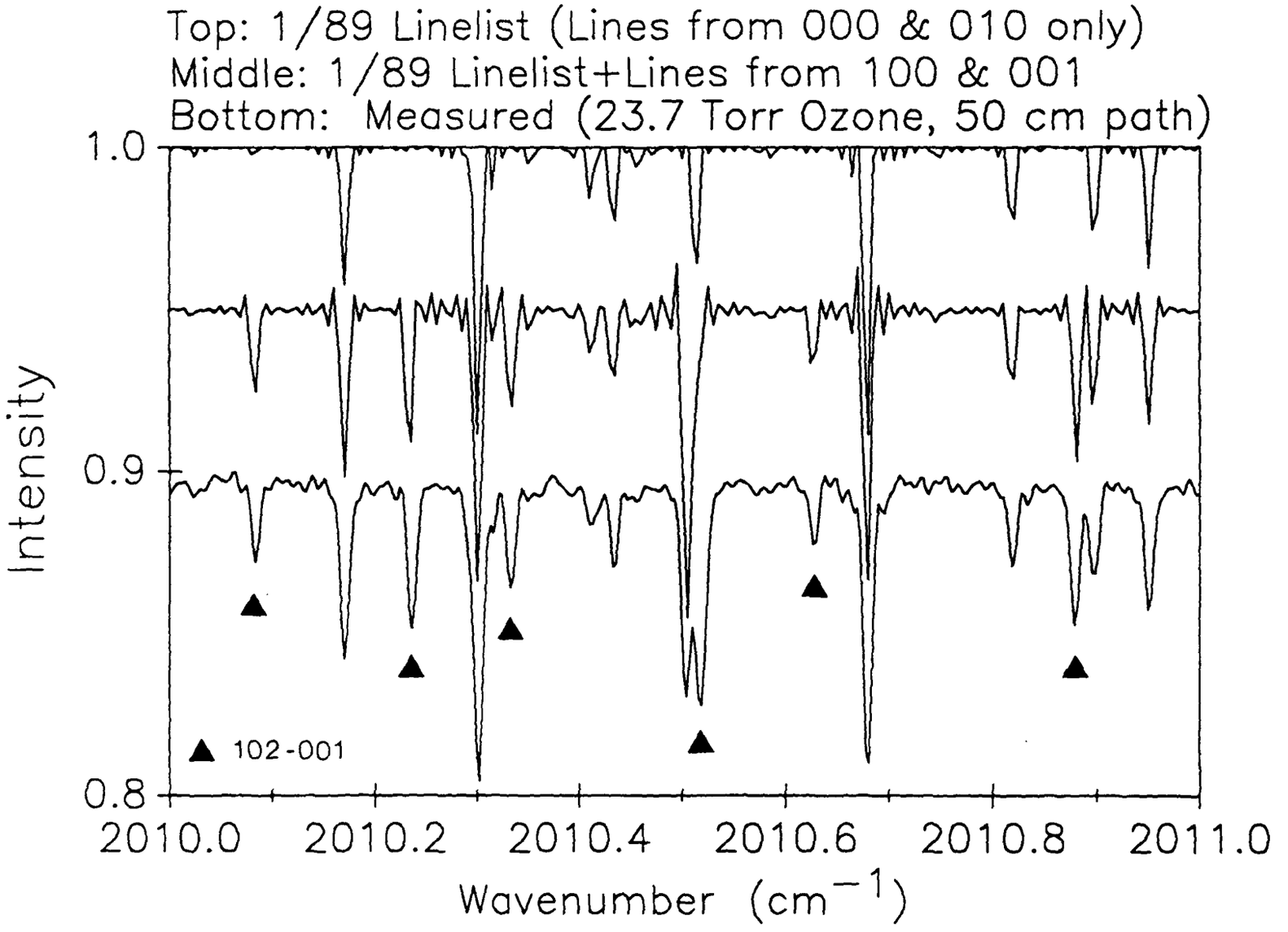
Top: 1/89 Linelist (Lines from 000 & 010 only)
Middle: 1/89 Linelist+Lines from 100 & 001
Bottom: Measured (23.7 Torr Ozone, 50 cm path)
1.0
0.9
0.8
Intensity
102-001
2010.0
2010.2
2010.4
2010.6
2010.8
2011.0
Wavenumber (cm^{-1})

ZANDER ET AL., J.G.R. 93, 1669, 1988.
TICK MARKS INDICATE OZONE LINES

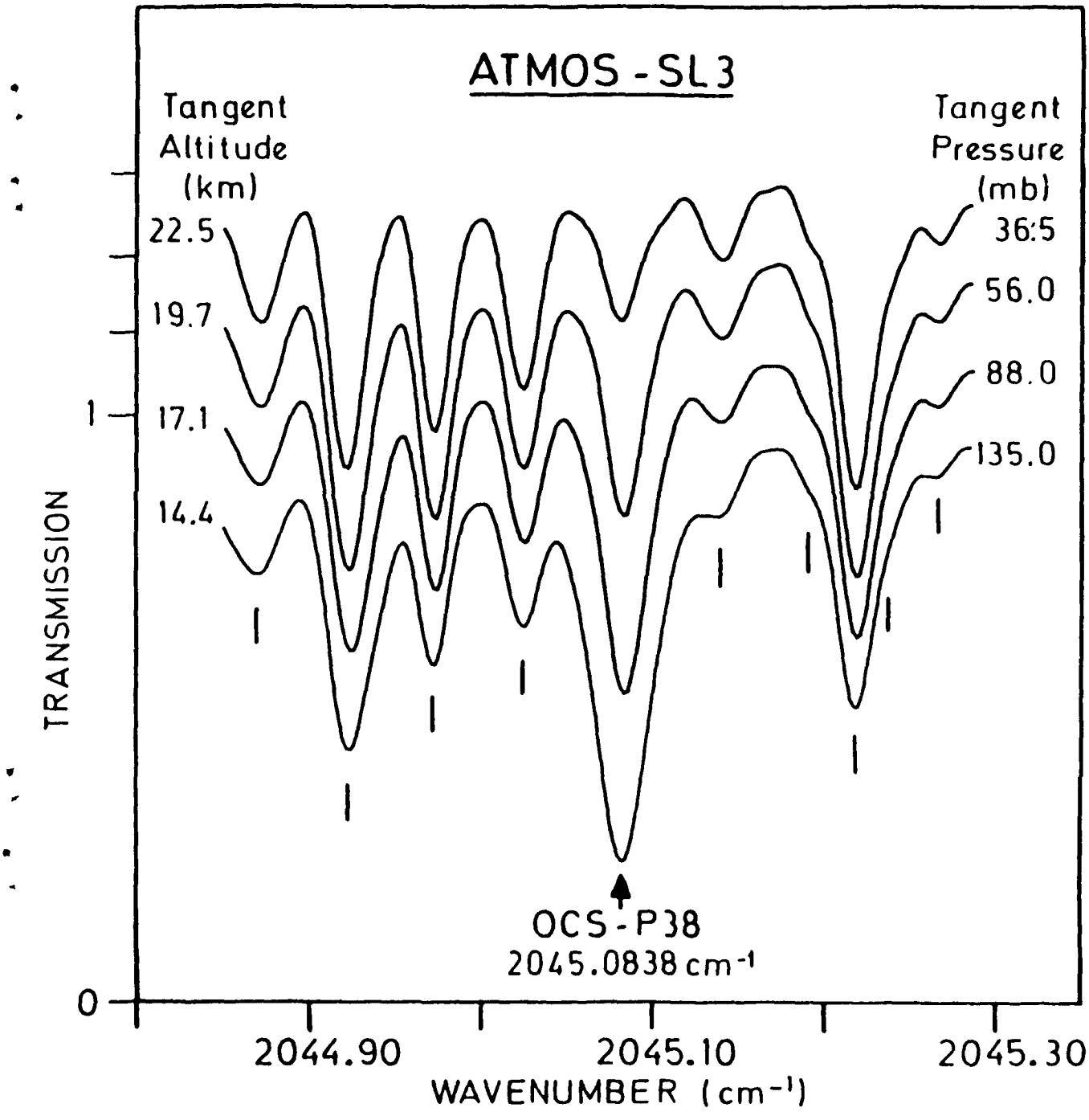

ATMOS/SPACELAB 3 SOLAR SPECTRUM
LINELIST INCLUDES OZONE FROM 1986 HITRAN

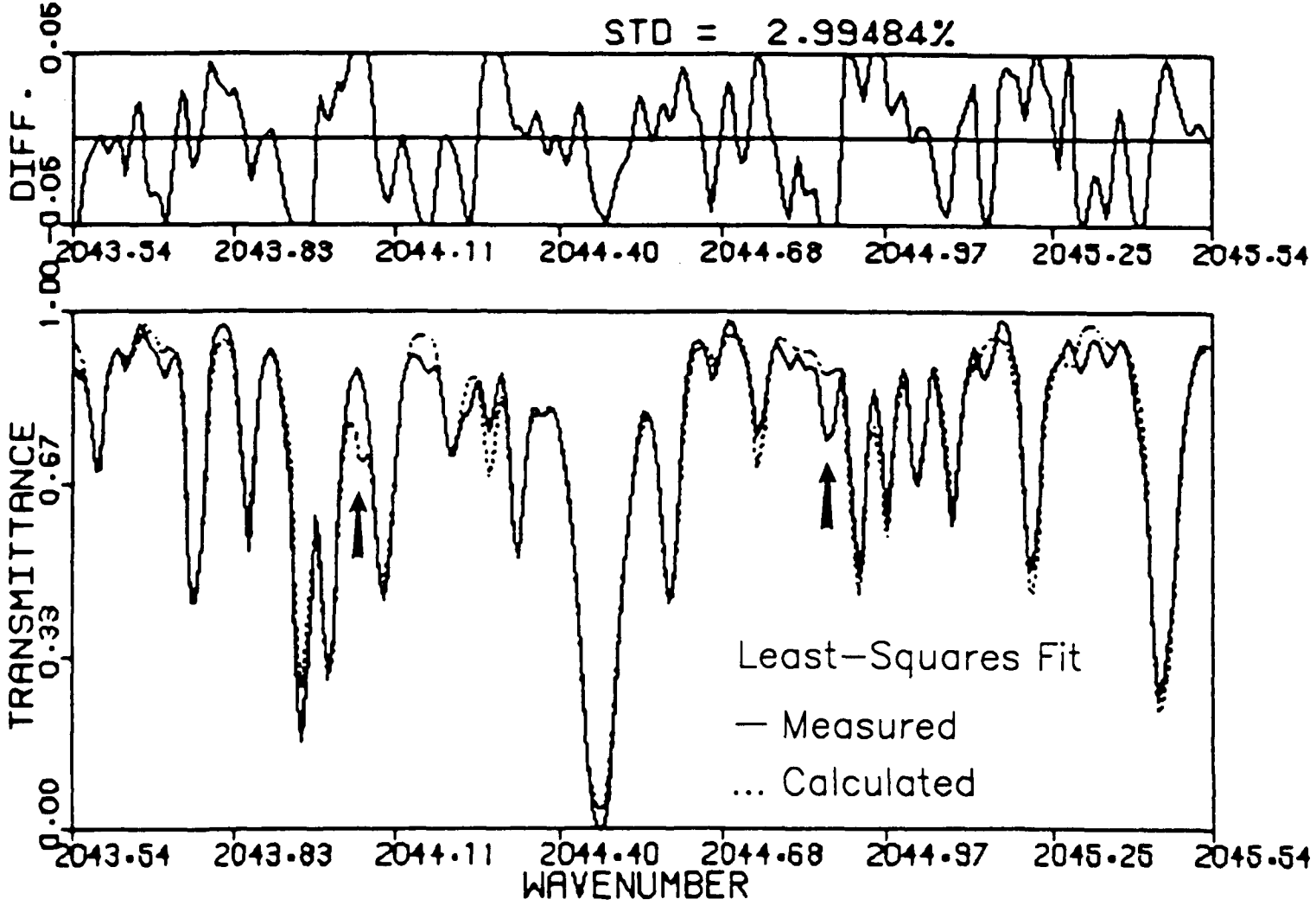

*ATMOS/SPACELAB 3 SOLAR SPECTRUM
LINELIST WITH UPDATED OZONE BANDS
[(002),(101),(200)] ← 000
[(012),(111),(210)] ← 010

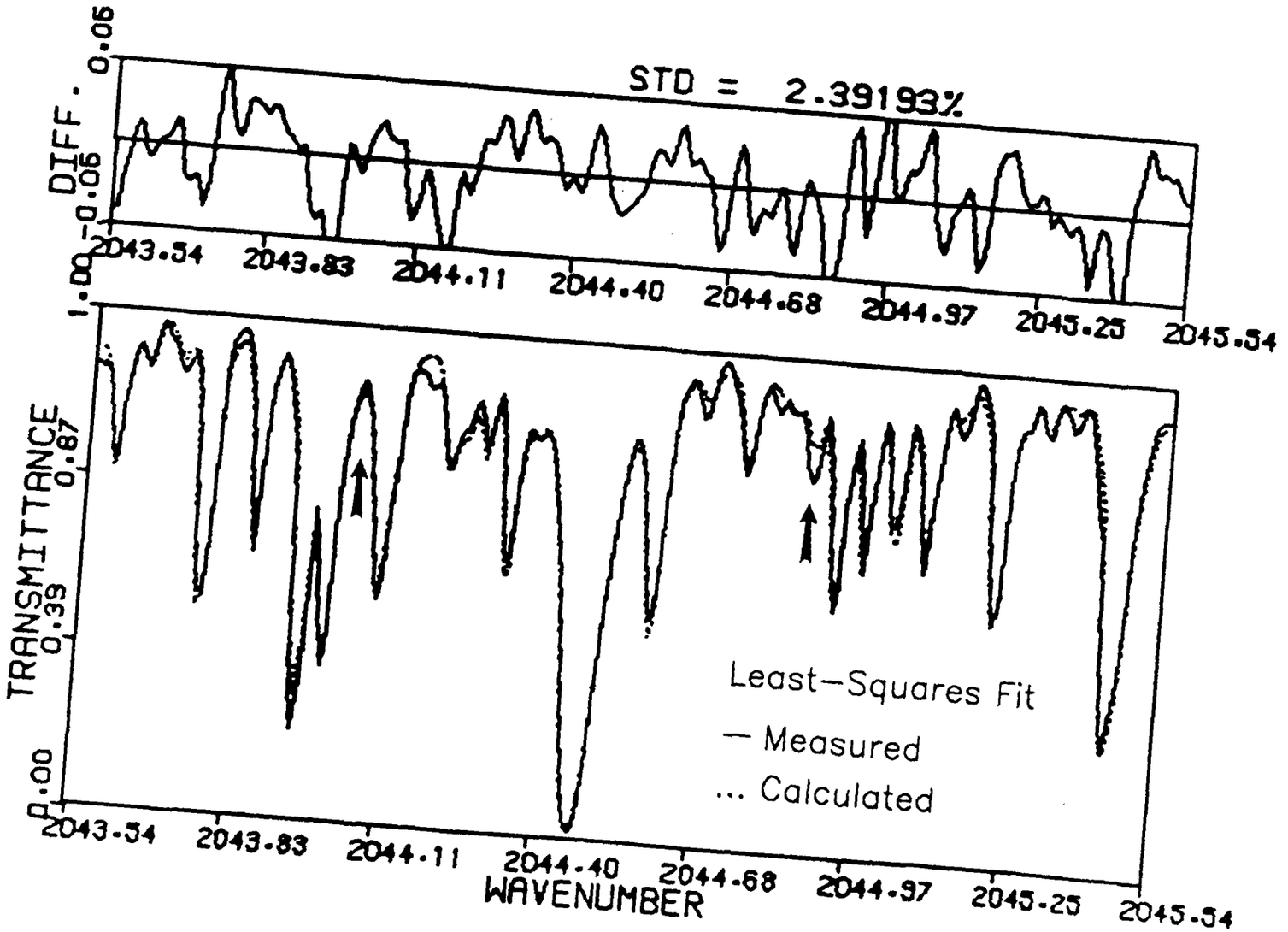

ATMOS/SPACELAB 3 SOLAR SPECTRUM
LINELIST WITH UPDATED OZONE BANDS
[(002),(101),(200)] ← 000
[(012),(111),(210)] ← 010
[(003),(102),(201),(300)] ← [(100),(001)]

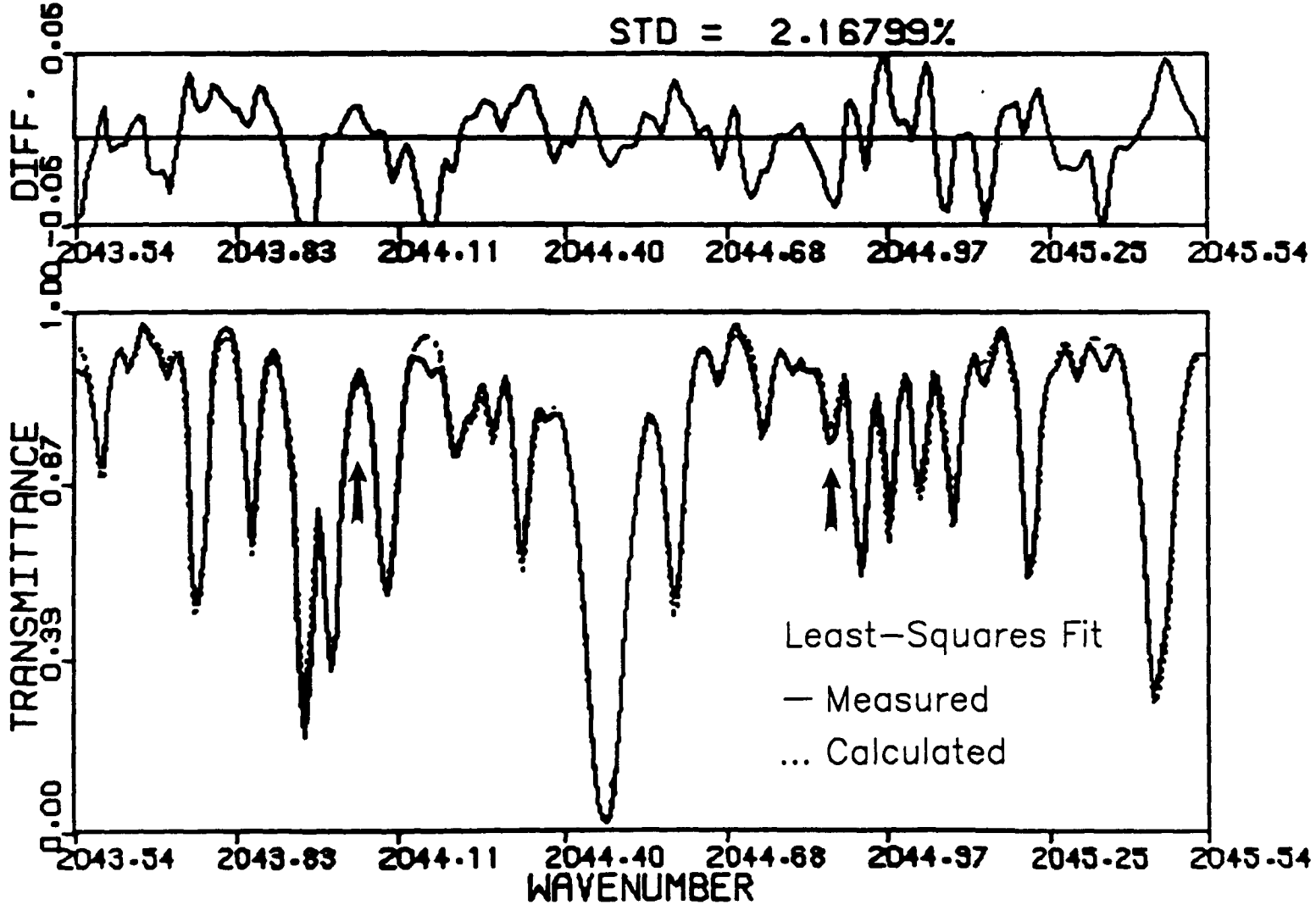

Table 1. Ozone Band Positions and Identifications

(See Barbe et al. 6, 7, 8)

Identification	Ozone Band Positions (cm^{-1}) Liquid Observed	Gas Observed (ref.8)	calc (ref.8)
ν_2	702.5	700.93[a]	
ν_3	1033	1042.096[b]	
ν_1	1105.5	1103.15[b]	
$2\nu_2$	1401.5	1400.[e]	
$\nu_2 + \nu_3$	1716	1726.4	1726.0
$\nu_1 + \nu_2$	1794	1795.3	1795.0
$2\nu_3$	2046	2058.0	2057.8
$\nu_1 + \nu_3$	2107	2110.79[c]	2110.5
$2\nu_1$	2199	2201.3	2201.6
$2\nu_2 + \nu_3$	2402	2409.5	2408.0
$2\nu_2 + \nu_1$	2485		
$2\nu_3 + \nu_2$	2716	2725.6	2725.5
$\nu_1 + \nu_2 + \nu_3$	2780	2785.24	2785.2
$2\nu_1 + \nu_2$			2884.2
$3\nu_3$	3029	3046.0	3045.2
$\nu_1 + 2\nu_3$		3084.1	3085.2
$2\nu_1 + \nu_3$	3179	3185.7	3186.5
$3\nu_1$			3291.3
$2\nu_2 + \nu_1 + \nu_3$	3445	3457.5	3458.1
$3\nu_3 + \nu_2$	3681	3697.1	3697.1
$2\nu_1 + \nu_2 + \nu_3$	3839	3849.4	3850.2
$4\nu_3$	4005	4024.5[f]	
$3\nu_3 + \nu_1$		4026	4026.9
$3\nu_1 + \nu_3$			4252.3
$3\nu_3 + 2\nu_2$	4325		
$4\nu_3 + \nu_2$	4639	4665[g]	

Notes to Table 1

a - T. Tanaka and Y. Morino, J. Mol. Spec. 33, 552 (1970).
b - S.A. Clough and F.X. Kneizys, J. Chem. Phys. 44, 1855 (1966).
c - S. Trajmar and D.J. McCaa, J. Mol. Spec. 14, 244 (1964).
d - D.E. Snider and J.H. Shaw, J. Mol. Spec. 44, 400 (1972).
e - D.J. McCaa and J.H. Shaw, J. Mol. Spec. 25, 374 (1968).
f - A. Barbe, C. Secroun, and P. Jouve, C. R. Acad. Sci. Paris 274B, 615 (1972).
g - A. Barbe and P. Jouve, C. R. Acad. Sci., Paris 268B, 1723 (1969).

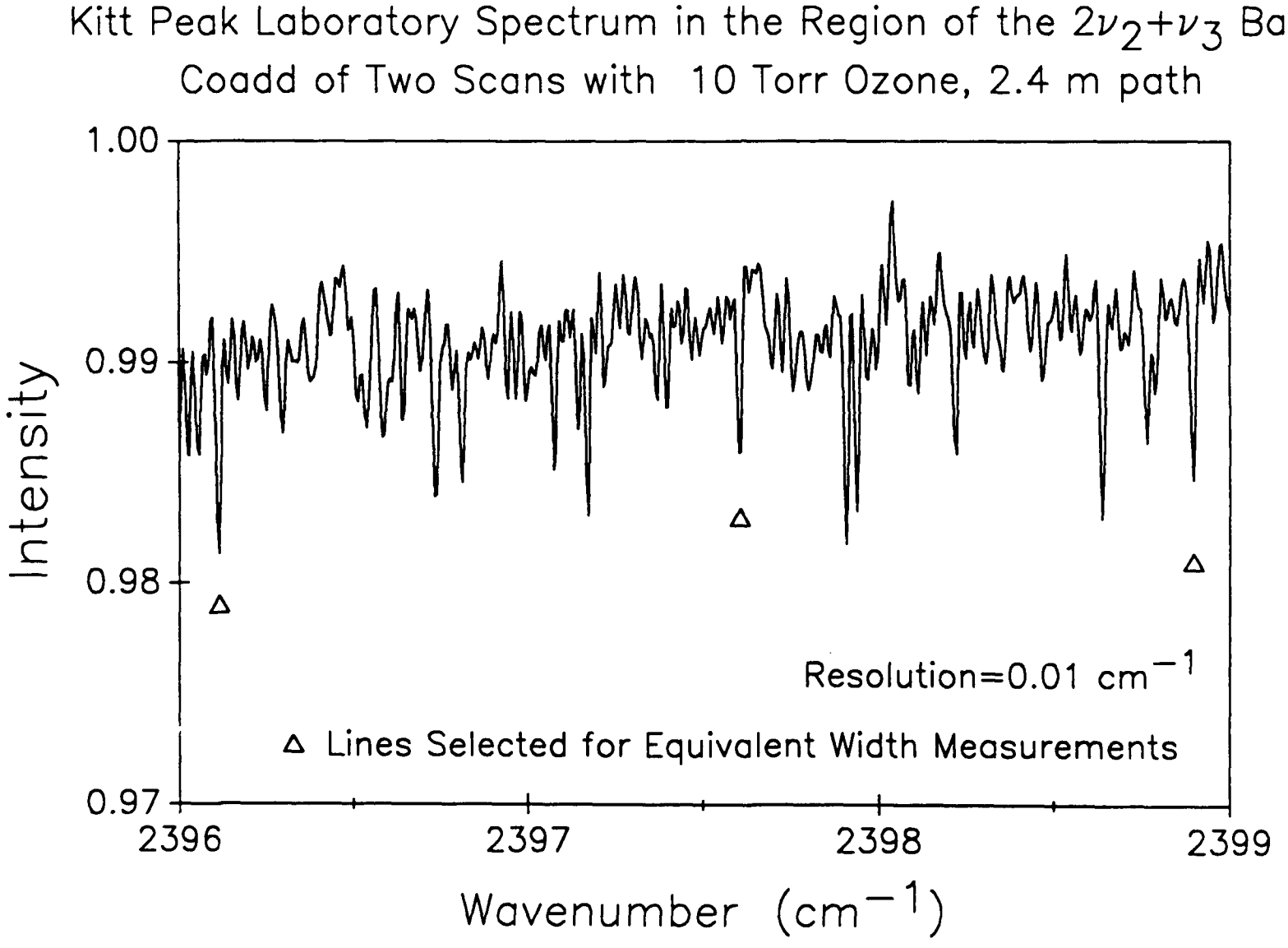
Kitt Peak Laboratory Spectrum in the Region of the $2\nu_2+\nu_3$ Band
Coadd of Two Scans with 10 Torr Ozone, 2.4 m path
1.00
0.99
0.98
0.97
Intensity
Resolution=0.01 cm^{-1}
Δ Lines Selected for Equivalent Width Measurements
2396
2397
2398
2399
Wavenumber (cm^{-1})

STATUS OF ANALYSIS

- ASSIGNMENTS OBTAINED FOR (120)←(000) BAND UP TO J=50, K_a=4 IN THE R BRANCH (P BRANCH IS VERY WEAK)

- ASSIGNMENTS OBTAINED FOR (021)←(000) BAND UP TO J=25, K_a=7 IN THE Q AND R BRANCHES (P BRANCH COVERED BY CO_2)

THE $\nu_2+2\nu_3$, $\nu_1+\nu_2+\nu_3$, AND $2\nu_1+\nu_2$ BANDS OF $^{16}O_3$ (3.6 μm REGION)

PARAMETER	1986 HITRAN DATA[a]	1989 HITRAN DATA[b]
SPECTRAL RESOLUTION	0.03 cm^{-1}	0.01 cm^{-1}
MAXIMUM QUANTUM NUMBERS		
$\nu_2+2\nu_3$	-	$J \leq 48$, $K_a \leq 11$
$\nu_1+\nu_2+\nu_3$	$J \leq 32$, $K_a \leq 8$	$J \leq 47$, $K_a \leq 13$
$2\nu_1+\nu_2$	-	$J \leq 46$, $K_a \leq 9$
STANDARD DEVIATION OF FIT	-	0.0009 cm^{-1}
INTENSITY ACCURACY	-	±5-10%
INTEGRATED INTENSITY (# LINES)		
$\nu_2+2\nu_3$	-	3.70×10^{-21} (2630)
$\nu_1+\nu_2+\nu_3$	3.140×10^{-20} (1449)	2.72×10^{-20} (2390)
$2\nu_1+\nu_2$	-	1.23×10^{-21} (1973)

[a]BARBE, A., C. SECROUN, A. GOLDMAN, AND J. R. GILLIS, "ANALYSIS OF THE $\nu_1+\nu_2+\nu_3$ BAND OF $^{16}O_3$," J. MOL. SPECTROSC., 100, 377-381 (1983).

[b]SMITH, M. A. H., C. P. RINSLAND, V. MALATHY DEVI, J.-M. FLAUD, AND C. CAMY-PEYRET, "THE 3.6 μm REGION OF OZONE: LINE POSITIONS AND INTENSITIES," TO BE SUBMITTED TO J. MOL. SPECTROSC.

KITT PEAK LABORATORY SPECTRUM OF OZONE
15.5 TORR 239 CM PATH 25.6° C

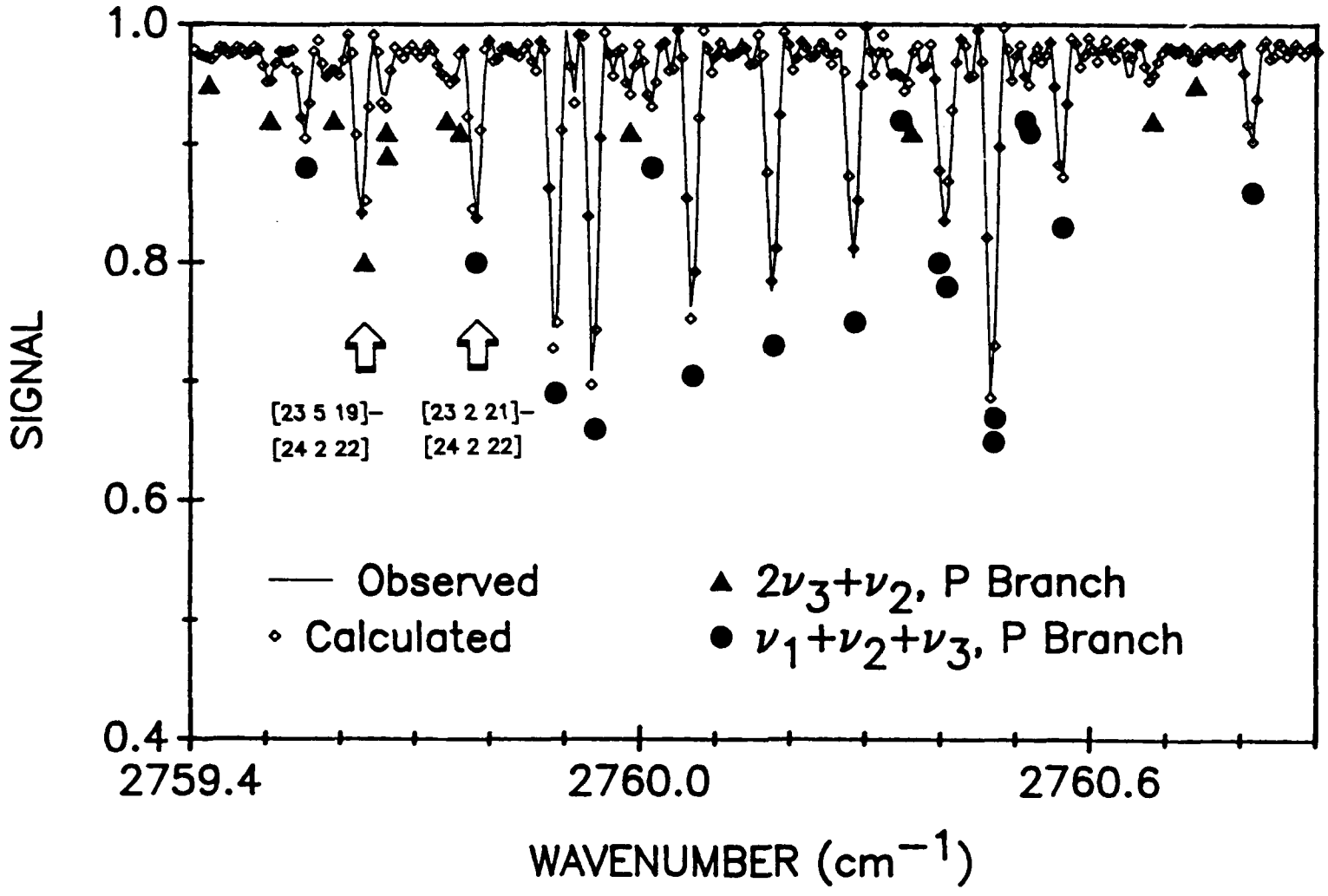

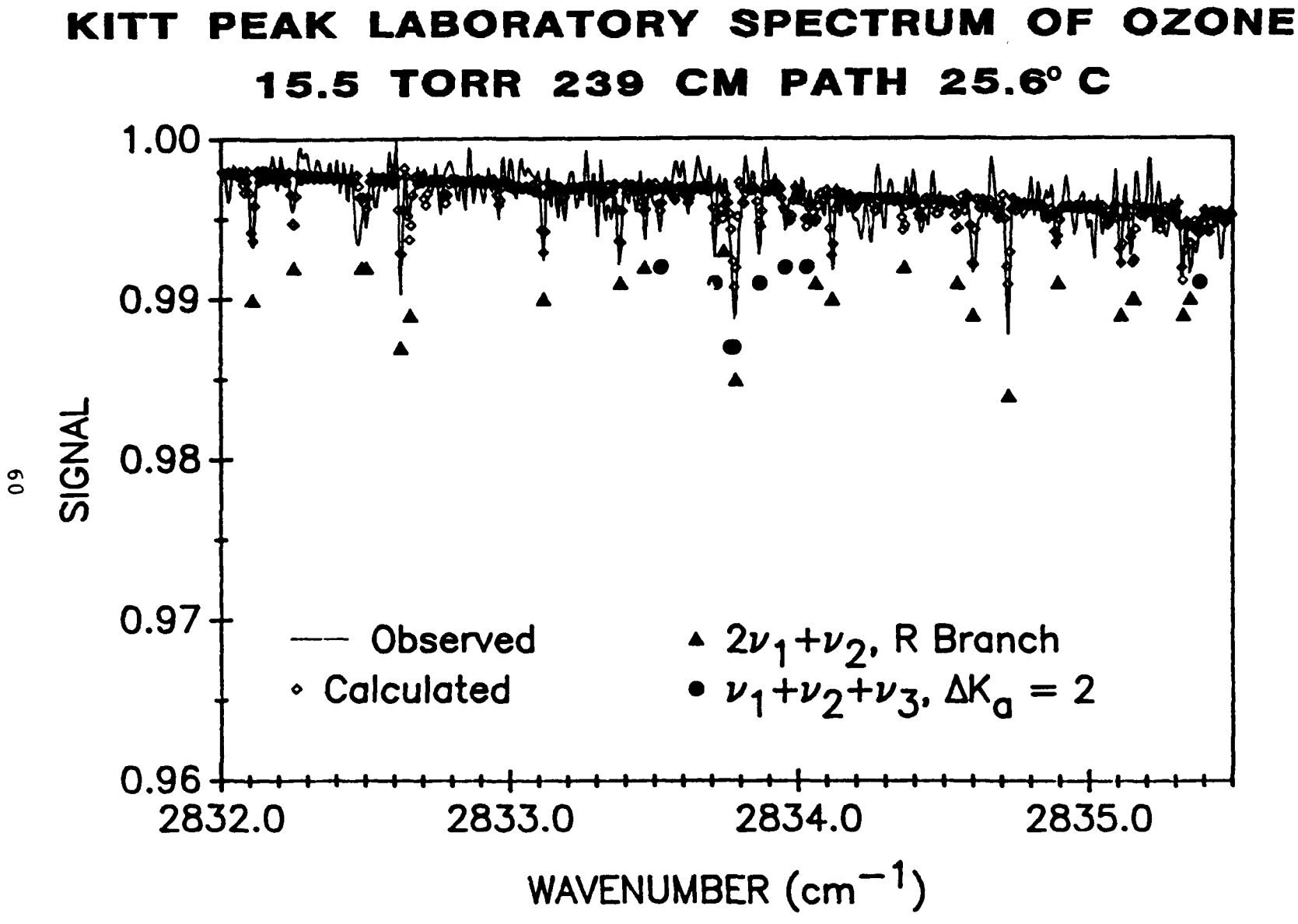
KITT PEAK LABORATORY SPECTRUM OF OZONE
15.5 TORR 239 CM PATH 25.6° C
1.00
0.99
0.98
0.97
0.96
SIGNAL
Observed
Calculated
▲ 2ν1+ν2, R Branch
● ν1+ν2+ν3, ΔKa = 2
2832.0
2833.0
2834.0
2835.0
WAVENUMBER (cm−1)

THE $3\nu_3$, $\nu_1 + 2\nu_3$, $2\nu_3$, $2\nu_1 + \nu_3$, AND $3\nu_1$ BAND SYSTEM OF $^{16}O_3$ AT 3.3 μm

PARAMETER	1986 HITRAN DATA[a]	PRELIMINARY CALCULATIONS
SPECTRAL RESOLUTION	-	0.01 cm^{-1}
POSITION ACCURACY		
$3\nu_3$	±5 cm^{-1}	~0.001 cm^{-1}
$\nu_1 + 2\nu_3$	-	
$2\nu_1 + \nu_3$	-	
$3\nu_1$	-	
INTENSITY ACCURACY	-	±10%
INTEGRATED INTENSITY		
$3\nu_3$	1.105×10^{-19} (1575)	1.385×10^{-19} (2650)
$\nu_1 + 2\nu_3$	-	1.305×10^{-20} (2863)
$2\nu_1 + \nu_3$	-	9.711×10^{-21} (1910)
$3\nu_1$	-	-

[a]CALCULATION DATES BACK TO 1973 AFCRL COMPILATION (McCLATCHEY ET AL., AFCRL-TR-73-0096, ENVIRON. RES. PAP. NO. 434, 1973).

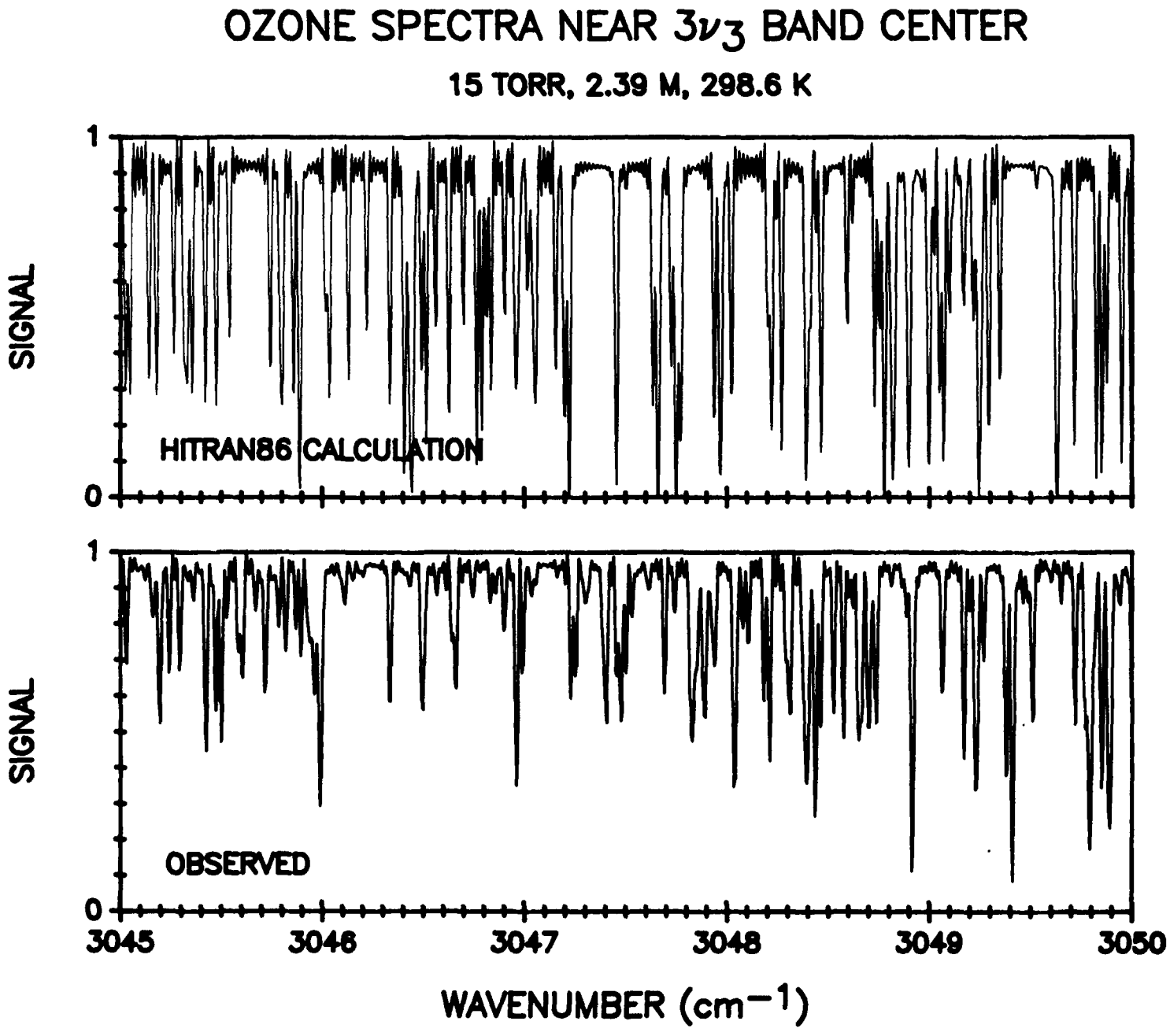
OZONE SPECTRA NEAR $3\nu_3$ BAND CENTER
15 TORR, 2.39 M, 298.6 K
SIGNAL
1
0
HITRAN86 CALCULATION
SIGNAL
1
0
OBSERVED
3045
3046
3047
3048
3049
3050
WAVENUMBER (cm^{-1})

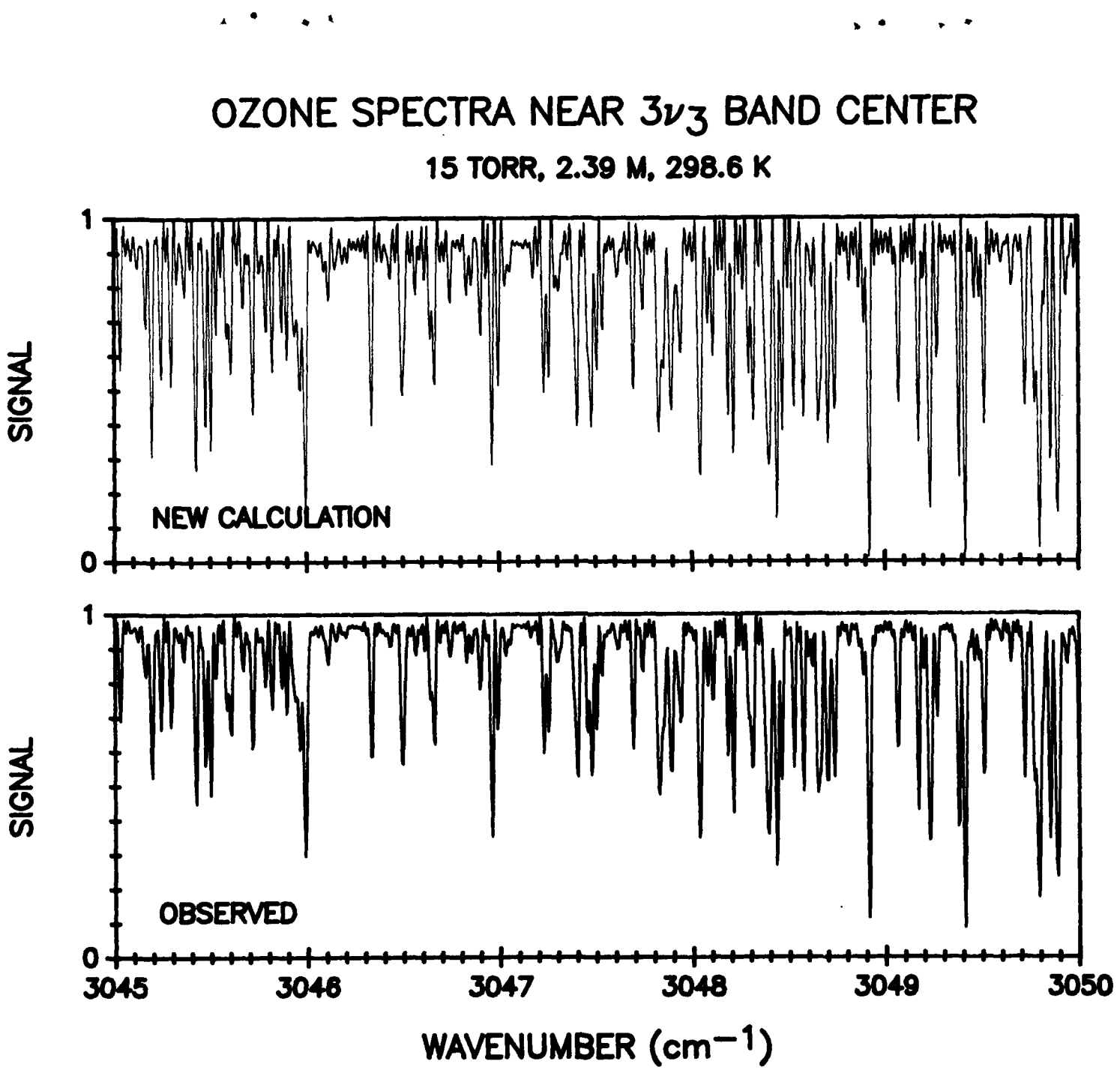
OZONE SPECTRA NEAR 3ν3 BAND CENTER
15 TORR, 2.39 M, 298.6 K
SIGNAL
1
0
NEW CALCULATION
SIGNAL
1
0
OBSERVED
3045
3046
3047
3048
3049
3050
WAVENUMBER (cm−1)

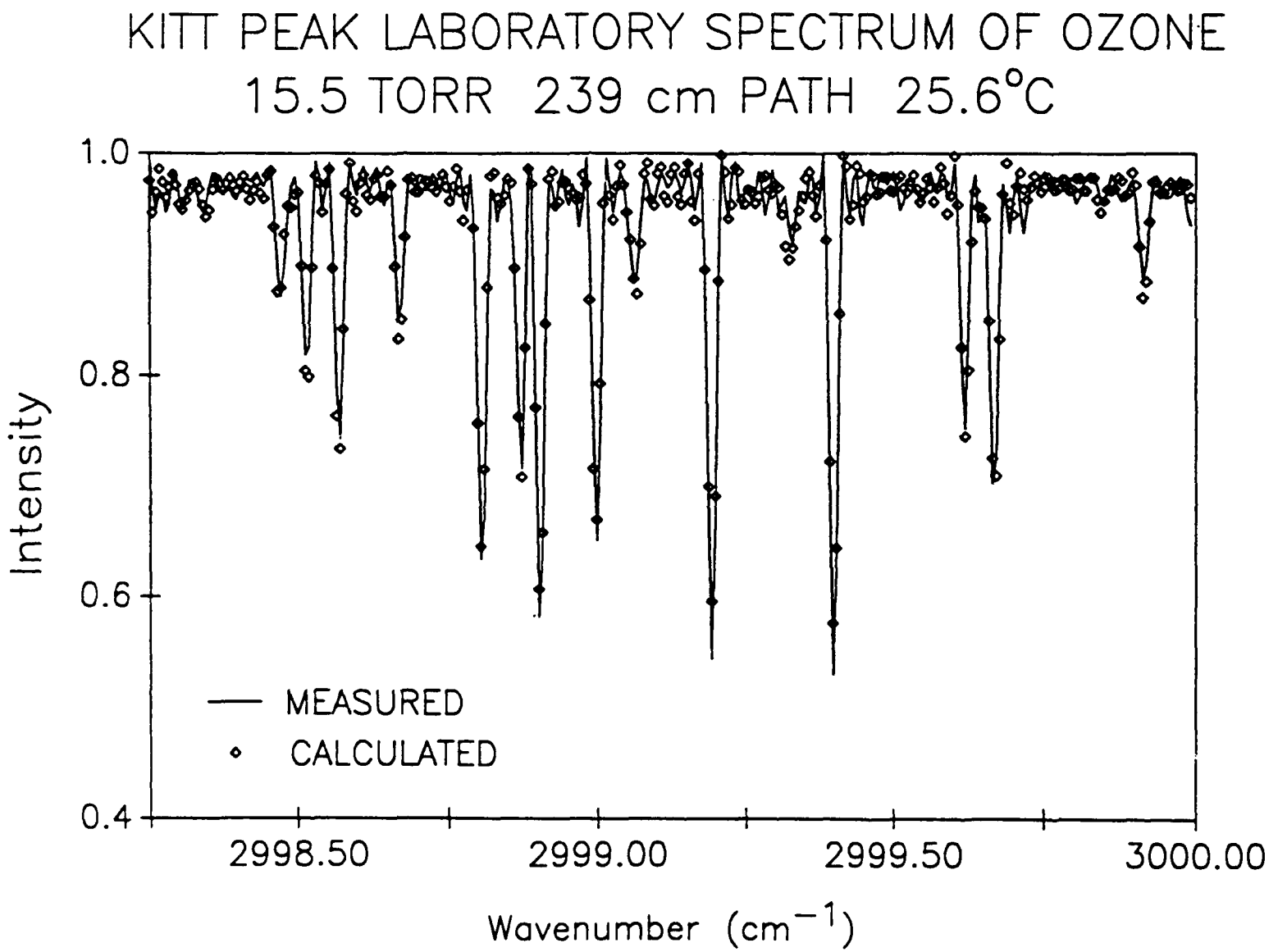
KITT PEAK LABORATORY SPECTRUM OF OZONE
15.5 TORR 239 cm PATH 25.6°C
1.0
0.8
0.6
0.4
Intensity
MEASURED
CALCULATED
2998.50
2999.00
2999.50
3000.00
Wavenumber (cm^{-1})

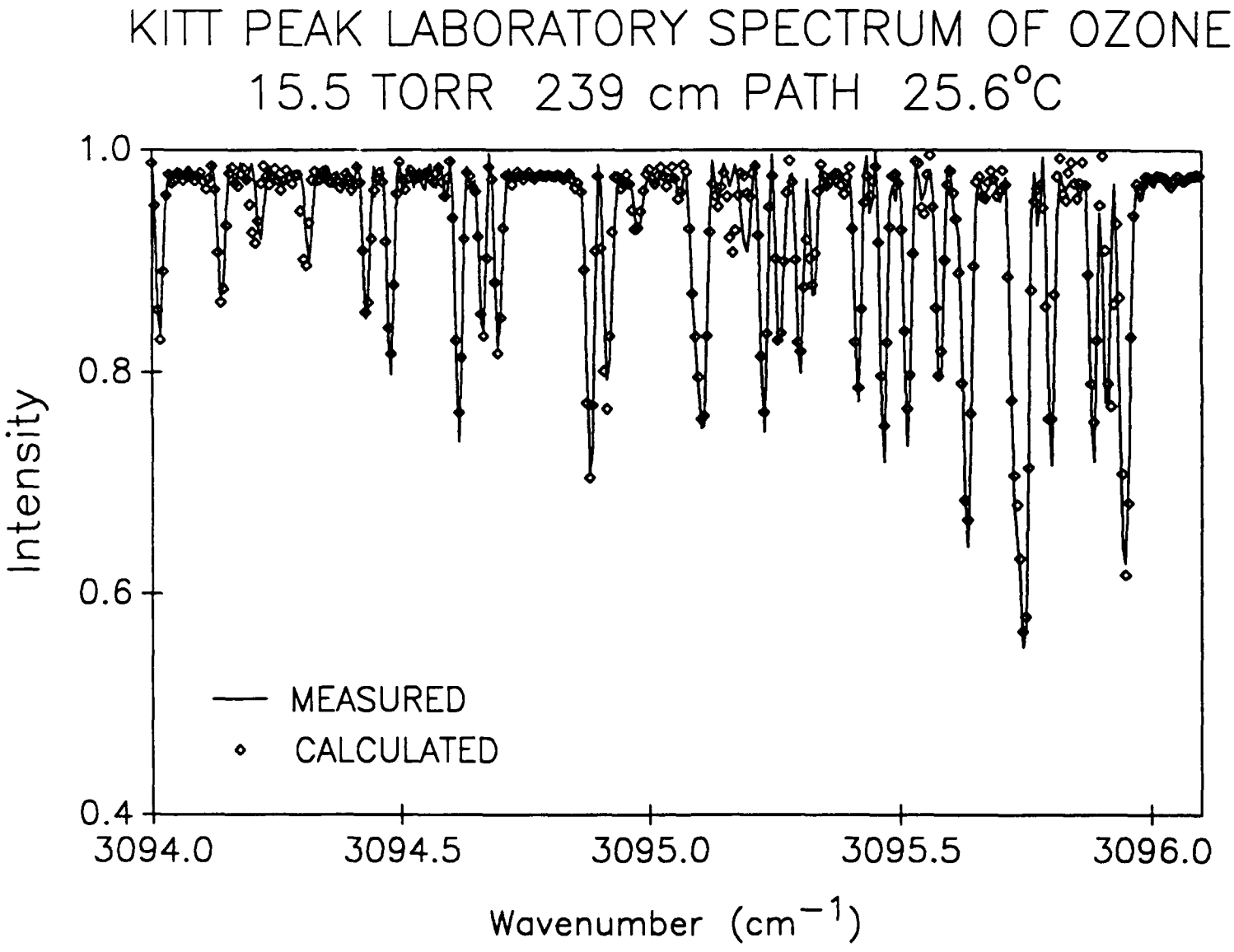
KITT PEAK LABORATORY SPECTRUM OF OZONE
15.5 TORR 239 cm PATH 25.6°C
Intensity
1.0
0.8
0.6
0.4
MEASURED
CALCULATED
3094.0
3094.5
3095.0
3095.5
3096.0
Wavenumber (cm⁻¹)

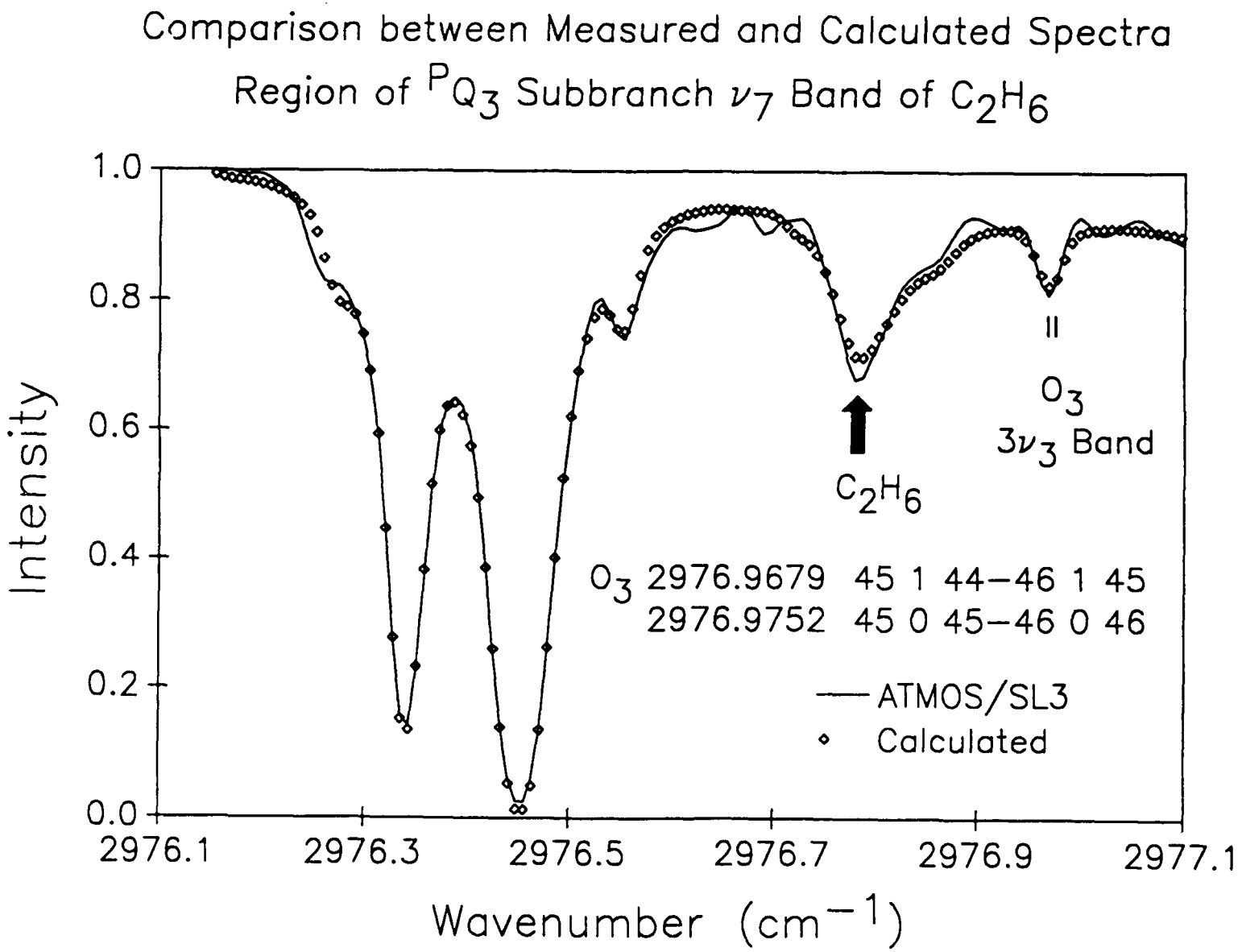
Comparison between Measured and Calculated Spectra
Region of $^{P}Q_3$ Subbranch ν_7 Band of C_2H_6
Intensity
1.0
0.8
0.6
0.4
0.2
0.0
2976.1
2976.3
2976.5
2976.7
2976.9
2977.1
Wavenumber (cm^{-1})
C_2H_6
O_3
$3\nu_3$ Band
O_3 2976.9679 45 1 44–46 1 45
2976.9752 45 0 45–46 0 46
ATMOS/SL3
Calculated

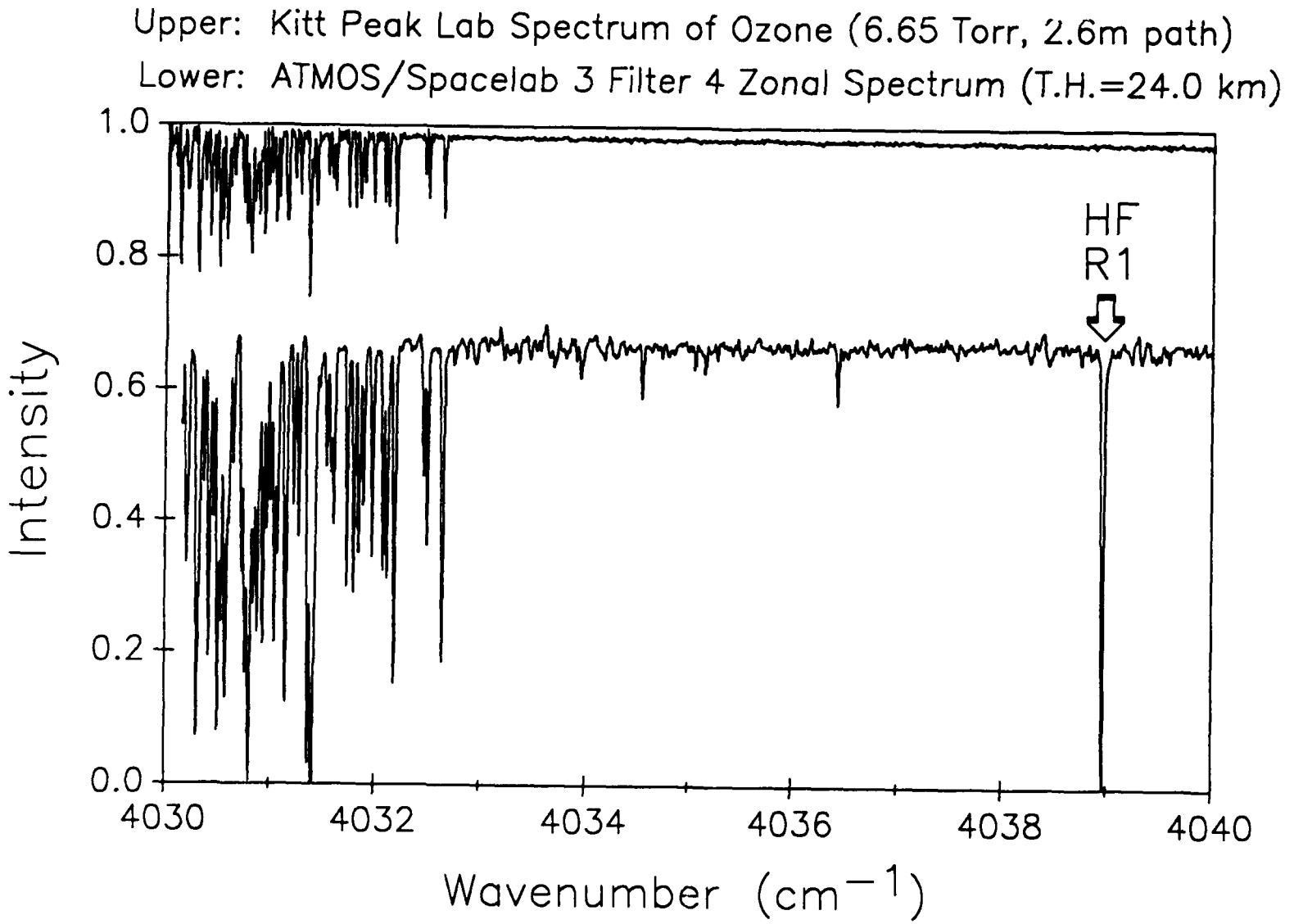
Upper: Kitt Peak Lab Spectrum of Ozone (6.65 Torr, 2.6m path)
Lower: ATMOS/Spacelab 3 Filter 4 Zonal Spectrum (T.H.=24.0 km)
HF
R1
Intensity
1.0
0.8
0.6
0.4
0.2
0.0
4030
4032
4034
4036
4038
4040
Wavenumber (cm^{-1})

FUTURE NEEDS

- ANALYSIS OF THE $^{16}O^{16}O^{17}O$ AND $^{16}O^{17}O^{16}O$ BANDS AT 10 μm.
- ANALYSIS OF OZONE BANDS ABOVE 3500 cm^{-1}.
- CALCULATION OF HOT BANDS IN THE 5.2 μm SPECTRAL REGION.
- IMPROVEMENT IN THE ABSOLUTE ACCURACIES OF THE INTENSITIES THROUGHOUT THE INFRARED.
- HIGH RESOLUTION (0.01 cm^{-1} OR BETTER) ATLAS OF LONG PATH, LOW PRESSURE OZONE LABORATORY SPECTRA.

N_2O LINE PARAMETERS IN THE 1000 TO 4000 cm^{-1} REGION NEW MEASUREMENTS IN THE ν_2 BAND OF $H_2^{16}O$

Robert A. Toth
Jet Propulsion Laboratory
Mail Stop T1166
4800 Oak Grove Drive
Pasadena, CA 91109

N_2O LINE PARAMETERS IN THE 1000 TO 4000 cm^{-1} REGION
NEW MEASUREMENTS IN THE ν_2 BAND OF $H_2^{16}O$

Robert A. Toth
Jet Propulsion Laboratory
Mail Stop T1166
4800 Oak Grove Drive
Pasadena, CA 91109

Abstract

N_2 line parameters in the 1000 to 4000 cm^{-1} region are discussed. New measurements in the (010) - (000) band of $H_2^{16}O$ are also discussed.

The infrared spectrum of N_2O and its isotopic derivatives has been measured from laboratory spectra obtained with a FTS located at the McMath Solar facility at the Kitt Peak National Observatory. A discussion will be given on the parameters involved in computing accurate line positions (0.00006 cm^{-1}) and strengths (5% uncertainty or better) for N_2O bands covering the 1000 to 4000 cm^{-1} region.

A discussion will also be given on new measurements and analysis of the (010) - (000) band of $H_2^{16}O$ centered at 1594.7463 cm^{-1}.

Explanation of Viewgraphs

1. Present and future studies of N_2O by R. Toth.
2. Overview of the present state of N_2O parameters.
3. F factor expressions used in the line strength, S, equation for N_2O.
4. Self broadening parameters obtained with high accuracy.
5. Frequency pressure shifts due to self broadening of N_2O.
6. Example of several bands of N_2O analyzed by R. Toth for the determination of the vibrational band strength, S_v, and F factor coefficients, $a1$ and $a2$.
7. Comparison of selected N_2O band strength values in the 1100 to 1900 cm^{-1} region.

N_2O LINE PARAMETERS IN THE 1000 TO 4000 cm^{-1} REGION
NEW MEASUREMENTS IN THE ν_2 BAND OF $H_2^{16}O$

Robert A. Toth
Jet Propulsion Laboratory
Mail Stop T1166
4800 Oak Grove Drive
Pasadena, CA 91109

Papers by R. Toth on N_2O

1. R.A Toth, "Line strengths of N_2O in the 1120 - 1440 cm^{-1} region", **Appl. Opt.**, **23**, 1825-1834 (1984).
2. R.A. Toth, "Frequencies of N_2O in the 1100 to 1440 cm^{-1} region", **Opt. Soc. Am.**, **B 3**, 1263-1281 (1986).
3. R.A. Toth, "N_2O vibration-rotation parameters derived from measurements in the 900-1090 and 1580-2380 cm^{-1} regions", **Opt. Soc. Am.**, **4**, 357-374 (1987).
4. R.A. Toth, "Line strengths (1100-2370 cm^{-1}), self broadended line widths and frequency shifts (1800-2630 cm^{-1}) of N_2O and isotopic variants", (in preparation).

To be analyzed during 1989-1991

1. Frequency measurements, 2400-5500 cm^{-1}
2. Line strengths, 2400-5500 cm^{-1}
3. N_2 and air broadened line widths and frequency shifts.

Figure 1

Presently good values

**E_v, B, D, H, and L for states with E_v<5320 cm^{-1} for $N_2{}^{16}O$

* Line strength parameters for bands with band centers < 3500 cm^{-1}

, Pressure broadening coefficients

* includes perturbed levels in the following states:
0400, 0420(e), 0510(e), 0510(f), 1001, 0600, 0620(e),
1111(e), 1111(f), and 1201(e)

Figure 2

F factors for N_2O

$S = S_v F$

$F = [1 + a_1 m + a_2 J'(J'+1)]^2 \cdot H$

$H = 1$ for $|l'-l| = 0, 1$

$H = [J'(J'+1)]^2$ for $|l'-l| = 2$

Figure 3

Smoothed values of self-broadening coefficients, b , of N_2O derived from measurements. b in $cm^{-1}/atm.$ times 10^4

lMl	This Work 446* (296K)	This Work 448* (296K)	Lacome et al. 446* (295K)	% diff.	lMl	This Work 446* (296K)	Lacome et al. 446* (295K)	% diff.
1	1270	1270	1214	4.4	44	809	808	0.1
2	1211	1229	1160	4.2	45	807	804	0.4
3	1190	1190	1131	5.0	46	803	799	0.5
4	1157	1143	1110	4.1	47	793	795	-0.3
5	1139	1133	1092	4.1	48	791	791	0.0
6	1126	1111	1076	4.4	49	792	787	0.6
7	1112	1108	1061	4.6	50	789	784	0.6
8	1099	1105	1048	4.6	51	788	780	1.0
9	1080	1077	1036	4.1	52	784	778	0.8
10	1069	1068	1024	4.2	53	77[illegible]	775	0.1
11	1050	1046	1014	3.4	54	778		
12	1041	1032	1004	3.6	55	781		
13	1039	1025	994	4.3	56	776		
14	1029	1018	985	4.3	57	777		
15	1020	1013	977	4.2	58	773		
16	1009	1010	969	4.0	59	776		
17	993	995	961	3.2	60	773		
18	987	990	954	3.3	61	765		
19	981	983	947	3.5	62	759		
20	974	977	940	3.5	63	766		
21	965	974	933	3.3	64	758		
22	961	963	927	3.5	65	757		
23	954	962	921	3.5	66	759		
24	944	950	915	3.1	67	765		
25	943	945	909	3.6	68	770		
26	939	945	903	3.8	69	767		
27	923	936	897	2.8	70	760		
28	917	930	892	2.7	71	750		
29	909	920	886	2.5	72	732		
30	897	910	881	1.8	73	728		
31	893	886	875	2.0	74	722		
32	876	874	870	0.7	75	717		
33	865	862	864	0.1	76	710		
34	860	851	859	0.1	77	710		
35	863	845	854	1.0	78	700		
36	851	840	848	0.4	79	697		
37	845	836	843	0.2	80	700		
38	832	833	838	-0.7	81	695		
39	830	830	833	-0.4	82	690		
40	825	828	828	-0.4	83	690		
41	823	824	823	0.0	84	685		
42	820	820	818	0.2	85	685		
43	818		813	0.6	86	680		

(*) value before asterisk denotes molecular species. Values of b listed under 446 and 448 were derived from measurements of lines of the 446 and 448 species, respectively.
% diff. is the percent difference between the value obtained in this work(446 species) and that of Lacome et al.

Figure 4

Measured pressure-shift coefficients, d, for self-broadened N_2O. d in cm^{-1}/atm times 1000 at 296K.

N	line	d	N	line	d	N	line	d	N	line	d
1	P5	-0.2	1	R24	-1.3	15	P41	-1.2	17	P18	-1.5
1	P10	-0.5	1	R28	-1.7	15	P43	-1.3	17	P20	-1.5
1	P25	-0.9	1	R29	-1.8	15	P44	-1.3	17	P21	-1.1
1	P27	-0.9	1	R30	-1.9	15	P45	-1.3	17	P22	-1.3
1	P28	-0.9	1	R31	-2.1	15	P46	-1.5	17	P23	-1.2
1	P29	-0.9	1	R32	-2.4	15	P47	-1.5	17	P28	-1.3
1	P30	-0.8	1	R36	-2.3	15	P48	-1.3	17	P30	-1.5
1	P31	-0.9	1	R38	-1.3	15	R13	-1.7	17	P31	-1.3
1	P32	-0.8	1	R40	-1.5	15	R25	-1.5	17	P32	-1.6
1	P33	-0.8	1	R42	-1.7	15	R29	-2.0	17	P38	-1.5
1	P34	-1.1	8	R72	-4.2	15	R30	-2.0	17	P39	-1.8
1	P35	-1.0	8	R73	-2.5	15	R31	-1.5	17	P40	-2.3
1	P36	-1.5	8	R74	-3.0	15	R39	-1.3	17	P41	-1.7
1	P37	-1.1	8	R75	-3.0	15	R43	-1.5	17	R28	-1.3
1	P38	-0.7	8	R76	-2.4	15	R45	-1.4	18	R36	-1.8
1	P41	-1.8	8	R78	-2.5	15	R46	-1.7	18	R37	-1.7
1	P42	-0.7	8	R80	-2.8	15	R49	-1.9	19	P11	-1.2
1	P43	-0.7	8	R81	-3.3	15	R50	-1.5	19	P12	-0.8
1	P44	-1.5	8	R83	-1.7	16	P11	-1.6	19	P19	-2.0
1	P46	-0.6	9	P54	-2.4	16	P12	-1.3	19	P20	-1.5
1	P47	-0.7	9	P56	-1.8	16	P13	-1.7	20	P13	-1.6
1	P48	-2.2	9	P57	-2.1	16	P16	-1.4	20	P15	-1.1
1	R1	-0.8	9	P58	-1.7	16	P27	-1.4	20	P19	-0.3
1	R2	-0.7	9	P61	-1.8	16	P28	-1.4	20	P22	-0.5
1	R8	-0.6	9	P63	-1.8	16	P29	-1.5	20	P24	-1.7
1	R13	-1.5	11	P42	-2.9	16	P30	-1.3	20	P25	-1.2
1	R15	-0.7	12	P42	-2.7	16	R14	-2.0	20	P26	-1.0
1	R16	-1.9	12	P50	-3.0	16	R41	-1.9	20	P27	-0.9
1	R18	-2.0	12	P53	-2.6	17	P11	-1.3	20	P29	-0.4
1	R19	-1.8	15	P1	-1.3	17	P12	-1.3	20	P30	-1.6
1	R20	-1.5	15	P28	-1.5	17	P13	-1.4	21	P65	-1.1
1	R21	-1.8	15	P29	-1.5	17	P14	-1.3	21	P66	-0.5
1	R22	-1.5	15	P31	-1.5	17	P16	-1.7	21	P67	-1.4
1	R23	-1.9	15	P40	-1.3	17	P17	-1.3	21	R54	-0.8

N represents the band number. Refer to Table 2. for the band and molecular specie listed with the band number.

Figure 5

Band strengths S_v, rotationless dipole moment matrix elements $|R|$, and F factor coefficients of N_2O; S_v in cm^{-2}/atm. at 296K and $|R|$ in Debye

mol	band	band center (cm^{-1})	S_v	$\|R\|$	$a_1 \times 10^4$	$a2 \times 10^5$	no. of lines	σ%
446	0200-0000	1168.132	7.00(6)E-00	2.57(1)E-02	-0.01(2)	2.48(10)	132	1.9
456	0200-0000	1144.333	1.09(2)E-02	1.69(2)E-02	-2.07(88)	2.58(57)	50	2.9
546	0200-0000	1159.972	2.84(4)E-02	2.71(2)E-02	1.14(40)	3.38(29)	81	2.2
448	0200-0000	1155.140	3.16(6)E-02	3.84(4)E-02	0.15(43)	3.54(32)	82	2.5
447	0200-0000	1161.545	4.03(6)E-03	3.20(3)E-02	0.76(79)		31	4.2
446	1000-0000	1284.903	2.080(7)E+02	1.336(2)E-01	-0.09(2)		144	2.1
456	1000-0000	1280.354	7.90(6)E-01	1.36(1)E-01			73	3.1
546	1000-0000	1269.892	7.00(5)E-01	1.29(1)E-01	-2.99(52)		73	2.9
448	1000-0000	1246.885	4.14(22)E-01	1.34(3)E-01			87	2.7
447	1000-0000	1264.704	7.98(34)E-02	1.37(3)E-01			54	2.1
556	1000-0000	1265.334	2.69(15)E-03	1.32(4)E-01			26	3.9
446	0310(e)-0000	1749.065	2.33(3)E-02	1.21(1)E-03	-58.26(47)	2.31(21)	91	1.8
446	0310(f)-0000	1749.065	2.26(4)E-02	1.19(1)E-03		3.38(28)	42	1.8
446	1110(e)-0000	1880.266	2.58(1)E-01	3.89(1)E-03	-108.88(30)	-0.07(7)	121	1.4
446	1110(f)-0000	1880.266	2.56(6)E-01	3.87(5)E-03			44	2.5
456	1110(e)-0000	1860.191	9.13(20)E-04	3.85(4)E-03	-107.3(67)	3.7(28)	35	4.1
456	1110(f)-0000	1860.191	9.01(19)E-04	3.82(4)E-03			30	2.1
546	1110(e)-0000	1862.767	9.37(16)E-04	3.88(3)E-03	-110.5(42)	-3.2(17)	38	3.2
546	1110(f)-0000	1862.767	9.11(18)E-04	3.83(4)E-03		-1.3(14)	23	4.1
448	1110(e)-0000	1839.936	4.78(10)E-04	3.74(4)E-03	-88.1(49)	2.6(22)	41	4.5
446	0001-0000	2223.757	1.238(4)E+03	2.477(4)E-01	-0.23(13)		164	1.7
456	0001-0000	2177.657	4.21(5)E-00	2.42(1)E-01	0.77(49)	0.22(18)	106	2.4
546	0001-0000	2201.605	4.42(1)E-00	2.45(1)E-01	-0.59(27)		103	1.9
448	0001-0000	2216.711	2.45(3)E-00	2.44(2)E-01	-0.10(40)	0.50(18)	108	2.9
447	0001-0000	2220.073	5.06(6)E-01	2.59(2)E-01	-1.52(76)		63	4.1
556	0001-0000	2154.726	1.55(8)E-02	2.44(7)E-01	-2.6(21)	-1.7(20)	33	4.9
458	0001-0000	2171.044	8.44(75)E-03	2.39(15)E-01			29	6.5
548	0001-0000	2194.046	9.87(80)E-03	2.57(95)E-01			21	4.0
446	0400-0000	2322.573	5.80(4)E-01	5.25(13)E-03	-1.86(34)		108	2.7
456	0400-0000	2278.193	5.83(72)E-04	2.78(16)E-03			12	6.7
546	0400-0000	2201.605	2.69(11)E-03	5.92(11)E-03	-1.1(19)	2.0(15)	26	3.7
448	0400-0000	2294.017	6.19(8)E-03	1.20(8)E-02	-3.9(14)		41	4.4
446	0220(e)-0000	1177.745	5.53(5)E-08	2.28(1)E-06	-1.57(43)		81	3.4
446	0420(e)-0000	2331.121	1.53(8)E-08	8.51(27)E-07	1.75(95)	-7.2(20)	46	4.1
446	0310(e)-0110(e)	1160.297	6.38(11)E-01	3.26(3)E-02	-1.48(39)	1.43(23)	82	2.7
446	0310(f)-0110(f)	1160.297	6.27(12)E-01	3.23(3)E-02	-2.05(41)	2.79(24)	96	3.0
446	0310(f)-0110(e)	1160.297	5.94(46)E-01	3.14(12)E-02			14	3.8
546	0310(e)-0110(e)	1151.336	2.62(4)E-03	3.42(3)E-02	-1.9(16)		31	4.2
546	0310(f)-0110(f)	1151.336	2.56(4)E-03	3.39(2)E-02	-3.1(15)		33	4.0
448	0310(e)-0110(e)	1145.122	2.60(3)E-03	4.56(3)E-02	-1.3(10)		44	3.7
448	0310(f)-0110(f)	1145.122	2.49(5)E-03	4.47(5)E-02	-2.4(22)		31	5.7
446	1110(e)-0110(e)	1291.498	1.249(8)E+01	1.366(4)E-01	-0.44(14)	-0.64(6)	123	1.4
446	1110(f)-0110(f)	1291.498	1.253(9)E+01	1.368(5)E-01	-1.48(17)	-0.36(7)	128	1.6
456	1110(e)-0110(e)	1284.757	4.61(14)E-02	1.33(2)E-01	-1.29(51)	0.83(48)	42	2.4
456	1110(f)-0110(f)	1284.757	4.65(28)E-02	1.34(4)E-01	-0.19(79)	0.90(78)	29	2.5
546	1110(e)-0110(e)	1277.455	3.91(15)E-02	1.26(3)E-01	0.79(73)	0.32(56)	38	3.2
546	1110(f)-0110(f)	1277.455	3.87(15)E-02	1.25(3)E-01	-1.50(51)	0.66(54)	42	2.1
448	1110(e)-0110(e)	1255.711	2.24(5)E-02	1.28(1)E-01	-2.24(85)	-0.43(48)	41	2.4
448	1110(f)-0110(f)	1255.711	2.36(6)E-02	1.31(2)E-01	-2.0(10)	-0.22(57)	38	3.0
447	1110(e)-0110(e)	1272.402	4.59(15)E-03	1.36(3)E-01	1.5(17)	1.23(84)	19	2.4
447	1110(f)-0110(f)	1272.402	4.47(20)E-03	1.34(3)E-01	-0.2(2)	2.4(13)	29	3.0
446	0001-0110(e)	1634.989	2.92(3)E-02	5.87(3)E-03	62.11(48)	-0.35(19)	95	1.6
446	0001-0110(f)	1634.989	2.97(20)E-02	5.92(21)E-03			46	3.6

Figure 6

Comparison of selected measurements of N_2O band strengths, S_v, in $cm^{-2}/atm.$ at 296K

mol	band	band center (cm^{-1})	this work	Toth ref. 1	other value	studies investigator(s)
446	1000-0000	1284.904	208.0(7)	205(2)	197(11)*	Kagann ref. 12
					229.8(45)	Levy et al. ref. 14
446	0200-0000	1168.133	7.00(6)	6.93(6)	7.28(38)*	Kagann ref. 12
					7.34(7)	Levy et al. ref. 14
446	1110(e)-0110(e)	1291.498	12.49(8)	11.8(2)		
446	1110(f)-0110(f)	1291.498	12.53(9)	11.8(2)		
446	0310(e)-0110(e)	1160.298	0.638(11)	0.649(18)		
446	0310(f)-0110(f)	1160.298	0.627(12)	0.632(18)		
446	1200-0200	1293.864	0.764(11)	0.699(20)		
446	2000-1000	1278.437	0.791(12)	0.767(22)		
446	2000-0200	1395.208	3.46(4)E-03	3.31(6)E-03		
446	1220-0220	1297.055	0.731(14)	0.688(24)		
456	1000-0000	1280.354	0.790(6)	0.802(22)		
546	1000-0000	1269.892	0.700(5)	0.698(22)		
448	1000-0000	1246.885	0.414(22)	0.414(8)		
446	0220(e)-0000	1177.745	5.53(5)E-08	5.69(52)E-08		
446	0001-0000	2223.757	1238(4)		1251(67)*	Kagann ref. 12
					1189(30)	Boissy et al. ref. 11
					1302	Lowder ref. 10
					1207(22)	Loewenstein et al. ref. 13
446	1110(e)-0000	1880.266	0.258(1)		0.214(10)	Toth and Farmer ref. 15
	F-Factor coef. a1		-1.089(3)E-02		-1.07(22)E-02	Toth and Farmer
446	1110(f)-0000	1880.266	0.256(6)		0.220(10)	Toth and Farmer
446	1200-0110(f)	1873.229	8.75(15)E-03		3.3(7)E-03	Toth and Farmer
446	1220(e)-0110(f) +1220(f)-0110(e)	1886.031	2.94(14)E-02		2.54(30)E-02	Toth and Farmer

* values calculated from dipole moment matrix elements given by Kagann
values given within parenthesis are uncertainties in the last digit(s)

Figure 7

THE ALPHA AND OMEGA OF CO AND THE HYDROGEN HALIDES

Richard Tipping
Department of Physics and Astronomy
University of Alabama
Tuscaloosa, AL 35487

THE ALPHA AND OMEGA OF CO AND THE HYDROGEN HALIDES

In this talk, I will outline the method used to calculate the most important spectroscopic parameters (specifically, the frequencies and intensities) and review the current status of the available spectroscopic information for the vibration-rotational transitions of CO and the hydrogen halides.

The outline of the computational scheme is shown in Figure 1. As can be seen from the figure, the basic experimental input data consist of frequency data in the form of Dunham parameters Y_{kl} and dipole moment function parameters obtained from analyses of laboratory intensity data. The first step is to calculate the vibration-rotational energy levels E_{vJ} from the well known series expansion given in Figure 2 in terms of the vibrational and rotational quantum numbers, v and J, respectively. The wavenumbers of the transitions ν_{if} can be calculated from the energy differences, subject to the usual selection rules for the allowed transitions. At the same time, one can calculate two other functions G(v) and B(v). These functions can then be used with a standard RKR program (Figure 3) to compute the two auxillary functions f(v) and g(v) from which one can easily determine two turning points R_{min} and R_{max} for each vibrational level as indicated in Figure 3. From the turning point data, one can construct the potential V(x), where x is the dimensionless displacement from equilibrium $x = (R - R_e)/R_e$. This potential is used as the input data in a numerical program for the solution of the vibration-rotational Schrodinger equation as outlined in Figure 4. The wavefunctions $\psi_{vJ}(x)$ can then be used in conjunction with the input parameters describing the dipole moment function, expressed either in terms of a series expansion or as a Padé approximant as illustrated in Figure 5, to calculate the dipole moment matrix elements M_{if}. Using these matrix elements, one can then calculate the transition moments R_{if} or the strengths S_{if} as defined in Figure 4. The output ν_{if}, R_{if}, and S_{if} are then combined with other experimental data (for instance, half widths, temperature coefficients, etc.) and the results in the correct AFGL tape format forwarded to Larry, the keeper of the "tape" (Figure 6).

Using the method just described, we have compiled data for the 5 most abundant isotopes of CO, and for the isotopes of the hydrogen halides listed in Figure 7. The vibrational bands and the rotational lines that have been calculated at present are also given in Figure 7. The accuracy, sources for the other spectroscopic parameters required for the tape, and status of the various data are given for CO, HF, HCl, and HBr and HI in Figures 8-11, respectively.

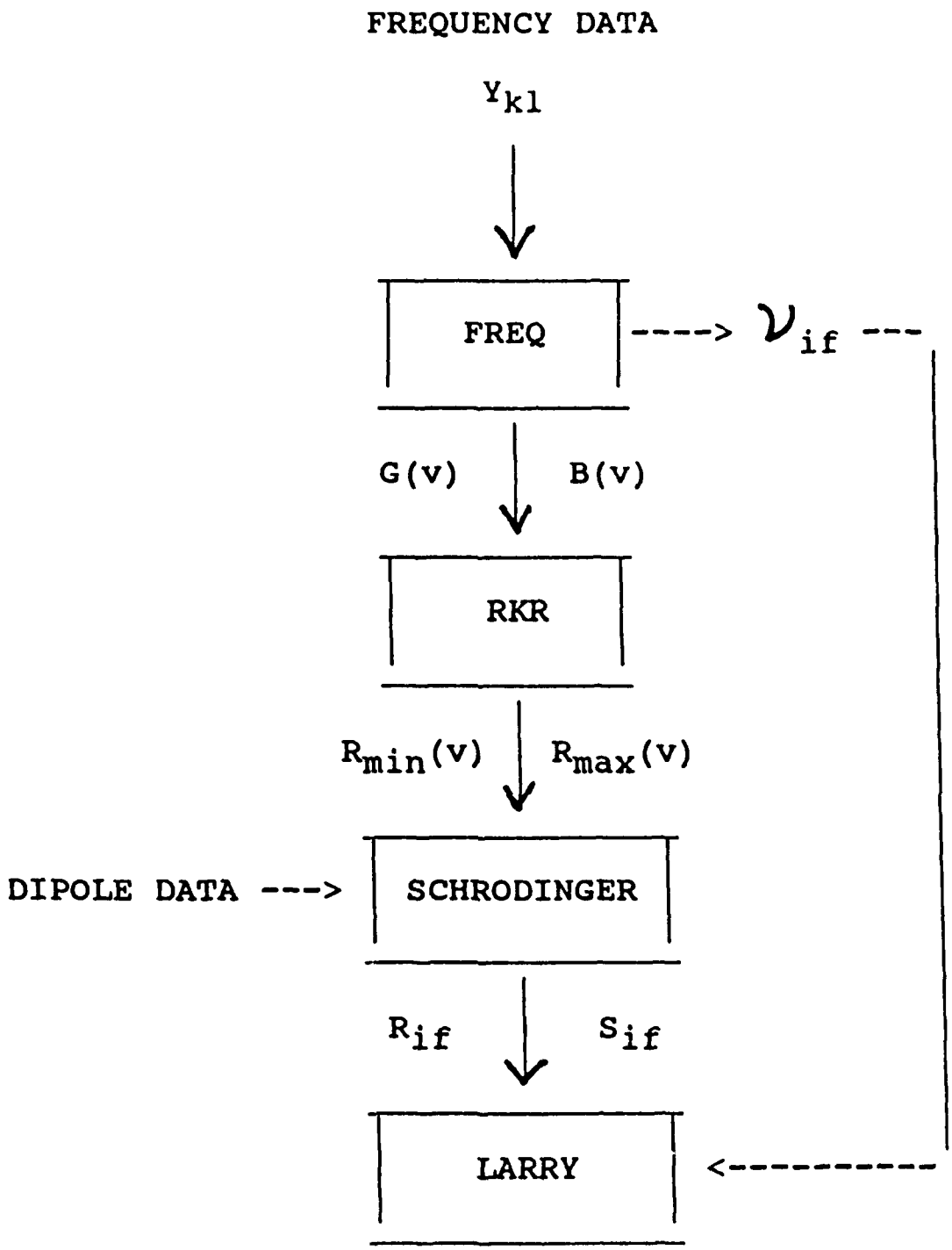
FREQUENCY DATA
Y_{kl}
FREQ
----> ν_{if} ---
G(v)
B(v)
RKR
$R_{min}(v)$
$R_{max}(v)$
DIPOLE DATA --->
SCHRODINGER
R_{if}
S_{if}
LARRY
<----------

Figure 1.

$$E_{vJ} = \sum_{k,l} Y_{kl} \, (v + 1/2)^k \, [J(J+1)]^l$$

$$\nu_{if} = E_{v'J'} - E_{vJ}$$

$$G(v) = \sum_{k} Y_{k0} \, (v + 1/2)^k$$

$$B(v) = \sum_{k} Y_{k1} \, (v + 1/2)^k$$

Figure 2.

RKR

$$f(v) = \int_{v_0}^{v} [G(v) - G(v')]^{-1/2}\, dv'$$

$$g(v) = \int_{v_0}^{v} B(v')[G(v) - G(v')]^{-1/2}\, dv'$$

$$R_{\substack{min \\ max}}(v) = (h/8\pi^2 c\mu)^{1/2}[(f^2 + f/g)^{1/2} \underset{+}{-} f]$$

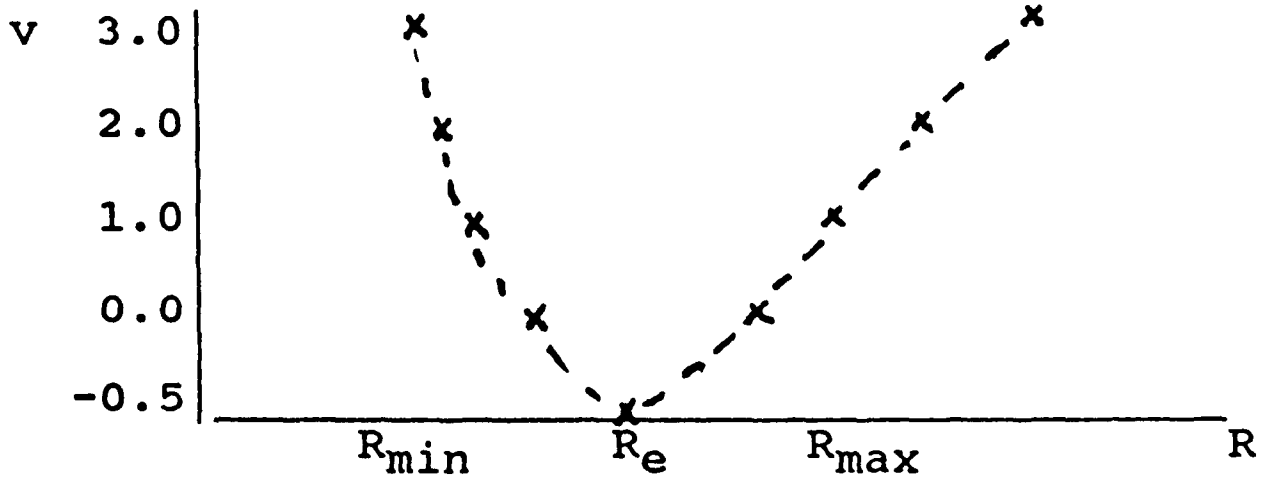

Figure 3.

SCHRODINGER

$$\frac{-\hbar^2}{2\mu}\frac{d^2\psi_{vJ}(x)}{dx^2} + V(x)\psi_{vJ}(x) = E_{vJ}\psi_{vJ}(x)$$

$$x = (R - R_e)/R_e$$

$$M_{if} = \int \psi_{v'J'}(x)\, M(x)\, \psi_{vJ}(x)\, dx$$

$$R_{if} = [(J'(J' + 1) - J(J + 1))/2]\, M_{if}^2$$

$$S_{if} = (8\pi^3/3hc)\nu_{if}\,[1 - \exp(-c_2\nu_{if}/T)]\, g_i I_a/Q(T)$$

$$\exp(-c_2E_i/T)\, R_{if} \cdot 10^{-36}$$

Figure 4.

DIPOLE DATA

$$M(x) = \sum_i M_i x^i \qquad \text{SERIES}$$

$$M(x) = \frac{M_0 + M_1 x + M_2 x^2}{1 + \sum_{i=1}^{6} e_i x^i} \qquad \text{PADE}$$

$$x = (R - R_e)/R_e$$

$$M(-1) = 0 \quad \text{AND} \quad M(x) \sim x^{-4}$$

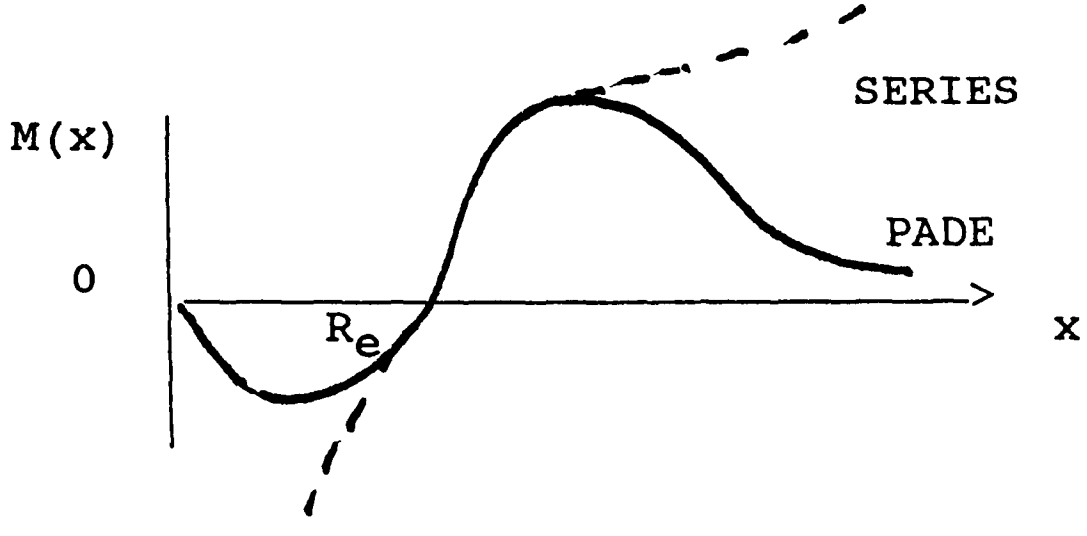

Figure 5.

?

Figure 6.

CALCULATED VIBRATION-ROTATIONAL LEVELS

CO (12,16) (13,16) (12,18) (12,17) (13,17)

VIBRATIONAL BANDS		ROTATIONAL LEVELS
0-0	1-1	
1-0	2-1	J = 0 --> 50
2-0	3-1	
3-0	4-1	
4-0		J = 0 --> 120 (12,16)

^{1}HX X = ^{19}F, ^{35}Cl, ^{37}Cl, ^{79}Br, ^{81}Br, ^{127}I

VIBRATIONAL BANDS			ROTATIONAL LEVELS
0-0	1-1	2-2	
1-0	2-1	3-2	
2-0	3-1	4-2	J = 0 --> 35
3-0	4-1	5-2	
4-0	5-1	6-2	
5-0	6-1	7-2	

Figure 7.

CO SOURCES AND STATUS

1. ν $\pm$ 0.0001 cm^{-1}

Guelachvili et al., J. M. S. 98, 64 (83)
Pollack et al., J. M. S. 99, 357 (83)

2. S $\pm$ 1 - 10%
Chackerian and Tipping, J. M. S. 99, 431 (83)
Chackerian et al., Can. J. Phys. 62, 1579 (84)

3. γ $\pm$ 1 - 2%
Nakazawa and Tanaka, J. Q. S. R. T. 28, 409, 471 (82)

4. γ_a $\pm$ 1 - 2%
Nakazawa and Tanaka, J. Q. S. R. T. 28, 409, 471 (82)

5. n $0.6 < n < 0.75$
Varanasi and Sarangi, J. Q. S. R. T. 15, 473 (75)
Lowry and Fisher, J. Q. S. R. T. 27, 585 (82)
Hartmann et al., J. Q. S. R. T. 35, 357 (86)

6. y
No data

Figure 8.

HF SOURCES AND STATUS

1. ν ± 0.001 cm^{-1}
Jennings et al., J. M. S. 122, 477 (87)
Guelachvili, Opt. Comm. 19, 150 (76)
Coxon, Private Comm. (87)

2. S ± 1 - 10%
Ogilvie et al., J. Chem. Phys. 73, 5221 (80)
Pine et al., J. M. S. 109, 30 (85)

3. γ ± 1 - 10%
Pine and Fried, J. M. S. 114, 148 (85)
Meredith, J. Q. S. R. T. 12, 485 (72)

4. γ_a ± 1 - 10%
Bachet, J. Q. S. R. T. 14, 1285 (74)
Pine and Looney, J. M. S. 122, 41 (87)
Meredith and Smith, J. Chem. Phys. 60, 3388 (74)

5. n ± 5% (1-0); no data for other bands
Pine and Looney, J. M. S. 122, 41 (87)

6. y ± 1 - 10%
Bachet and Coulon, Infra. Phys. 18, 585 (87)
Pine and Looney, J. M. S. 122, 41 (87)

Figure 9.

HCl SOURCES AND STATUS

1. ν ± 0.001 cm^{-1}
Guelachvili, Opt. Comm. 19, 150 (76)
Coxon and Ogilvie, J. Chem. Soc. Far. Trans. 78, 1345 (82)

2. S ± 1 - 10%
Ogilvie et al., J. Chem. Phys. 73, 5221 (80)
Pine et al., J. m. S. 109, 30 (85)

3. γ ± 1 - 10%
Pourcin et al., J. M. S. 90, 43 (81)
Pine and Fried, J. M. S. 114, 148 (85)

4. γ_a ± 1 - 10
Sergent-Rozey et al., J. M. S. 120, 403 (86)
Pine and Looney, J. M. S. 122, 41 (87)
Stanton and Silver, Appl. Opt. 27, 5009 (88)

5. n ± 5% (1-0); no data for other bands
Chackerian et al., J. M. S. 113, 373 (85)
Pine and Looney, J. M. S. 122, 41 (87)

6. y ± 1 - 10%
Guelachvili and Smith, J. Q. S. R. T. 20, 35 (78)
Pine and Looney, J. M. S. 122, 41 (87)

Figure 10.

NEW DATA FOR HBr AND HI

1. ν (DBr)
Wells et al., J. M. S. 107, 48 (84)

2. S (HBr)
Carlisle et al., J. M. S. 130, 395 (88)

S (HI)
Riris, Private Comm. (89)

3. γ (HBr)
Seoudi et al., J. M. S. 112, 88 (85)

Figure 11.

THE STATUS OF LINE PARAMETERS OF METHANE

Linda R. Brown
Jet Propulsion Laboratory
4800 Oak Grove Drive
Pasadena, CA 91109

V. Malathy Devi
Department of Physics
College of William and Mary
Williamsburg, VA 23185

1. Methane absorption spectra in four spectral intervals:

$0 - 600\ cm^{-1}$
$900 - 2350\ cm^{-1}$
$3700 - 4136\ cm^{-1}$
$5500 - 6185\ cm^{-1}$

2. The new studies involved:

(a) Measurements of self–, N_2, and air–broadened widths and shifts
(b) Theoretical modeling of energy levels
(c) Positions and intensities of the lowest fundamentals in all three isotopes
(d) Predictions of $^{12}CH_4$ and $^{13}CH_4$ hot bands
(e) Measurements of positions and intensities in two new spectral regions not included previously in the compilation

NEW METHANE LINE PARAMETERS

Bands	Iso	Region	type	source
gs-gs	1,2	00 - 300	new	Dijon
dyad-dyad	1,2	00 - 579	new	Dijon
dyad (ν_2,ν_4)	1,2	994 - 1798	chg	JPL/Dijon
pentad-dyad	1	1109 - 1798	new	JPL/Dijon
ν_3,ν_5,ν_6	3	904 - 1968	chg	Orsay
ν_2	3	2000 - 2355	new	Ames/Orsay
unassigned	1	3700 - 4136	new	JPL
$3\nu_4$	1	3871 - 3890	new	JPL
unassigned	1	5500 - 6184	new	JPL
$2\nu_3$	1	5891 - 6106	chg	JPL
$2\nu_3$	2	5898 - 6069	chg	JPL

ISO 1, 2, 3 = $^{12}CH_4$, $^{13}CH_4$, CH_3D respectively

JOURNAL OF MOLECULAR SPECTROSCOPY 133, 273–311 (1989)

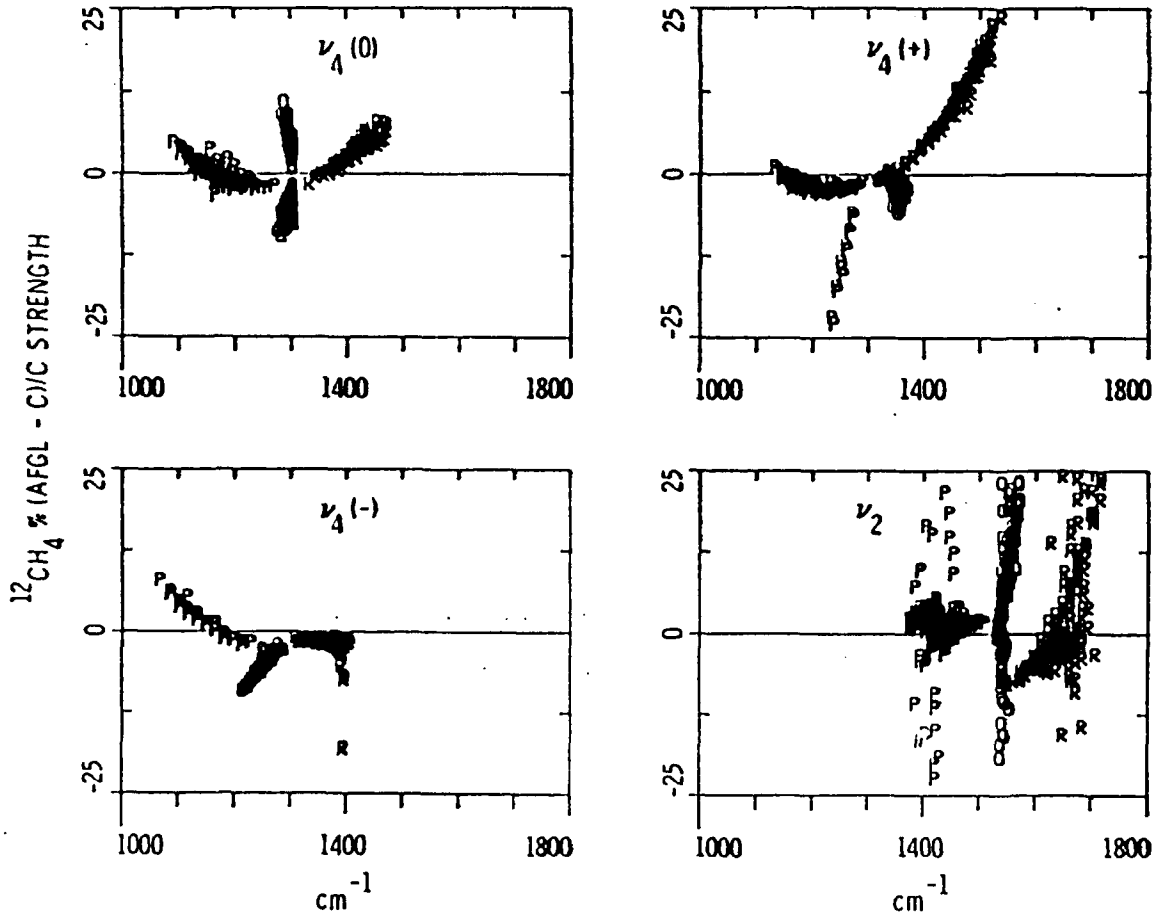

FIG. 8. Comparison of the present $^{12}CH_4$ calculated strengths with the calculated values from the 1986 AFGL HITRAN compilation (*35*) for the *P*, *Q*, and *R* transitions arising from the four level sets.

TABLE V

Summary of the Atlas (in Natural Isotopic Abundance)

Iso.	Band Id	Center(cm^{-1})	Str-sum	Max str.	Range(cm^{-1})	#Lines
CH_3D	ν_6	1161.	0.038	0.0005	1040 - 1250	490
$^{13}CH_4$	ν_4	1302.	1.376	0.04	1090 - 1730	1200
CH_3D	ν_3	1306.	0.031	0.006	1170 - 1420	320
$^{12}CH_4$	$2\nu_4-\nu_4$	1310.	0.91	0.01	1110 - 1600	2420
$^{12}CH_4$	$\nu_2+\nu_4-\nu_2$	1310.	0.14	0.001	1120 - 1480	1800
$^{12}CH_4$	ν_4	1310.	127.5	4.	1040 - 1570	3230
$^{12}CH_4$	$\nu_1-\nu_2$	1384.	0.0008	0.00002	1220 - 1490	220
CH_3D	ν_5	1472.	0.007	0.00007	1340 - 1600	220
$^{12}CH_4$	$\nu_3-\nu_2$	1485.	0.009	0.0001	1330 - 1600	780
$^{12}CH_4$	ν_2	1533.	1.35	0.01	1350 - 1770	1930
$^{13}CH_4$	ν_2	1533.	0.0128	0.0001	1400 - 1720	700
$^{12}CH_4$	$2\nu_2-\nu_2$	1533.	0.002	0.00003	1410 - 1670	480
$^{12}CH_4$	$\nu_2+\nu_4-\nu_4$	1533.	0.008	0.00008	1310 - 1720	1320
$^{12}CH_4$	$\nu_1-\nu_4$	1607.	0.0006	0.00001	1430 - 1700	170
$^{12}CH_4$	$\nu_3-\nu_4$	1710.	0.047	0.0006	1500 - 1910	1830
$^{12}CH_4$	$2\nu_2-\nu_4$	1750.	0.0002	0.00001	1730 - 1970	80

Tabulation of Integrated Sums

$^{12}CH_4$ dyad	(ν_2,ν_4)	128.9 (4)
$^{13}CH_4$ dyad	(ν_2,ν_4)	1.39(6)
$^{12}CH_4$ hot bands (pentad - dyad)		1.12
CH_3D fundamentals		0.08
$^{13}CH_4$ hot bands (pentad - dyad)		0.01 (not included in above list)
Integrated strength for region		131.5 (4.) $cm^{-2}\cdot atm^{-1}$ at 296 K

Note. Strengths are in units of $cm^{-2}\cdot atm^{-1}$ at 296 K in natural isotopic abundance. For all bands, 10^{-6} $cm^{-2}\cdot atm^{-1}$ is the weakest line in the prediction. For the averaging of strength measurements, a prediction of H_2O lines (*15*) was also included to detect residual absorption in the FTS.

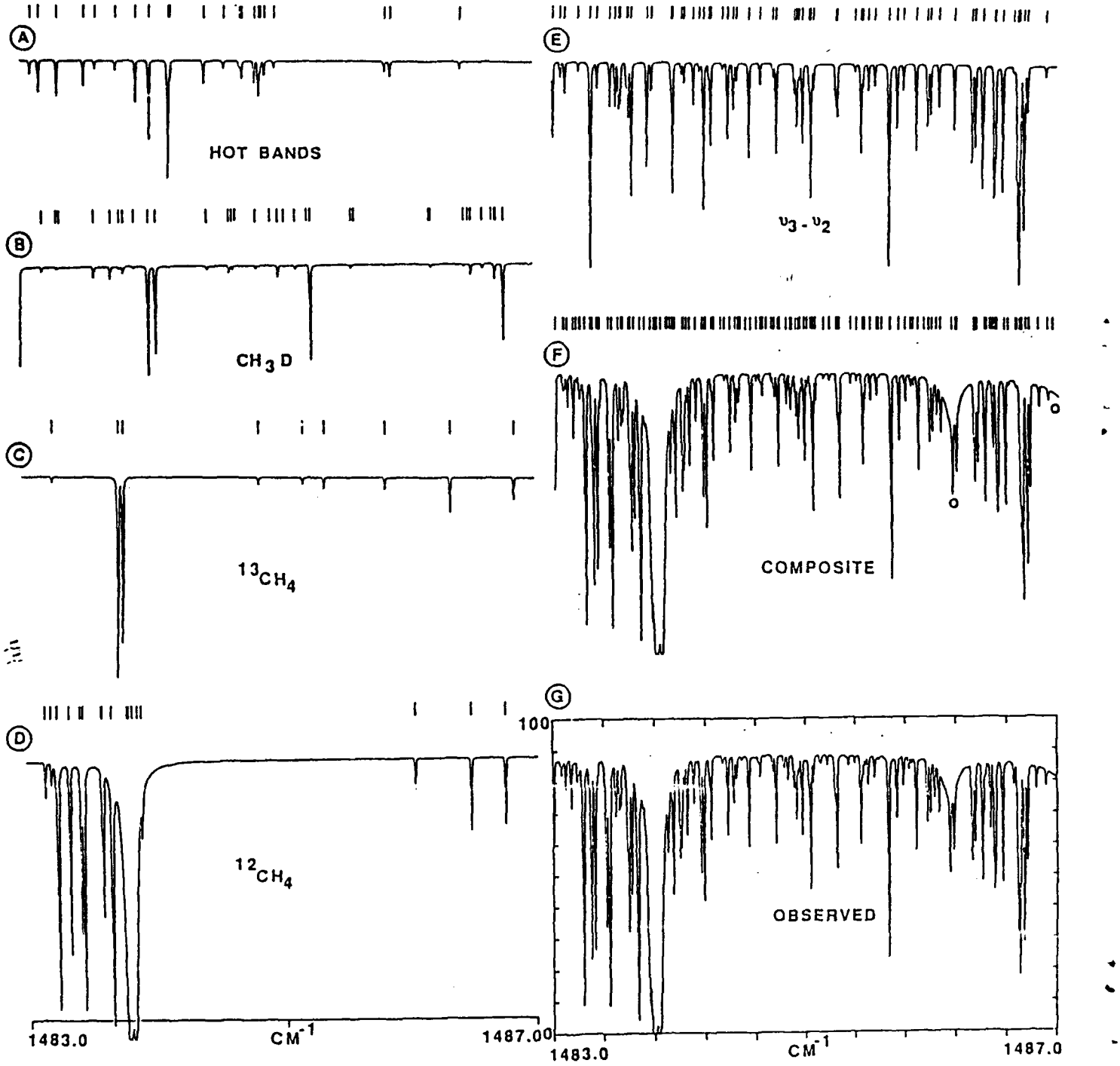

Fig. 2. The methane spectrum in the region of the Q branch of the ν_3 - ν_2 band (1483 - 1487 cm^{-1}). Spectra A -- F are computed at the conditions of the observed spectrum G (0.008 cm^{-1} resolution (apodized), 10.0 Torr, 193 m, 297.4 K). The composite F spectrum includes residual H_2O, marked by o. The fundamental transitions of CH_3D, $^{13}CH_4$ and $^{12}CH_4$ are shown in panels B, C and D respectively, while absorptions arising from hot bands are shown in A (all but the ν_3 - ν_2 band) and E (ν_3 - ν_2 alone).

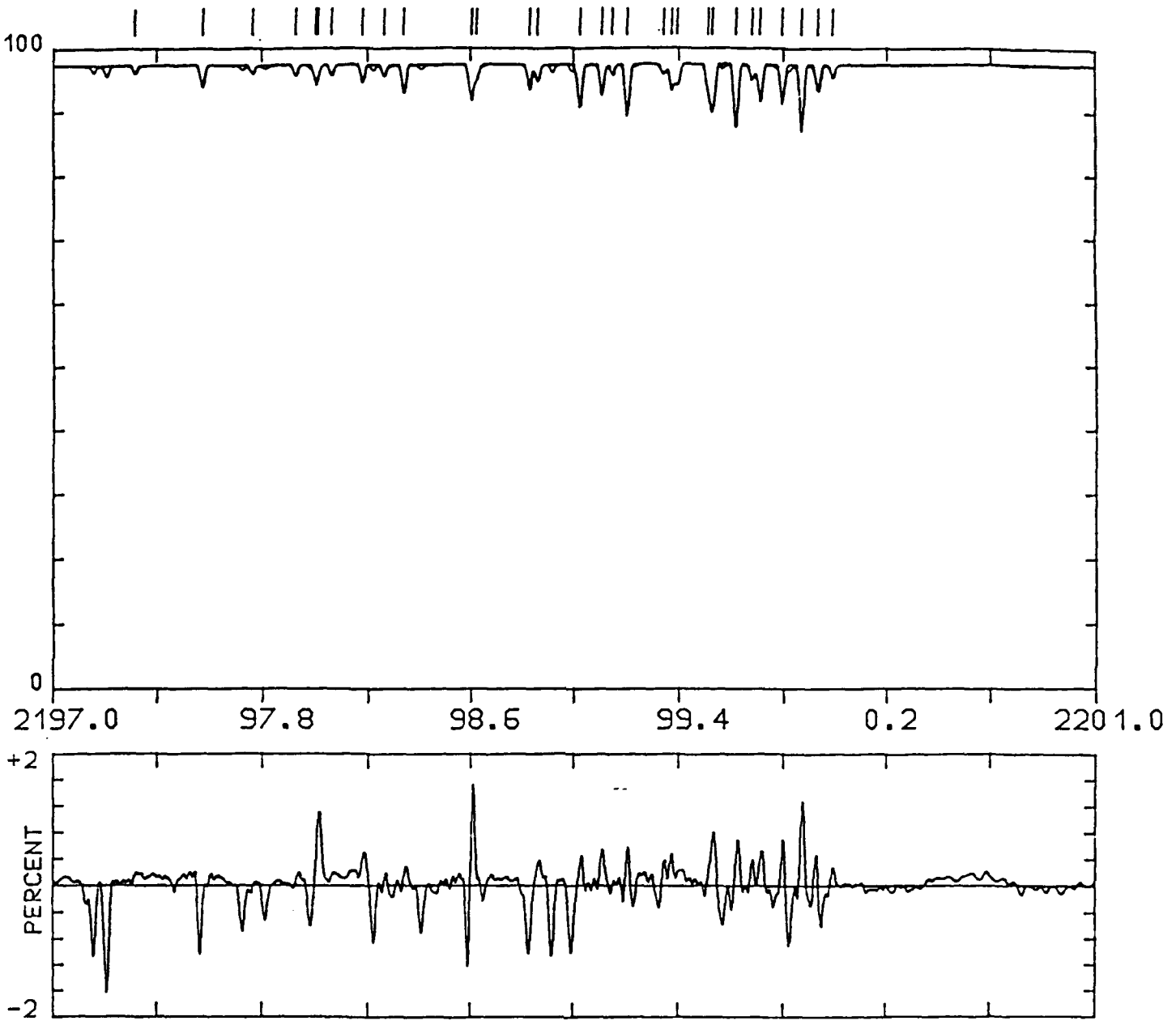

Fig. 1 Comparison of observed and calculated spectra in the ν_2 region of CH_3D. In the upper panel two spectra are overlaid. The synthetic spectrum is computed using the experimental conditions of the observed data (3.4 torr of normal methane at room temperature and a path length of 25 meters). The observed spectrum was recorded at 0.012 cm^{-1} resolution using the FTS at Kitt Peak. The lower panel shows the percentage differences of the transmission values.

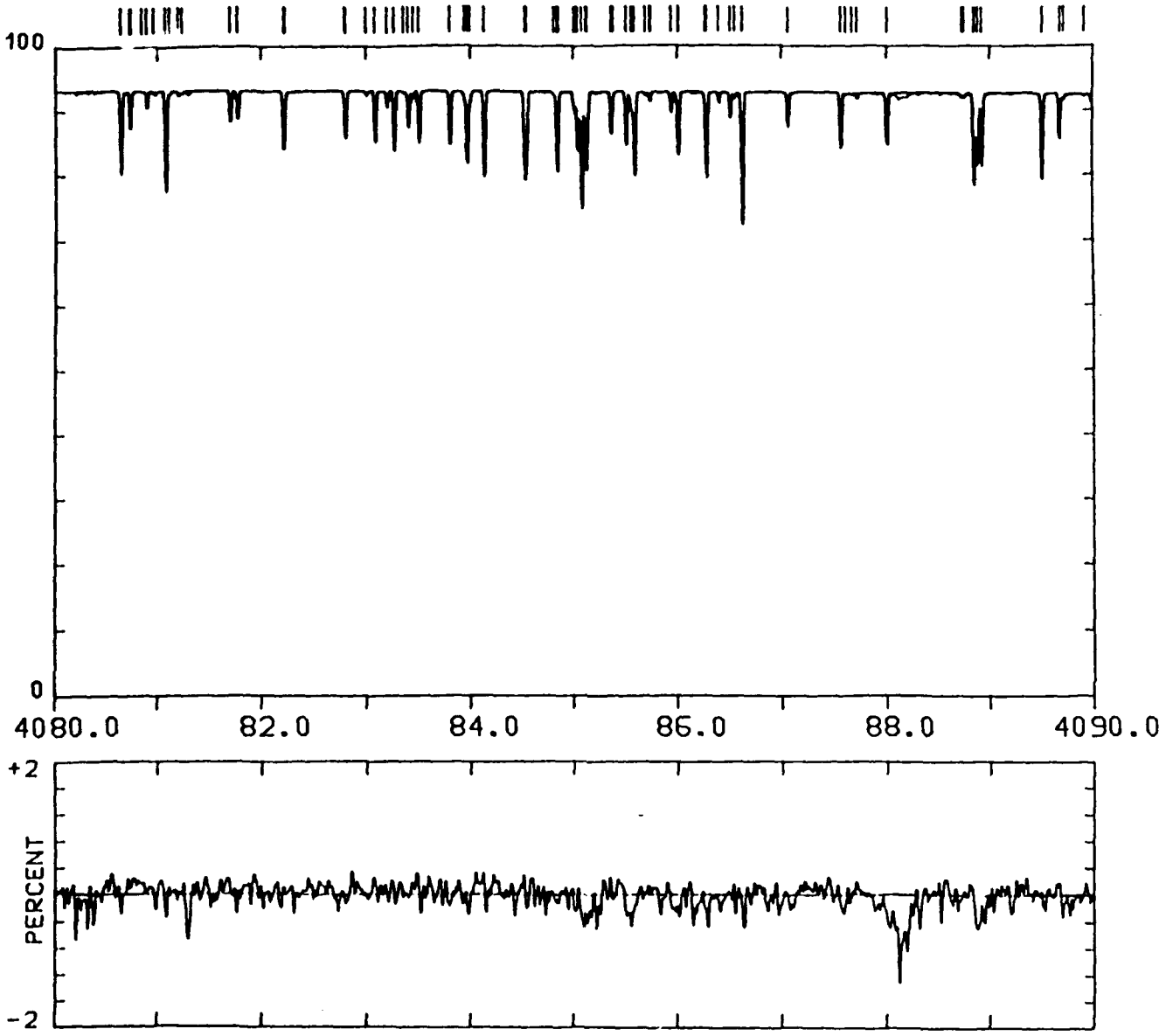

Fig. 3. Comparison of the observed and computed methane spectra near 4085 cm^{-1}. The synthetic spectrum is computed from the experimentally-determined parameters of Ref. 16 using the experimental conditions of the observed spectrum (10 torr at room temperature with a path length of 1.5 m). No quantum assignments are available for these features at this time, and so lower state energies are set to 300 cm^{-1}.

SYNTHETIC SPECTRA FROM 1989 METHANE PARAMETERS

IPL

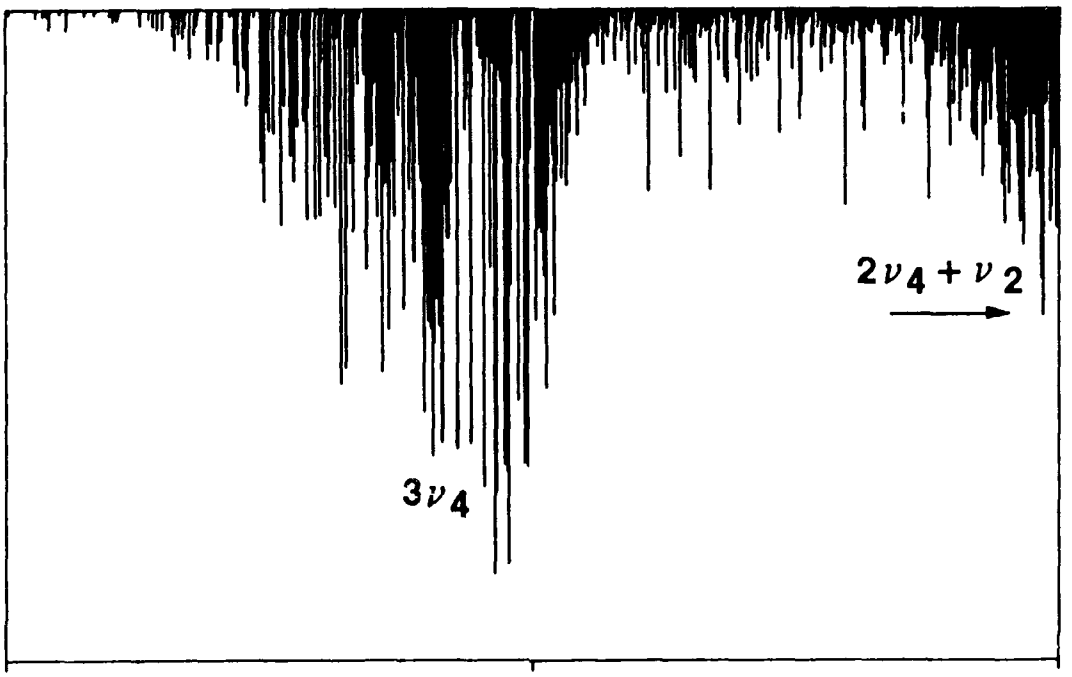

3700.00 3900.00 4100.00

cm^{-1}

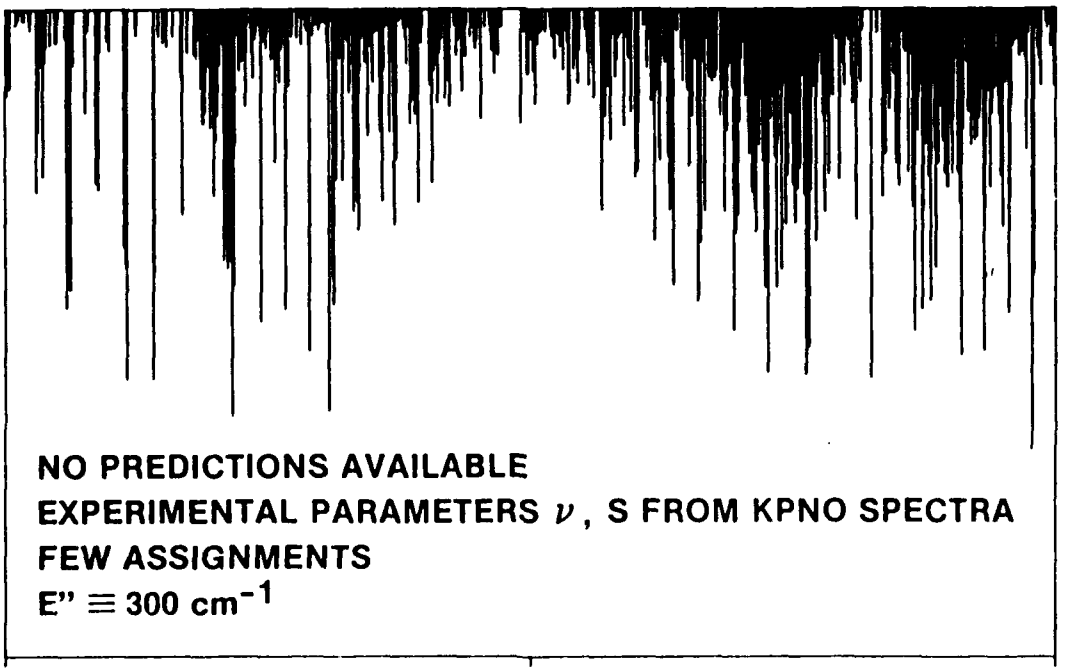

NO PREDICTIONS AVAILABLE
EXPERIMENTAL PARAMETERS ν, S FROM KPNO SPECTRA
FEW ASSIGNMENTS
E" $\equiv$ 300 cm^{-1}

5500.00 5700.00 5900.00

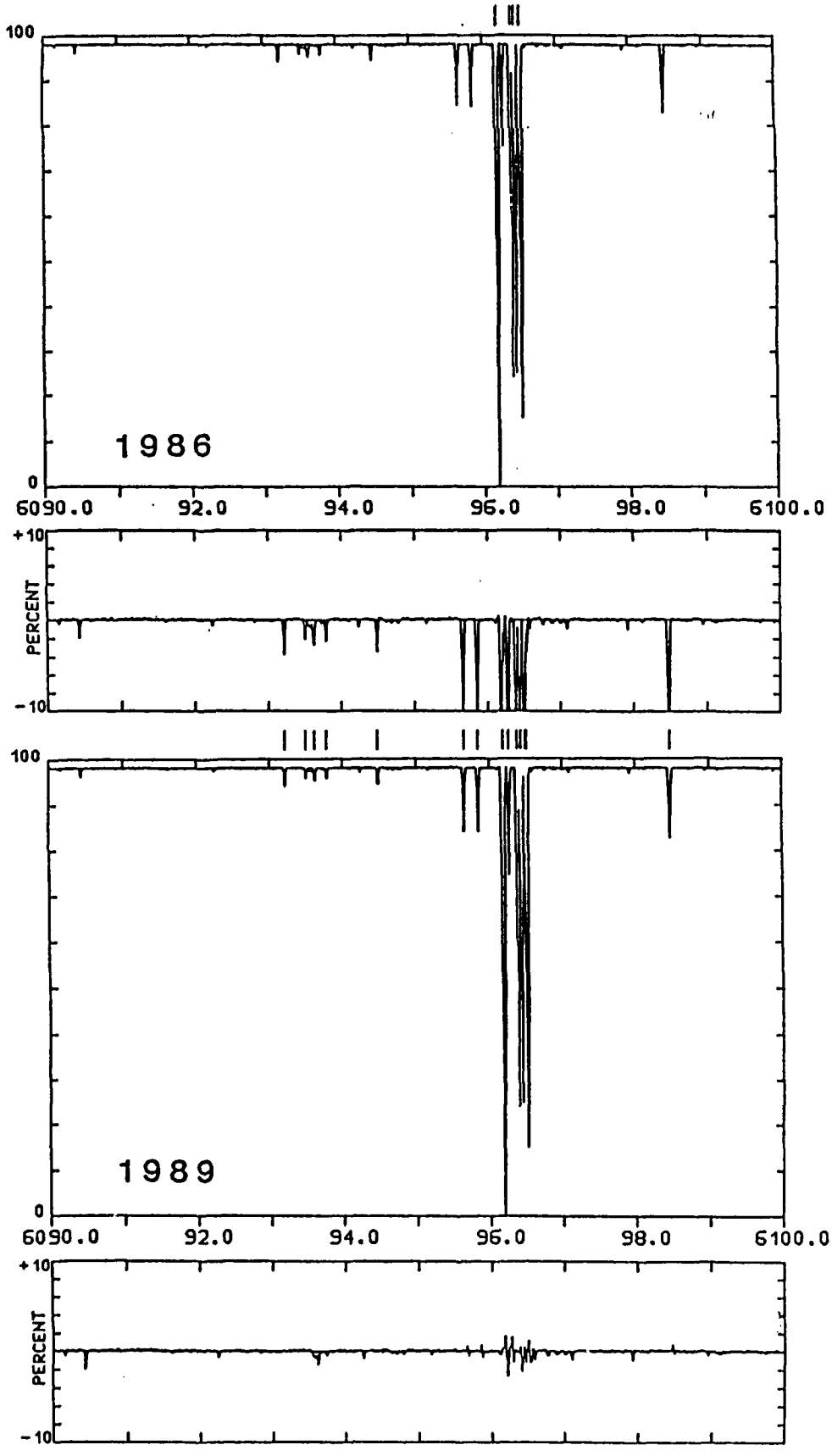

Fig. 4. Comparison of observed and calculated methane spectra near 6100 cm^{-1} In the top panel, 1986 HITRAN parameters are used for the synthetic spectrum, while in the lower panel, the revised methane parameters are used. The observed spectrum is recorded at 0.012 cm^{-1} resolution with the FTS at Kitt Peak using a 1 torr sample at room temperature and a 25 meter path.

Reprinted from Applied Optics, Vol. 27 page 631, February 1, 1988

Measurements of air-broadened and nitrogen-broadened Lorentz width coefficients and pressure shift coefficients in the ν_4 and ν_2 bands of $^{12}CH_4$

Curtis P. Rinsland, V. Malathy Devi, Mary Ann H. Smith, and D. Chris Benner

Air-broadened and N_2-broadened halfwidth and pressure shift coefficients of 294 transitions in the ν_4 and ν_2 bands of $^{12}CH_4$ have been measured from laboratory absorption spectra recorded at room temperature with the Fourier transform spectrometer in the McMath solar telescope facility of the National Solar Observatory. Total pressures of up to 551 Torr were employed with absorption paths of 5–150 cm, CH_4 volume mixing ratios of 2.6% or less, and resolutions of 0.005 and 0.01 cm^{-1}. A nonlinear least-squares spectral fitting technique has been utilized in the analysis of the twenty-five measured spectra. Lines up to $J'' = 18$ in the ν_4 band and $J'' = 15$ in the ν_2 band have been analyzed.

Reprinted from Applied Optics, Vol. 27 page 2296, June 1, 1988

Air-broadened Lorentz halfwidths and pressure-induced line shifts in the ν_4 band of $^{13}CH_4$

V. Malathy Devi, Curtis P. Rinsland, Mary Ann H. Smith, and D. Chris Benner

Air-broadened halfwidths and pressure-induced line shifts in the ν_4 fundamental of $^{13}CH_4$ were determined from spectra recorded at room temperature and at 0.01-cm^{-1} resolution using a Fourier transform spectrometer. Halfwidths and pressure shifts were determined for over 180 transitions belonging to J'' values of ≤ 16. Comparisons of air-broadened halfwidths and pressure-induced line shifts made for identical transitions in the ν_4 bands of $^{12}CH_4$ and $^{13}CH_4$ have shown that $^{13}CH_4$ air-broadened halfwidths are ~5% smaller than the corresponding $^{12}CH_4$ halfwidths, and the pressure shifts for $^{13}CH_4$ lines are ~5–15% larger than those for $^{12}CH_4$.

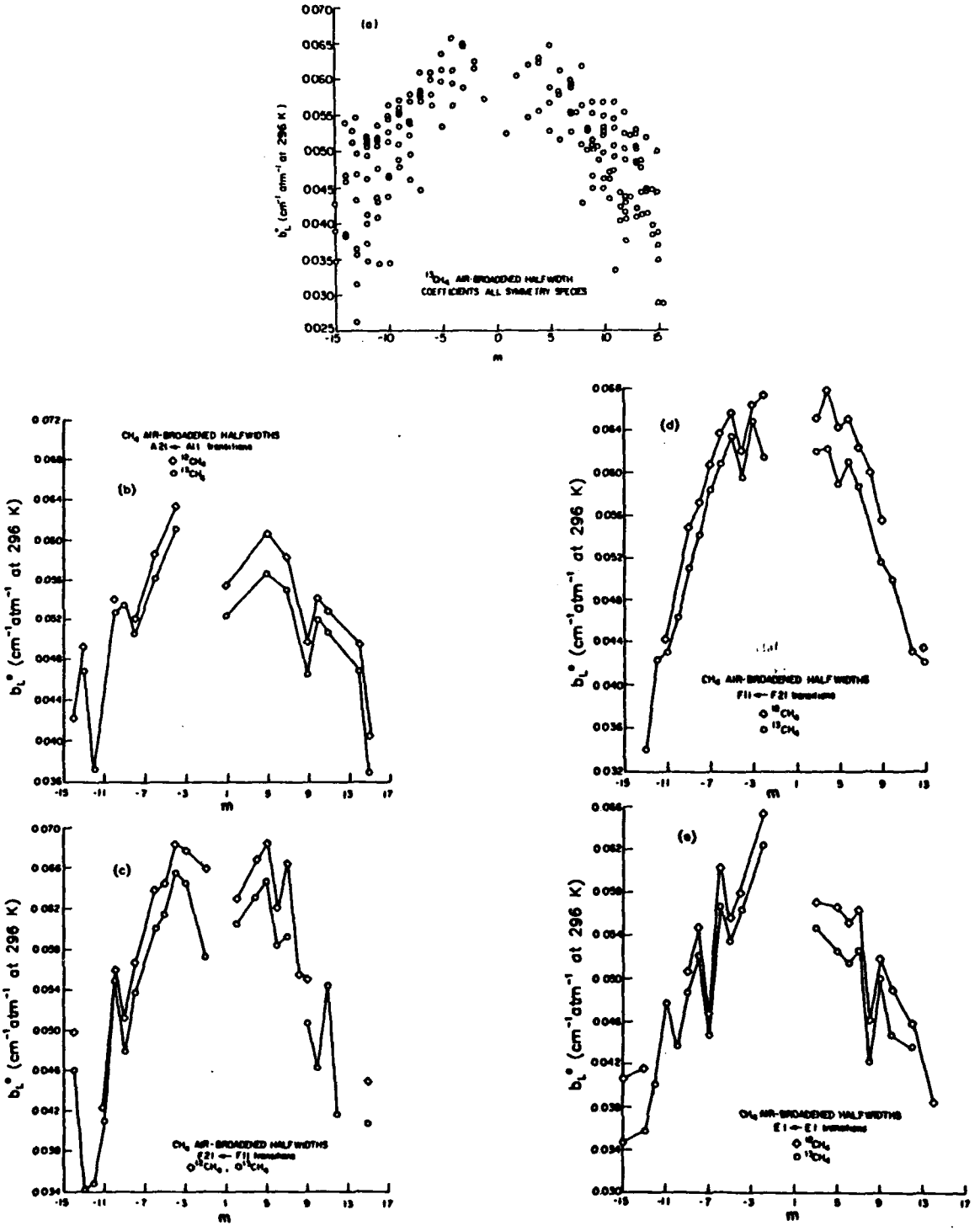

Fig. 5. Plots of measured air-broadened Lorentz halfwidth coefficient vs m: (a) for all measured transitions in $^{12}CH_4$; (b) $A21 \leftarrow A11$ transitions; (c) $F21 \leftarrow F11$ transitions; (d) $F11 \leftarrow F21$ transitions; (e) $E1 \leftarrow E1$ transitions. In (b)–(e), solid lines connect measurements to help distinguish $^{12}CH_4$ from $^{13}CH_4$ data. Discontinuity in solid lines joining the symbols indicate halfwidth values were not available. Plots (b)–(e) contain measurements for both $^{12}CH_4$ and $^{13}CH_4$.

TABLE I SUMMARY OF MOLECULAR LINE PARAMETERS FOR METHANE[+]

VIBRATIONAL BAND		STATUS	ISO	#LINES	FMIN	FMAX	SMIN	SMAX	S-SUM
00000000	00000000	ADD	211	1747	0.010	312.781	4.06-34	6.87-25	1.975E-23
00000000	00000000	ADD	311	1286	0.032	309.132	4.10-34	7.62-27	2.192E-25
00000111	00000111	ADD	211	2207	2.537	367.116	4.04-29	5.99-25	2.205E-23
GROUND	GROUND		212	79	7.760	99.950	5.57-30	1.51-27	4.235E-26
00000111	00000111	ADD	311	508	19.009	340.125	4.03-29	7.04-27	2.458E-25
01100001	00000111	ADD	211	2297	26.675	578.722	4.04-29	1.35-25	8.700E-24
01100001	01100001	ADD	211	110	62.558	197.878	4.05-29	5.00-28	1.255E-26
01100001	00000111	ADD	311	446	78.511	401.385	4.04-29	1.63-27	9.388E-26
ν_6	GROUND	REP	212	2081	904.489	1486.185	1.00-27	1.94-23	1.461E-21
00000111	00000000	REP	211	3198	992.256	1766.145	4.05-26	9.68-20	4.782E-18
ν_3	GROUND	REP	212	1003	1035.840	1478.250	1.01-27	2.16-23	1.049E-21
00000111	00000000	REP	311	1246	1089.040	1685.139	4.05-26	1.01-21	5.025E-20
00000222	00000111	ADD	211	2397	1109.032	1605.075	4.04-26	3.82-22	3.659E-20
01100112	01100001	ADD	211	1813	1127.955	1480.889	4.04-26	5.34-23	5.734E-21
01100001	00000000	REP	211	1973	1149.156	1798.069	4.06-26	5.58-20	4.151E-19
01100001	00000000	REP	311	724	1170.554	1732.358	4.06-26	5.90-22	4.316E-21
10000001	01100001	ADD	211	342	1223.613	1502.333	4.05-26	1.60-24	7.219E-23
ν_5	GROUND	REP	212	1873	1250.525	1695.368	1.01-27	4.90-24	3.534E-22
00011001	01100001	ADD	211	768	1329.298	1605.861	4.04-26	5.24-24	3.449E-22
01100112	00000111	ADD	211	1214	1341.112	1716.667	4.04-26	3.15-24	3.040E-22
02200002	01100001	ADD	211	500	1412.719	1671.395	4.05-26	1.30-24	8.581E-23
00011001	00000111	REP	211	1828	1505.569	1900.154	4.03-26	2.34-23	1.905E-21
10000001	00000111	ADD	211	135	1553.652	1695.967	4.19-26	4.05-25	2.023E-23
02200002	00000111	ADD	211	189	1700.850	1968.837	4.05-26	6.71-25	2.203E-23
ν_2	GROUND	ADD	212	502	2005.045	2355.045	1.26-28	9.12-24	4.635E-22
$2\nu_6$	GROUND		212	609	2088.463	2433.369	9.55-27	2.14-24	1.146E-22
00000222	00000000		211	1266	2255.492	2847.219	1.32-24	8.39-22	5.500E-20
00000222	00000000		311	36	2461.590	2727.654	1.23-24	2.20-23	1.771E-22
01100112	00000000		211	2300	2573.103	3167.121	1.22-24	5.18-21	3.767E-19
01100112	00000000		311	208	2659.654	2998.601	2.08-24	5.96-23	2.805E-21
10000001	00000000		211	90	2764.931	3091.442	1.52-24	6.82-22	2.510E-21
00011001	00000000		211	1903	2809.526	3209.940	1.48-24	2.13-19	1.080E-17
00011001	00000000		311	355	2832.715	3167.050	1.94-24	2.25-21	8.549E-20
00011112	00000111		211	712	2880.787	3135.543	2.20-24	6.17-22	4.445E-20
01111002	01100001		211	264	2898.463	3105.094	1.40-24	2.77-22	6.801E-21
$2\nu_5$	GROUND	REP	212	39	2902.494	3129.538	2.01-24	9.87-23	3.832E-22
ν_1	GROUND	REP	212	28	2902.562	3070.791	2.29-24	9.87-23	4.485E-22
ν_4	GROUND	REP	212	242	2903.131	3146.460	1.94-24	4.03-22	5.865E-21
02200002	00000000		211	755	2906.842	3253.323	1.00-24	7.16-22	3.435E-20
00011112	00000111		311	12	3034.350	3090.330	3.41-24	1.05-23	5.906E-23
UNASSIGNED			311	4	3157.869	3174.954	1.28-23	6.49-23	1.302E-22
00000333	00000000	ADD *	211	11	3871.563	3890.856	1.91-22	5.25-22	3.386E-21
10000111	00000000		211	172	4136.165	4278.242	1.90-22	5.24-21	2.399E-19
00011112	00000000		211	958	4147.842	4489.168	1.56-23	5.53-21	4.077E-19
01111002	00000000		211	388	4409.945	4666.560	2.05-23	1.21-21	6.246E-20
00022002	00000000	REP	211	144	5891.064	6106.283	4.06-23	1.32-21	5.973E-20
00022002	00000000	REP	311	85	5898.248	6069.084	1.15-24	1.94-23	5.222E-22
UNASSIGNED		ADD	211	5910	2511.381	6184.491	4.03-25	1.87-21	2.174E-19

+ FMIN AND FMAX ARE IN UNITS OF CM^{-1}. SMIN, SMAX AND S-SUM ARE IN UNITS OF $CM^{-1}/(MOLECULE \cdot CM^{-2})$. LINE WIDTHS ARE BASED ON REFS. 2-6.

* NEW VIBRATIONAL CODE.

COMPARISON OF 1986 AND 1989 METHANE LINE PARAMETERS

SUMMATIONS	1986	1989
TOTAL NUMBER OF BANDS	30	48
TOTAL NUMBER OF LINES	17000	47000
NUMBER OF UNASSIGNED LINES	3000	5900
MINIMUM IR STRENGTH+	1×10^{-24}	4×10^{-26}
TOTAL ABSORPTION+	1.74×10^{-17}	1.77×10^{-17}
MAXIMUM CM^{-1} INCLUDED	6107	6185
TOTAL CM^{-1} INCLUDED	3100	4500

+ IN UNITS OF $CM^{-1}/(MOLECULE\text{-}CM^{-2})$ AT 296K

JPL

STATUS OF 1989 METHANE

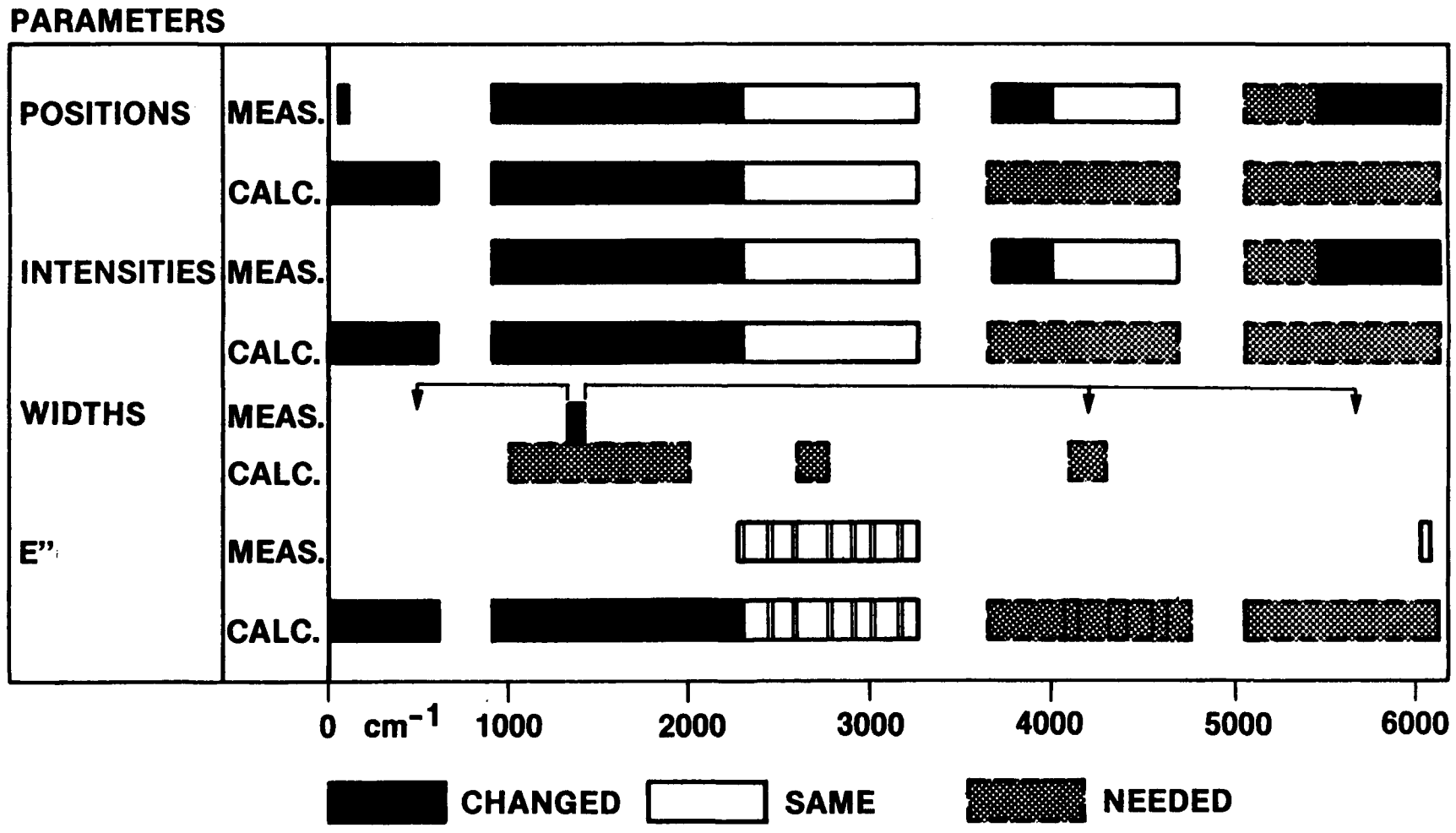

This viewgraph shows the four spectral regions in the methane absorption spectrum where new studies have been completed.

The reseach work performed in these four spectral intervals are listed under section (2) a, b, c, d, and e.
Most of the experimental data used in these studies were obtained at 0.005 to 0.02 cm^{-1} resolution spectra recorded with the Fourier transform spectrometer (FTS) at the National Solar Observatory facility at Kitt Peak, Arizona.

VUGRAPH 2

This Table shows the spectral regions for which new line parameters are available. The Table identifies the various bands, isotope, spectral regions in cm^{-1}, and the source. Source gives the various spctroscopists who worked on the different projects and made this update possible.

Sources include the following groups:

Dijon (Champion, Loete, Hilico etc.)
JPL (Linda Brown, Margolis)
Orsay (Tarrago, Guelachvili)
Nasa Ames (Chackerian)

Let us start with the second set:

1. Dyad refers to the ν_2 and ν_4 fundamentals of ^{12}CH and ^{13}CH. Positions and intensities of the ν_2 and ν_4 bands of $^{12}CH_4$ & $^{13}CH_4$ were measured with high precision from spectra recorded using the FTS at Kitt Peak and successfully modeled by the JPL / Dijon group. Positions for the two bands in both isotopes are now determined with accuracies ranging from 0.0001 cm^{-1} (fitted well) to 0.001 cm^{-1} (extrapolated to J values beyond 20); intensities for the two bands are known with accuracies from 3% (fitted well) to 15% (for lines extrapolated to high J valus).
2. Hot bands of $^{12}CH_4$ predicted in the 1000 to 2000 cm^{-1} region.
3. Positions and intensities for the three lowest fundamentals of CH_3D have been revised. Parameters for the ν_2 band of CH_3D in the 5 micron region are added in the update.

4. First set: The results achieved in the dyad region were used in a theoretical prediction of weak "rotational" transitions in the 0 – 600 cm^{-1} region for the two main isotopes of methane. Transitions were computed for the ground – ground, ν_4 to ν_4, and ν_4 to ν_2. A few dozen observations of these transitions were measured but no intensity measurements are done in this region. Intensities may be off by 30% in this region.

5. Experimental measurements of positions and intensities with little modeling to quantum mechanics are available in the 3700 – 4136 cm^{-1} and 5500 – 6185 cm^{-1} regions.

Some examples from these studies will be illustrated in the following viewgraphs.

As an example we show in this viewgraph how the computed intensities for the $^{12}CH_4$ dyad have changed. Dyad work involved fitting over 1200 measured intensities with RMS of 3%. This plot has the percent differences between the 1986 HITRAN line intensities and the new calculations. The transitions of four subsets are shown: The 3 degeneracies of ν_4 (−, 0, +1) and ν_2. The symbole P,Q, and R stand for delta J. The residuals for the strong allowed lines correspond to R(−), Q(+), and P(+). The remaing large residuals are for the weaker forbidden transitions. Overall, the effective band intensity has been raised by 2.5%. The biggest change has been in the $\nu_2$band.

The new dyad calculations are based on the Hamiltonin developed by Champion et al.
The new intensity calculations required an expansion of the dipole momet to seven terms, rather than the two terms (main dipole and Herman–Wallis factor) used before.

In this viewgraph we list the various bands occurring in the dyad region. The 1000 to 2000 cm^{-1} region contains preleminary predictions of several hot bands in the region totaling more than 10000 lines with intensities of the order of 10^{-6} cm^{-2} atm^{-1} at 296 K. This table is a summary of the atlas from which these predictions were made.

The hot band positions are predicted with the pentad levels (ν_1, ν_3, $2\nu_4$, $\nu_2+\nu_4$, $2\nu_2$) as the upper state and the dyad as the lower state. The accuracies of positions for these hot bands are good only to 0.001 cm^{-1} to 0.01 cm^{-1} because positions are computed using well determined predicted dyad levels and either the experimentally determined or not so well determined pentad levels. Better positions for these hot bands await successful treatment of pentad bands. Intensities are believed to be accurate in the 5 – 30% range.

Notice that the intensities of these hot bands are extremely weak in comparison with the total integrated intensities for the region.

This Figure clearly illustrates the need to include these hot bands. The seven panels show the calculated (A, B, C, D, E, F) and the observed (G) spectra between 1483 and 1487 cm^{-1} near the Q branch of $\nu_3 - \nu_2$, a very weak band of $^{12}CH_4$. The panels A to E are synthetic spectra computed from the revised parameters of the (A) hot bands other than $\nu_3 - \nu_2$, (B) CH_3D (C) $^{13}CH_4$ (D) $^{12}CH_4$ (E) $\nu_3 - \nu_2$. Panel F is the calculated composite of the first five spectra and compares well with the high density observed spectrum (G) recorded with the Kitt Peak FTS with a pathlength of 193m and 3 torr methane. Comparison of spectra (F) & (G) shows that even weak hot band transitions need to be considered. Extend of methane spectrum in this region is very good. Notice that there is very little visual difference seen between the observed and the calculated spectra.
Additionl studies are needed to refine the predicted values of the upper state pentad levels.A new study in the pentad region 2200 – to 3300 cm^{-1} by JPL / DIJON group is beginning this fall with hopes of achieving similar good results. It is a very difficult region to analyze which requires the simultaneous treatment of 5 bands.

The new list contains 160 transitions in this 4 wavenumber interval, 28 of which have intensities greater than 10^{-24} cm^{-1}/ (molecule.cm^{-2}); the 1986 compilation has 13 lines, all with intensities greater than 10^{-24} cm^{-1}/ (molecule.cm^{-2})

The studies involving the positions and intensities of the ν_6, ν_5, ν_3 and ν_2 fundamentals of CH_3D between 900 and 2350 cm^{-1} were completed by researchers at the Laboratoire de Infrarouge, Orsay, France, Ispra, Italy and NASA Ames research center, using spectra obtained with Fourier tranform and tunable diode laser spectrometers. The rms values of the observed minus calculated values of the analysis of triad ν_3, ν_5, and ν_6 were 0.0003 cm^{-1} for positions and 3.4% for intensities. The accuracies for corresponding measurements in the ν_2 band of CH_3D were difficult to charecterize. This viewgraph shows the CH_3D absorptions in the ν_2 Q branch region. The observed spectrum and the synthetic spectrum based on the retrieved parameters are overlaid with the observed minus calculated transmission values plotted below. The deviations in positions are as much as 0.003 cm^{-1}. However, since the band is completely missing in the 1986 edition, the new parameters will be included in the present update.

Figure of spectra in the 2.5 and 1.7 micron regions.

Measurements of positions and intensities obtatained from spectra recorded with the FTS at Kitt Peak are tabulated for the 3700 – 4136 cm^{-1} and 5500 – 6185 cm^{-1} regions. In both cases, few quantum assignments and lower state energies are reported. This plot shows representative calculated spectra based on the new parameters. Much work is needed to assign the spectra and then model the measurements by quantum mechanics. Both regions shown in this figure are very difficult to analyse. The upper panel shows two of the eight bands (octade) absorbing in the 3700 – 4136 cm^{-1} spectral region. The lower panel is part of the 5000 – 6300 cm^{-1} region containing 40 possible states in interaction involving all three isotopes.

Examples of short segments from these two intervals will be shown in the next two viewgraphs.

This figure shows the comparison between the observed and calculated spectra in the 4080 to 4090 cm^{-1}region. The synthetic spectrum is computed from the experimentally determined parameters from analysing spectrum containing 10 torr methane at room temperature in a 1.5m path. No quantum assignments are available for these features at this time, and therefore the lower state energies are set to 300 cm^{-1}. The 1986 database contained an unpublished version of the list from 3900 – 4136 cm^{-1}. For the present update, new measurements have been added to this interval and parameters for the 3700 – 3900 cm^{-1} region are included.

The low frequency fundamentals of methane were also used for experimental measurements of halfwidth and pressure shift coefficients. A comprehensive and extensive research work on methane halfwidths and pressure shifts has been undertaken by the group at NASA Langley Research Center. Several hundred experimental measurements on air– and nitrogen–broadened widths and shift coefficients in the ν_4 and ν_2 bands of $^{12}CH_4$ and air–broadened widths and shifts in the ν_4 band of $^{13}CH_4$ have been reported by them. The air–broadened halfwidths in the new list have been changed in all spectral regions except 2200 – 3350 cm $^{-1}$ region using the results published by the Langley group. This view graph shows the references to those two articles based on which the revised half widths were incorporated in the new update.

Analysis on similar measurements in the ν_3 band of $^{12}CH_4$ is in progress while the measurements for the ν_3 band has just been completed.

Observed and calculated spectra near the 6089 cm^{-1} region: 1986 versus 1989.

The strongest band in th1s short wavelength region is the $2\nu_3$ band of $^{12}CH_4$. For this band the line intensities in the P, Q, R branches through J=10 were measured and fitted to obtain a band intensity and Herman–Wallis coefficients. The 1986 compilation included a total of 142 lines belonging to $^{12}CH_4$ and 93 lines for $^{13}CH_4$ calculated for the $2\nu_3$ region in the 5897 – 6107 cm^{-1} region. The new list now has over 2000 entries to represent the methane absorption between 5500 and 6185 cm^{-1}. This figure shows observed and calculated spectra overlaid with the residual differences plotted below. In the top panel the 1986 HITRAN list is used while in the bottom panel the new list is used. In both cases the observed spectrum is data recorded at Kitt Peak. It is clear that the new parameters give a much better representation of the existing strong lines and now include many of the weak features as well.

But the problem is that the new lines are generally unassigned. The lower states energies are set to 300 cm^1 except for the 200 $2\nu_3$ lines. The net change for $2\nu_3$ band is that the band intensity has increased by 11% and the P– and R– branch lines are different because of large Herman–Wallis factors (A= 0.03, B= 0.0054)

This view graph shows plots of measured air–broadened Lorentz halfwidths versus m: (a) for all measured transitions in $^{13}CH_4$; (b) A21<– A11 transitions; (c) F21<– F11 transitions; (d) F11<– F21 transitions; (e) E1<– E1 transitions. In (b) – (e), solid lines connect measurements to help distinguish $^{12}CH_4$ from $^{13}CH_4$ data.Plots (b) – (e) contain measurements for both the isotopes. From our analyses in the ν_4 bands of $^{12}CH_4$ and $^{13}CH_4$ we have found that for a given transition, $^{13}CH_4$ widths are about 5% narrower than the corresponding $^{12}CH_4$ widths. From the above plots it is clear that the variation of widths as a function of "m" is not smooth for any symmetry transitions.

This table gives the summary of molecular line parameters for methane. It shows the total # of vibration–rotation bands that could be included at this time. The columns indicate the vibrational quanta of the upper and lower states, status of each band after update, the isotope code,# of lines in each band, beginning and ending wave–number for each band, min. and max.intensity range and the total band intensity for each band.

The status indicator column shows whether the parameters for the band were unaltered (blank), replaced (rep), or added (add) during the revision. Eighteen new bands (including the unassigned) are now in the database. Many of these additional bands fall in regions not previously included in the compilation. Below 2350 cm^{-1} region, a smaller minimum intensity cutoff was applied: $4*10^{-26}cm^{-1}/$ (molecule.cm^{-2}) rather than $1*10^{-26}cm^{-1}/$ (molecule.cm^{-2}). This choice will broaden the usefulness of the methane database. As a result of the lower minimum intensity cutoff value and the addition of new bands, the number of methane parameters has increased from 17774 to about 46000 lines.

This table shows a comparison between the 1986 and the 1989 methane line parameters.It is interesting to note that while the total # of bands has increased from 30 to 48 and the total # lines has increased by almost a factor of 2, the total absorption has only increased by ~2%. It may be noted that the the minimum intensity cutoff value has been lowered by almost two orders of magnitude in the new linelist.

This figure shows the status of methane parameters for the new update of the HITRAN database. This figure gives at a glance the status of line positions, intensities, halfwidths, assignments (lower states) versus available measurements and modeling by quantum mechanics(calc.) by region, from 0 – 6000 cm^{1} . Regions coded by black, white, and gray correspond to parameters changed, not changed and completely missing, respectively. The need for additional studies in the pentad region is obvious. Such studies should prove useful not only in improving the parameters for the pentad levels but also the hot band studies. Experimental results as well as quantum mechanical modeling of pressure–broadened halfwidth measurements are urgently needed.

REFERENCES

L. S. Rothman, R. R. Gamache, A. Goldman, L. R. Brown, R. A. Toth, H. M. Pickett, P. L. Poynter, J. -M. Flaud, C. Camy- Peyret, A. Barbe, N. Husson, C. P. Rinsland, and M. A. H. Smith, " The HITRAN database: 1986 edition," Appl. Opt. 26, 4058 - 4097 (1987) .

C. P. Rinsland, V. Malathy Devi, M. A. H. Smith, and D. C. Benner, "Measurements of air-broadened and nitrogen-broadened Lorentz width coefficients and pressure shift coefficients in the ν_4 and ν_2 band of $^{12}CH_4$," Appl. Opt. 27, 631 - 651 (1988).

J. Ballard and W. B. Johnston, "Self-broadened widths and absolute strengths of $^{12}CH_4$ lines in the 1310 - 1370 cm^{-1} region," J. Quant. Spectrosc. Radiat. Transfer. 36, 365 - 371 (1986).

V. Malathy Devi, C. P. Rinsland, M. A. H. Smith, and D. C. Benner, "Air-broadened Lorentz halfwidths and pressure induced line shifts in the ν_4 band of $^{13}CH_4$," Appl. Opt. 27, 2296 - 2308 (1988).

V. Malathy Devi, C. P. Rinsland, D. C. Benner, M. A. H. Smith, and K. B. Thakur, "Absolute intensities and self-, N_2 and air-broadened Lorentz halfwidths for selected lines in the ν_3 band of $^{12}CH_3D$ from measurements with a tunable diode laser spectrometer," Appl. Opt. 25, 1848 - 1853 (1986).

V. Malathy Devi, D. C. Benner, C. P. Rinsland, M. A. H. Smith, and K. B. Thakur, "Absolute intensities and self–, N_2 and air–broadened Lorentz halfwidths for selected lines in the ν_6 band of $^{12}CH_3D$ from measurements with a tunable diode laser spectrometer," J. Mol. Spectrosc. 122, 182 – 189 (1987).

J. P. Champion, J. C. Hilico, and L. R. Brown, "The vibrational ground state of $^{12}CH_4$ and $^{13}CH_4$," J. Mol. Spectrosc. 133, 244 – 255 (1989).

J. P. Champion, J. C. Hilico, C. Wenger, and L. R. Brown, "Analysis of the ν_2 / ν_4 dyad of $^{12}CH_4$ and $^{13}CH_4$," J. Mol. Spectrosc. 133, 256 – 273 (1989).

L. R. Brown, M. Loete, and J. C. Hilico, "Linestrengths of the ν_2 and ν_4 bands of $^{12}CH_4$ and $^{13}CH_4$," J. Mol. Spectrosc. 133, 273 – 311 (1989).

G. Tarrago, M. Delaveau, L. Fusina, and G. Guelachvili, "Absorption of $^{12}CH_3D$ at 6 – 10 μm: triad ν_3, ν_5, ν_6," J. Mol. Spectrosc. 126, 99 – 158 (1987).

G. Tarrago, G. Restelli, and F. Cappellani, "Absolute absorption intensities in the triad ν_3, ν_5, ν_6 of $^{12}CH_3D$ at 6 – 10μm," J. Mol. Spectrosc. 129, 326 – 332 (1988).

C. Chackerian, Jr. and G. Guelachvili, "Direct retrieval of lineshape parameters: absolute line intensities for the ν_2 band of CH_3D," J. Mol. Spectrosc. 97, 316 (1983).

M. Oldani, A. Bauder, J. C. Hilico, M. Loete, and J. P. Champion, Europhys. Lett. 4, 29 – 33 (1987).

J. C. Hilico, M. Loete, J. P. Champion, J. L. Destomes and M. Bogey, "The millimeter–wave spectrum of methane," J. Mol. Spectrosc. 122, 381 – 389 (1987).

O. Ouardi, "Intensities des bands chaudes du ethane dans la region de 8 microns," thesis, *Universite de Bourgogne*, 1988.

L. R. Brown, "Methane line parameters from 3700 to 4136 cm $^{-1}$" Appl. Opt. 27, 3275 – 3279 (1988).

J. S. Margolis, "Measured line positions and strengths of methane between 5500 and 6180 cm^{-1}," Appl. Opt. 27, 4038 – 4051 (1988).

L. R. Brown, C. B. Farmer, C. P. Rinsland, "Molecular line parameters of the atmospheric trace molecule spectroscopy experiment," Appl. Opt. 26, 5154 – 5182 (1987).

UV ABSORPTION PARAMETERS: O_2 AND O_3

L. A. Hall
GL/LIU
Hanscom AFB, MA 01731-5000

Gail P. Anderson
GL/OPE
Hanscom AFB, MA 01731-5000

June 1989

UV Absorption Parameters: O2 and O3

ABSTRACT:

Spectroscopic data describing the ultraviolet absorption properties of molecular oxygen and ozone has been collected for incorporation into FASCODE and LOWTRAN. The data include the O2 Herzberg continuum and Schumann-Runge bands and the O3 Hartley and Huggins bands. All of these systems result in the dissociation of the parent molecule and the creation of atomic oxygen. The non-dissociative Herzberg bands are not currently part of the data set although they may be important for accurate transmittance calculations near the surface.

INTRODUCTION:

The dissociation of oxygen allotropes is of paramount importance to the chemical makeup of the earth's atmosphere. The strongly absorbing Schumann-Runge and weaker Herzberg systems influence different altitude regimes in the atmosphere because of the relative strengths of their respective transition probabilities (permitted and forbidden, respectively, Fig. 1); Fig. 2 (after Watanabe, 1958) shows the approximate depth of penetration of solar irradiance throughout the UV spectral range. In general, solar radiation in the 0.175 to 0.2μ spectral region is completely absorbed by the Schumann-Runge [S/R] system at altitudes above 40 km. Towards longer wavelengths (greater than 0.2μ) absorption by ozone begins to compete with the residual [S/R] and Herzberg absorption; the combination allows no solar energy at wavelengths less than 0.3μ to penetrate to the surface. In addition to this shielding of high energy solar radiation, ozone dissociation between 0.2 and 0.3μ provides the dominant source of stratospheric heating.

HERZBERG CONTINUUM:

While the Herzberg continuum absorption is small relative to both the [S/R] and ozone contributions, it is very important to the maintainance of stratospheric photochemical balance. Until recently the Herzberg continuum was thought to be almost 40% more effective than the current estimate. Because it lacks any detailed spectral structure, the

absorption properties are readily described by an analytic function proposed by Johnston et.al. (1984). Fitting the combined measurements of Harvard-Smithsonian and the French UER Molecular and Atmospheric Spectrometry Lab (Yoshino et.al. 1988) yields:

$$\sigma(o,\mu) =$$

$$6.88e\text{-}24 \quad R \quad \exp\left[-69.7374 \{ \ln (R) \}^2 \right]$$

where: $R = 0.20487/(\mu)$
μ = wavelength in μ

This equation reproduces both data sets to within 5%.

The longevity of the erroneously large Herzberg values can be traced to their pressure dependence, related to dimer formation. The cross sections are so small that older laboratory determinations relied on high pressure techniques to create the necessary opacities. In all cases, extrapolation to zero pressure was attempted, but with poor success. In fact, long-path, low pressure stratospheric measurements of attenuation of solar irradiance provided the first verification that the lab results were seriously wrong (Frederick and Mentall, 1981, Anderson & Hall, 1981, etc.)

Accurate determination of the pressure dependence of O2 within an O2 environment is part of the laboratory procedure when measuring the cross section since elevated pressure and extrapolation are still necessary (Yoshino, et.al. 1988). A marked similarity in spectral shape of the pressure dependence to the cross section itself (Fig. 3) has been employed to simplify the calculation within FASCODE and LOWTRAN. Where Yoshino et.al. provide an equation of the form:

$$\sigma(p,\mu) = \sigma(o,\mu) + (\alpha(\mu) \times P(\text{Torr}))$$

and a table of $\alpha(\mu)$, the FASCODE/LOWTRAN formulations replace the spectrally dependent α with a proportionality constant ($\alpha(\mu)/\sigma(\mu) = 1.72e\text{-}3$) that is good to within 2% for most of the Herzberg spectral range (between 0.20 and 0.23μ). Errors between 0.23 and 0.24μ gradually increase to 30%. The magnitude of this error is generally tolerable because the pressure contribution is still a fractionally small portion of the cross section which is diminishing while the ozone cross section is increasing dramatically. The adopted formalism for pressure broadening in an O2 environment is then:

$$\sigma(p,\mu) = \sigma(o,\mu) \ (1.+ \ 1.72e\text{-}3 \times P(\text{Torr})).$$

However, atmospheric pressure dependence is also governed by interaction with N2 (O2-N2 dimer formation). Shardanand (1977) has provided an estimate of this effect, N2 being approximately 45% as efficient as pure O2 (Fig. 3). The pressure dependence of the Herzberg continuum for a combination of 21% O2 and 78% N2, including the 45% efficiency factor is:

$$1.72e\text{-}3\ (\ .21 \times P(Torr) + .45 \times .78 \times P(Torr))$$

$$= 9.65e\text{-}4 \times P(Torr) = .73 \times P(atm)$$

Both transmittance codes employ a normalized density algorithm rather than pressure, so the final Herzberg cross section is given as:

$$\sigma(p,\mu) = \sigma(o,\mu)\ (1.+ .73\ (P/P_o)(T_o/T))$$

and P_o and T_o are at STP. .

As mentioned above, the Herzberg bands are not included explicitly in FASCODE and LOWTRAN. While they would not contribute to the photochemical production of odd oxygen, some contribution is expected in the total transmittance calculations. This has been approximated in LOWTRAN7 and *FASCOD3 by extending the Herzberg analytic equation to longer* wavelengths (0.277μ or 36000cm-1) with a linearly smooth damping to zero absorption at that arbitrary cutoff. The errors introduced by this approximation are admittedly serious but relatively small. Eventually a more correct band model approximation will be developed within the context of LOWTRAN. Line-by-line corrections for FASCODE must await preparation of an appropriate line file; (see the [S/R] description below).

SCHUMANN-RUNGE BANDS:

The O2 Schumann-Runge band analysis has been addressed in two ways: (1) a line-by-line spectroscopic atlas, similar in format to the HITRAN database, has been calculated from published energy levels; and (2) a one parameter (P-dependent) 20cm-1 resolution band model has been generated for incorporation into LOWTRAN. Both studies are considered preliminary, although the line atlas, when coupled with an "exact" line shape (Lorentz) algorithm will produce cross sections comparable to those of Nicolet (1987).

The line-by-line synthesis of the [S/R] cross section, including temperature dependence of the vibronic population levels, has been accomplished with both a special version of FASCODE and a standard fixed-frequency Lorentz fitting function. Standard FASCODE could not be used in the calculations because the predissociation (natural) half widths of the [S/R] lines are too large. FASCODE, of course, was designed for vibrational energy levels where the half widths are of order 0.08cm-1 and the line shape algorithm only calculates individual line shapes to ±25cm-1 (VBOUND) about line center. The Schumann-Runge half widths vary between 0.1 and 1.8cm-1 (Table 1), so that the existing VBOUND limit can be almost a factor of 10 too small. For the special [S/R] version of FASCODE, VBOUND has been reset to 250cm-1 and the pressure-dependent terms in the Lorentz calculation have been eliminated. Figure 4 compares cross sections calculated by FASCODx and the fixed frequency Lorentz synthesis for two different temperatures.

The line parameters required for these calculations (as in Table 2 and described below) have been generated by Hall (private communication). The ground state energy levels (v"= 0,1,2) are from Blake et al. (1984) with additional triplet splitting constants from Babcock and Herzberg (1948). The corresponding upper state (v'= 0-19) data are from Nicolet et.al. (1987). The rotational line width assignments, also from Nicolet et.al., are currently being reassessed by Harvard Smithsonian (Freeman, private communication).

The equations describing the rotational energy levels of the triplet sigma ($^3\Sigma$) state are from Herzberg (1950). The P and R line positions are then simply the differences between upper and lower energy levels for each allowed transition. The selection rules for the triplet transitions are:

$$\text{with:} \quad \Delta(K) = \pm 1, \quad \Delta(J) = \pm 1$$

where: K = rotational quantum number
J = total angular momentum quantum number.

and: J = K+1, K, or K-1.

Note that for R lines, J'= J"+1 with the triplet components, R(1,K), R(2,K), and R(3,K), having:

J"= K+1, J" = K, and J" = K-1, respectively.

For P lines the same is true except that J'= J"-1.

The variation of the intensity of absorption lines in a vibronic band as a function of J is given essentially by the thermal distribution of the rotational levels. The individual relative intensities are calculated from Herzberg (1950) as a product of the frequency, a total angular momentum term, and an expontial term proportional to the population of the lower (initial) state:

$$I = \nu\ (J'+J"+1)\ \exp(-B"\ J"\ (J"+1)\ hc/kT)$$

These intensities can be calculated separately for the P and R branches using the above selection rules, such that:

$$I_R\ (N,K) = 2\nu\ (K+3-N)\ \exp(-B"(K+2-N)(K+3-N)hc/kT)$$

and

$$I_P\ (N,K) = 2\nu\ (K+2-N)\ \exp(-B"(K+2-N)(K+3-N)hc/kT)$$

where: B"= rotational constant
and: N = 1,2,3 for the triplet components.

The total intensity for a particular band is defined as the integrated cross section over its full spectral range, this quantity being equal to the product of a front factor, the band absorption oscillator strength and the fractional population of the lower vibrational states (Ackerman et.al., 1970). The oscillator strengths (f(v',v") are taken from Nicolet et.al. while the lower state population is simply the Boltzman term for the initial state energy level. Inherent in this calculation is the assumption of a Lorentz line shape profile. [Again, the use of a Lorentz line shape in this case is not just easier than using a Voigt; it is actually justified, since the lines are so strongly predissociated that the Doppler broadening is negligible in comparison to the natural width.]

Table 2, then, is a portion of the output from the above sequence of calculations, providing a frequency sorted database of line positions, strengths, half widths, ground state energies, and spectroscopic identifications in the typical HITRAN-type format. All calculations were done for 296K temperature suitable for quasi-direct input into FASCODE. Figure 5 shows a portion or the available database, giving line positions and relative strengths at line center. The individual band groupings are easily identified.

The 20cm-1 band model for the Schumann-Runge system (as currently available in LOWTRAN7) was developed from a similar line-by-line formulation developed by Frederick and

Hudson (1979) with additional laboratory input from Yoshino et.al. (1987). It is both preliminary and inadequate for detailed spectroscopic calculations because it does not properly handle the strong temperature dependence of the O2 cross sections brought about by the change in population of the v"=1 state. This effect is strongest in the spectral regions away from the v"=0 band heads (i.e. in the window regions); see Figure 4. Solar energy penetrates deepest into the atmosphere in just these window regions so improvement in the model formulation is mandatory if it is to be used for photochemical calculations.

Given these stated inaccuracies, the band model does show reasonable agreement with in situ measurements of the depleted solar irradiance (Figure 6). The band model algorithm is patterned on that developed for the IR by Pierluissi and Maragoudakis (1986), including the use of their fitting parameters for O2. The form of the double exponential is outlined in Figure 7. A single spectral function [C(μ)] has been calculated for the wavelength range from 0.1875 to 0.203μ. When a more sensitive band model is developed, the wavelength range will be extended to include the entire [S/R] system. It is expected that this new band model will separate the v"=0 from the v"=1 bands, with the ground state transitions fit as described here. The temperature-dependent v"=1 transitions will require a more sensitive treatment. [NOTE: while the band model parameters are available within the LOWTRAN7 coding, they are not directly accessible for wavelengths smaller than 0.2μ. This limitation is imposed by an "if-test" related only to the nonavailablility of the aerosol functions for these wavelengths.]

As a final comment on the Schumann-Runge bands, band model parameters and/or some equivalent description are not intuitively compatible with a line-by-line algorithm. Therefore, there is no plan to incorporate the [S/R] bands into FASCODE. Rather, a version of FASCODE suitable for generic electronic transitions must be developed for general distribution. There is some possibility, however, of designing a two-part (v"=0 and 1) cross section capability, similar to that being developed to handle the cross sections of heavy molecules (CF-11, CF-12, etc.).

OZONE:

Absorption by ozone, the remaining UV-active oxygen allotrope, is described in both FASCODE and LOWTRAN by a temperature-dependent (quadratic) continuum. The overlapping Hartley and Huggins systems are spectrally continuous although they lead to either the ground or first excited state for atomic oxygen, $O(^1D)$ and $O(^3P)$, respectively:

$$O_3 + h\nu \text{ ----> } O_2(^3\Sigma) + O(^3P) \quad : \text{Huggins } \lambda > 0.31\mu$$

and $$O_3 + h\nu \text{ ----> } O_2(^1\Delta) + O(^1D) \quad : \text{Hartley } \lambda < 0.31\mu$$

Photochemically sufficient excitation energy for $O(^1D)$ formation occurs near 0.31μ, although that division is not exact. The difference in atomic oxygen excitation state is, however, critical to subsequent photochemical reactions because $O(^1D)$ is the preferred reactant. The Hartley band is very strong, exhibiting only marginal structure and generally no temperature dependence. The Huggins system has a much more pronounced band structure and moderate to strong T-dependence, although the features are still broad enough (because of predissociation) to not be amenable to detailed line-by-line identification or representation (Figure 8).

Studies of the ozone absorption cross section have been available since the early 1900's. The relatively recent measurements of Bass and Paur (1985) form the basis of LOWTRAN7-FASCOD3 formulation. Their values, including quadratic temperature dependence, are provided at 5cm-1 intervals from 41000 to 30000cm-1 (0.24 to 0.33μ). Figure 9 shows the form of the equation. Subsequent measurements of Molina and Molina (1986) have been used in combination with those of Yoshino et.al. (1988) to expand the temperature dependent range to 0.34μ, with a final extension to 0.36μ using the values of Cacciani, et.al. (1987). At the short wavelength range, the temperature-independent values of Molina and Molina were again adopted between 0.18 and 0.24μ. The various data sources agree very well (usually better than 3%) in the regions of overlap. All feature replication is real and suitable; that is, the small spectral features are represented at their natural resolution and a line-by-line representation would not provide greater spectral detail.

SUMMARY:

As an adjunct to the preparation of LOWTRAN7 and FASCOD3, a set of UV spectroscopic data has been compiled. The new data set includes an analytic function which describes the O2 Herzberg continuum absorption (0.19-0.244μ) with an extension of that function to approximate the Herzberg bands. The functional dependence provides an atmospheric (O2 and N2) pressure dependent term. The total estimated accuracy over the Herzberg continuum is 5-10%. A separate line atlas has been calculated for the O2 Schumann-Runge bands. Using these

spectroscopic parameters, [S/R] absorption cross sections have been derived using a special version of FASCODE (FASCODx). Again, the results agree with both theory and experiment to within approximately 10%. A 20cm-1 band model developed for portions of the [S/R] system has been incorporated into LOWTRAN7. It is adequate (10-20%) for frequency ranges dominated by transitions to the ground level (v"=0) but cannot replicate the behavior of the weaker T-dependent v"=1 transitions. Finally, the Hartley-Huggins O3 absorption cross section has been collated from 4 different sets of measurements. The resultant continuum formulation incorporates a quadratic T-dependence for the wavelength range from 0.19-0.36μ with an expected accuracy of 3-5% for the Hartley system and 3-10% for the Huggins.

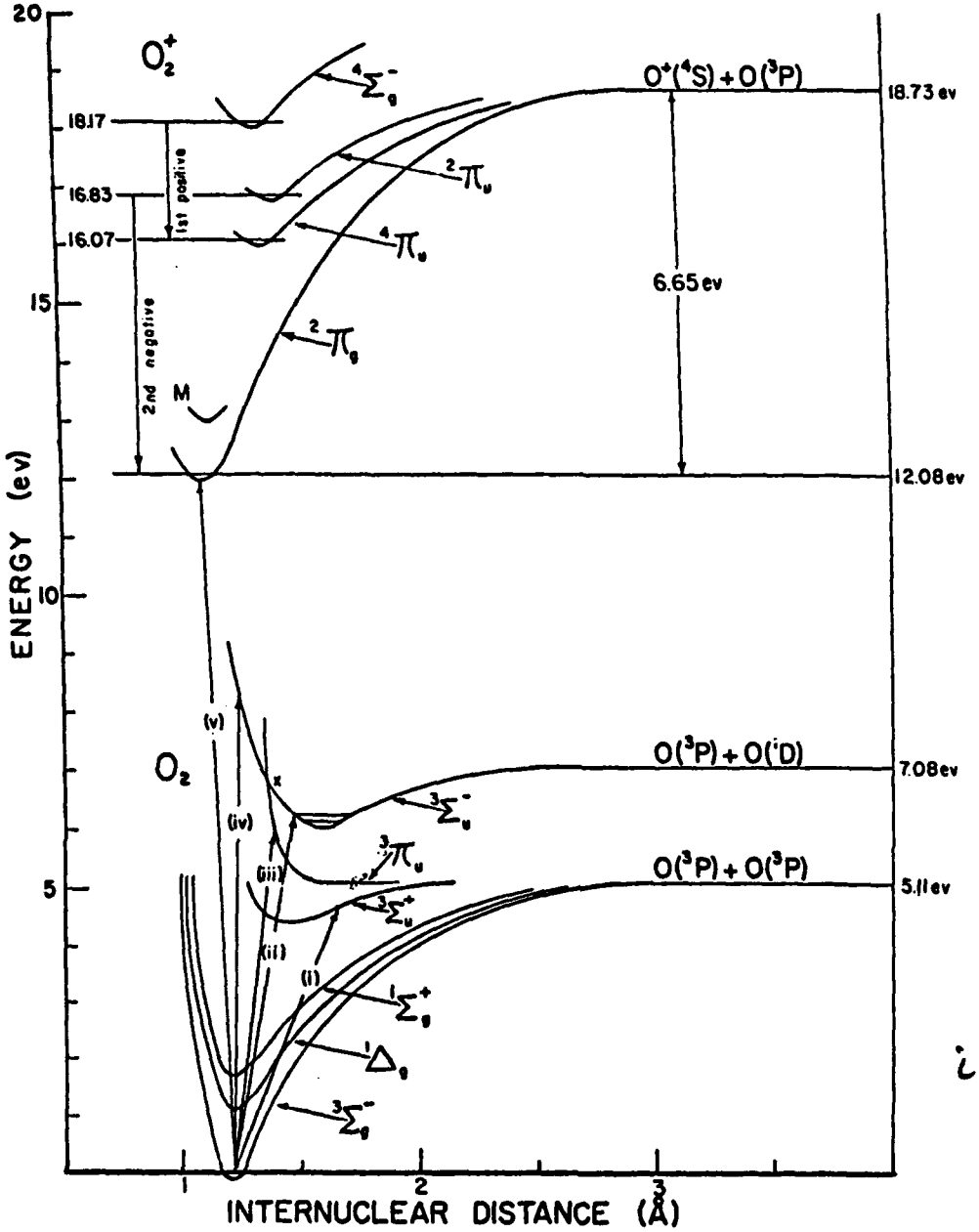

FIG. 1. Potential curves of the observed states of O_2 and O_2^+.

transitions to discrete excited electronic states, and in absorption spectra such transitions appear as discrete bands. Transition (*i*) gives the Herzberg bands, and transition (*ii*) gives the Schumann–Runge bands. Molecules in excited states usually return by emission of light to the ground state in a very short time of the order of 10^{-8} sec, but some excited states have much longer life. In any case, photochemical reaction may result if a molecule in an excited state collides with another molecule.

i = Herz
ii = [S/R]

Fig 1

Figure 24 shows the altitude at which the intensity of solar radiation at vertical incidence is reduced by a factor of e. The reference atmosphere given in Table VII was used for computing optical densities.

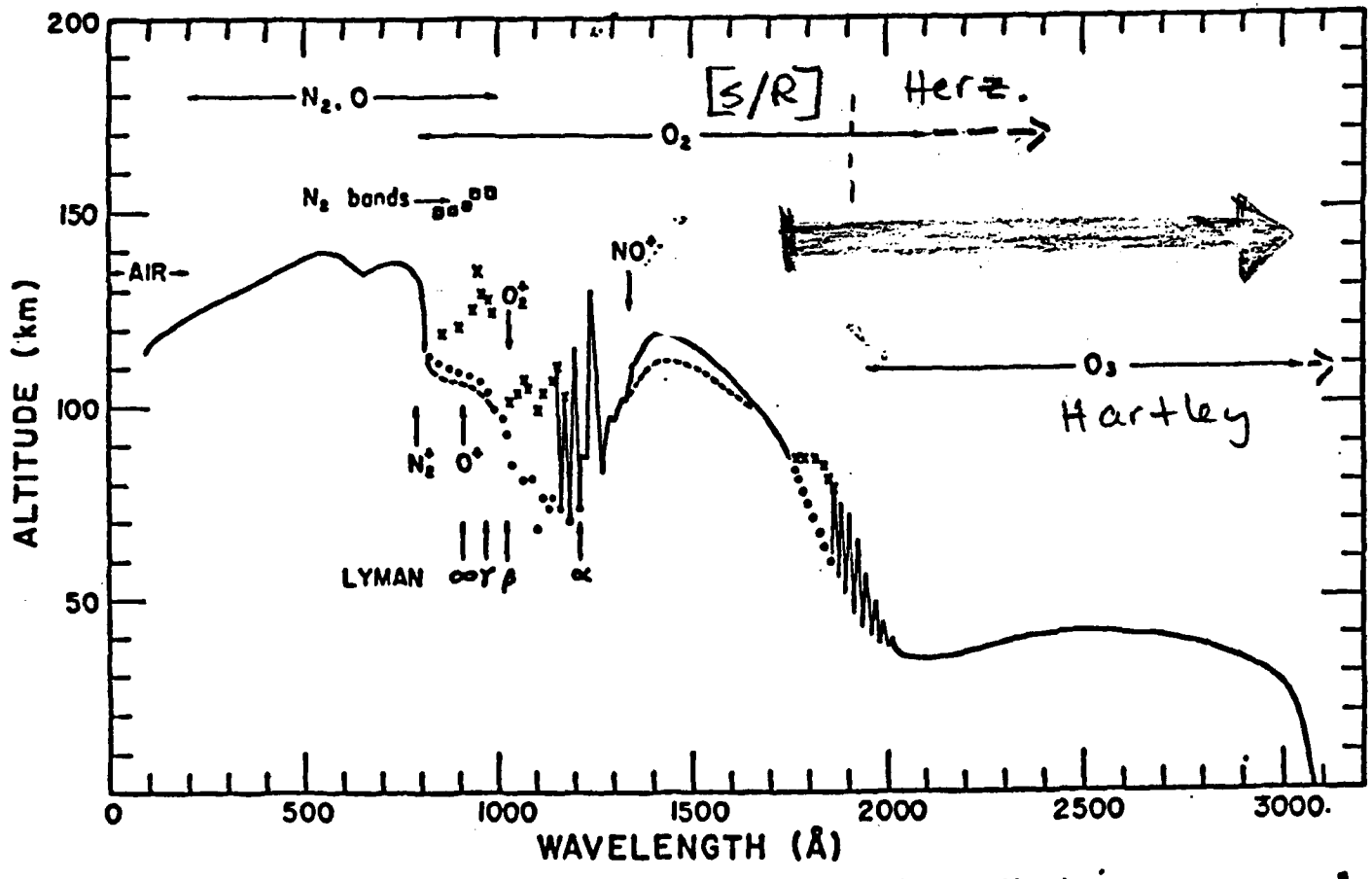

FIG. 24. Penetration of solar ultraviolet radiation.

Fig. 2

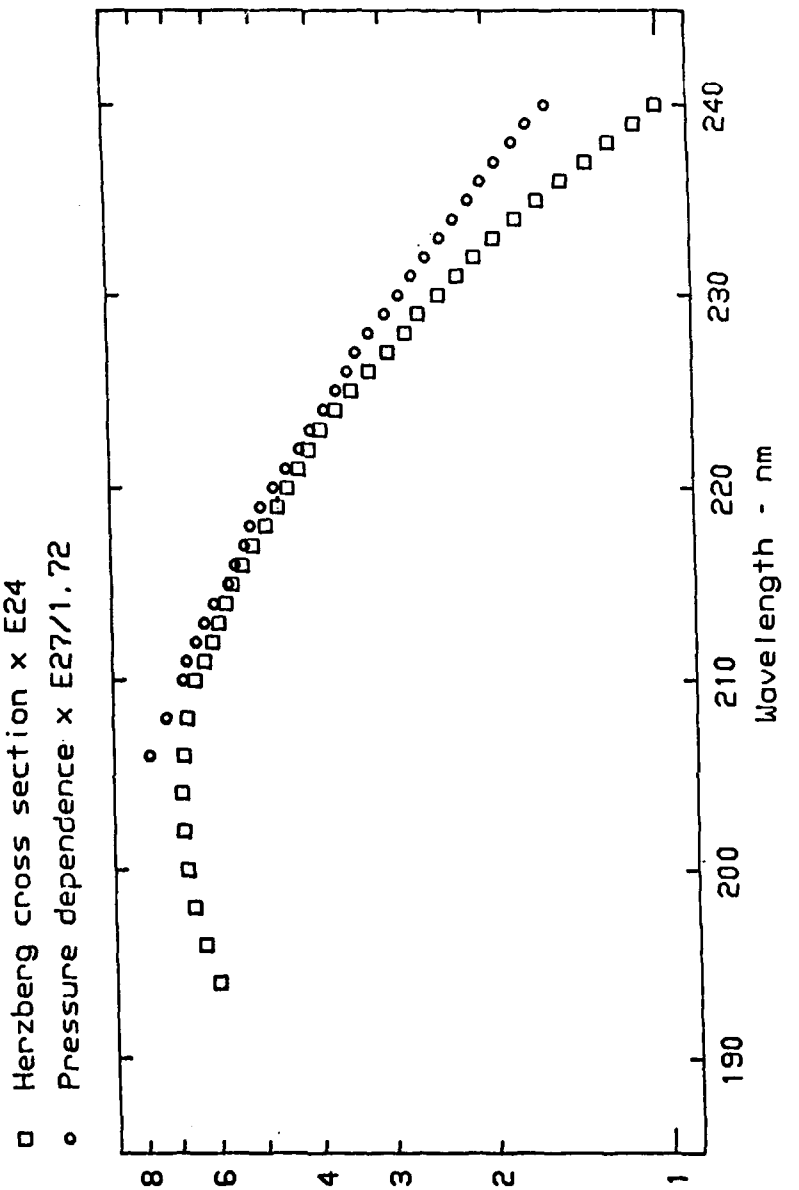
□ Herzberg cross section x E24
○ Pressure dependence x E27/1.72
8
6
4
3
2
1
190
200
210
220
230
240
Wavelength - nm

Fig 3

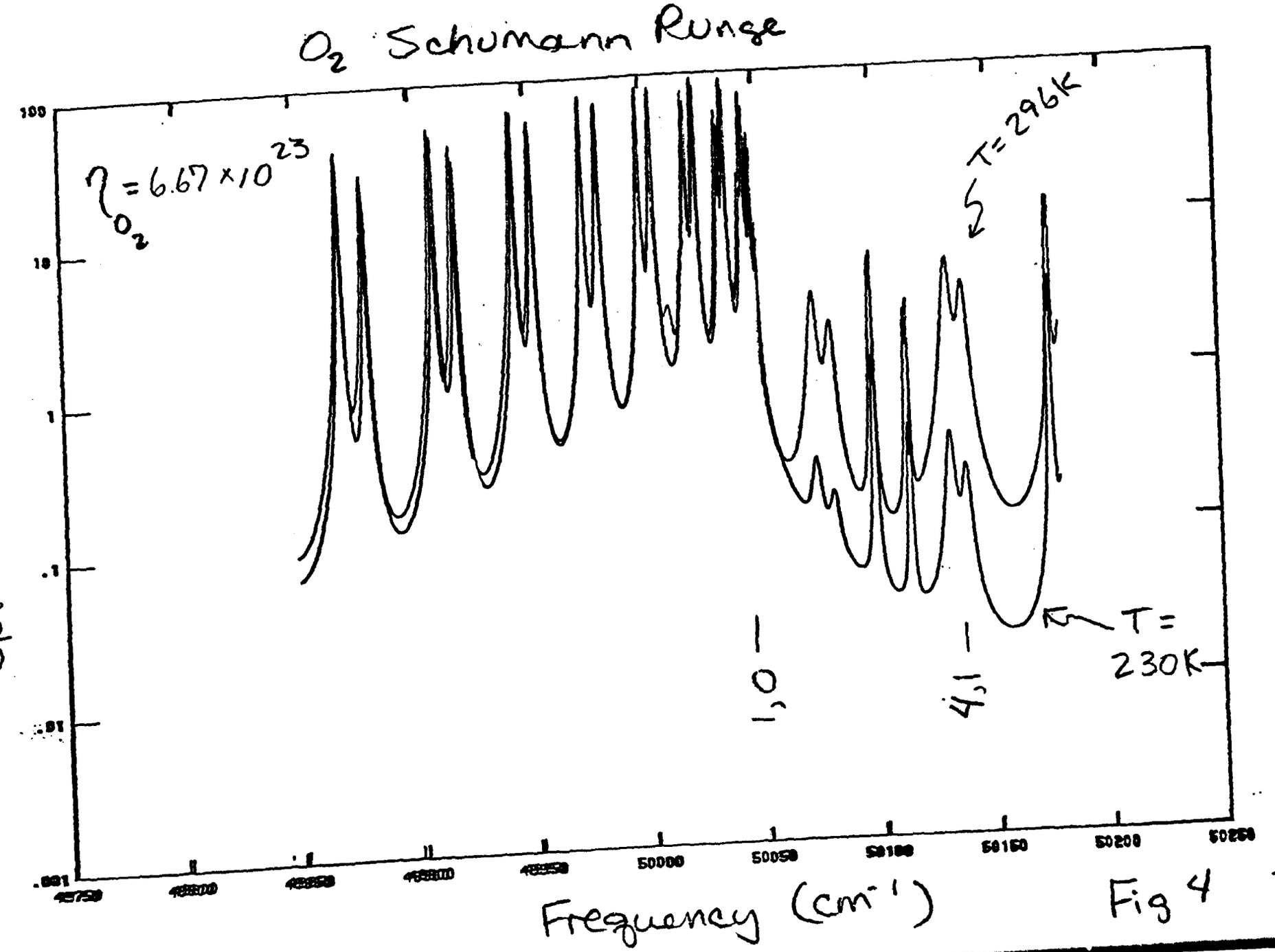
O_2 Schumann Runge
$\eta_{O_2} = 6.67 \times 10^{23}$
T=296K
T=230K
1,0
4,1
Optical Depth
139
100
10
1
.1
.01
.001
50000
50050
50100
50150
50200
50250
Frequency (cm⁻¹)

Fig 4

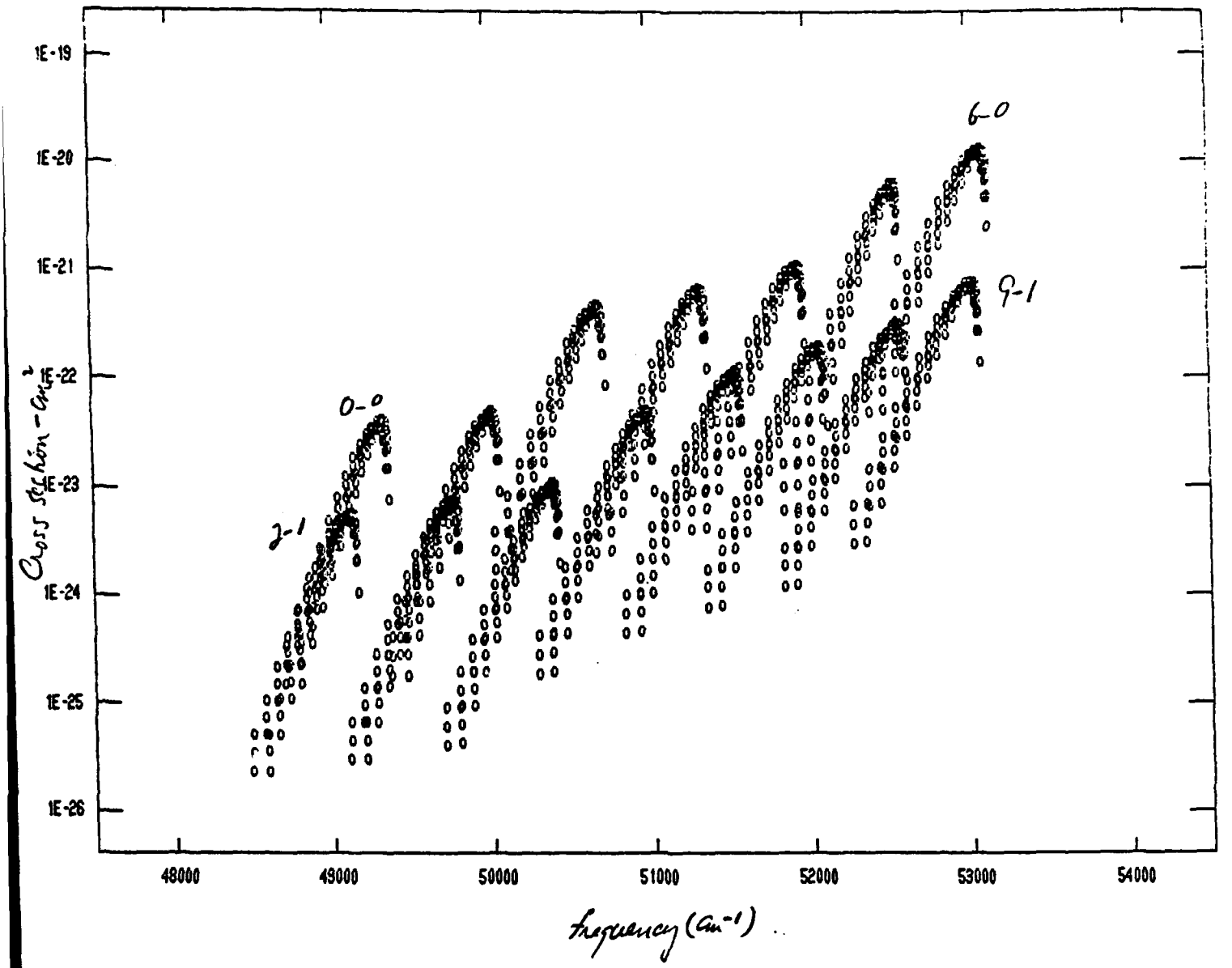
1E-19
1E-20
1E-21
1E-22
1E-23
1E-24
1E-25
1E-26
Cross section - cm²
48000
49000
50000
51000
52000
53000
54000
frequency (cm⁻¹)
0-0
2-1
6-0
9-1

Fig 5

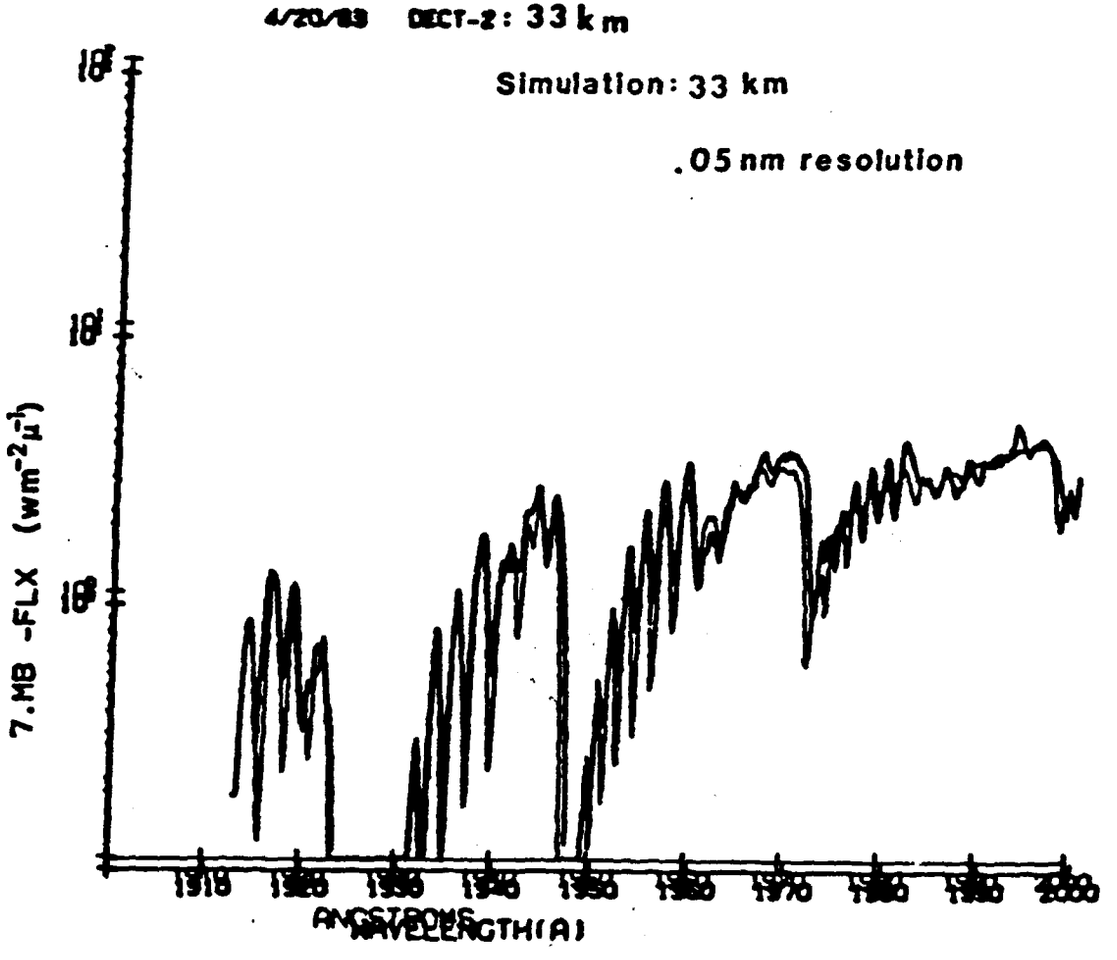
4/20/88 DECT-2: 33 km
Simulation: 33 km
.05 nm resolution
7.MB -FLX (wm⁻²μ⁻¹)
ANGSTROMS
WAVELENGTH(A)

Fig 6

O_2 Attenuation:

Schumann-Runge Bands

LOWTRAN6: *NONE*

FASCOD2: *NONE*

LOWTRAN7: Schumann-Runge Bands

1 Set of line-by-line Calculations (Frederick & Hudson, 1979)
(3 Temperatures, Based on Old Data, and Omits 1-0 Band)

1 Set of Cross Section Measurements (Yoshino et. al., 1987)
(300K and 79K, Fine Resolution, and includes 1-0 Band))

[NOTE: M. Nicolet is redoing line-by-line with Yoshino data]

Chose to: Adopt LOWTRAN "IR" Band Model Approach

$$T = \exp\{ -(C*W)^a \}$$

Where: C = Spectrally Dependent "Weighted" Cross Section
(derived from above data)

W = "Weighted Density" Parameter

$= (P/P_o)^n * (T_o/T)^m * .209$

a = Fitting Parameter

['n','m', and initial 'a' adopted from Pierluissi, 1987]

Errors: 10-30% in Band Model Parameterization
10-30% in F&H Cross Sections

Assumptions:

Appropriateness of IR Band Model Parameters

Appropriateness of Frederick & Hudson

Fig 7

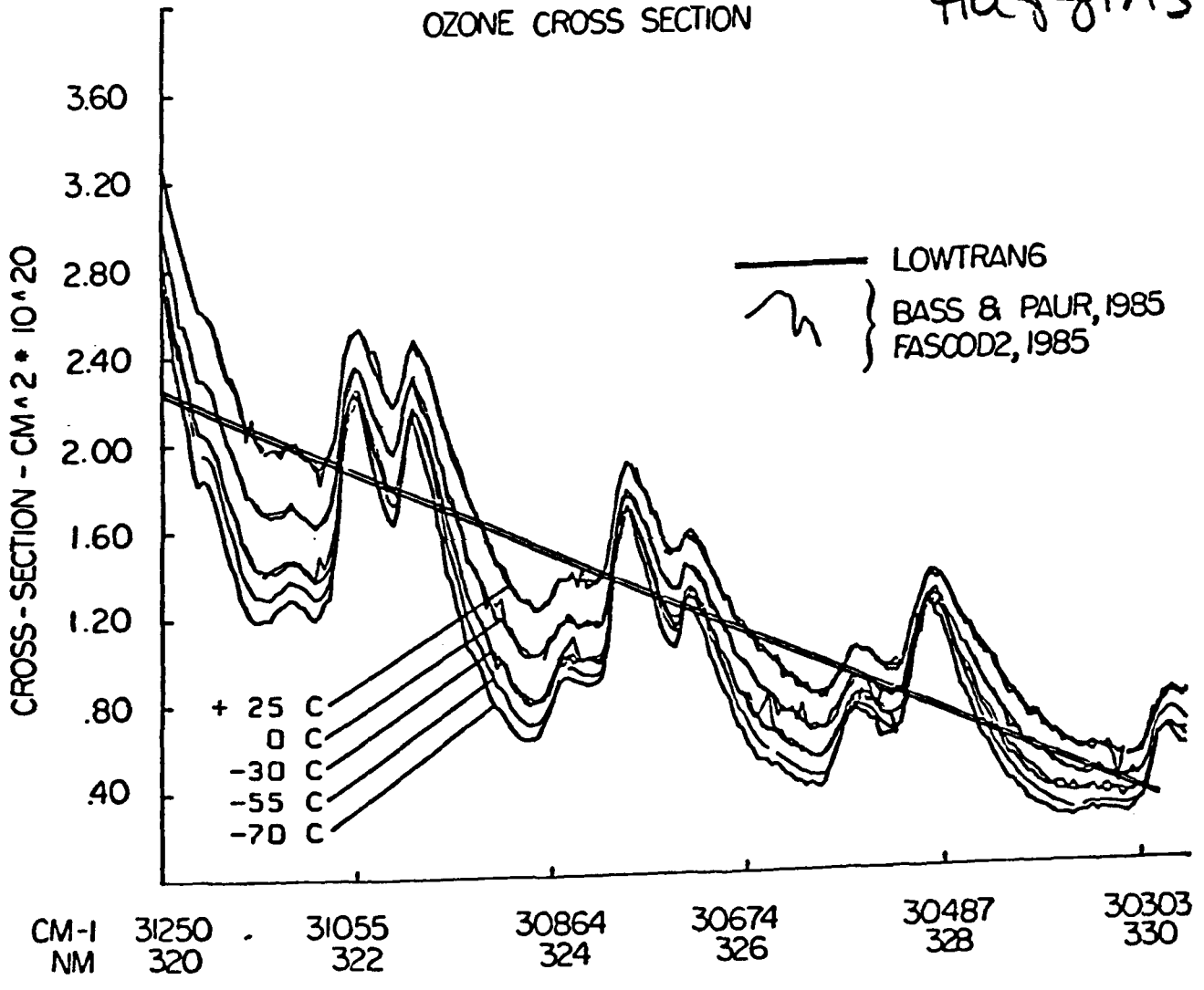
OZONE CROSS SECTION
Huggins
CROSS-SECTION - CM^2 * 10^20
3.60
3.20
2.80
2.40
2.00
1.60
1.20
.80
.40
LOWTRAN6
BASS & PAUR, 1985
FASCOD2, 1985
+ 25 C
0 C
-30 C
-55 C
-70 C
CM-1 31250 31055 30864 30674 30487 30303
NM 320 322 324 326 328 330

Fig 8

Ozone Attenuation:

Hartley-Huggins Bands

LOWTRAN6: Inn & Tanaka, '53

~ 500cm^{-1} Resolution

2000-3500A

FASCOD2: Bass & Paur, '85 ✓

20cm^{-1} Resolution

Temperature Dependence (30% at 3200A, 1%at 2550A)

$$(C = C_0 + C_1 * T + C_2 * T^2)$$

Range: 2440-3400A

LOWTRAN7: 3 Data Sets Available

Including: Bass & Paur
Molina & Molina '86 (1900-3500A) ✓
Yoshino & Freeman '85-'87 (2400-3400A)
Cacciani et al '87 (3400-3600Å)

Chose: REnormalized Bass & Paur plus Molina2 near 200(

Errors: 3- 5% relative
3- 5% absolute

Fig 9

O_2 Schumann-Runge (UV)

PARTIAL LISTING: O2 SCHUMANN-RUNGE BAND PARAMETERS
HALL & ANDERSON, 1988
AFTER NICOLET, ET AL, 1988 AND CHEUNG ET AL., 1987

ν	S	α	E''	V'	V''		±D
							K J
49980.97	.638943E-22	.450	158.145	1	0	BX	RR1110
49998.60	.593211E-22	.450	80.510	1	0	BX	PP 7 7
49998.73	.606238E-22	.450	103.513	1	0	BX	PP 7 8
49999.04	.560733E-22	.450	60.383	1	0	BX	PP 7 6
50004.05	.668297E-22	.450	129.391	1	0	BX	RR 9 9
50004.10	.639239E-22	.450	158.145	1	0	BX	RR 910
50004.57	.682097E-22	.450	103.513	1	0	BX	RR 9 8
50009.87	.403662E-231	.800	2409.388	4	1	BX	PP2324
50010.20	.539046E-231	.800	2341.133	4	1	BX	PP2323
50010.87	.708616E-231	.800	2275.722	4	1	BX	PP2322
50014.96	.156435E-23	.300	1518.190	2	0	BX	PP3132
50015.30	.237020E-23	.300	1426.179	2	0	BX	PP3131
50016.22	.353771E-23	.300	1337.042	2	0	BX	PP3130
50017.55	.224414E-231	.800	2554.430	4	1	BX	RR2526
50017.98	.309570E-231	.800	2480.487	4	1	BX	RR2525
50018.39	.508350E-22	.450	43.130	1	0	BX	PP 5 5
50018.53	.560952E-22	.450	60.383	1	0	BX	PP 5 6
50018.75	.420556E-231	.800	2409.388	4	1	BX	RR2524
50018.82	.436120E-22	.450	28.754	1	0	BX	PP 5 4

where J= K
K±1

Table 2

NLTE EMISSION FROM HIGH VIBRATIONAL LEVELS OF OZONE

Steven Adler-Golden
Spectral Sciences, Inc.
99 South Bedford Street.
Burlington, MA 01803

Donald R. Smith
GL/OPB
Hanscom AFB, MA 01731-5000

SPECTRAL SCIENCES INCORPORATED

NLTE PROBLEM

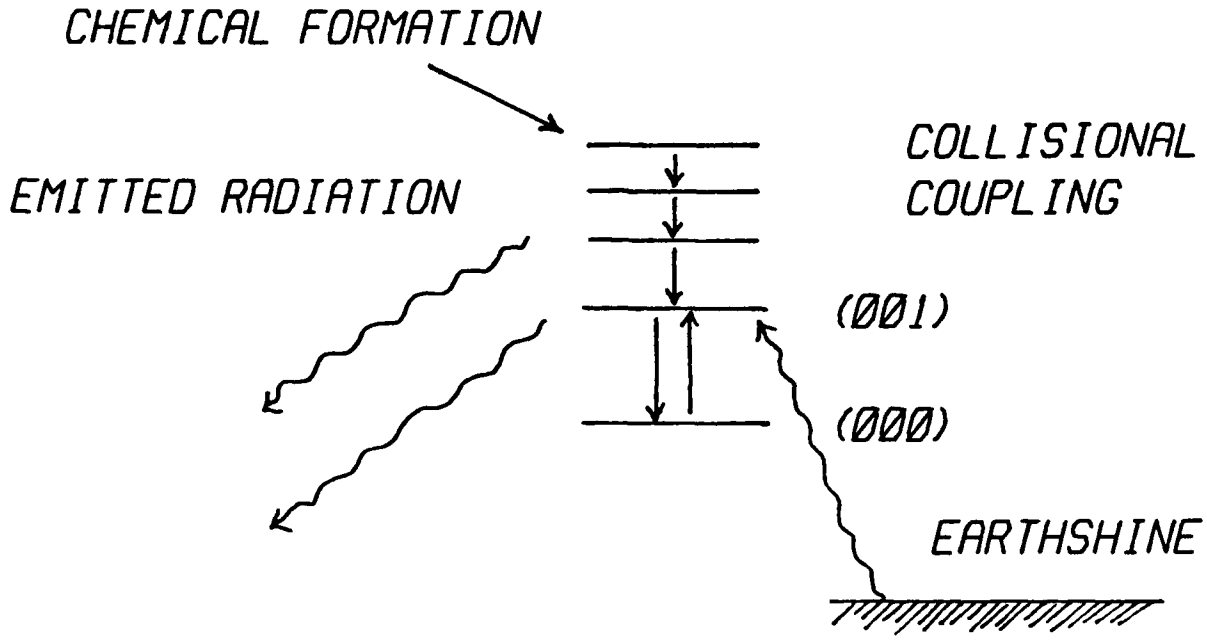

SPECTRAL SCIENCES INCORPORATED

EXAMPLES OF NLTE EMISSION

OZONE ν_3

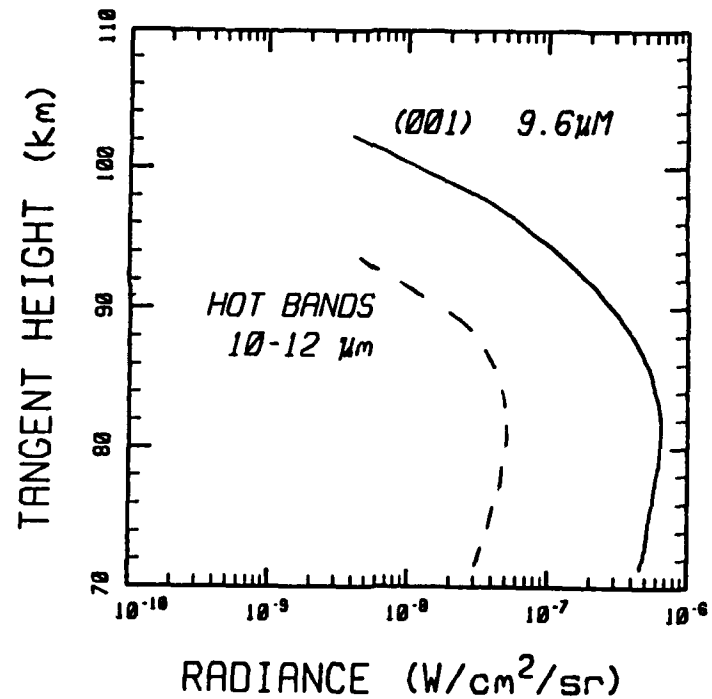

OTHER EXAMPLES: CO_2 (V); NO, OH (HIGH V AND J)

SPECTRAL SCIENCES INCORPORATED

OZONE ν_3 HOT BAND SPECTRUM FROM SPIRIT 1 ROCKET EXPERIMENT

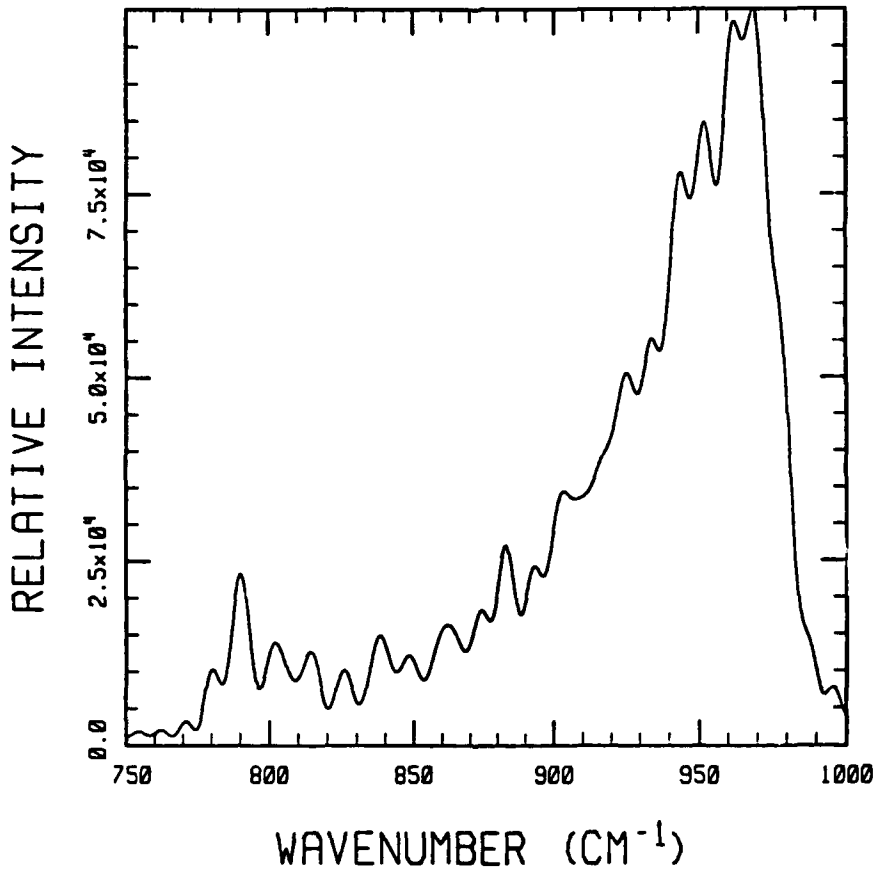

4/8/86 Nighttime

~80 km limb 63° N

4 cm^{-1} Resolution
Unapodized

Bandpass Filter 1
Uncalibrated

- NEED TO UNDERSTAND SPECTRUM TO MODEL WINDOW RADIANCE

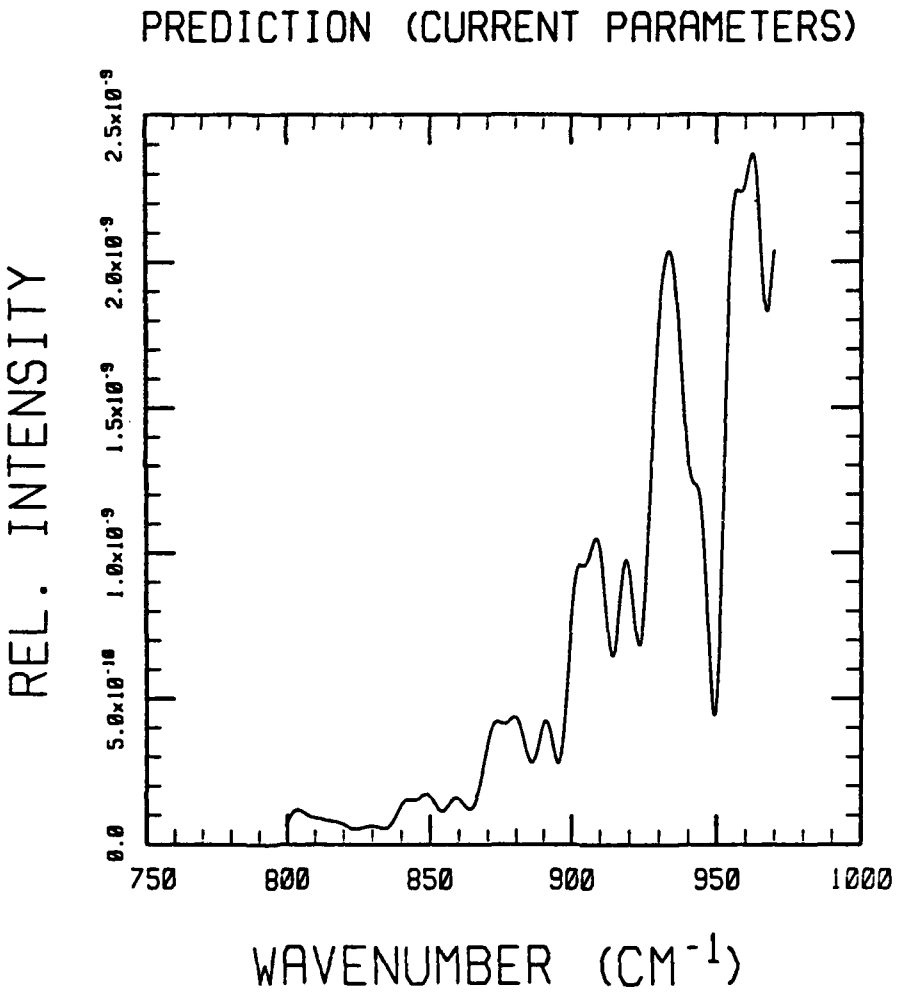
PREDICTION (CURRENT PARAMETERS)
REL. INTENSITY
0.0
5.0x10⁻¹⁰
1.0x10⁻⁹
1.5x10⁻⁹
2.0x10⁻⁹
2.5x10⁻⁹
750
800
850
900
950
1000
WAVENUMBER (CM⁻¹)

SPECTRAL SCIENCES INCORPORATED

METHODS OF ANALYSIS

HIGH RESOLUTION

- DETAILED V-R LINE ANALYSIS: DETERMINE SPECTROSCOPIC CONSTANTS FOR SUCCESSIVELY HIGHER V. CURRENT LIMIT: $V_1+V_3=2$
- ULTIMATE GOAL: HIGH V LINES FOR HITRAN

LOW RESOLUTION

- DERIVE APPROXIMATE BAND CENTERS AND CONTOURS
- COMMENSURATE WITH CURRENT REQUIREMENTS AND DATA

SPECTRAL SCIENCES INCORPORATED

SPIRIT I DATA ANALYSIS

METHOD

- DARLING-DENNISON-TYPE VIBRATIONAL ENERGY FORMULA
- BAND CONTOURS FROM SYMMETRIC TOP V-R LINES COMPARE WELL WITH "FULL" CALCULATIONS

RESULTS

- BANDS IDENTIFIED WITH UP TO 7 VIBRATIONAL QUANTA
- BAND CENTERS ACCURATE TO ~2 CM^{-1}

SPECTRAL SCIENCES INCORPORATED

OZONE HOT BAND ASSIGNMENTS

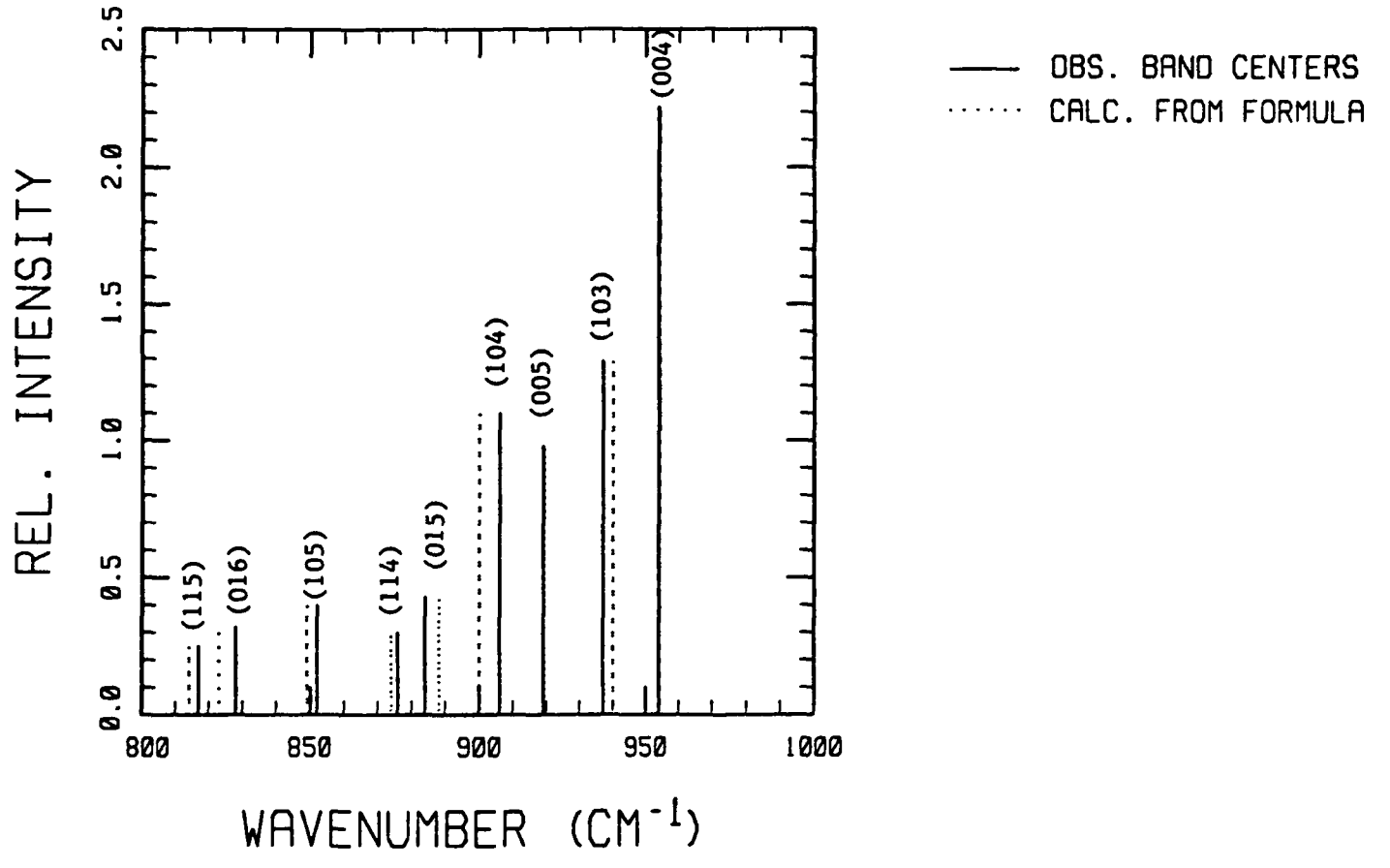

RELATIVE INTENSITY
0.0
2.5x10⁴
5.0x10⁴
7.5x10⁴
1.0x10⁵
800
850
900
950
1000
WAVENUMBER (CM⁻¹)

SPECTRAL SCIENCES INCORPORATED

SYNTHETIC OZONE SPECTRUM

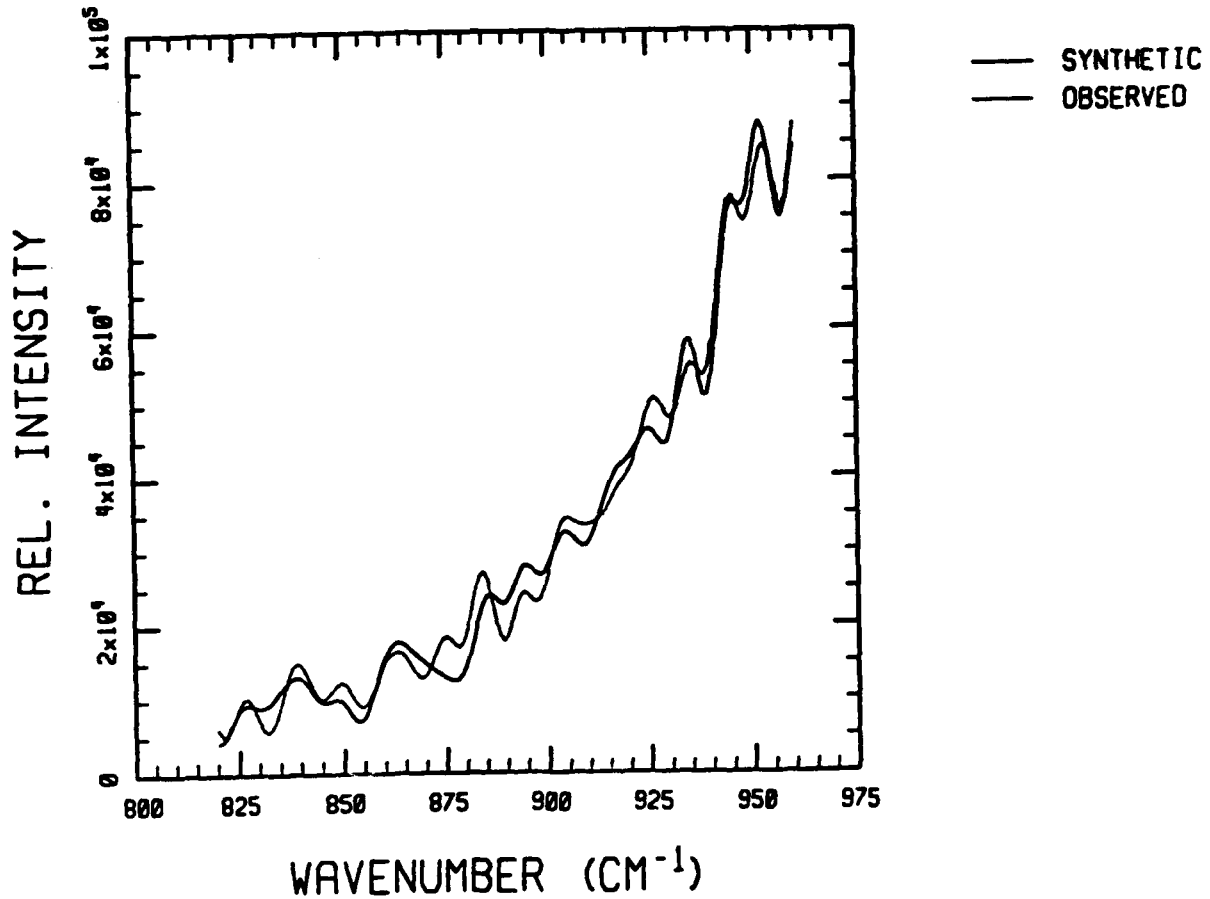

SPECTRAL SCIENCES INCORPORATED

SUMMARY

CONCLUSION

- LINES WITH HIGH V AND/OR J ARE REQUIRED FOR UPPER ATMOSPHERIC NLTE PROBLEMS

APPLICATION

- ANALYSIS OF OZONE HOT BAND EMISSION IS UNDERWAY TO UPDATE PARAMETERS FOR UPPER ATMOSPHERIC CODES

PHILOSOPHICAL ISSUE

- WHAT ACCURACY SHOULD BE REQUIRED FOR INCLUSION OF NLTE LINES IN HITRAN?

NLTE EMISSION FROM HIGH-LYING VIBRATIONAL LEVELS OF OZONE

S. M. Adler-Golden
Spectral Sciences, Inc.

D. R. Smith
Geophysics Laboratory, Hanscom AFB

8 June 1989

This presentation is intended to provide a brief introduction to the NLTE concept in upper atmospheric radiation, focusing on ozone as an example, and will describe some recent progress in understanding the NLTE emission from high vibrational levels of ozone.

NLTE, or non-local-thermodynamic equilibrium, occurs in molecules in the upper atmosphere as the result of low number densities, hence collision rates that are too slow to bring the steady-state energy level distributions into equilibrium with the kinetic temperature. Processes which require consideration in NLTE problems include chemical formation of high-energy states, radiative loss, and earthshine and/or solar pumping from the ground vibrational state. These processes produce vibrational, and occasionally rotational, distributions characterized by temperatures which may be much higher or lower than kinetic.

One of the most important NLTE radiators in the atmosphere is ozone. High vibrational levels of ozone are formed in recombination and emit in the "window" region to the red of the 9.6 μm cold band, which is also in NLTE. This emission is important in limb views between 70-100 km tangent heights. Other molecules in NLTE include CO_2, NO and OH, and in the latter two cases highly excited rotational distributions have been observed.

An example of the ozone hot band spectrum is shown. It was taken in the SPIRIT 1 rocket experiment, which employed a cryogenic interferometer viewing the atmospheric limb. The unapodized resolution is approximately 4 cm^{-1}, and represents the best achieved to date. The spectral structure is all real, and arises from the P, Q and R branches of overlapping ν_3 bands of high-lying vibrational levels.

These high-v bands have been poorly understood, and have not been included in HITRAN. An "extended" data base containing estimated bands has been developed for use with upper atmospheric radiance codes. However, the calculated spectra are seen to agree rather poorly with the SPIRIT 1 data, as shown. To better model this "window" region, more accurate spectroscopic parameters for ozone are required.

Two general approaches have been used in the past to analyze ozone vibrational states. Detailed vibration-rotation analyses based on absorption spectra have been carried out by many workers; currently, these extend to states with up to two stretching quanta. It should be possible,

with further work, to "bootstrap" up to higher levels, using the rotational constants from the lower levels. This approach would result in accurate high-v vibration-rotation lines suitable for HITRAN. However, above perhaps four quanta the absorption lines may be too weak to analyze. A second line of attack has been to extract information from the emission spectra using a low-resolution approach. This approach, although not ideal, is commensurate with available data as well as current modeling requirements.

We have recently begun analyzing the SPIRIT 1 ozone data using a low-resolution model. Initial vibrational energies were predicted from a Darling-Dennison-type formula. The band contours were estimated using a symmetric top model. The contour model has been tested against an elaborate calculation using an asymmetric rotor program generously provided by Herb Pickett of JPL, the same program that has been used to generate JPL's spectral line atlas. This calculation incorporated Darling-Dennison and coriolis interactions as well as high-order centrifugal distortion constants. The results were found to differ little from the approximate model for the highest energy calculation that could be run, which was for bands of the 4-quantum stretching states. This has given us confidence in our method of analysis.

Next, the SPIRIT spectrum was examined, and with the aid of band center predictions and spectral simulations the major bands were identified. They are associated with states having up to seven quanta. The band centers are accurate to within 1-3 cm^{-1}.

A sampling of the hot band assignments are shown. These bands have Q branches which are clearly visible in the spectrum. Several had been previously identified in the COCHISE experiment at AFGL. The (0 0 5) state has been seen in a long-path absorption spectrum taken by Damon, Hawkins and Shaw. The other bands were assigned by finding Q branches close to the Darling-Dennison formula predictions, which are seen to be accurate to within a few cm^{-1}.

A synthetic spectrum using the new band centers is shown along with the SPIRIT I spectrum. While there are some differences, the level of agreement is satisfying, and represents a vast improvement on the current models.

In conclusion, we reiterate the point that upper atmospheric NLTE radiance modeling requires spectral lines with high v and/or J which are currently not in HITRAN. In the case of ozone, progress has been made in understanding the spectroscopy of NLTE emission from high v levels. However, there is long way to go before line positions of the usual HITRAN precision are obtained. This leads to the philosophical question of how accurate the lines should be before they are included in HITRAN. We note that HITRAN is the basis for NLTE radiance codes such as HAIRM, FASCODE and SHARC. Since NLTE bands of ozone and other species are very important in atmospheric backgrounds, a case can be made for including them, perhaps on an extended HITRAN tape, even if the line locations are only approximate.

SUMMARY OF COLLISION-BROADENED HALFWIDTHS FOR HITRAN

Robert R. Gamache
The University of Lowell
Center for Atmospheric Research
450 Aiken Street
Lowell, MA 01854

Laurence S. Rothman
GL/OPI
Hanscom AFB, MA 01731-5000

Summary of Collision-broadened Halfwidths for HITRAN

Robert R. Gamache, The University of Lowell
Center for Atmospheric Research,
Lowell, MA

Laurence S. Rothman, Optical Physics Division
Geophysical Laboratory
Hanscom AFB
Bedford, MA

ULCAR

In this talk, we will briefly review the halfwidths that are on the HITRAN database and review the updates that will be incorporated into the next edition of the database.

If you know of any ongoing determinations of halfwidths or of any data not mentioned here that you feel is essential for the next edition of the database, please let us know.

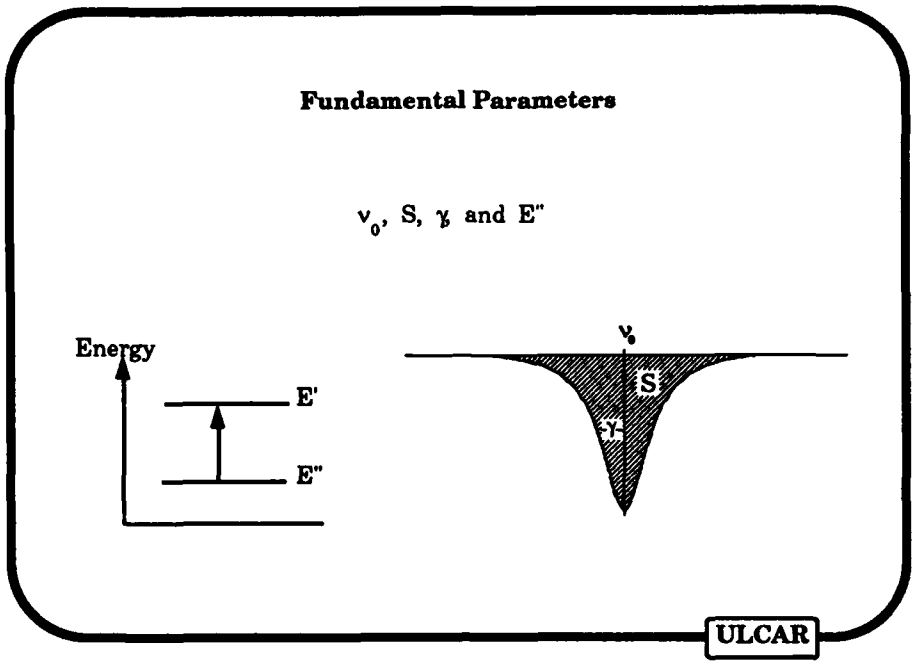

The fundamental parameters on the database are the wave number of the transition, the line intensity, the halfwidth of the transition and the lower state energy.

Here we are concerned with the halfwidth at half max for **air**-broadening.

On the HITRAN database, the halfwidth is reported in units of inverse centimeters per atmosphere at 296 K.

$$\text{i.e. } cm^{-1}/atm$$

Often N2-broadened values are scaled to give the air-broadened results.

H2O constant = 0.90

O3 constant = 0.95

$$\gamma_{air} = C \bullet \gamma_{N_2}$$

Temperature Dependence of the Halfwidth

Assuming the optical cross section varies as $\sigma(T) = \sigma_0 \cdot T^m$,
the halfwidth in units of cm^{-1}/atm as a function of temperature is

$$\gamma(T) = \gamma(T_0) \cdot \left(\frac{T_0}{T}\right)^n$$

The temperature dependence of the halfwidth is contained in the value of the exponent n.

ULCAR

Assuming that the optical cross-section varies with temperature according to a power law gives the temperature dependence of the halfwidth as above.

This assumption appears to be valid for small temperatures ranges e.g. 70 - 400 K. It becomes more approximate as the range increases.

Range of Air-Broadened Halfwidths and Temperature Dependences

Molecule	γ min.	γ max.	n min.	n max.
H2O	0 0061	0.1046	-- 0.64 --	
CO2	0.0659	0 08990 75		0.79
O3	0 045	0 077	-- 0.76 --	
N2O	0 0686	0 09740.64		0.82
CO	0 047	0 068	-- 0.69 --	
CH4	0 0445	0 09200.63		1.00
O2	0 032	0 062	-- 0.5 --	
NO	0 043	0 063	-- 0.5 --	
SO2	0 110	0 152	-- 0.5 --	
NO2	0 062	0 073	-- 0.5 --	
NH3	0 043	0 090	-- 0.5 --	
HNO3	-- 0 13 --		-- 0.5 --	
OH	-- 0 083 --		-- 0.5 --	
HF	0 020	0 126	-- 0.5 --	
HCl	0 0135	0 09530.20		0.88
HBr	0 015	0 123	-- 0.5 --	
HI	0 008	0 100	-- 0.5 --	
ClO	-- 0 085 --		-- 0.5 --	
OCS	-- 0 07 --		-- 0.5 --	
H2CO	0 107	0 108	-- 0.5 --	
HOCl	-- 0 06 --		-- 0.5 --	
N2	-- 0 06 --		-- 0.5 --	
HCN	0 0619	0 1566	-- 0.5 --	
CH3Cl	-- 0 08 --		-- 0.5 --	
H2O2	-- 0 10 --		-- 0.5 --	
C2H2	0 0400	0 1158	-- 0 75 --	
C2H6	-- 0 10 --		-- 0.5 --	
PH3	-- 0 075 --		-- 0.5 --	

ULCAR

The range of air-broadened halfwidths that are present on the 1986 version of the HITRAN database and the associated temperature exponents are given here. For the cases with a single value these represent constant values which are inferred values or are based on single (or few) measurements. Below we discuss some of the updates that are schedules for the 1989 version of the database.

Water Vapor

HITRAN 1986

R. R. Gamache and R. W. Davies, Appl. Opt. **22**, 4013(1983).

New data

S. D. Gasster, C. H. Townes, D. Goorvitch, and F. P. J. Valero, J. Opt. Soc. Am. B **5**, 593(1988). *Exp; 161 species; 297 K; O2- and N2-broadening.*

T. G. Adiks, A. A. Vinogradova, and I. P. Malkov, Zhurnal Prikladnoi Spektroskopii **45**, 194(1986). *Exp; 161 species; 294 K; air-broadening.*

V. Malathy Devi, D. Chris Benner, C. P. Rinsland, M. A. H. Smith, and B. D. Sidney, J. Mol. Spectrosc. **117** 403(1986). *Exp; 161, 181, and 162 species; 296 K; N2- and air-broadening.*

R. R. Gamache and R. W. Davies, Appl. Opt. **22**, 4013(1983). *Theory; 161 species; 296K; self-broadening.*

ULCAR

For water vapor, we plan to augment the existing database with the results of experiment.

With the updates, the error flag and reference codes will be implemented to keep track of the changes.

Self-broadened halfwidths will also be added to this version.

Gasster - FTS Bomem

Adiks - Diode laser

Devi - Diode laser

Carbon dioxide

HITRAN 1986

E. Arié, N. Lacome, P. Arcas, and A. Levy, Appl. Opt. **25**, 2584 (1986).

New data

L. Rosenmann, M. Y. Perrin, and J. Taine, J. Chem. Phys. **88**, 2995(1988). *Exp; 626 species; 295 - 815 K; N2-broadening*

L. Rosenmann, J. M. Hartmann, M. Y. Perrin, and J. Taine, J. Chem. Phys. **88**, 2999(1988). *Theory; 626 species ; 295 - 815 K; N2-, O2-, and self-broadening.*

T. Huet, N. Lacome, and A. Levy, J. Mol. Spectrosc. **128**, 206(1988). *Exp; 626 species ; 296K; self-broadening.*

M. Margottin-Maclou, P. Dahoo, A. Henry, A. Valentin, and L. Henry, J. Mol. Spectrosc. **131**, 21(1988). *Exp; 626 species ; 296 K; N2-, O2-, and self-broadening.*

V. Dana, A. Valentin, A. Hamdouni, and L. S. Rothman, Submitted to Appl. Opt. *Exp; 626 species ; 296 K; N2-, O2-, and self-broadening.*

ULCAR

For carbon dioxide, new data is available for many bands at many temperatures. All of this data will be used to determine a "best set" to be used on the next HITRAN.

Rosenmann - I; diode-laser; II; theory

Huet - TDL

Margottin-Maclou - FTS

Dana - FTS

Ozone

HITRAN 1986

R. R. Gamache and L. S. Rothman, Appl. Opt. **24**, 1651(1985).

New data

M. A. H. Smith, C. P. Rinsland, V. Malathy Devi, D. Chris Benner, and K. B. Thakur, J. Opt. Soc. Am. B 5, 585(1988), and private communications.
Exp; 666 species; 296 K; N2-, and self-broadening.

ULCAR

For ozone, the experimental values of Smith et. al. will be added to the database of ozone halfwidths. FTS

CO

HITRAN 1986

R. H. Hunt, R. A. Toth, and E. K. Plyer, J. Chem. Phys. 49, 9(1968).

New data

T. Nakazawa and M. Tanaka , J. Quant. Spectrosc. Radiat, Transfer 28, 409(1982); ib. id. 28, 471(1982). *Exp; 26 species; 81, 99, 150, 200, and 300 K; N2-, O2-, and self-, and CO2-broadening.*

ULCAR

For CO, air-broadened halfwidths determined from Nakazawa and Tanaka's N2- and O2-broadened half widths will be used.

The temperature exponent can be determined form this work as well.

This was discussed by Dick Tipping.

double beam spectrometer

Methane

HITRAN 1986

G. D. T. Tejwani and Fox, J. Chem. Phys. 60 2021(1974); J. Chem. Phys. 61, 759(1974).

New data

C. P. Rinsland , V. Malathy Devi, M. A. H. Smith, and D. Chris Benner, Appl. Opt.27, 631(1988). *Exp; 211 species; 296K; N2-, and self-broadening.*

V. Malathy Devi, C. P. Rinsland , M. A. H. Smith, and D. Chris Benner, Appl. Opt. 27, 2296(1988). *Exp; 311 species; 296K; N2-, and self-broadening.*

V. Malathy Devi, D. Chris Benner, C. P. Rinsland, M. A. H. Smith, and K. B. Thakur, J. Mol. Spectrosc. 122, 182(1988). *Exp; 212 species; 296K; N2-, O2-, and self-broadening.*

V. Malathy Devi, C. P. Rinsland, D. Chris Benner, M. A. H. Smith, and K. B. Thakur, Appl. Opt. 25,1848(1986). *Exp; 212 species; 296K; N2-, O2-, and self-broadening.*

ULCAR

The halfwidths from Devi, Rinsland, Smith, and Benner will be added to the methane lines.

This has already been discussed by Malathy Devi.

Hydroxyl Radical

HITRAN 1986

constant value 0.083 cm^{-1}/atm

New data

G. Buffa, O. Tarrini, and M. Inguscio, Appl. Opt. **26**, 3066(1987). *Theory; 16 species; 200, 300, and 400 K; N2-broadening.*

I. G. Nolt, K. V. Chance, L. R. Zink, D. A. Jennings, K. M. Evenson, M. D. Vanek, and J. V. Radostitz, in *Conference Digest, Eleventh International Conference on Infrared and Millimeter Waves*, Pisa, G. Moruzzi, Ed.(1986), pp. 286-288. *Exp; 16 species; 300 K; N2-broadening.*

ULCAR

The constant value of 0.083 cm-1/atm based on a single measurement will be replaced by the work of Nolt et. al. (diode laser) and that of Buffa et. al..

Although not a large change, this will help keep HITRAN at the forefront of spectroscopy.

HF, HCl

HITRAN 1986

R. E. Thompson, J. H. Park, M. A. H. Smith, G. A. Harvey, and J. M. Russell III, J. Mol. Spectrosc. 106, 251(1984).

J. Ballard, W. B. Johnston, P. H. Moffat, and D. T. Llewellyn-Jones, J. Quant. Spectrosc. Radiat, Transfer 33, 365(1985).

New data

A. S. Pine and J. P. Looney, J. Mol. Spectrosc. 122, 41(1987). *Exp; HF, H ^{35}Cl; 202, 295 K; N2-, air-broadening.*

A. S. Pine and A. Fried, J. Mol. Spectrosc. 114, 148(1985). *Exp; HF, H ^{35}Cl; 295 K; self-broadening.*

G. Bachet, C. R. Acad. Sci. Paris 274, 1319(1972); J. Quant. Spectrosc. Radiat, Transfer 14,1285(1974). *Exp and Theory; HF and H ^{35}Cl; 296 K; N-2-broadening.*

R. E. Meredith and F. G. Smith, J. Chem. Phys. 60, 3388(1974). *Exp; HF; 373K; N2-broadening.*

ULCAR

As discussed by Dick Tipping, for HF and HCl, the work of Al Pine et. al. will be used when possible. For HF the values of Bachet were used for the 0-0 band, and Meredith and Smith for the 3-0 band.

Halfwidths and line shifts.

OCS

HITRAN 1986

constant value 0.083 cm^{-1} /atm

New data

J. C. Depannemaecker and J. Lemaire, J. Mol. Spectrosc. 128, 350(1988). *Exp; 624 species; 295K; self-broadening.*

J. -P. Bouanich, G. Blanquet, J. Walrand, and C. P. Courtoy, J. Quant. Spectrosc. Radiat. Transfer 36, 295(1986). *Exp; 624 species; 200 and 298 K; self-broadening.*

ULCAR

For OCS, self-broadening data is available from Depannemaecker and Lemaire (double beam diode laser) and Bouanich et. al.(diode laser).

This data will be added to the self-broabening field.

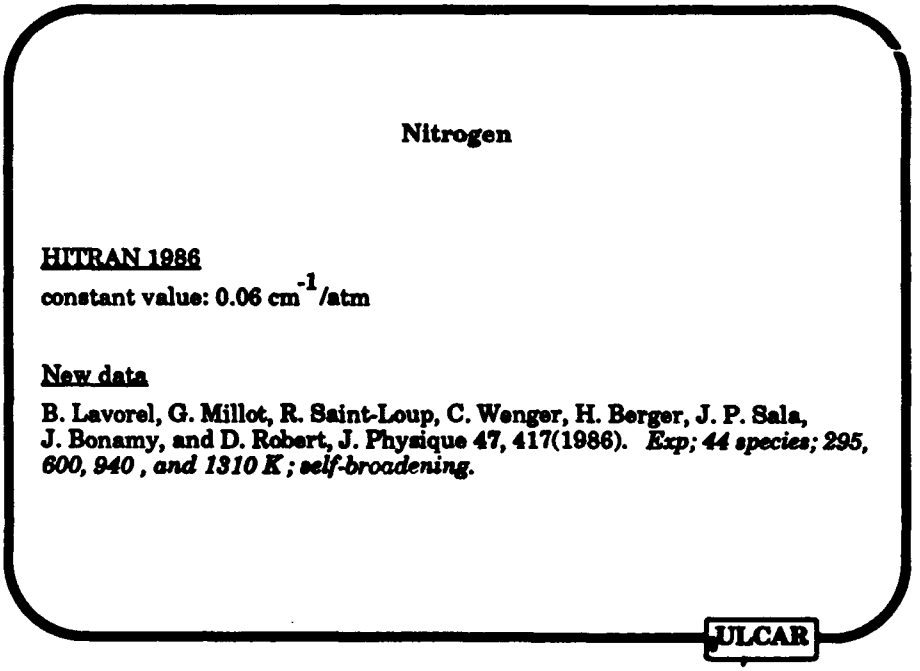

For N2, data is available for the fundamental Q-branch from Lavorel et. al. This will be used to replace the constant value of 0.06 cm-1/atm.

RAMAN

Hydrogen Peroxide

HITRAN 1986

constant value: 0.10 cm^{-1}/atm

New data

V. Malathy Devi, C. P. Rinsland , M. A. H. Smith, D. Chris Benner, and B. Fridovich, Appl. Opt. **25**, 1844(1986). *Exp; 1661 species; 296K; air-broadening.*

ULCAR

The experimental values of Devi et. al. will replace the constant value of 0.10 cm-1/atm on the database.

TDL measurements

STATUS OF LINE PARAMETERS OF H_2CO, HCN, AND C_2H_2

MaryAnn H. Smith
NASA Langley Research Center
Mail Stop 401A
Hampton, VA 23665

BANDS USED FOR ATMOSPHERIC MEASUREMENTS

MOLECULE	BAND	REGION (cm^{-1})	REFERENCE
C_2H_2	ν_5	750– 780	Rinsland et al. (1987)
C_2H_2	$\nu_2+\nu_4+\nu_5$	3230–3240	Rinsland et al. (1985)
HCN	$2\nu_2$	1435–1445	Zander et al. (1988)
HCN	ν_3	3270–3310	Zander et al. (1988)
HCN	rot.	32– 56	Abbas et al. (1987)

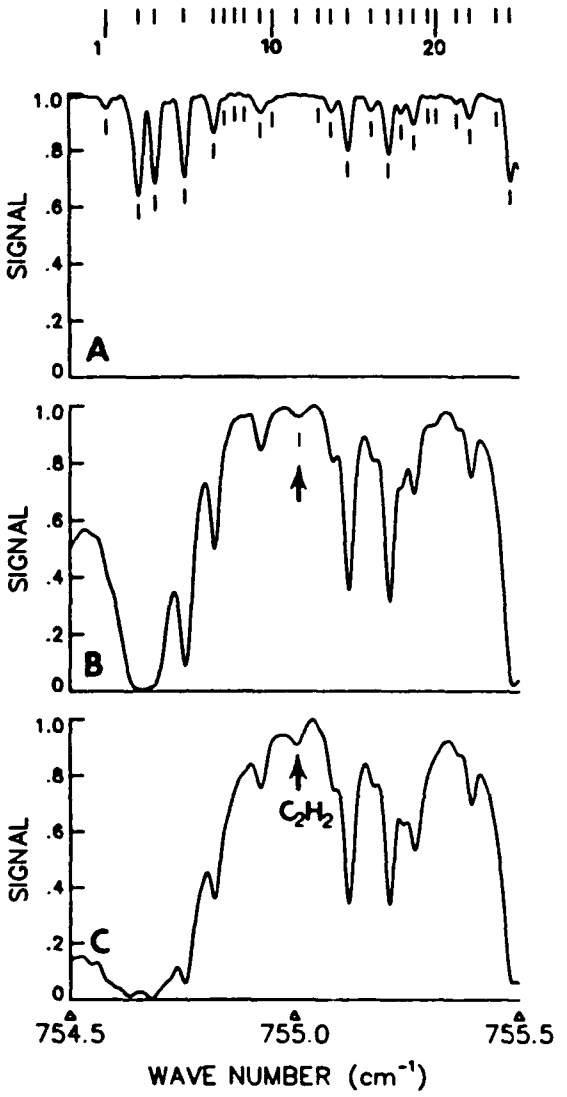

Fig. 6. ATMOS spectra in the region of the $R10$ line of the ν_5 band of C_2H_2 at tangent heights of(*a*) 36.4, (*b*) 11.6, and (*c*) 8.2 km, corresponding to tangent pressures of 4.8, 221, and 371 mbar, respectively. The uppermost spectrum is the result of coadding nearly equal tangent altitude scans from three occultations at 30°–33°N; spectra in Figures 6*b* and 6*c* are from occultation SS08. Ratios of the spectra to a high-Sun spectrum have been used to remove solar features. Tick marks correspond to the positions and identifications from Table 5. Absorption by C_2H_2 is indicated in Figures 6*b* and 6*c*.

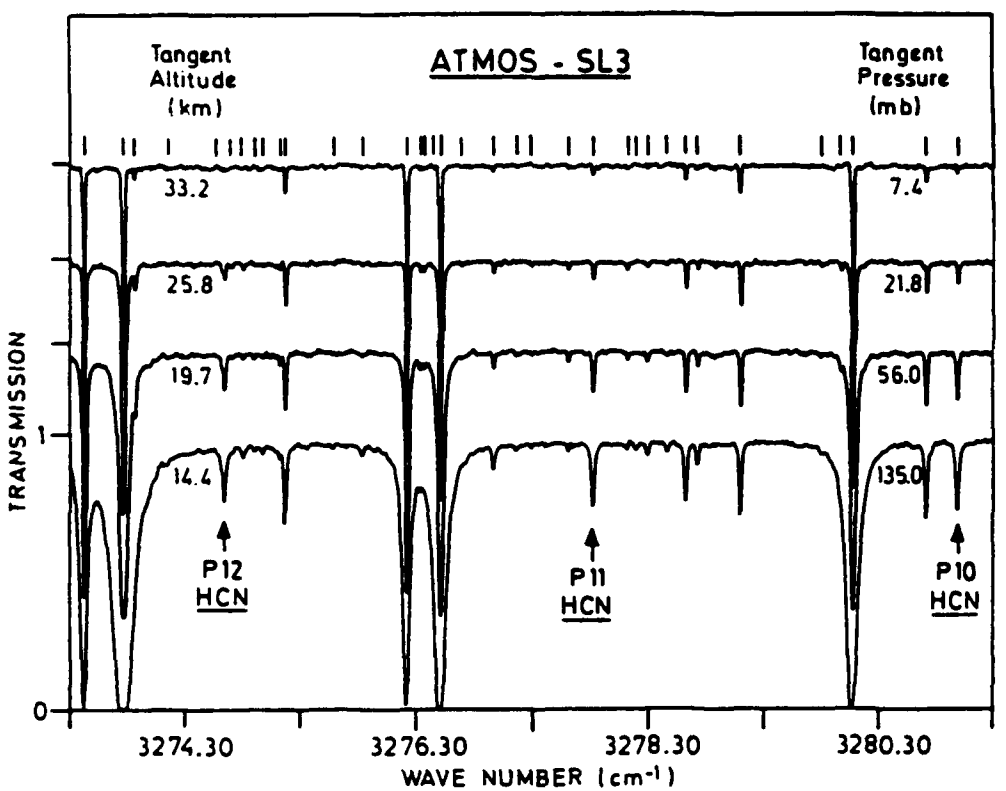

Fig. 7. High sun-ratioed ATMOS/SL3 sample spectra, showing the P10, P11, and P12 transitions of the ν_3 band of HCN. The saturated lines are due to telluric H_2O. All genuine absorptions detected in one or more runs are indicated by tick marks at the top of the figure. See text for details and discussion.

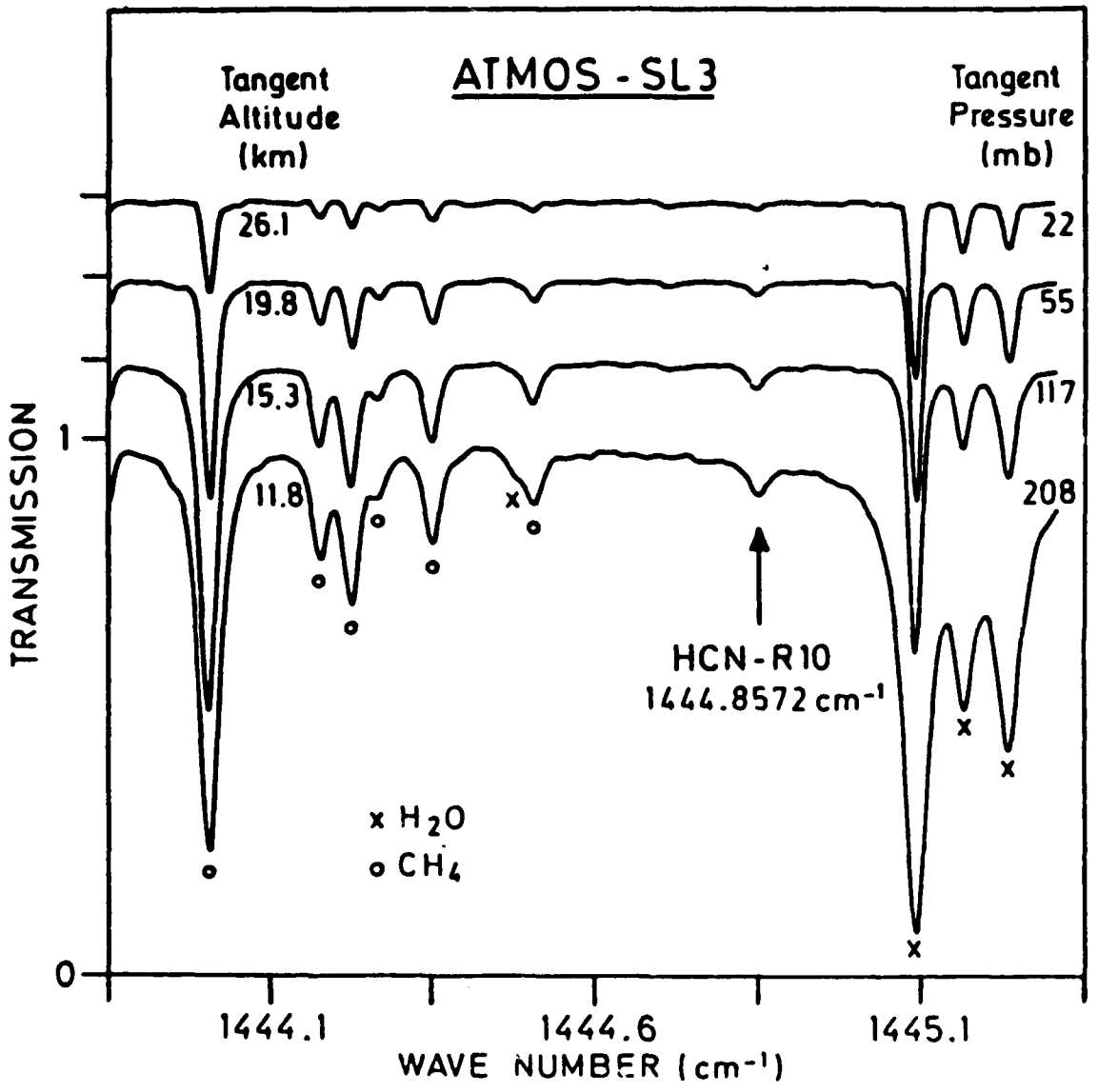

Fig. 9. Four high sun-ratioed sample spectra observed by TMOS, showing the R10 line of the $2\nu_2$ band of HCN. Correspond-g tangent pressures and altitudes are indicated below each trace.

SUNSET SPECTRA OBTAINED AT 30°S, 23 MARCH 1977

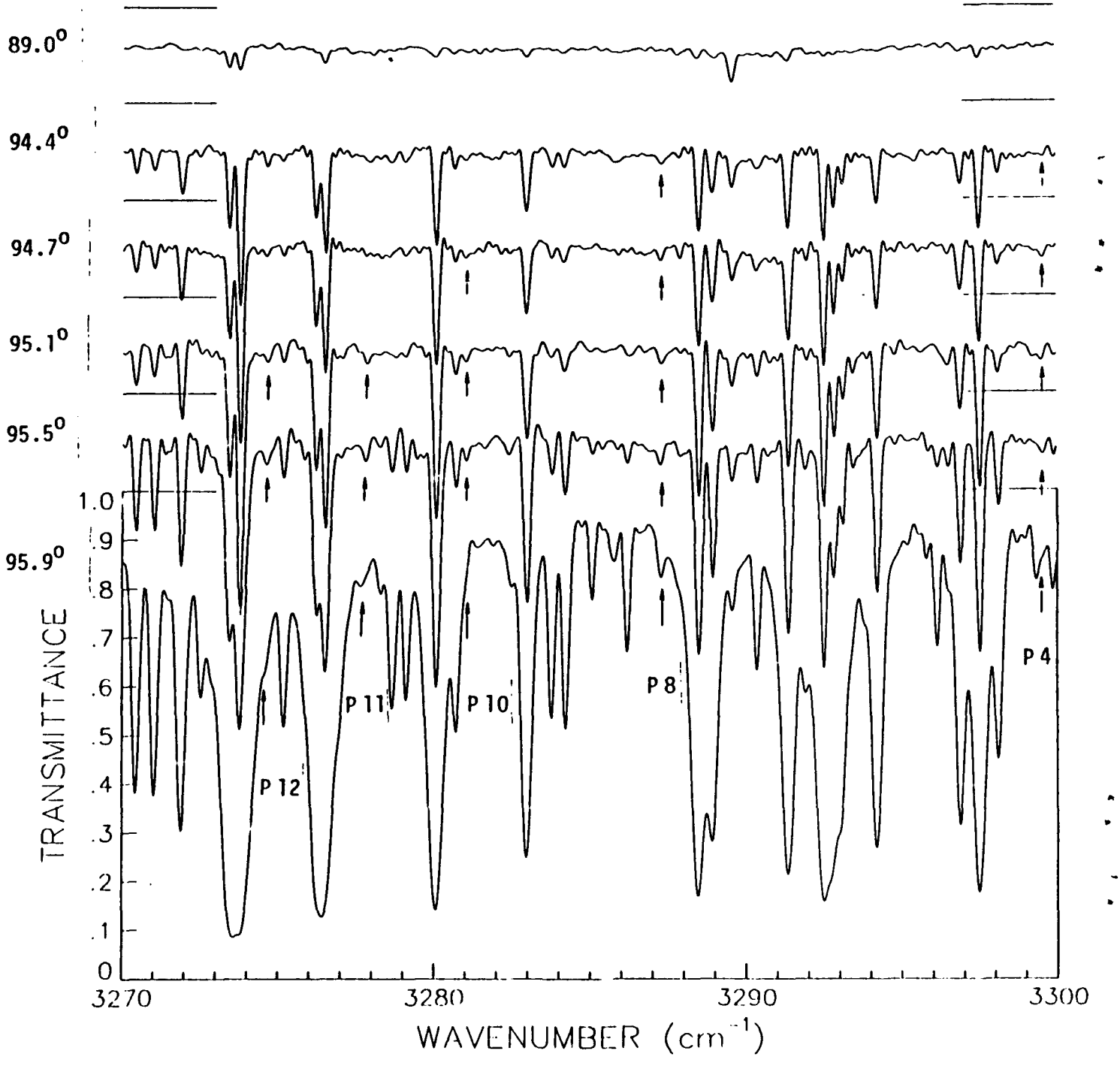

H2CO Molecule: # lines= 2702

Band Centers	Isotope	Vibrational Band upper	lower	Frequency min	max	number lines	Sum of Intensity	
	126	000000-	000000	0-	100	611	3.265E-18	N
	136	000000-	000000	0-	73	563	5.633E-20	
	128	000000-	000000	0-	48	367	6.941E-21	
2500.	126	000002-	000000	2743-	2812	5	4.548E-20	
2655.	126	001100-	000000	2734-	2735	1	5.890E-21	
2719.156	126	001001-	000000	2700-	2879	105	1.386E-18	
2782.457	126	100000-	000000	2723-	2843	424	8.288E-18	
2843.326	126	000010-	000000	2703-	2982	595	9.742E-18	
2905.	126	010100-	000000	2734-	2999	28	3.813E-19	
3000.066	126	010001-	000000	2896-	2957	3	8.550E-20	

RECOMMENDATIONS FOR H_2CO UPDATE

- Modify air-broadened halfwidths using work of Nadler et al. (1987) (Present: constant 0.1080 $cm^{-1}atm^{-1}$)
- Add constant self-broadened halfwidth 0.6 $cm^{-1}atm^{-1}$ (Kline and Penner, 1980; Sulzmann et al., 1983)

HCN Molecule: # lines= 772

Band Centers	Isotope	Vibrational Band upper	lower	Frequency min	max	number lines	Sum of Intensity
	124	0000-	0000	2-	132	47	1.026E-17
	134	0000-	0000	2-	98	34	1.223E-19
	125	0000-	0000	2-	101	35	4.036E-20
697.957	124	0200-	0110	587-	823	119	2.498E-19
713.076	124	0220-	0110	595-	851	232	1.033E-18
713.459	124	0110-	0000	579-	844	134	8.230E-18
1426.535	124	0200-	0000	1298-	1537	81	1.399E-18
331 .4772	124	0001-	0000	3158-	3422	90	9.516E-18

RECOMMENDATIONS FOR HCN UPDATE

- Add hot bands and isotopic bands in 3 μm region
  (Choe et al., 1986; Kyro et al., 1985; Goldman 1983 calculation)
- Add bands in 2100 cm^{-1} region (Choe et al., 1987)
- Add variable self-broadened halfwidths, range 0.5 to 3.0 $cm^{-1}atm^{-1}$
  (Hochard-Demolliere at al., 1967; Pigott and Rank, 1957)

LABORATORY SPECTRUM OF HCN BROADENED BY N_2

(P = 700 torr, VMR = 0.1%, T = 299.1 K, RES = 0.06 cm^{-1})

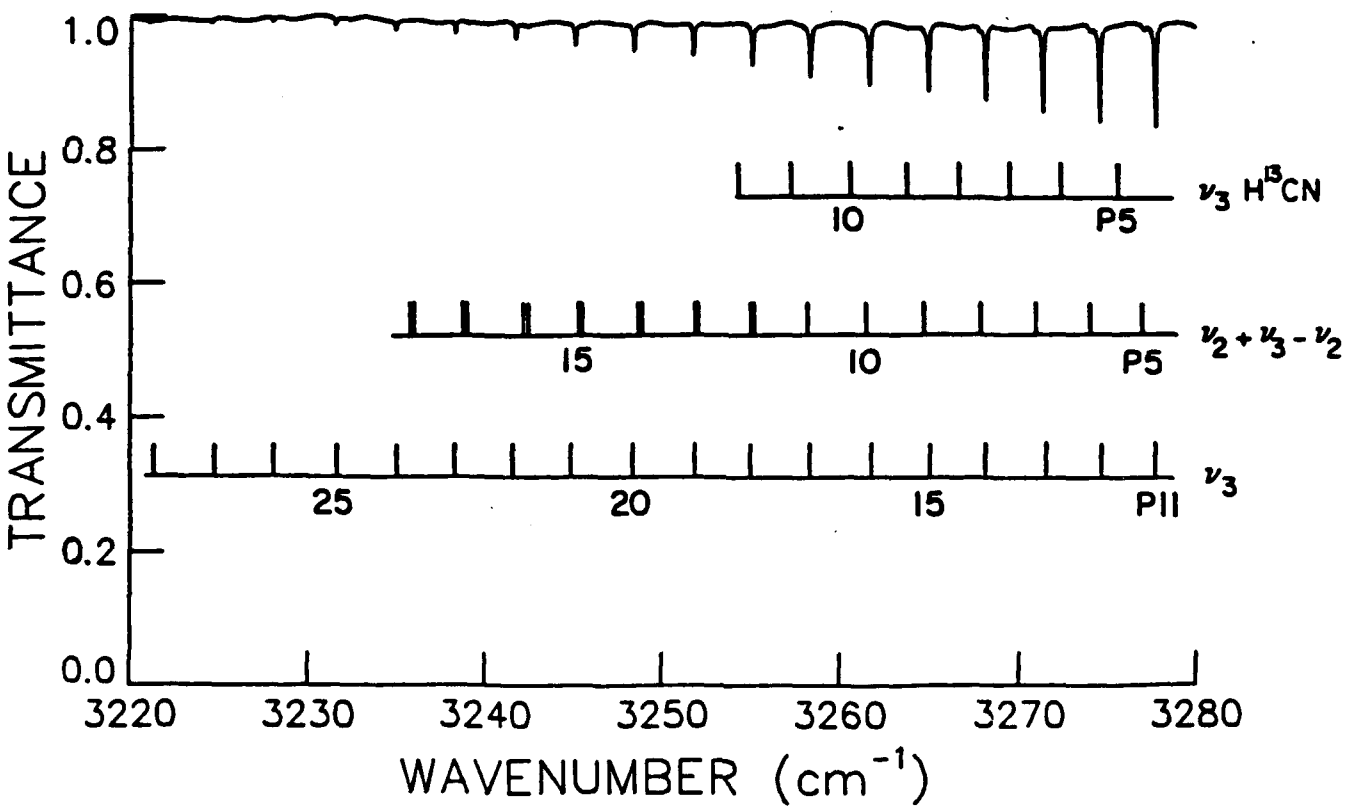

COMPARISON OF HCN BAND INTENSITIES

Band Center	Isotope	Upper Level--Lower Level	Intensity
1426.535	124	0200 - 0000	1.399E-18
3292.1807	124	0111 - 0110	6.663E-19
3293.515	134	0001 - 0000	1.035E-19
3311.4772	124	0001 - 0000	9.516E-18

MEASURED SELF–BROADENED HALFWIDTHS OF HCN

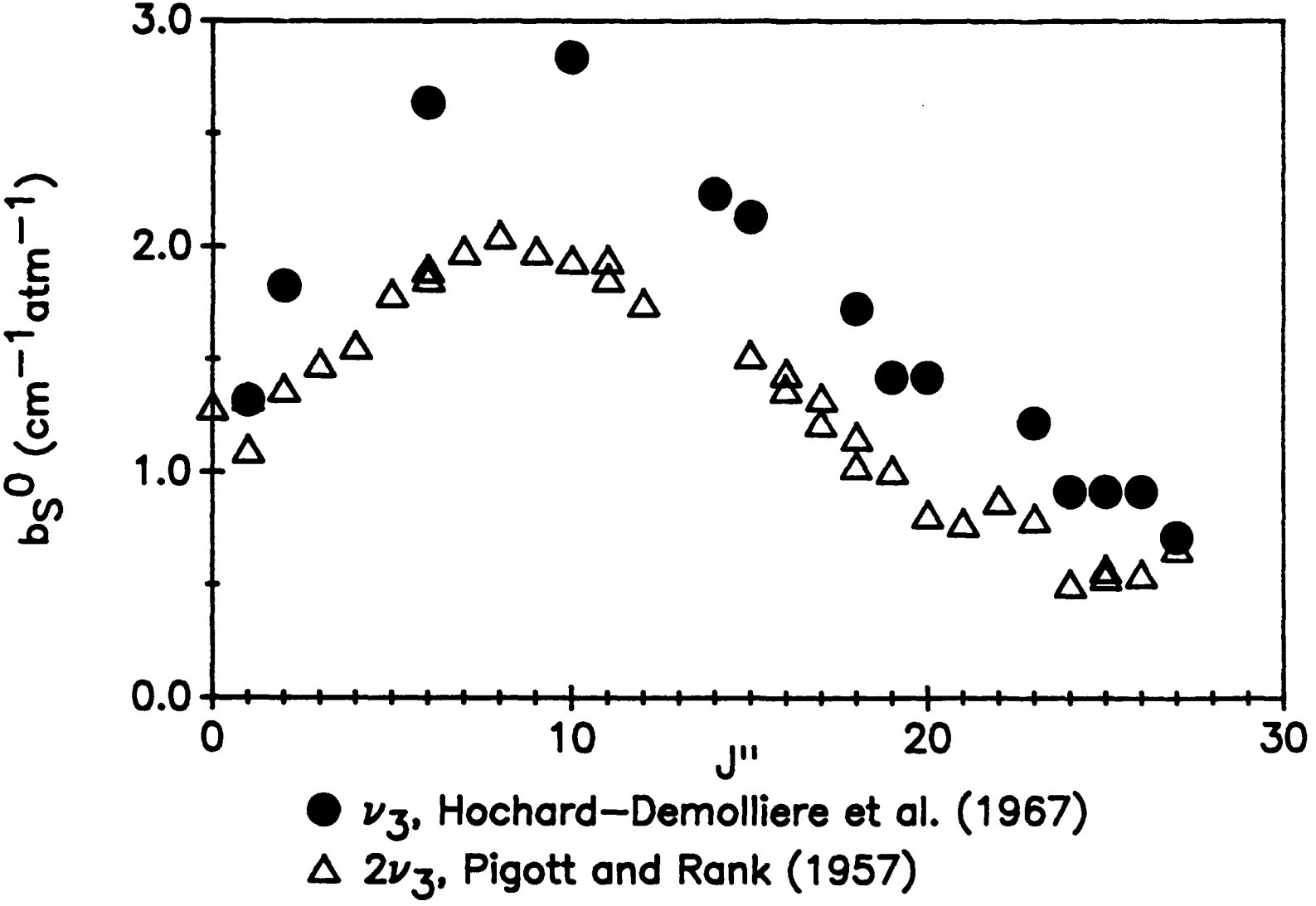

C2H2 Molecule: # lines= 1139

Band Centers	Isotope	Vibrational Band upper	lower	Frequency min	max	number lines	Sum of Intensity	
719.9658	1221	00000200-00000111		640-	805	93	9.430E-19	N
728.8574	1221	00011110-00011001		638-	811	198	1.439E-18	N
729.1365	1221	00000222-00000111		655-	820	187	1.119E-18	N
729.1553	1221	00000111-00000000		646-	811	182	2.383E-17	N
731.1074	1221	00011112-00011001		650-	822	191	1.355E-18	N
3281.9020	1221	01011110-00000000		3151-	3387	101	5.004E-18	N
3284.1904	1231	00100000-00000000		3178-	3375	86	1.835E-19	N
3294.8406	1221	00100000-00000000		3162-	3398	101	4.420E-18	N

RECOMMENDATIONS FOR C_2H_2 UPDATE

- Add line parameters for the $(\nu_4+\nu_5)^0$ band (Rinsland calculation)

Band Center	Isotope	Vibrational Band Upper	Vibrational Band Lower	Frequency Min.	Frequency Max.	Number of Lines	Sum of Intensities
1328.0735	1221	00011110	00000000	1192	1470	119	2.664E-18

- Add hot bands in 3 μm region (low priority)

LINE PARAMETERS FOR THE $(\nu_4 + \nu_5)^0$ BAND OF $^{12}C_2H_2$

Below is a lising of the band center, isotope code, vibrational band code, minimum and maximum frequencies, number of lines, and intensity sum for the $(\nu_4 + \nu_5)^0$ band of $^{12}C_2H_2$:

Band Center	Isotope	Vibrational Band Upper	Vibrational Band Lower	Frequency Min.	Frequency Max.	Number of Lines	Sum of Intensities
1328.0735	1221	00011110	00000000	1192	1470	119	2.664E-18

A. Line Positions and Intensities

The calculated line positions have been obtained from the molecular constants reported in Table I of Palmer, Mickelson, and Rao.[1]

The intensities have been calculated from the experimental R-branch line intensities measured by Podolske, Loewenstein, and Varanasi[2] with a tunable diode laser system. The F factor has been assumed to be unity.

B. Halfwidths

The halfwidths are the same as used for the C_2H_2 bands on the 1986 HITRAN compilation.[3] The air-broadened halfwidths are the experimental values measured by Malathy Devi et al.[4] P- and R-branch widths corresponding to the same value of $|m|$, where $m = J + 1$ for the R-branch and $m = -J$ for the P-branch, have been averaged, except for $|m| = 1$ (R0 and P1) where the experimental results indicate significant differences between the widths. Beyond the range of measurements ($|m| \leq 31$), the halfwidths have been arbitrarily extrapolated to an asymptotic value of 0.04 cm^{-1} atm^{-1} at 296 K.

The self-broadened halfwidths have been computed using a polynomial in $|m|$ expansion derived from experimental data by Varanasi et al.[5] Above $|m| = 25$, a constant value of 0.11 cm^{-1} atm^{-1} at 296 K has been assumed.

C. Temperature Dependence of the Air-Broadened Halfwidths

As on the 1986 HITRAN compilation,[3] a value of $n = 0.75$ has been assumed for all lines based on the N_2-broadening measurements of Varanasi et al.,[6] which were obtained at 153 and 200 K.

REFERENCES

1. K. F. Palmer, M. E. Mickelson, and K. Narahari Rao, "Investigations of Several Infrared Bands of $^{12}C_2H_2$ and Studies of the Effects of Vibrational Rotational Interactions," J. Mol. Spectrosc., 44, 131-144 (1972).

2. J. R. Podolske, M. Loewenstein, and P. Varanasi, "Diode Laser Line Strength Measurements of the $(\nu_4 + \nu_5)^0$ Band of $^{12}C_2H_2$, "J. Mol. Spectrosc., 107, 241-249 (1984).

3. L. S. Rothman, R. R. Gamache, A. Goldman, L. R. Brown, R. A. Toth, H. M. Pickett, R. L. Poynter, J.-M. Flaud, C. Camy-Peyret, A. Barbe, N. Husson, C. P. Rinsland , and M. A. H. Smith, "The HITRAN Database: 1986 Edition," Appl. Opt., 26, 4058-4097 (1987).

4. V. Malathy Devi, D. C. Benner, C. P. Rinsland, M. A. H. Smith, and B. D. Sidney, "Tunable Diode Laser Measurements of N_2- and Air-Broadened Halfwidths: Lines in the $(\nu_4 + \nu_5)^0$ Band of $^{12}C_2H_2$ Near 7.4 μm," J. Mol. Spectrosc., 114, 49-53 (1985).

5. P. Varanasi, L. P. Giver, and F. P. J. Valero, "Infrared Absorption by Acetylene in the 12-14 μm Region at Low Temperatures," J. Quant. Spectrosc. Radiat. Transfer, 30, 497-504 (1983).

6. P. Varanasi, L. P. Giver, and F. P. J. Valero, "Measurements of Nitrogen-Broadened Line Widths of Acetylene at Low Temperatures," J. Quant. Spectrosc. Radiat. Transfer, 30 505-509 (1983).

LAB SPECTRUM OF C_2H_2 NEAR 4090 cm^{-1} (0.1 torr, 24 m)

(G. Guelachvili, K. Narahari Rao, R. D'Cunha, V. Malathy Devi)

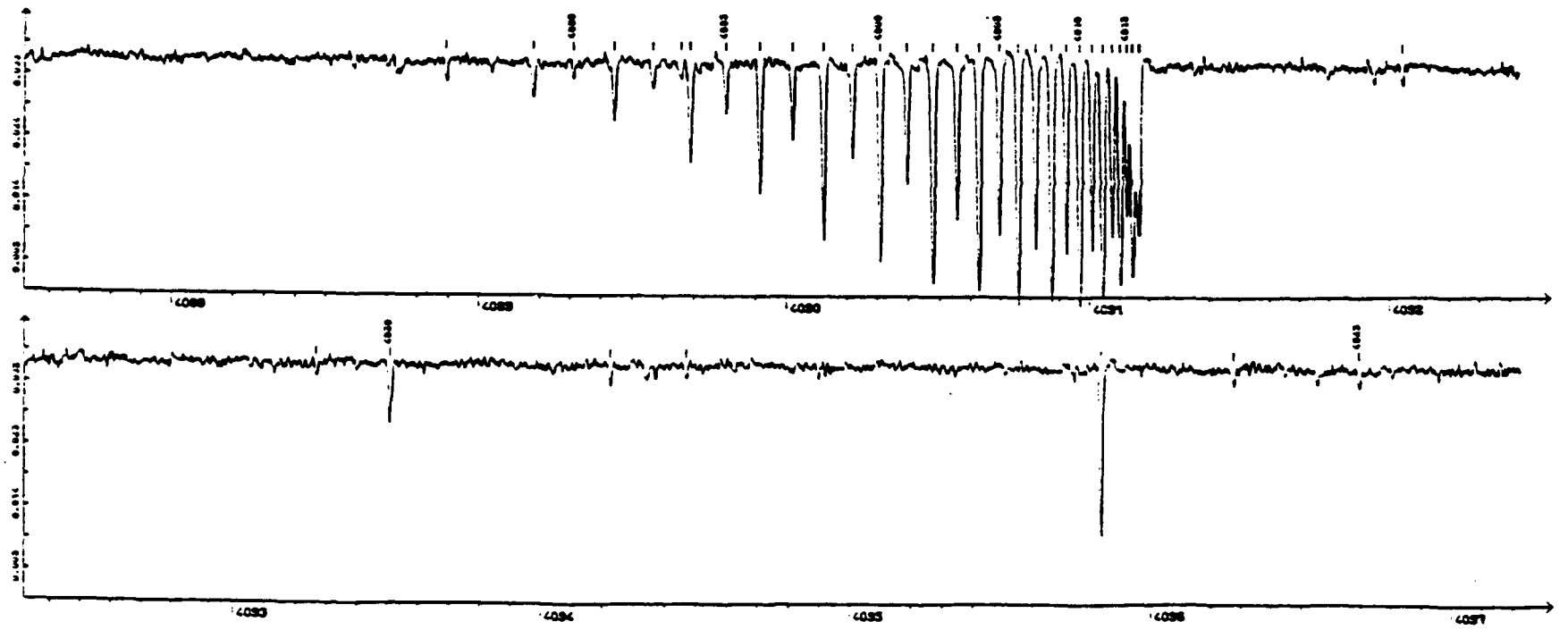

REFERENCES FOR ATMOSPHERIC MEASUREMENTS

M. M. Abbas, J. Guo, B. Carli, F. Mencaraglia, M. Carlotti, and I. G. Nolt, Stratospheric distribution of HCN from far infrared observations, Geophys. Res. Lett. 14, 531-544 (1987).

C. P. Rinsland, A. Goldman, and G. Stokes, Identification of atmospheric C_2H_2 lines in the 3230-3340-cm^{-1} region of high resolution solar absorption spectra recorded at the National Solar Observatory, Appl. Opt. 24, 2044-2046 (1985).

C. P. Rinsland, R. Zander, C. B. Farmer, R. H. Norton, and J. M. Russell III, Concentrations of ethane (C_2H_6) in the lower stratosphere and upper troposphere and acetylene (C_2H_2) in the upper troposphere deduced from Atmospheric Trace Molecule Spectroscopy/Spacelab 3 spectra, J. Geophys. Res. 92, 11951-11964 (1987).

R. Zander, C. P. Rinsland, C. B. Farmer, J. Namkung, R. H. Norton, and J. M. Russell III, Concentrations of carbonyl sulfide and hydrogen cyanide in the free upper troposphere and lower stratosphere deduced from ATMOS/Specelab 3 infrared solar occultation spectra, J. Geophys. Res. 93, 1669-1678 (1988).

REFERENCES TO CONSIDER FOR UPDATES OF H_2CO

M. Dang-Nhu and J. C. Deroche, Absolute intensities of H_2CO in the 9-11 μm region, J. Chem. Phys. 89, 3407-3409.

J. M. Kline and S. S. Penner, Measurements of off-peak spectral absorption coefficients (in CH_2O) for an isolated Voigt line, J. Quant. Spectrosc. Radiat. Transfer 24, 185 (1980).

S. Nadler, S. J. Daunt, and D. C. Reuter, Tunable diode laser measurements of formaldehyde foreign-gas broadening parameters and line strengths in the 9-11 μm region, Appl. Opt. 26, 1641-1646 (1987).

A. S. Pine, Doppler-limited spectra of the C-H stretching fundamental of formaldehyde, J. Mol. Spectrosc. 70, 167 (1978).

K. G. P. Sulzmann, A. Hamins, and S. Y. Tang, 3.508 μ-HeXe-laser line absorption by formaldehyde monomer and dimer and by nitrogen dioxide monomer and dimer without and in the presence of argon, J. Quant. Spectrosc. Radiat. Transfer 29, 31 (1983).

REFERENCES TO CONSIDER FOR UPDATES OF HCN

J.-I. Choe, T. Tipton, and S. G. Kukolich, Fourier transform spectra of the 3300 cm^{-1} bands of HCN, J. Mol. Spectrosc. 117, 292-307 (1986).

J.-I. Choe, D. K. Kwak, and S. G. Kukolich, Fourier transform spectra of the 2100 cm^{-1} bands of HCN, J. Mol. Spectrosc. 121, 75-83 (1987).

J. M. Colmont, Collisional broadening of the J = 1 - 0 transition of $HC^{15}N$ by nitrogen, oxygen, helium and air, J. Mol. Spectrosc. 114, 298-304 (1985).

R. L. DeLeon and J. S. Muenter, The vibrational dipole moment function of HCN, J. Chem. Phys. 80, 3992-3999 (1984).

W. L. Ebenstein and J. S. Muenter, Dipole moment and hyperfine properties of the ground state and the C-H excited vibrational state of HCN, J. Chem. Phys. 80, 3989-3991 (1984).

J. Hietanen, K. Jolma, and V.-M. Horneman, The infrared calibration lines of HCN in the region of ν_2 with the resolution of 0.003 cm^{-1}, J. Mol. Spectrosc. 127, 272-274 (1988).

L. Hochard-Demolliere, C. Alamichel, and P. Arcas, Etude des largeurs de raies de la bande ν_3 de HCN et la bande fondamentale de NO, J. Phys. (Orsay, Fr.) 28, 421-426 (1967).

G. Kortüm and H. Verleger, The pressure broadening of the vibration rotation band of the HCN molecule at 10380 A, Proc. Phys. Soc., London 63, 462-469 (1950).

E. K. Kyrö, P. Shoja-Chaghervand, M. Eliades, D. Danzeiser, S. G. Lieb, and J. W. Bevan, Broadband ν_3 sub-Doppler spectrum of HCN: application of a color center laser optothermal molecular beam spectrometer, Can. J. Chem. 63, 1870-1873 (1985).

M. T. Pigott and D. H. Rank, Measurements of self-broadening in HCN, J. Chem. Phys. 26, 384-391 (1957).

ADDITIONAL REFERENCE TO CONSIDER FOR UPDATES TO C_2H_2

W. E. Blass and V. W. L. Chin, Hydrogen and nitrogen broadening of the lines of C_2H_2 at 14 μm, J. Quant. Spectrosc. Radiat. Transfer 38, 185-188 (1987).

STATUS OF LINE PARAMETER LISTINGS BETWEEN 400 AND 700 cm^{-1}

Kelly Chance
Harvard Center for Astrophysics
60 Garden Street
Cambridge, MA 02138

Status of Line Parameter Listings Between 400 and 700 cm^{-1}

Kelly Chance

Harvard-Smithsonian Center for Astrophysics

The ongoing program of balloon-borne spectroscopic measurements of the atmosphere using far infrared emission spectroscopy at the Smithsonian Astrophysical Observatory has recently been extended to include an infrared channel. This channel currently includes useful emission spectra from 400 to 700 cm^{-1} (the Nyquist sampling cutoff is 790 cm^{-1}); we plan to extend the channel to 800 cm^{-1} in the near future. Our purpose in adding the infrared channel is to increase the number of interrelated chemical species that can be measured simultaneously by our instrument during balloon flights. This paper discusses needs for molecular spectroscopic parameters in the current 400 to 700 cm^{-1} range, with an emphasis on the parameters needed to retrieve abundances of trace gases involved in the photochemistry of the ozone layer.

An example of the type of spectroscopic information that has been available from the SAO far infrared balloon measurements is shown in Figure 1. This figure shows 1 cm^{-1} of a limb-scan sequence of spectra taken from a balloon gondola at 39 km. The useful far infared range in these spectra is 70-200 cm^{-1}. The Q_2 rotational branch of HOCl, at 99.53 cm^{-1}, is included in the portions of spectra shown in this figure.

The far infrared spectrum of the atmosphere, which consists primarily of rotation lines, is at present known (in terms of line identifications) to about the 0.5% level. For example, Figure 2 shows an 0.2 cm^{-1} portion of an atmospheric spectrum containing seven different types of ozone transitions, all assignable with the present spectroscopic databases.

Figure 3 shows the altitude limits for atmospheric constituent measurements that are attainable, or should be attainable, by the SAO FIRS-2 instrument, with the infrared channel included. Not included is O^3P, which is measured, but whose emission originates primarily in the thermosphere. The only constituents given in Figure 3 which we have not yet measured are $ClNO_3$ and N_2O_5. The limits shown are estimated from the limited spectroscopic information currently available. Extension of the infrared channel to 800 cm^{-1} will add several new species, notably CCl_4 and several of the CFCs, to this set.

The infrared channel of the FIRS-2 instrument was operated successfully during our balloon flight of May 15, 1989. Several regions of a spectrum obtained during this flight are shown in Figure 4. The spectrum was obtained at an elevation angle of -2.31°, corresponding to a tangent altitude of 35 km. The figure includes several CO_2-rich regions, the ν_9 band of HNO_3 and the ν_2 band of N_2O. This is a preliminary, uncalibrated, spectrum, which includes some channeling effects. Additionally, coadding will significantly increase the signal to noise ratio in final spectra from this flight.

For analysis of balloon flight spectra in the 400-700 cm^{-1} range improved spectroscopic parameters are needed for a number of molecules. Figure 5 summarizes the current needs for the major species which can be observed in this spectral range.

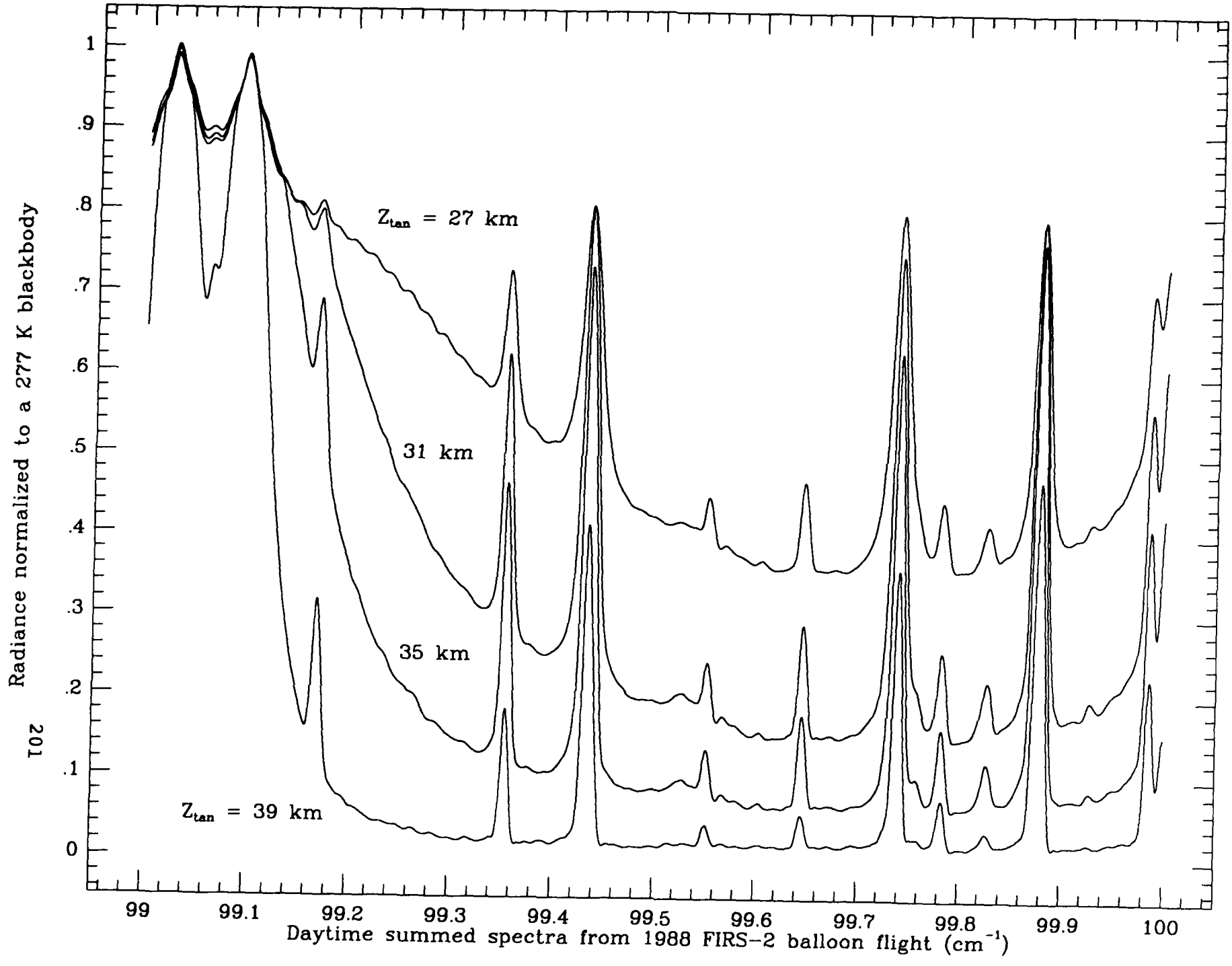
Radiance normalized to a 277 K blackbody
1
.9
.8
.7
.6
.5
.4
.3
.2
.1
0
Z_{tan} = 27 km
31 km
35 km
Z_{tan} = 39 km
99
99.1
99.2
99.3
99.4
99.5
99.6
99.7
99.8
99.9
100
Daytime summed spectra from 1988 FIRS-2 balloon flight (cm^{-1})

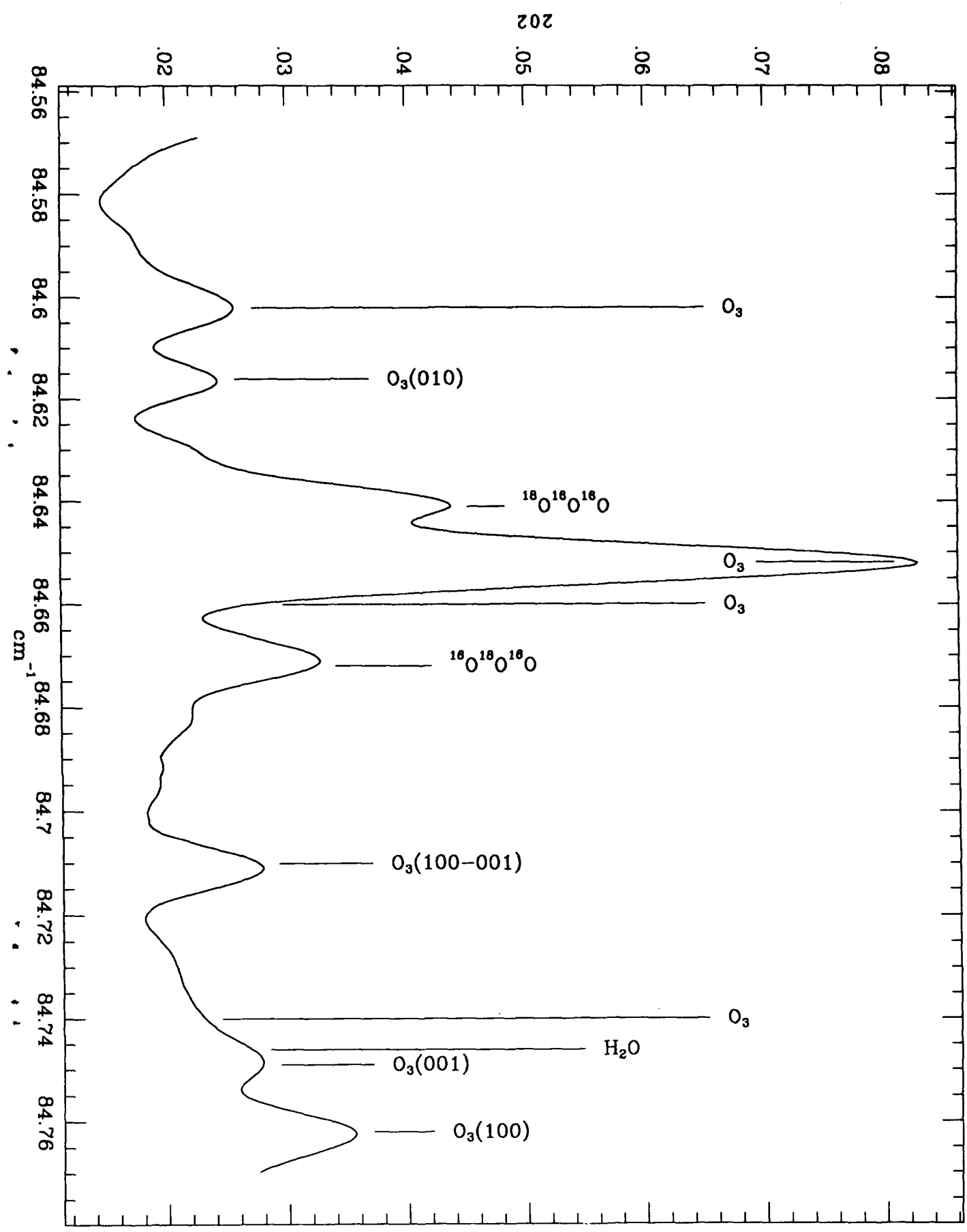
202
.02
.03
.04
.05
.06
.07
.08
84.56
84.58
84.6
84.62
84.64
84.66
84.68
84.7
84.72
84.74
84.76
cm^{-1}
O_3
$O_3(010)$
$^{18}O^{16}O^{16}O$
O_3
O_3
$^{16}O^{18}O^{16}O$
$O_3(100-001)$
O_3
H_2O
$O_3(001)$
$O_3(100)$

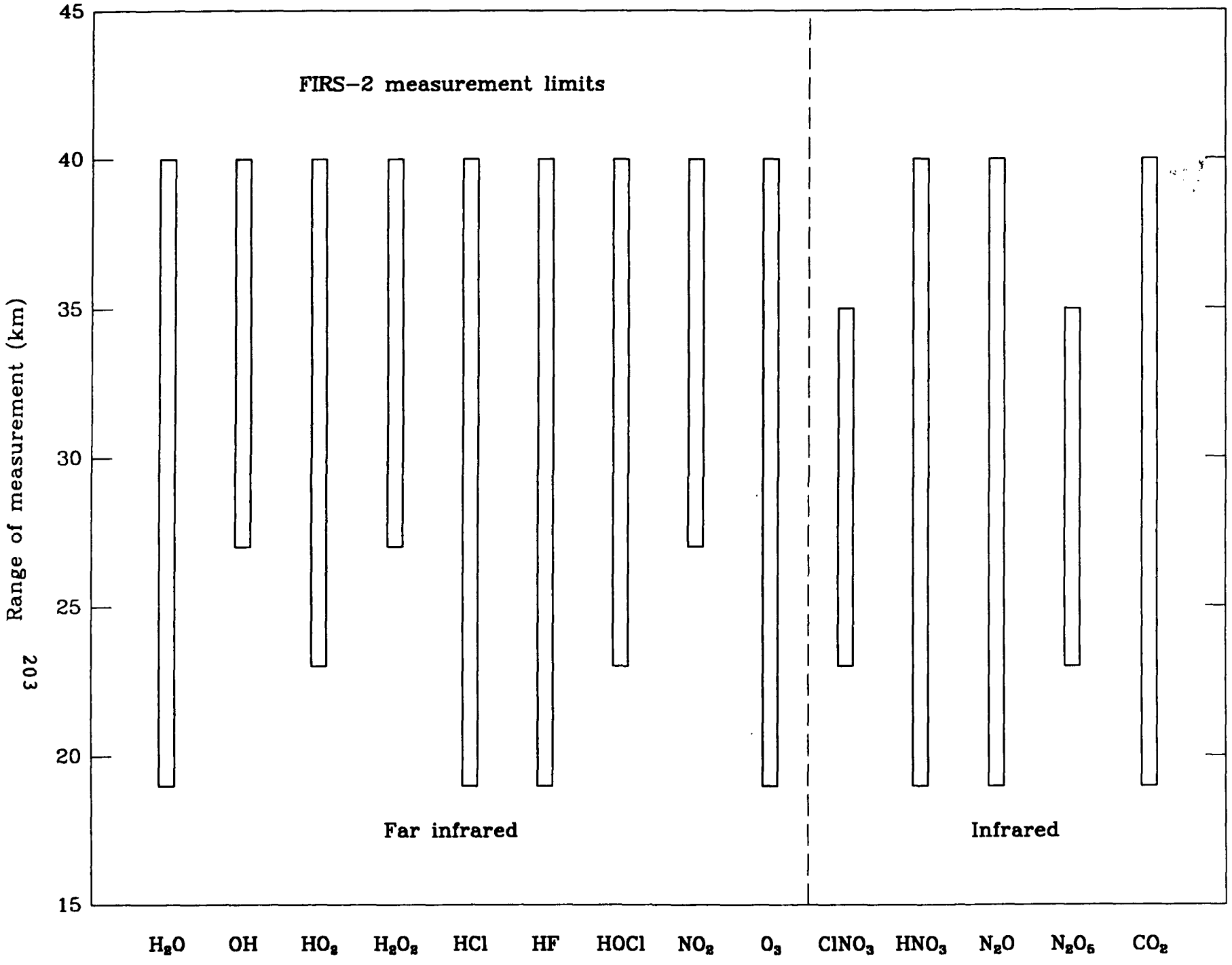
FIRS–2 measurement limits
Range of measurement (km)
45
40
35
30
25
20
15
Far infrared
Infrared
H_2O
OH
HO_2
H_2O_2
HCl
HF
HOCl
NO_2
O_3
$ClNO_3$
HNO_3
N_2O
N_2O_5
CO_2

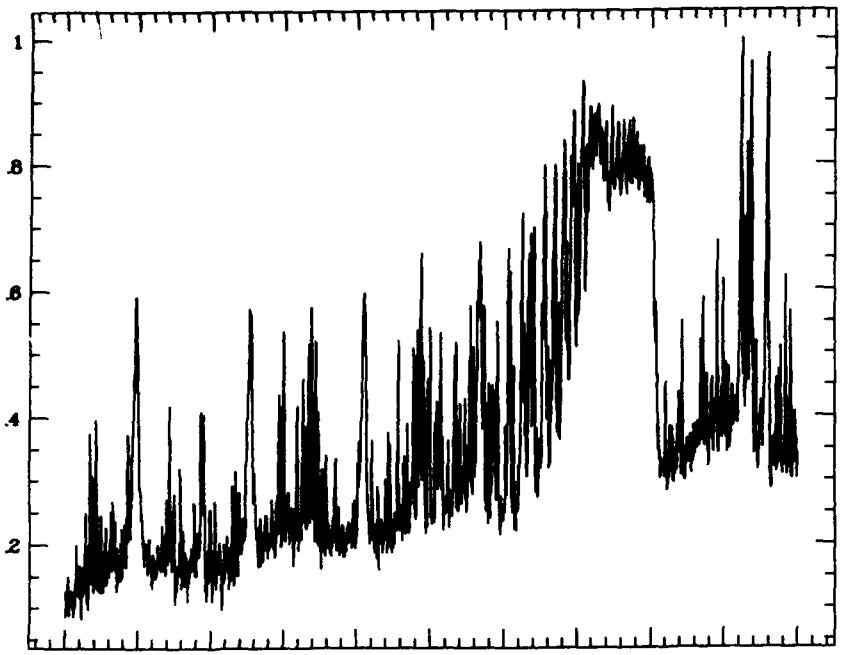

CO_2 in FIRS-2 1989 flight spectrum

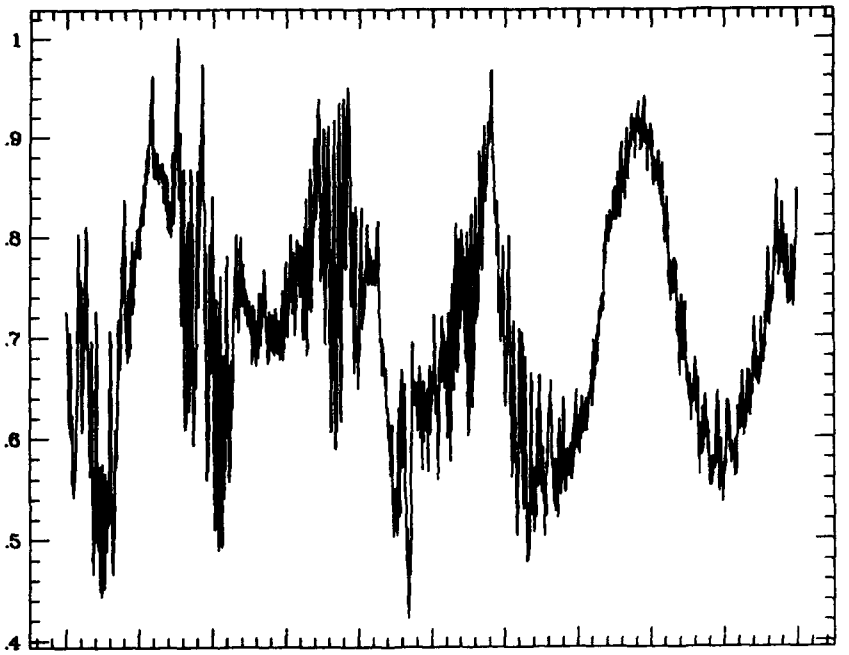

CO_2 in FIRS-2 1989 flight spectrum

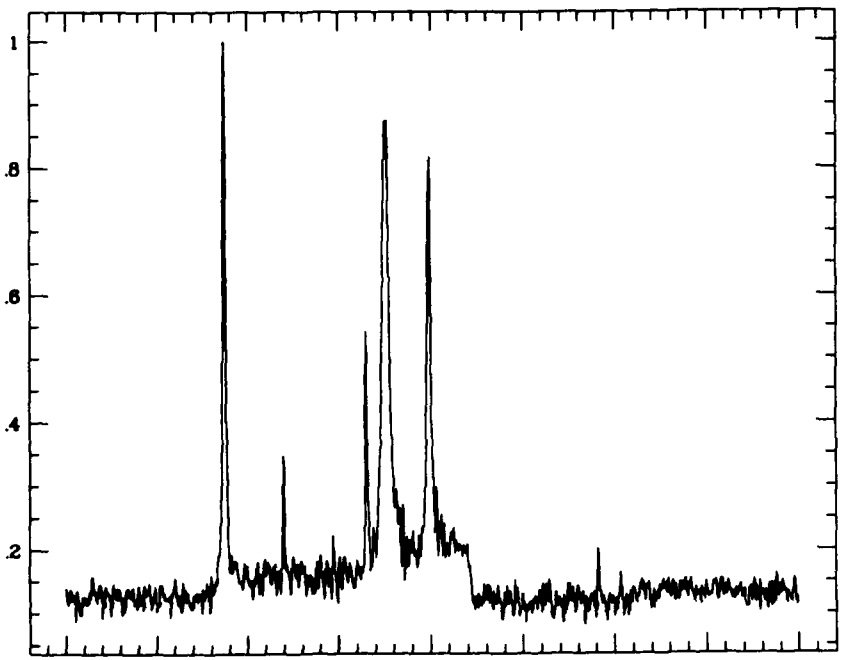

ν_9 band of HNO_3, plus H_2O lines, in FIRS-2 1989 flight spectrum

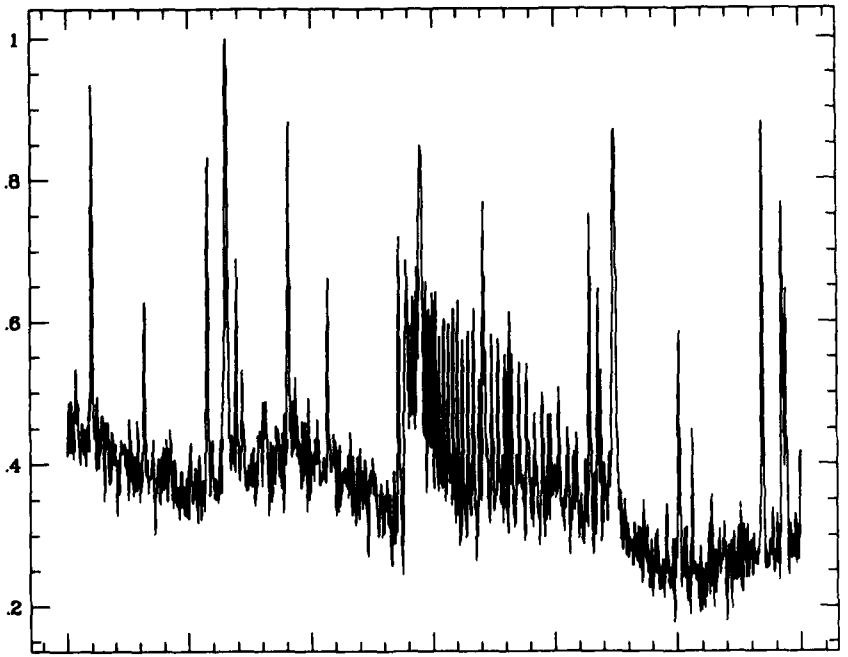

ν_2 band of N_2O, plus CO_2 lines, in FIRS-2 1989 flight spectrum

DATABASE NEEDS IN THE 400-700 CM^{-1} REGION

This is a limited set of parameter needs, oriented toward the measurement of trace species concentrations in the stratospere.

CO_2 Parameters in 1986 HITRAN database are adequate for CO_2 measurement, but not for a complete description of the radiative balance of the atmosphere. Necessary updates include: line-mixing; strengths for isotopic bands.

H_2O Parameters in 1986 HITRAN database are adequate for atmospheric measurement needs.

N_2O Positions and band strength of ν_2 (589 cm^{-1}) band are adequate. Evaluation of Herman-Wallis factors and pressure-broadening coefficients are needed.

HNO_3 Further studies are needed on the ν_6 (647 cm^{-1}), ν_7 (580 cm^{-1}) and ν_9 (458 cm^{-1}) bands, with emphasis on the ν_9 band. The strength of the ν_9 band is good to 15%; 5% is needed, as well as Herman-Wallis factors. Positions in the ν_9 band are currently known very accurately.

$ClNO_3$ High resolution studies of ν_5 and ν_6 bands (560 and 434 cm^{-1}), for band shapes and strengths, are needed.

N_2O_5 The 557 cm^{-1} band needs study at high resolution, and a more accurate band strength (the strength is currently reported with 20% uncertainty).

NEW MOLECULAR PARAMETERS FOR HIGH RESOLUTION STRATOSPHERIC SPECTRA: COF_2, HNO_3, $ClONO_2$, HNO_4

Aaron Goldman
Department of Physics
University of Denver
Denver, CO 80208

HITRAN Workshop
8-9 June, 1989
AFGL

New Molecular Parameters for High Resolution Stratospheric Spectra: COF_2, HNO_3, $ClONO_2$, HNO_4

A. Goldman

Department of Physics

University of Denver

Denver, CO 80208

Abstract

Infrared high resolution (0.002-0.003 cm^{-1}) solar absorption spectra of the stratosphere show new spectral features of several trace gases. Spectral simulations show that previous line parameters and cross sections are often inadequate at the high resolution, and new analysis of laboratory and atmospheric spectra are required. Several sets of improved molecular parameters are discussed, with examples from COF_2, HNO_3, $ClONO_2$ and HNO_4.

New Molecular Parameters for High Resolution Stratospheric Spectra: COF_2, HNO_3, $ClONO_2$, HNO_4

A.Goldman
Department of Physics
University of Denver

HITRAN Workshop
8-9 June 1989
AFGL

Atmospheric Spectroscopy Group at DU

R.D Blatherwick, F.S. Bonomo,
A. Goldman, J.J. Kosters,
D.G. Murcray, F.H. Murcray,
F.J. Murcray, J. VanAllen,
W.J. Williams

Coinvestigators and Contributors

A. Barbe, L.R. Brown, J.B. Burkholder,
C. Camy-Peyret, J.C. Deroche,
J.-M. Flaud, A.G. Maki, S.T. Massie,
C.P. Rinsland, L.S. Rothman

High Res Spectra at DU

Balloon-borne Stratos. Spectra

37km, medium-long optical path
0.002-0.003 cm^{-1} 700-1950 cm^{-1}
Most stratospheric species

Ground-base spectra

Lab. spectra: Select. bands room temp.
CCl_4, CCl_2F_2, CCl_3F, CF_4, $CHClF_2$, CH_2O, $ClONO_2$, COF_2, $COCl_2$, $COClF$, $HCOOH$, HNO_3, HNO_4, H_2O_2, NO_2, N_2O_5, More

High Res 700-1950cm^{-1} stratospheric spectra show cases of:
1. Discrepancies with existing line parameters
2. Need for new line parameters

Much update needed for:
O_3, CH_4, NO_2,HNO_3, COF_2, $ClONO_2$, HNO_4, CF_4, ...
Less update needed for:
H_2O, CO_2, N_2O, O_2, NO

Recently publ. and in progress parameters improvements used:
Lines: O_3(Orsay), CH_4(JPL), HNO_3(NBS,DU), COF_2(DU)
Cross Sec: $ClONO_2$(DU), HNO_4(DU)

Examples From:

Line Parameters

COF_2

ν_2, ν_6, ν_4

$\nu_1, 2\nu_2$

HNO_3

ν_6, ν_7, ν_8, $\nu_8 + \nu_9$, ν_9

$\nu_5, 2\nu_9$, ν_3, ν_4

Cross Sections

$ClONO_2$ ν_4, ν_3, ν_2, ν_1

HNO_4 ν_6

COF_2

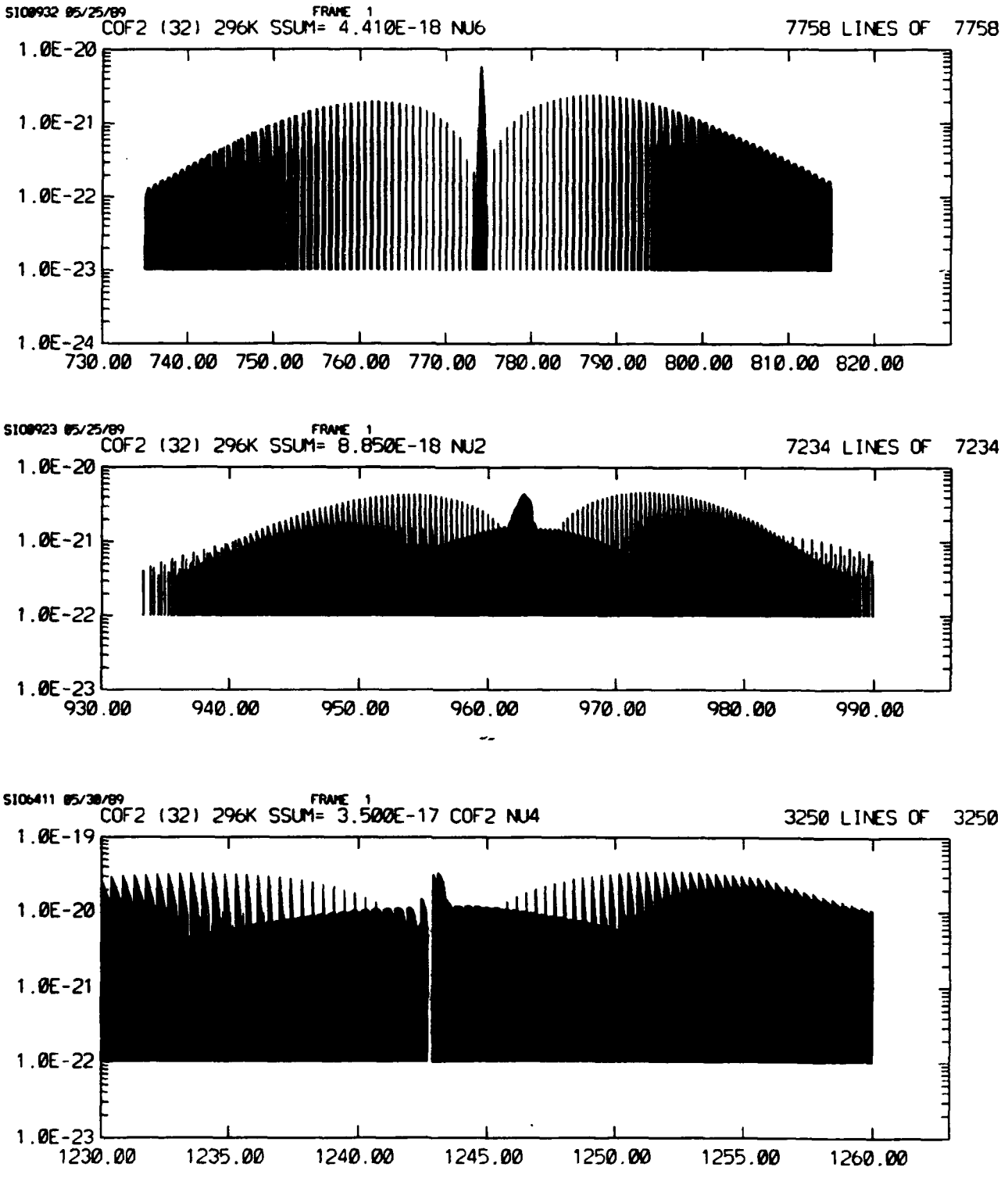
S108932 05/25/89
FRAME 1
COF2 (32) 296K SSUM= 4.410E-18 NU6
7758 LINES OF 7758
1.0E-20
1.0E-21
1.0E-22
1.0E-23
1.0E-24
730.00 740.00 750.00 760.00 770.00 780.00 790.00 800.00 810.00 820.00
S108923 05/25/89
FRAME 1
COF2 (32) 296K SSUM= 8.850E-18 NU2
7234 LINES OF 7234
1.0E-20
1.0E-21
1.0E-22
1.0E-23
930.00 940.00 950.00 960.00 970.00 980.00 990.00
S106411 05/30/89
FRAME 1
COF2 (32) 296K SSUM= 3.500E-17 COF2 NU4
3250 LINES OF 3250
1.0E-19
1.0E-20
1.0E-21
1.0E-22
1.0E-23
1230.00 1235.00 1240.00 1245.00 1250.00 1255.00 1260.00
INTENSITY
WAVENUMBER (CM-1)

HNO_3

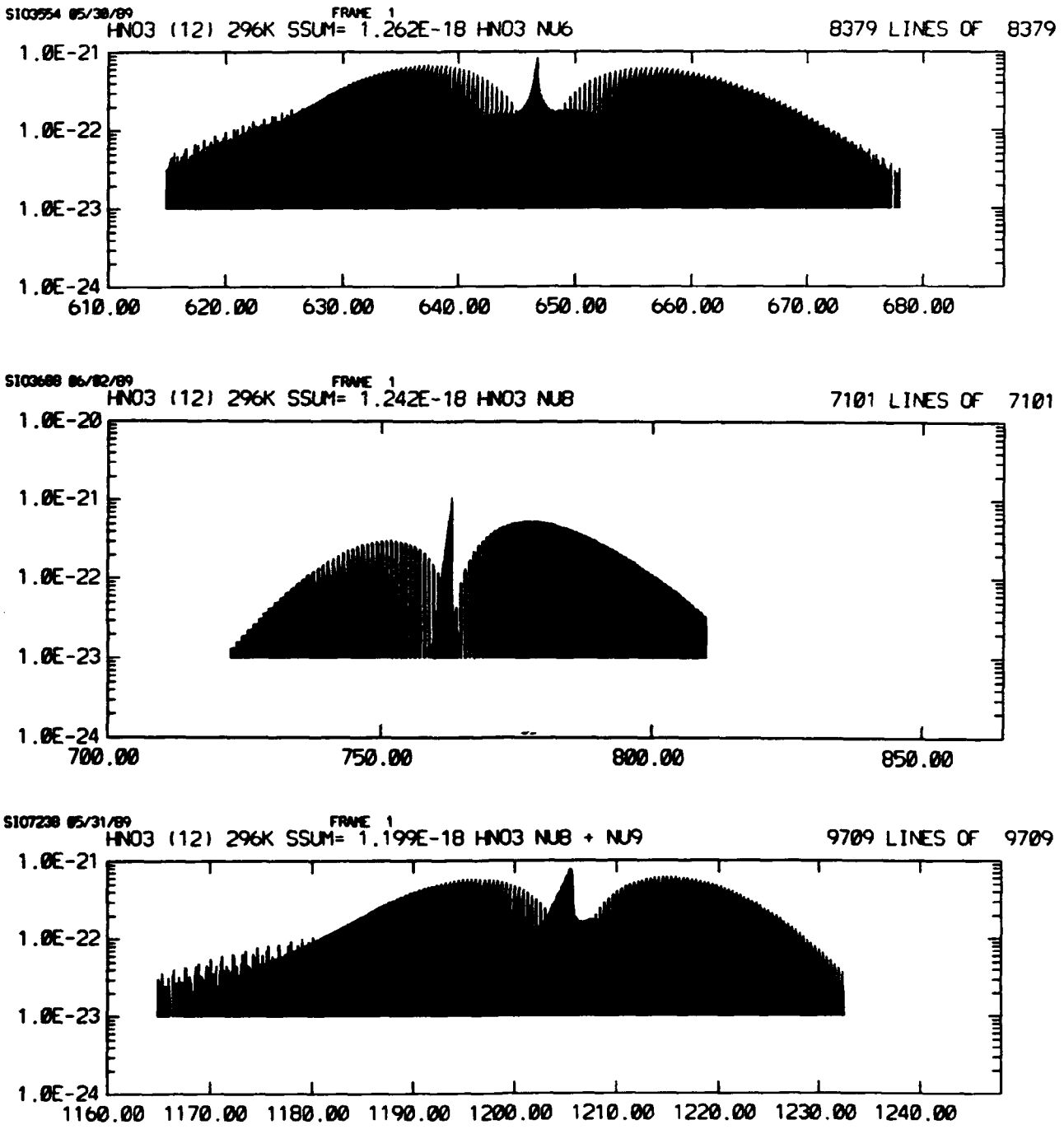

INTENSITY

WAVENUMBER (CM-1)

HNO_3

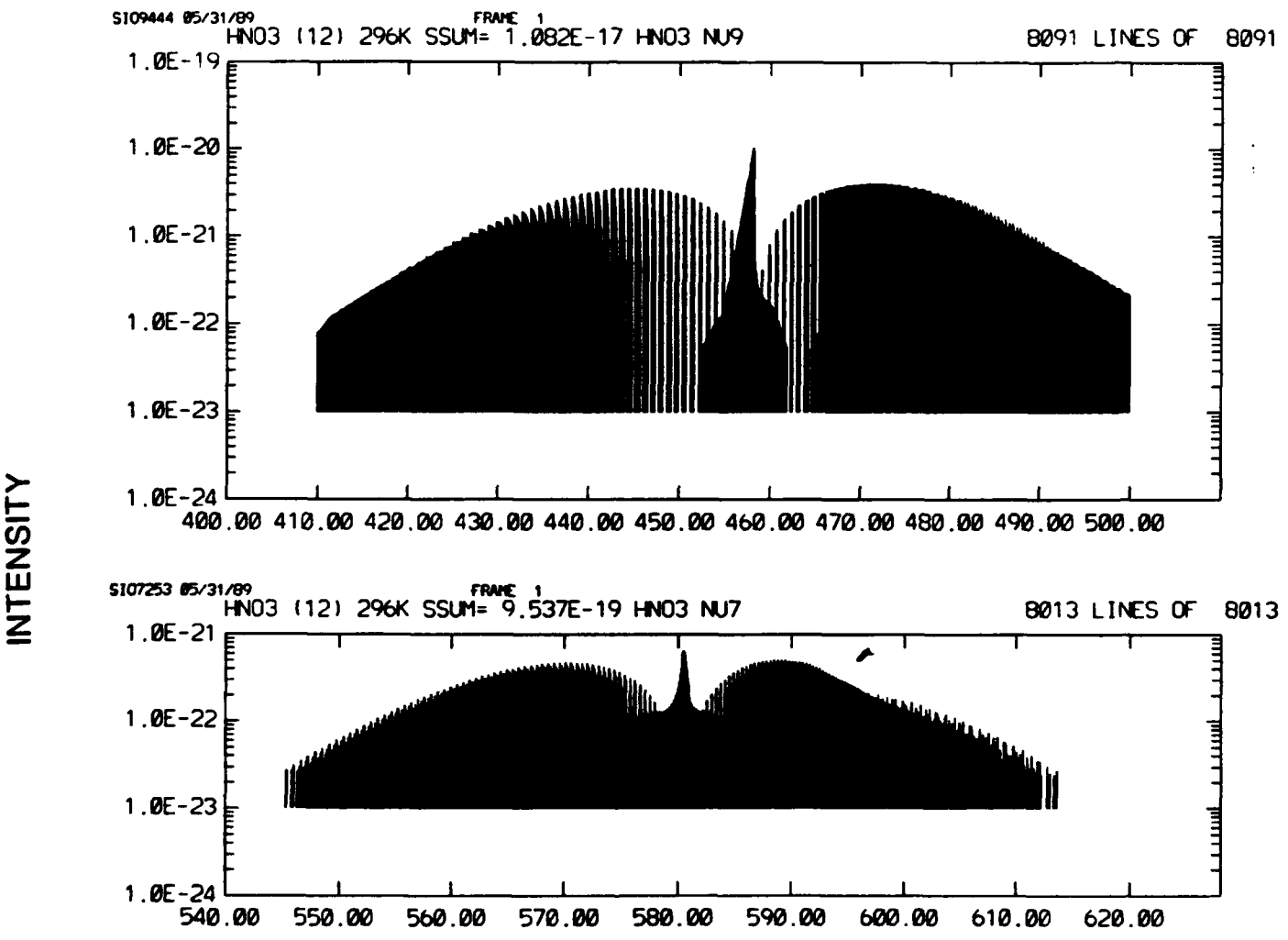
S109444 05/31/89
FRAME 1
HNO3 (12) 296K SSUM= 1.082E-17 HNO3 NU9
8091 LINES OF 8091
1.0E-19
1.0E-20
1.0E-21
1.0E-22
1.0E-23
1.0E-24
400.00 410.00 420.00 430.00 440.00 450.00 460.00 470.00 480.00 490.00 500.00
S107253 05/31/89
FRAME 1
HNO3 (12) 296K SSUM= 9.537E-19 HNO3 NU7
8013 LINES OF 8013
1.0E-21
1.0E-22
1.0E-23
1.0E-24
540.00 550.00 560.00 570.00 580.00 590.00 600.00 610.00 620.00
INTENSITY
WAVENUMBER (CM-1)

$CLONO_2$

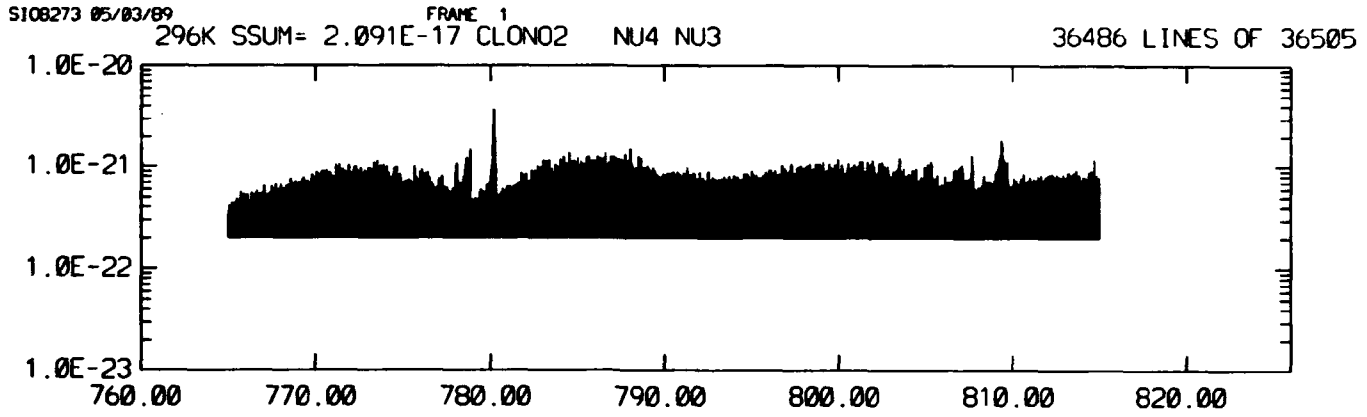

INTENSITY

WAVENUMBER (CM-1)

HNO_4

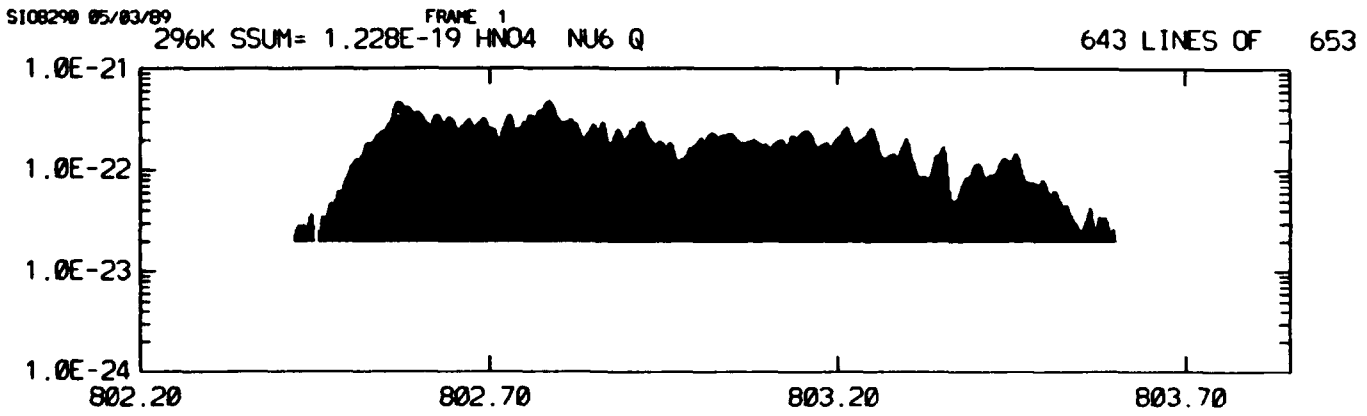

INTENSITY

WAVENUMBER (CM-1)

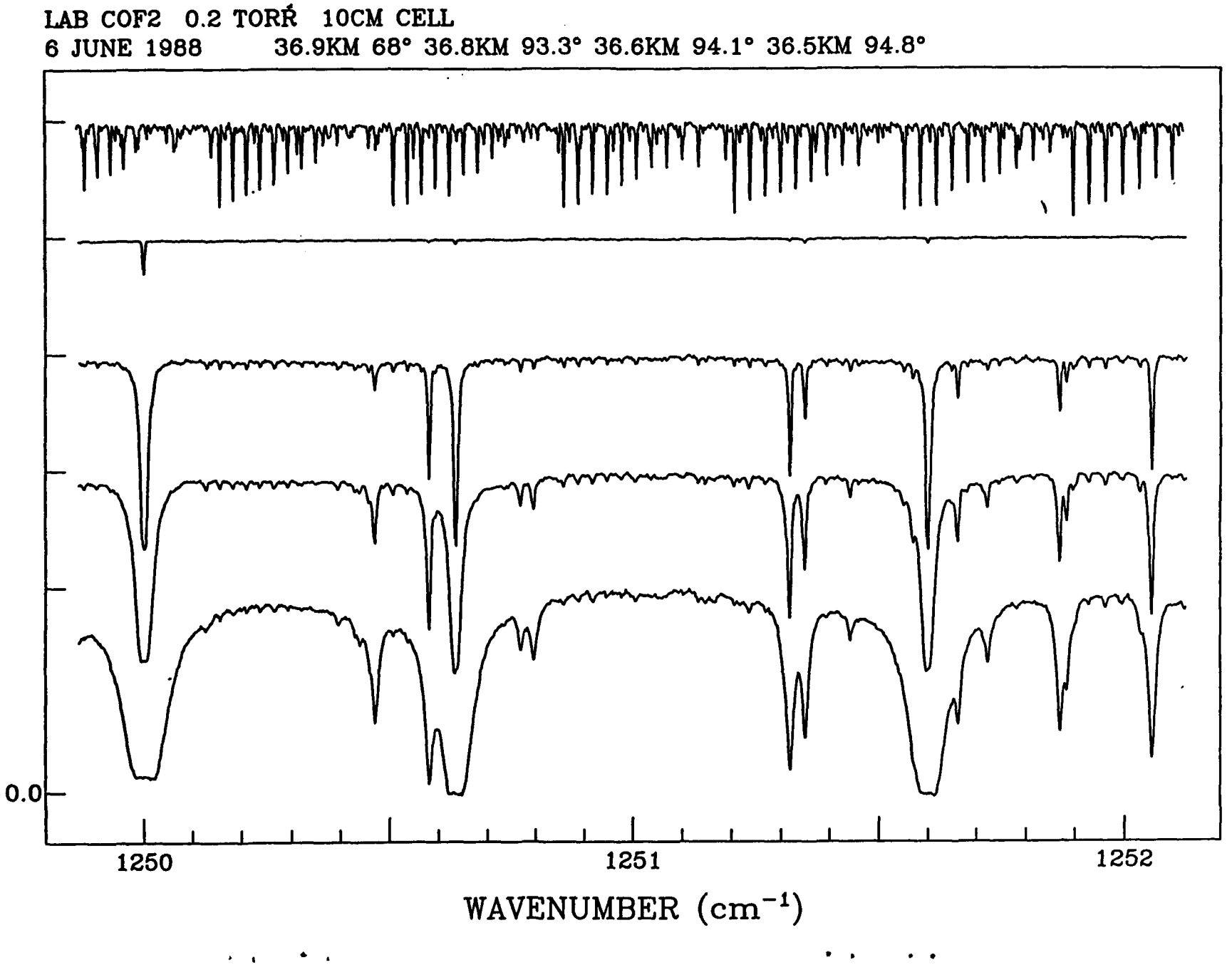
LAB COF2 0.2 TORR 10CM CELL
6 JUNE 1988 36.9KM 68° 36.8KM 93.3° 36.6KM 94.1° 36.5KM 94.8°
SIGNAL
0.0
1250
1251
1252
WAVENUMBER (cm^{-1})

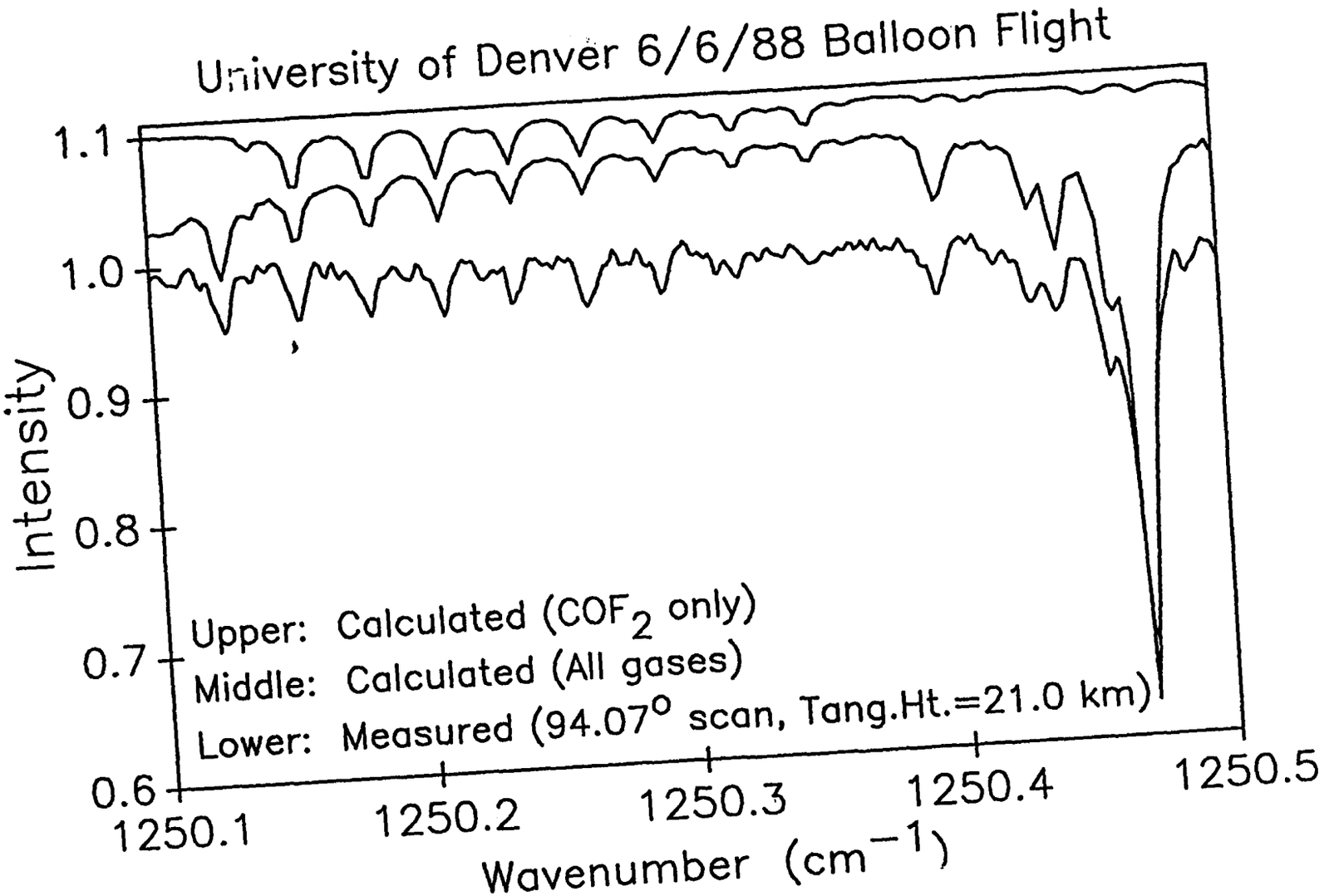
University of Denver 6/6/88 Balloon Flight
Intensity
1.1
1.0
0.9
0.8
0.7
0.6
Upper: Calculated (COF_2 only)
Middle: Calculated (All gases)
Lower: Measured (94.07° scan, Tang.Ht.=21.0 km)
1250.1
1250.2
1250.3
1250.4
1250.5
Wavenumber (cm^{-1})

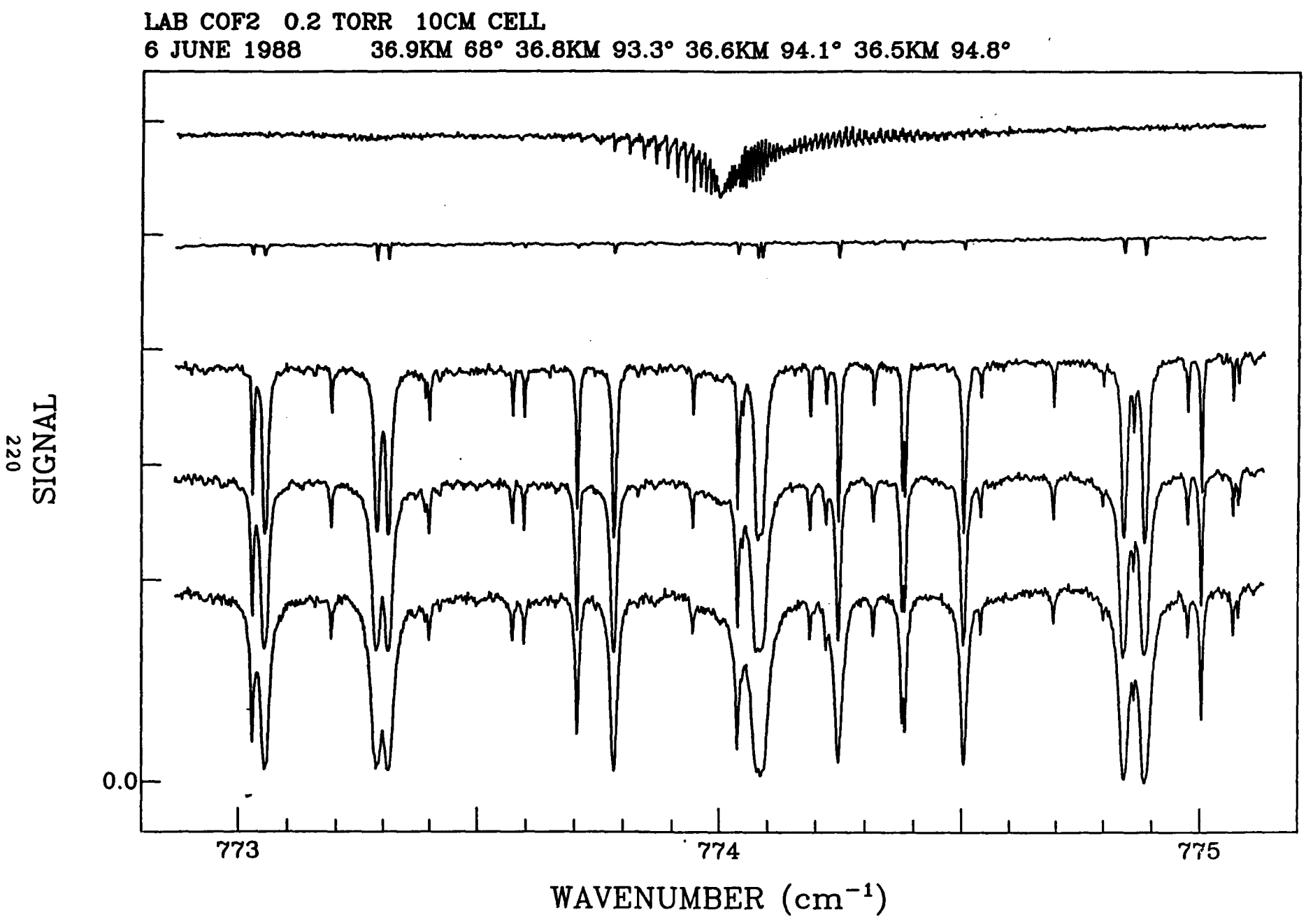
LAB COF2 0.2 TORR 10CM CELL
6 JUNE 1988 36.9KM 68° 36.8KM 93.3° 36.6KM 94.1° 36.5KM 94.8°
SIGNAL
220
0.0
773
774
775
WAVENUMBER (cm⁻¹)

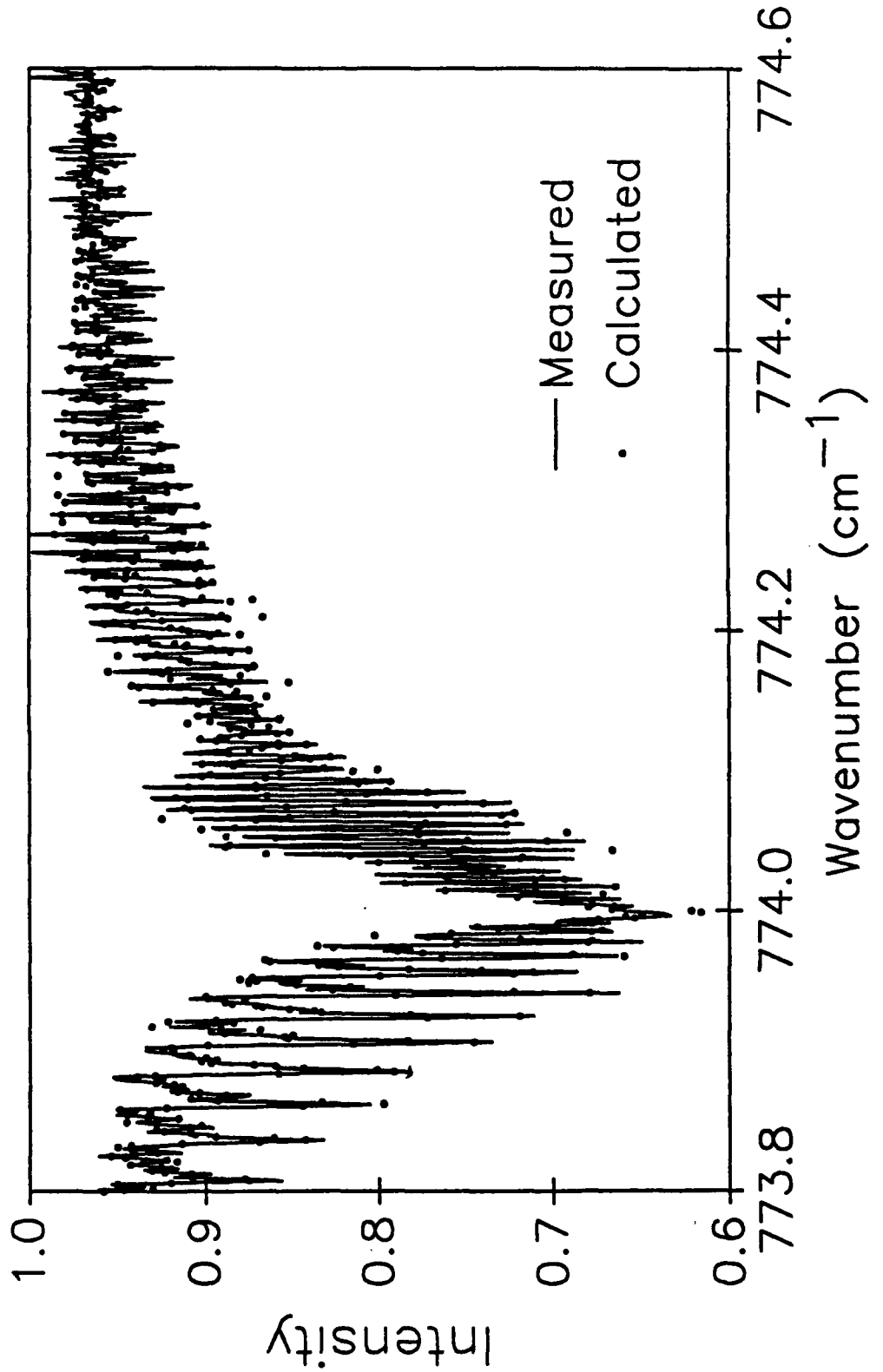
Intensity
1.0
0.9
0.8
0.7
0.6
773.8
774.0
774.2
774.4
774.6
Wavenumber (cm^{-1})
Measured
Calculated

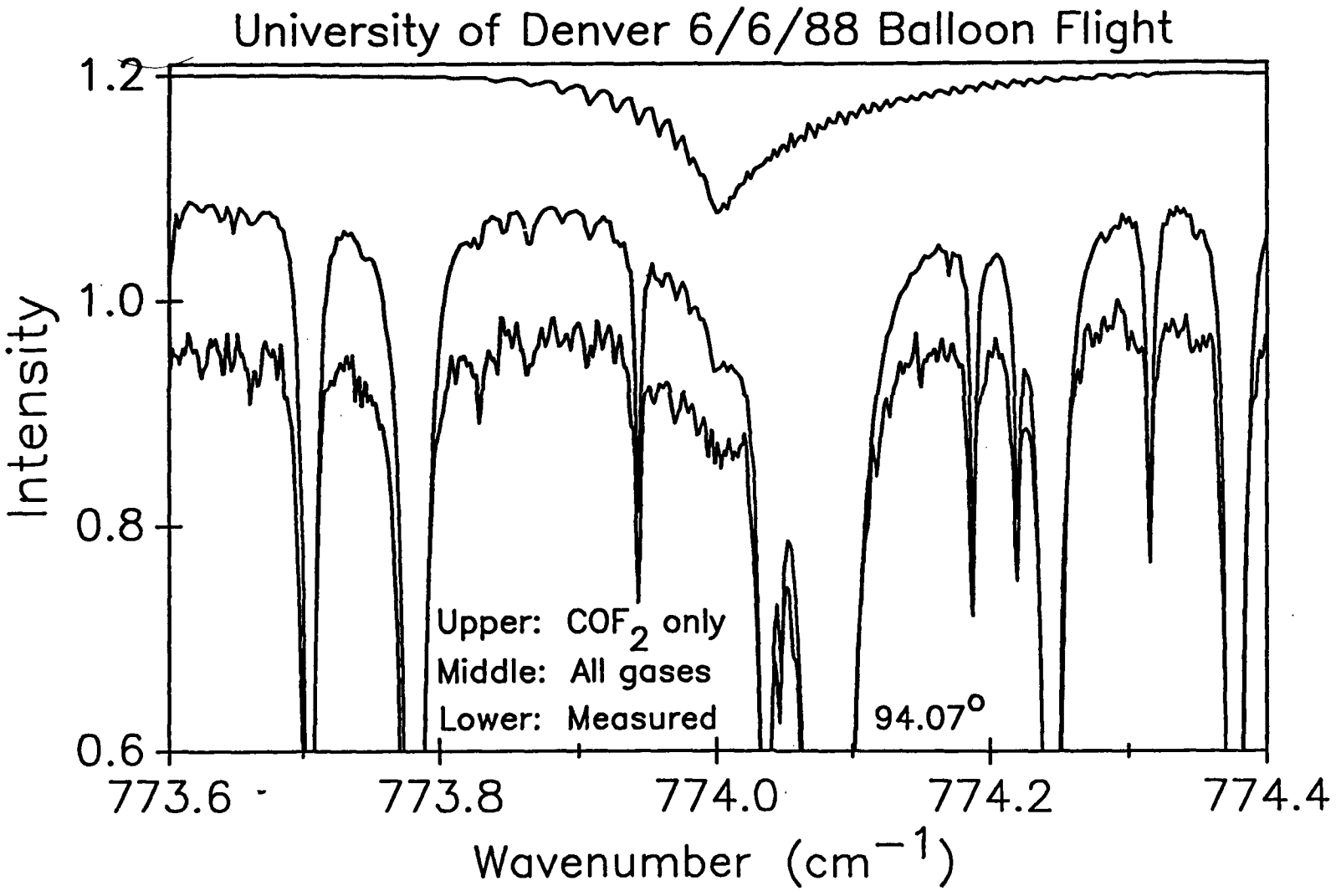
University of Denver 6/6/88 Balloon Flight
1.2
1.0
0.8
0.6
Intensity
222
Upper: COF2 only
Middle: All gases
Lower: Measured
94.07°
773.6
773.8
774.0
774.2
774.4
Wavenumber (cm−1)

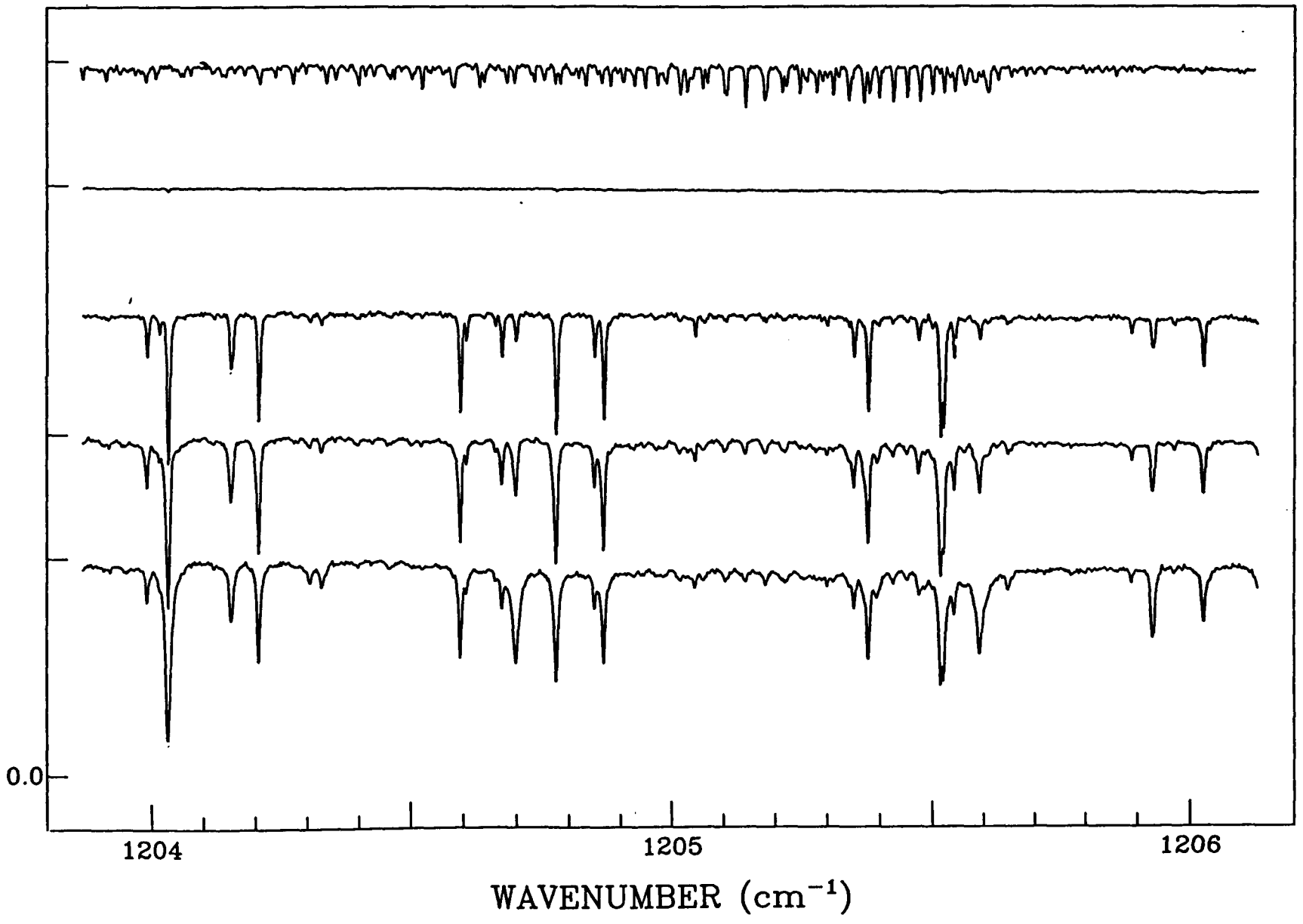
LAB HNO3 1.0 TORR 22CM CELL
6 JUNE 1988 36.9KM 68° 36.8KM 93.3° 36.6KM 94.1° 36.5KM 94.8°
SIGNAL
0.0
1204
1205
1206
WAVENUMBER (cm⁻¹)

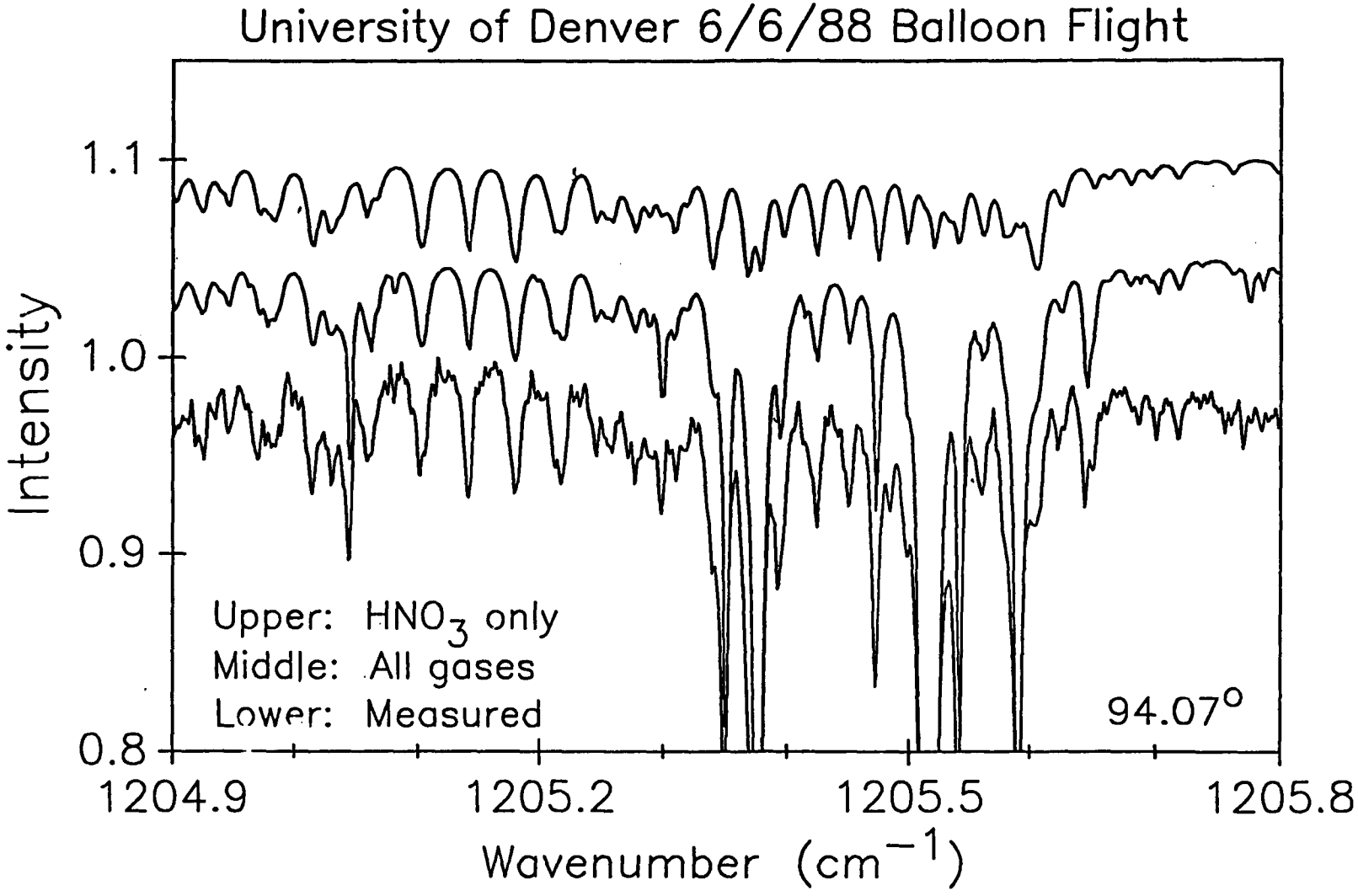
University of Denver 6/6/88 Balloon Flight
Intensity
1.1
1.0
0.9
0.8
Upper: HNO_3 only
Middle: All gases
Lower: Measured
94.07°
1204.9
1205.2
1205.5
1205.8
Wavenumber (cm^{-1})

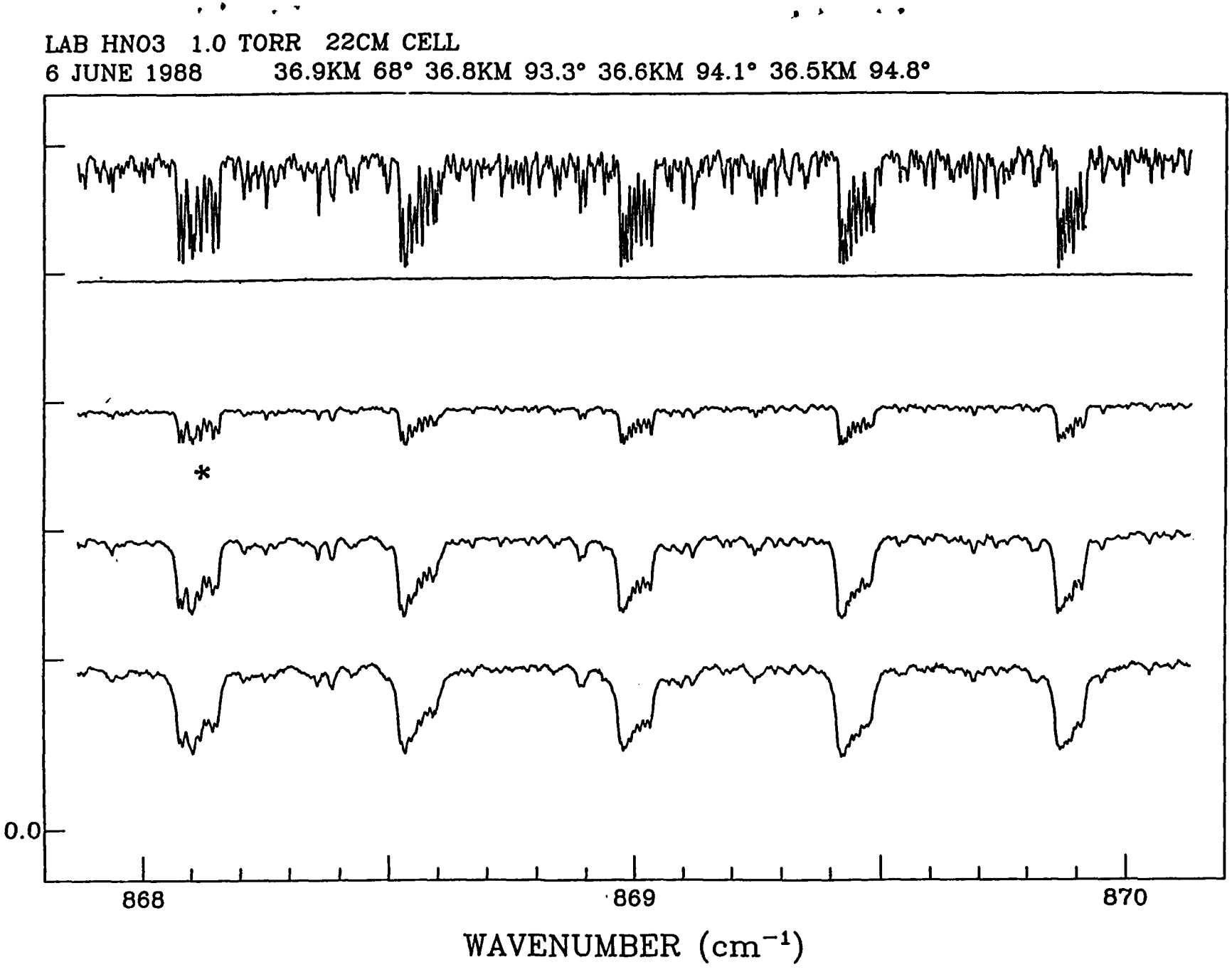
LAB HNO3 1.0 TORR 22CM CELL
6 JUNE 1988 36.9KM 68° 36.8KM 93.3° 36.6KM 94.1° 36.5KM 94.8°
SIGNAL
225
0.0
*
868
869
870
WAVENUMBER (cm^{-1})

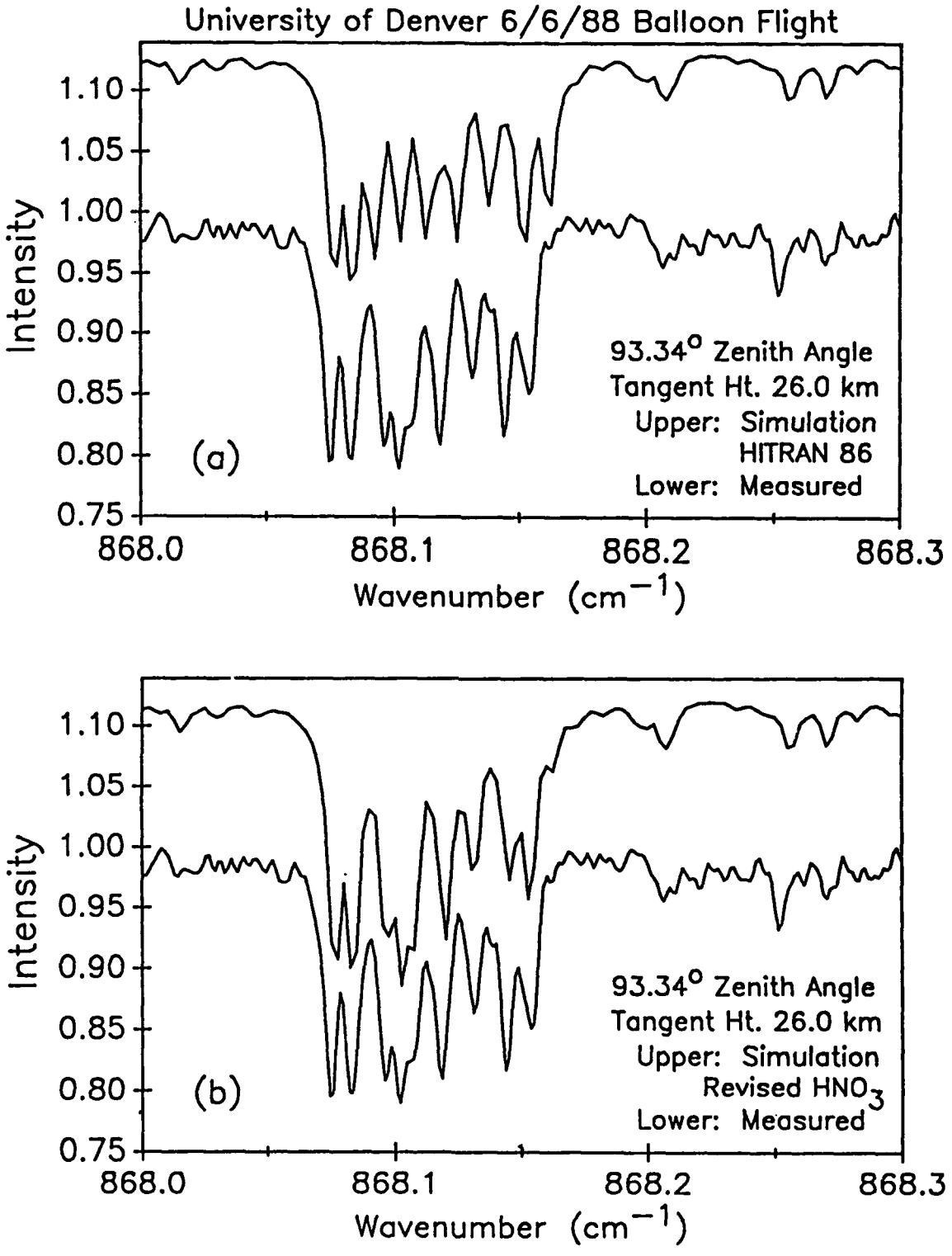
University of Denver 6/6/88 Balloon Flight
Intensity
1.10
1.05
1.00
0.95
0.90
0.85
0.80
0.75
(a)
93.34° Zenith Angle
Tangent Ht. 26.0 km
Upper: Simulation
HITRAN 86
Lower: Measured
868.0
868.1
868.2
868.3
Wavenumber (cm⁻¹)
Intensity
1.10
1.05
1.00
0.95
0.90
0.85
0.80
0.75
(b)
93.34° Zenith Angle
Tangent Ht. 26.0 km
Upper: Simulation
Revised HNO3
Lower: Measured
868.0
868.1
868.2
868.3
Wavenumber (cm⁻¹)

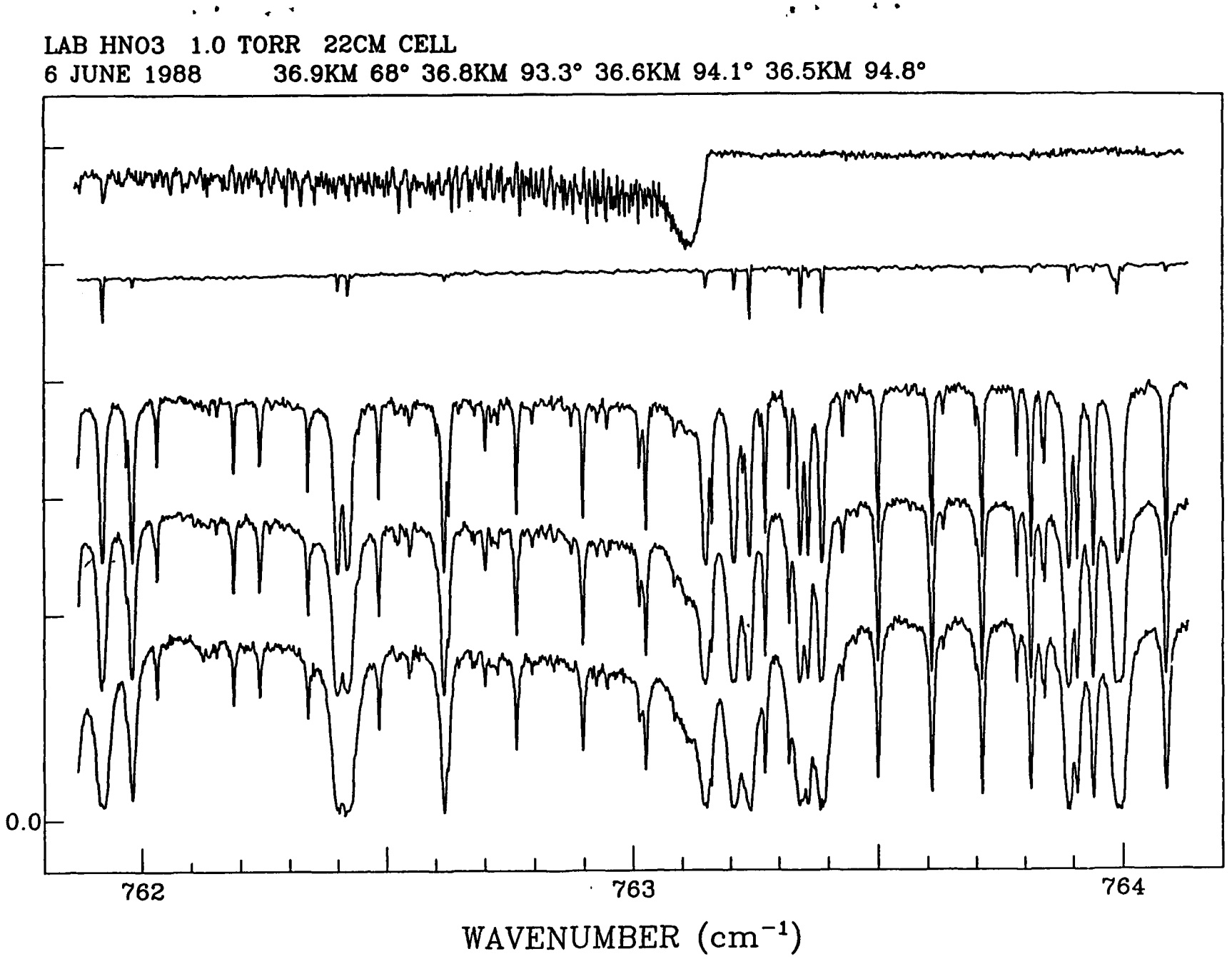
LAB HNO3 1.0 TORR 22CM CELL
6 JUNE 1988 36.9KM 68° 36.8KM 93.3° 36.6KM 94.1° 36.5KM 94.8°
SIGNAL
0.0
762
763
764
WAVENUMBER (cm^{-1})

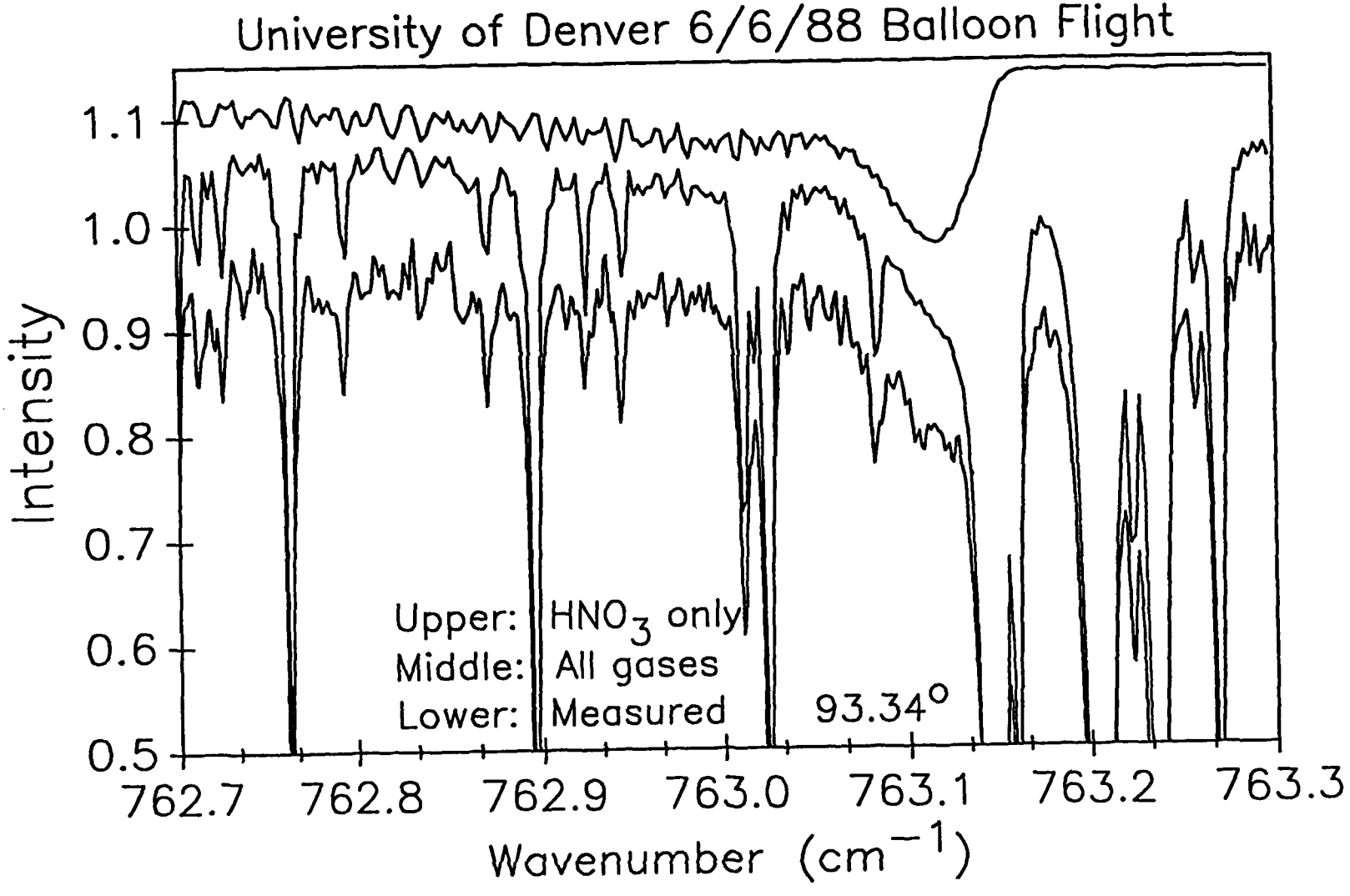
University of Denver 6/6/88 Balloon Flight
Intensity
1.1
1.0
0.9
0.8
0.7
0.6
0.5
Upper: HNO3 only
Middle: All gases
Lower: Measured
93.34°
762.7
762.8
762.9
763.0
763.1
763.2
763.3
Wavenumber (cm−1)

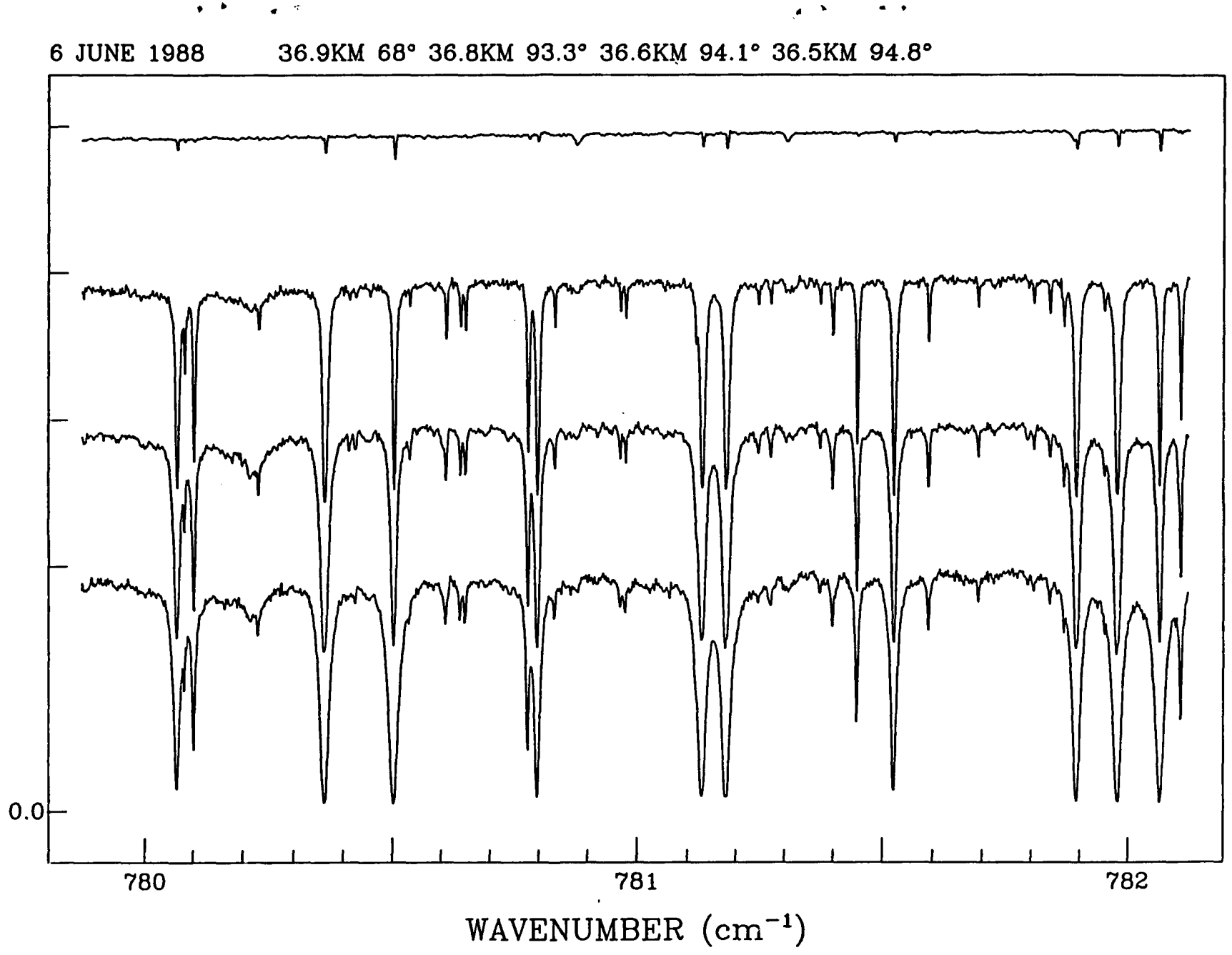
6 JUNE 1988 36.9KM 68° 36.8KM 93.3° 36.6KM 94.1° 36.5KM 94.8°
SIGNAL
0.0
780
781
782
WAVENUMBER (cm^{-1})

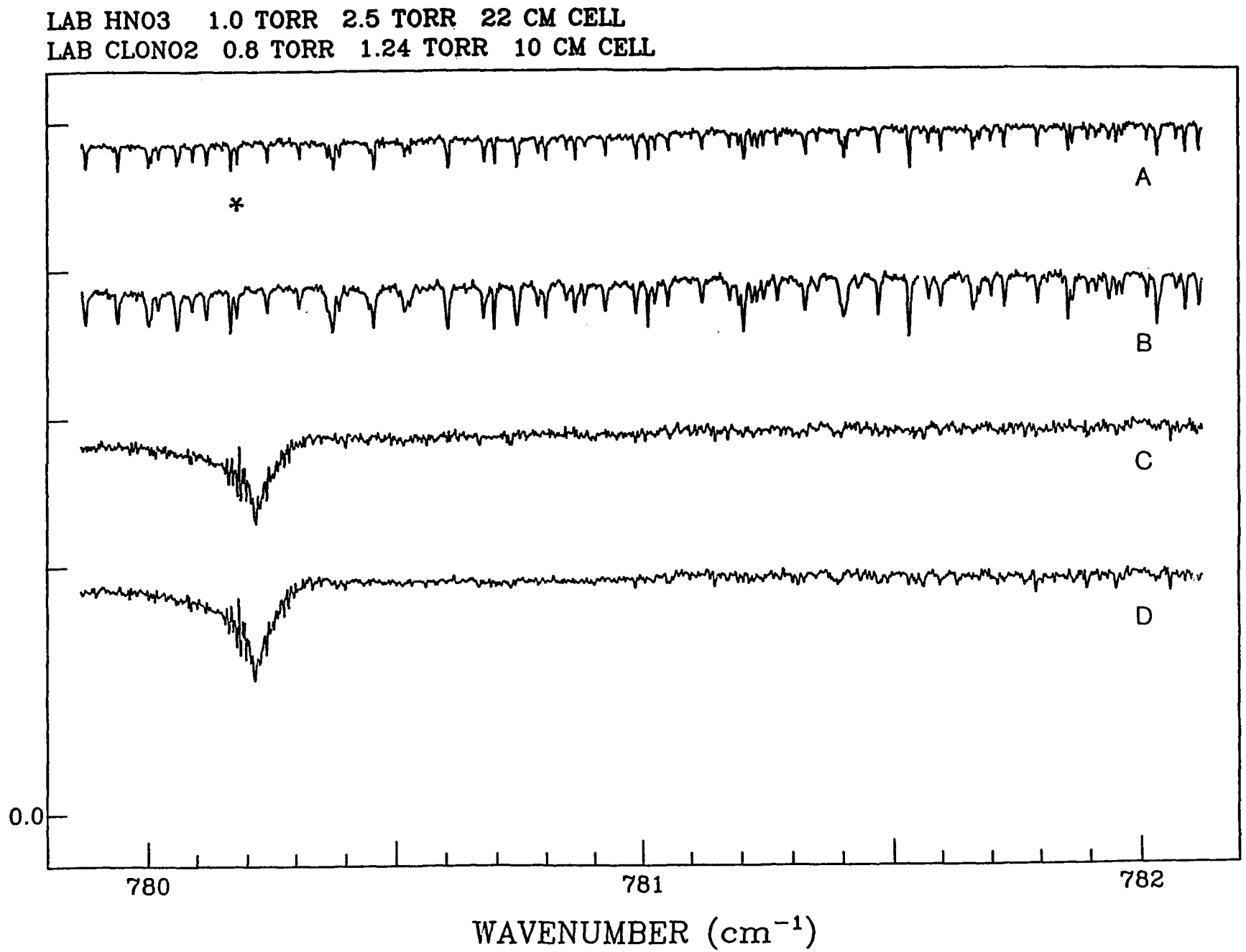
LAB HNO3 1.0 TORR 2.5 TORR 22 CM CELL
LAB CLONO2 0.8 TORR 1.24 TORR 10 CM CELL
A
B
C
D
*
SIGNAL
230
0.0
780
781
782
WAVENUMBER (cm^{-1})

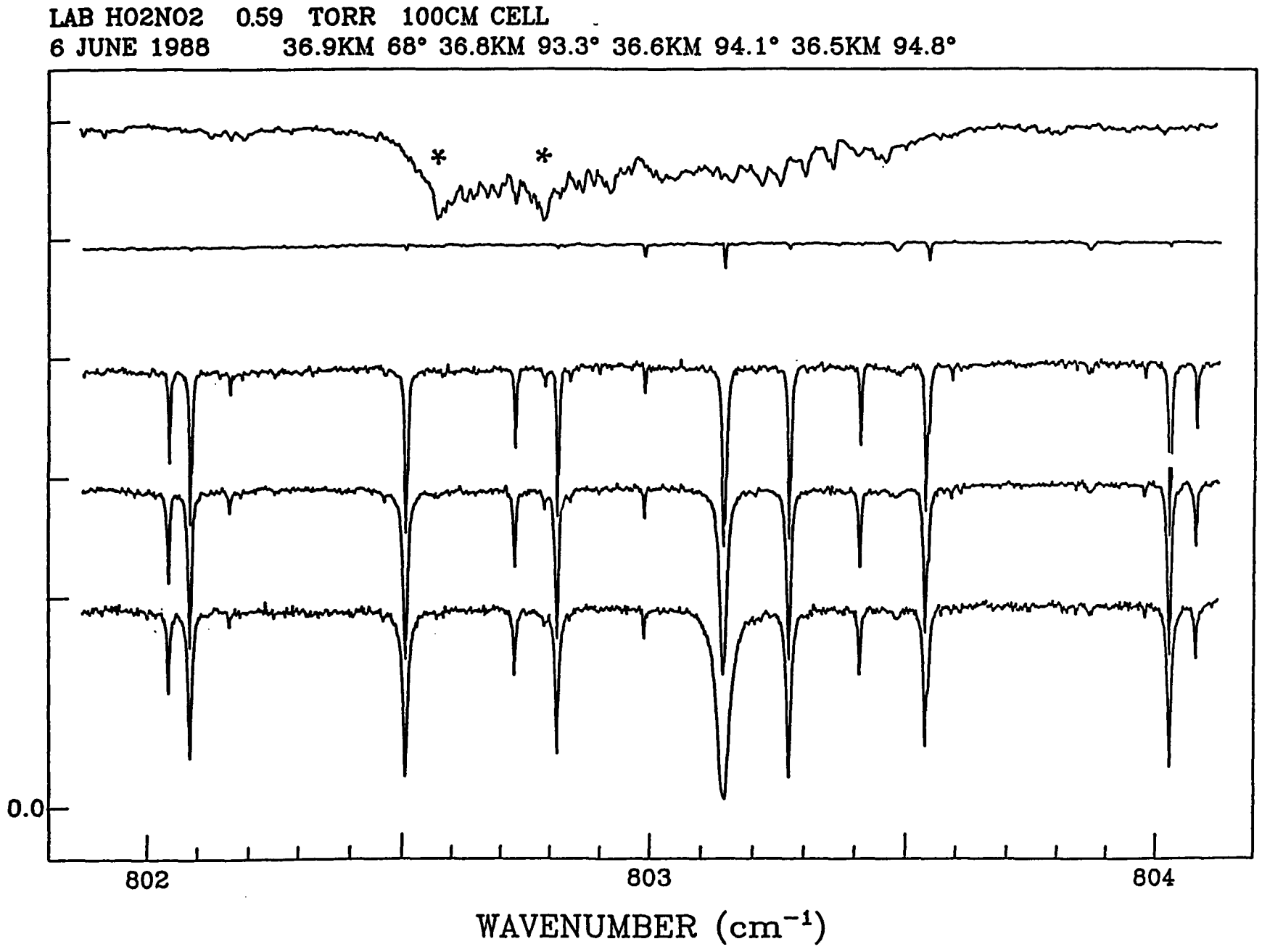
LAB H02N02 0.59 TORR 100CM CELL
6 JUNE 1988 36.9KM 68° 36.8KM 93.3° 36.6KM 94.1° 36.5KM 94.8°
SIGNAL
0.0
802
803
804
WAVENUMBER (cm⁻¹)

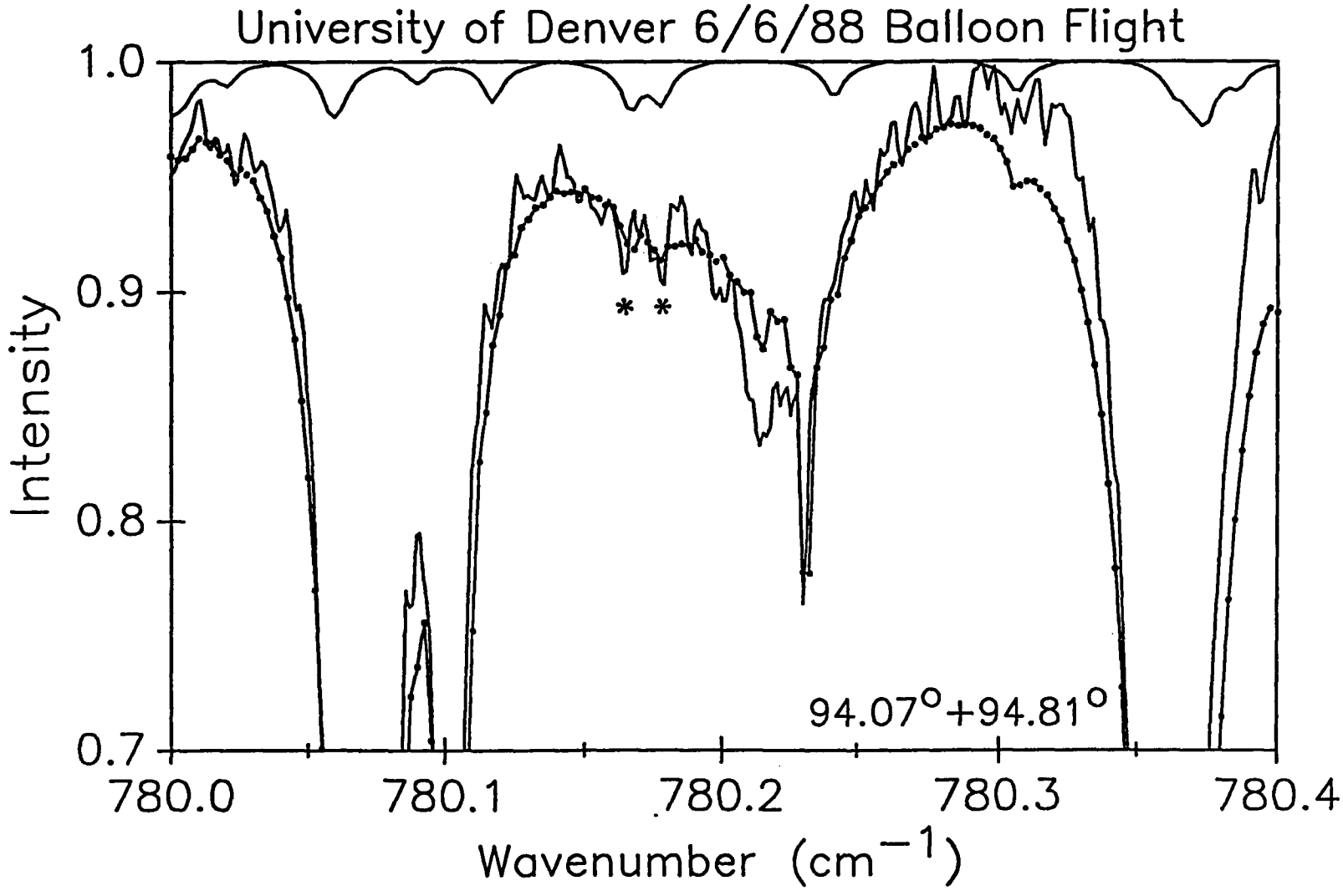
University of Denver 6/6/88 Balloon Flight
1.0
0.9
0.8
0.7
Intensity
* *
94.07°+94.81°
780.0
780.1
780.2
780.3
780.4
Wavenumber (cm^{-1})

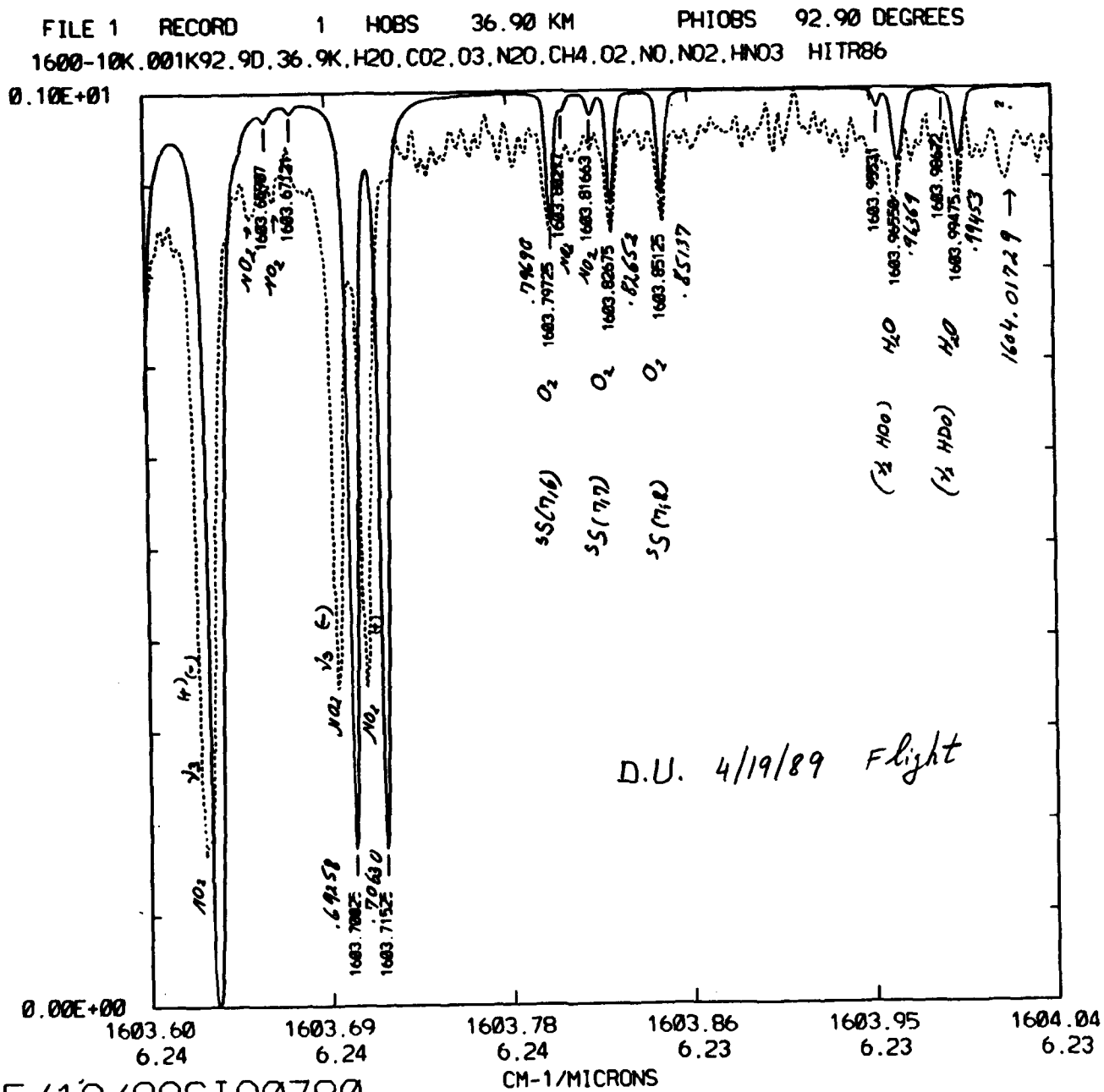
FILE 1 RECORD 1 HOBS 36.90 KM PHIOBS 92.90 DEGREES
1600-10K.001K92.9D.36.9K.H2O.CO2.O3.N2O.CH4.O2.NO.NO2.HNO3 HITR86
0.10E+01
0.00E+00
1603.60
6.24
1603.69
6.24
1603.78
6.24
1603.86
6.23
1603.95
6.23
1604.04
6.23
CM-1/MICRONS
D.U. 4/19/89 Flight
05/19/89SI00780

Conclusions

1. High resolution stratospheric spectra show many new spectral features

2. Several new sets of improved line parameters and cross sections are available and in progress

ADEOS SATELLITE SENSOR SENSITIVITY ESTIMATION USING THE FASCODE PROGRAM

Makoto Suzuki
T. Yokota
National Institute for Environmental Studies
16-2 Onogawa, Yatabe-Machi
Tsukuba-gun, Ibaraki 305
Japan

Shooichi Taguchi
National Research Institute for Pollution and Resources
16-3 Onogawa
Tsukuba-gun, Ibaraki 305
Japan

N. Takeuchi
National Institute for Environmental Studies
16-2 Onogawa, Yatabe-Machi
Tsukuba-gun, Ibarki 305
Japan

ADEOS Satellite Sensor Sensitivity Estimation using the FASCODE program

M.Suzuki,
T.Yokota,
S.Taguchi,*
and
N.Takeuchi,

National Institute for
Environmental Studies,
Environment Agency,

*National Research Institute for
Pollution and Resources,
MITI.

Abstract::

Ministry of International Trade and Industry (MITI) and Japan Environment Agency (J-EA) have proposed satelliite atmospheric sensors for the ADEOS (Advanced Earth Observation Satellite) to be launched in Feb 1995. MITI's proposal is based upon NADIR looking FTIR with 0.1 cm^{-1} resolution for the measurement of "greenhouse gases" in the troposphere. J-EA's poposal, ILAS, is based upon solar occultation measurement in the IR region for the ozone depletion in the stratosphere. This paper presents the current results on sensitovity analysis of both MITI's and J-EA's groups. The usage of FASCODE in Japan is very rare, eventually, we are the only active user of FASCOE in JAPAN.

ILAS Hardware Development Team

M.Suzuki, Y.Yokota, and N.Takeuchi,
National Institute for Environmental Studies
and
A.Matsuzaki
The Institute of Space and Astronautical Science.

The ILAS is officially come from Improved Limb Atmospheric Spectrometer, which is also meaning Infrared -LAS. The original "LAS" was flown in Feb 1984 mounted on EXOS-C, "Ohzora". Unfortunately, attitude control of Ohzora was missed 40 days after the launch, no conclusive results was reported for the LAS. The Ohzora was sun-spotting satellite with sun-asynchronized orbit. Several instruments were mounted on Ohzora most of which were targeted to the observation of stratosphere and mesosphere during the MAP campaign.

The LAS was based upon the solar occultation technique in the Infrared region. Three wave-length regions of LAS, 1.6-2.4μm, 2.8-4.8μm, and 8.8-10.2μm covered species H_2O, CO_2, CH_4, N_2O, O_3, and aerosol. Because the light scattering in the Infrared region is much weaker than the visible region, the inversion process of solar-occultation observation was supposed to be easy, which give the vertical profile of ozone in the stratosphere, 10-60 km altitude, together with the profile of other spices.

The principal feature of ILAS is the accurate and stable ozone trend monitoring. The ozone depletion in the mid-low latitude area has been slow, and previous satellite monitoring instruments, TOMS, SBUV, and SAGE I&II faced tough situations to certify their long term stability. Of these three instruments, SAGE-type instruments were proved to be most reliable, which is based upon its measurement technique, the solar occultation. Main reason of the stability of solar occultation is its self-calibration capability, since the 100% is observed by the direct view of sun and 0% is given by the deep space in each sun-rise or sun-set. The solar-occultation method of ILAS assures its long-term reliability. The use of Pyroelectric detector of ILAS, which works at room-temperature, assures the long life of instrument.

The second feature of ILAS is in its measuring wavelength in Infrared region. The SAGE I&II used visible wavelength, 600 nm, for the ozone measurement, where the scattering by aerosols and air is significant and multiple

scattering problem cause the difficulty in the inversion of vertical profile. Since the measurements are carried in the infrared region, the ILAS is insensitive against aerosols and Rayleigh scattering is negligible in those wavelengths. This gives the simplicity in the inversion problem of ILAS observation.

The third feature of ILAS is in its coverage of species. Currently seven spices are targeted in ILAS project, O_3, HNO_3, NO_2, N_2O, H_2O, CH_4, and CO_2. Temperature, density and aerosol will be measured together. Although no Clx species is included, these combined observation will provide the adequate informations about the chemical-dynamical phenomena on-going in the stratosphere.

ADEOS

Feb 1995, by H-II Rocket
Sun-synchronized orbit 800km

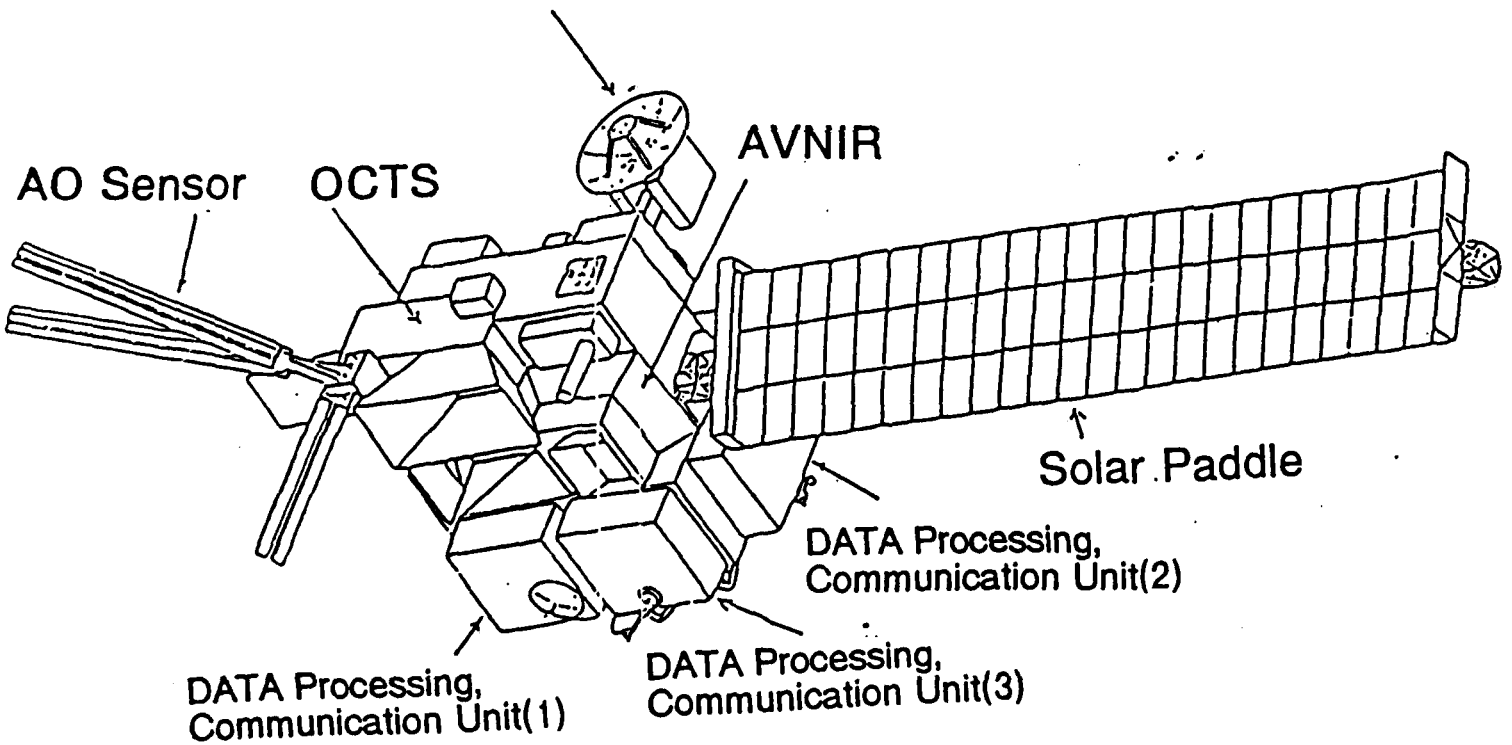

ADEOS Specification

Launch	Feb 1995
Weight	2.8 t
Payload	>0.8 t
Orbit	quasi-Sun synchronized
	41 days period
	800 km
	98.6deg.inclination
Life	3 years
Power	3.5 KW (EOL)

The specification of ADEOS satellite are as follows: the ADEOS will be launched on Feb 1st, 1995, the first launch using new H-II type rocket. The total payload will be 0.8 t or more. The orbit is quasi-Sun synchronized with 41 days period, 800 km altitude, and 98.6 deg. inclination. The life of the spacecraft is 3 years in nominal which is determined by the life of battery in full power operation, 3.5 KW at the end of life. Fewer instruments can be operated after 3 years.

ADEOS proposed sensors

OCTS Ocean Color & Temperature Spectrometer

AVNIR Advanced Visible & NearInfraredRadiometer

NSCAT NASAScatterometer

TOMS Total Ozone Mapping Spectrometer

POLDER Polarization & Bidirectionality of Earth's Surface

MITI-NADIR-FTIR Infrared Mapper for Greenhouse Gases

ILAS Improved Limb Atmospheric Spectrometer

Retro-Reflector

Eight instruments are considered to be mounted on ILAS. Two come from NASDA itself, OCTS and AVNIR targeted to ground and ocean surface. Two other instruments come from NASA, one of them is TOMS, total ozone mapping spectrometer. And one french instruments also will be mounted. Three Japanese instruments for atmospheric instruments, which are presented in this paper. Japan Environment Agency also has plan to mount a retro-reflector for long range absorption experiment, from ground to space and back-to ground. TOMS and ILAS are supposed to collaborate to give more accurate total ozone value at polar region.

LAS

Limb Atmospheric infrared Spectrometor

Institute of Space and Astronoutical Science

Dr. A. Matsuzaki,
Dr. T. Itoh, and
Dr. Y. Nakamura

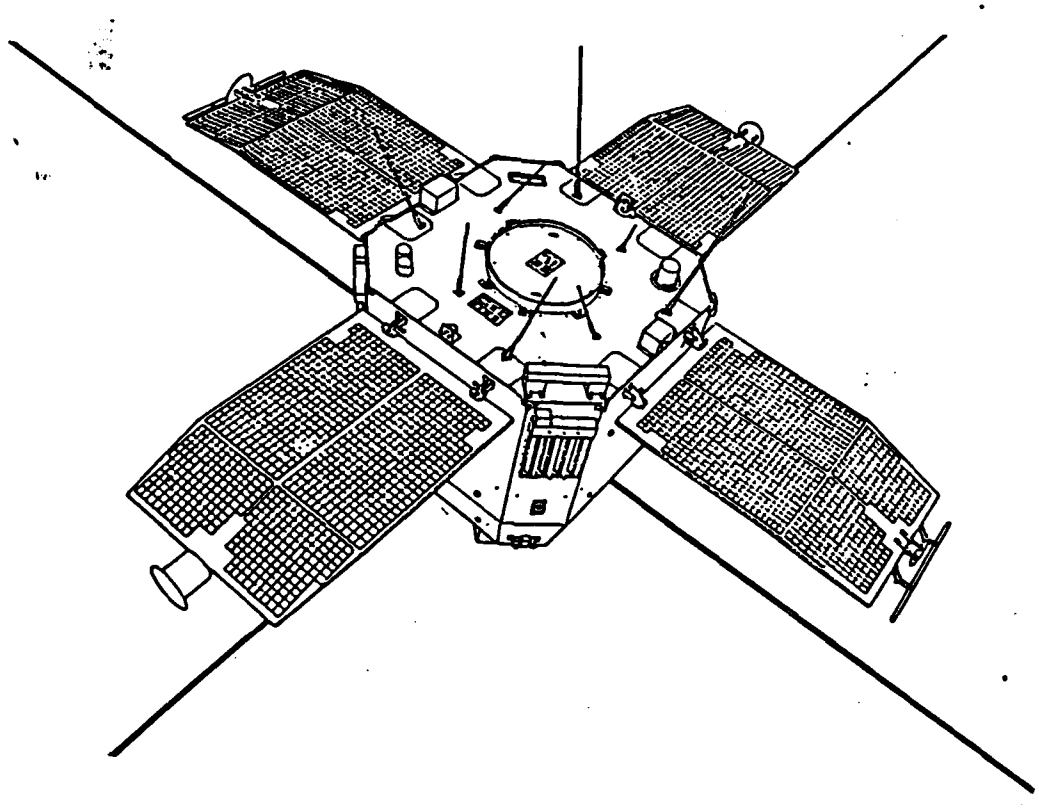

EXOS-C

The wavelength ranges for the LAS observation

range	wavelength	sensor	constituents
1	1.6-2.4 μm	32 ele. LiTaO3	H2O, aerosol
2	2.8-4.8 μm	64 ele. LiTaO3	CO2, CH4, N2O, H2O aerosol
3	8.8-10.2 μm	16 ele. PbTiO3	O3

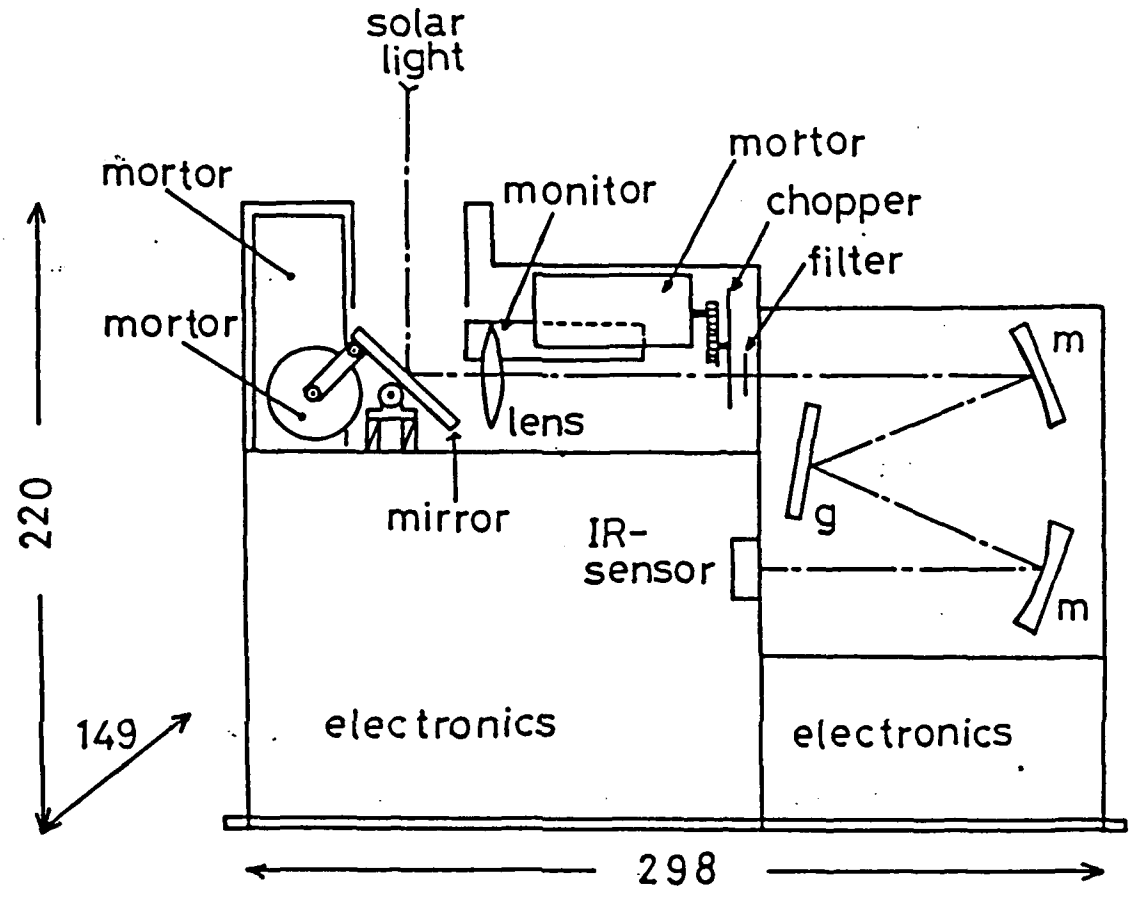

LAS Sensor Head

Targets and Requirements, ILAS

Ozone Trend
Ozone Hall

Sensitivity and long term stability
Temperature
Aerosol
Chemical spices
- HNO_3, NO_2,
- N_2O,
- CH_4, H_2O

ILAS Specification

Observation

Observing height	10-60 km
Vertical resolution	2 km
Latitude	N56-70 deg.
	S63-88 deg.

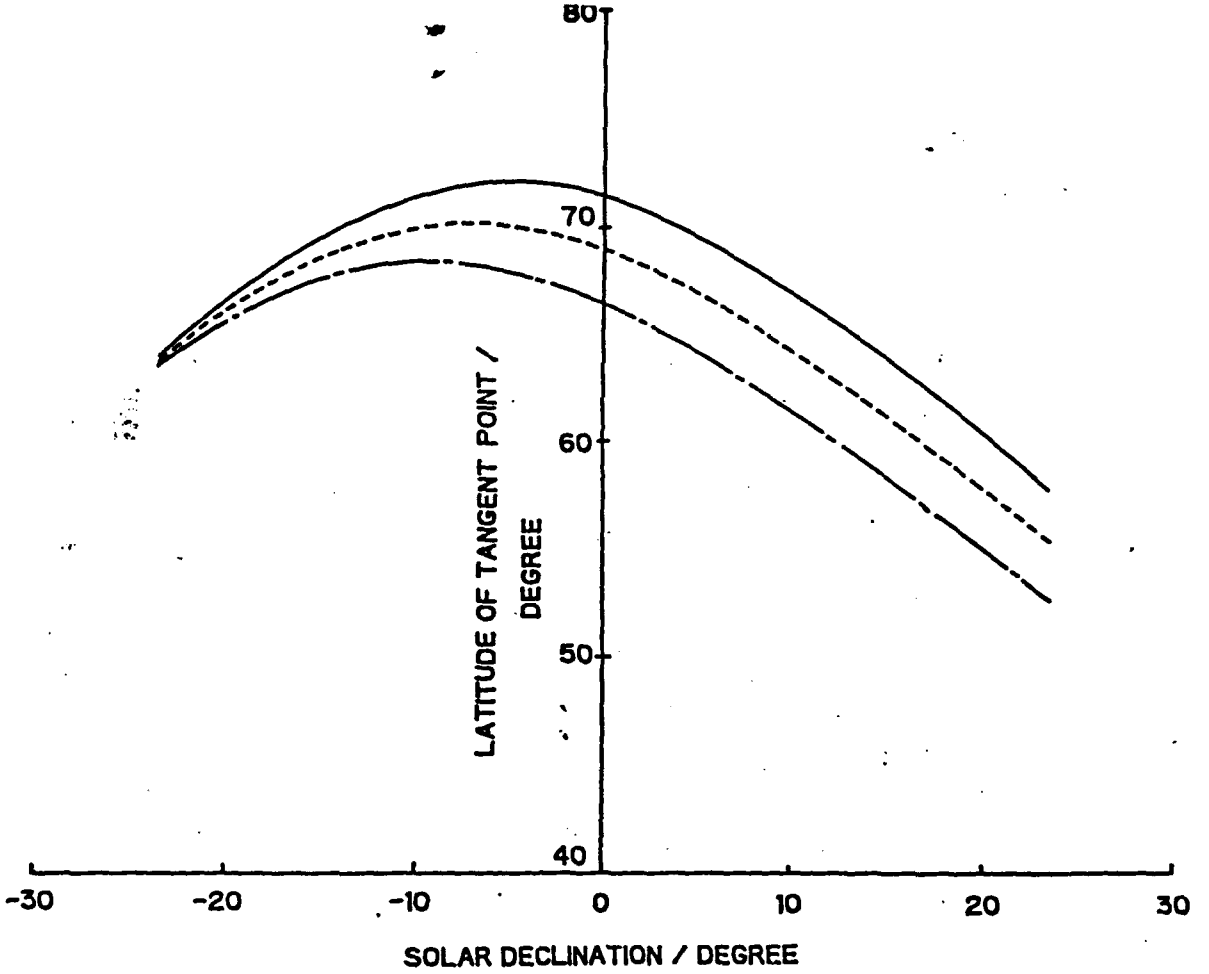
80
70
60
50
40
LATITUDE OF TANGENT POINT / DEGREE
-30
-20
-10
0
10
20
30
SOLAR DECLINATION / DEGREE

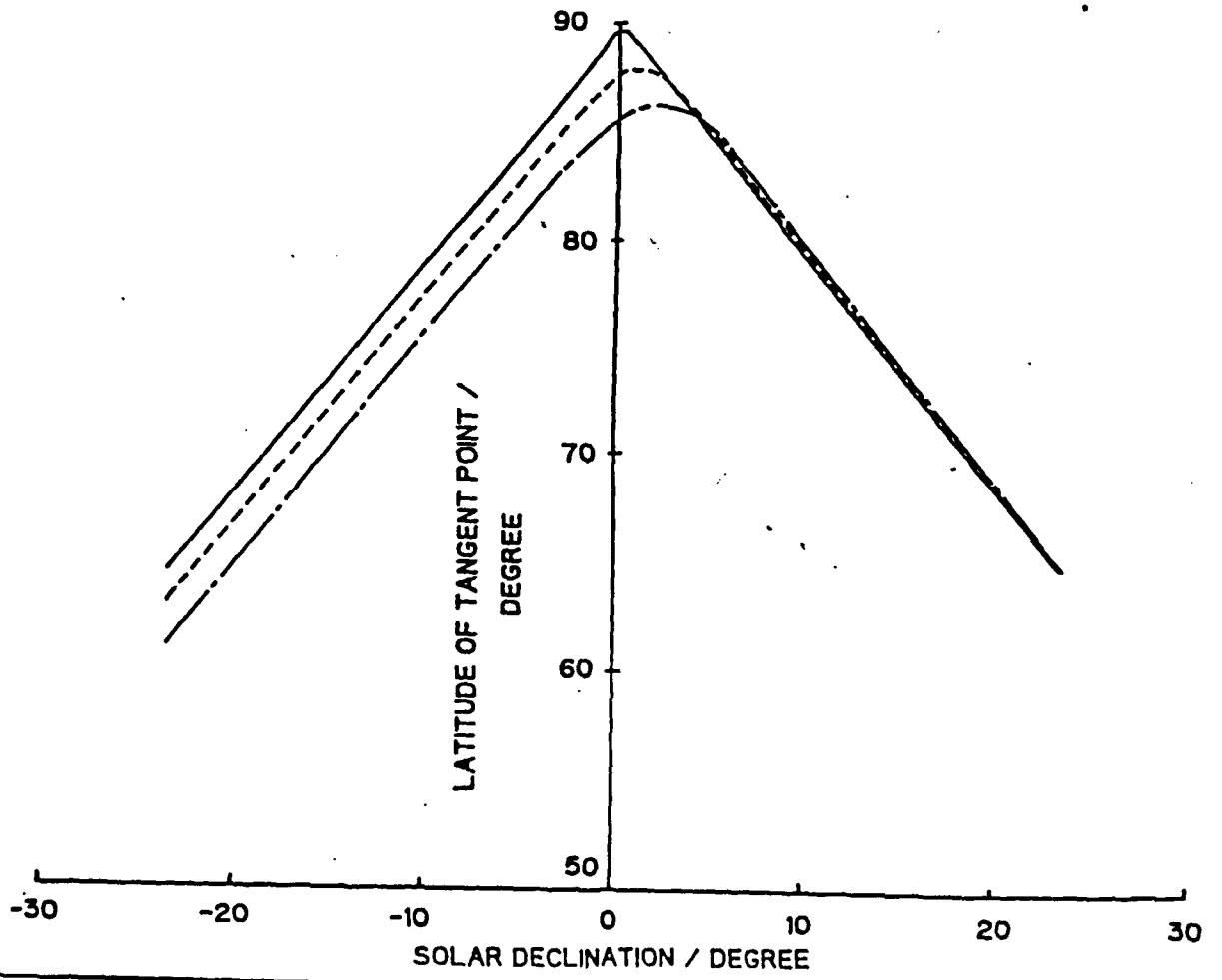
90
80
70
60
50
LATITUDE OF TANGENT POINT / DEGREE
-30
-20
-10
0
10
20
30
SOLAR DECLINATION / DEGREE

ILAS Spcification

Design Target

	ILAS	GLS (GOMR)
Obs. Height	10-60km	10-60km
O_3 Acc.	<10%	<10%
Stab.		<0.5%
Obs. Lat.	NS60-80	N80 to S80
Temp	1K acc.	1K acc., 0.2K res.
Aerosol	yes	yes
H_2O	yes	yes(Tropo. to Strato.)
NO_2	may be	<20%
HNO_3	yes	<25%
N_2O	yes	<25%
CH_4	yes	<25%

ILAS Specification

Wavelength and Targets

	cm^{-1}	Spices
ch1	850-1370 16cm^{-1}	O_3,HNO_3,CH_4, N_2O,H_2O
ch2	1450-2410 30 cm^{-1}	O_3,N_2O,CO_2, NO_2,H_2O
ch3	753-784nm 1000pixels	Temp. Dens. & Aerosol

The targets of ILAS are carefully selected to cover the long-term trend of ozone and to study the ozone hole phenomena. Two infrared channels cover the region, 850-2410 cm^{-1}, which includes most major species related to ozone depletion such as O_3, HNO_3, and NO_2. Temperature drop and subsequent Polar Stratospheric Clouds formation is considered to trigger the ozone hole, the temperature and aerosol measurements is useful for the ozone hole study. The temperature and density measurements is also help to identify the chemistry from dynamics where is happening, which should be useful to the long-term observation.

The spectral resolution of ILAS in the infrared region is poor, 16-30 cm^{-1} per pixels, but ILAS targets the main components which have broad and strong absorption band. Someone might worry about the resolution of CH_4, N_2O, and H2O around 1300 cm^{-1}. We will measure the H_2O and N_2O at ch2 starting from 1450 cm^{-1} which will give us more accurate concentrations of them. Then applying these concentration to the bands around 1300 cm^{-1} and it can be solved about methane. Following two figures depicts the calculated transmission by FASCODE, one is at 0.01 cm^{-1} resolution from 10-50 km tangent height, and the other is at the 1160-1400 cm^{-1} region in 20 cm^{-1} resolution at 30 km.

Detector

Pyroelectric Array
32 Elements
0.3nm/$Hz^{1/2}$
$PbTiO_3$
0.38 x 2 x 0.03 mm

0.4 mm x 2 mm = 2 arc min x 10 arc min
= 2 km altitude x 10 km horizontal
320 V/W

The infrared detector of ILAS are Pyroelectric array detector. The detector is made of PbTiO3 which will be produced one of the subsidiary of Panasonic. The array has 32 pixels to cover the spectral region, and each pixel coincide to the view area, 2 km altitude and 10 km horizontal. The main drawback of choosing the Pyroelectric detector is its poor sensitivity, but our sensitivity analysis shows which is enough to get the proper vertical profile. The main reason choosing the Pyroelectric detector is, it does not need any cryogenic cooling, which gives longer lifetime to the ILAS instrument necessary for the ozone trend monitoring. The chopper frequency is 15 Hz. Out puts of the detectors are connected parallel to separate lock-in amplifiers, those time constant is about 1 sec, or 1 km altitude during the observation. This means the ILAS simply track the Sun and not scan over the solar disk, the ILAS will track the radiometric-center of Sun with proper indicator of viewing point on the solar disk.

Detector

Pyroelectric Array

32 Elements

0.3 $nW/Hz^{1/2}$

$PbTiO_3$

0.38 x 2 x 0.03 mm

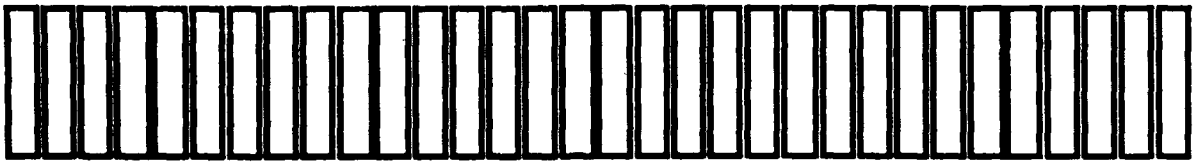

0.4 mm pitch

320 V/W

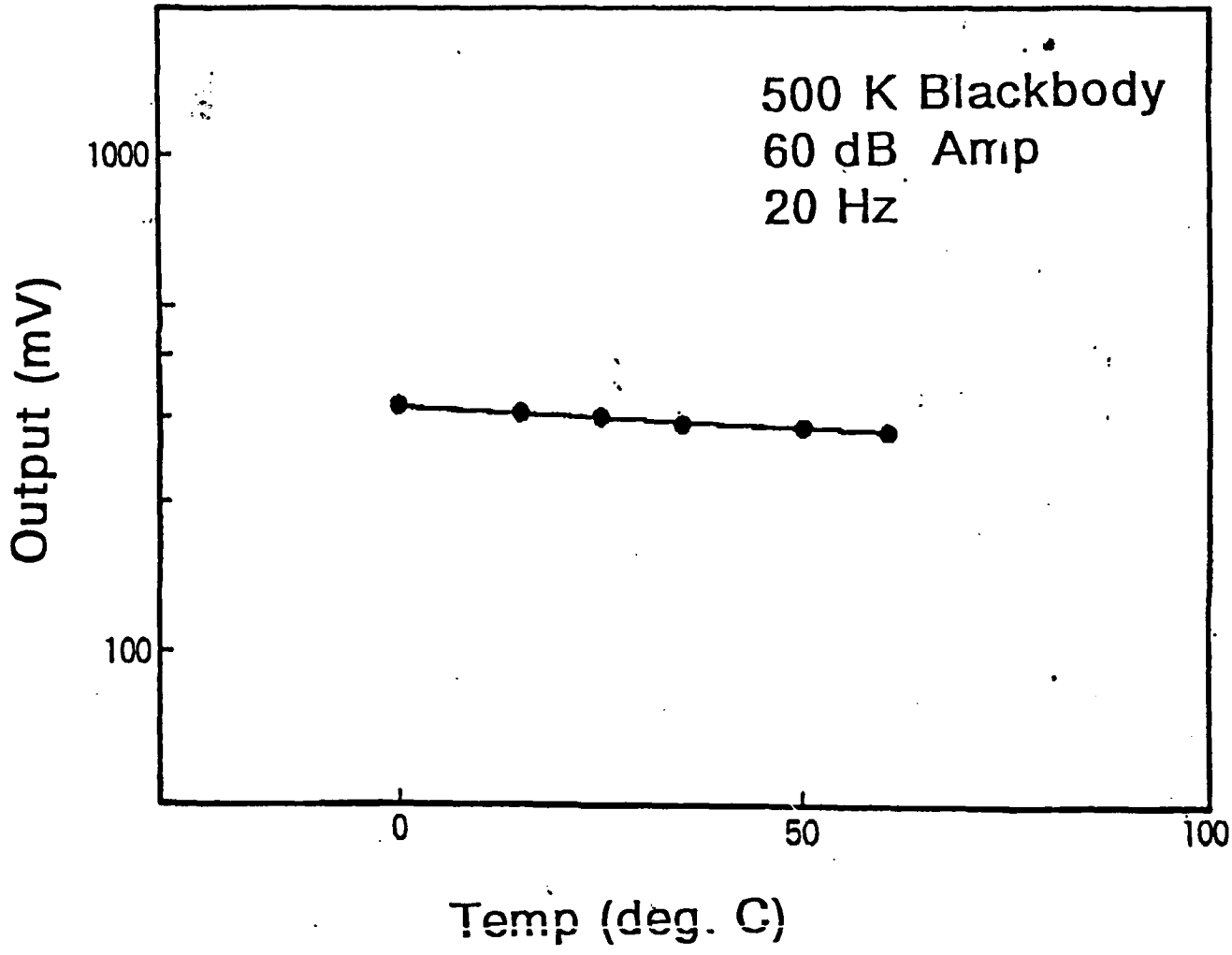

Temperature Dependence of
16-elements PLA detector

ILAS Specification

Optics and Monochrometer

Monochrometer

F=6.6
f=100 mm
Czerny-TurnerType
Slit 0.4 x 2 mm

Telescope

ClassicalCassegraintype
f=660 mm
D=100 mm

The instrument of ILAS is consist of a Sun-tracking mirror, a telescope, a chopper, a monochrometer, and a detector. The monochrometer is a simple Czerny-Turner type, which slit size coincides to that of the detector pixel and the view area. Currently, the telescope is classical cassegrain type with a diameter, 100 mm.

The next drawing shows the preliminary ILAS, which simply an arrangement of specified parts without any size reducing effort. Fortunately, we got a foot-print 775x705 mm with 540 mm height for each head. Total weight is 95 kg, and Power is 120W at maximum.

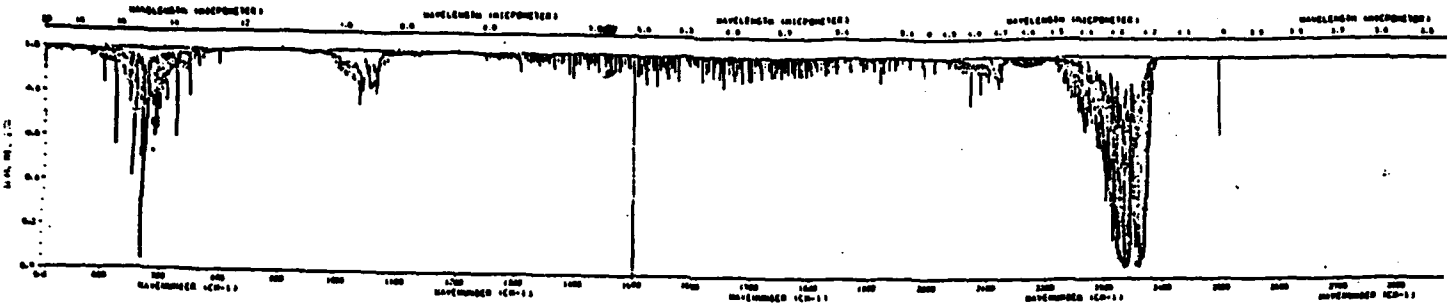

TH = 50 K

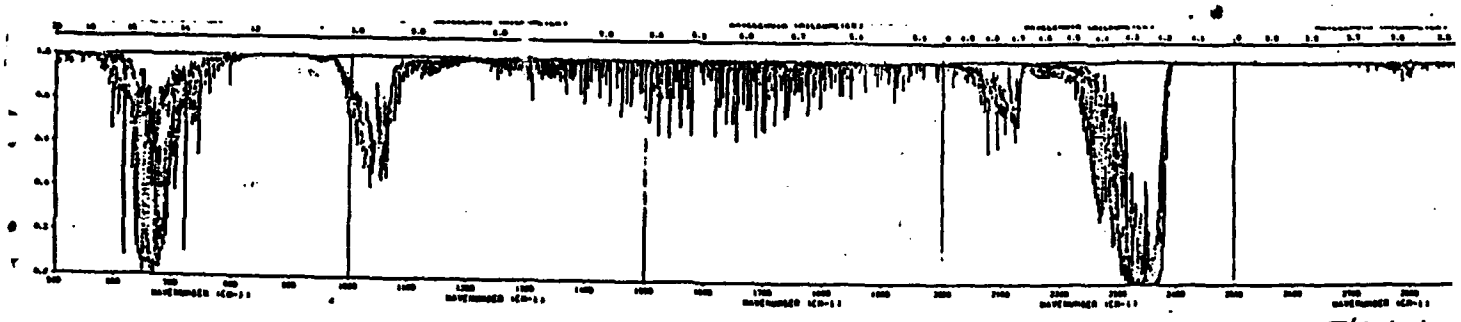

TH = 40 K

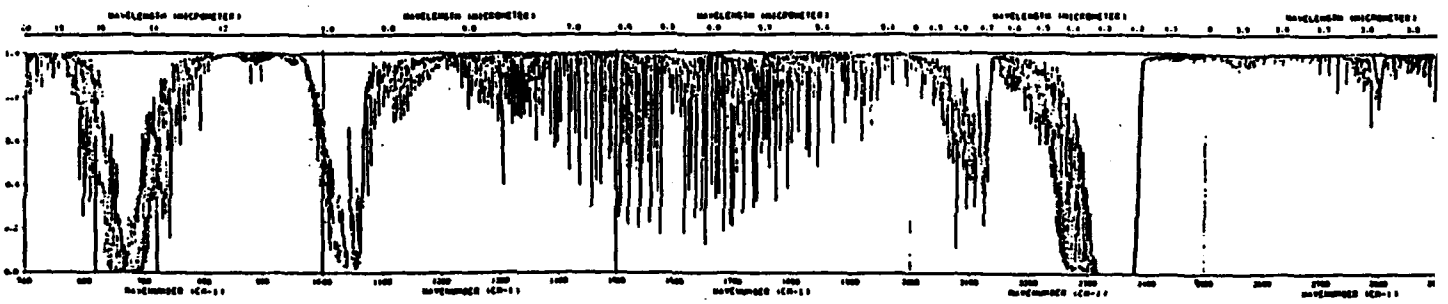

TH = 30 K

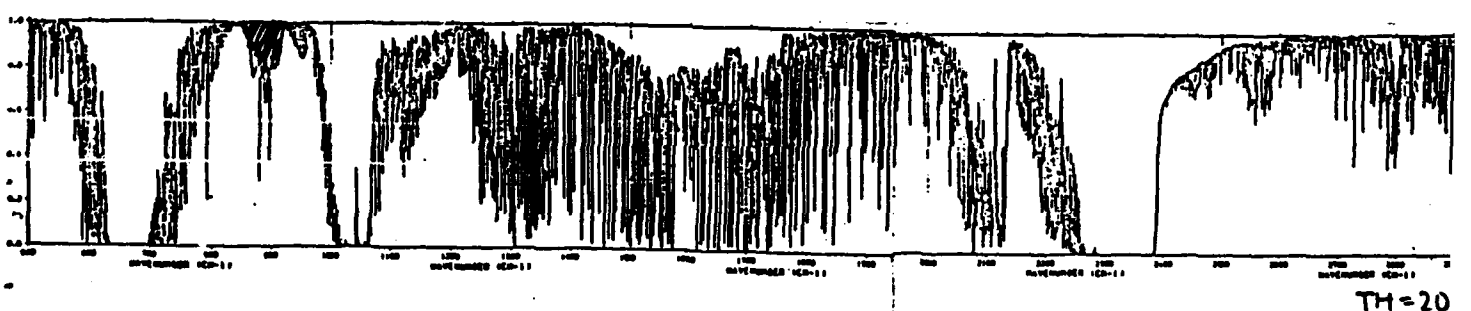

TH = 20

HNO_3

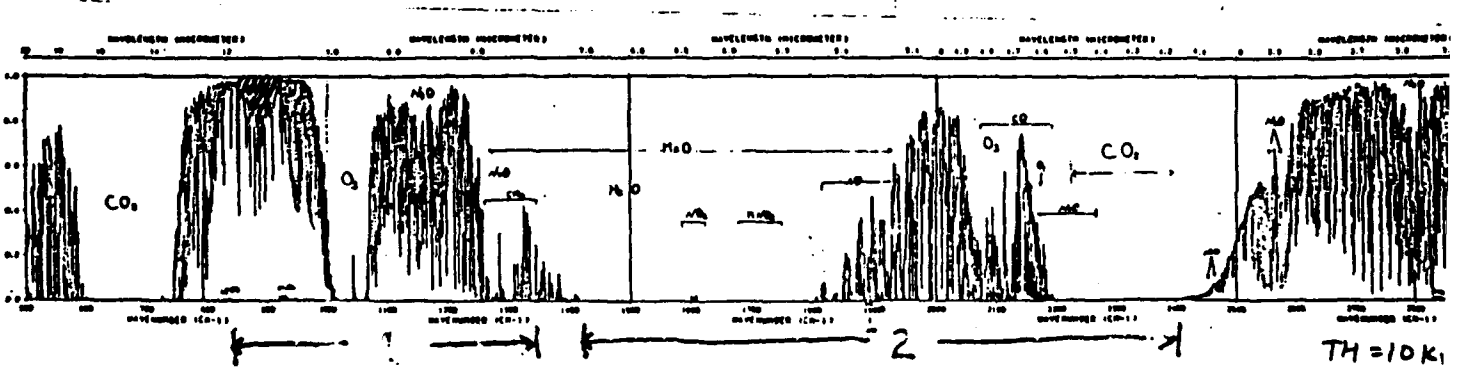

TH = 10 K

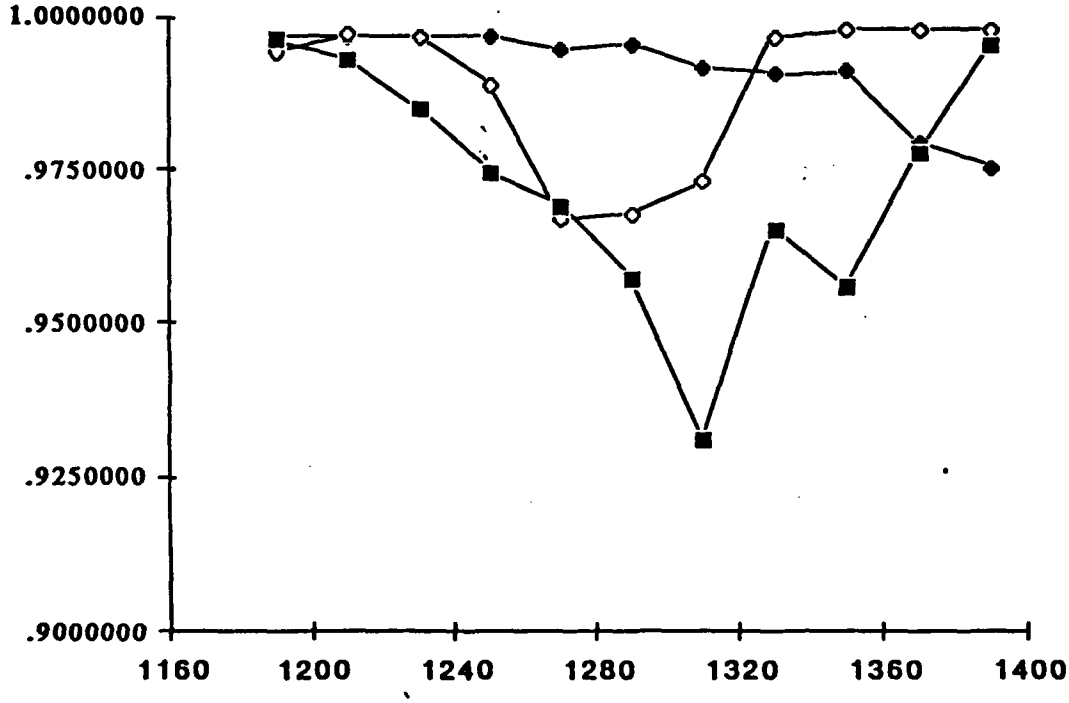
1.0000000
.9750000
.9500000
.9250000
.9000000
1160
1200
1240
1280
1320
1360
1400

Following several figures show the Signal to Noise estimation of ILAS using FASCODE. To reduce the computation load, the calculation was carried for 20 and 30 km altitude 300 km horizontal path, which give almost same transmissionspectra.

The basic parameters are

NEP of detector	$0.3 nW/Hz^{1/2}$
Accumulation	1/15 sec
Telescope	100 mm ø
Opticaleff.	0.1
view angle	2 arc min x 10 arc min

using these parameters and given solar spectral power, the SN in vacuum can be calculated easily. FASCODE tells us the transmission at desired wavelength, thus the optical SN at the target region can be calculated. The optical SN does not mean the SN in concentration, thus we estimated the SN in concentration as,

$SN_{conc} = SN_{opt}$ x optical depth.

By these calculation, the SN ratio for HNO_3 is a little bit poor but other components can be measured at SN>1000 after 1 sec integration which resembles the 1 km vertical resolution from the spacecraft.

The FASCODE is powerful and very useful for these kind of estimation, but if it can provide the 1 % accuracy for these spectral regions, it will really help us.

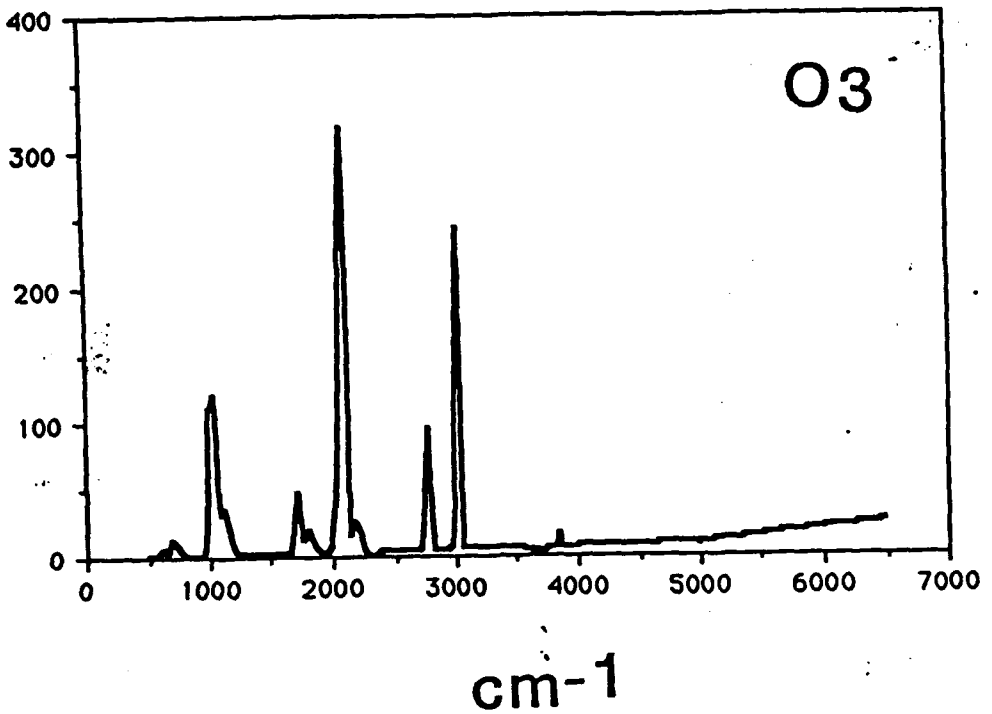

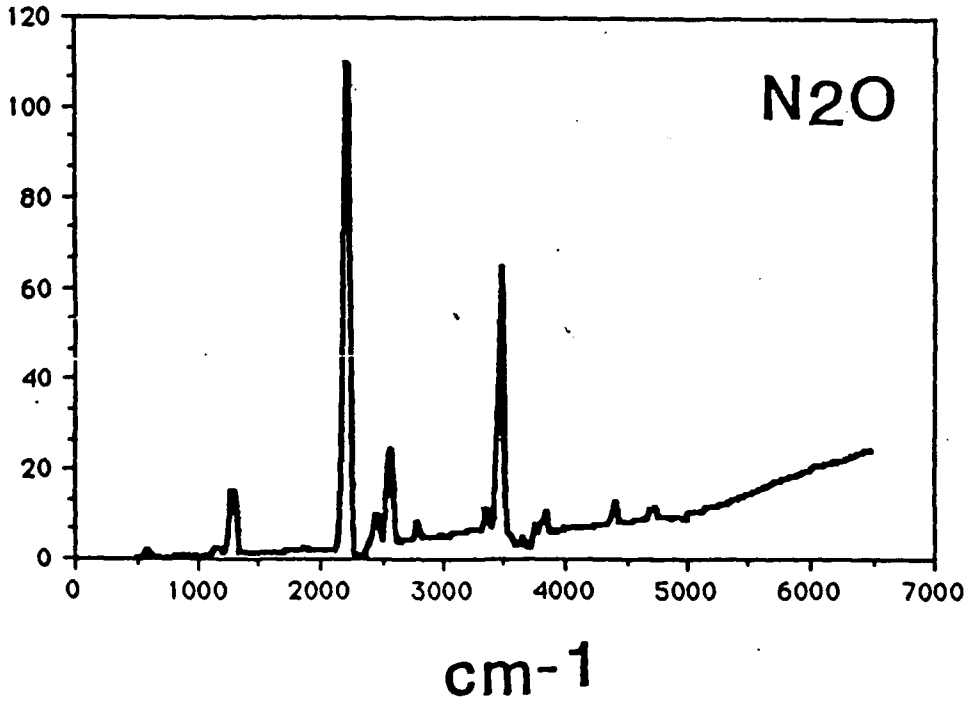

Estimated SN H=30km

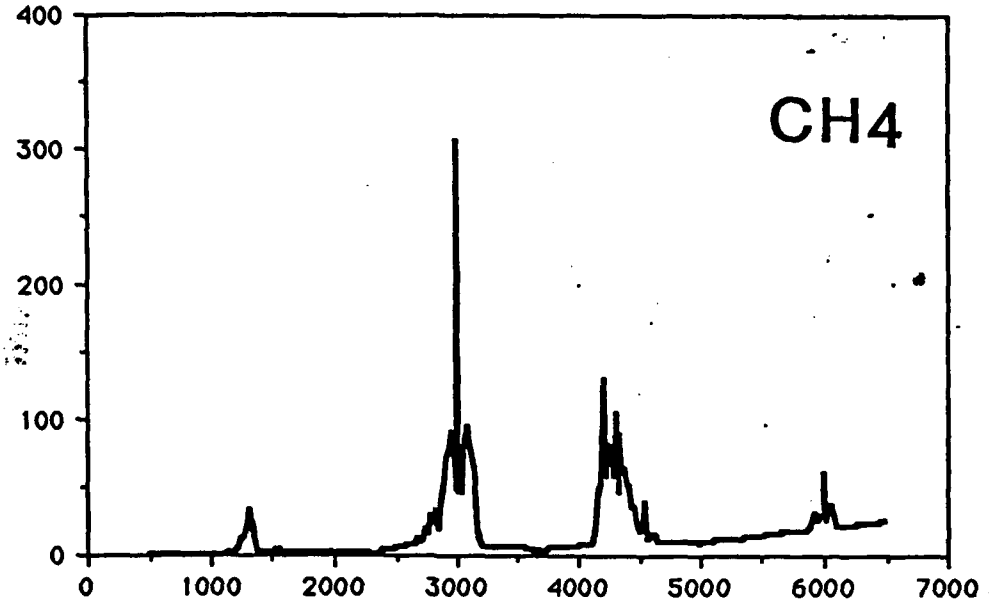

cm-1

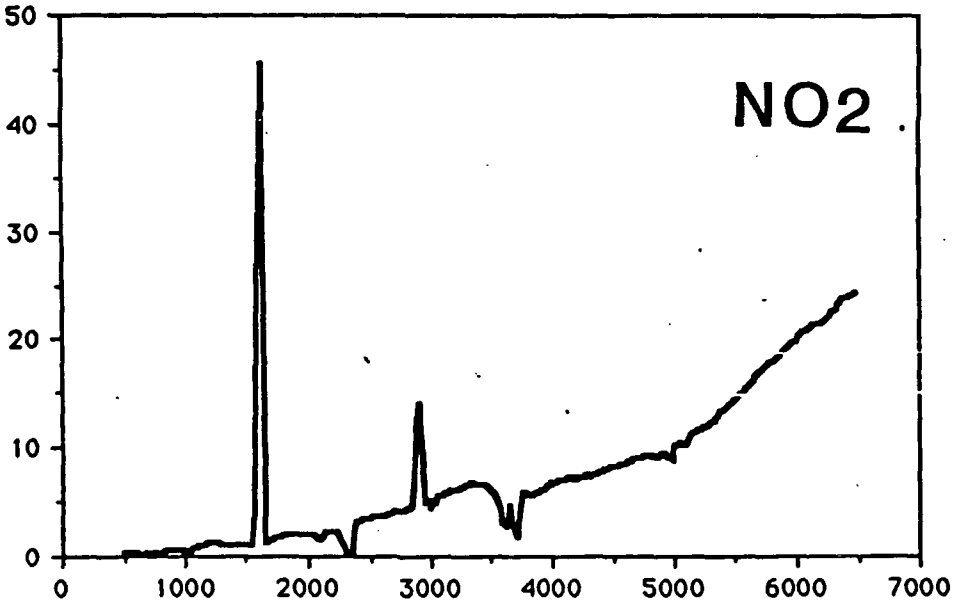

cm-1

Estimated SN H=30km

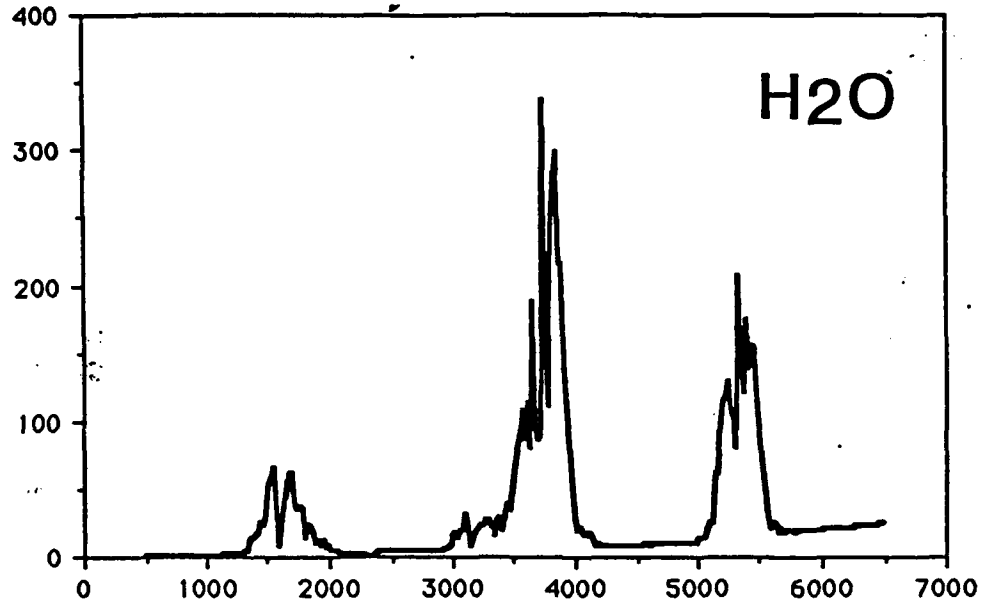

cm-1

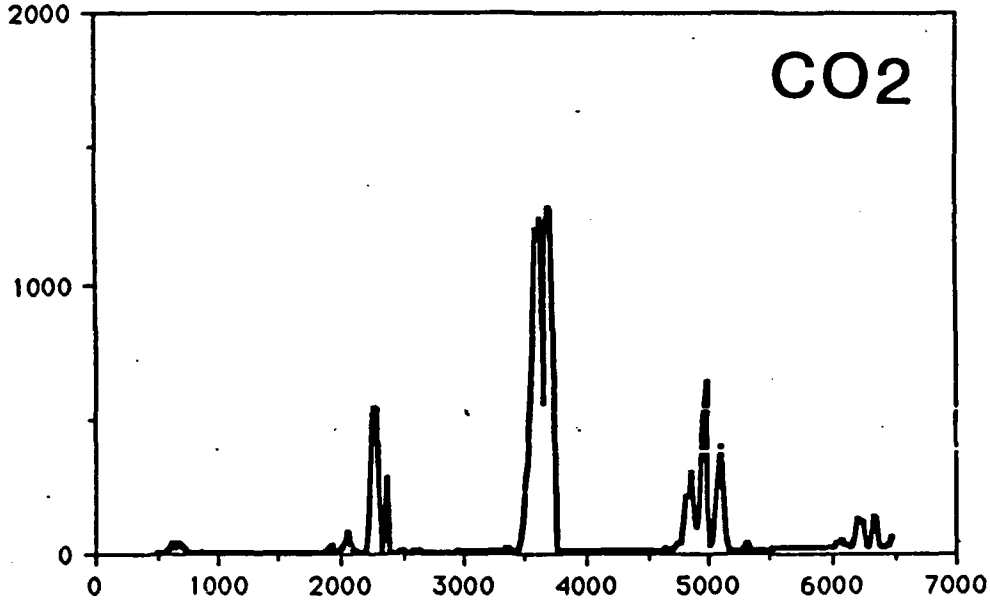

cm-1

Estimated SN H=30km

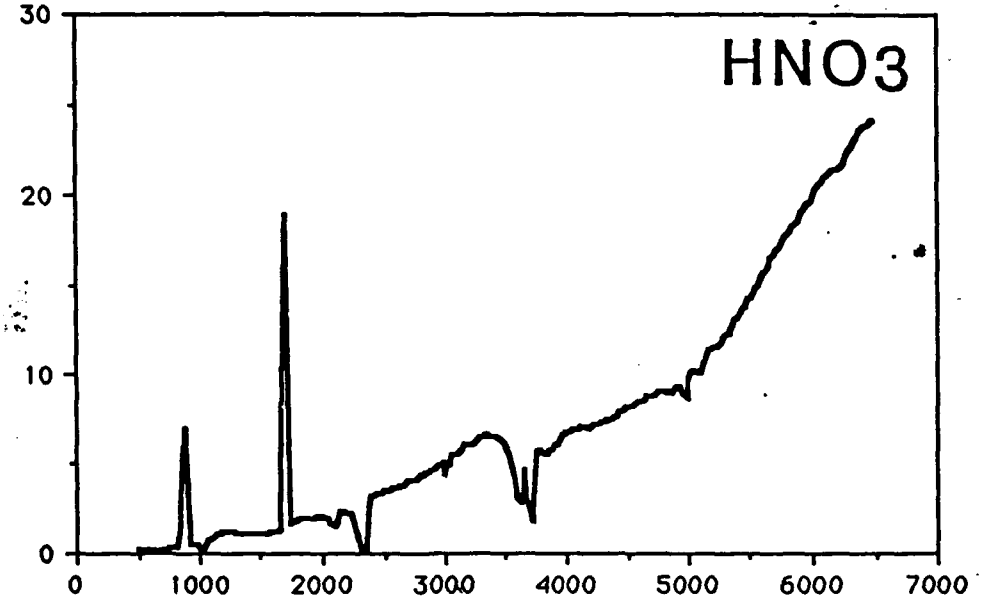

cm-1

Estimated SN H=30km

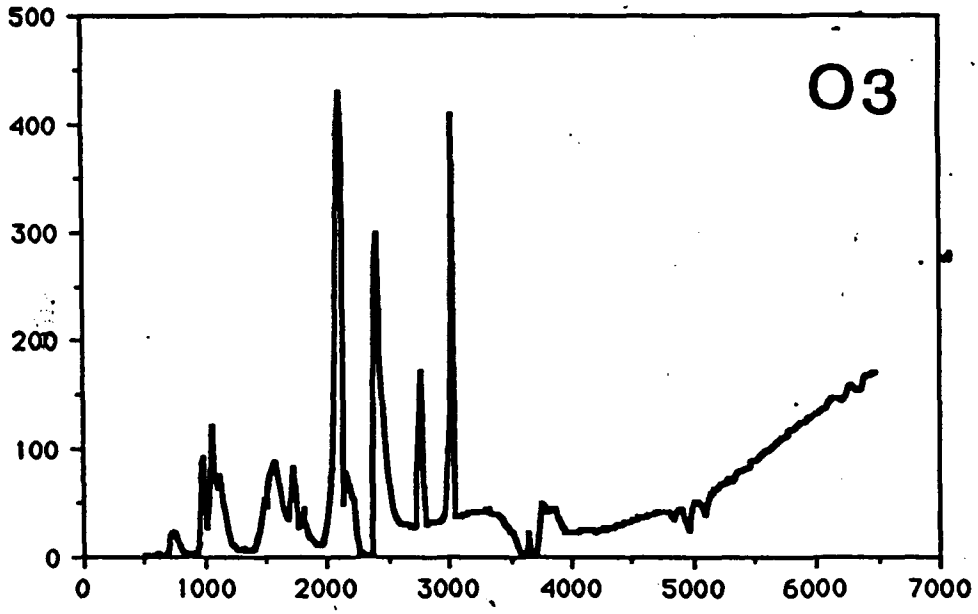

cm-1

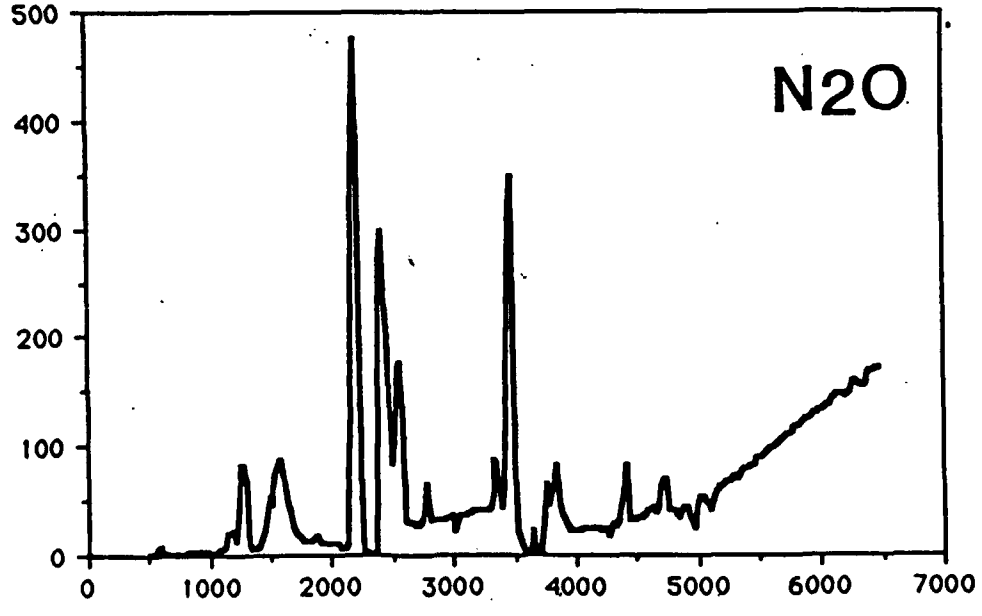

cm-1

Estimated SN H=20km

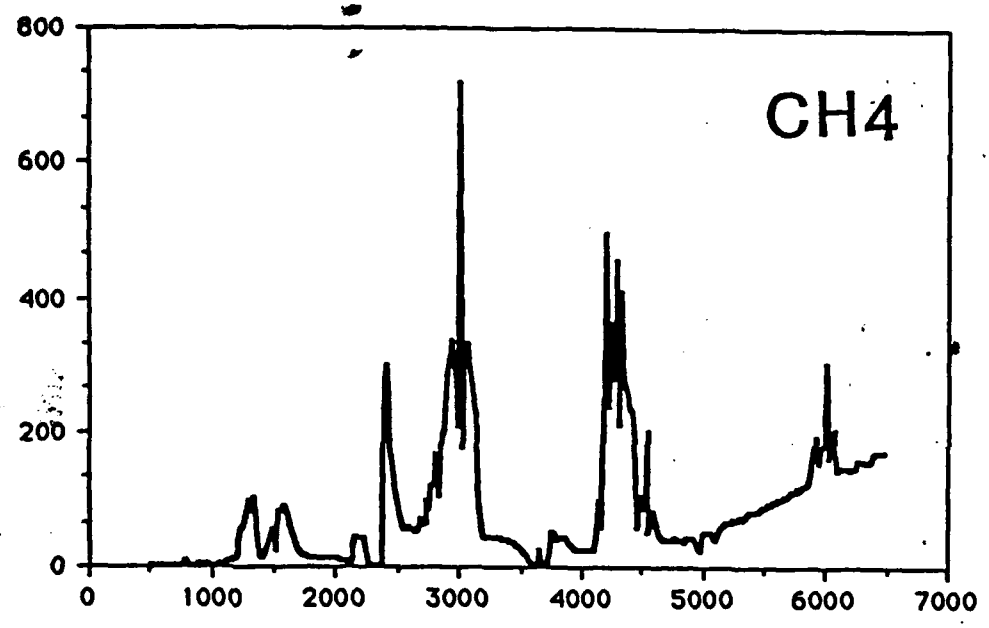

cm-1

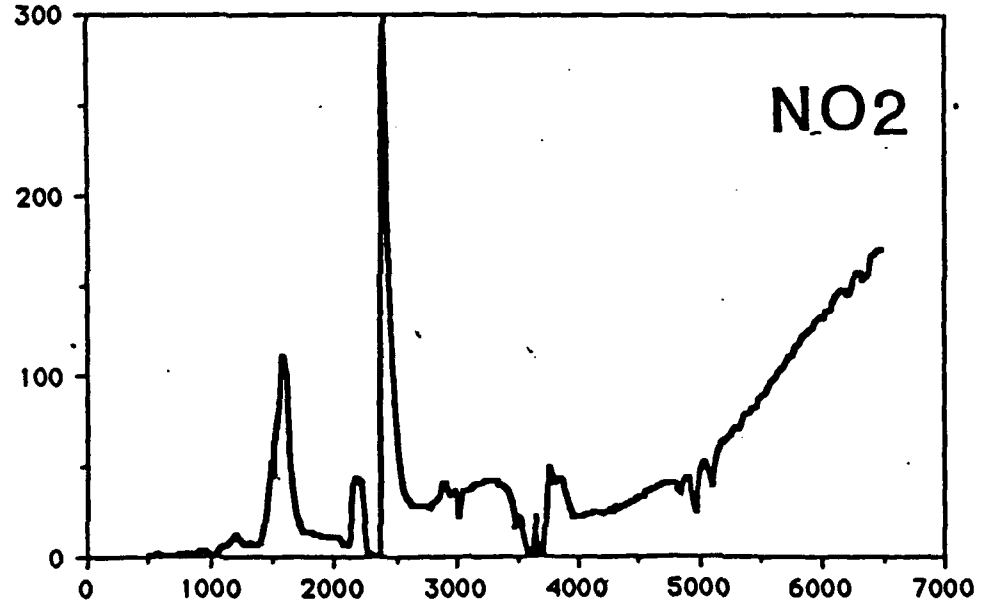

cm-1

Estimated SN H=20km

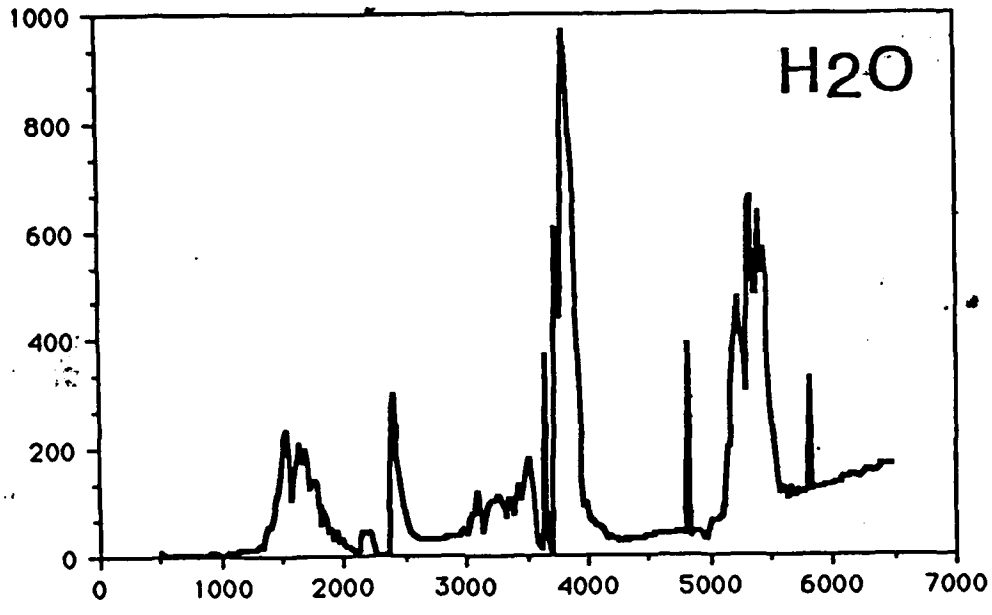

cm-1

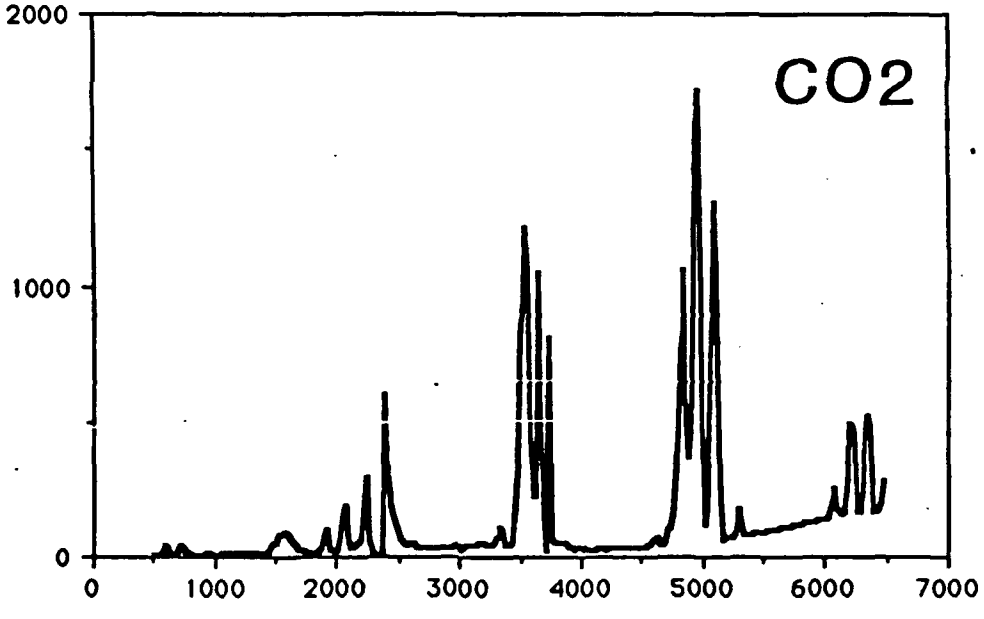

cm-1

Estimated SN H=20km

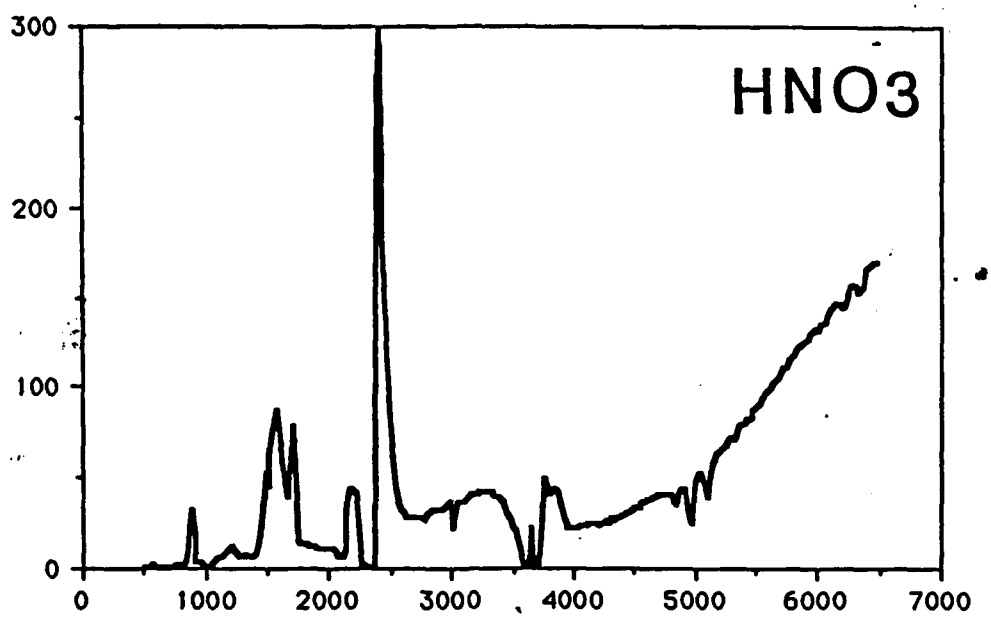

cm-1

Estimated SN H=20km

Temperature measurement of stratosphere using molecular oxygen A band.
Proposed for ILAS,
Observed in 1983 by rocket experiment

Dr. A. Matsuzaki

Anther feature of ILAS is temperature and density measurement. The ch 3 of ILAS is targeted to molecular oxygen A band around 760 nm. Our plan is to obtain the rotational line profile of oxygen molecule, then fitting the temperature and fitting the total absorption which gives the density.

This kind of instruments was flown in 1983 by rocket experiment. Following figure shows the obtained spectra, fitting procedure and the schematics of instrument. About 1000 pixels of photodiode-CCD array with intensifier was used to obtain the spectra.

The fit temperature was about 217 K which sounds reasonable for that of stratosphere, but no cross checking was carried out at that time. The residual of fitting is pretty large, 3 sigma, which means there was something not oxygen molecule. Today, we can assume that is O4. We hope people working with the database will provide a precise simulation for this band soon.

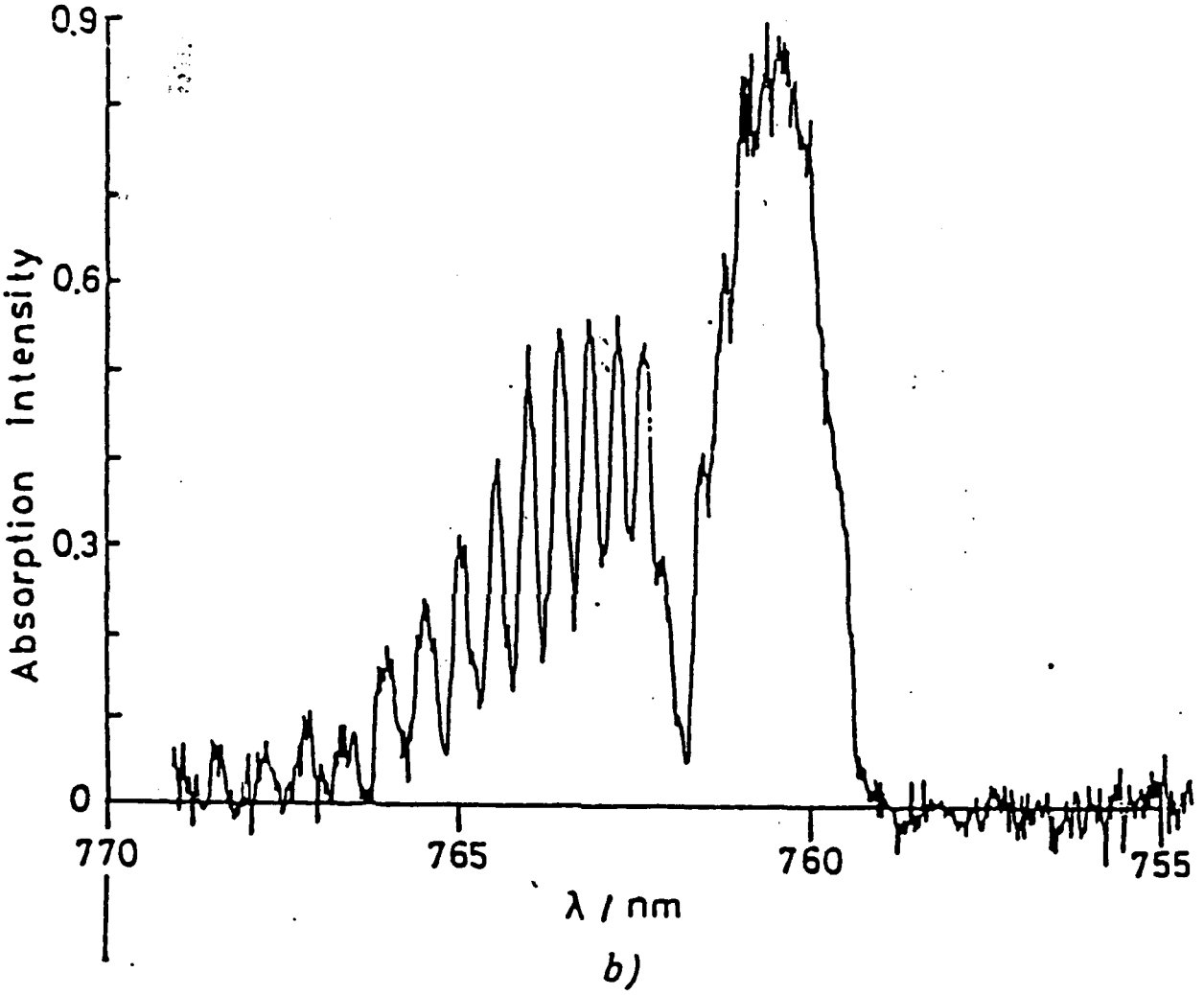

Figure 3(*b*).

The absorption intensity obtained from the plot in figure 3(a).

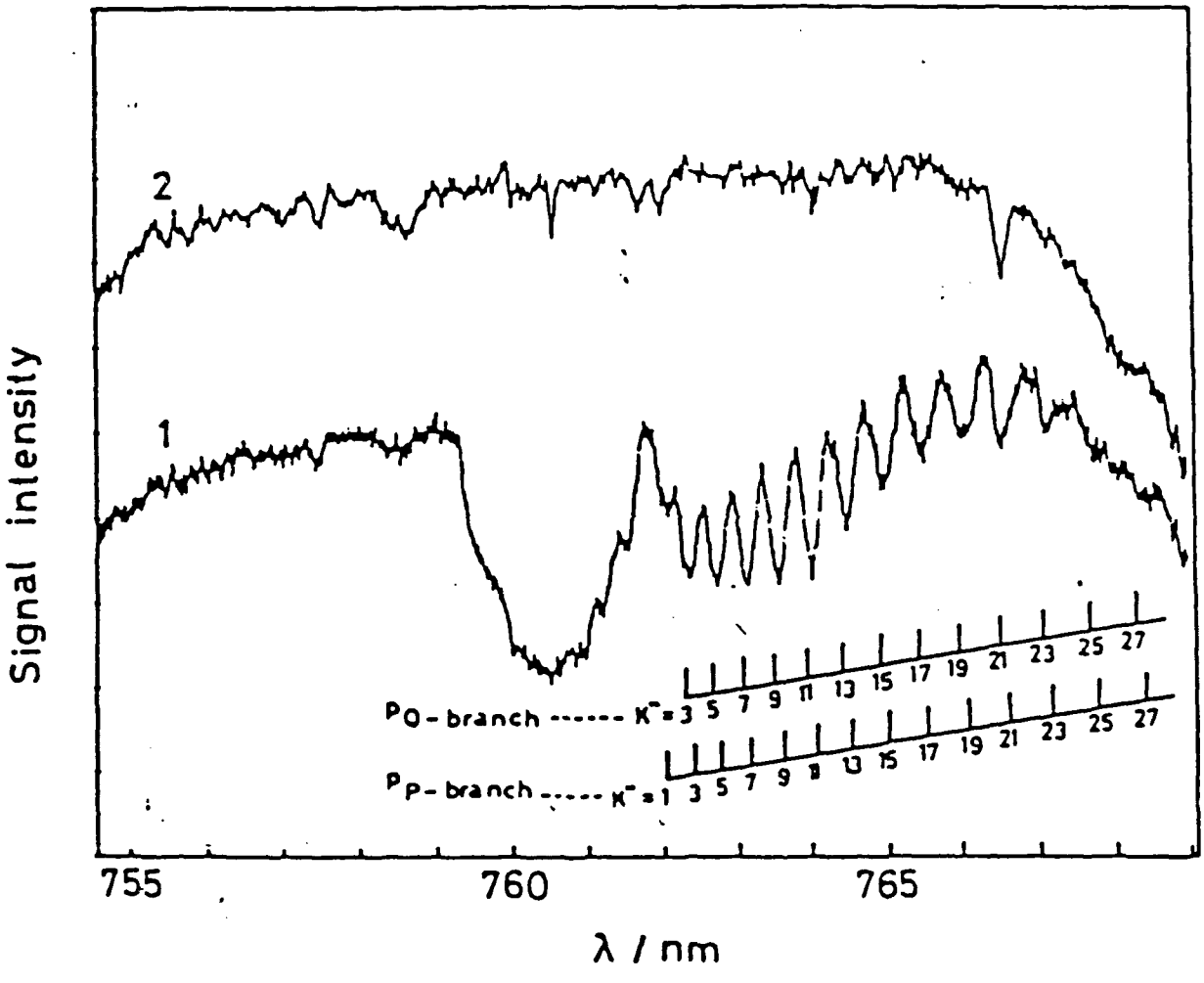

Figure 2.

The spectra measured by the S-310-11 *rocket observation. Spectrum* 1 : 24.8 km, *Spectrum* 2 : 190 km *in the altitude of the rocket.*

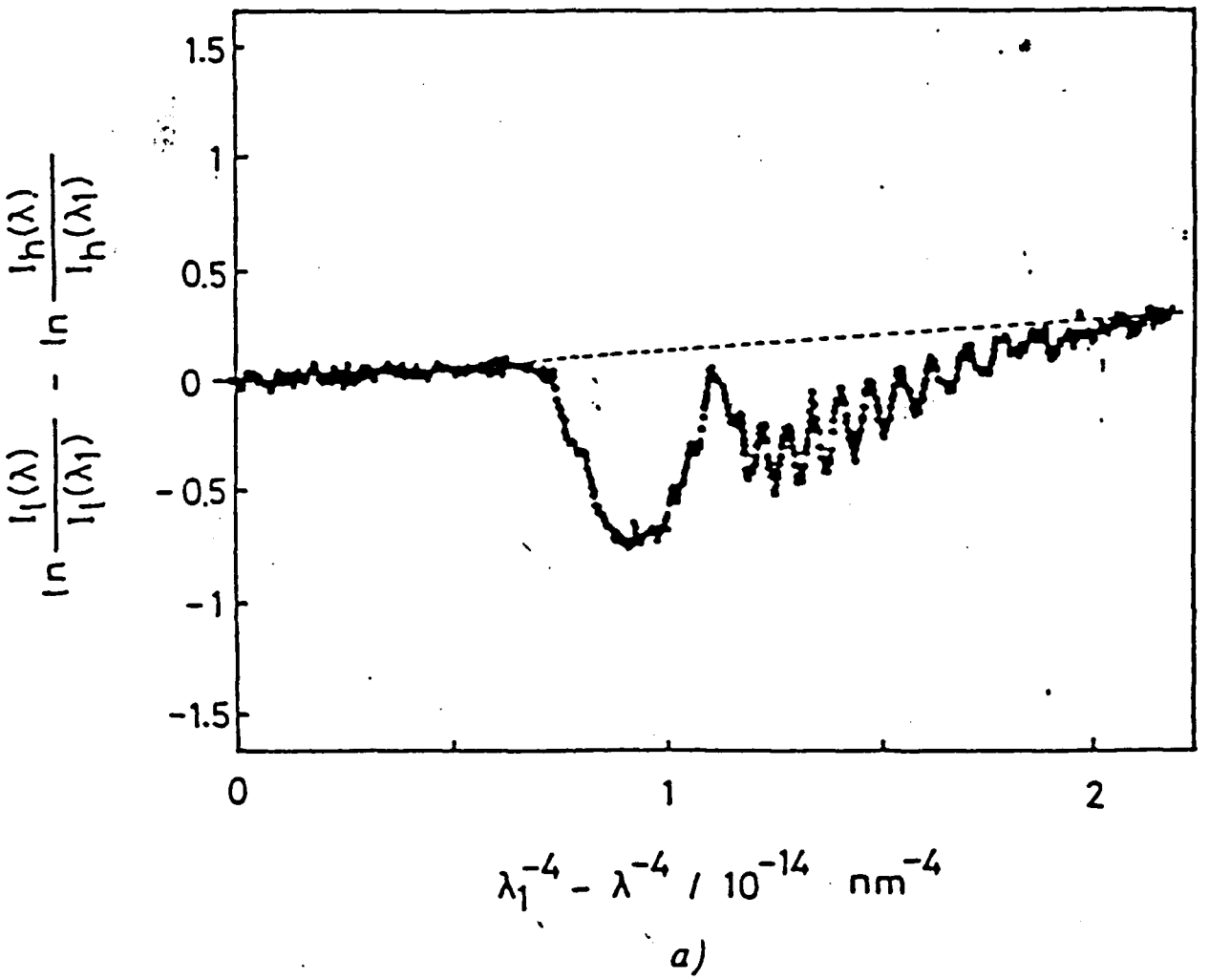

Figure 3(*a*).

Plot of the $\{ \ln [I_l(\lambda)/I_l(\lambda_1)] - \ln [I_h(\lambda)/I_h(\lambda_1)] \}$ *value as a function of the* $(\lambda_1^{-4} - \lambda^{-4})$ *value. Here,* $I_l(\lambda)$ *and* $I_h(\lambda)$ *are the signal intensities of spectra* 1 *and* 2 *of figure* 2, *respectively, at the wavelength* λ. *The wavelength* λ_1 *is* 755.0 nm.

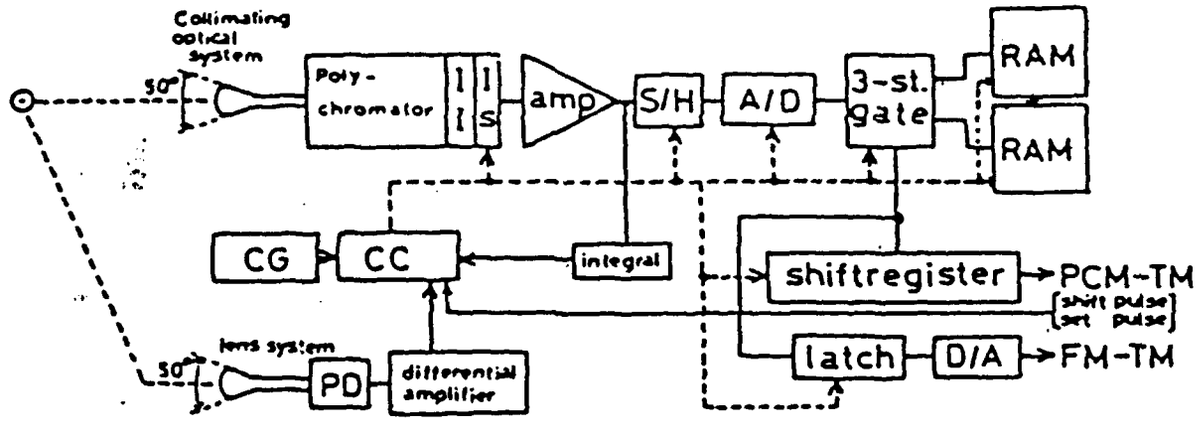

a)

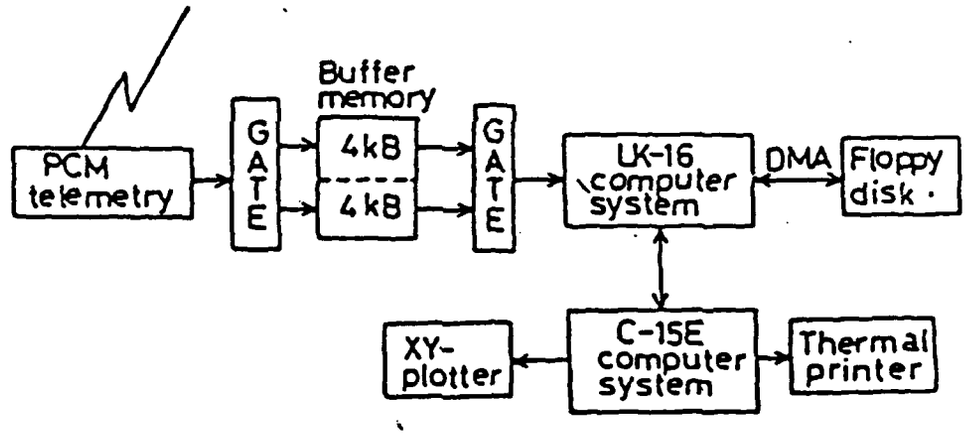

b)

Figure 1(*a*).

The schematic diagram of the rocket-borne spectrometer. II : *an image intensifier,* IS : *a photodiode array,* CG : *a clock generator,* CC : *a clock controller,* PD : *a photodiode.*

Figure 1(*b*)

The schematic diagram of the PCM *data processing system.*

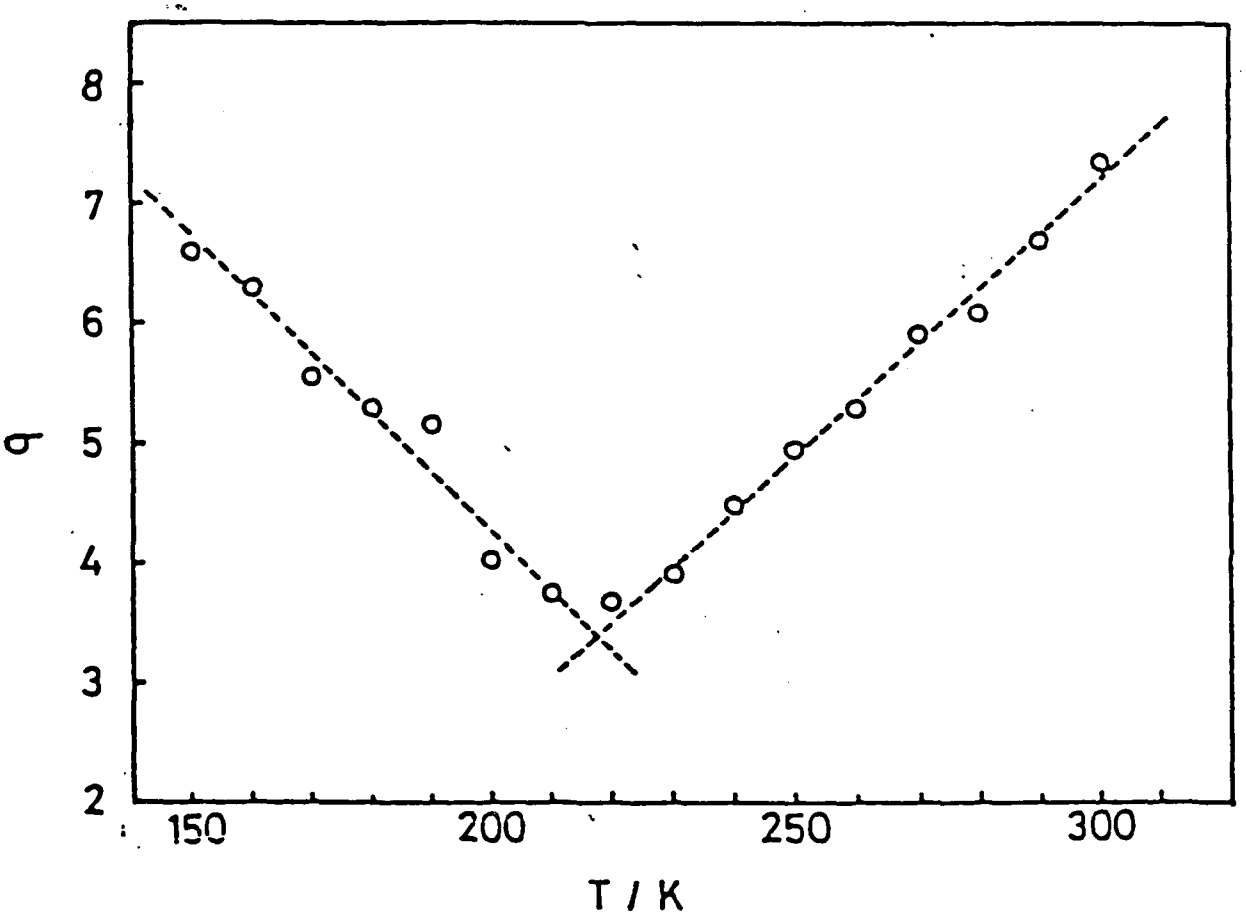

Figure 8.

Standard deviations, σ, obtained at various temperatures, T.

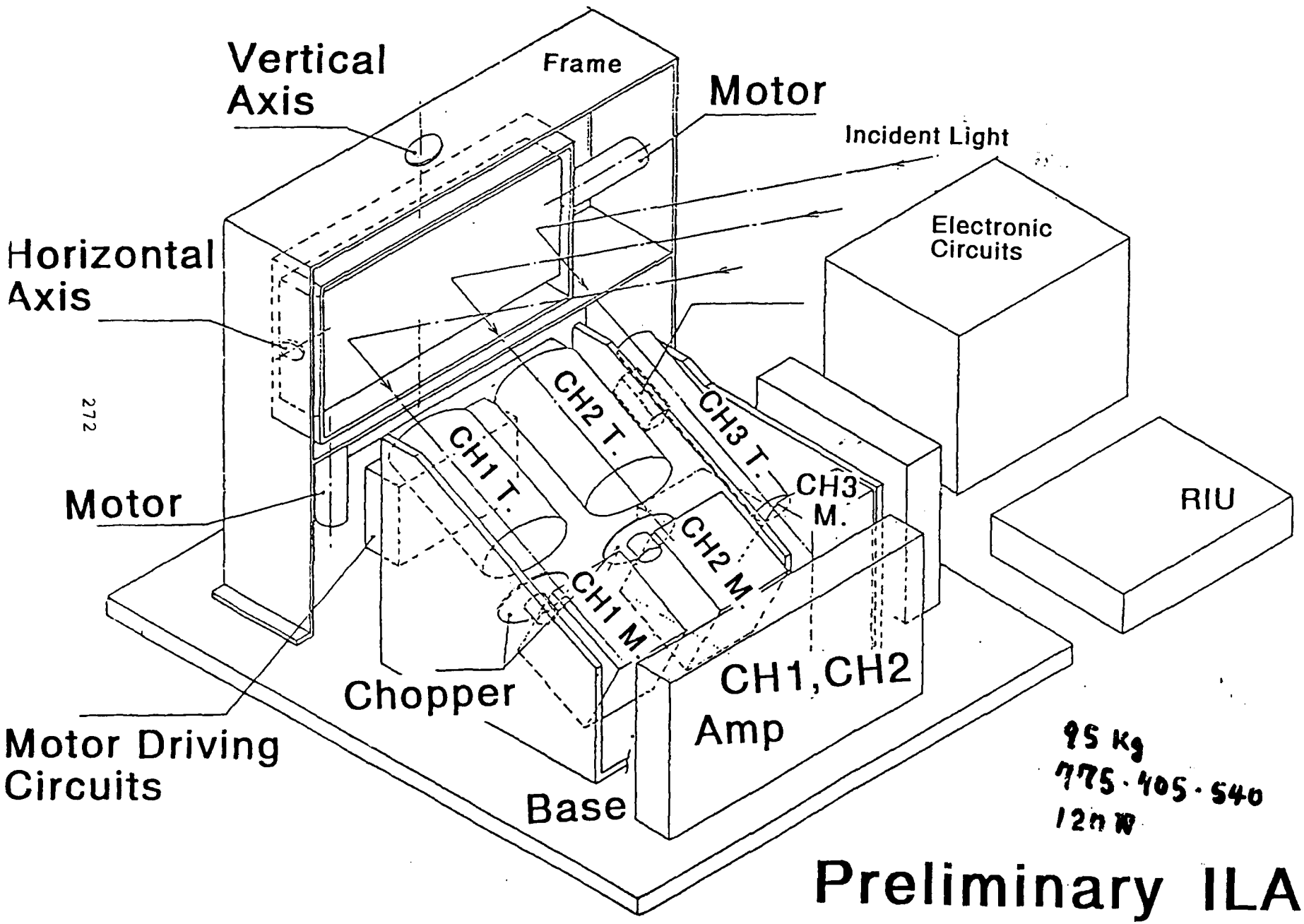

272

95 kg
775 · 405 · 540
120 W

Preliminary ILAS

Retro-reflector

Dr. Nobuo Sugimoto
Dr. Yasuhiro Sasano
Lidar group,
National Institute for
Environmental Studies

5
60 cmø corner cube, IR to UV
will be mounted on ADEOS.

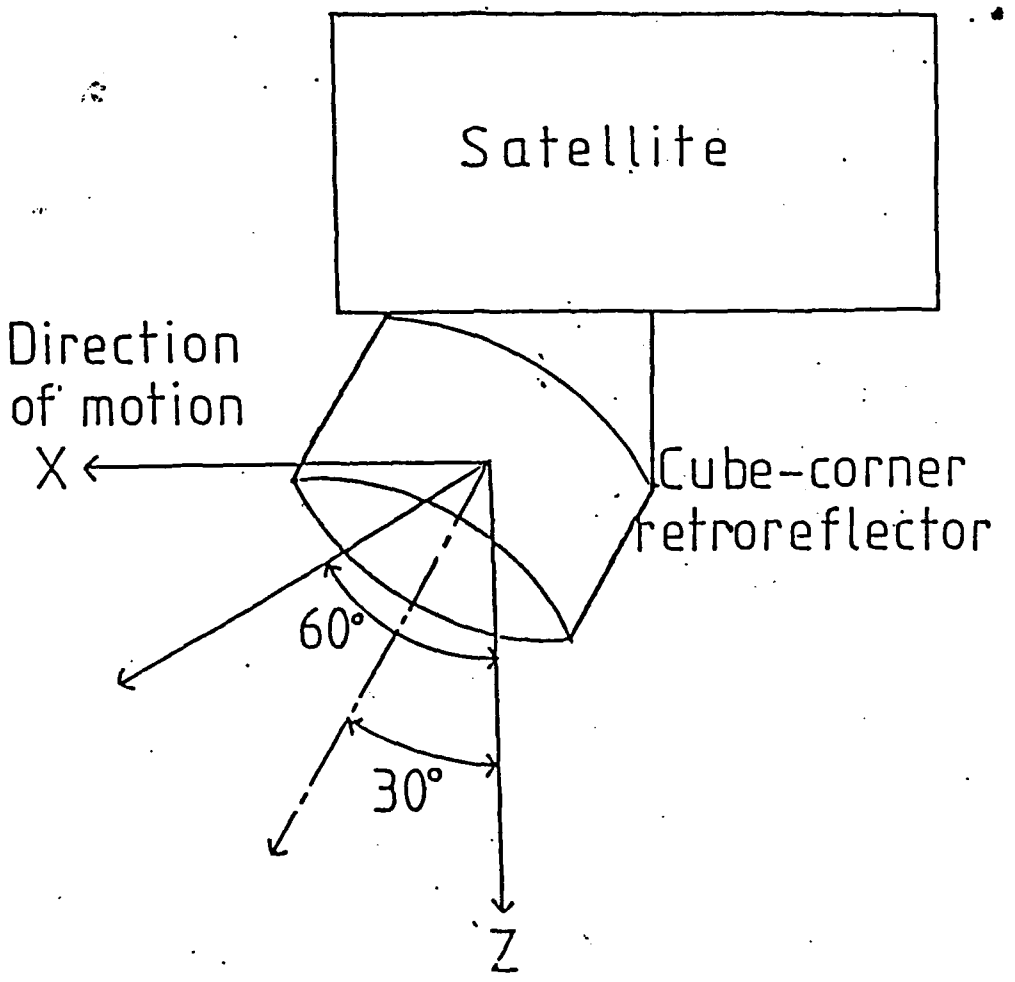
Satellite
Direction
of motion
X
Cube-corner
retroreflector
60°
30°
Z

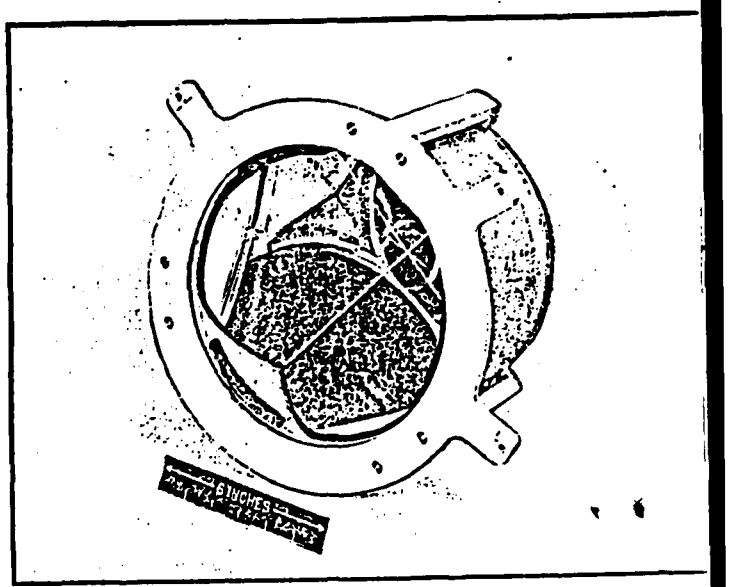

Precision Lapping's 8-inch retroreflector, enclosed in the bracket by which it was attached to the space shuttle Discovery for the laser targeting experiment last Jun

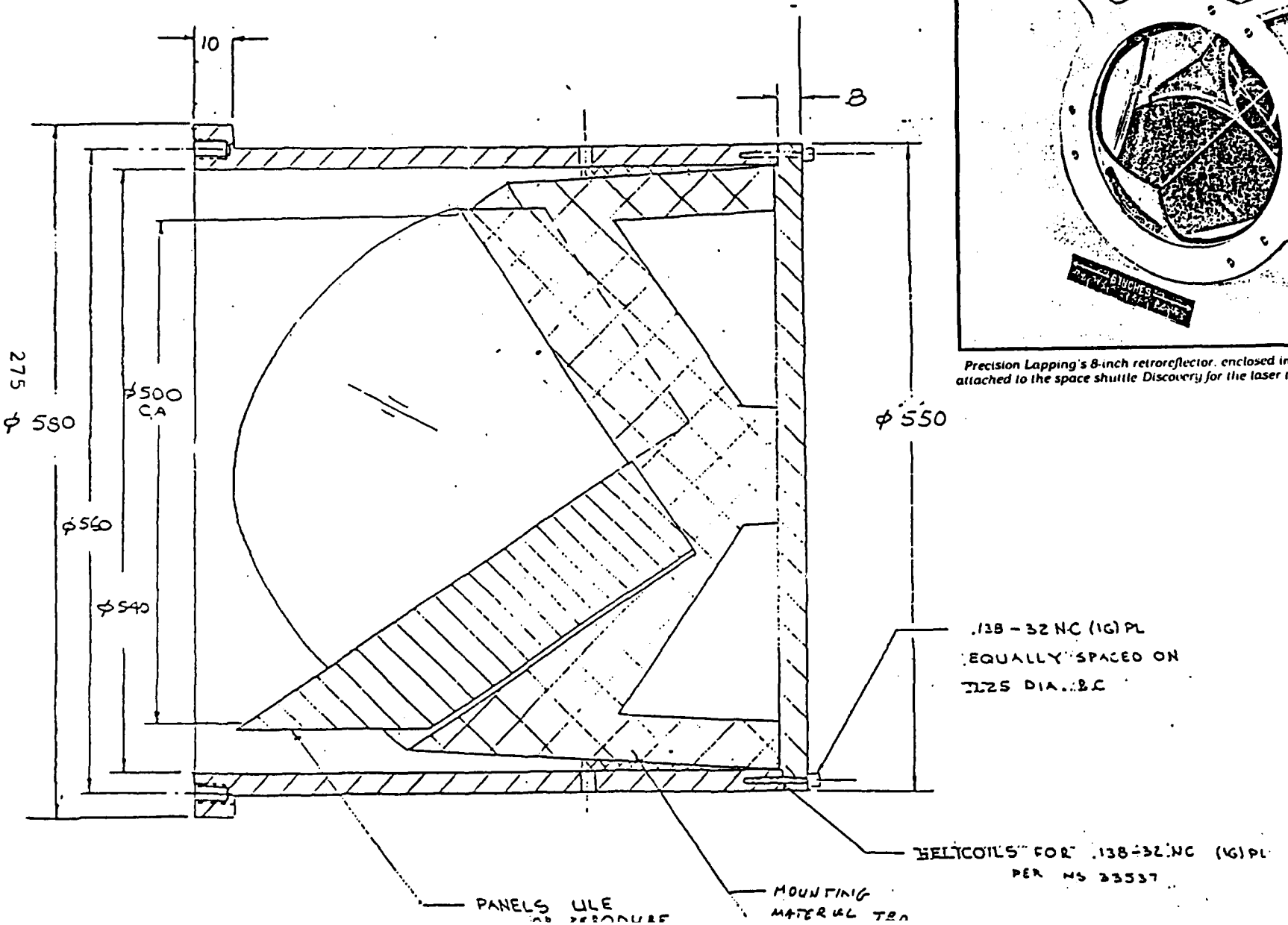

THE HITRAN DATABASE FROM A USER'S PERSPECTIVE

Shepard A. Clough
Atmospheric & Environmental Research, Inc.
840 Memorial Drive
Cambridge, MA 02138

THE HITRAN DATABASE: A USER'S PERSPECTIVE

GENERAL ISSUES

- TRANSMITTANCE/RADIANCE ACCURACY REQUIREMENTS
- SCOPE
- ASSOCIATED PROGRAMS

DATABASE

- LINE PARAMETERS
- MOLECULAR PARAMETERS (PARTITION FUNCTIONS)
- ACCURACIES

'STRATEGIC' ISSUES

- INTERIM LINE DATA
- FREQUENCY OF RELEASE/REFERENCE FUNCTION

STRUCTURAL ISSUES

- SEQUENTIAL
- RECORD LENGTHS
- ADDITIONAL NECESSARY INFORMATION

HIGH SPECTRAL DENSITIES

- HIGH TEMPERATURE
- HEAVY MOLECULES
- HYPERFINE STRUCTURE

S.A. CLOUGH AER

General Issues: Transmittance/Radiance Accuracy Requirements

Transmission

$$T(\nu) = e^{-\kappa(\nu)L}$$

$\kappa(\nu)$ absorption coefficient
L optical path length

long path transmission $\frac{\delta T}{T} = L \delta k$

Radiance

$$R(\nu) = (1-T(\nu))\, U(\nu)$$

$U(\nu)$ Planck function

forward problem $\frac{\delta R}{R} = \frac{\delta T}{T} \left(\frac{T}{1-T} \right)$

path characterization

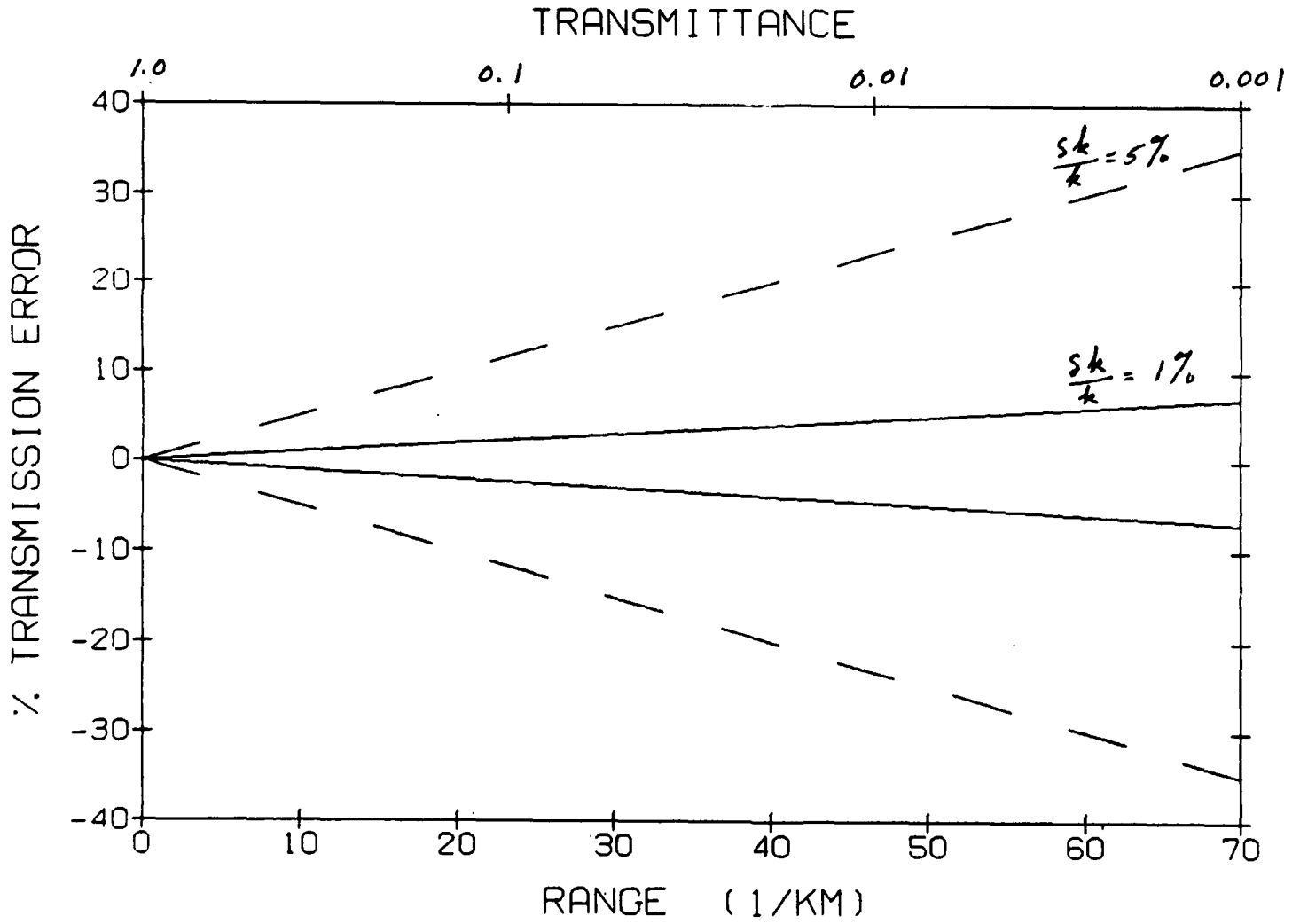

absorption coefficient

$k = 0.1$

Physical Retrieval/Path Characterization Problem

$$Y = (A^T A)\, X$$

$$X = (A^T A)^{-1}\, Y$$

$$\begin{bmatrix} 1 \\ -1 \end{bmatrix} = \begin{bmatrix} .550 & .423 \\ .484 & .372 \end{bmatrix}^{-1} \begin{bmatrix} .127 \\ .112 \end{bmatrix}$$

$$(A^T A) + \delta(A^T A)$$

$$\begin{bmatrix} -.4535 \\ .8899 \end{bmatrix} = \begin{bmatrix} .550 & .423 \\ .483 & .372 \end{bmatrix}^{-1} \begin{bmatrix} .127 \\ .112 \end{bmatrix}$$

$Y + \delta Y$:

$$\begin{bmatrix} 1 \\ -1.91 \end{bmatrix} = \begin{bmatrix} .550 & .423 \\ .484 & .372 \end{bmatrix}^{-1} \begin{bmatrix} .12707 \\ .11228 \end{bmatrix}$$

X atmospheric state vector

$A = \frac{\partial R}{\partial X}$ radiance derivatives

$Y = y \frac{\partial R}{\partial X}$ y measured radiances

cond $(A^T A)$ = 7622

SCOPE

TEMPERATURE REGIME

PRESSURE REGIME

MOLECULES

INTENSITY CUTOFF

EARTH'S ATMOSPHERE (QUIESCENT)

DISTURBED ATMOSPHERE (NLTE, RADICALS), plumes

OTHER PLANETS, cool stars

diffuse spectra (UV, ...)

ASSOCIATED PROGRAMS

SELECT

MOLECULAR CONSTANTS

PROGRAMS FOR LINE PARAMETER GENERATION

OTHER DATABASES

GEISA

JPL

ATMOS

SLP

a single principal reference source

Line Parameters

$$\kappa_i(\nu) = \nu \tanh(hc\nu/2\kappa T)\left\{\bar{S}_i(T)\,\frac{\gamma_i(p,T)}{\left[\nu-\nu_i-\delta_i(p,T)\right]^2+\left[\gamma_i(p,T)\right]^2}\,\chi(\nu-\nu_i)\right\}$$

$$\bar{S}_i(T) = \frac{R_i \exp(-E_i'' hc/\kappa t)}{Q(T)}$$

$$= \bar{S}_i(T_o)\exp\left[-E_i''(hc/\kappa T - hc/\kappa T_o)\right]\left[\frac{Q(T_o)}{Q(T)}\right]$$

$\chi(\nu-\nu_i)$ chi factor

$p = P/P_o$

$$\left[\frac{Q(T_o)}{Q(T)}\right] = a^{[\log_a Q(T_o) - \log_a Q(T)]}$$

$\left(\frac{T_o}{T}\right)^{3/2}$ triatomic +

$\left(\frac{T_o}{T}\right)$ diatomic

$$Q = \sum e^{-(v+1/2)hc\nu_o/kT} e^{-E_i'' hc/kT}$$

tables of $\log_a Q(T_i)$ linear interpolation
improved extrapolation

T_i: ___, ___, 200K, 250K, 296K, 350K, ___, ___.

T_o

Line Parameters

		Current	Requirement	
intensity	$\bar{S}_i(T)$	→ 2%	→ 0.5%	
transition probability	R_i		→ 0.5%	
partition sum	$Q(T)$	→ 2%	→ 0.2%	molecular par.
lower state energy	E_i''	→ 0.1 cm^{-1}	0.1 cm^{-1}	
resonant frequency	ν_i		→ $\frac{\gamma(P,T)}{\delta}$	lidar
pressure shift	$\delta_i(p,T) = p\,\delta_i^{\circ}$			lidar
air halfwidth	$\gamma_i(p,T) = p\left[\frac{T}{T_o}\right]^{n}\gamma_i^{\circ}$	→ 5%	0.2%	
temp. dep.	(n)	20% → 10%	5% 2%	
self halfwidths	$\gamma_i^{s}(p,T)$	→ 5%	0.2%	water (earth)
Tony	M_S			

Line Parameters (Line Coupling)

$$\kappa_i(\nu) = \nu \tanh(hc\nu/2kT) \left\{ \bar{S}_i(T) \frac{\gamma_i(p,T)\,[1+g_i(p,T)] + y_i(p,T)\,[\nu-\lambda_i(p,T)]}{[\nu-\lambda_i(p,T)]^2 + [\gamma_i(p,T)]^2} \right\}$$

quantity	no coupling	2nd order	exact
$g_i(p,T)$	0	$p^2\, g_i^{\circ}(T)$	$p^2 g_i^{\circ}(p,T)$
$y_i(p,T)$	0	$p\, y_i^{\circ}(T)$	$p\, y_i^{\circ}(p,T)$
$\lambda_i(p,T)$	ν_i	$\nu_i - p^2\delta_i^{\circ}(T)$	$\nu_i - p^2\delta_i^{\circ}(p,T)$
$\gamma_i(p,T)$	$p\,\gamma_i^{\circ}$	$p\,\gamma_i^{\circ}(T)$	$p\,\gamma_i^{\circ}(p,T)$
$\sum_{\text{band}_i} y_i(p,T) = 0$	$\sum_{\text{band}_j} g_i(p,T) = 0$		
2nd order	$y_i^{\circ}(T)$		T = 200,250,296,340
	$g_i^{\circ}(T)$		linear interpolation
exact	$y_i^{\circ}(p,T)$ $S_i^{\circ}(p,T)$		tabulated for temperature and pressure
	$g_i^{\circ}(p,T)$ $\alpha_i^{\circ}(p,T)$		

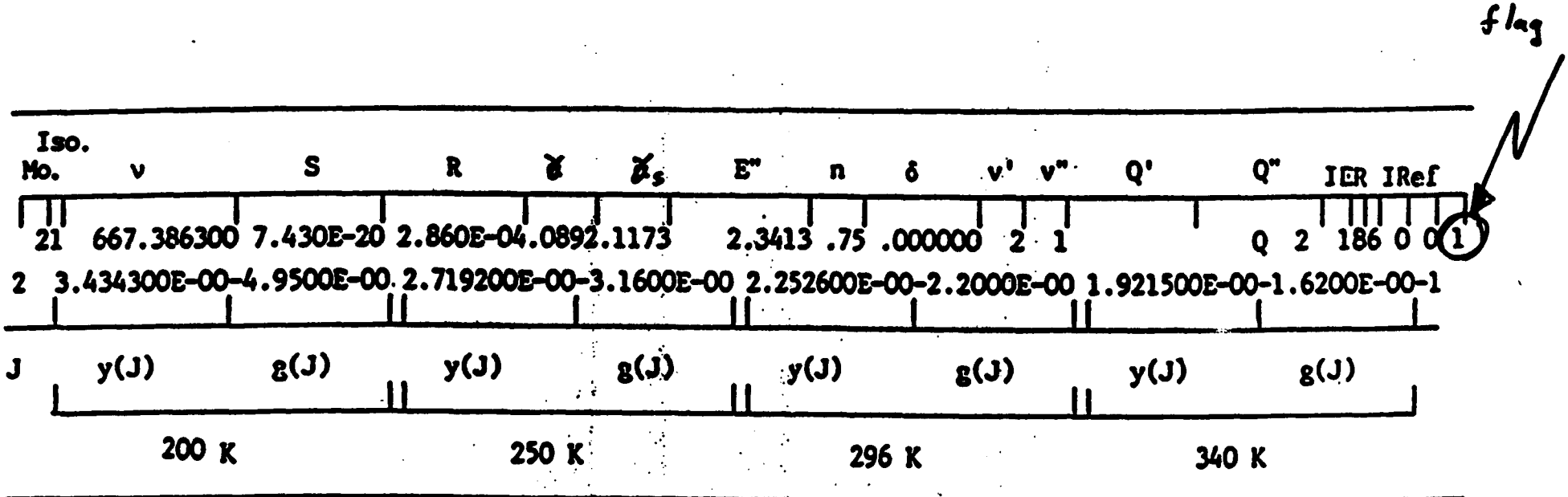

1) 2nd order

2) $\beta_i^\circ(T)$ $\gamma_i^\circ(T) = \rho\,\gamma_i^\circ(T)\,(1-\rho\,\beta_i^\circ(T))$

3) $g_i^\circ(P,T)$, $g_i^\circ(P,T)$, $\delta_i^\circ(P,T)$, $\kappa_i^\circ(P,T)$

H104R8

HIS Equivalent Brightness Spectrum

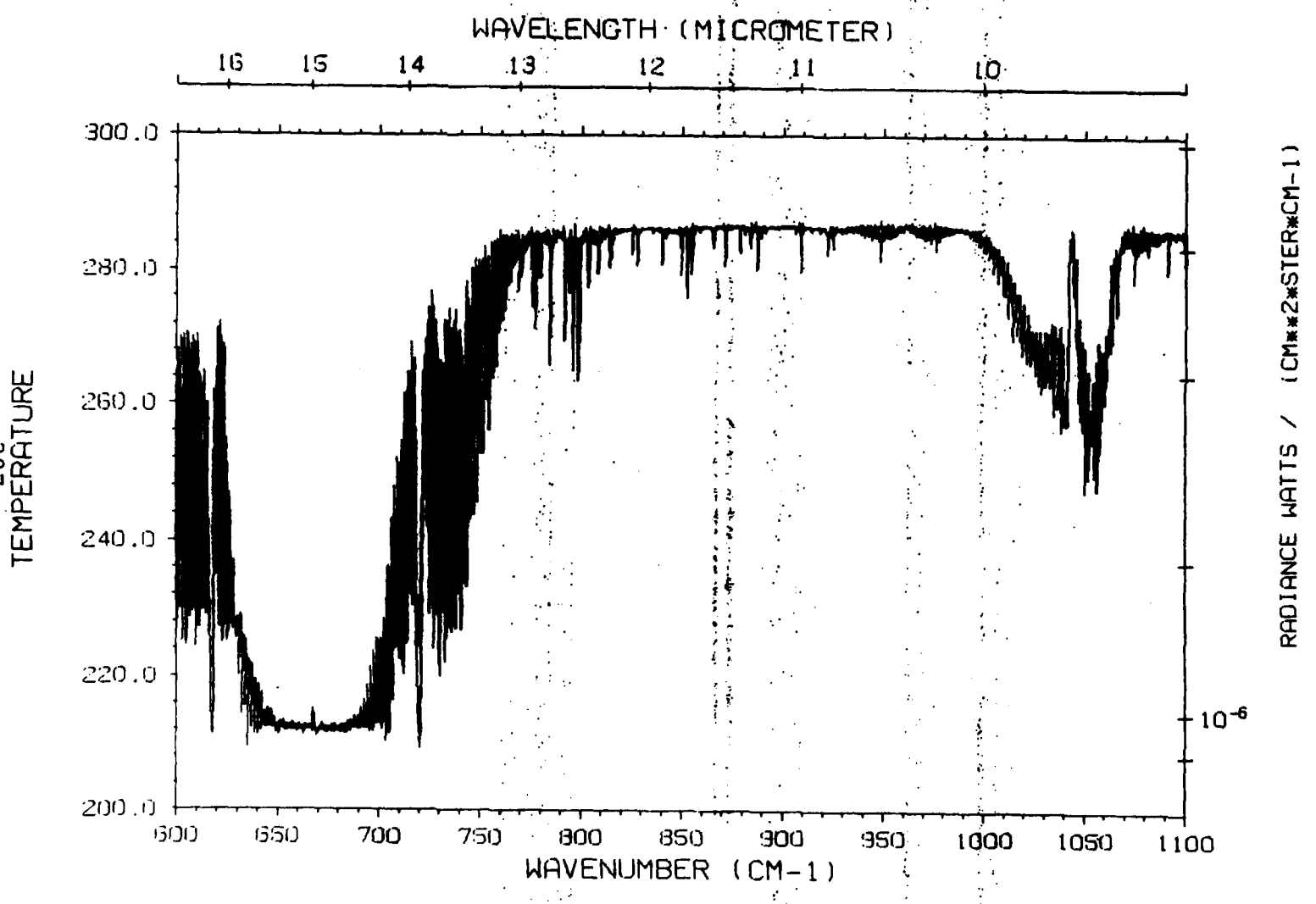

U. of Wisconsin
Smith et al

April 14, 1982
ocean surface
nadir view 19.6 km

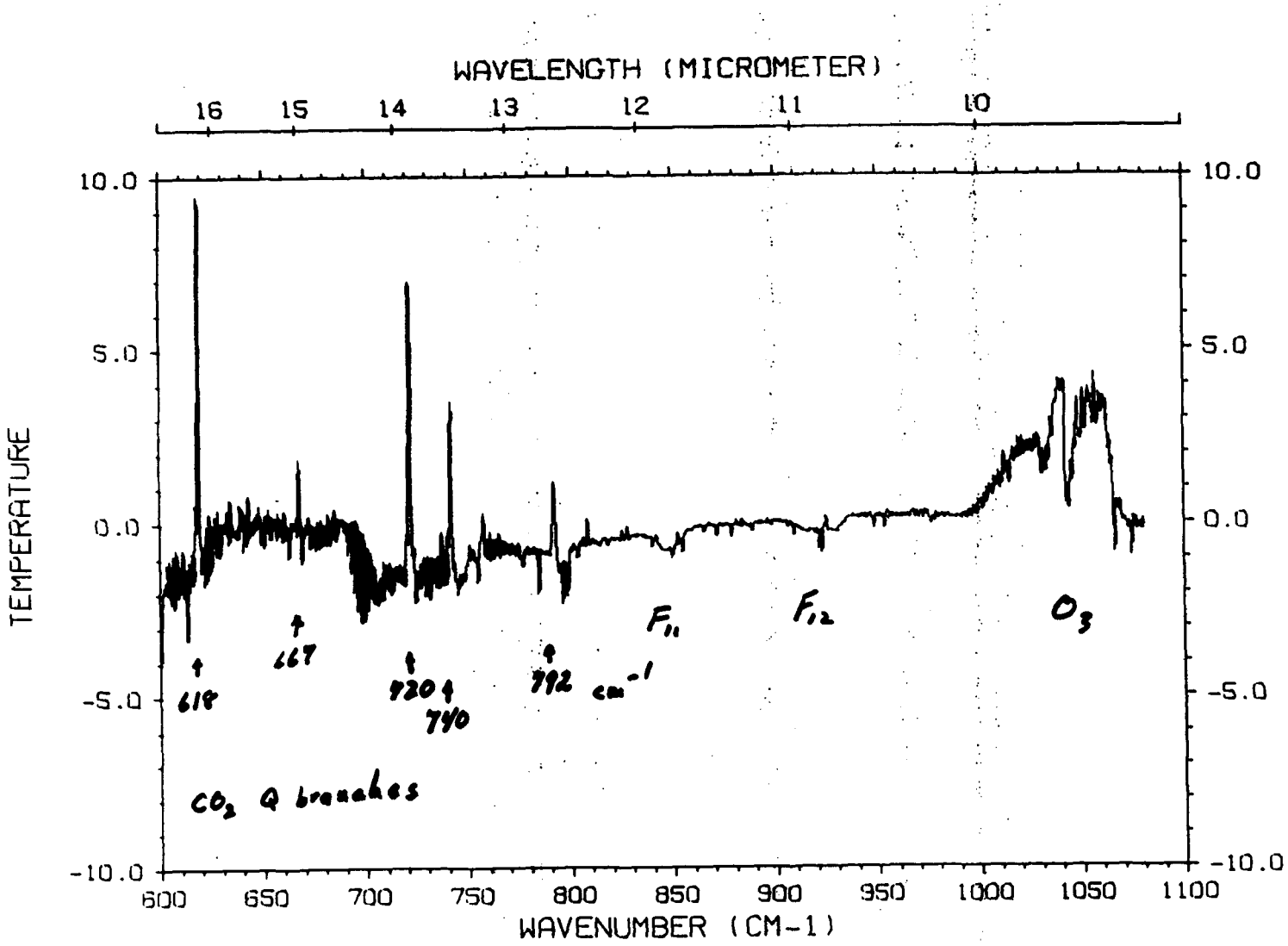

CO_2 line coupling
618
720
740
792

CFC's
850 CFC 11
920 CFC 12

ozone profile
1000 - 1070

warm gas in pod
667

$F_3 - F_2$

Humm = .219

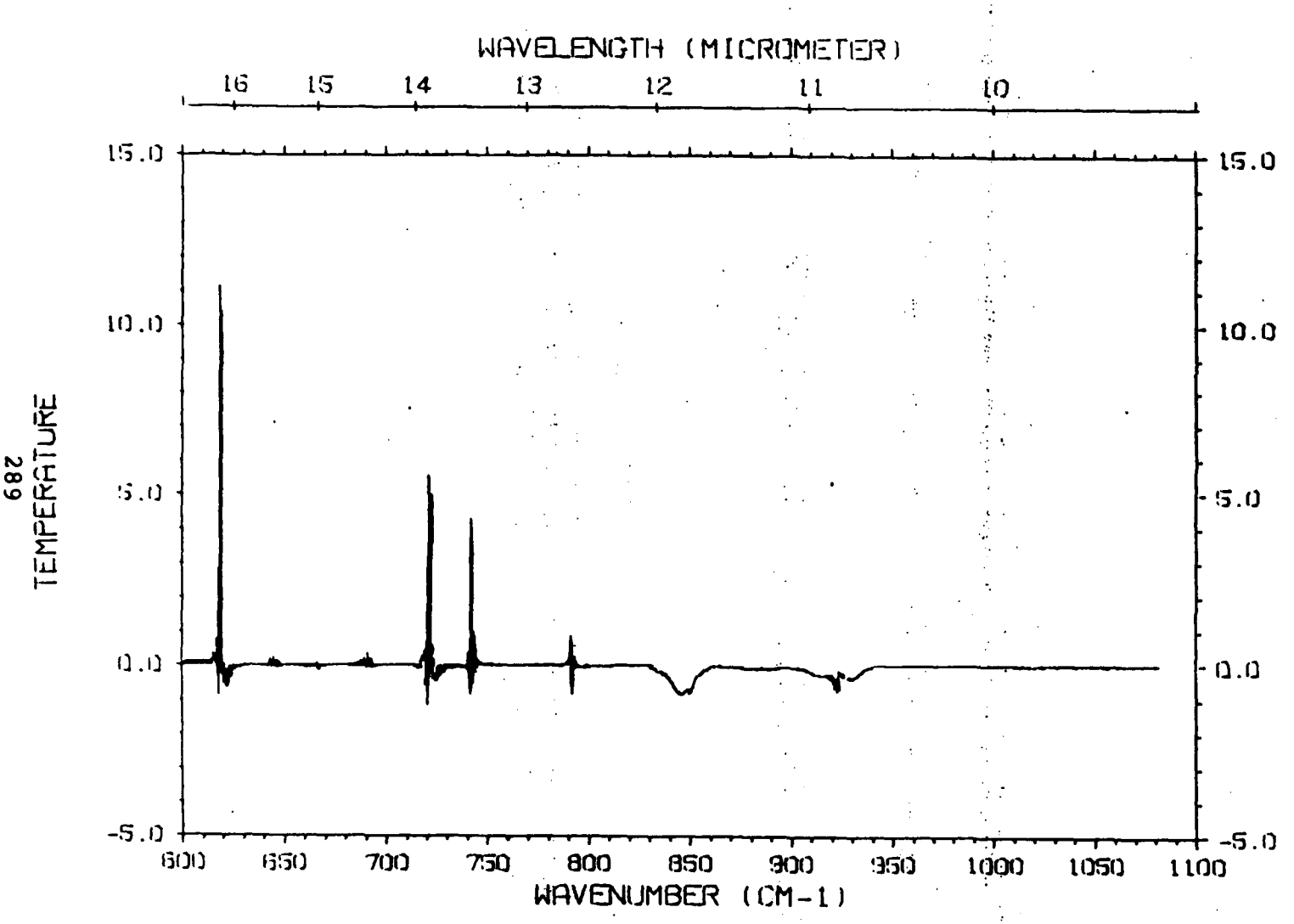

line coupling
Hake + Clough
cross sections
CFC 11
CFC 12
Massie et al

9/88

$F_{3\,MS} - F_2$
.314 Sine

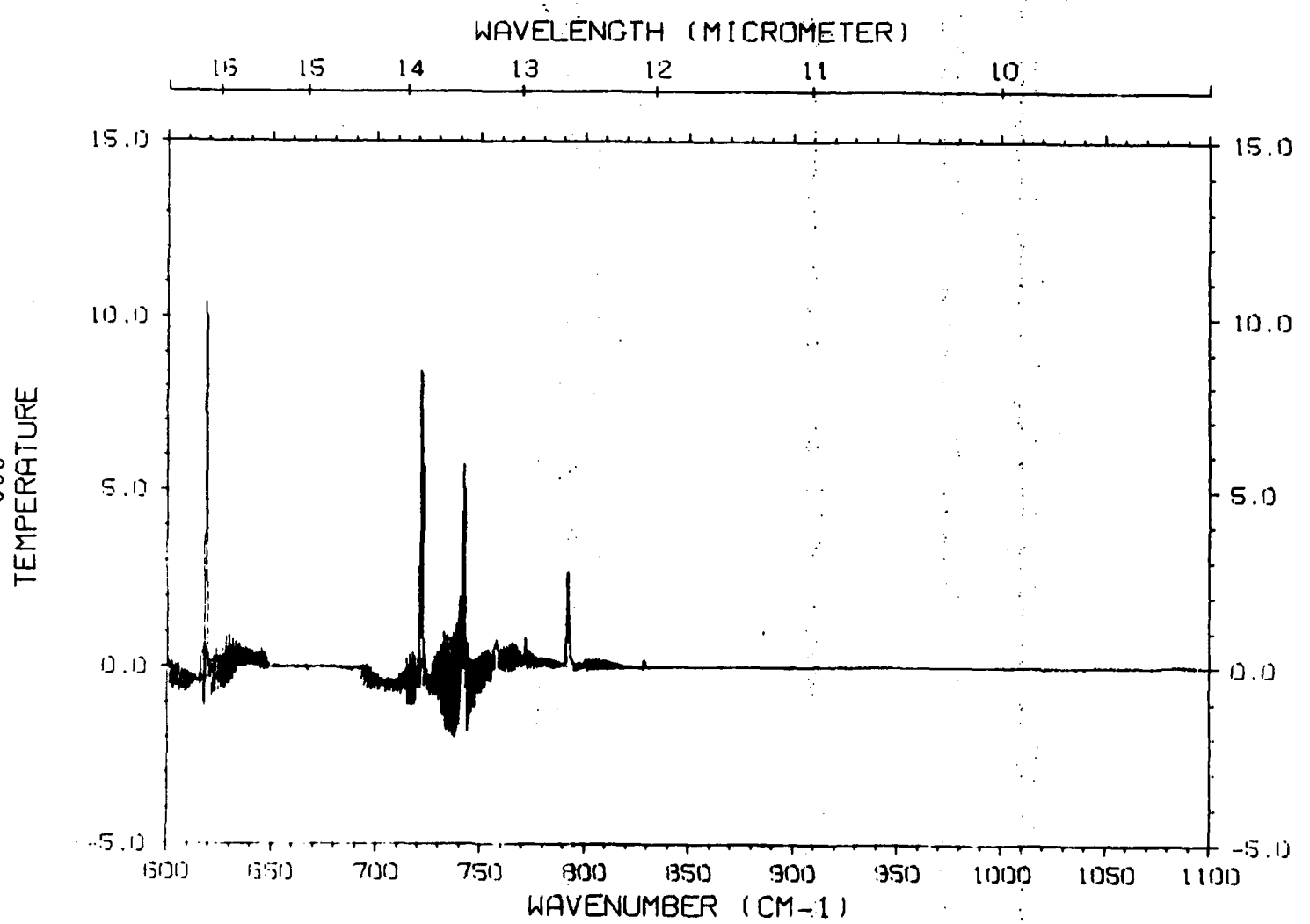

line coupling
12/88 CO_2 line Site
Hake + Clough

'STRATEGIC' ISSUES

- INTERIM (TRANSITION) LINE FILE
  - A) REFINED LINE PARAMETERS
  - B) ADDITIONAL LINE PARAMETERS
  - C) LINE PARAMETERS FOR ADDITIONAL MOLECULES
  - D) FREQUENCY OF UPDATE
  - E) METHOD OF ACCESS

communication:
bulletin board
newsletter

- CARBON DIOXIDE EXAMPLE

- FREQUENCY OF RELEASE

  CURRENCY VS. REFERENCE

Structural Issues

- SEQUENTIAL ACCESS A MAJOR ISSUE

- FILE FORMAT/STRUCTURE SHOULD NOT BE DRIVER

  - o I.E. RECORD LENGTH SHOULD NOT LIMIT DATA

- ADDITIONAL INFORMATION

  - o LINE COUPLING

    A) EFFECTIVE HALFWIDTH
    B) 2ND ORDER PARAMETERS
    C) EXACT TREATMENT

  - o Zeeman Effect

    - O_2

  - o Hyperfine Structure

    - NO_2

1 JUNE 1989
SCRIBE DATA

SCRIBE

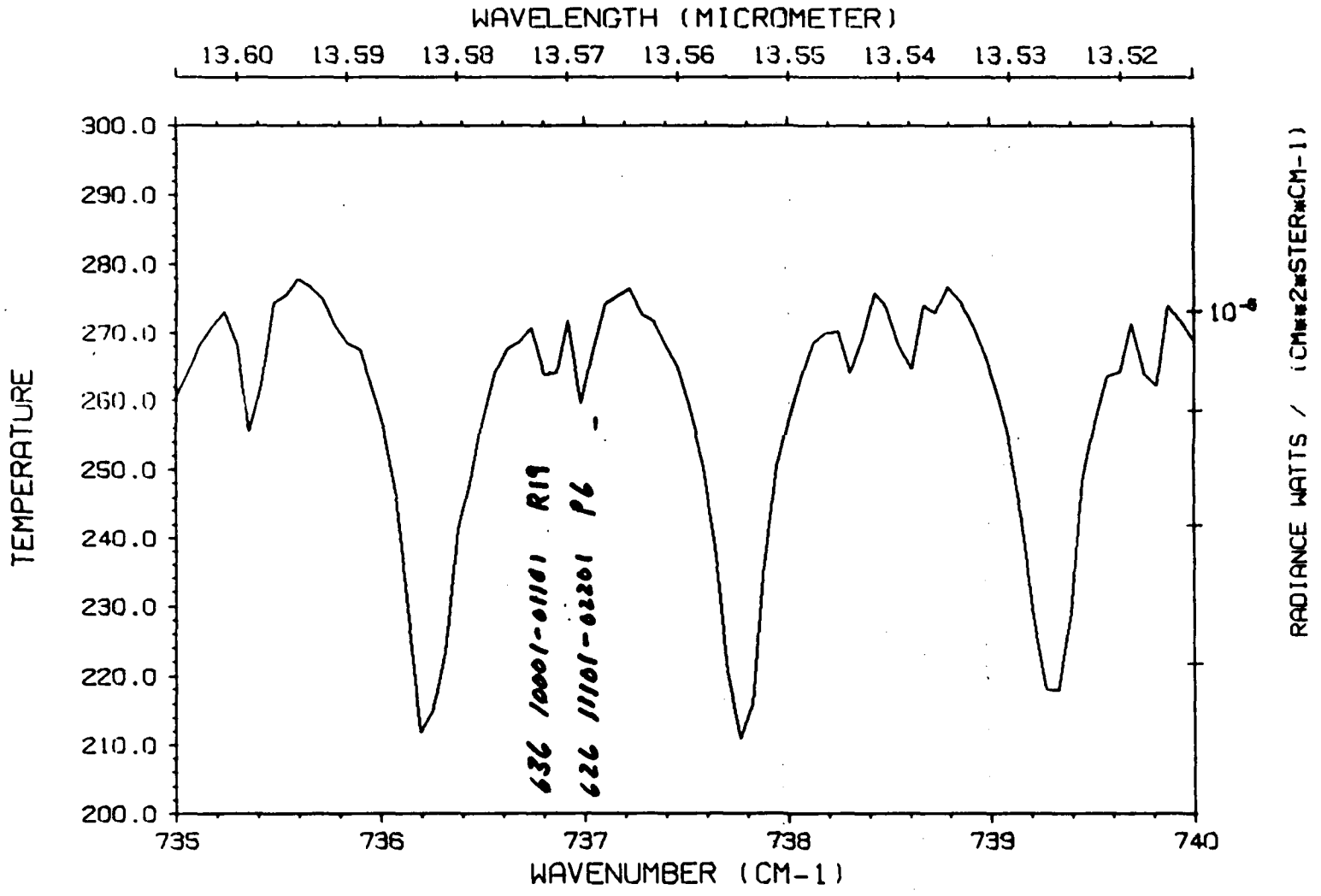

Q 721 cm^{-1}

Q 740 cm^{-1}

1 June 1989
Scribe (TSHB)

FASCODE
'86 lines

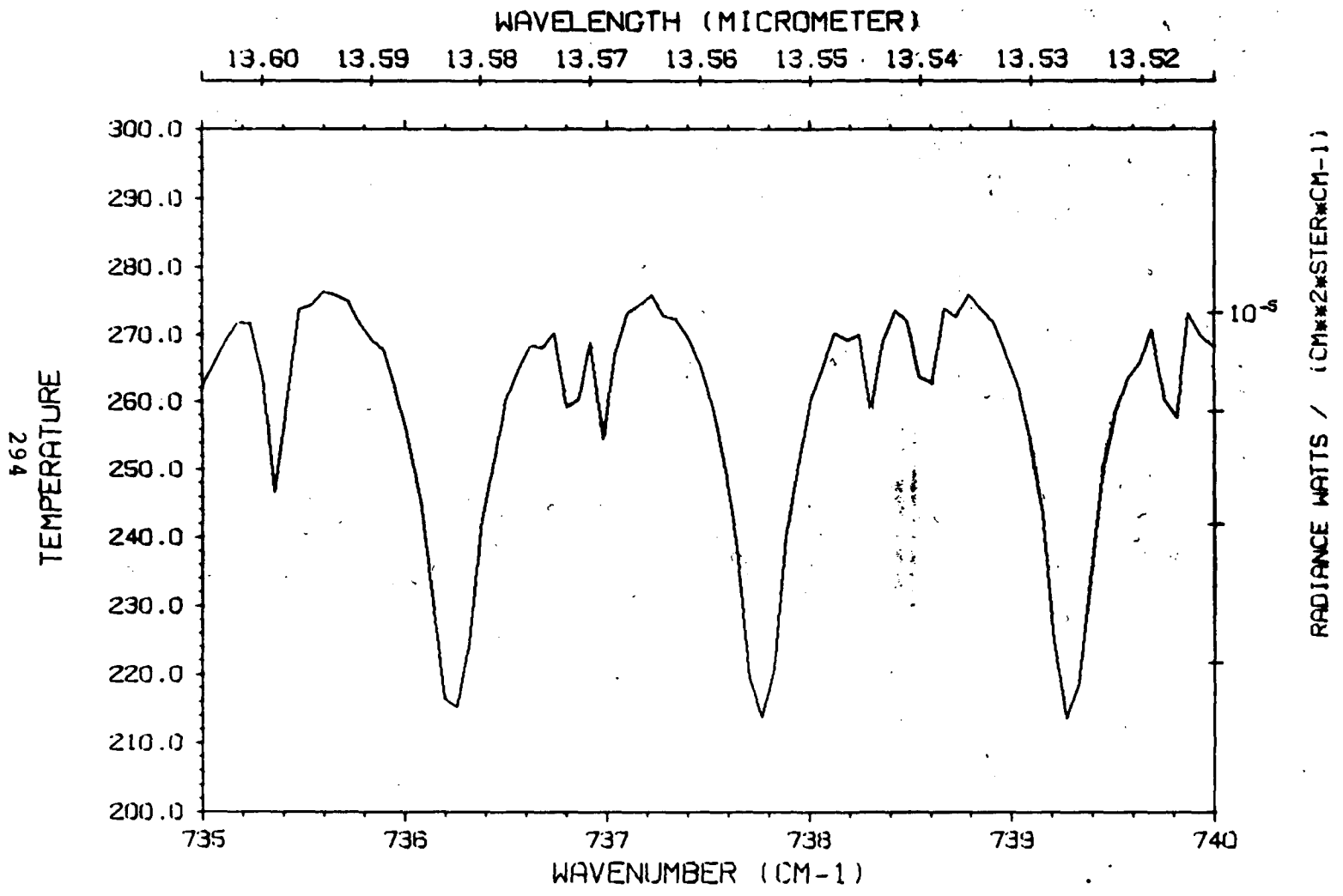

1 June 1989
Scribe (T3HIS2)

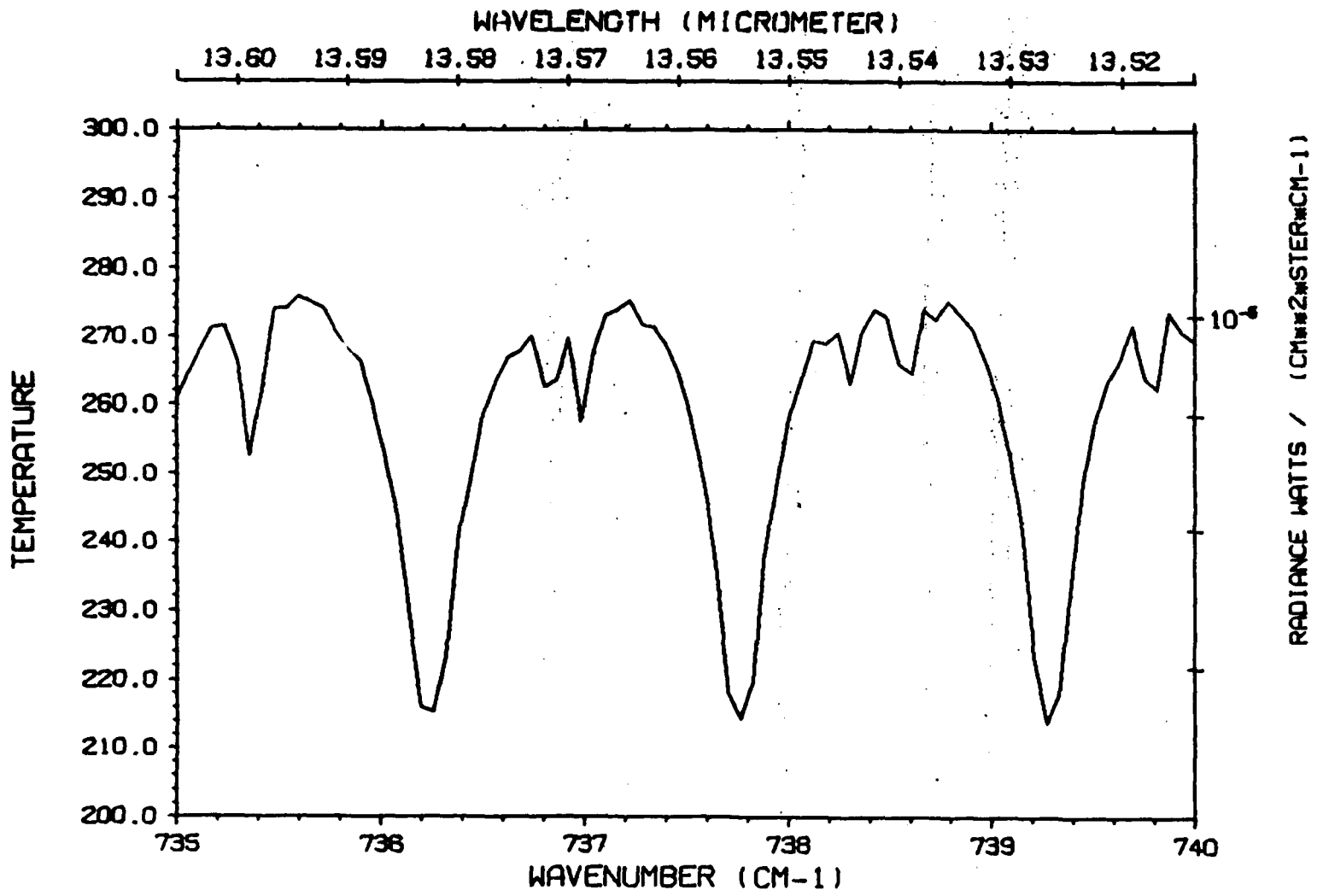

FASCODE
new CO_2 lines

HIGH SPECTRAL DENSITIES

HIGH TEMPERATURE

* o TEMPERATURE DEPENDENT CROSS SECTIONS (CALCULATED FROM HOT GAS TAPE)

Emissivity (T)

HEAVY MOLECULES

*** o TEMPERATURE DEPENDENT CROSS SECTIONS

o PRESSURE DEPENDENCE

PRINCIPAL CONCLUSIONS

		short term	long term
** Accuracy:	Strength	1%	<1%
	Air halfwidth	1%	<1%
	Air halfwidth temperature dep.	10%	2%
	Self broadened halfwidth	1%	<1%

** Include temp. dep. of self broadened HW — new parameter!

* Emphasis on pressure shifts for lidar purposes

** Include line coupling with temp. dep.

Include partition function tabulated as log Q at appropriate temp.

** Database structure should not constrain science

** User community should have access to a transition or supplemental data base

** Extended communications: Bulletin board and/or newsletter

** A single principal archive: AFGL

** Temp. dependent cross sections

THE STATUS OF H_2O AND NO_2

Jean-Marie Flaud
Laboratoire de Physique Moléculaire et Atmosphérique
CNRS and Université Pierre et Marie Curie
Tour 13, 4 Place Jussieu
75252 Paris Cedex 05
France

WATER VAPOR

	$H_2{}^{16}O$	$H_2{}^{17}O$	$H_2{}^{18}O$	HDO
				ν_2: 1986
0 - 4500 cm^{-1}	1981	1981	1981	$\nu_1, 2\nu_2$: 1985
4500 - 5900 cm^{-1}	1977		1985	
5900 - 7900 cm^{-1}	1986 (strong lines)		1986	
8000 - 9500 cm^{-1}	1988			
9500 - 11 500 cm^{-1}	1989		1987	
11500 - 13200 cm^{-1}				
13200 - 22700 cm^{-1}	1988			

Calculated
Only measured if not underlined

Main contributors

J.-M. FLAUD
C. CAMY-PEYRET
R.A. TOTH
J.-Y. MANDIN
J.-P. CHEVILLARD
A. PERRIN

SCHEMATIC DIAGRAMM OF ENERGY LEVELS $\omega_1 \approx \omega_3 \approx 2\omega_2$

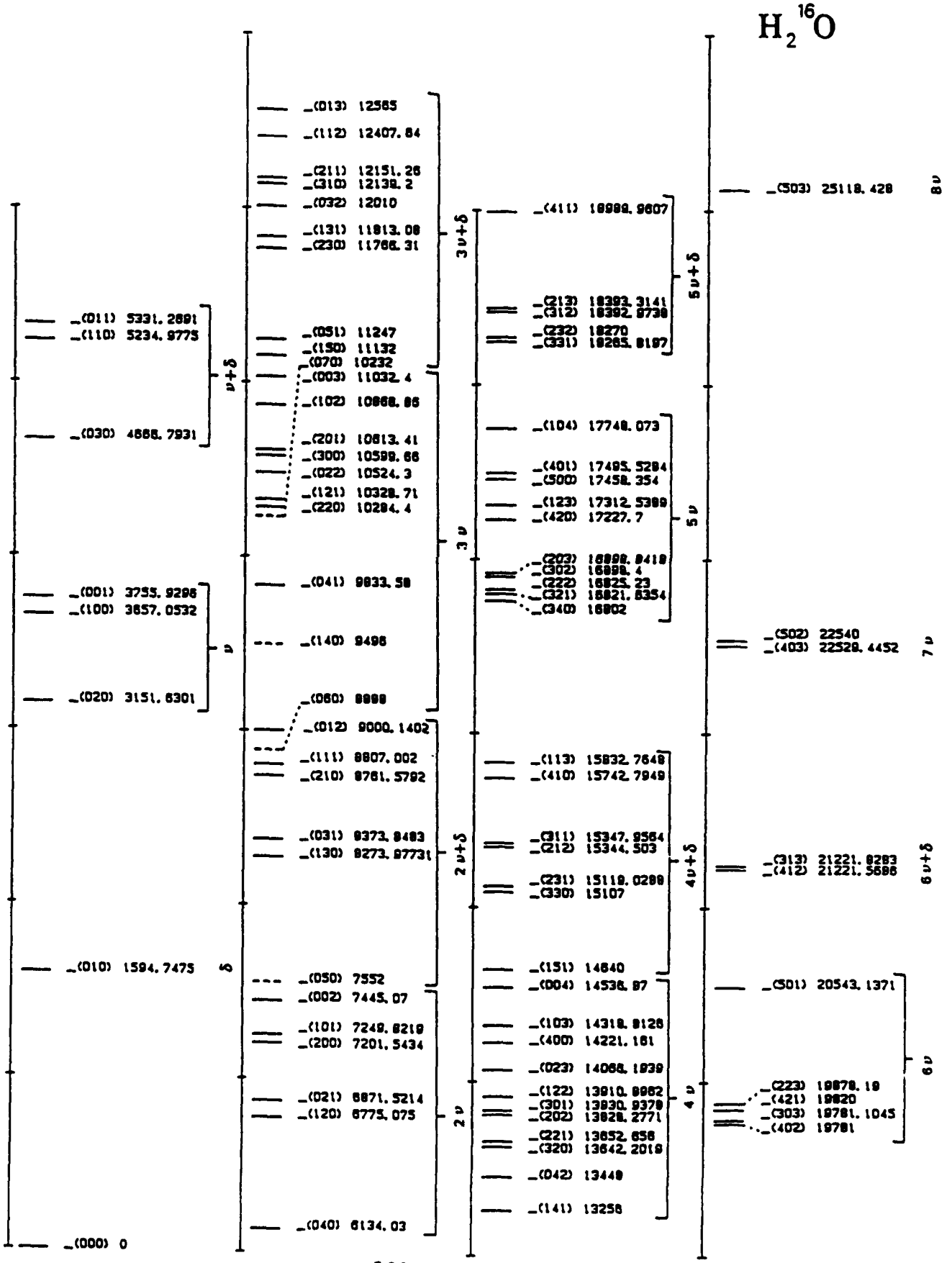

BRAULT FTS

AT KITT PEAK (N.S.O.)

4 400 to 25 250 cm^{-1} (about 60 spectra)

Natural

^{18}O and ^{17}O enriched spectra

Resolution: 0.020 to 0.010 cm^{-1}

SNR: 500 to 2 300

Collaborators: J.-M. FLAUD C. CAMY-PEYRET

J.-Y. MANDIN J.-P. CHEVILLARD

$H_2^{18}O$

LINE INTENSITIES

Statistical analysis

853 measured intensities	**107**	for	$3\nu_2$
	240	for	$\nu_1 + \nu_2$
	506	for	$\nu_2 + \nu_3$

Mean uncertainty:

13 % for $3\nu_2$ lines

8 % for $\nu_1+\nu_2$ and $\nu_2+\nu_3$ lines

$$\% = 100\ |Obs - Calc| / Obs$$

$0 < \% \leq 8$	73 %	of the lines
$8 < \% \leq 13$	16.5 %	
$13 < \% \leq 25$	9 %	
$25 < \% \leq 40$	1.5 %	

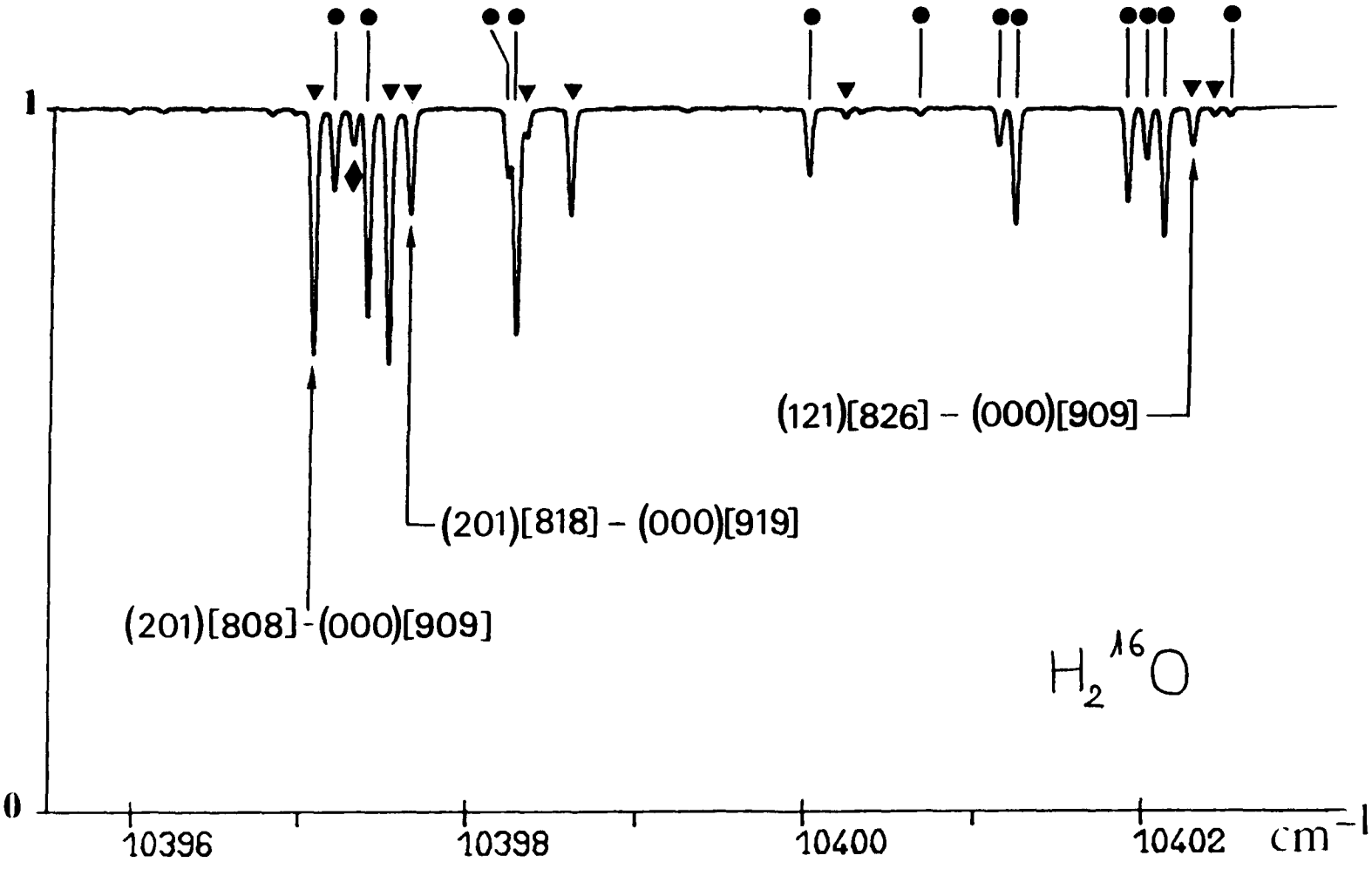

The resonances are different for $H_2{}^{16}O$ and $H_2{}^{18}O$
(see next figure)

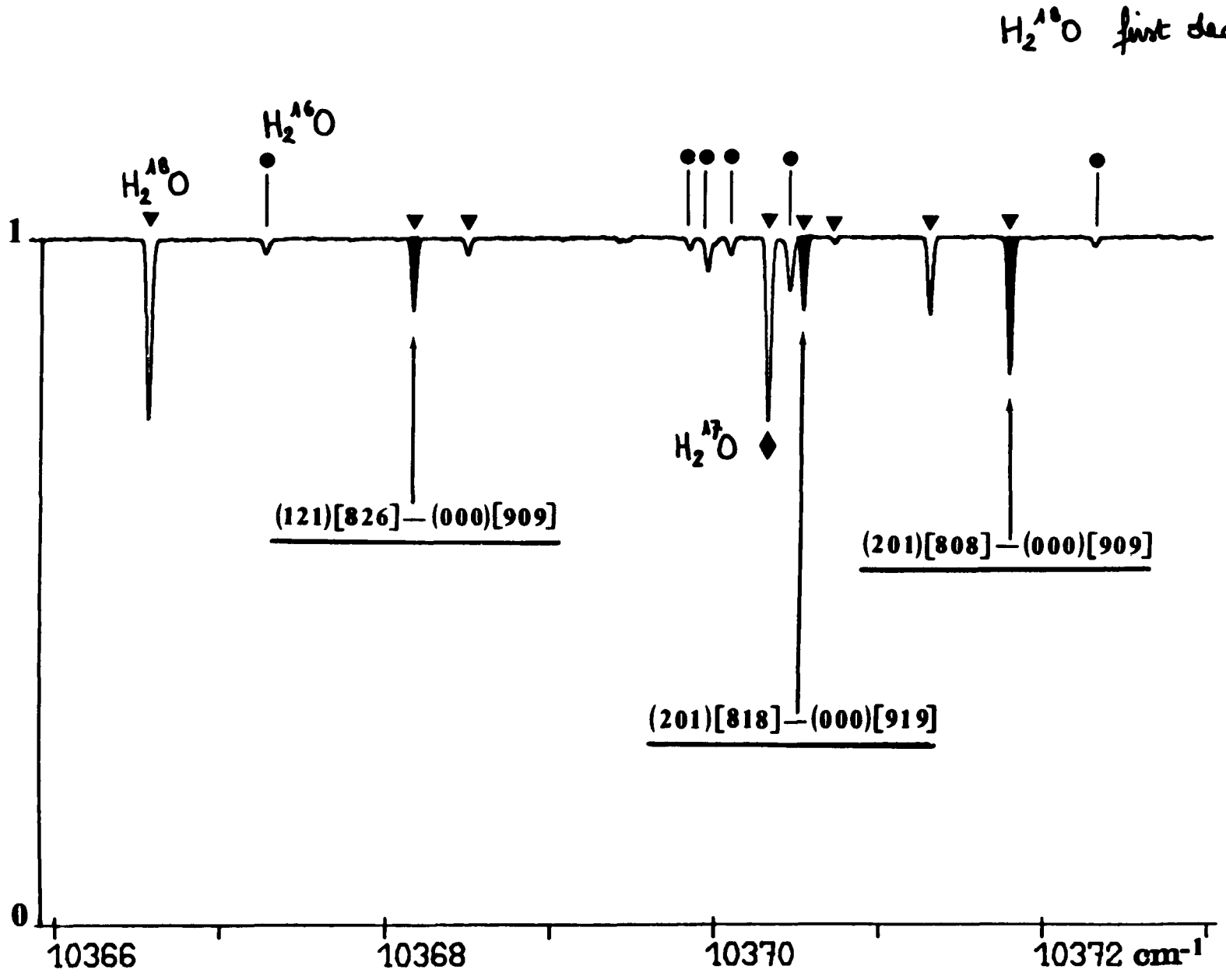
$H_2^{16}O$ first decad
$H_2^{18}O$
$H_2^{16}O$
$H_2^{17}O$
1
0
(121)[826]—(000)[909]
(201)[818]—(000)[919]
(201)[808]—(000)[909]
10366
10368
10370
10372 cm-1

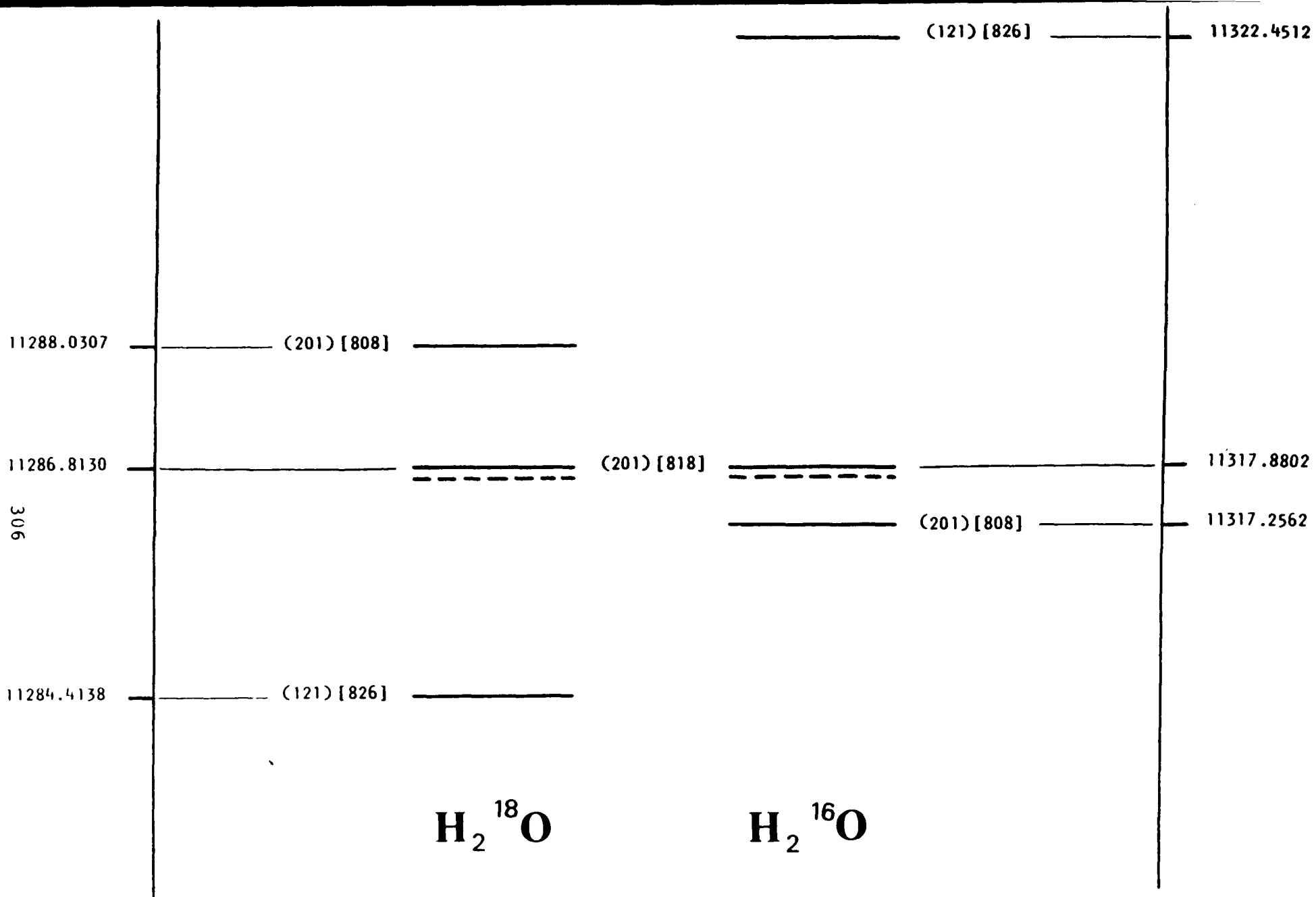
11288.0307
(201) [808]
11286.8130
11284.4138
(121) [826]
(201) [818]
(121) [826]
11322.4512
11317.8802
(201) [808]
11317.2562
$H_2{}^{18}O$
$H_2{}^{16}O$

$\gamma^\circ 10^{-4}$ cm^{-1}.atm^{-1} (width).

$S^\circ 10^{-4}$ cm^{-2}.atm^{-1} (strength). Measured this work.

HITRAN: Calculated γ°

MES: This work. Measured γ°.

MES/HITRAN.

H_2O

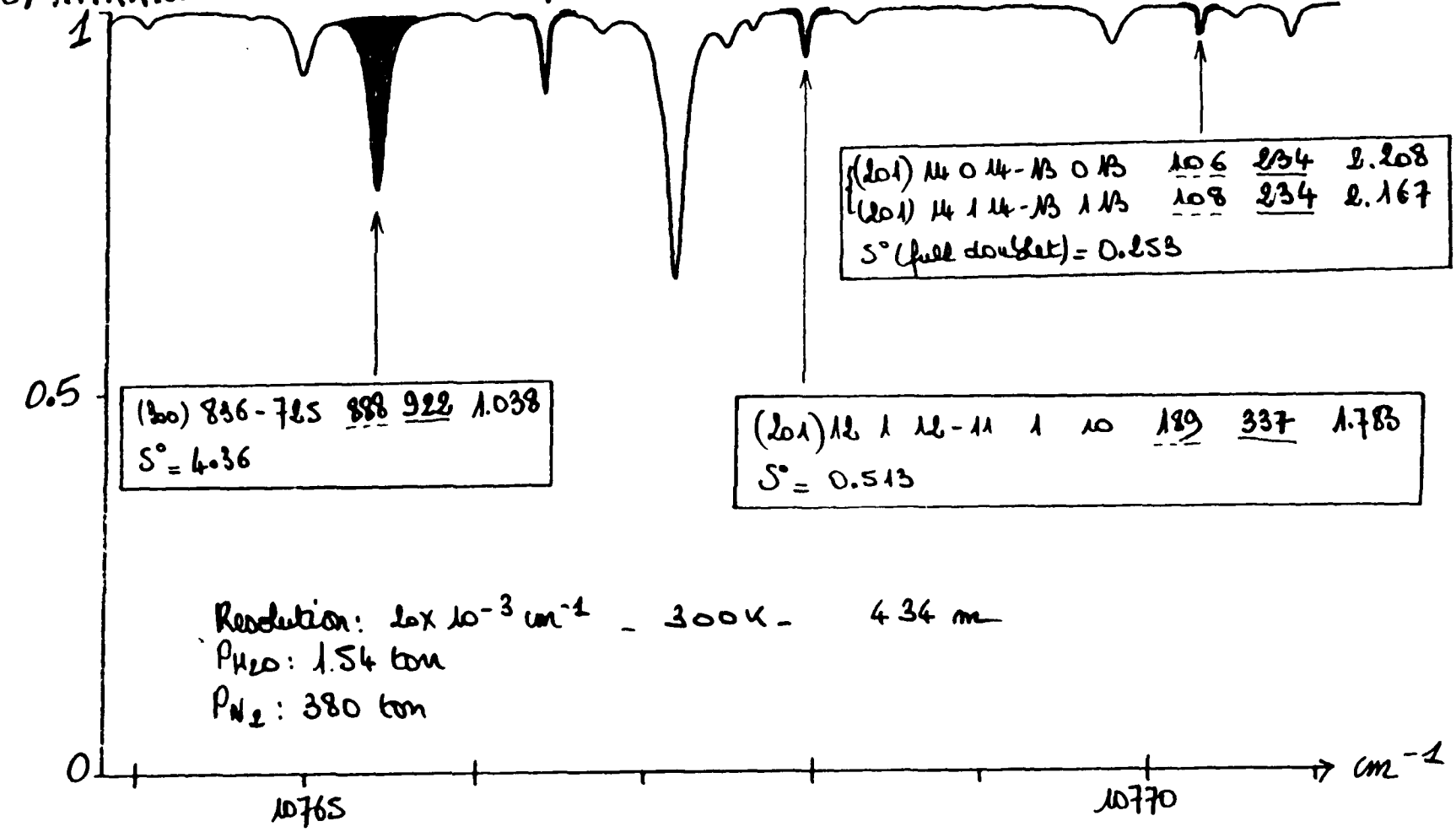

307

H_2O. For the doublets, the broadening coefficients are clearly calculated too low.

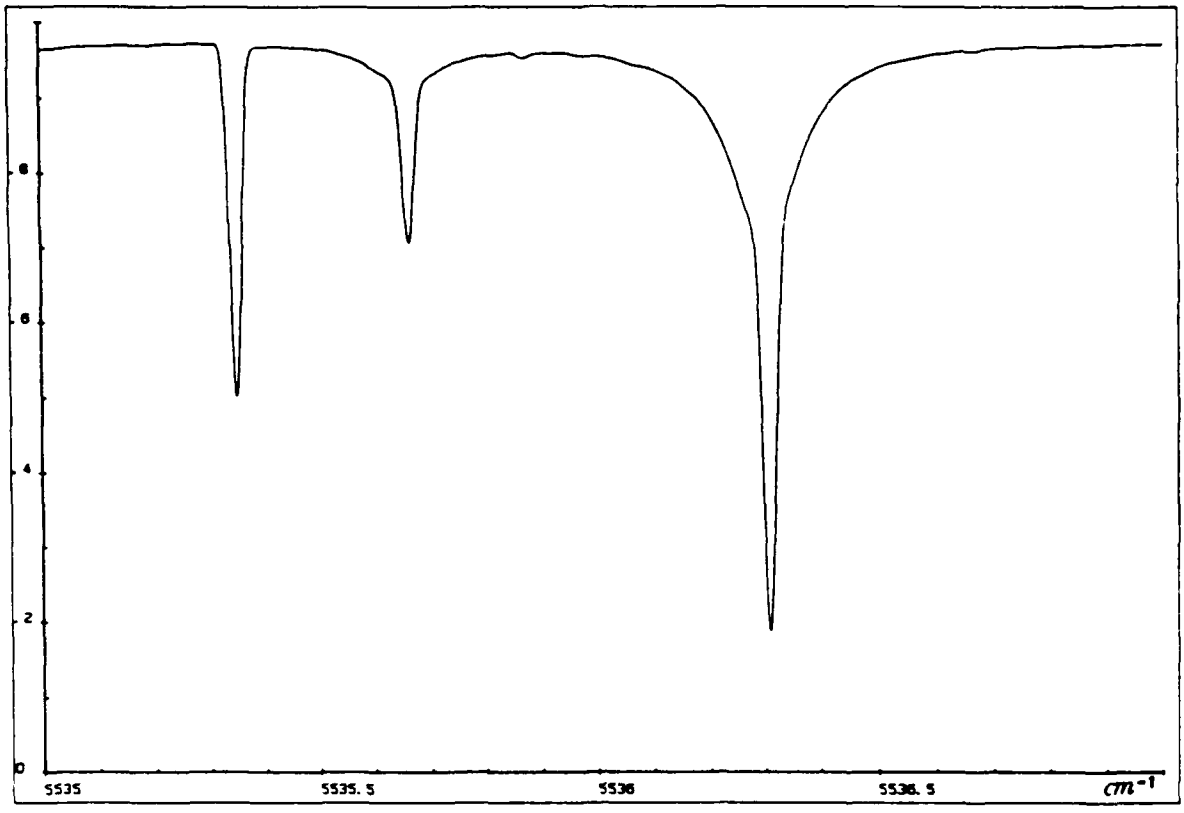

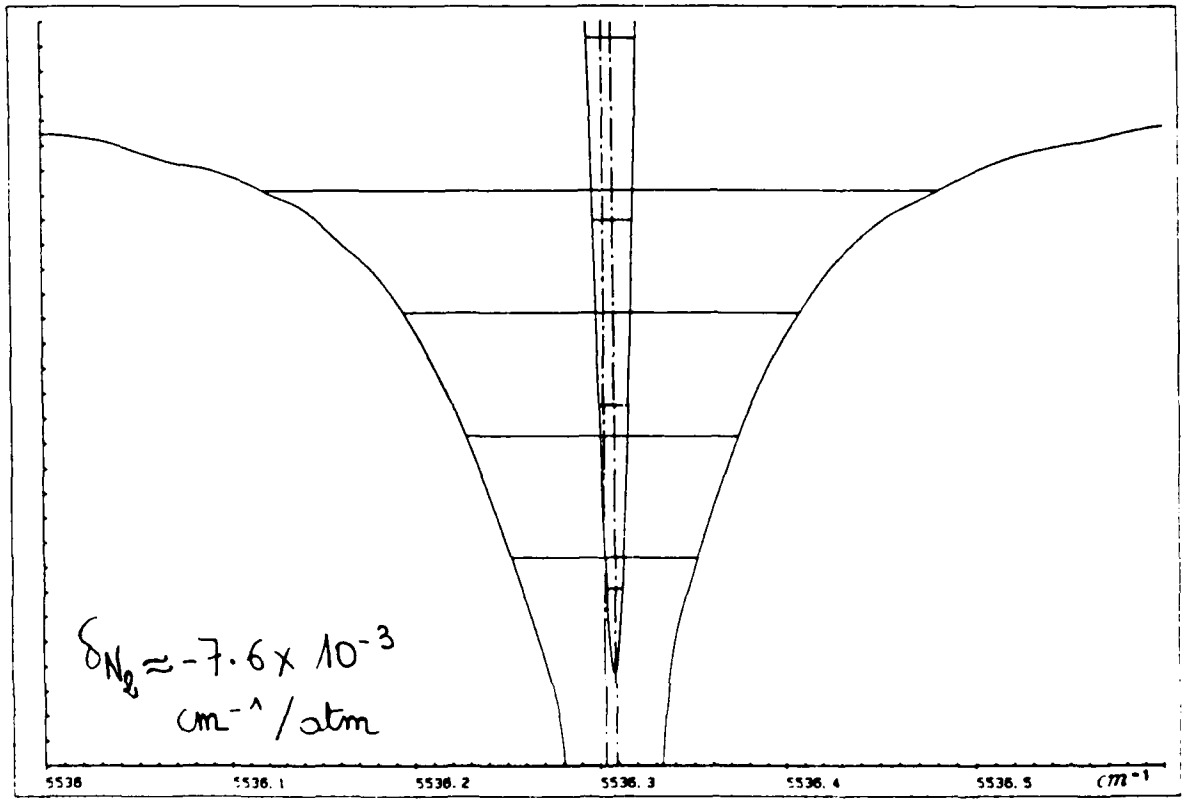

Example of PRESSURE LINE SHIFT of H_2O

(from J.-P. CHEVILLARD and J.-Y. MANDIN)

NO_2

(000) ⟷ (000) (010) ⟷ (010)	MW + FIR	1988	Rotation + Spin-Rotation + Hyperfine
(010) ⟵ (000)	14 μm	1988	" " + " "
(100) (020) (001) ⟵ (000)	6.3 μm	1982	Vibration-rotation + Spin-Rotation (Perturbation)
(011) ⟵ (010)			
(120) (101) ⟵ (000)	3.4 μm	1982	Vibration-rotation + Spin. Rotation (Perturbation)
(111) (130) ⟵ (010)			

(Calculations performed by A. Perrin, J.M Flaud and C. Camy-Peyret).

$(v_1\ v_2\ v_3=1)$	N	Ka	K_c	Energy en cm^{-1}	type of the resonance	WATSON'S TYPE HAMILTONIAN ONLY $E_{obs}-E_{calc}$
(001)	48	12	37	3622.3344	(1)	+ 0.097
	49	12	37	3663.6030		+ 0.110
	49	5	44	2827.2280	(2)	- 0.450
	50	5	46	2869.1760		- 0.513
(011)	46	4	43	3383.5100		0.076
	46	5	42	3451.7303		- 0.155
(101)	45	4	41	3887.3370		0.075
	46	5	42	3991.6340		- 0.035
(111)	38	4	35	4379.0664		- 0.085

(This Work)
Coriolis resonances taken into account:

	$E_{obs}-E_{calc}$
(100) $\overset{C}{\longleftrightarrow}$ (001) et (020) $\overset{C}{\longleftrightarrow}$ (001)	0.0002
	0.0039
	0.0049
	0.0059
(030) $\overset{C}{\longleftrightarrow}$ (001)	-0.0020
	-0.0032
(120) $\overset{C}{\longleftrightarrow}$ (101)	0.0013
	-0.0021
(130) $\overset{C}{\longleftrightarrow}$ (111)	0.0075

(1) $(100) \overset{C}{\longleftrightarrow} (001)$

(2) $(v_1\ v_2+2\ 0) \overset{C}{\longleftrightarrow} (v_1\ v_2\ 1)$

NO_2 - THE VIB-ROTATION RESONANCES ARE TO BE CONSIDERED TO REPRODUCE CORRECTLY THE LEVELS

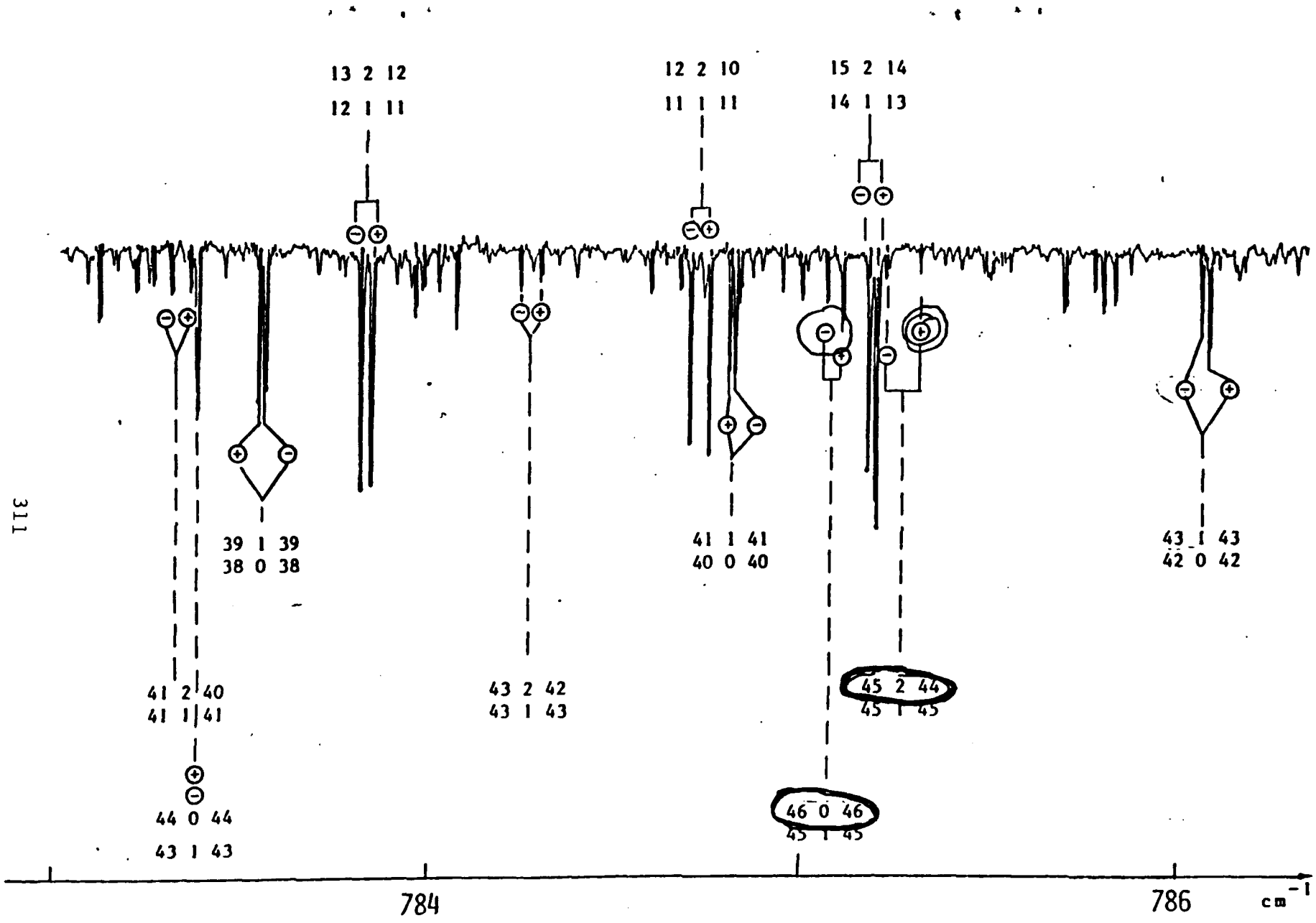

NO_2 : THE ν_2 band. spin-rotation resonance : [46 0 46] is resonating with [45 2 44]

NO_2 : EVIDENCE FOR HYPERFINE STRUCTURE

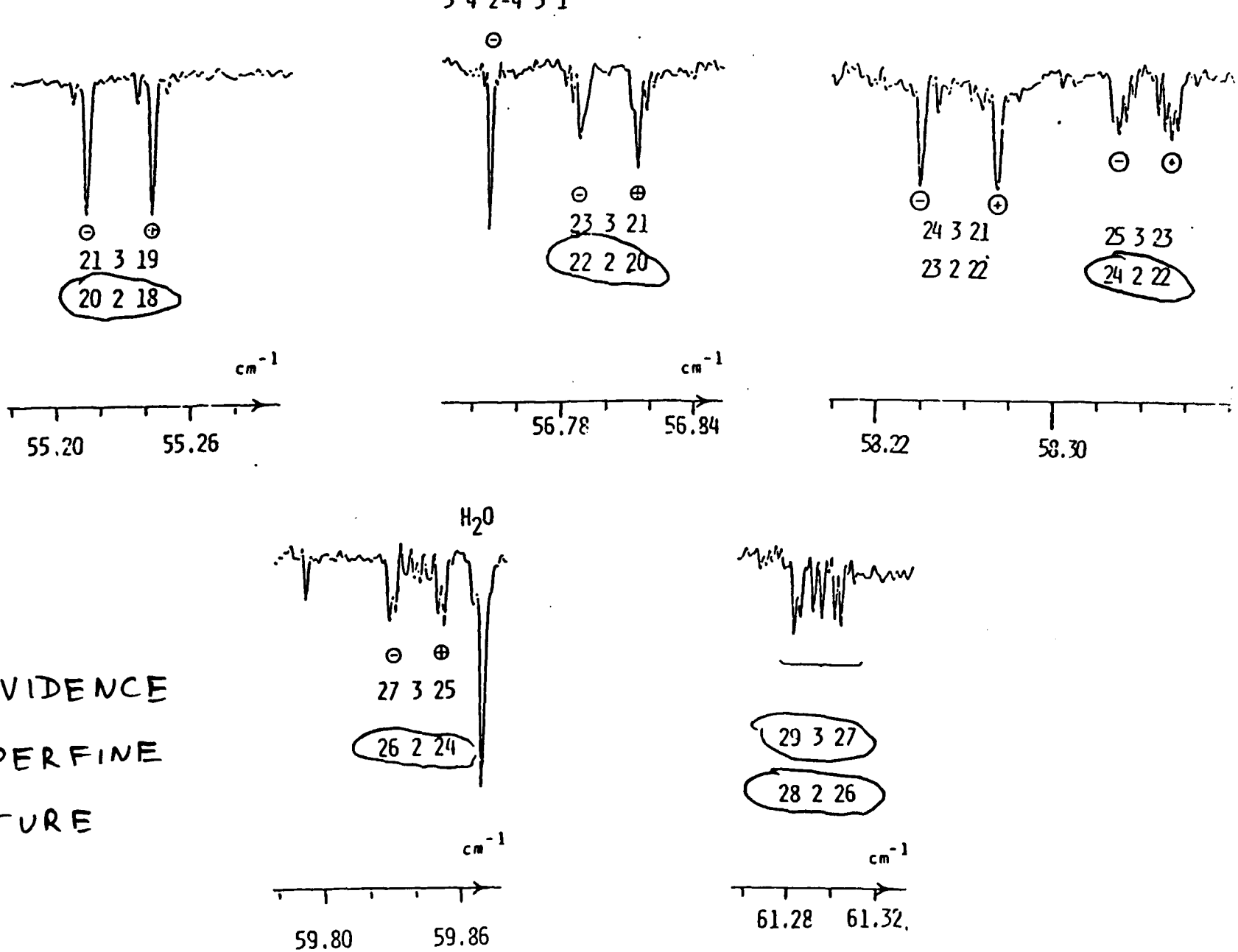

NO_2

EFFECTIVE ZERO-FIELD HAMILTONIAN

$$H = H_{ROT} + H_{SPIN\text{-}ROT} + H_{HFS} + H_Q$$

** H_{ROT} = WATSON-TYPE ROTATIONAL HAMILTONIAN

(I_R REPRESENTATION)

$$= A N_z^2 + B N_x^2 + C N_y^2 + \ldots$$

** $H_{SPIN\text{-}ROT}$ = ELECTRON SPIN-ROTATION INTERACTION

$$= \epsilon_{aa} N_z S_z + \epsilon_{bb} N_x S_x + \epsilon_{cc} N_y S_y + \ldots$$

* H_{HFS} = MAGNETIC HYPERFINE INTERACTION

$$= a_c T^1(\mathbf{I}) \cdot T^1(\mathbf{S}) - \sqrt{10}\, T^1(\mathbf{I}) \cdot T^1(\mathbf{S}, C^2)$$

Fermi constant — 2 constants

* H_Q = NUCLEAR ELECTRIC QUADRUPOLE INTERACTION

$$= e\, T^2(\mathbf{Q}) \cdot T^2(\nabla E)$$

2 constants

* Hyperfine constants derived from MW

** The higher order constants are derived from the high K_a and J levels observed in the infrared.

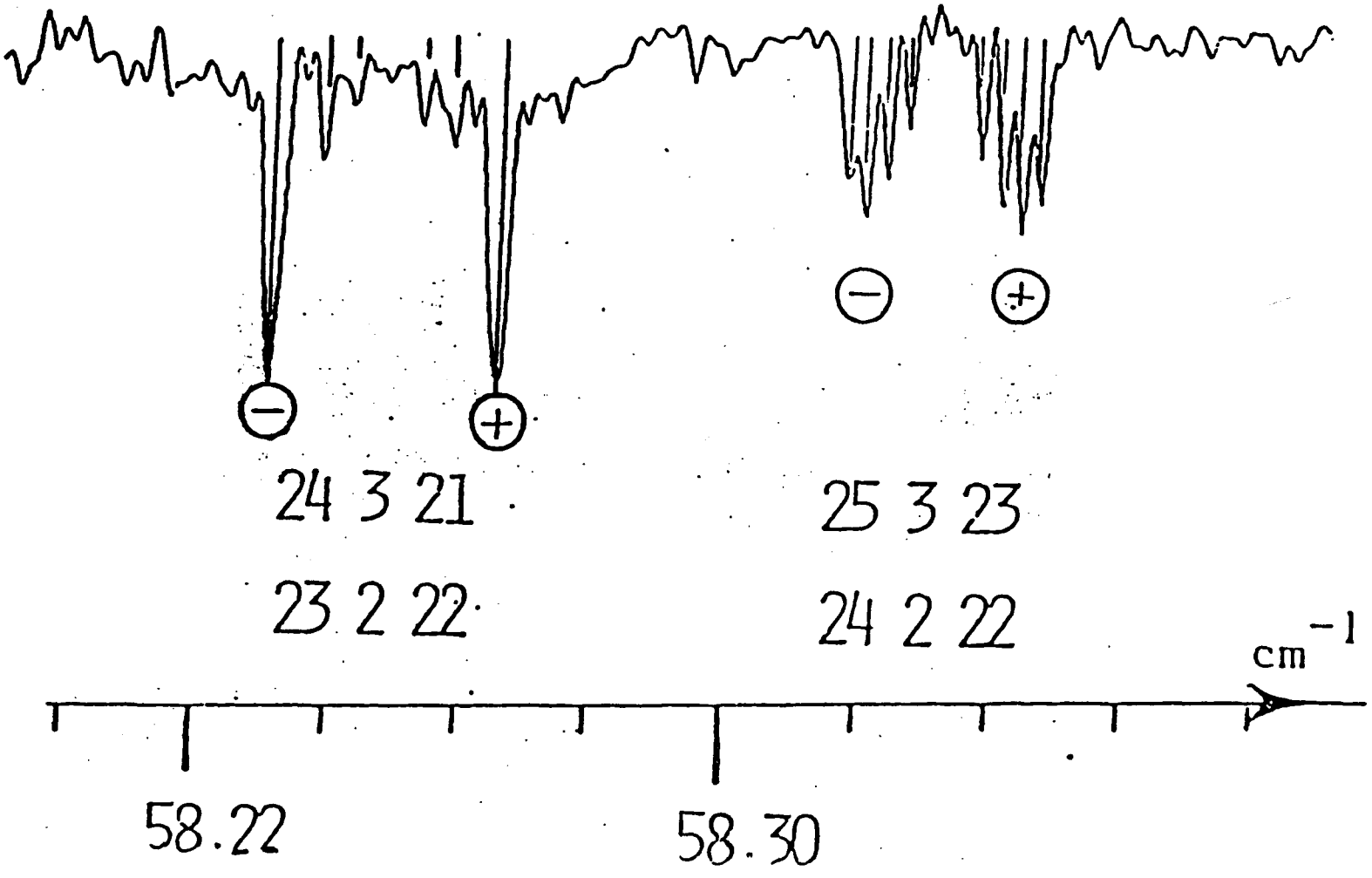

NO_2

THE CALCULATION (BARS) IS EXCELLENT

(A. Perrin et al. J. M. S 130, 168-182 (1988))

CONCLUSION

A Lot of work still to be done !!

H_2O

Below 6000 cm^{-1}

* New intensity measurements (Mainly in the band wings)
* New position measurements $\Rightarrow$ 0.1 or 0.2 $\times 10^{-3}$ cm^{-1} accuracy.

Above 6000 cm^{-1}

* Improve theory to refine the assignments.

General problem of broadening coefficients and line shifts.

NO_2

* Pure rotation, ν_2 OK
* Other bands : improve theory to treat simultaneously the vibration-rotation, spin-rotation and Hyperfine interactions.

(Problem of the number of lines : 33000 lines between 0 - 230 cm^{-1} for the pure rotation NO_2 spectrum)

SELECT: THE USER-FRIENDLY INTERFACE TO HITRAN

Robert R. Gamache
The University of Lowell
Center for Atmospheric Research
450 Aiken Street
Lowell, MA 01854

Laurence S. Rothman
GL/OPI
Hanscom AFB, MA 01731-5000

SELECT: the User-friendly Interface to HITRAN

Robert R. Gamache, The University of Lowell
Center for Atmospheric Research,
Lowell, MA

Laurence S. Rothman, Optical Physics Division
Geophysical Laboratory
Hanscom AFB
Bedford, MA

ULCAR

SELECT is a user-friendly interface to HITRAN which allows the selection from the database of up to ten choices of molecule, isotope, vibrational bands, and a cutoff in line intensities.

All selections are checked for validity of the input.

Output file format can be 1982/1986 AFGL format, line listings are available.

User specified formats are straightforward.

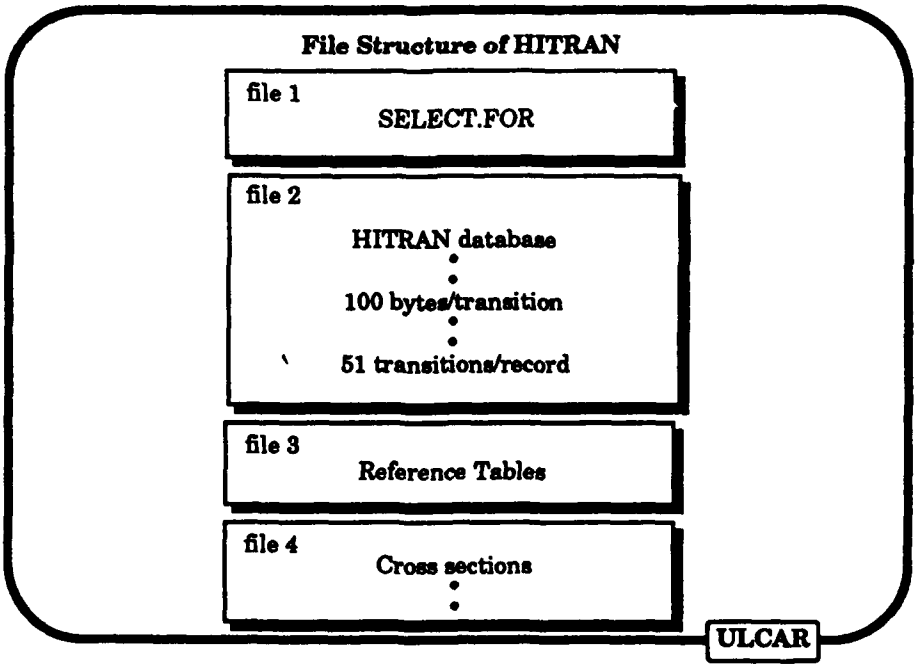

This is the file structure of the distributed HITRAN tape. It consist of:

the SELECT program

the HITRAN database

a file of reference tables, e.g. isotopic abundance, atomic masses, etc.

a file of absorption cross sections for heavy molecular species such as chlorofluorocarbons (CFC's) and oxides of nitrogen which are not amenable to line-by-line representation.

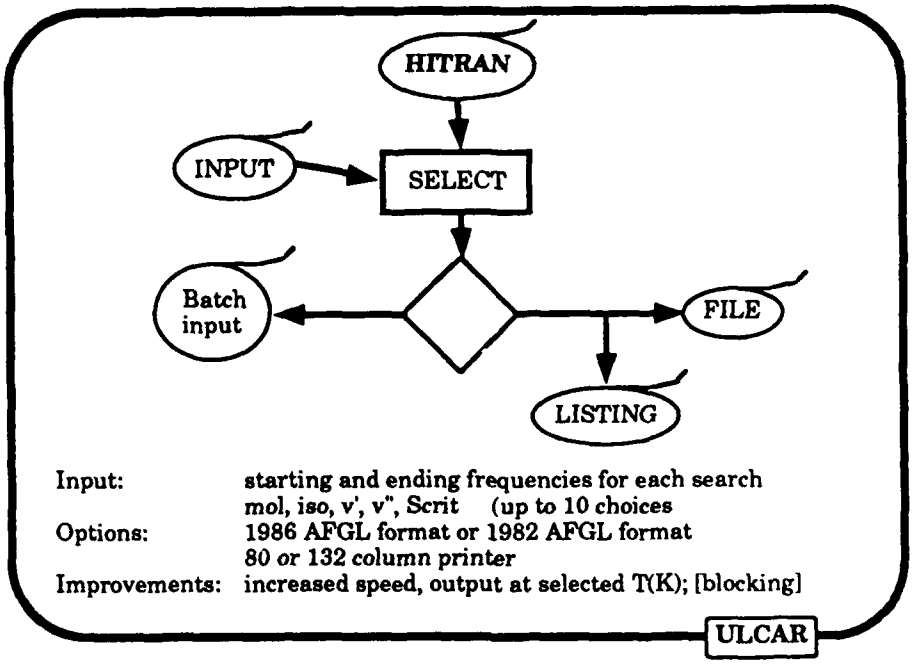

This shows schematically the functions of SELECT.

User specified input are used to select the particular transitions from the HITRAN database.

The program also allows batch input files to be generated in the user-friendly mode.

Files and **listings** of the selected data are the output of SELECT.

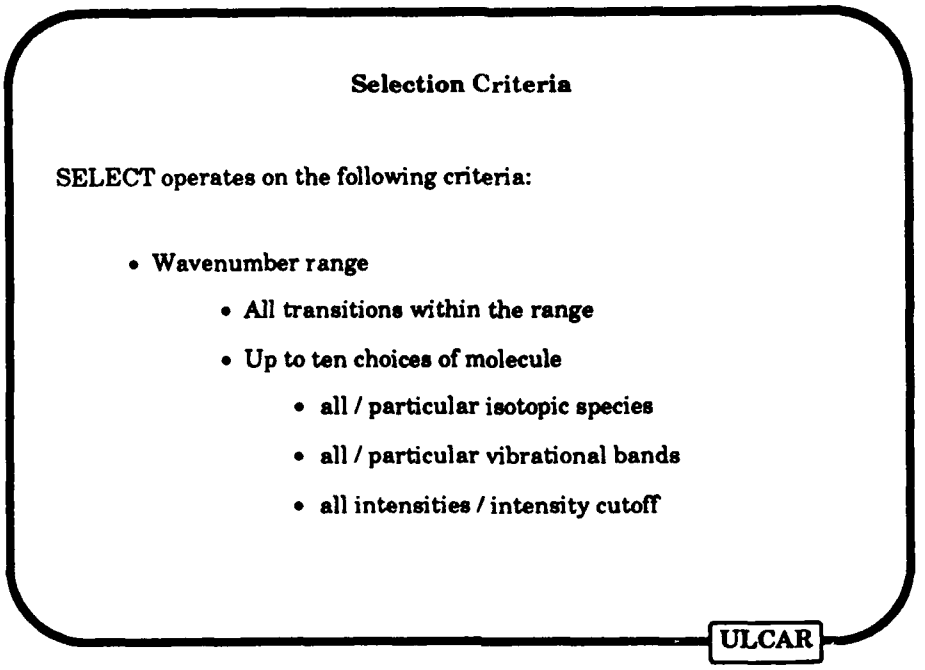

After defining a wavenumber interval, one can select all transitions within the interval **or** up to ten combinations of molecules, isotopic species, vibrational bands, and intensity.

For example; in a given range, one can select the ν2 band of HDO, all CO2 lines, the ν3 band of O3, etc.

HITRAN version 1989

The first block HITRAN will contain a version number and a wavenumber - block correspondence table to decrease the time necessary to read the database.

Advancing to block with first frequency - 2.8 times faster

Reading and selecting data - 2.5 times faster

all molecules (~9), molecule, and molecule-isotope searches

SELECT will now couple to a version number of HITRAN. If the wrong version of HITRAN is being read a warning is issued and the speed factor will be lost. This change will be upward compatible.

ULCAR

New features of the 1989 version of SELECT

New routines have been written to speed up certain selection choices, i.e. all molecules, all of one molecule

1986 HITRAN format as default for speed

~9 times faster for an all transition selection

Output files at a specified temperature within the range 70 - 2005 K

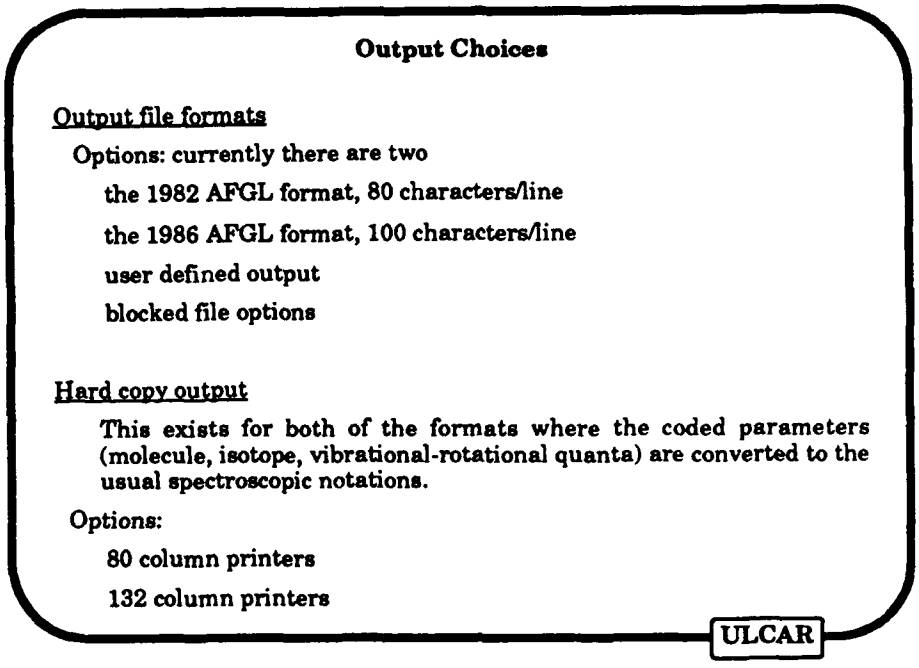

Output consist of:

line files in the **1986** or 1982 AFGL formats (we recommend the 1986 format to take advantage of the speed)

hard copy output for 80 or 132 character width printers

User defined output is straightforward and is noted in the program.

Partition Sums

Partition sums calculated for all species on database.

70 - 425 K in 5K steps

405 - 2005 K in 20 K steps

Polynomial representation of temperature dependence

$$Q(T) = a + bT + cT^2 + dT^3$$

Accuracy :

low temperature range a few tenths of a percent error in fit

high temperature range one percent error in fit

ULCAR

Partition sums were explicitly calculated for all isotopic species on the database over a temperature range of 70 to 2005 K.

These were done in two ranges 70 to 425 K in 5K steps and from 405 to 2005 K in 20K steps.

The temperature dependence of the partition sum was fit by a polynomial and the coefficients determined by a minimax fit . low range a few tenths of a percent error in the fit (except CO2 ~1%), high range about 1% error in the fits (except CO2 ~5%)

Temperature Dependent Output Files

A new feature is the creation of output files for specific temperatures. Current range is from 70 -2005 K. Note there is an increase in run time.

$$S(T) = S(T_0)\frac{Q(T_0)}{Q(T)}\exp\left(\frac{c_2 E''(T-T_0)}{T\,T_0}\right)\left[\frac{\left(1 - e^{-c_2\nu_0/T_0}\right)}{\left(1 - e^{-c_2\nu_0/T}\right)}\right]$$

$$Q(T) = a + bT + cT^2 + dT^3$$

$$\gamma(T) = \gamma(T_0)\left(\frac{T_0}{T}\right)^n$$

ULCAR

The feature now exist for the output line files to be at temperatures other than the standard temperature of 296K.

The current limitations are temperatures from 70 to 2005K.

The line intensities and the air-broadened halfwidths are converted to the appropriate temperatures.

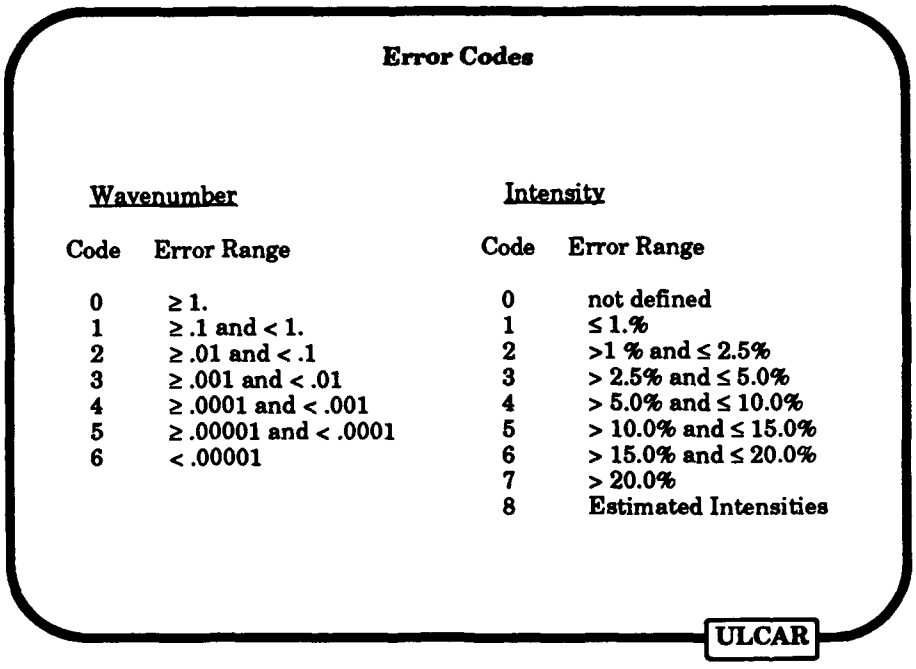

Error codes are now used to indicate the quality of the data for the line position, the line intensity, and the air-broadened halfwidth.

Above are the values used for the position and intensity.

Discussions at the Workshop suggested the codes all follow the same form. Using the wavenumber code as a model the following codes are suggested for the intensities.

code	error range
0	estimated
1	> 20 %
2	≤ 10 % and < 20 %
3	≤ 5 % and < 10 %
4	≤ 2 % and < 5 %
5	≤ 1 % and < 2 %
6	≤ 1 %

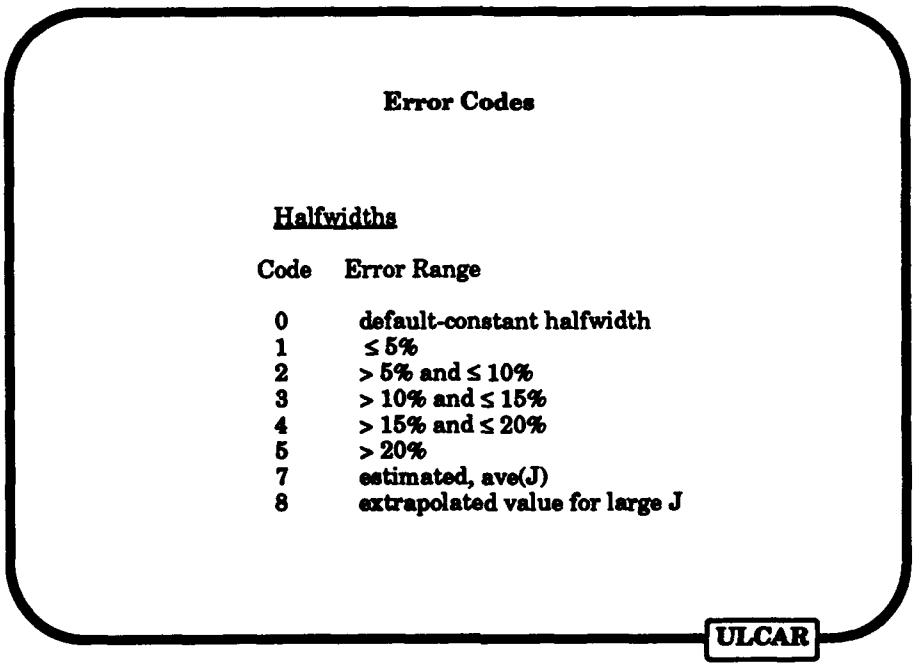

Error codes are now used to indicate the quality of the data for the line position, the line intensity, and the air-broadened halfwidth.

Above are the values for the air-broadened halfwidths. Discussions at the Workshop suggested the codes all follow the same form. Using the wavenumber code as a model the following codes are suggested for the halfwidths.

code	error range
0	default-constant halfwidth
1	> 20 %
2	≤ 20 % and > 10 %
3	≤ 10 % and < 5 %
4	≤ 5 % and < 2 %
5	≤ 2 % and < 1 %
6	≤ 1 %

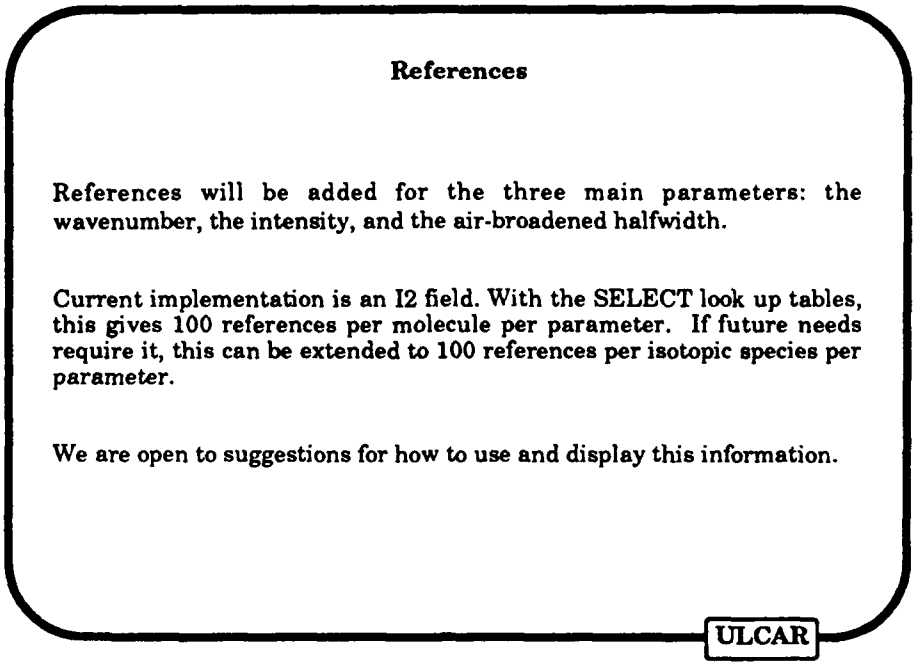

Although not fully implemented, provisions have been made for adding references for the three main data; the wavenumber, the intensity, and the air-broadened halfwidth of the transitions.

HITEMP: THE HOT GAS COMPILATION STATUS AND COMPARISON WITH OBSERVATIONS

John E.A. Selby
Grumman Corporate Research Center
Mail Stop A08-35
Bethpage, NY 11714

Laurence S. Rothman
GL/OPI
Hanscom AFB, MA 01731-5000

Richard B. Watson
Visidyne, Inc.
South Bedford Street
Burlington, MA 01803

Robert R. Gamache
Center for Atmospheric Research
University of Lowell Research Foundation
450 Aiken Street
Lowell, MA 01854

Jean-Marie Flaud
C. Camy-Peyret
Laboratoire de Physique Moléculaire et Atmosphérique
CNRS and Université Pierre et Marie Curie
Tour 13, 4 Place Jussieu
75252 Paris Cedex 05
France

OUTLINE

OBJECTIVES

APPLICATIONS

HISTORY

OUTLINE OF CONTRACT

VALIDATION & TESTING

STATUS

ISSUES

SUMMARY & CONCLUSIONS

RECOMMENDATIONS

HITEMP OBJECTIVES

- HIGH TEMPERATURE DATA BASE FOR LINE-BY-LINE CALCULATIONS (FASCODE)
- SAME FORMAT AS GL HITRAN 86 DATA BASE
- TEMPERATURE RANGE 1000K TO 2500K
- WAVELENGTH RANGE (A) 2.2 - 10- MICROMETERS (PHASE 1)
  (B) 1-20 MICROMETERS (PHASE 2)
- ALL IMPORTANT COMBUSTION SPECIES

  CO2, H2O, CO, Hf, HCL, OH, NO, HBOx. ETC
- (C - H FAMILY FUTURE CANDIDATE)

APPLICATIONS

HIGH RESOLUTION

- SIMULATION OF HOT GASEOUS SOURCES (SPECIES DISCRIMINATION, CHARACTERIZATION)
- ATMOSPHERIC PROPAGATION OF HOT GASEOUS SOURCES (PLUMES ETC).
- LASER PROPAGATION THROUGH PLUMES
- NARROW BAND DETECTION/OPTIMIZATION

MEDIUM/LOW RESOLUTION

- PLUME DETECTION/SPECTRAL OPTIMIZATION
- BAND MODEL APPLICATION/SUPPLEMENT

HISTORY

- 1977/78 — GRUMMAN HOT GAS TAPE (SELBY/CALFEE)
  EXTRAPOLATION FROM KNOWN CO2 & H2O CONSTANTS 2.7 & 4.3 μm
- 1978/83 — GRUMMAN HOT GAS TAPE
  INCLUDED NEW H2O CALCULATIONS (FLAUD & CAMY-PEYRET)
  1000 – 4500 CM $^{-1}$ (2.2 -- 10 μm)
- 1984/87 — GRUMMAN/AFGL COLLABORATION
  - REPLACED CO2 USING BEST CONSTANTS (ROTHMAN/WATTSON)
  - INCLUDED H2O HALF WIDTHS (R. GAMACHE)
- 1988 — AFGL CONTRACT WITH GRUMMAN (HITEMP) – DEC 88
  - NEW CO2 (WATTSON/ROTHMAN)
  - NEW CO (TIPPING)
  - EXTEND HOT H2O (SELBY/FLAUD/CAMY-PEYRET) (2.2 – 10 μm)

FUTURE

PHASE 2 – VERSION 2 1989 (→ 1990)
PHASE 3 – VERSION 3 1990 (→ 1991)

CONTRACT STATUS

- HITEMP WAS SUPPORTED BY AFAL UNDER AFGL CONTRACT

- NOT FUNDED IN FY 89

OUTLINE OF CONTRACT

TASK 1 - CONSTRUCT USER TAPES IN 3 PHASES

TASK 2 - VALIDATE TAPE AGAINST SELECTED LAB & FIELD MEASUREMENTS (3 PHASES)

TASK 3 - MAKE COMPARISON BETWEEN LINE-BY-LINE & SIRRM CALCULATIONS

TASK 4 - PROVIDE GUIDANCE TO POTENTIAL USERS

TASK 5 - CONDUCT ADDITIONAL LAB OR FIELD MEASUREMENTS

TASK 1 CONSTRUCTION OF TAPE

PHASE 1 2-10 μM FOR H_2O, CO_2, CO (SEPT. '88)

PHASE 2 UPDATE H_2O, INCLUDE HF, HCl, OH, NO, N_2O MAY/SEPT '89

PHASE 3 ADDITIONAL SPECIES HBO, BO ETC. (AS PRIORITIZED BY AFAL) MAY/SEPT. 90

TASK 2 VALIDATION AND TESTING

- HIGH RESOLUTION (1000 - 3000K) FLAME SPECTRA/HOT CELL
  - AFGL (.005 cm^{-1})
  - CNRS (.05 cm^{-1})
  - GRUMMAN (0.05 cm^{-1})
  - ERIM (0.3 cm^{-1})
- MEDIUM/LOW RESOLUTION (300 - 1000 K) - HOT CELL
  - ERIM
  - OPTIMETRICS
  - AEDC
  - ECOLE CENTRALE
  - CNRS
  - AERONUTRONIC FORD
- OTHER - EARLY CLASSICAL MEASUREMENTS (PENNER, FERRISO, LUDWIG ET AL.)
- FIELD MEASUREMENTS

PROGRESS H2O

- JAN – JULY 88
- REANALYSED GRUMMAN/CNRS H2O DATA BASE FOR HITRAN 86 (SELBY/FLAUD/CAMY-PEYRET)
- RECALCULATED H2O HALF WIDTHS (R. GAMACHE)
- COMBINED GRUMMAN/CNRS AND AFGL HITRAN 86 (ELIMINATING DUPLICATE LINES FROM HITRAN 86)
- COMPARISONS WITH MEASUREMENTS (2.7, 6.3 μm)

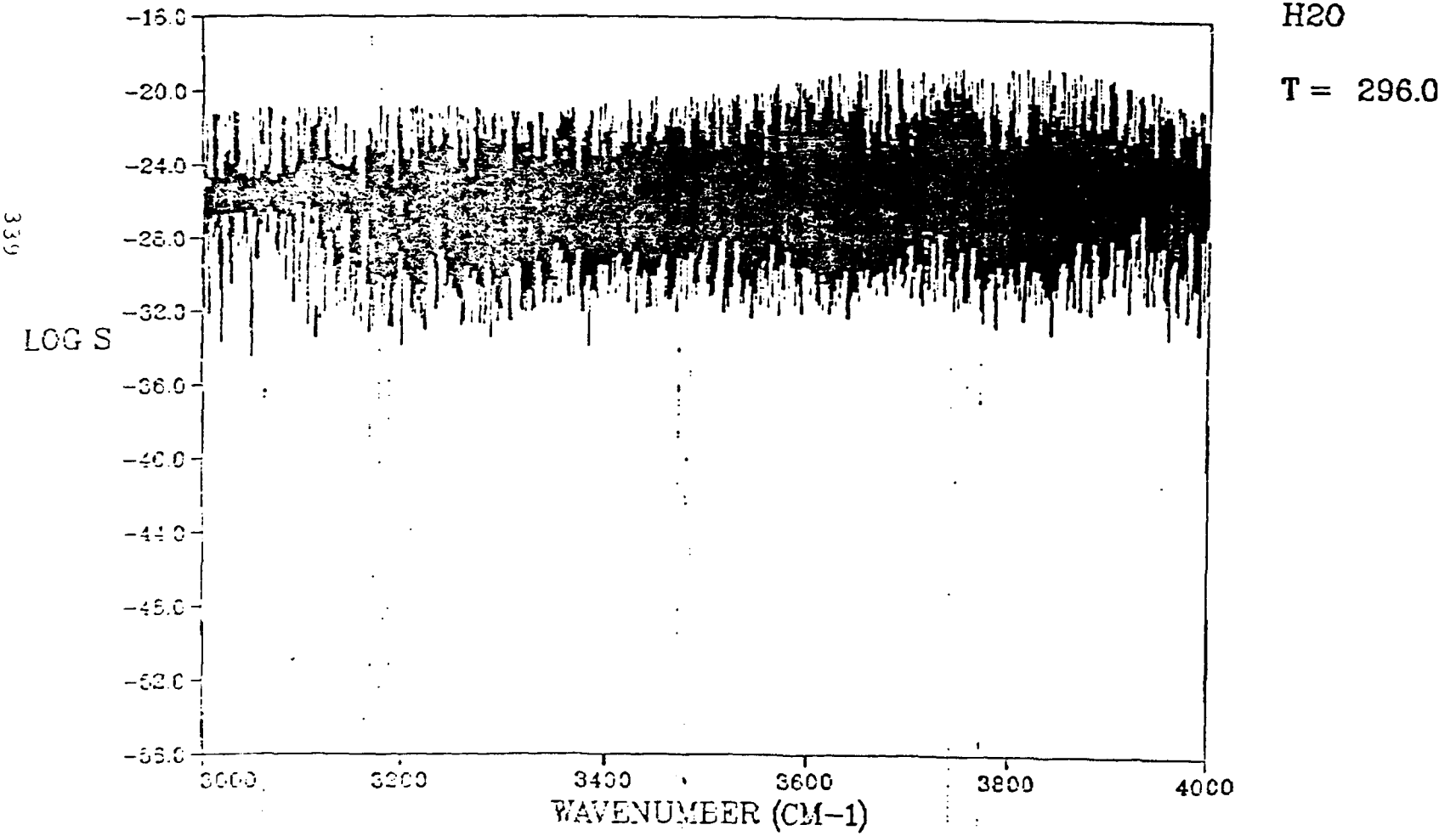
H20
T = 296.0
LOG S
-16.0
-20.0
-24.0
-28.0
-32.0
-36.0
-40.0
-44.0
-48.0
-52.0
-56.0
3000
3200
3400
3600
3800
4000
WAVENUMBER (CM-1)

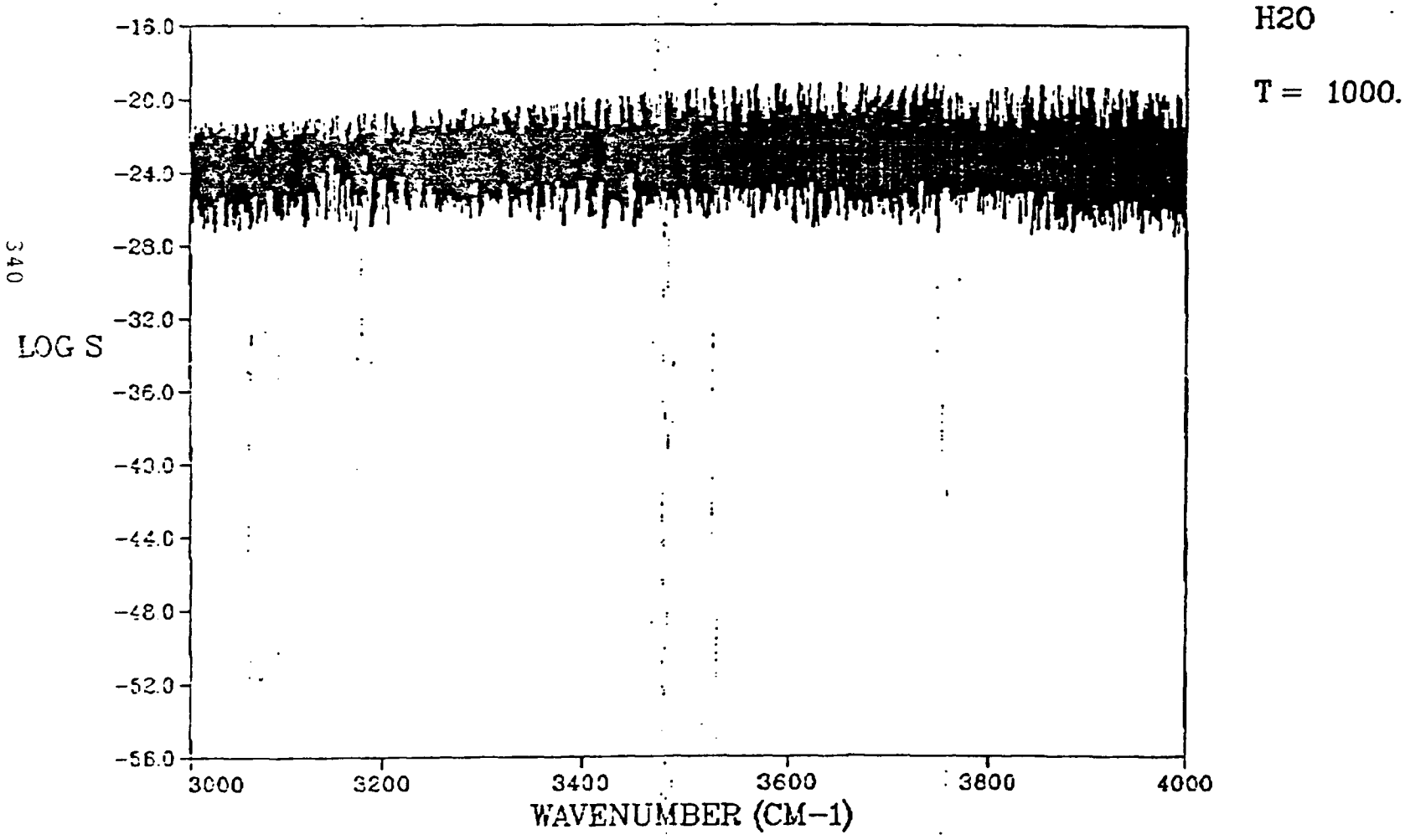
H20
T = 1000.
-16.0
-20.0
-24.0
-28.0
-32.0
-36.0
-40.0
-44.0
-48.0
-52.0
-56.0
LOG S
3000
3200
3400
3600
3800
4000
WAVENUMBER (CM-1)

PROGRESS CO2

- DEC 88 RECEIVED CO2 DATA (WATTSON/ROTHMAN)
- 2.2×10^6 LINES
- ASSESSMENT
  - TRANSITION ID FOR HIGH VIB STATES LOST
  - DUPLICATE OR SPLIT LINES
  - UNUSUAL Q BRANCHES
  - PARTITION SUM QUESTION
- TEST CALCULATIONS
- COMPARISON WITH MEASUREMENTS

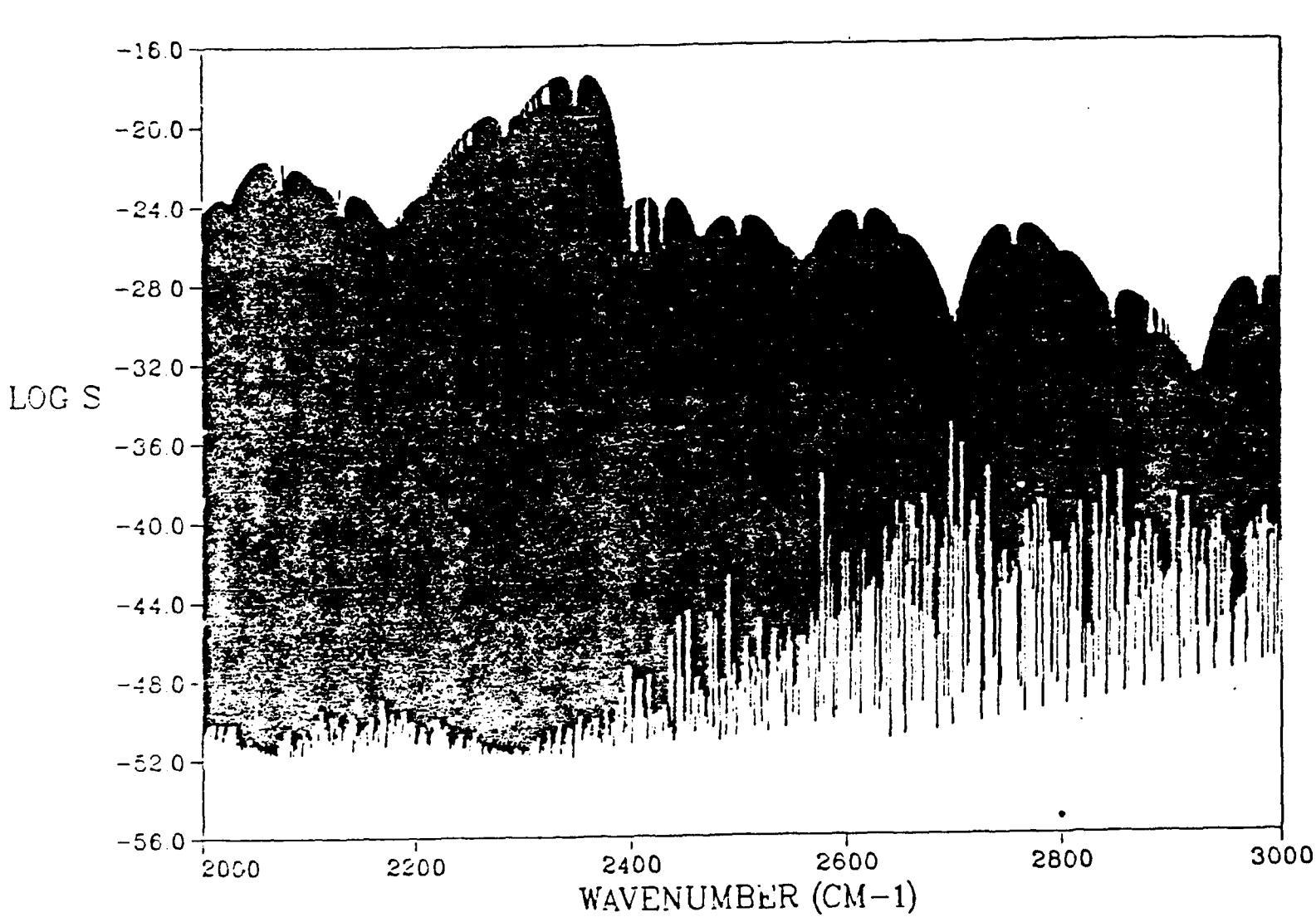
CO2
T = 296.0
LOG S
-16.0
-20.0
-24.0
-28.0
-32.0
-36.0
-40.0
-44.0
-48.0
-52.0
-56.0
2000
2200
2400
2600
2800
3000
WAVENUMBER (CM-1)

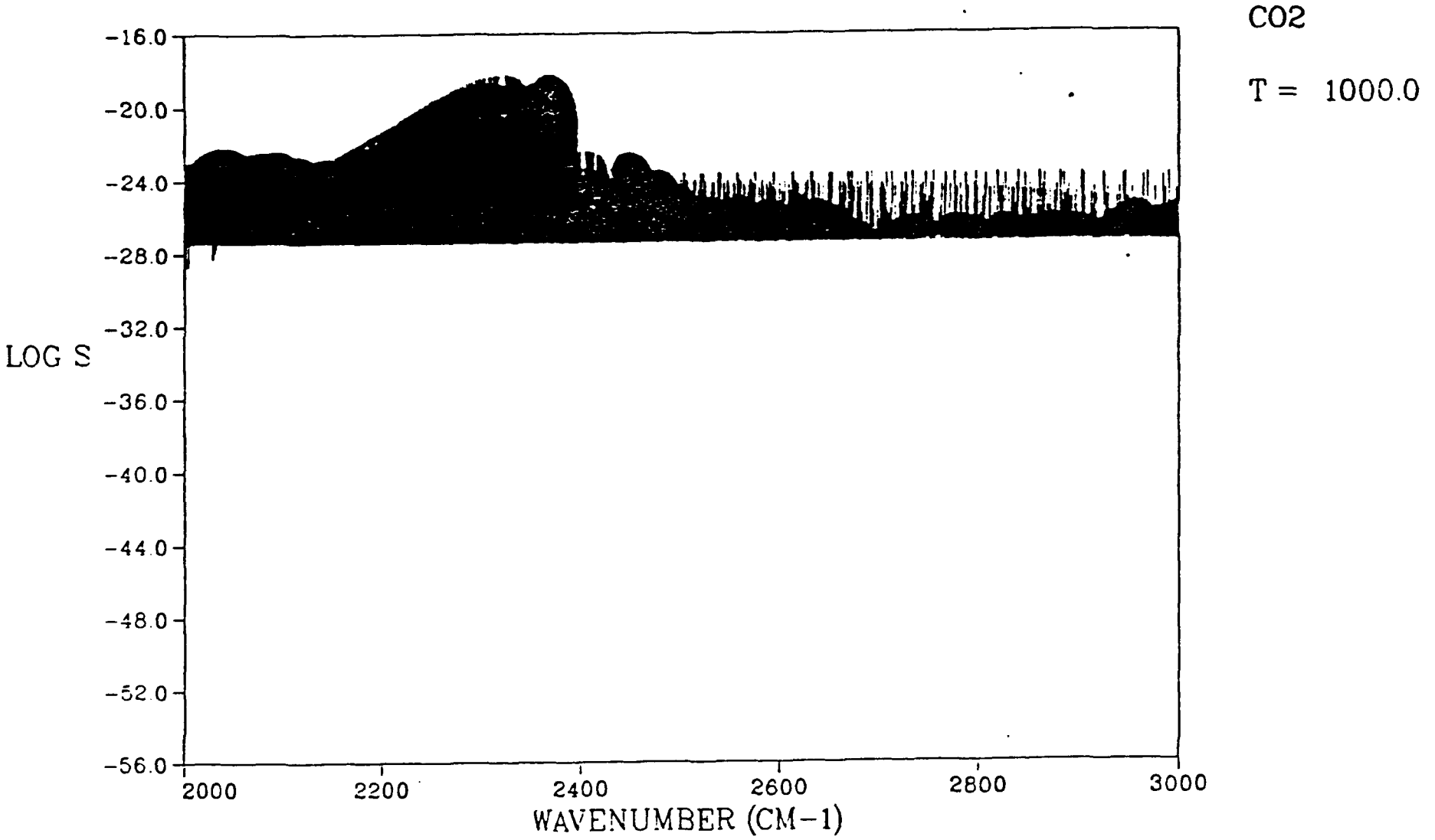
CO2
T = 1000.0
-16.0
-20.0
-24.0
-28.0
-32.0
-36.0
-40.0
-44.0
-48.0
-52.0
-56.0
LOG S
2000
2200
2400
2600
2800
3000
WAVENUMBER (CM-1)

HITEMP CO2 ANOMALIES

- 12000 DUPLICATE LINES ?
- UNUSUAL Q BRANCHES (e.g. 22201 → 11101)*

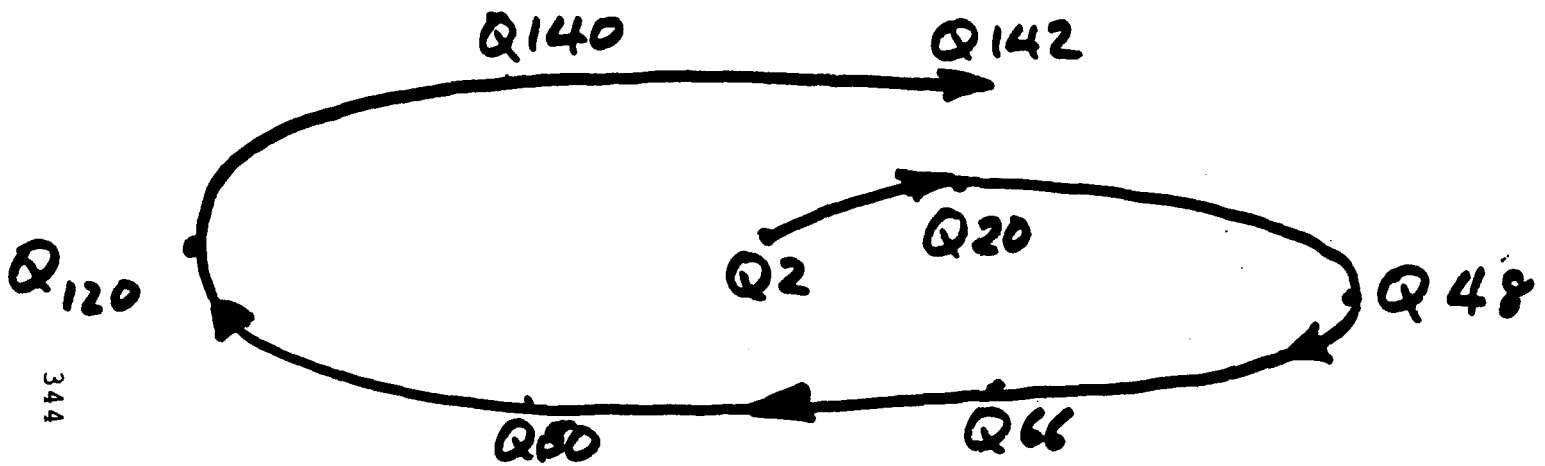

Q3	Q13	Q21	QH43
2116.6	2119.8	2120.7	2121.	2146

* NOTE 22201 $B = 0.39159593$
11101 $B_f = 0.3913397$

PROGRESS CO

- MAY 89 RECEIVED CO DATA (R. TIPPING)
- QUICK EVALUATION
- NOT ADEQUATE FOR HITEMP
  (NEED HIGHER VIB TRANSITIONS
  AND TO EXTEND J TO 150 ———)
- CO LINE INTENSITIES 7 TO 10% HIGHER
  THAN HITRAN 86 (AND OTHER DATA)?

U. OF ALABAMA

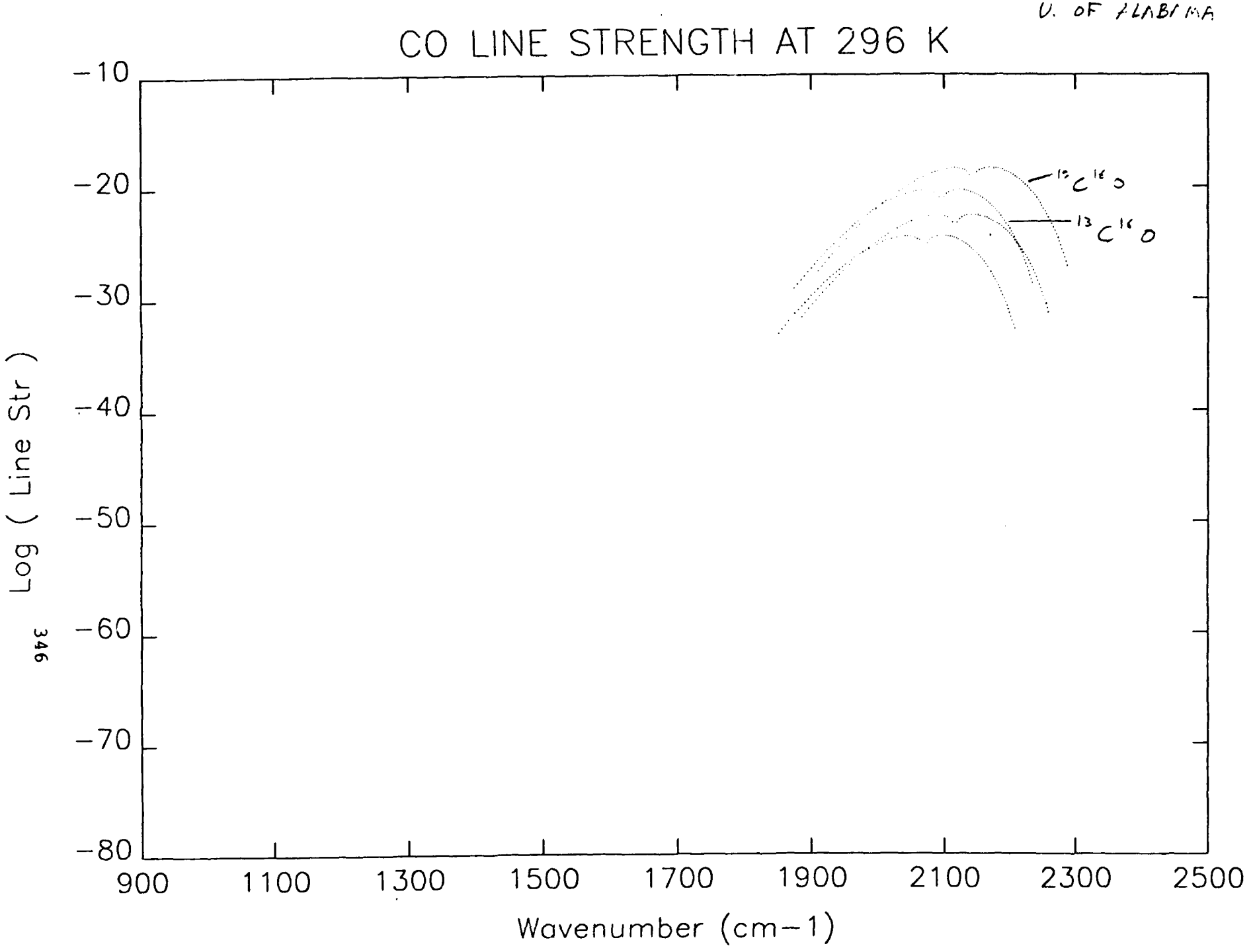
CO LINE STRENGTH AT 296 K
-10
-20
-30
-40
-50
-60
-70
-80
Log (Line Str)
900
1100
1300
1500
1700
1900
2100
2300
2500
Wavenumber (cm-1)
$^{12}C^{16}O$
$^{13}C^{16}O$

GRUMMAN

CO LINE STRENGTH AT 296 K

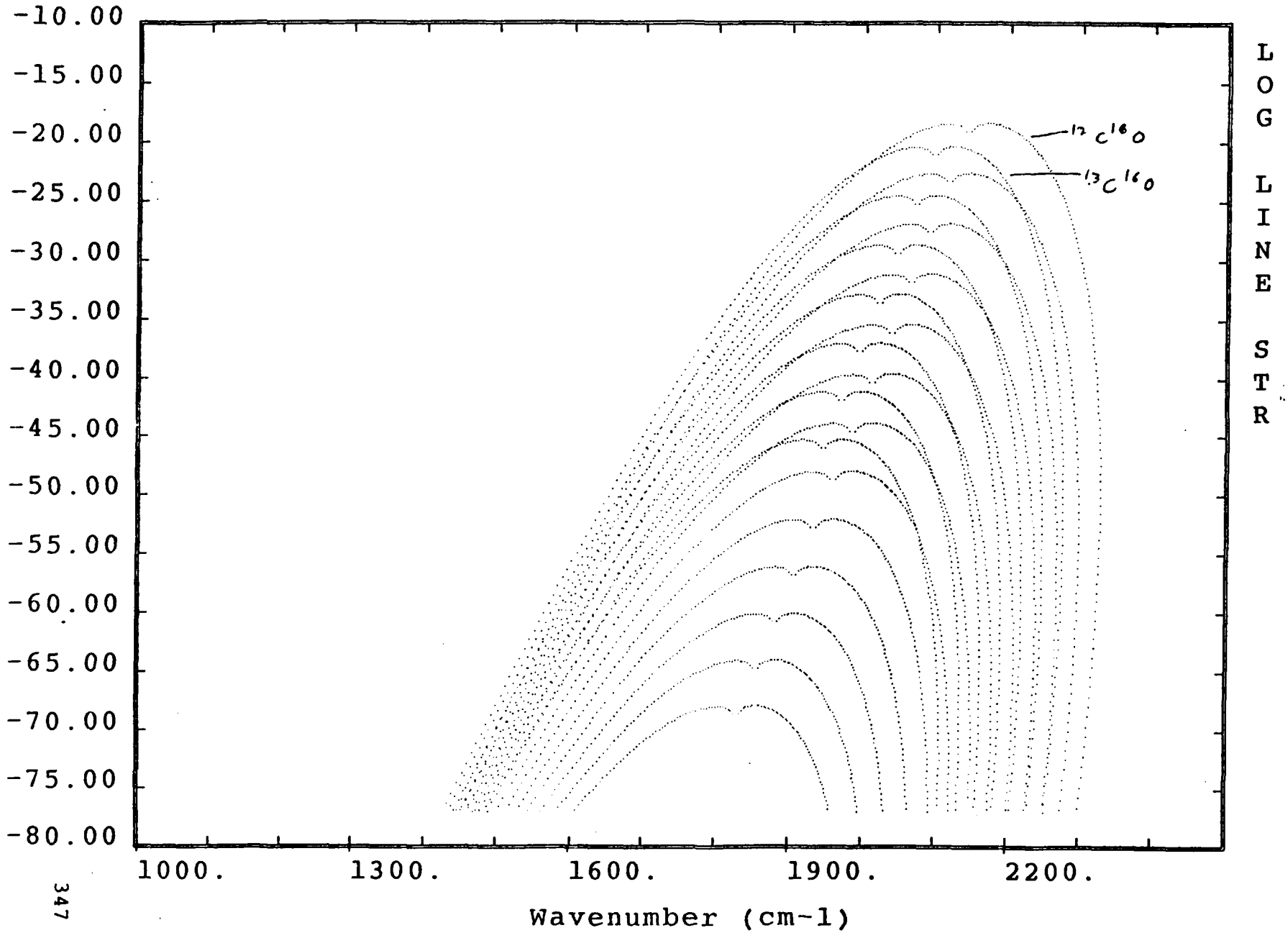

C0796P

UNIV OF ALABAMA

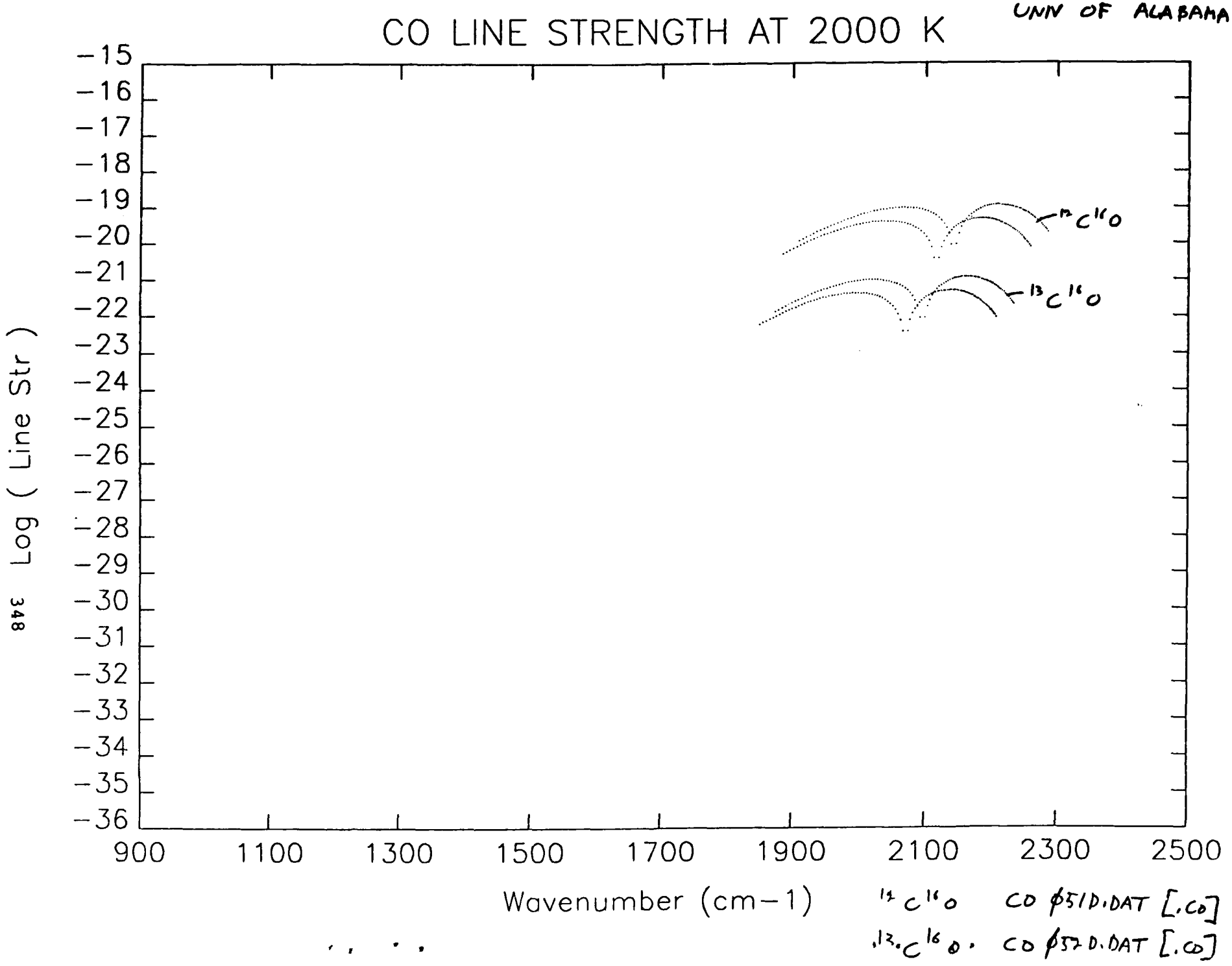

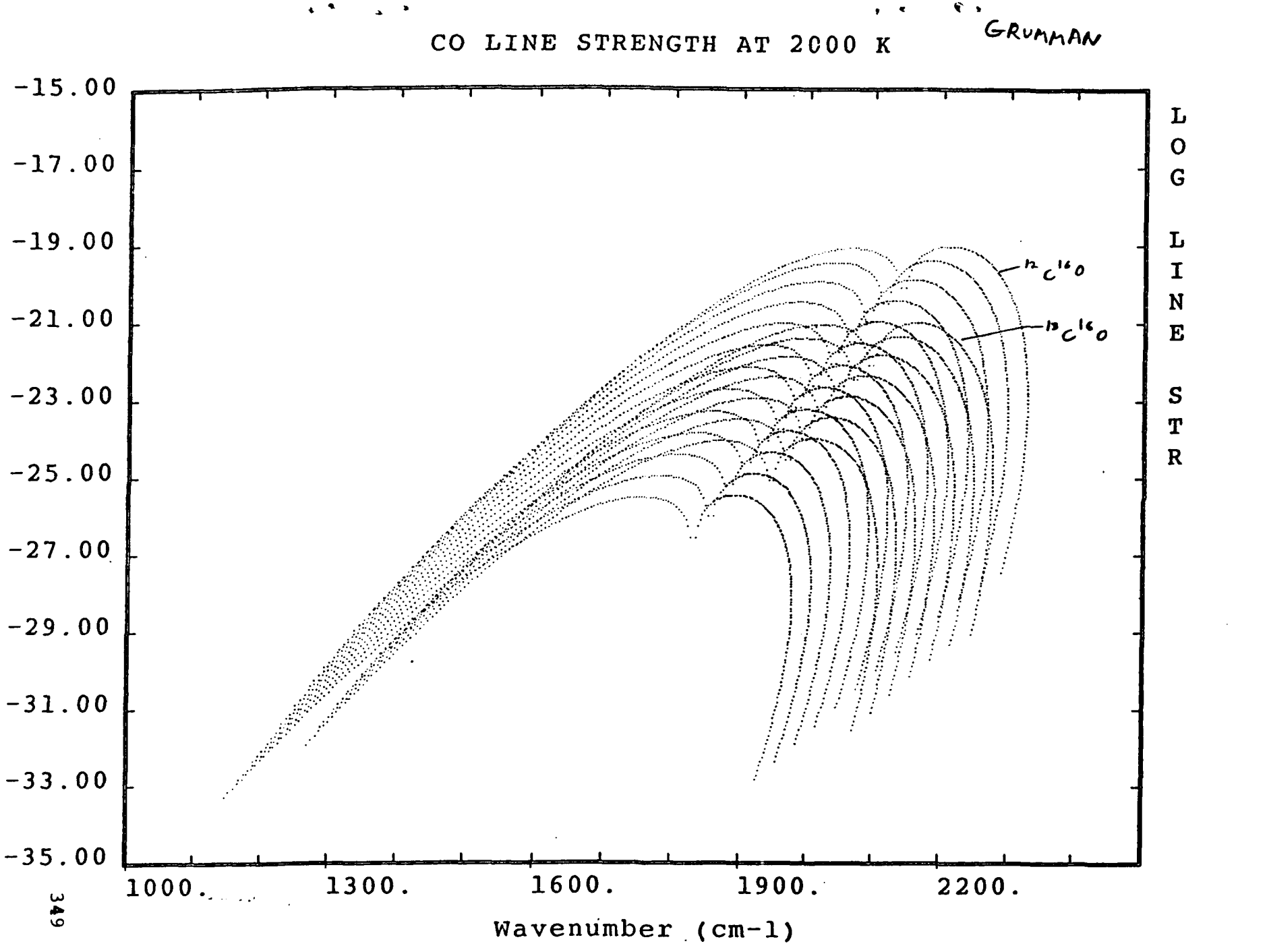
CO LINE STRENGTH AT 2000 K
GRUMMAN
-15.00
-17.00
-19.00
-21.00
-23.00
-25.00
-27.00
-29.00
-31.00
-33.00
-35.00
LOG LINE STR
$^{12}C^{16}O$
$^{13}C^{16}O$
1000.
1300.
1600.
1900.
2200.
Wavenumber (cm-1)

CO2000P

ISSUES

- CONTINUED SUPPORT FOR THIS WORK!
- HOW TO COPE WITH LARGE NUMBER OF LINES (OVER 2.2 MILLION)

  (PSEUDO-CONTINUUM FOR EACH SPECIES AT EACH TEMPERATURE)
- ACCURACY OF SPECTRAL DATA AT HIGH TEMPERATURE
- ADEQUACY FOR LASER PROPAGATION CALCULATIONS
- QUANTUM NUMBER/IDENTIFICATION FOR TRANSITIONS
- PARTITION FUNCTION DEFINITION

CONCLUSIONS

- HAVE 2.2 - 10μm COMPILATION FOR HITEMP FOR CO2 + H2O ONLY
- NEED TO INCORPORATE CO AFTER RE-CALCULATIONS FROM R. TIPPING TO COMPLETE PHASE 1
- H2O AND CO2 COMPARISONS AGREE WELL WITH LOW RESOLUTION MEASUREMENTS FOR CO2, 2.7, 4.3μm, H2O, 2.7, 6.3μm (BURCH,ERIM,AEDC)
- JUST STARTED HIGH RESOLUTION VALIDATION AGAINST FLAME SPECTRA
- NEED TO RESOLVE CO2 ISSUES (SPLIT/DUPLICATE LINES/Q-BRANCH ANOMALIES)
- HITEMP USEFUL FOR EVALUATING/VALIDATING BAND MODELS (eg. SIRRM etc)
- FUNDS NEED TO CONTINUE

RECOMMENDATIONS

- H2O
  - RECALCULATE USING DND APPROACH (WATTSON/ROTHMAN)
  - EXTEND WAVELENGTH RANGE 0.8 - 25μm
  - HIGH RESOLUTION VALIDATION
- CO2
  - ADD MISSING HERMAN WALLACE FACTORS
  - RESOLVE ISSUES (QUANTUM ID, LINE SPLITTING, ETC)
  - HIGH RESOLUTION VALIDATION
- CO
  - EXTEND DATA TO HIGH J (J=35 → 150)
  - INCLUDE HIGHER VIB TRANSITIONS (TO 8-7)
- CREATE PHASE 1 HITEMP TAPE WITH AVAILABLE PHASE 2 MOLECULES
  (ie. HF, HCL, HBr IN 2.2 - 10 μm REGION)
- FUNDING TO FINISH WORK

LINE POSITIONS OF HIGH TEMPERATURE CO_2 IN THE 15 μm REGION

Mark P. Esplin
Stewart Radiance Laboratory
Utah State University
139 The Great Road
Bedford, MA 01730

Michael L. Hoke
GL/OPI
Hanscom AFB, MA 01731-5000

LINE POSITIONS OF HIGH TEMPERATURE CO_2 IN THE 15 μm REGION

MARK P. ESPLIN AND MICHAEL HOKE

A CO_2 sample of natural isotopic abundance has been heated to 800 K in a high temperature absorption cell of pathlength 1 3/4 meters. Spectra were taken using the AFGL (Air Force Geophysics Laboratory) high resolution Fourier transform spectroscopy with a resolution of 0.004 cm^{-1}. Many "hot bands" in the ν_2 region were observed. Effective vibration-rotation constants for these bands will be presented.

This work was supported by the Air Force Office of Scientific Research (AFOSR) as part of AFGL Task 2310G1.

Address of Esplin: Stewart Radiance Laboratory, Utah State University, 139 The Great Road, Bedford, Ma 01730.

Address of Hoke: OPI/Air Force Geophysics Laboratory, Hanscom AFB, Bedford, Ma 01730.

Time required: 10 minutes

Session in which paper is
recommended for presentation: (5) High Resolution IR

FIGURE 1 HIGH RESOLUTION INTERFEROMETER

The experimental components include an infrared source, high temperature gas sample absorption cell and high resolution interferometer. The "step and hold" Michelson interferometer employs "cat's-eye" mirrors and a stepping mirror displacement, for this study, of 74 cm; this corresponds to an unapodized resolution of approximately 0.004 cm^{-1}. The input and output beams of the cat's eye mirrors are laterally displaced making both accessible. Since the two beams are complementary, two detectors are used and the signals differenced to yield the interferometric signal and reduce the effect of systematic errors, such as source fluctuations and instrumental drifts. The liquid helium cooled detectors are housed in the same dewar to keep their experimental conditions the same. In practice this arrangement is very stable over the fifteen hour data collection period necessary for a single high resolution interferogram. For operation in the fifteen micron spectral region a potassium bromide beam splitter and copper doped germanium detectors were used. The interferometer chamber, which contains the transfer optics and optical filter wheel, is evacuated during operation.

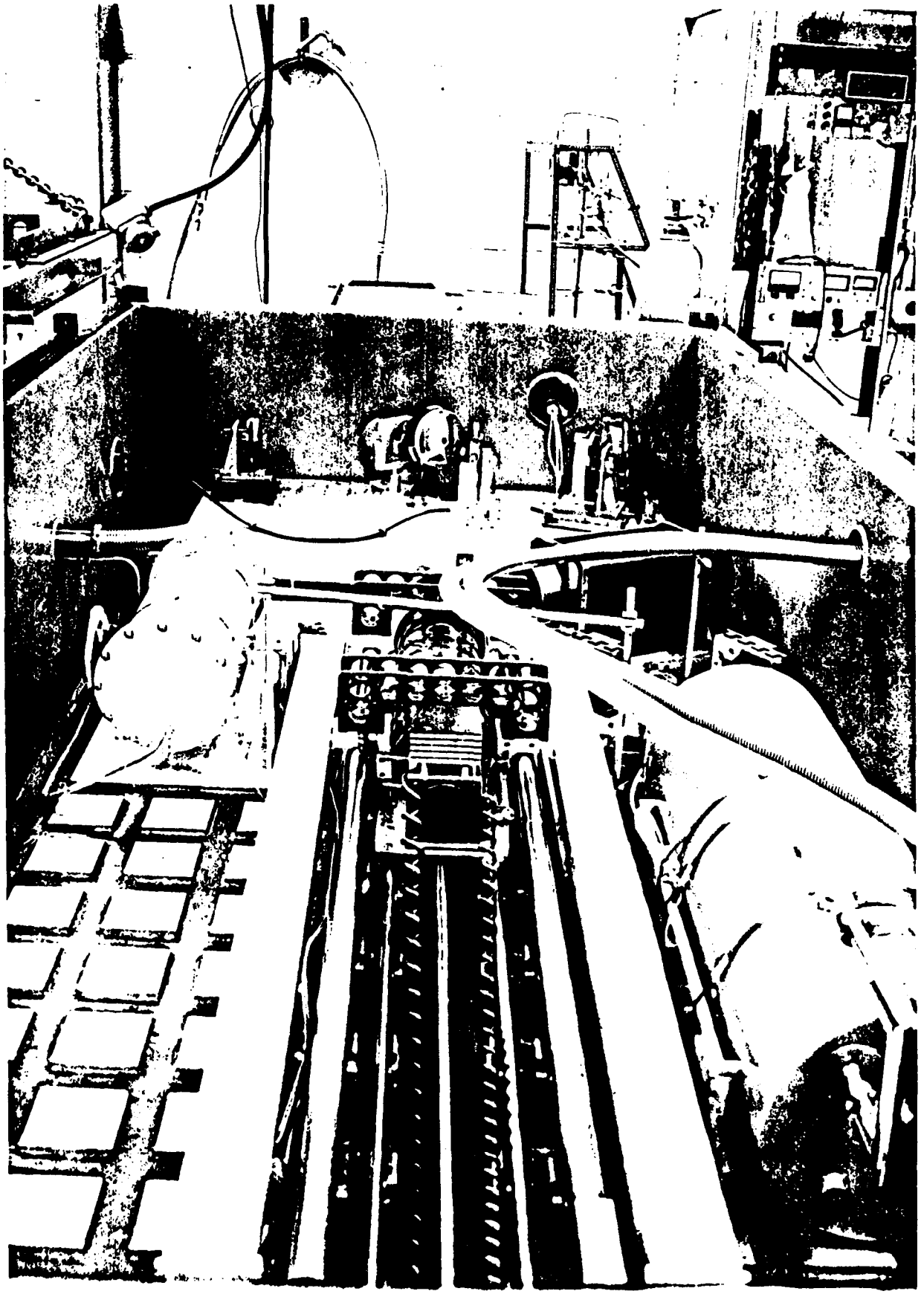

FIGURE 2 HIGH TEMPERATURE SAMPLE CELL AND SOURCE CHAMBER

The single pass stainless steel gas sample cell is coupled to the interferometer chamber with a purged expansion bellows. The cell is housed in a commercial electric furnace and for our studies was heated to 800 K. The single pass length is 1.75 meters. However only the central one meter portion of the cell was near the furnace temperature, with temperature gradients in the end portions and the zinc selenide cell windows at room temperature.

The source chamber contains a Nernst glower, radiation chopper and collimation optics. It is mounted rigidly to the absorption cell and evacuated during operation. The hot gas sample not only absorbs but radiates. Locating the chopper in the source chamber in the optical path before the sample cell prevents the gas emissions from being modulated and recorded.

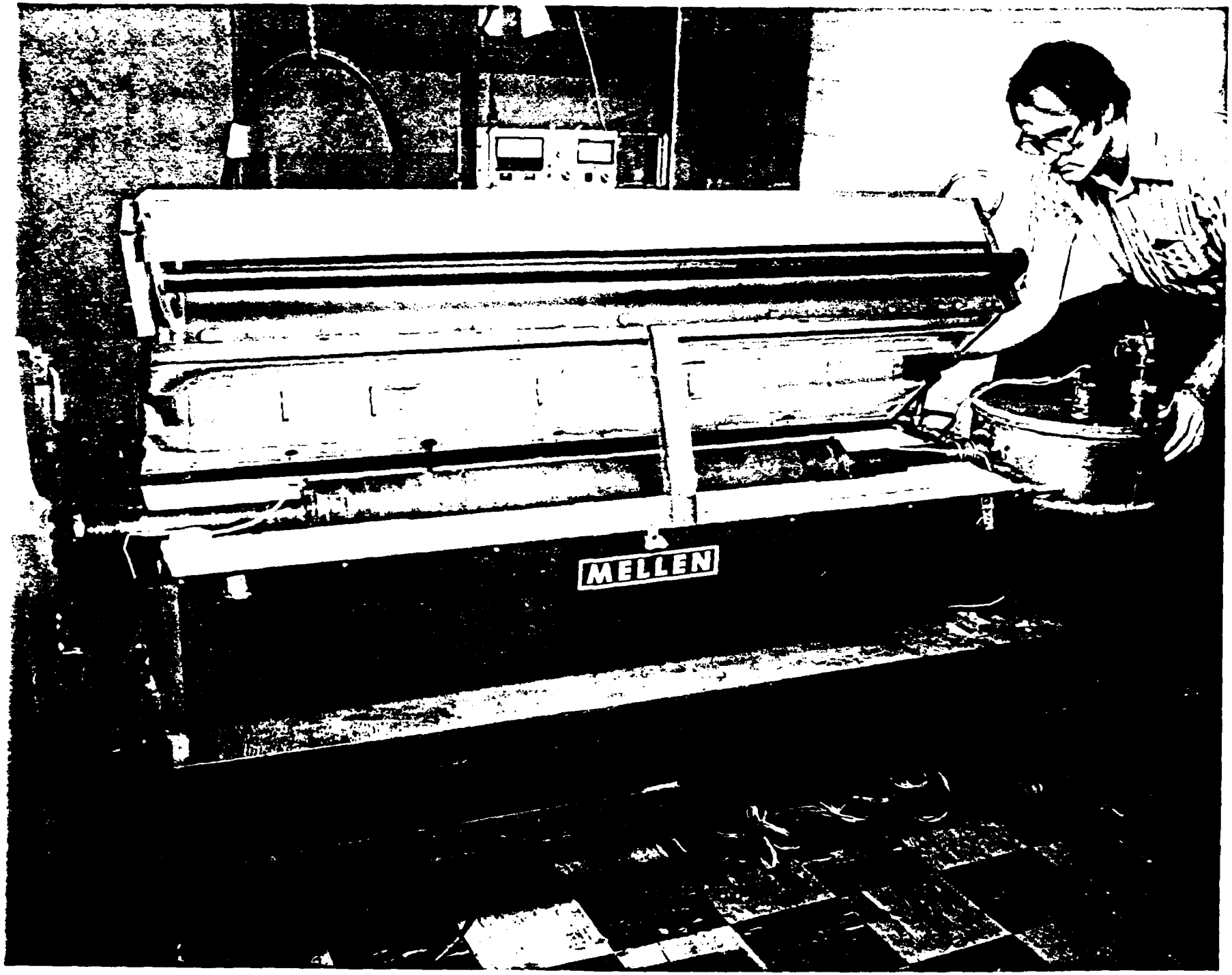
MELLEN

EXPERIMENTAL CONDITIONS

RESOLUTION: $\frac{1}{2(114\ \text{CM})} = 0.004\ \text{CM}^{-1}$

APSORPTION PATH LENGTH: 1 3/4 METER

TEMPERATURE: 800 K

PRESSURE: 5 TORR

FIGURE 3 MEASUREMENTS

Several interferograms of high temperature (800 K), low pressure (5 Torr) naturally occurring carbon dioxide samples were collected for analyses of the vibrational, rotational bands in the fifteen micron spectral region. Each high resolution interferogram included approximately 300,000 data points, sampling the interferogram every sixth NeHe laser fringe. A consequence of the interferometer optical design is that very little non-linear optical phase error is ever present. In practice phase error is easily corrected using the technique of Forman et al(*).

The figure shows a portion of a transmittance spectrum which is the ratio of two co-added high resolution scans collected alternately with two co-added low resolution empty cell background scans. The upper portion of the figure is a survey of the fifteen micron and shows many carbon dioxide spectral lines which result only in studies of high temperature gas samples. The loss of instrumental sensitivity is evidenced near 600 cm^{-1}. The approximate signal-to-noise ratio can be inferred from the spectral region above 800 cm^{-1}. The lower portion of the figure shows a detail of the upper portion; a 1 cm^{-1} region, including Q branch lines of the transition 10001-01101 of $^{12}C^{16}O_2$ located at 720.8 cm^{-1}.

* Michael L. Forman, W. Howard Steel and George A. Vanasse, "Correction of Asymmetric Interferograms Obtained in Fourier Spectroscopy", Journal of the Optical Sociery of America, Vol. 56, pp. 59-63, 1966.

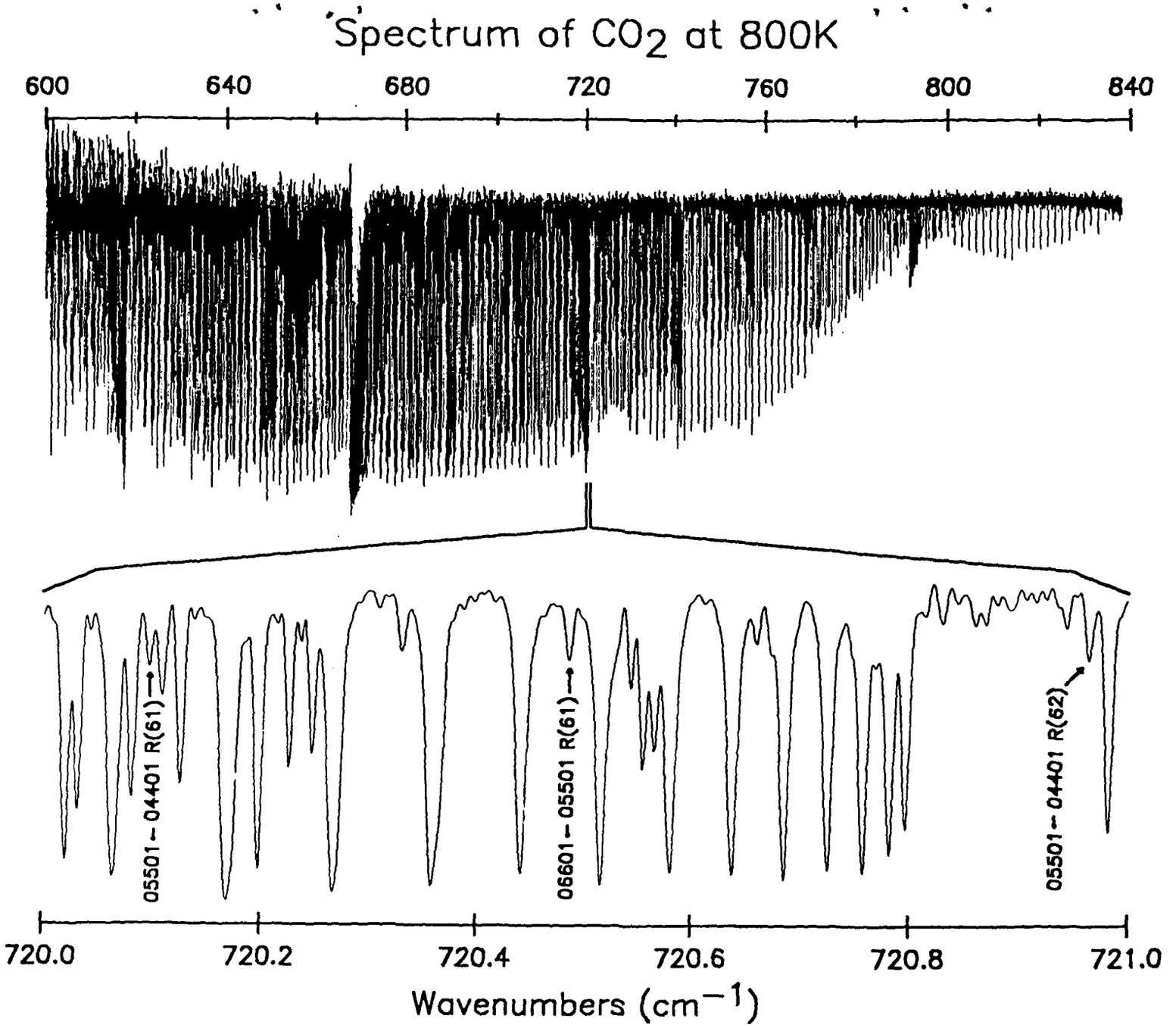
Spectrum of CO_2 at 800K
600
640
680
720
760
800
840
05501 ← 04401 R(61)
06601 ← 05501 R(61)
05501 ← 04401 R(62)
720.0
720.2
720.4
720.6
720.8
721.0
Wavenumbers (cm^{-1})

FIGURE 4 ENERGY LEVEL DIAGRAM OF CARBON DIOXIDE

The figure shows a partial energy level diagram of carbon dioxide, and indicates the fifteen micron transitions which have been measured.

BANDS OBSERVED

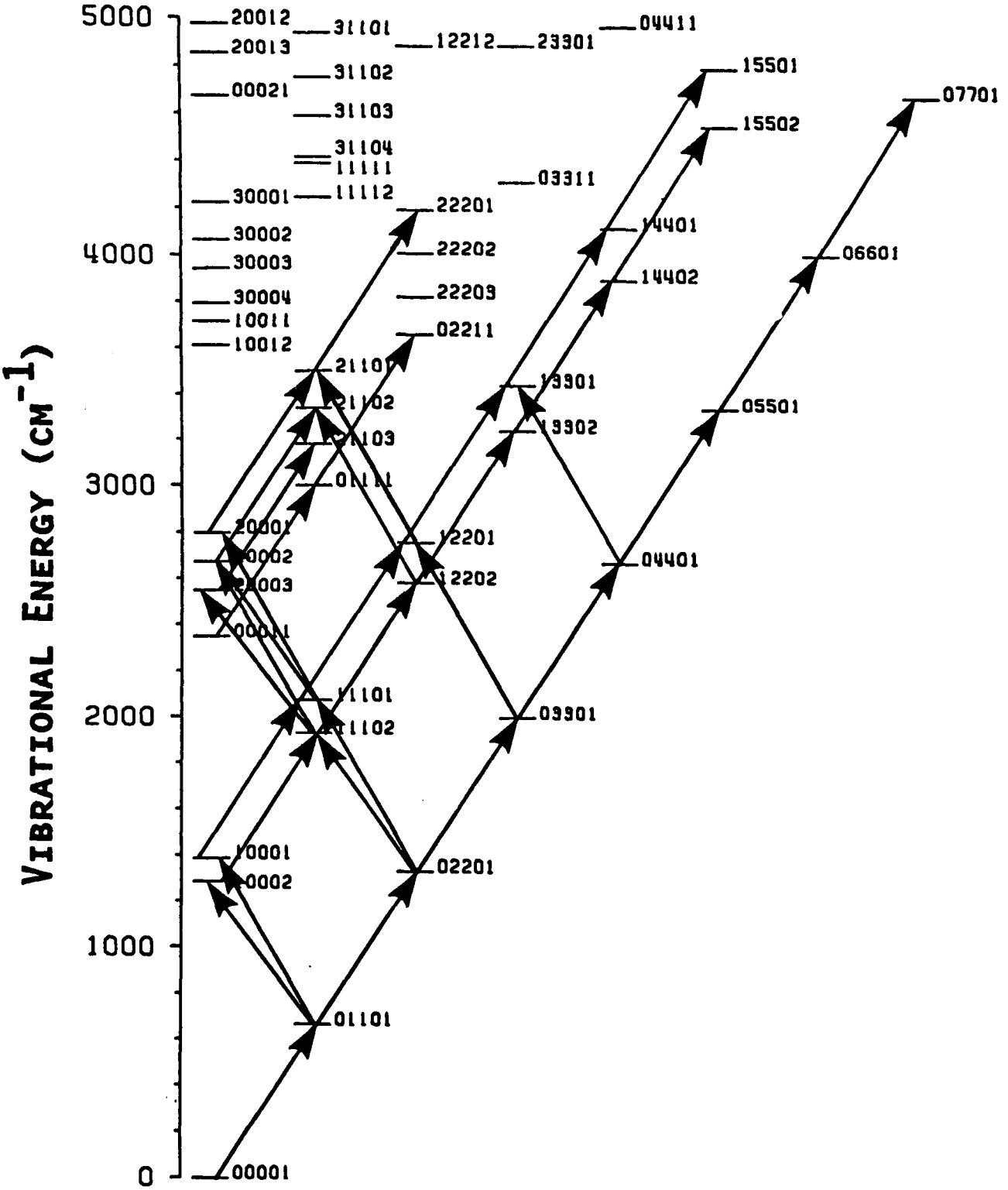

FIGURE 5 GRAPHICAL COMPARISON
OF OBSERVED AND CALCULATED LINE POSITIONS

The position of each spectral line is calculated and a slice of the spectrum is plotted contered on the calculated line position. For this example each spectral slice is 0.4 cm^{-1} wide. To assist in the identification, the absorption spectra have been plotted inverted (absorption lines become peaks).

This figure shows the spectral segments for the P_{60} through P_{50} lines of the 01101 - 00001 band of $^{12}C^{16}O_2$.

The graphical technique is based on an original scheme of Loomis and Wood(*).

* F. W. Loomis and R. W. Wood, Phys. Rev., Vol. 32, pp. 223, 1928.

P(60) TO P(50) OF 01101 ◄ 00001 BAND

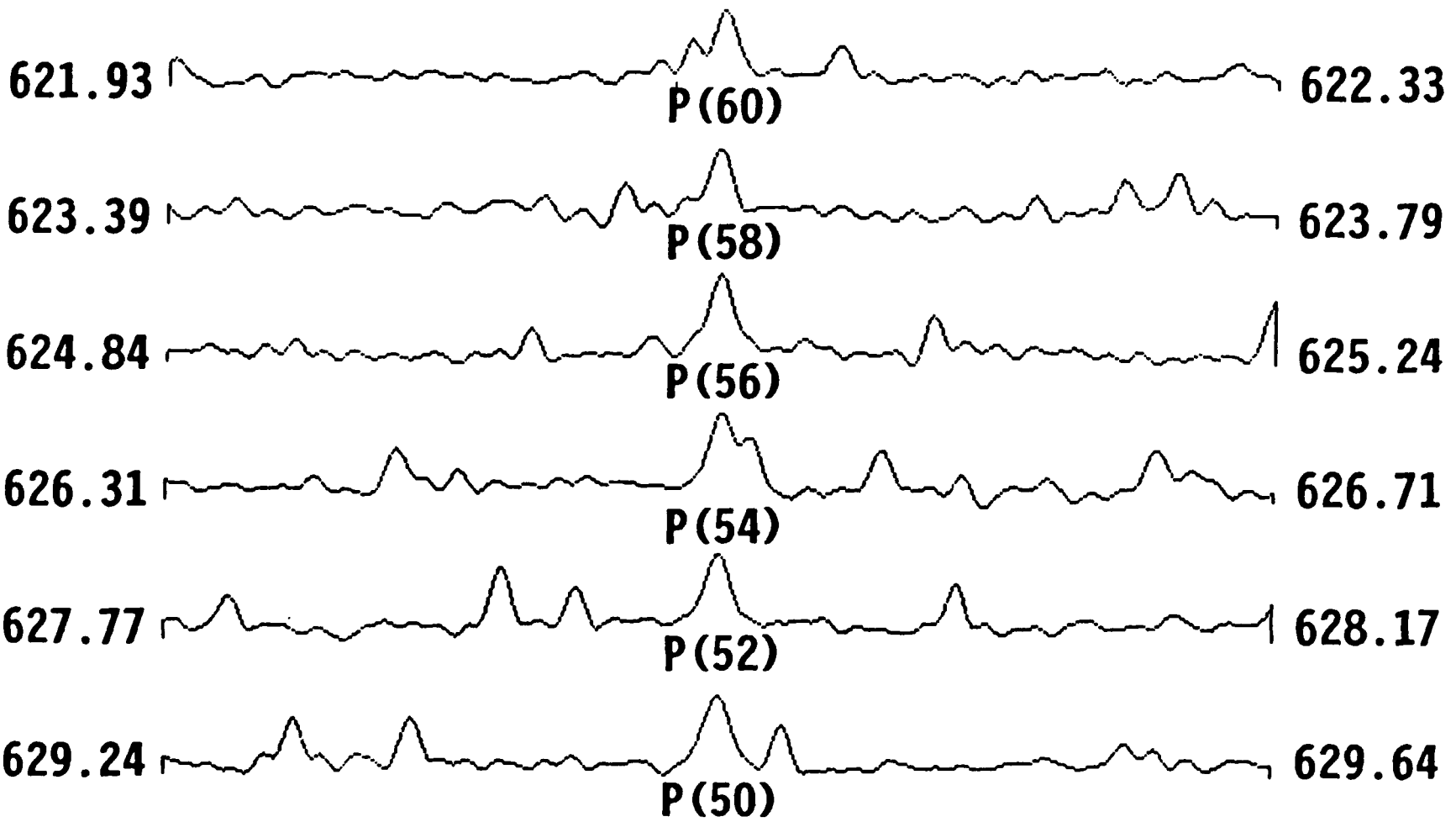

FIGURE 6

When the slices are plotted close together in the Y-direction and each slice is slightly offset in the X-direction a 3-D effect is achieved. A band then appears as a "mountain range".

This is a compressed plot of Figure 5.

P(60) TO P(50) OF 01101 ◄ 00001 BAND

FIGURE 7 GRAPHICAL REPRESENTATION
FOR THE P BRANCH OF 01101 - 00001

This figure shows the graphical representation of the spectral data based on the P branch of the 01101 - 00001 band of CO_2. To the extent that the "mountain range" forms a straight line the observed and calculated line positions agree.

The figure is a full representation of which Figure 6 is a part.

P(100) TO P(2) OF 01101 ◄ 00001 BAND, 0.4 CM^{-1} PER SLICE

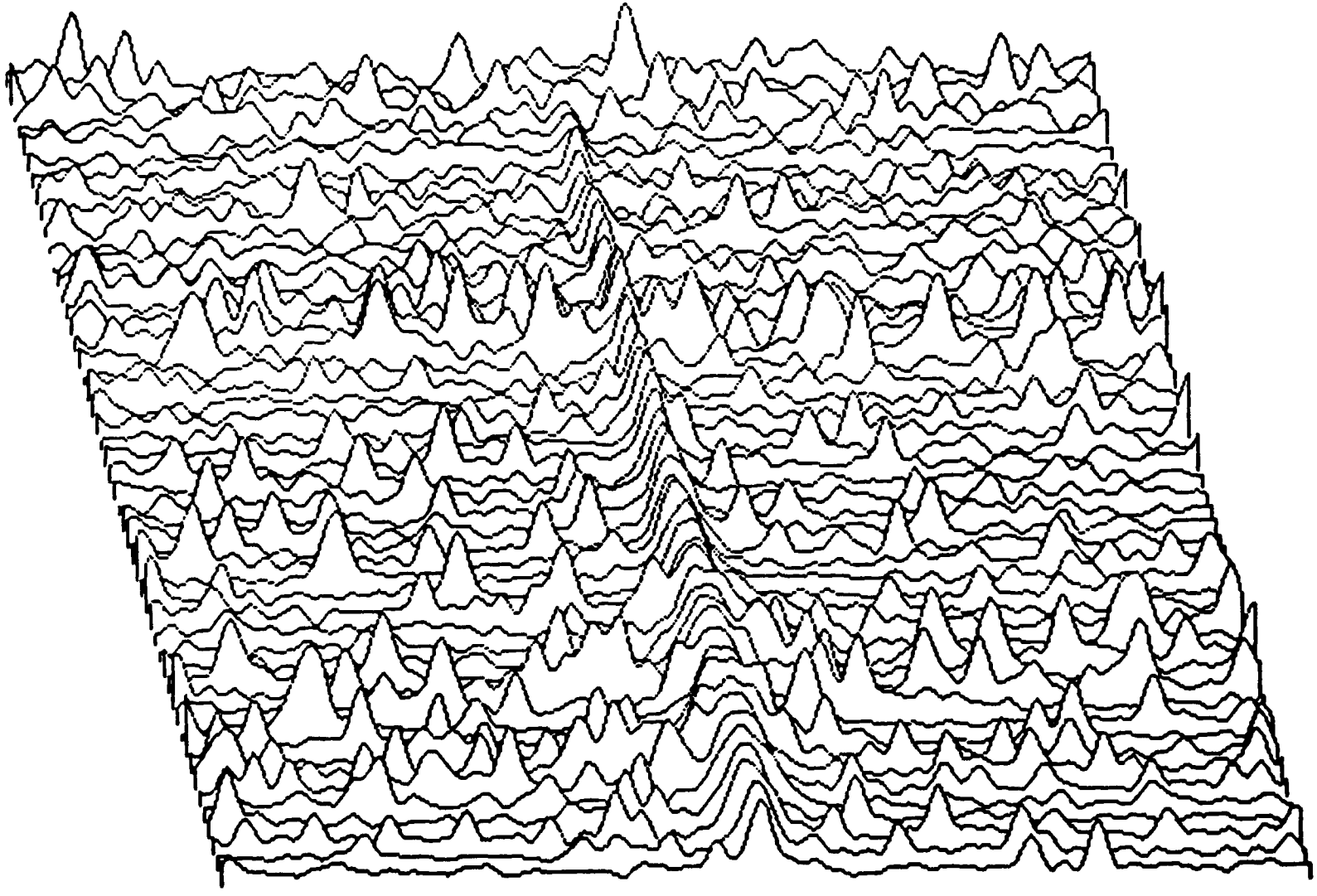

FIGURE 8 GRAPHICAL REPRESENTATION
OF THE P BRANCH OF 05501 - 04401

One difficluty with this 3-D technique is that the plots become too chaotic to effectively visualize the different bands. For example, while the line position comparison "peaks" in the "mountain range" for the P branch of 05501-04401 are clearly discernible in the figure those for other bands are not.

One solution is to change the perspective and switch to color. Instead of viewing the topographical features oblique, as in Figures 7 and 8, view them from above. In addition represent the changing transmittance with color; high transmittance (tops of tall "peaks") as red and the average of background above which the peaks rise by black or dark blue. Transmittance values in between the two extremes will be represented by shades of color between red and blue.

P(54) TO P(6) OF 05501 ◄ 04401 BAND, 0.8 CM^{-1} PER SLICE
WATTSON'S MOLECULAR CONSTANTS

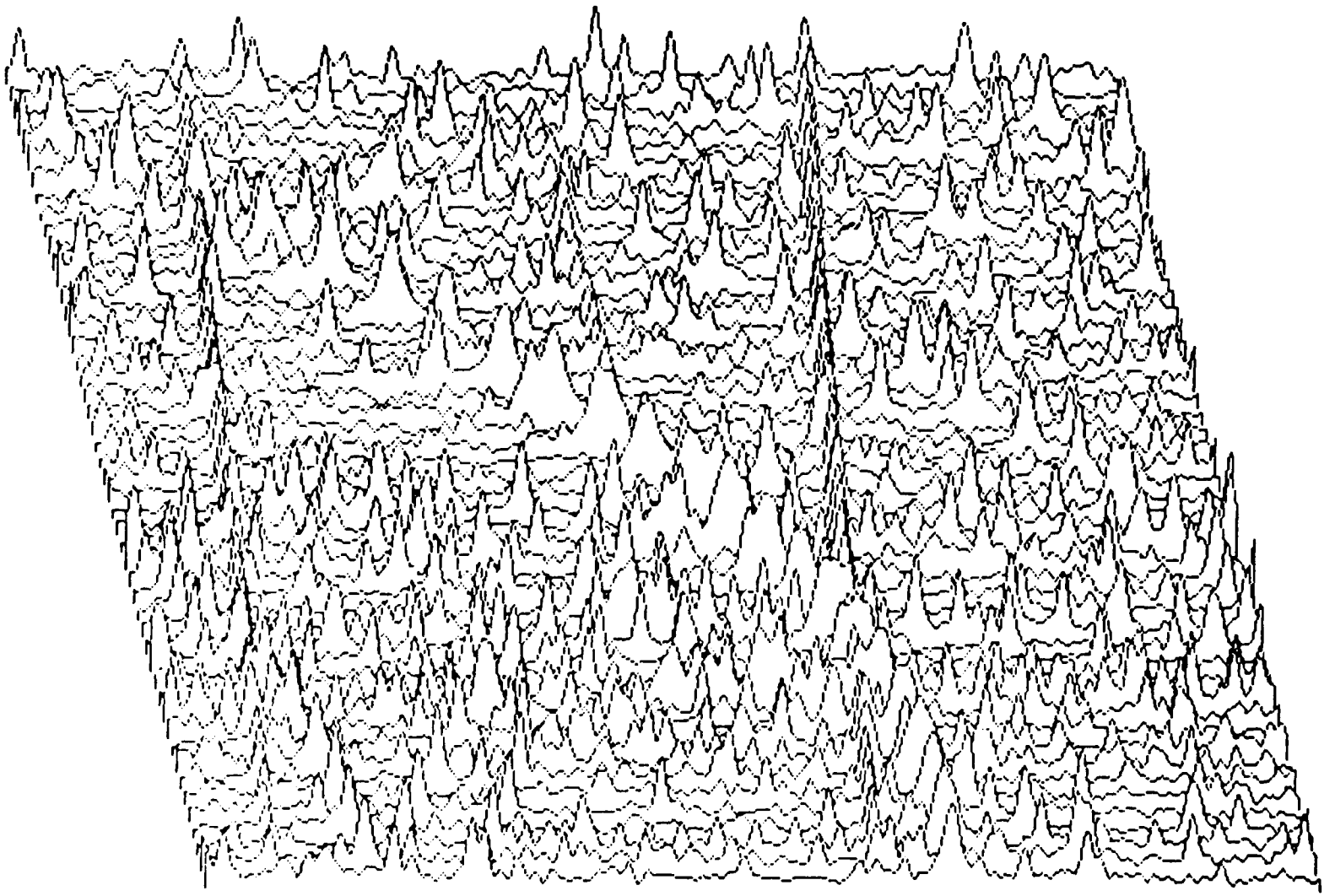

FIGURE 9 COLOR LOOMIS-WOOD DIAGRAM FOR 05501-04401

The figure shows the P and R branches of the band 05501-04401. In this figure, as compared to Figure 8, bands of spectral lines which did not show up clearly in the previous figure are now clearly seen.

An immediate consequence of the application of the color graphical technique to the spectral data was the identification of the bands 07701-06601 and 06601-05501 of $^{12}C^{16}O_2$ which would not have been seen otherwise.

With the aid of the new graphical technique, a preliminary analyses of the fifteen micron carbon dioxide bands has been performed. More than 2500 rotational line positions, of the principal isotope of carbon dioxide, were measured and assigned to the 35 vibrational bands indicated in Figure 4. Upper and lower state rotational constants were determined for each of these 35 bands from weighted linear least squares fits to the measured line positions.

Color Loomis-Wood Diagram For 05501◄04401

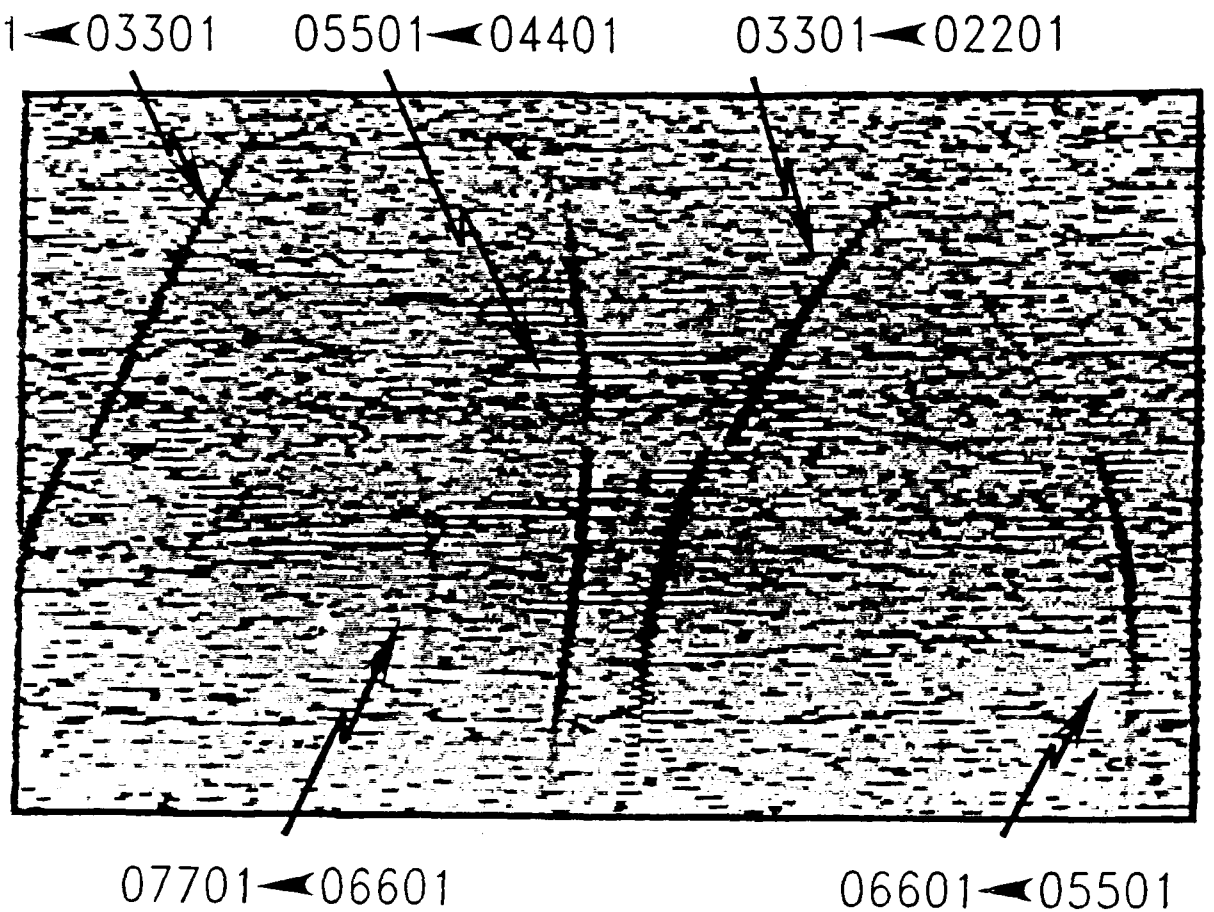

FIGURE 10 LINE POSITION COMPARISONS

Line positions calculated from our estimated rotational constants were compared with the values on HIGH86, the most recent version of the HITRAN line parameter data base(*). As an example, Figure 10 is a comparison for the well known fundamental band 01101-00001 located near 667 cm^{-1}. In this figure the dots represent the differences between the measured line positions and the line positions calculated from the estimated rotational constants. The solid line, marked HITRAN86, represents the fifferences between the line positions calculated using our estimated rotational constants and the line positions on the HITRAN86 data base. As the figure shows some improvement was obtained, for P and R branch lines with rotational quantum number greater than about 80.

Figure 11 shows the same comparison for the Q branch of the same fundamental band; 01101-00001.

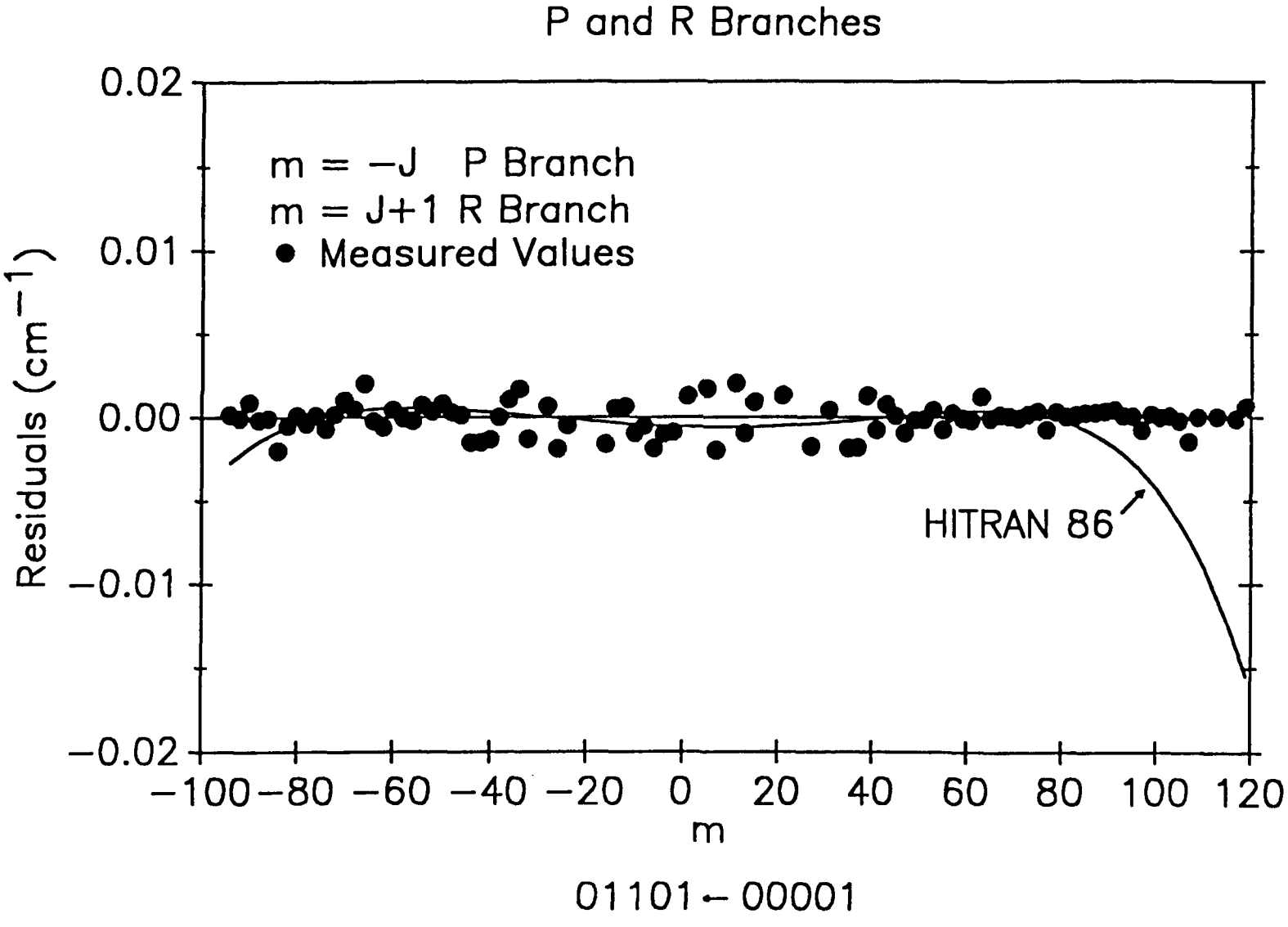
P and R Branches
m = −J P Branch
m = J+1 R Branch
● Measured Values
HITRAN 86
Residuals (cm⁻¹)
0.02
0.01
0.00
−0.01
−0.02
−100 −80 −60 −40 −20 0 20 40 60 80 100 120
m
01101 ← 00001

FIGURE 11 LINE POSITION COMPARISONS
FOR Q BRANCH OF 01101-00001

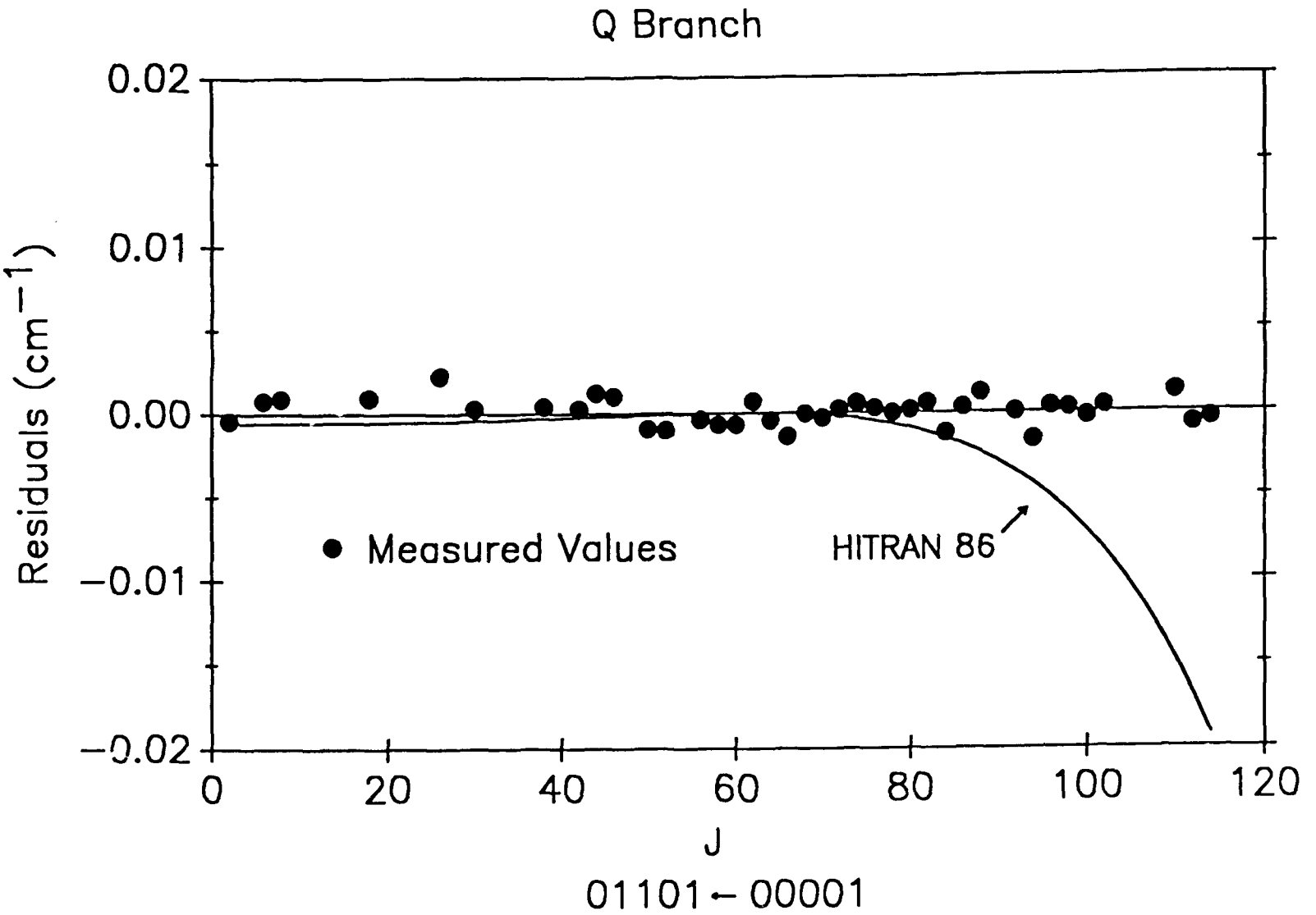
Q Branch
0.02
0.01
0.00
−0.01
−0.02
Residuals (cm⁻¹)
Measured Values
HITRAN 86
0
20
40
60
80
100
120
J
01101 ← 00001

FIGURE 12 LINE POSITION COMPARISONS
FOR P AND R BRANCHES OF 14402-13302

The comparisons shown in this figure for 14402-13302 are more typical. The comparisons in this figure are the same as in the two previous figures, figures 10 and 11.

The solid line in this figure, marked Wattson, represents the differences between the line positions calculated using our estimated rotational constants and the theoretical line positions calculated by Wattson and Rothman(*) using their Direct Numerical Diagonalization (DND) technique. The good agreement indicates the excellent predictive power of their DND technique.

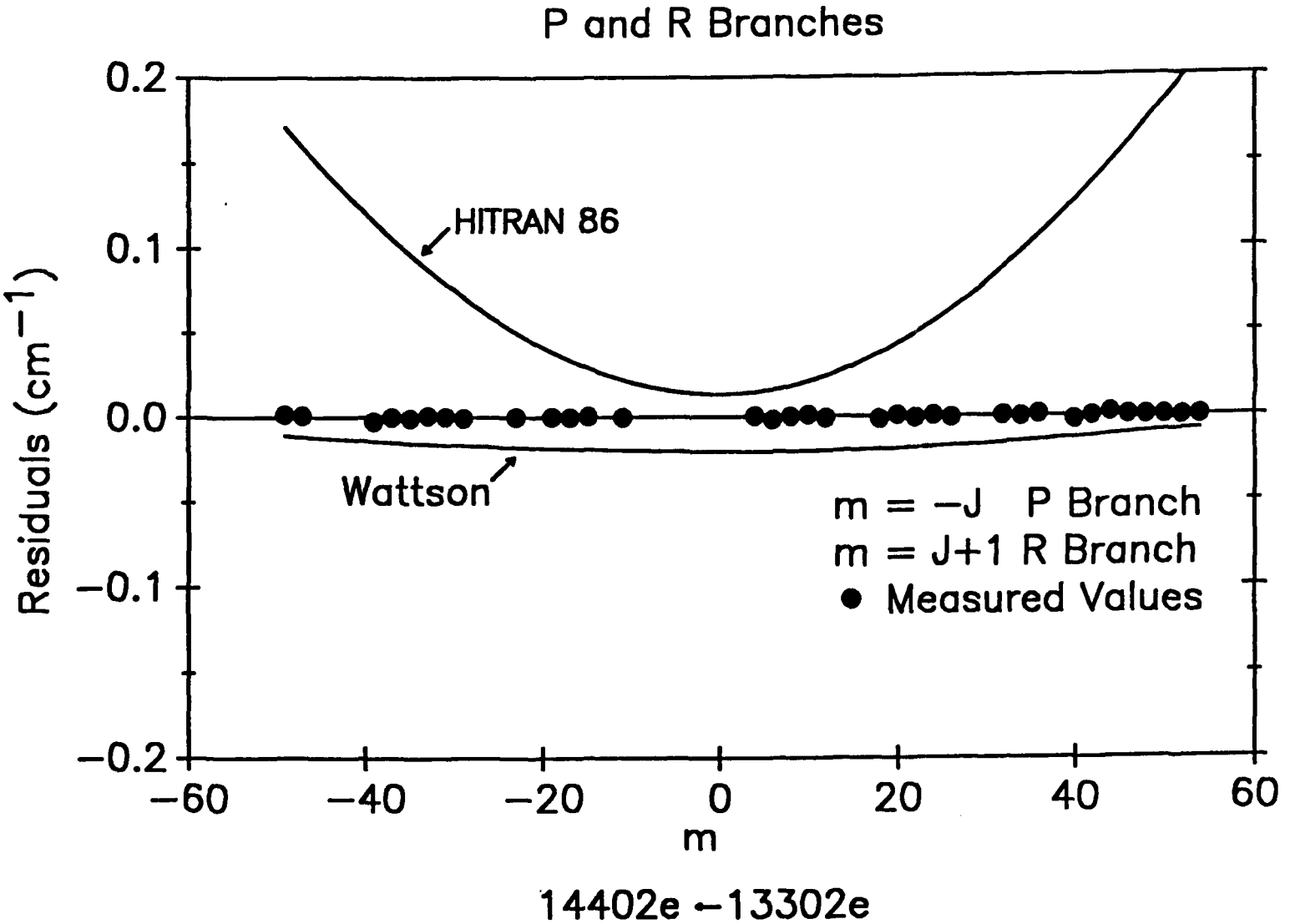
P and R Branches
0.2
0.1
0.0
−0.1
−0.2
Residuals (cm^{-1})
HITRAN 86
Wattson
m = −J P Branch
m = J+1 R Branch
● Measured Values
−60
−40
−20
0
20
40
60
m
14402e −13302e

SPECTROSCOPIC PARAMETERS AT HIGH TEMPERATURE

Laurence Rosenmann
Laboratoire E.M2.C du CNRS et de l'E.C.P.
Ecole Centrale des Arts et Manufactures
Grande voie des Vignes
92295 Châtenay-Malabry Cedex
France

SPECTROSCOPIC PARAMETERS AT HIGH TEMPERATURE

Laurence Rosenmann

Laboratoire E.M2.C du CNRS et de l'Ecole Centrale des Arts et Manufactures

Ecole Centrale, Grande voie des Vignes, 92295 Châtenay-Malabry Cedex, FRANCE

The temperature dependence of N_2 and H_2O- broadened linewidths of CO_2, CO and H_2O is deduced from diode laser measurements up to 900 K.

A theoretical model is widely and successfully tested by comparison with available data : it leads to accurate predictions for both the rotational quantum number and temperature dependences of linewidths.

We have made systematic calculations of CO_2 and CO line broadening by CO_2, H_2O, N_2 and O_2 in the 200-3000 K temperature range. The results can be easily introduced in molecular data bases. They should improve spectra calculations through the accounting for correct line, perturber, and temperature dependences of linewidths.

Our plans concerning measurements of CO_2 line-intensities at elevated temperatures are also presented.

SPECTROSCOPIC PARAMETERS AT HIGH TEMPERATURE

Laurence Rosenmann
Laboratoire E.M2.C du CNRS et de l'Ecole Centrale des Arts et Manufactures
Ecole Centrale, Grande voie des Vignes, 92295 Châtenay-Malabry Cedex, FRANCE

Aim Modeling of radiative properties of gas mixtures CO_2, CO, H_2O

Applications Radiative transfers in industrial systems
I.R plume signature
Laser diagnostics (temperature or mole-fraction measurements)
.....

Required data for absorption / emission IR spectra

Positions and intensities of lines which contribute in the **300-3000 K** range

Pressure line-broadening by **air, CO_2, H_2O,** ..... in the **300-3000 K** range

Example of CO_2 base : $\gamma_{|m|}(300\ K)$ (in $10^{-3}\ cm^{-1}\ atm^{-1}$) and $N_{|m|}$

Linc	CO_2-CO_2		CO_2-H_2O		CO_2-N_2		CO_2-O_2	
|m|	$\gamma(300)$	N	$\gamma(300)$	N	$\gamma(300)$	N	$\gamma(300)$	N
1	119.9	0.723	117.7	0.726	95.0	0.737	85.9	0.721
41	85.5	0.583	147.6	0.800	72.7	0.674	61.0	0.640
101	55.4	0.482	126.7	0.634	56.9	0.550	51.4	0.573

$\gamma_{|m|}(300\ K)$ and $N_{|m|}$ are very dependent on both the value of |m| and the perturber

Data used

- in optics diagnostics in flames
- to determine energy transfer rates which are responsible of line-interferences
- in line-by-line calculations

Air-broadened half-widths of CO and CO_2 lines at 296 K and N coefficients deduced from calculated values at 200 and 296 K will be incorporated in the GEISA data bank

HITRAN and GEISA data bases : room temperature applications

- Positions extensive effort (recent measurements at high temperature)
- Widths air and self-broadening at 296 Kwith the same temperature dependence
- Intensities sometimes not sufficiently well known for transitions of high initial energy level

⟶ Lack of data for elevated temperature applications

⟶ **High temperature measurements**
Development of accurate theoretical models

1. Studies on pressure-broadened line-widths

   1.1 experimental studies
   1.2 line-broadening calculations
   1.3 calculated tabulations

2. Study starting on CO_2 line-intensities at elevated temperatures

1. PRESSURE BROADENED LINE-WIDTHS γ

1.1 Experimental studies

Measurements of linewidths for some lines in mixtures

$CO_2 - N_2$	$CO_2 - H_2O$	(ν_3 band)	(first measurements)
$CO - N_2$	$CO - H_2O$	(1-0 band)	
$H_2O - N_2$	$H_2O - H_2O$	(ν_2 band)	

Accuracy 1 - 10 %

Determination of the temperature dependence of γ such as

$$\gamma(T) = \gamma(T_0)\ (T_0/T)^N$$

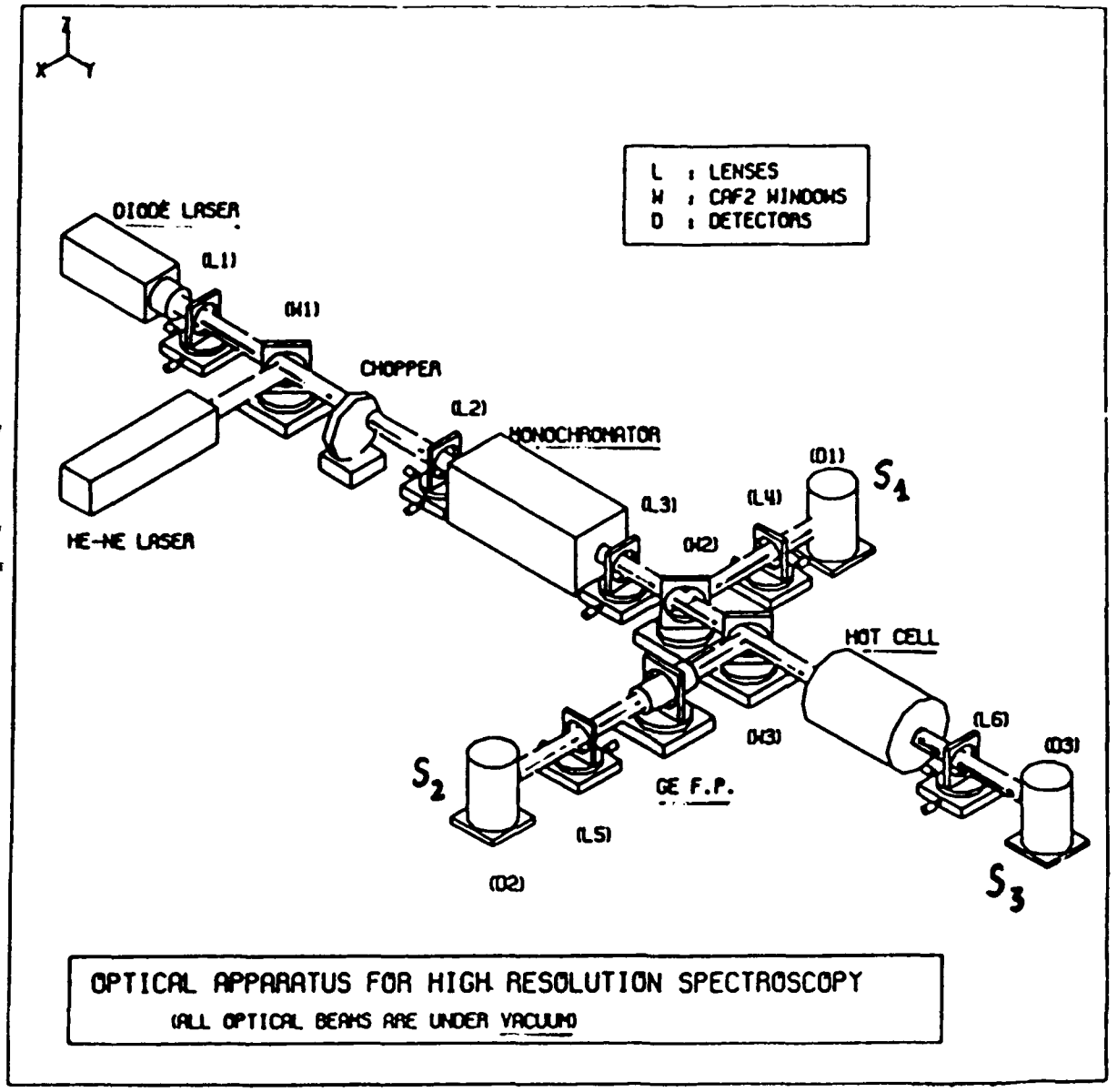

OPTICAL APPARATUS FOR HIGH RESOLUTION SPECTROSCOPY
(ALL OPTICAL BEAMS ARE UNDER VACUUM)

resolution $\simeq$ 0.0005 cm^{-1}

hot cell $\delta T \lesssim 1K$

T: 296 - 900 K

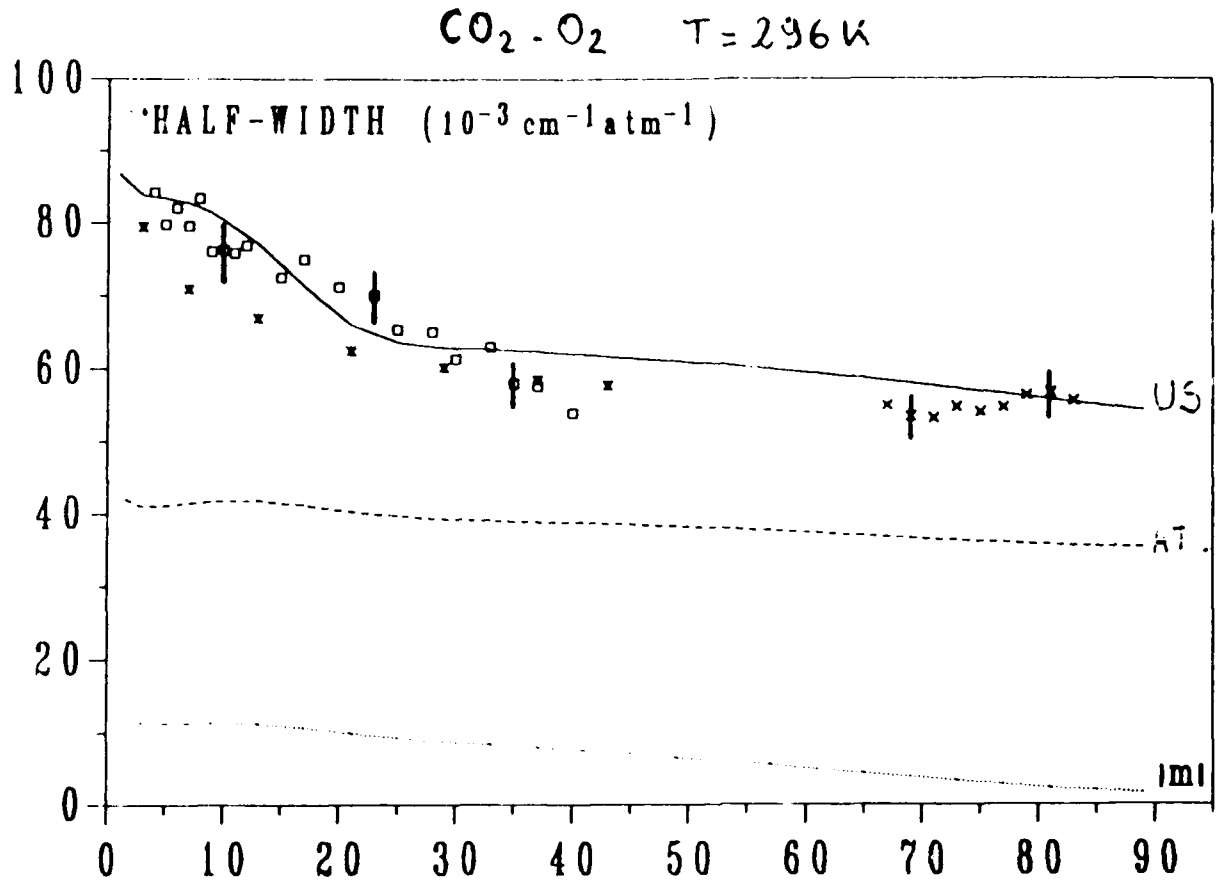

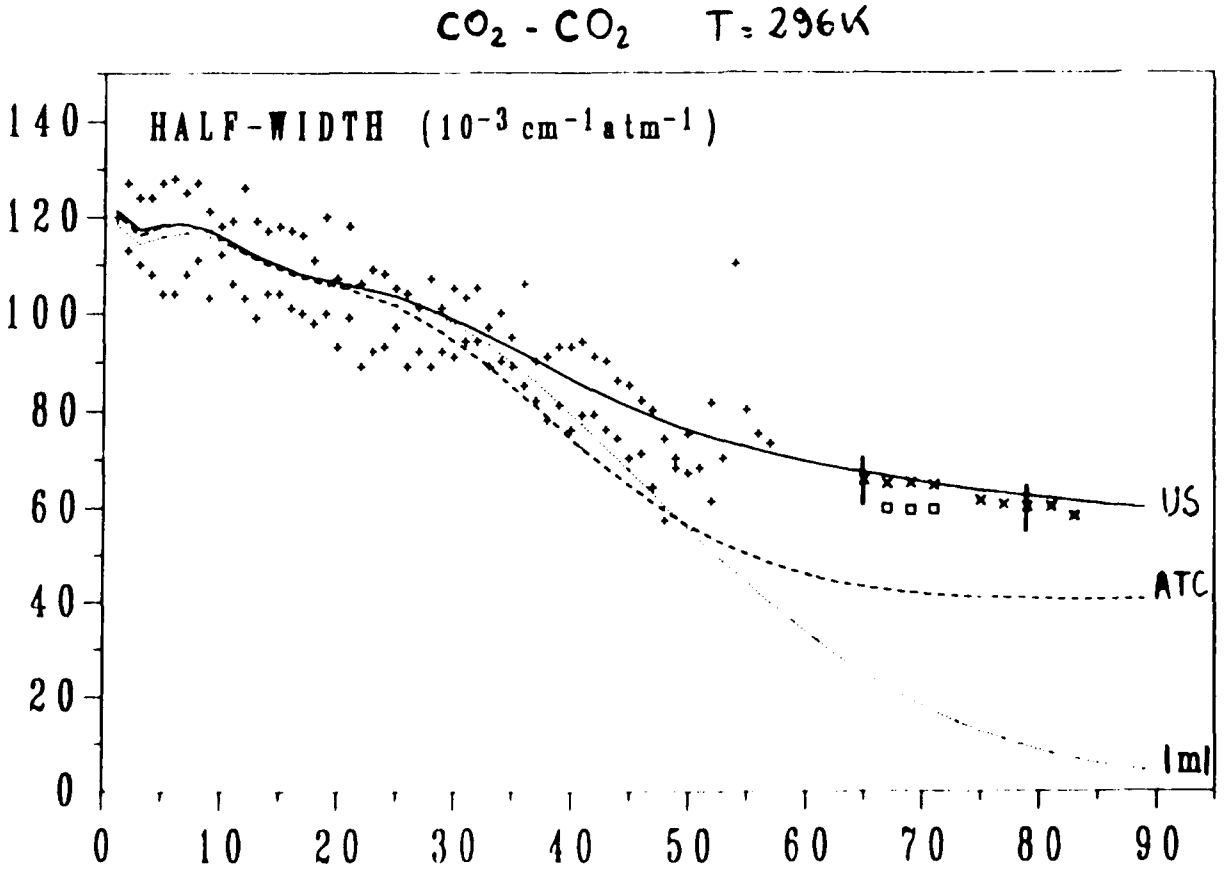

m: J+1, J, -J for P, Q, R branches

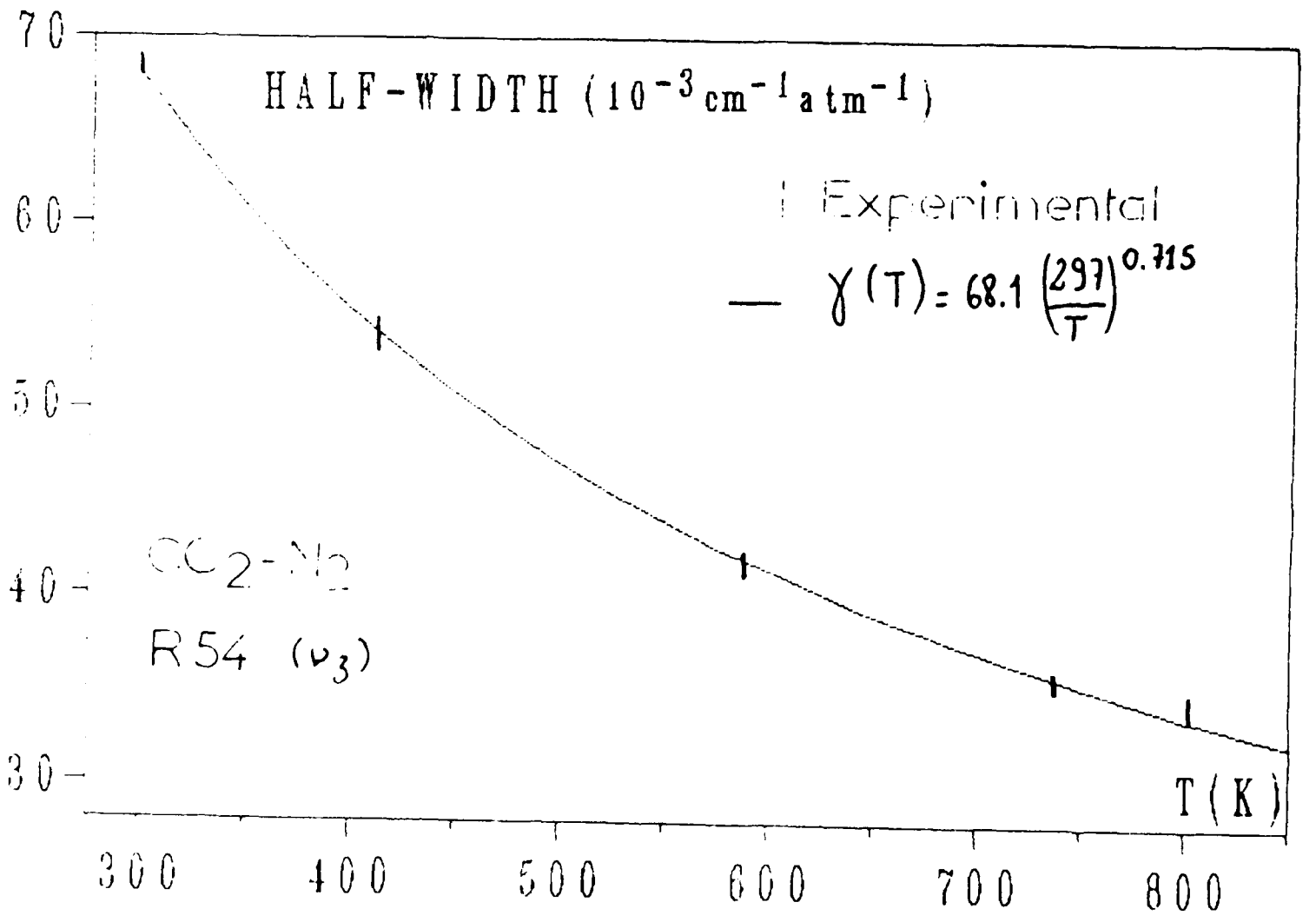

Temperature dependence of γ

1.3 Calculated tabulations

The theoretical model has been widely and successfully tested

tabulations of half-widths in the **300-2400 K** temperature range

radiative molecule: CO_2, CO

broadening partners: CO_2, H_2O, O_2, N_2

$\gamma_{|m|}$ **(300 K) and** $N_{|m|}$ are deduced from a fit of the calculated values by using

$$\gamma_{|m|}(T) = \gamma_{|m|}(300)\,(300/T)^{N_{|m|}}$$

$|m| = 1 - 101$ for CO_2

$|m| = 1 - 77$ for CO

The discrepancies between the calculated broadening coefficients and those obtained by this equation do not exceed 7 % in the **200 - 3000 K** range

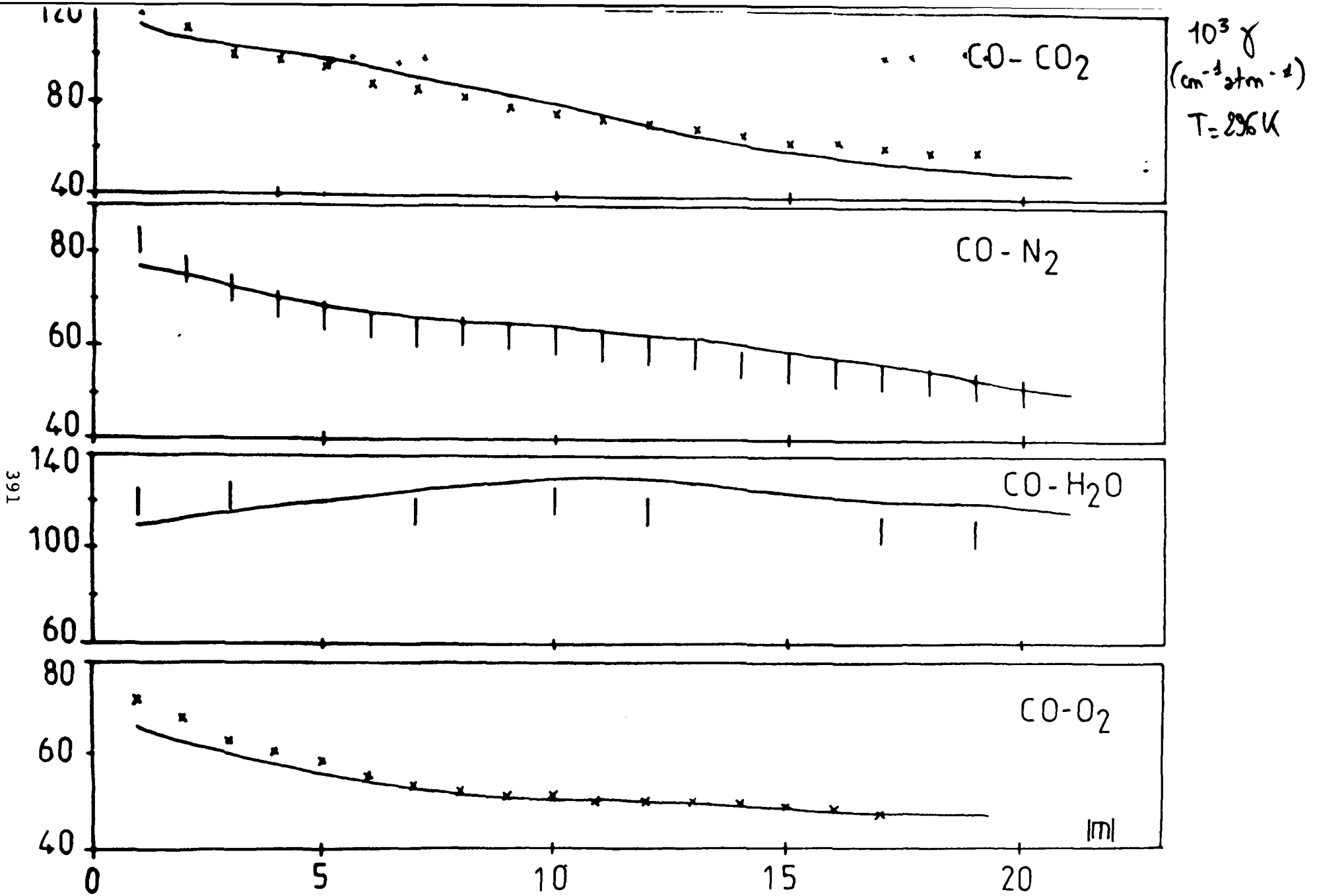
120
80
40
CO - CO2
10³ γ
(cm⁻¹ atm⁻¹)
T = 296 K
80
60
40
CO - N2
140
100
60
CO - H2O
80
60
40
CO - O2
0
5
10
15
20
ml

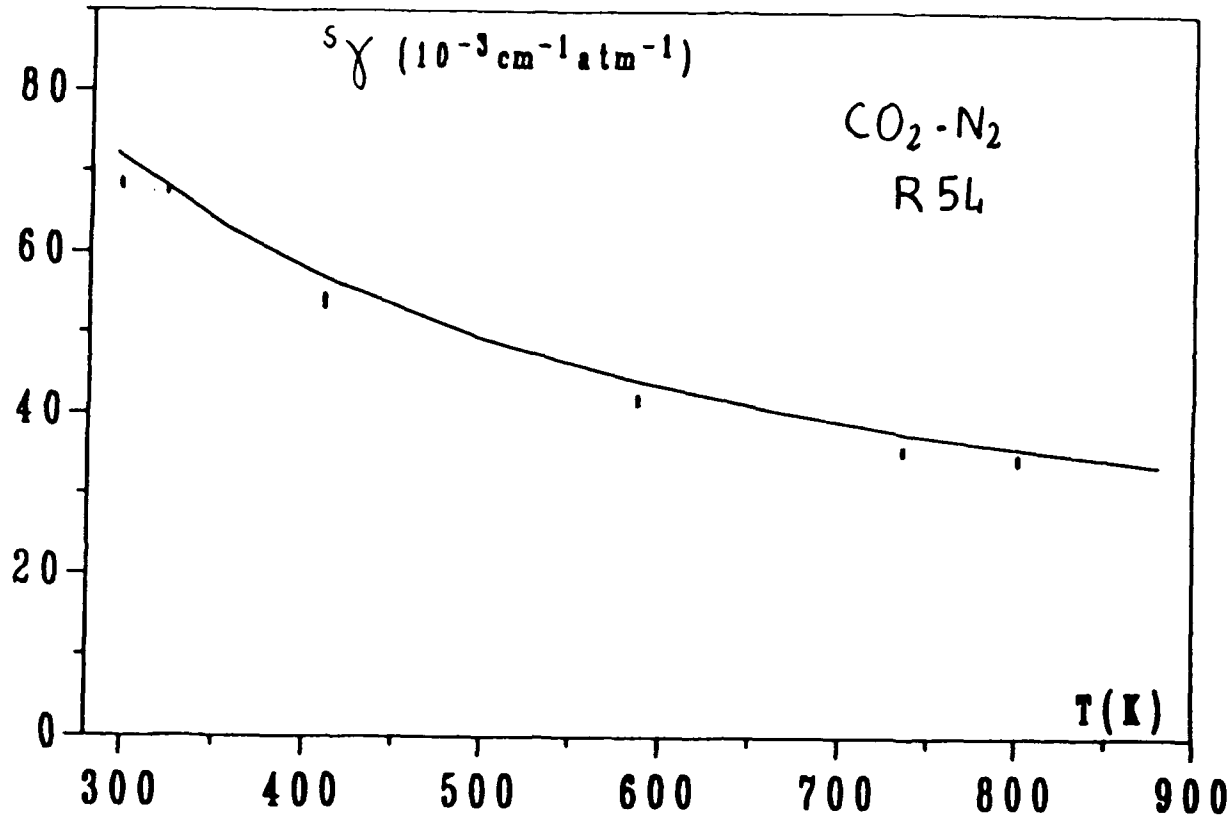

I experimental ___ calculation

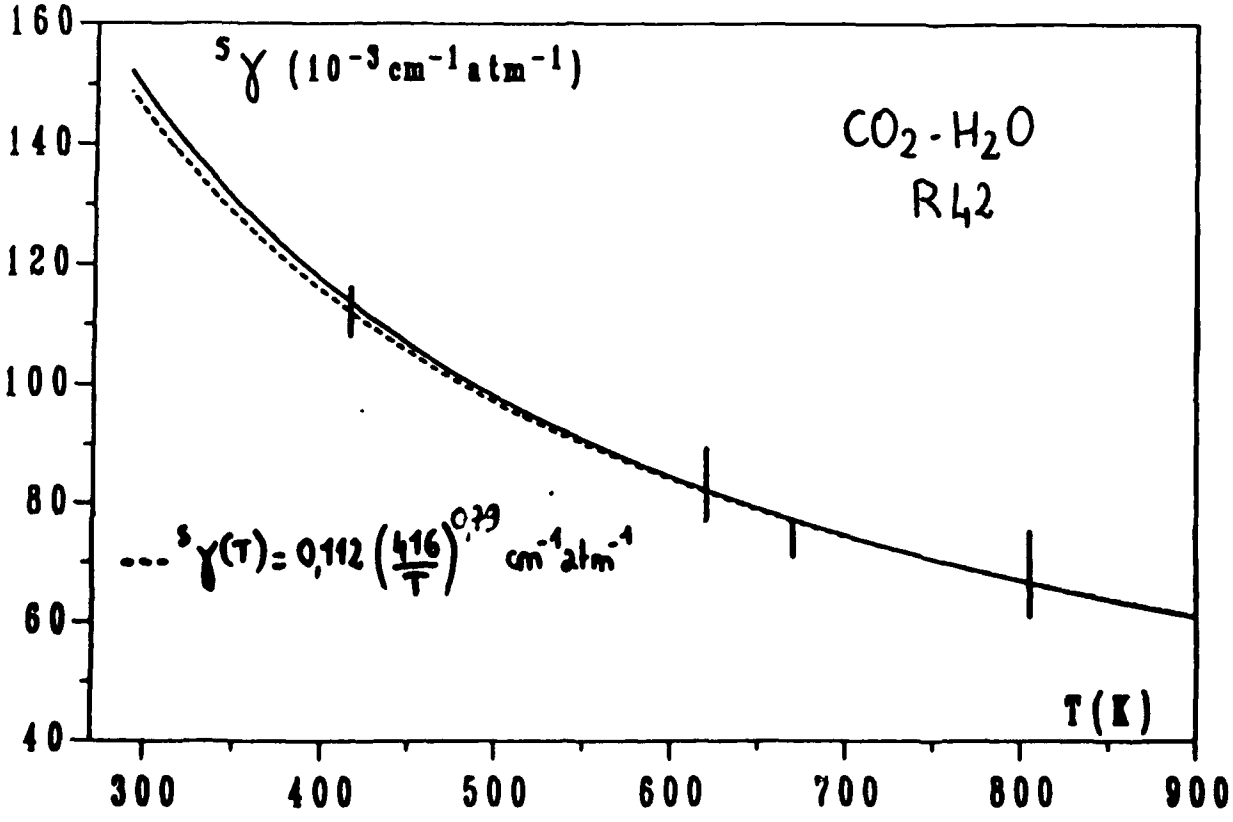

2. STUDY STARTING ON CO_2 LINE - INTENSITIES AT ELEVATED TEMPERATURE

Aim : Determination of line-intensities associated with transitions originate from high vibrational-rotational energy levels

High temperature ⟶ line density becomes very high

⟶ very high resolution spectroscopy ⟶ use of a diode laser

Similar experimental set up — cell (11 cm long) operating up to 900 K; diode laser working around 2300 cm^{-1}

\+ a reference cell operating at room temperature for line identifications

new high temperature cell of 1 m long

Improve the knowledge of band-intensities and Herman-Wallis coefficients for transitions of $E'' > 3500\ cm^{-1}$

Comparisons with calculations (with the DND method)

The results could be incorporated into a global theoretical model of the CO_2 molecule in order to improve the dipole moment function coefficients

SPECTROSCOPIC RESULTS ON CFC-12. HOW TO USE THEM TO MODEL STRATOSPHERIC ABSORPTIONS

Jean-Claude Deroche and Georges Graner
Laboratoire d'Infrarouge
Université de Paris-Sud
Bât.350 - Campus d'Orsay
91405 Orsay Cedex
France

SPECTROSCOPIC RESULTS ON CFC-12. HOW TO USE THEM TO MODEL STRATOSPHERIC ABSORPTIONS

Two regions are convenient for the atmospheric detection of CF_2Cl_2 alias CFC-12: near υ_8 at 1160 cm^{-1} and near υ_6 at 920 cm^{-1} (cf. Figure 1 which shows a balloon spectrum recorded by A. Goldman et al.) We have studied in detail this second region.

The first problem to solve is the **vibrational** assignment. Figure 2 shows the difficulties due to the isotopic species and to the low vibrational levels. Figure 3 shows a medium resolution spectrum of CFC-12 near 920 cm^{-1}, with at least seven Q branches, which were assigned in different ways by various authors. Finally, by preparing a sample containing only ^{35}Cl, Diallo, Deroche, and Morillon have given the vibrational assignments shown on Figures 4 and 5 for both regions.

The **rotational** assignment is a formidable challenge since there are more than 10,000 lines per cm^{-1} near 920 cm^{-1}, i.e. more than 10 lines per Doppler width. Fortunately, this is the region of the CO_2 laser. Therefore, it was possible to use microwave-infrared double resonance techniques, developed at Ulm. Several years of hard work allowed Jones, Morillon, and Traubmann to assign many coincidences between CFC-12 and the various CO_2 lasers. Figure 6 gives the six vibrational bands for which rovibrational constants were derived and also the three other ones for which we estimated the constants.

The constants of these nine bands were used to predict transitions, as detailed in Figure 7. The tape containing the 376,961 transitions is available from the authors. This is far from being perfect, as explained in Figure 8.

To test the quality of the prediction, we have made several simulations:

a. M. Sneels & W.L. Meerts have published in Appl. Phys. B 45, 27-31 (1988), spectra recorded with a molecular jet of CFC-12, either pure or diluted, in rare gases. Figure 9 shows a comparison of their diode laser spectrum with a synthetic spectrum computed at 15K in a region of R lines. Figure 10 shows a comparison near a Q branch (the vertical scale is not correct).

b. Linda Brown has recorded on the Kitt Peak interferometer several spectra at different temperatures. Figure 11 shows a spectrum recorded at 208K with an unapodized resolution of 0.005 cm^{-1}.

We are still working on the problem of absolute intensities. We are in the process of recording diode spectra in several zones between 921 and 933 cm^{-1}, with a 4 m absorption length and small pressures (0.03 to 0.7 Torr). Of course, we cannot measure line intensities but only the total absorption in small region and compare it to a synthetic spectrum. Figures 12, 13, and 14 show one of such comparisons (NB: the horizontal scale is different on the synthetic spectrum). A problem appears clearly above 923.250 cm^{-1}. There is a pressure dependent background which does not appear in the synthetic spectrum although the latter was done with a cutoff of 200 times the linewidth or 0.2 cm^{-1}. Should we use many more than 9 bands in the computation?

The last transparency discusses proposals on how to deal with the large file for atmospheric calculations.

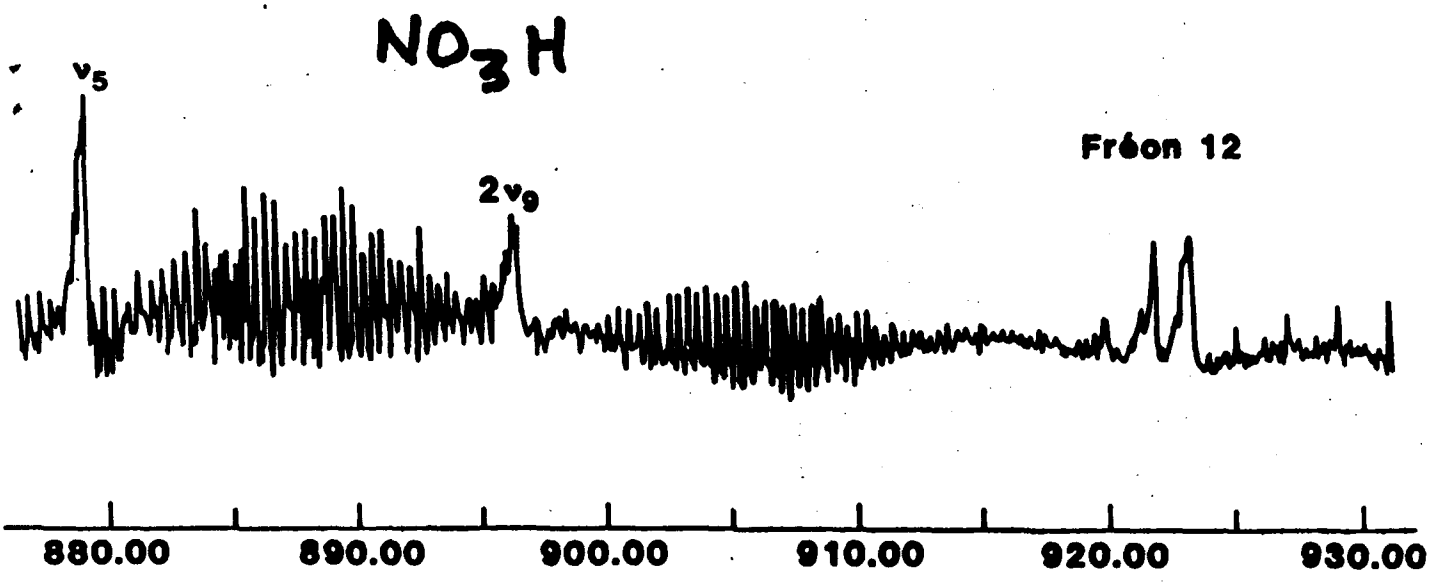

Figure 1.

GOLDMAN

21

Freon-12 CF_2Cl_2

a) Cl has 2 isotopes

^{35}Cl / ^{37}Cl proportion 3/1

Therefore F-12 has 3 isotopic varieties

35-35	9	} or	57.05 %
35-37	6		36.96 %
37-37	1	}	5.99 %

b) The lowest levels of CF_2Cl_2 are

$\nu_4 = 1$ 261.6 cm^{-1}

$\nu_5 = 1$ 320.7 cm^{-1}

$2\nu_4 = 2$ ≃520 cm^{-1}

hence strong hot bands

ν	at 300K	at 210 K
$\nu_4 = 1$	0.285	0.181
$\nu_5 = 1$	0.215	0.123
$\nu_4 = 2$	0.082	0.033

relative intensities
cold band = 1

Figure 2.

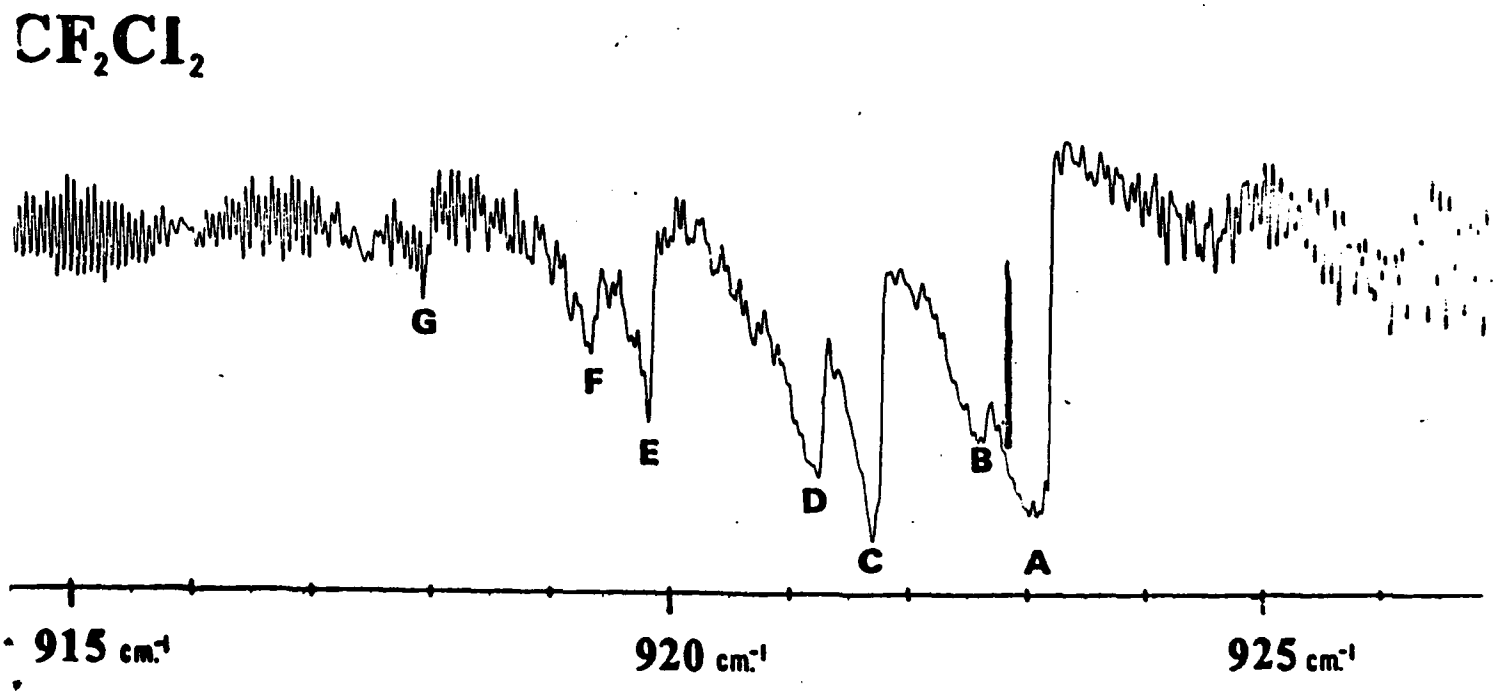

Figure 3.

3

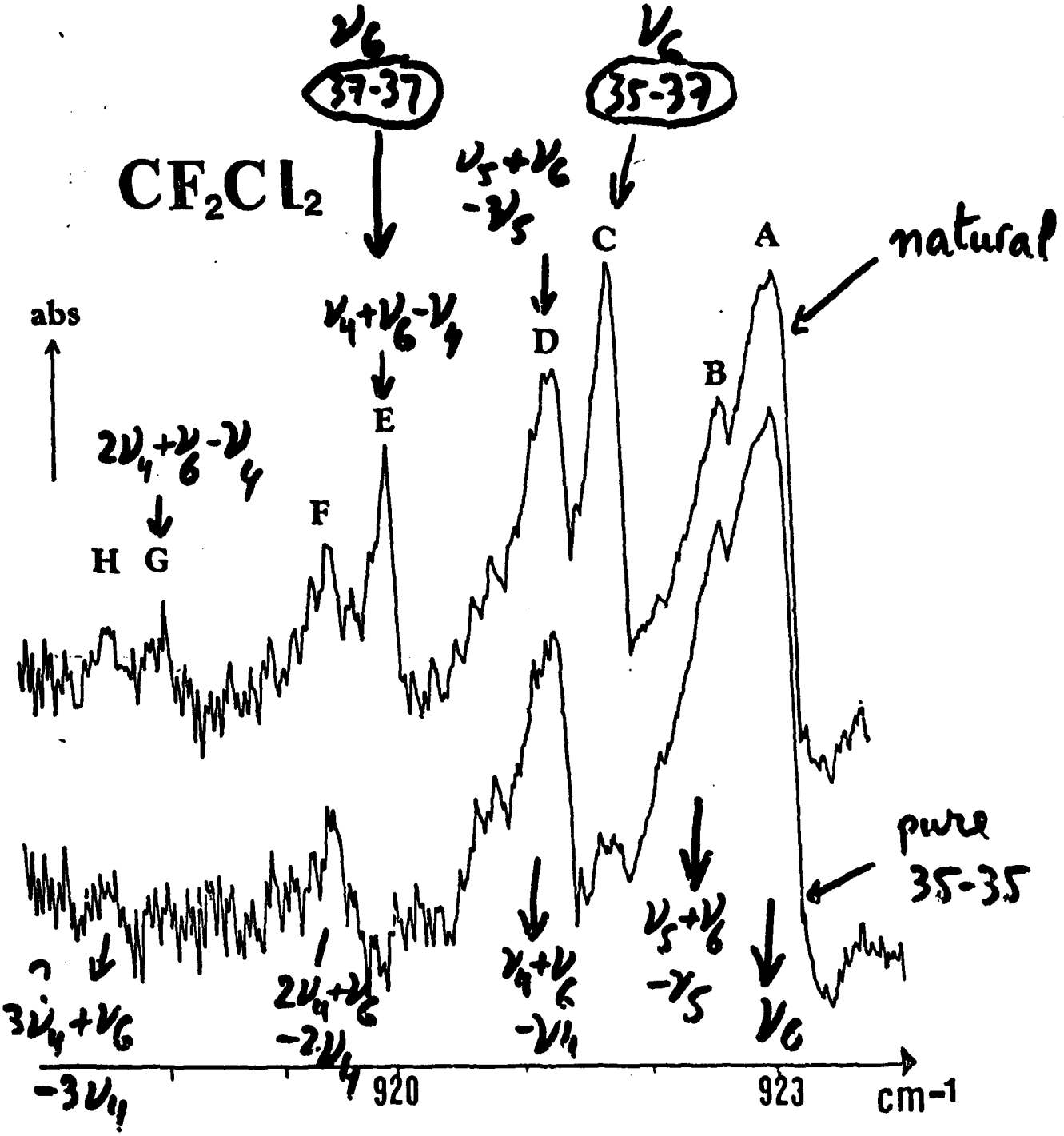

GREEN : 35-35
RED : 35-37
BLACK : 37-37

Figure 4.

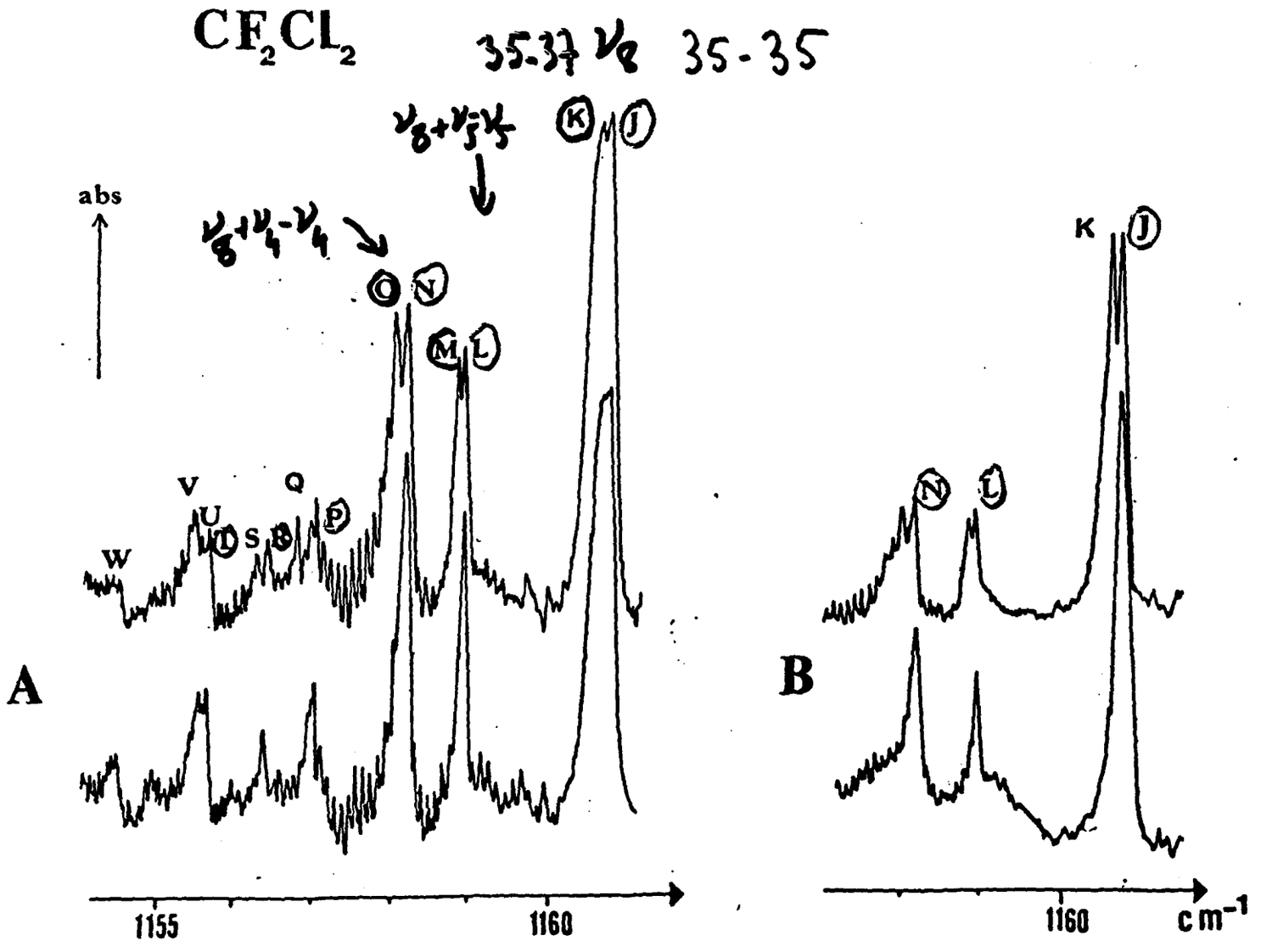
CF_2Cl_2
35.37 ν_8 35-35
$\nu_8+\nu_5-\nu_5$
$\nu_8+\nu_4-\nu_4$
abs
K
J
O
N
M
L
V
Q
U
T
S
R
P
W
A
B
1155
1160
1160
cm^{-1}

Figure 5.

Bands analysed

by | Harry JONES (Ulm)
Mireille MORILLON (Orsay)
Gerhard. TRAUBMANN (Ulm)

ν_6 35-35
ν_6 35-37
ν_6 37-37
$\nu_4 + \nu_6 - \nu_4$ 35-35
$\nu_4 + \nu_6 - \nu_4$ 35-37
$\nu_5 + \nu_6 - \nu_5$ 35-35

Other bands used by J.C. DEROCHE for the predictions.

$\nu_5 + \nu_6 - \nu_5$ 35-37
$2\nu_4 + \nu_6 - 2\nu_4$ 35-35
$2\nu_4 + \nu_6 - 2\nu_4$ 35-37

Figure 6.

PREDICTION OF TRANSITIONS OF CFC-12

Number of vibrational transitions used: 9

Prediction made at 296K

Intensity criterion: all lines > 10^{-4} of the strongest line.

All asymmetry doublets are merged if their separation is smaller than 0.0005 cm^{-1}.

Grand total: **376961** transitions listed between 850 and 946 cm^{-1}.

Some partial densities of lines:

916 - 917 cm^{-1}:	11927 lines
917 - 918 cm^{-1}:	15190 lines
918 - 919 cm^{-1}:	15036 lines
919 - 920 cm^{-1}:	17626 lines
920 - 921 cm^{-1}:	18498 lines
921 - 922 cm^{-1}:	17025 lines
922 - 923 cm^{-1}:	14516 lines
923 - 924 cm^{-1}:	10208 lines
924 - 925 cm^{-1}:	9792 lines

The list gives for each line: wavenumber, lower level energy,
relative intensity at 296K and all the vibrational and rotational quantum numbers of the transition.

Figure 7.

SOME PROBLEMS LEFT IN THE PREDICTION

1) The rovibrational constants of some of the 6 first bands are not all perfect (perturbations ignored).

2) The rovibrational constants of the 3 last bands have been extrapolated.

3) Many other hot bands exist, giving transitions with intensities larger than 10^{-4}. But they are relatively weak in the region of the main Q branches.

4) All intensities have been calculated as if all bands were unperturbed. No Herman-Wallis coefficient was introduced.

5) Self-broadening coefficients (*to simulate laboratory spectra*) and air-broadening coefficients (*for atmospheric spectra*) have been measured* but not their J and K dependence. Their temperature dependence is totally unknown.

6) With such a high density of lines, line-mixing effects are probably not negligible.

* 0.790 cm^{-1}/atm self-broadening
0.210 cm^{-1}/atm air-broadening

Figure 8.

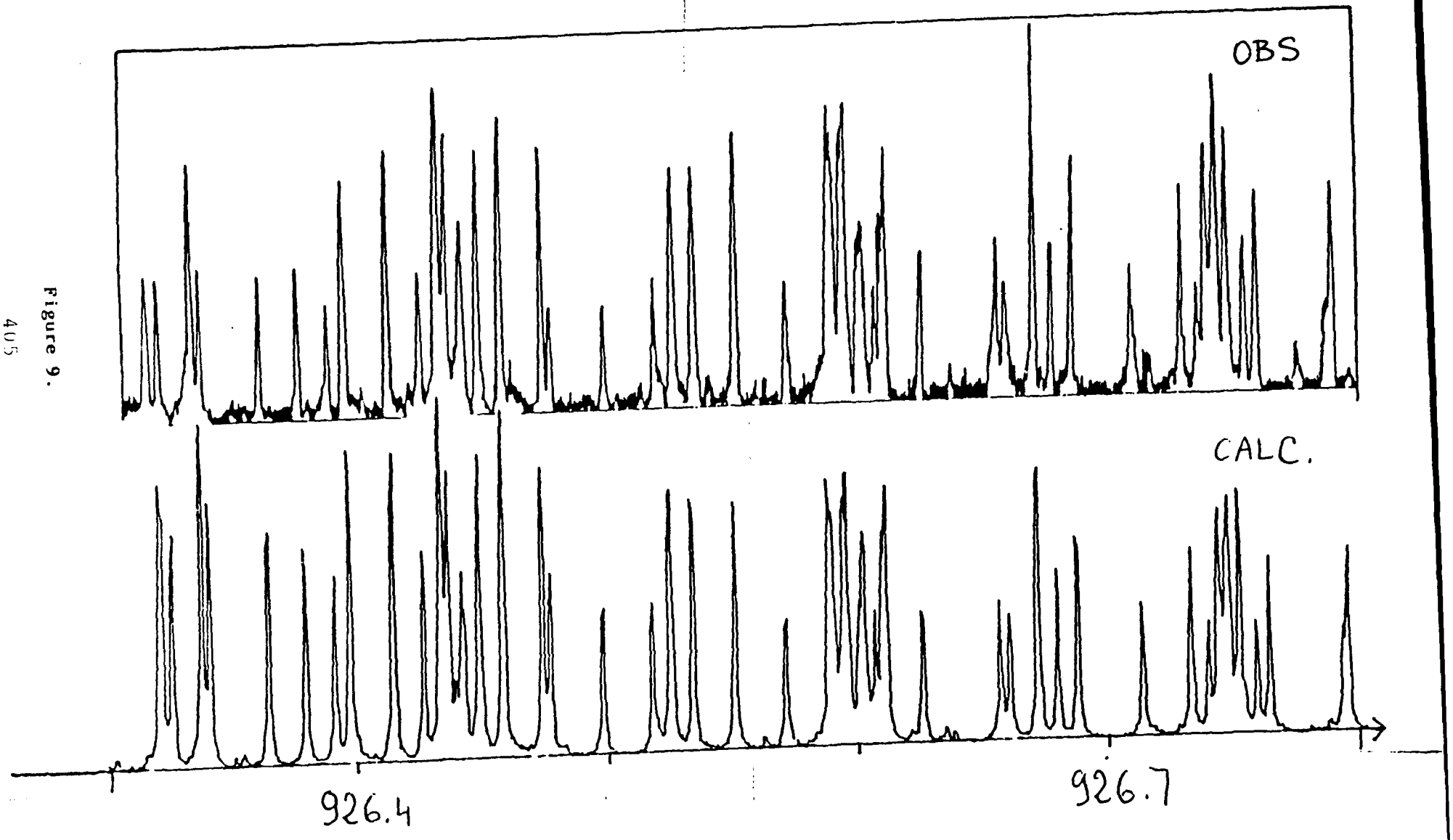

Figure 9.

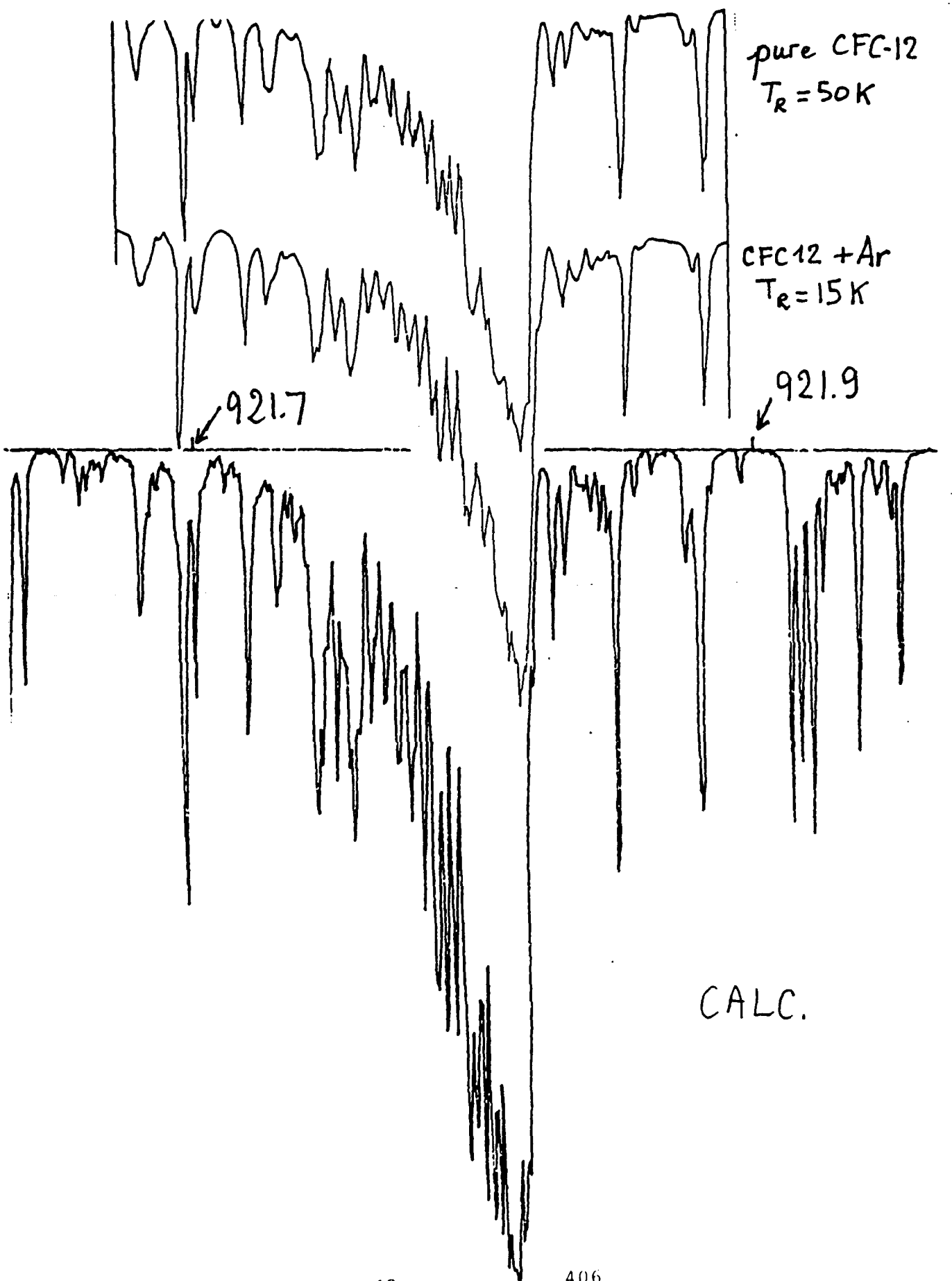

Figure 10.

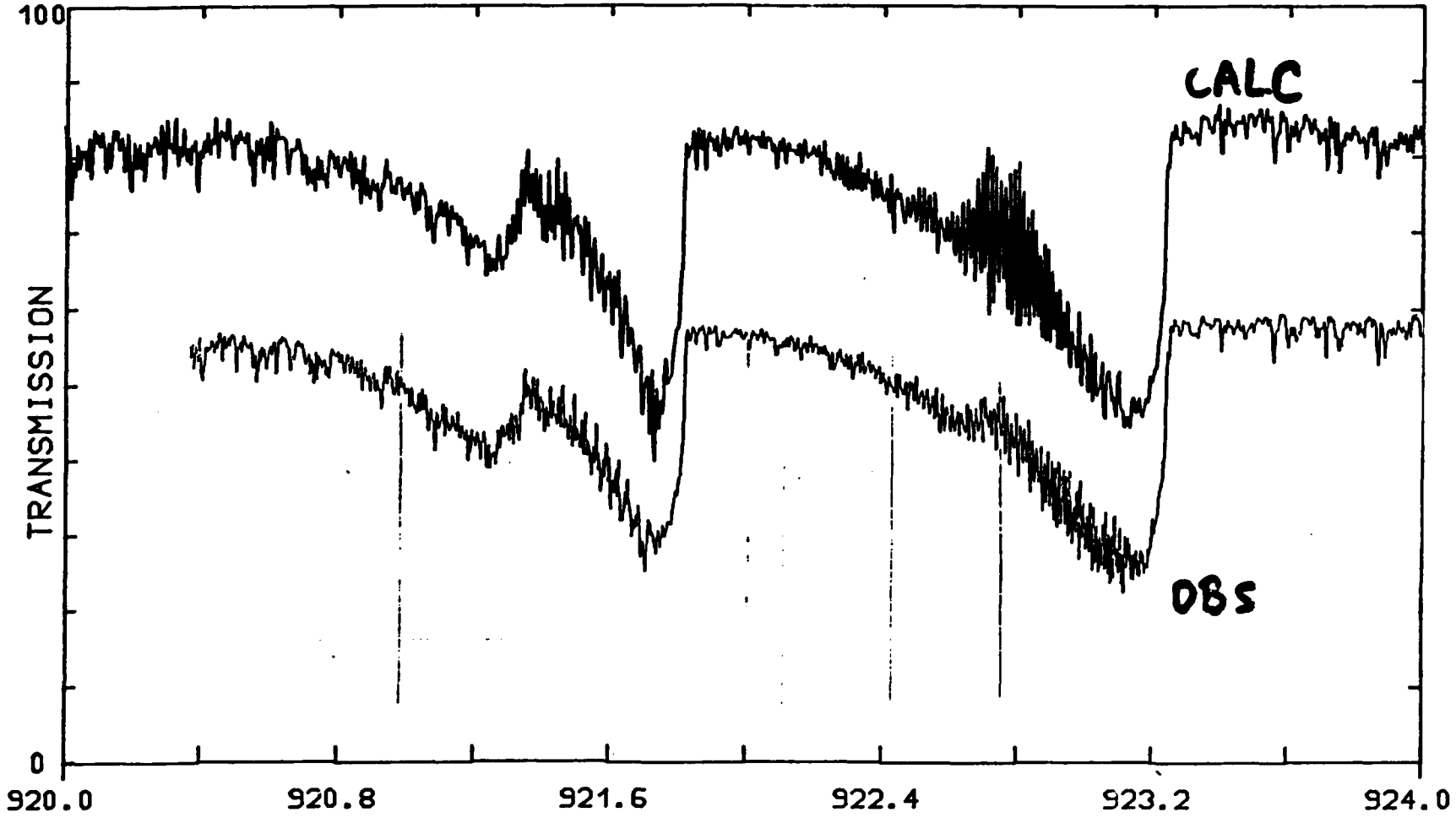

RUN: J53.1.3
PATH: 0.300000 M
APODIZATION: 0
DATE: 07/09/85

MOLECULE: FREON12
PRES: 0.047 TORR
GAS TEMP: 208.00 K

Figure 11.

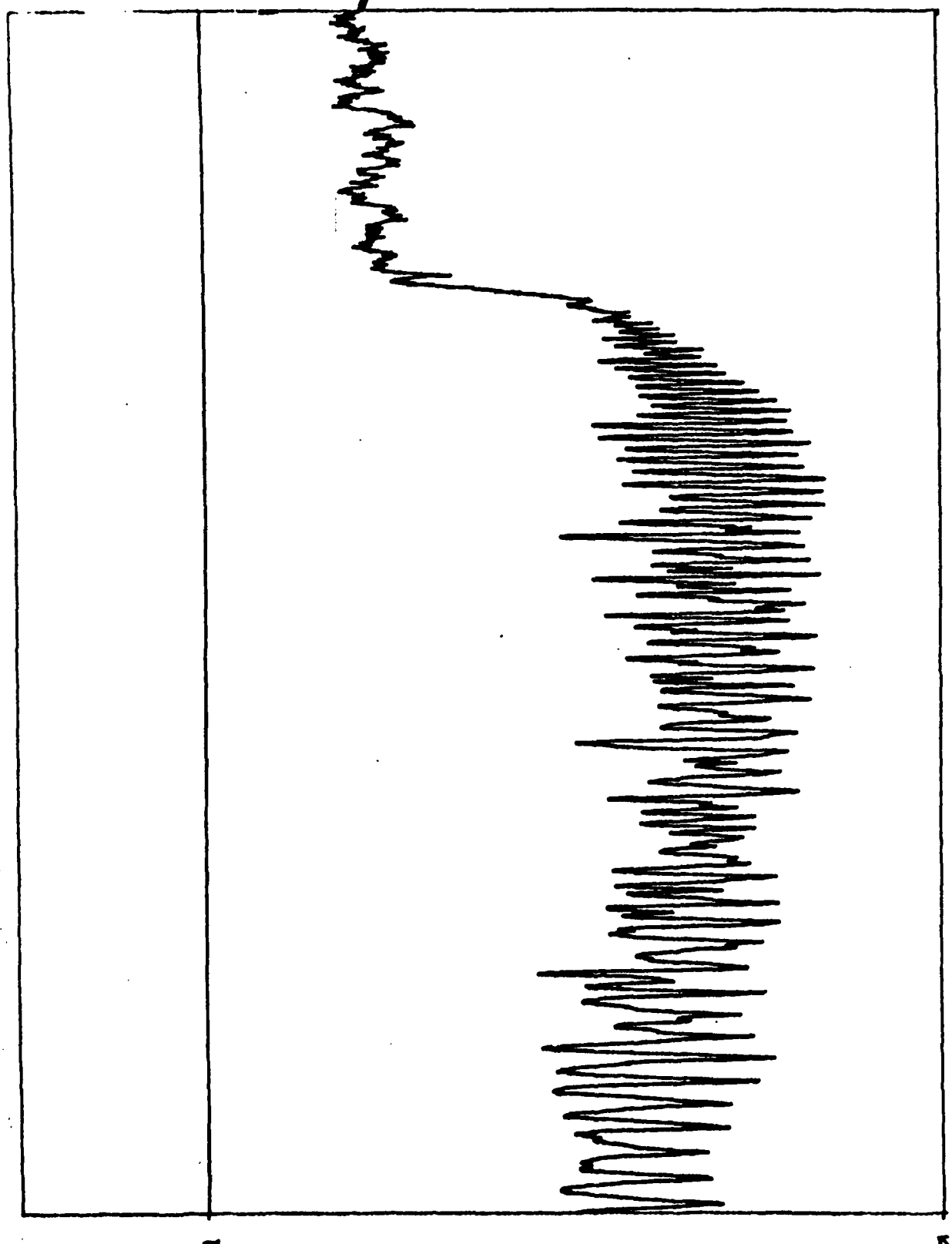

Figure 12.

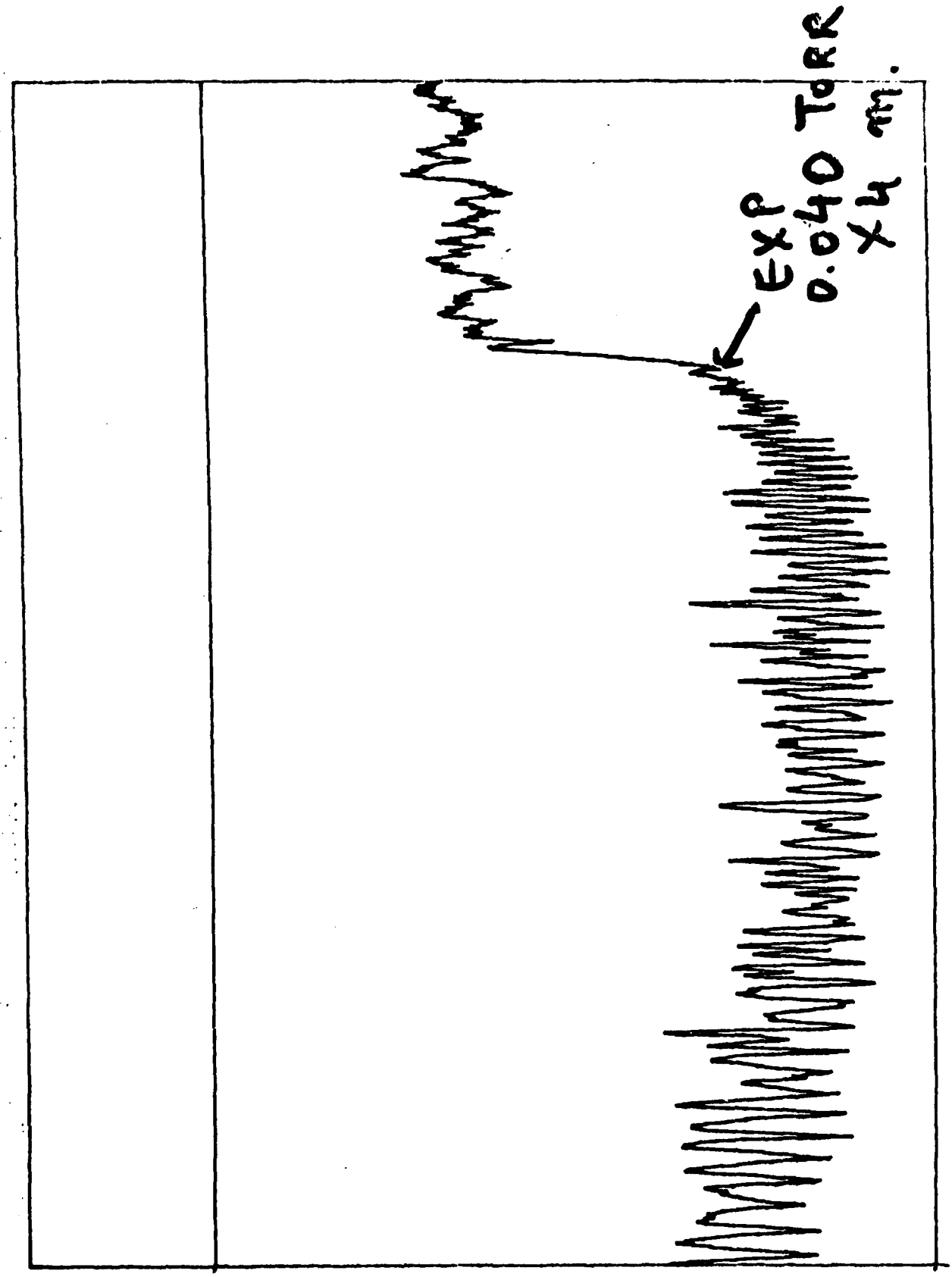

Figure 13.

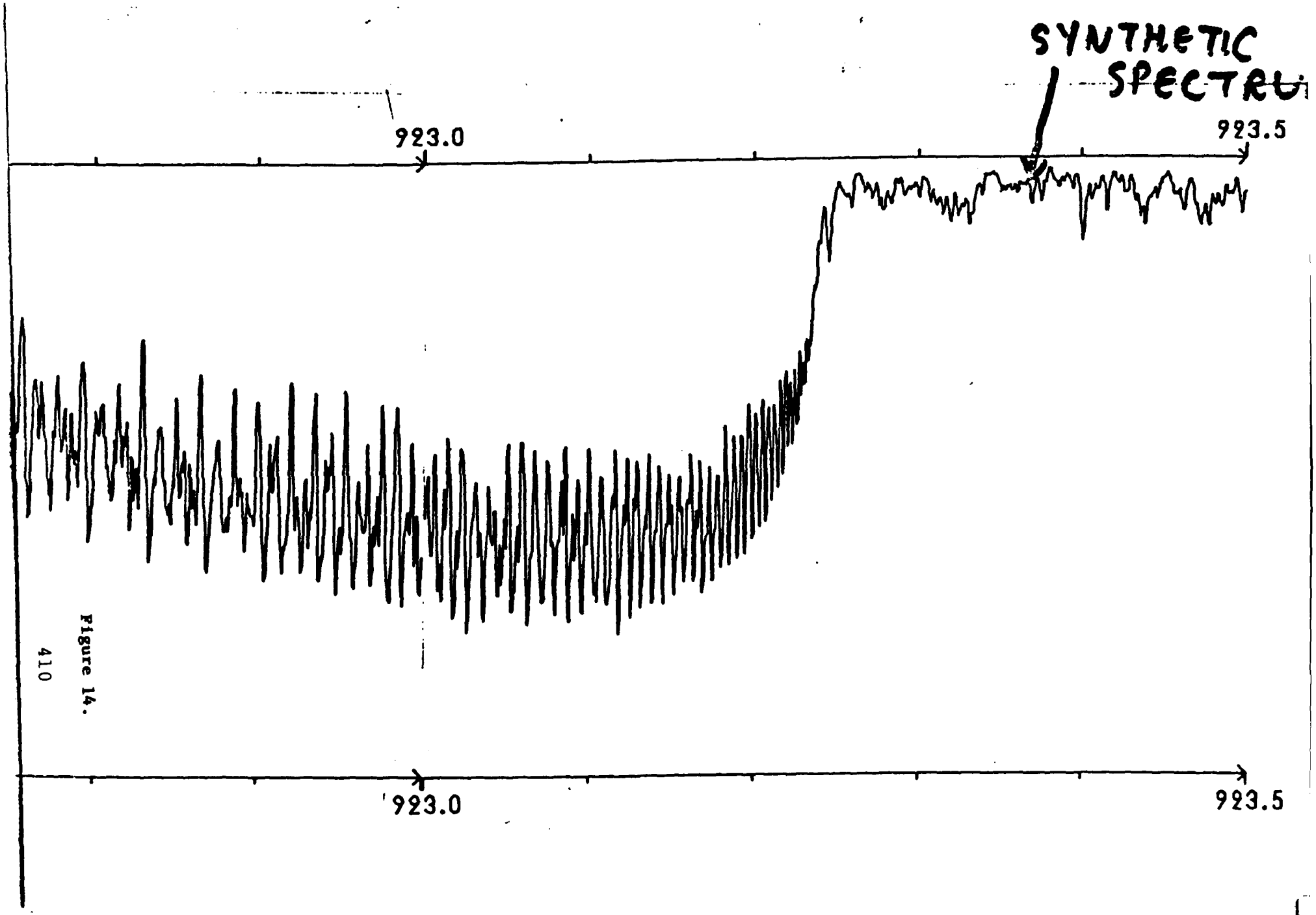

Figure 14.

410

HOW TO DEAL WITH THIS LARGE FILE ?

1) It is easy to compute from this file the relative intensities at any other temperature T. If the lower level of a transition has an energy E", the intensity at T is given by

$$I_T = I_{296} \frac{\exp(-hcE''/kT)}{\exp(-hcE''/296k)}$$

2) For most uses, the resolution can be very much degraded. If $\Delta\nu$ is the useful resolution, it is likely that a sampling step of $\Delta\nu$ / 10 is sufficient. Therefore, the suggested procedure might be the following:

a)produce **complete** lists of transitions at several temperatures: e.g. 200 K, 220 K, 240 K, 260 K, 280 K, 300 K.

b)for each temperature, merge all lines located within a box of width $\Delta\nu$ / 10, adding their intensity **at this temperature.** We have thus produced a much shorter list of "pseudo-lines".

(e.g. for a resolution of 1 cm^{-1}, one is left with 10 pseudo-lines per cm^{-1} for each temperature, instead of 10 - 18000 : a gain factor of more than 1000). (for a resolution of 0.01 cm^{-1}, the gain is still 10 to 18)

c) AFGL or any other user could keep these 6 lists for 3 typical resolutions (1 , 0.1 and 0.01 cm^{-1}).

d) For resolutions better than 0.01 cm^{-1} , the use of the complete list seems preferable. Most users can probably easily compute the corresponding list for any desired temperature. If not, AFGL could keep the list for the 6 above-mentioned temperatures.

Figure 15.

RECOMMENDATIONS FOR THE SUPPLEMENTARY ABSORPTION PARAMETERS FOR HEAVY MOLECULES IN THE AFGL COMPILATION

Aaron Goldman
Physics Department
University of Denver
Denver, CO 80208

Steven T. Massie
National Center for Atmospheric Research
P. O. Box 3000
Boulder, CO 80307

ABSTRACT

Current usuage of HITRAN 86 cross-sections for heavy molecules is reviewed. The need for pressure-temperature dependence and band contours of the cross-sections is illustrated, with examples from CF_2Cl_2, N_2O_5, and $ClONO_2$ laboratory spectra. Recommendations for extending the cross-section data base are presented.

1986 HITRAN DATABASE

Table VI. Species Included in Cross-Sectional File

Species		# cross sections	Frequency cm^{-1} Minimum	Maximum
$ClONO_2$		5020	765.002	819.998
HNO_4		5476	770.007	829.999
$CHCl_2F$	(CFC21)	5020	785.000	839.995
CCl_4		1826	786.001	805.998
$CFCl_3$	(CFC11)	2738	830.009	859.999
CF_2Cl_2	(CFC12)	7301	860.008	939.996
$C_2Cl_2F_4$	(CFC114)	12320	1025.009	1159.992
$CHCl_2F$	(CFC21)	4563	1050.004	1099.992
$CFCl_3$	(CFC11)	3651	1060.004	1099.998
CF_2Cl_2	(CFC12)	10039	1070.005	1179.994
$C_2Cl_3F_3$	(CFC113)	12777	1090.008	1229.998
$C_2Cl_2F_4$	(CFC114)	11771	1160.025	1288.992
N_2O_5		4647	1225.001	1265.000
HNO_3		7301	1270.004	1349.993
$ClONO_2$		3650	1270.007	1309.991
CF_4		1095	1275.003	1286.990
N_2O_5		11616	1680.003	1780.000

Rothman, L. S., et. al., Applied Optics, vol. 26, pg. 4058-4097, 1987.

1986 HITRAN DATABASE

Cross section specifications

Format wavenumber, cross section

Resolution 0.03 cm^{-1}

Temperature 296 K

Pressure single value

Accuracy 10 to 25 %

Limitations

Single resolution, temperature, pressure and amount.

Pure gas broadening.

Incomplete spectral intervals.

Beer's law assumption.

1986 HITRAN DATABASE

Cross section advantages

(i) First approximation for non-existing line parameters.

(ii) Small dataset size.

Present usuage

(i) Interpolate for Beer's law approx

(ii) Delta lines

(iii) Fit pseudolines
ν , S, broadening, effective E"

(iv) Partition function temperature dependence for vibrational and rotational degrees of freedom.

BAND CONTOURS

$S_{vibration}(T)$

Dominates for heavy molecule with low vibrational levels.

$S_{rotation}(T)$

Small dependence for
($200 < E < 400$ 1/cm)

Small B rotational constant
(< 0.1 1/cm)

Wings and Q-branch narrow at lower temperature.

Fundamental bands
Total band intensity/molecule constant with temperature.

Hot bands
Contour narrows at lower frequency.

VIBRATIONAL PARTITION FUNCTION

T(K)	CFC-12	$ClONO_2$	N_2O_5
200	1.48	2.16	1.23
220	1.65	2.45	1.32
240	1.85	2.79	1.43
260	2.09	3.18	1.56
296	2.64	4.04	1.87

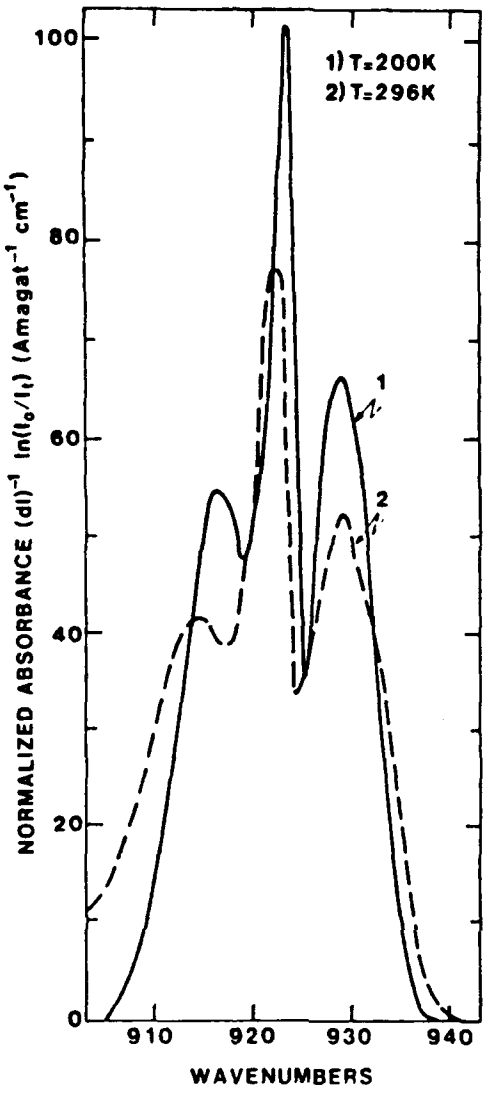

CF_2Cl_2

Fig. 4. Temperature dependence of the absorption coefficient of the ν_8 band for CF_2Cl_2 in the 900-950 cm^{-1} region with 1.6 cm^{-1} resolution. The line labeled "1" represents T = 200 K, dl = 27 x 10^{-4} amagat cm of F-12, P_{F12}/P_{F12+N_2} = 1/200. The dashed line labeled "2" represents T = 296 K, dl = 26 x 10^{-4} amagat cm of F-12, P_{F12} / P_{F12+N_2} = 1/200. Spectral data are listed in Table 4.

N-V-Thanh, et al., "Infrared Band Shapes and Band Strengths of CF2Cl2 from 800 to 1200 cm-1 at 296 and 200 K", JGR, vol 91, 4056-4062, 1986.

Elkins, J. W. and R. L. Sams,
NBS Rept. 553-K-86,
CMA Ref. Rept. FC 83-473, 1986.

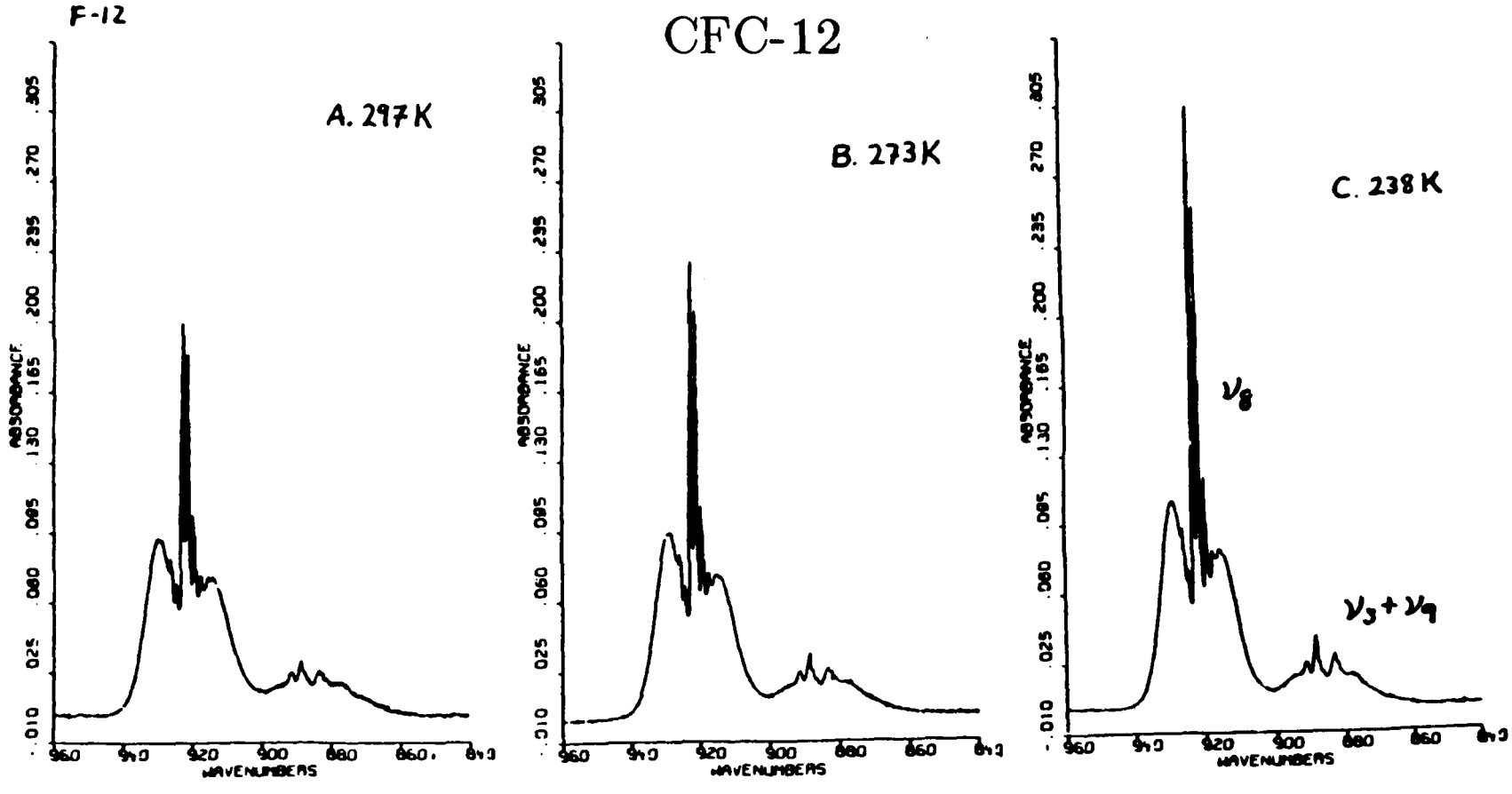

Figure 2 The absorption band system (BS#1) between 855 and 950 cm^{-1} of F-12 at 297, 273, and 238 K for the 286.7 ppm gas standard. Spectra have been corrected to the same number of halocarbon molecules for each temperature, a pl product of 4.2799 x 10^{-3} atm cm.

Cantrell et. al., preliminary

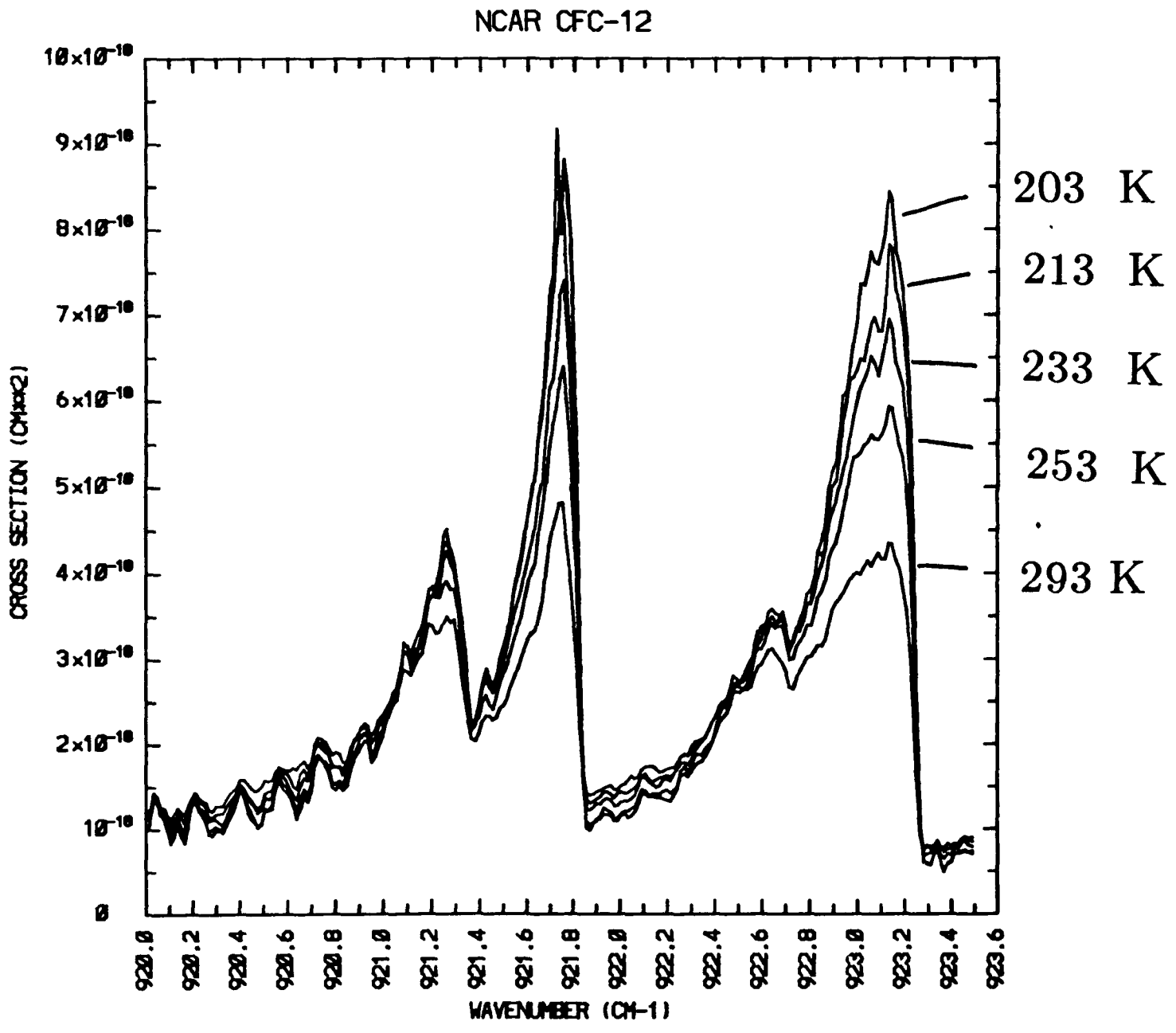

Cantrell, et al., Chem. Phys. Lett. 148 (1988), 358.

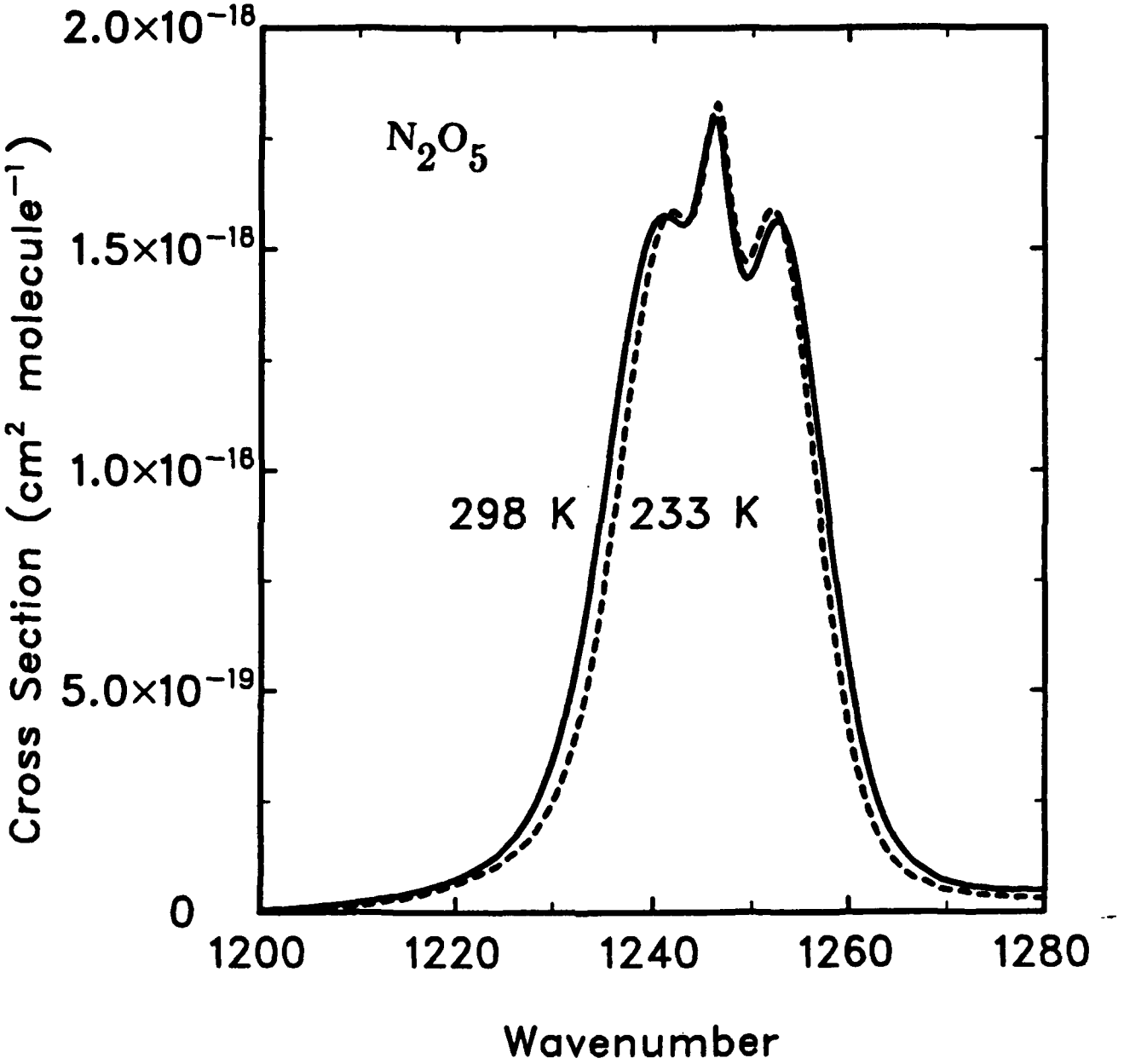

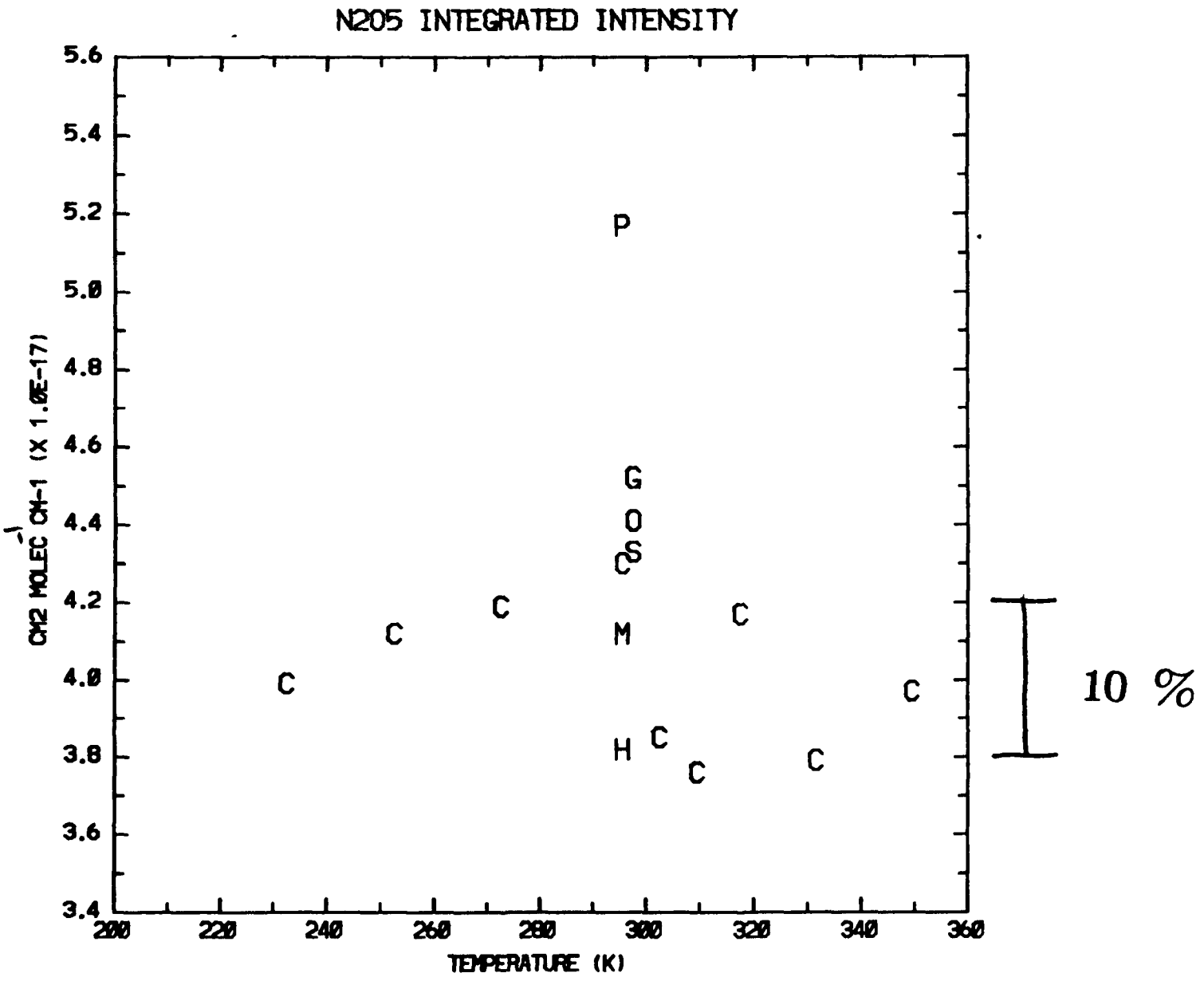
N2O5 INTEGRATED INTENSITY
CM2 MOLEC-1 CM-1 (X 1.0E-17)
TEMPERATURE (K)
5.6
5.4
5.2
5.0
4.8
4.6
4.4
4.2
4.0
3.8
3.6
3.4
200
220
240
260
280
300
320
340
360
P
G
O
S
C
M
H
10 %

$ClONO_2$

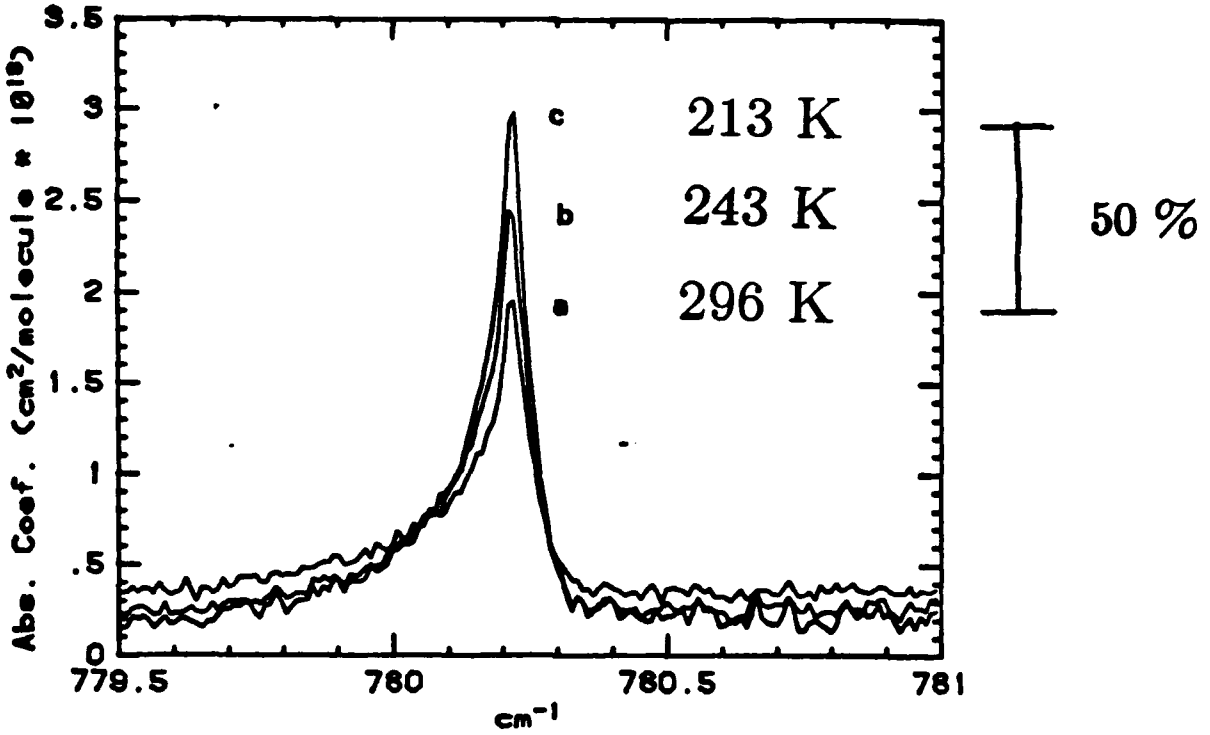

Fig. 8. Temperature dependence of absorption coefficients in the ν_4 Q branch at 0.02 cm^{-1} resolution. Curve a indicates 296 K; curve b, 243 K; curve c, 213 K.

Ballard, J., et al., "Absolute Absorption Coefficients of ClONO2 Infrared Bands at Stratospheric Temperatures", JGR, vol 93, 1659-1665, 1988.

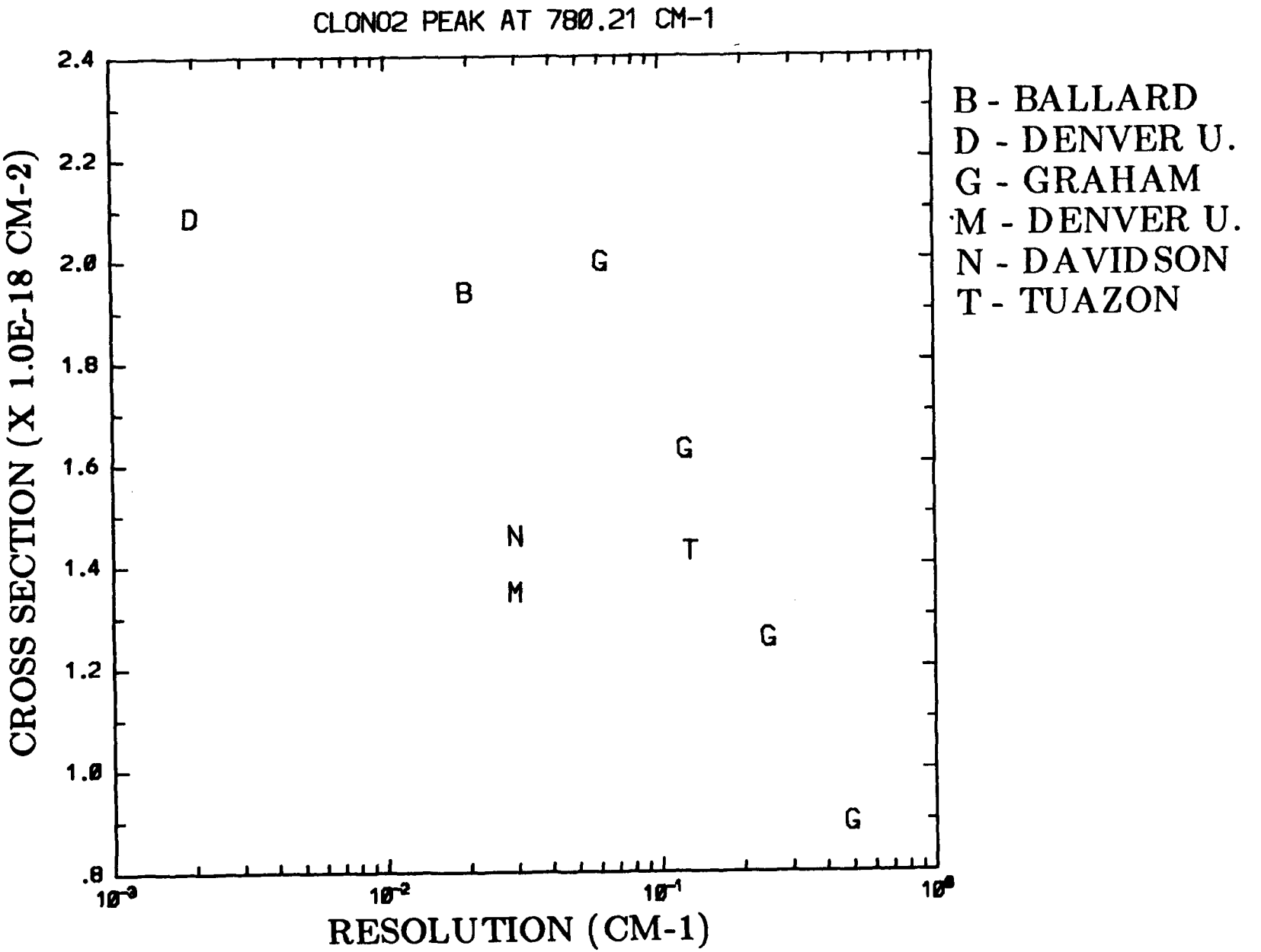
CLONO2 PEAK AT 780.21 CM-1
CROSS SECTION (X 1.0E-18 CM-2)
2.4
2.2
2.0
1.8
1.6
1.4
1.2
1.0
.8
RESOLUTION (CM-1)
B - BALLARD
D - DENVER U.
G - GRAHAM
M - DENVER U.
N - DAVIDSON
T - TUAZON

RECOMMENDATIONS

1. Approach

   Cross sections

   Empirical lines

2. Extensions of present lab data

   Spectral intervals

   Species

   Resolution

   Temperature-Pressure dependence

3. Laboratory and analysis intercomparison.
   (Denver University, JPL,
   NASA AMES, NBS, NCAR, Orsay,
   RAL, SUNY, UC Riverside)

RECOMMENDATIONS

4. Update molecular parameters

(i) Moderately heavy molecules
Replace with line parameters.
(example: CFC-12)
Compress number of lines.
(similar ν and E)

(ii) Heavy molecules
Fit pressure-temperature dependence.
(example: N_2O_5).

Effective E, fitting coefficients for temperature-pressure dependence.
Band contours.

5. File Structure for HITRAN 89
Various formats.
(σ, ν) at several temperatures.
$\sigma = f(\nu, T, P)$
Empirical lines: ν, S, broadening, E"
Partition function: $Q_v(T)$

HITRAN IN THE 1990's

John Schroeder
ONTAR Corporation
129 University Road
Brookline, MA 02146-4532

HITRAN IN THE 1990's
DISTRIBUTION AND MANAGEMENT

HITRAN WORKSHOP

8 - 9 June 1989

Air Force Geophysics Laboratory

Hanscom Air Force Base, Massachusetts

John Schroeder, ONTAR Corporation

129 University Road, Brookline, MA 02146-4532

Tel: 617-731-9619, FAX: 617-277-2374

ONTAR

HITRAN 1986

Line Data on ~ 300,000 Molecular Transitions

28 Atmospheric Gases

~ 40 Mbytes on 9-track, 1600 bpi tape in ASCII Format

Wide Distribution of Users

- DOD Community
- FASCODE
- NASA
- EPA
- University Laboratories and Private Industry

ONTAR

HITRAN IN THE 1990's

Big and Getting Bigger: 200, 500, 1000 Mbytes !!

Hot Gases,

Incorporate Other Databases

Should AFGL Continue to Distribute HITRAN on 9-track Tape ?

Tape is Unwieldy and "Difficult" to Use

Tape Handling is an Art and Differs from System to System

Costly for Users -- Ties Up a Lot of Disk Space

Costly for AFGL -- To Update, Reproduce and Distribute

Not "User-Friendly"

Evolution of Data Storage Devices . . .

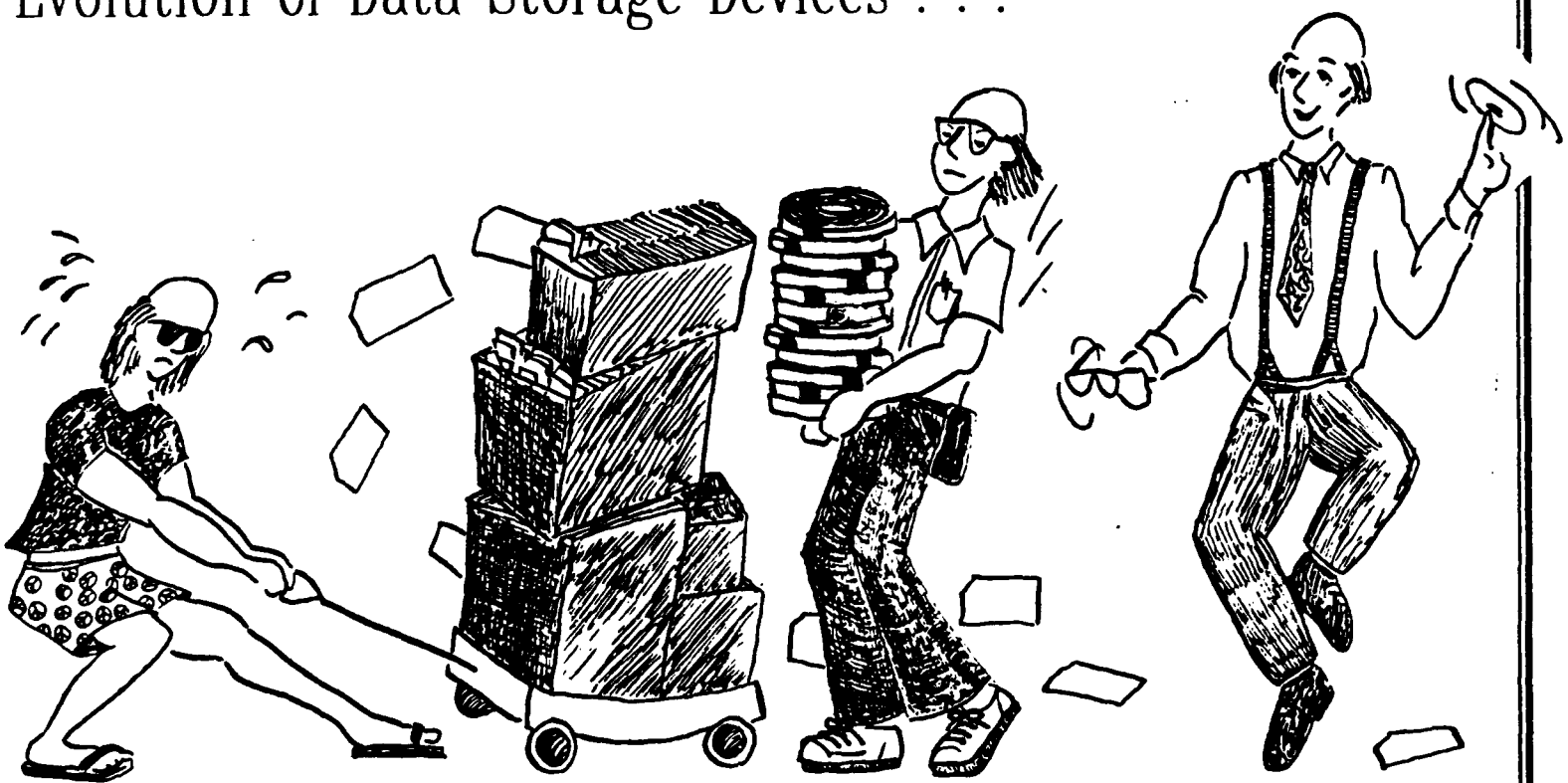

ONTAR

HITRAN ATMOSPHERIC WORK STATION

HAWKS

OBJECTIVE: Allow Users to Quickly USE HITRAN, Not Spend Their Time Trying to Figure Out How to Read and Manage the Database.

A Not User Abusive System Built Around PC Technology

CD - ROM Technology for Data/Software Distribution and Storage

Database Management Software

Incorporate (where feasible) Literature Sources

Interface Software for Main Frame and Minicomputers

HAWKS HARDWARE

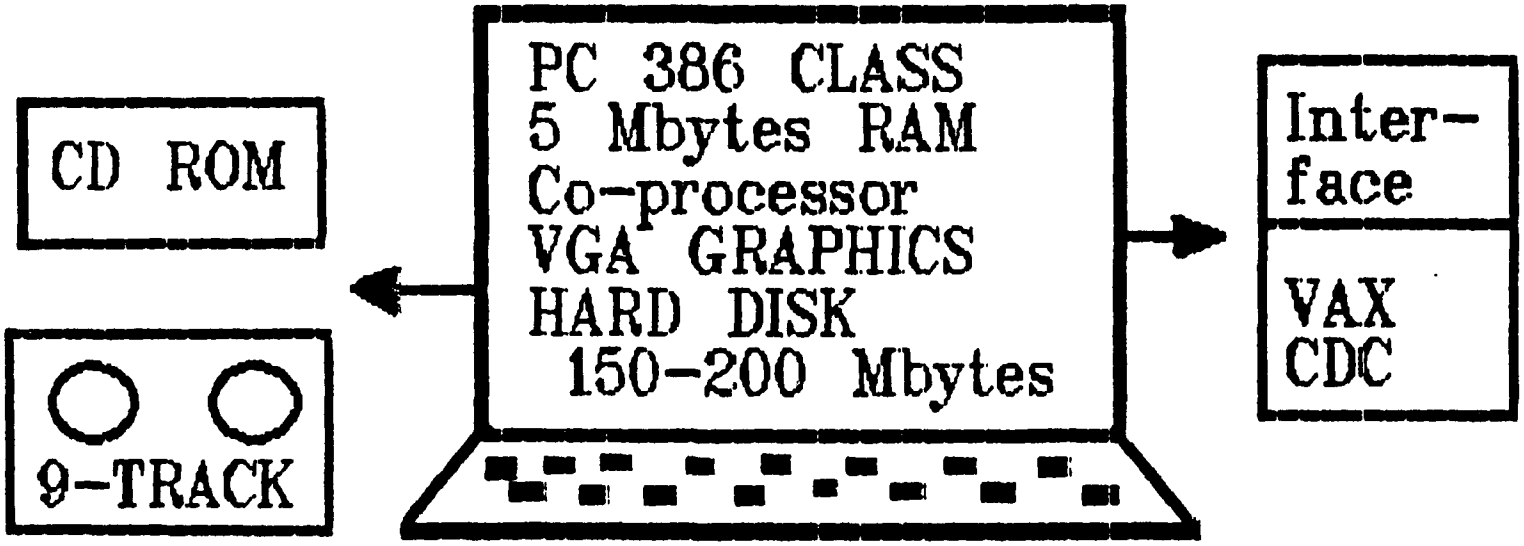

ICON DRIVEN from MOUSE or KEYBOARD

HAWKS MANAGEMENT CAPABILITIES

HITRAN Data Display

Readily Access Any Part of The Database With Identifying Headers, and On-line Help Including Literature References

Graphical Data Display

X - Y Data Plots, Histograms, etc.

Database Functions

Data Editing, Insertions, Deletions, Searching, Sorting, Moving, Saving, etc.

Data Output

Tape ?, WORM, Diskette, Hard Copy, etc.

SUMMARY

Community Should Spend Their Time Using HITRAN NOT Trying To Figure Out How To Use IT !

CD-ROM Technology Has Storage Capability For Present and Anticipated Growth

- Archival (Cannot be Erased)
- Sufficient Storage for Multiple Versions, Literature References, etc.

HAWKS For Database Management

- Not User Abusive
- Bulletin Board

A Happy HITRAN User

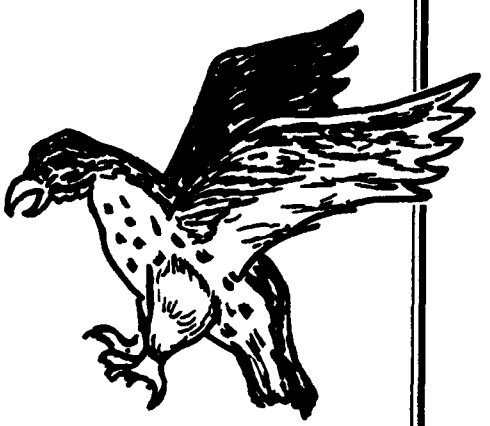

HITRAN In The 1990's

Viewgraph #1: Title

This presentation will described some ideas for distribution and management of future release of the HITRAN database. For anyone desiring additional information, please contact:

John Schroeder, ONTAR Corporation
129 University Road, Brookline, MA 02146-4532
Tel: 617-731-9619, FAX: 617-277-2374

Viewgraph #2 HITRAN 1986

The AFGL, under the direction of Dr. Laurence S. Rothman (OPI), has developed the HITRAN database which is universally recognized as one of the preeminent compilations of spectroscopic data for atmospheric gases. HITRAN contains data on approximately 300,000 molecular transition for 28 atmospheric species, and in an ASCII format is approaching 40 megabytes in size.

HITRAN is widely used within the Department of Defense (DOD), the National Aeronautics and Space Administration (NASA), the Environmental Protection Agency (EPA), numerous university laboratories and private industry to solve a wide range of scientific and engineering problems. For example, it is the molecular input data used by the AFGL FASCODE 2/3 atmospheric transmission/radiance code and is used to generate several of the bandmodels contained in the LOWTRAN code. It is gaining acceptance as the standard for atmospheric molecular gasses and is frequently cited in the literature.

Viewgraph #3: HITRAN In The 1990's

AFGL plans to significantly add to the HITRAN database in the near future, for example by adding lines for high temperature molecular bands, and within a few year the size is likely to exceed 200, 500, 1000 megabytes.

Currently the database is being used for applications that run on computers ranging from PC class machines to Cray's. Simply put, HITRAN is used on all classes of computers. The transfer is often a cumbersome process where a user must first read the tape which can differ from system to system and is more an art than a science. Second, the user must figure out how the data is organized within the database, and finally write a "patch" program to convert the data into a form usable by their software. While none of these steps are overly difficult, they do take a great deal of time which could be better spent. Furthermore, as the database get larger the situation will only become more difficult.

The questions that beg themselves are: Should AFGL continue to distribute HITRAN on digital tape? What other media should be considered? What can be done to make the database easier to use?

Viewgraph #4: Evolution of Data Storage Devices

In the beginning the HITRAN database was stored on punch cards. As long as you had a good heart and a strong back, and you didn't drop any them, everything was fine. As the database grew 9-track tape was the media for distribution. But, as pointed out above, tape is at its limit.

CD-ROM disks (Compact Disk Read Only Memory) represent a relatively new mass storage technology for computers. These disks are physically small (less than 5 inches diameter) and yet hold an enormous quantity of information (550 - 1000 megabytes per disk). The disks are removable from the disk drive, so many disks can be used in a single disk drive.

Another advantage of CD-ROM technology is its read-only capability. Since the disks cannot be written to, users cannot modify the information stored and distributed, which maintains the integrity of the database. However, the user can read part (or all) of the database onto normal magnetic media, and then modify or work with it, so that flexibility will be maintained. The basic database is not changed.

Finally, standard data formats have emerged for CD-ROM's. The current standard is known as the High Sierra ISO format, and it defines the physical layout of the disk and directory structures required. The widespread acceptance of this standard means that CD-ROM's can be read on a variety of different players and a wide range of computers.

Viewgraph #5: HITRAN ATMOSPHERIC WORK STATION (HAWKS)

The HITRAN ATMOSPHERIC WORK STATION (HAWKS) is designed to allow a user to quickly access and manage the HITRAN database. It will provide capabilities to:

1. Display HITRAN data in a "friendly" way ie. be able to readily access any portion of the database, with identifying headers at the top of the screen, and provide on line help functions for each data type.
2. Display data in a graphical format: (screen and hard copy) linear plots with user defined "X and Y variables", histograms, etc. with axis labels and titles.
3. All normal database functions including: data editing, insertions, deletions, searching, sorting, moving, saving, etc.
4. Data Output to tape, diskettes, and hard copy (either the entire database or selected portions). The system will also have the capability to output data in different formats eg. in a format compatible with FASCODE, a HITRAN format, user defined etc. This will also allow the user to create subset databases of larger ones.
5. Automatically incorporate other databases (eg. HOT Gases, or others) with different formats.

Viewgraph #6: HAWKS Hardware

HAWKS (HITRAN Atmospheric Work Station) will be based on a PC 386 (or 486). It will combine the function of a complete

database management system with the scientific computational capabilities needed to develop new databases, make copies for distribution and perform various housekeeping functions. The other major components will be a large hard disk (~300-800 Mbytes), a 9-track 1600/6250 bpi tape drive, a CD-ROM player, a printer/plotter and high resolution VGA graphics.

This system has several advantages that make it suitable for this application. First it is readily available high power stand alone system. The 386 class PC's, using 32 bit software compilers, have speeds equivalent equal to a DEC MicroVax III. These machines should soon become available under the government contract and are routinely used at industrial and university facilities. Consequently the user community probably will not need to make a large investment in computer equipment. Second, inexpensive large hard disks are readily available thus alleviating any "fights" with systems managers over storage of custom databases derived from the archival source. Finally they are easy to interface with main frame and mini- computers either directly or via a network.

Viewgraph #7: HAWKS Data Management Capabilities

The HAWKS database commands will provide all of the traditional functions associated with managing a large database. The user will be able to access data based upon searching criteria that will locate only data of interest. Thus, for example, a researcher studying selected vibrational states of high temperature carbon dioxide in a small wavelength band would be able to display spectral lines meeting all of those criteria. If he wanted to restrict his searches to a single database, he could, or by using a simple command he could extend his search across all of the databases contained on the CD-ROM (note that this example search would turn up no lines in the current HITRAN database). He could then print out (on the screen, printer, or a disk file) the information associated with these lines (line strength, half-width, etc.) Additional functions will be provided to manipulate this

data. Using the example above, the data could be plotted (screen or hard copy) as line strength vs. wavenumber. The user will be able to extract this data into a smaller subset of the database that is stored on his local magnetic hard disk, which he can then process further. He will be able to sort his subset database based upon numerous criteria (sorting by wavenumber value, or by line strength, etc.). He will be able to delete selected information from it, or add his own (additional lines, or new measurements). This limited discussion illustrates the power of the proposed HAWKS software system: the researcher will have a powerful set of database tools to manipulate the data, while the original is maintained in an unmodified form on the CD-ROM.

Viewgraph #7: A Happy HITRAN User

What could be better than a happy HITRAN user!

Appendix

HITRAN WORKSHOP

8-9 June 1989
Air Force Geophysics Laboratory
Hanscom Air Force Base

AFGL Science Center, Bldg. 1106

Thursday, 8 June 1989
(0845-1200)

WELCOMING ADDRESS - Col. John Kidd

WORKSHOP OVERVIEW - L. S. Rothman

SESSION I: Chairperson M.L. Hoke (AFGL)

"New Carbon Dioxide Line Parameters for Atmospheric and High Temperature Applications"
L.S. Rothman (AFGL), R.B. Wattson (Visidyne, Inc.), and R.L. Hawkins (AFGL)

"Infrared Ozone Line Positions and Intensities: Improvements for the 1989 HITRAN Database"
C.P. Rinsland (NASA Langley) and J.-M. Flaud (University of Paris)

"N_2O Line Parameters in the 1000 to 4000 cm^{-1} Region. New Measurements in the ν_2 Band of $H_2^{16}O$"
R.A. Toth (Jet Propulsion Laboratory)

BREAK (1000 - 1030)

"The Alpha and Omega of CO and the Hydrogen Halides"
R. Tipping (University of Alabama)

"The Status of Line Parameters of Methane"
L.R. Brown (Jet Propulsion Laboratory) and V.M. Devi (College of William and Mary)

"UV Absorption Parameters: O_2 and O_3"
L.A. Hall and G.P. Anderson (AFGL)

"NLTE Emission from High Vibrational Levels of Ozone"
S. Adler-Golden (SSI, Inc.) and D.R. Smith (AFGL)

LUNCH (1200 - 1330)

Thursday, 8 June 1989
(1330-1700)

SESSION II: Chairperson F.X. Kneizys (AFGL)

"Summary of Collision-broadened Halfwidths for HITRAN"
R.R. Gamache (University of Lowell)

"Status of Parameters of H_2CO, HCN, and C_2H_2"
M.A.H. Smith (NASA Langley)

"Status of Line Parameter Listings Between 400 and 700 cm^{-1}"
K. Chance (Harvard Smithsonian Center for Astrophysics)

BREAK (1500 - 1530)

"New Molecular Parameters for High-Resolution Stratospheric Spectra: COF_2, HNO_3, $ClONO_2$, and HNO_4"
A. Goldman (University of Denver)

"ADEOS Satellite Sensor Sensitivity Estimation Using the FASCODE Program"
M. Suzuki[1], T. Yokota[1], S. Taguchi[2], and N. Takeuchi[1] ([1]National Institute for Environmental Studies, Japan and [2] National Research Institute for Pollution and Resources, Japan)

"The HITRAN Database from a User's Perspective"
S.A. Clough (Atmospheric and Environmental Research, Inc.)

RECEPTION Officers Club (1700 - 1900)

Friday, 9 June 1989
(0830-1200)

SESSION III: Chairperson R. H. Picard (AFGL)

"The Status of H_2O and NO_2"
J.-M. Flaud (University of Paris)

"SELECT: The User-friendly Interface to HITRAN"
R.R. Gamache (University of Lowell) and L.S. Rothman (AFGL)

"HITEMP: The Hot Gas Compilation. Status and Comparison with Observations"
J.E.A Selby[1], L.S. Rothman[2], R.B. Wattson[3], R.R. Gamache[4], J.-M. Flaud[5], and C. Camy-Peyret[5] ([1]Grumman Corporation, [2]AFGL, [3]Visidyne, Inc., [4]University of Lowell, [5]University of Paris)

"Line Positions of High Temperature CO_2 in the 15 μm Region"
M.P. Esplin (Utah State University) and M.L. Hoke (AFGL)

Friday, 9 June 1989
(Continued)

"Spectroscopic Parameters at High Temperature"
L. Rosenmann (Ecole Central, France)

BREAK & GROUP PHOTO (1000 - 1045)

"Spectroscopic Results on CFC-12. How to Use Them to Model Stratospheric Absorptions"
J-C. Deroche and G. Graner (University of Paris at Orsay)

"Recommendations for the Supplementary Absorption Parameters for Heavy Molecules in the AFGL Compilation"
A. Goldman (University of Denver) and S.T. Massie (National Center for Atmospheric Research)

"HITRAN in the 1990's"
J. Schroeder (ONTAR Corporation)

LUNCH (1200 - 1330)

Friday, 9 June 1989
(1330)

PANEL SESSIONS

HITRAN Workshop Attendance **Appendix**

Name	Affiliation	Phone Number
Mr. Leonard Abreu	AFGL/OPE Hanscom AFB, MA 01731-5000	(617)377-2337
Dr. Steve Adler-Golden	Spectral Sciences, Inc. 99 South Bedford St. Burlington, MA 01803	(617)273-4770
Dr. Gabriele Adrian	Institut fuer Meteorologie und Klimaforschung Postfach 3640 D-7500 Karlsruhe Federal Republic of Germany	/49/721-823644
Ms. Gail P. Anderson	AFGL/OPE Hanscom AFB, MA 01731-5000	(617)377-2335
Ms. Heide Arneson	Texas Instruments MS 3402 P.O. Box 405 Lewisville, TX 76205	(214)466-4322
Dr. John Ballard	Rutherford Appleton Laboratory Chilton, Didcot Oxfordshire OX11 OQX *England*	/44/0235-29100 x5132
Dr. D. Chris Benner	Department of Physics The College of William and Mary Williamsburg, VA 23185	(804)253-4471
Dr. Heiner Billing	Freie Universitat Berlin Institut für Meteorologie Dietrich-Schafer Weg 6-8 D-1000 Berlin 41 Federal Republic of Germany	/49/030-838-3822
Dr. William Blumberg	AFGL/OPI Hanscom AFB, MA 01731-5000	(617)377-2810
Dr. Susan L. Bragg	McDonnell Douglas Research Lab St. Louis, MO 63166	(314)232-7126
Mr. Bruce Briegleb	Climate & Global Dynamics Division NCAR P.O. Box 3000 Boulder, CO 80307	(303)497-1345

Name	Affiliation	Phone Number
Dr. Mark W.P. Cann	Centre for Research in Experimental Space York University 4700 Keele Street Downsview, Ontario M3J 1P3 Canada	(416)736-2100 x3508
Dr. Charles Chackerian	NASA Ames Research Center Mail Stop 245-6 Moffet Field, CA 94035	(415)694-6300
Dr. Kenneth Champion	AFGL/LY Hanscom AFB, MA 01731-5000	(617)377-3033 (617)377-2978
Dr. Kelly Chance	Harvard Center for Astrophysics 60 Garden Street Cambridge, MA 02138	(617)495-7389
Mr. James H. Chetwynd	AFGL/OPE Hanscom AFB, MA 01731-5000	(617)377-2613
Capt. Mark Clausen	AFGWC/WSO Offutt AFB, NE 68113-5000	(402)294-3700
Mr. Tony Clough	Atmospheric & Environmental Research, Inc. 840 Memorial Drive Cambridge, MA 02138	(617)547-6207
Dr. William M. Cornette	Photon Research Associates, Inc. 9393 Towne Centre Dr., Suite 200 San Diego, CA 92121	(619)455-9741
Dr. Owen Coté	EOARD Box 14 FPO, NY 09510	/44/14094437
Lt. Col. Winston Crandall	AFSTC/WE Kirtland AFB, NM 87117	(505)844-0451 AV 244-0451
Dr. Earl C. Curtis	M/S FA 28 Rocketdyne International Corp. 6633 Canoga Avenue Canoga Park, CA 93105	(818)700-4893

Name	Affiliation	Phone Number
Dr. Steve A. Davidson	MIT Lincoln Laboratory 244 Wood Street Lexington, MA 02173	(617)981-3901
Dr. Anthony Dentamaro	AFGL/LIU Hanscom AFB, MA 01731-5000	(617)377-3484
Dr. V. Malathy Devi	Department of Physics The College of William and Mary Williamsburg, VA 23185	(804)864-5677
Maj. Greg J. Donovan	AFCSA/SAGW Washington, DC 20330	(202)697-5793
Dr. David P. Edwards	Hooke Inst. for Coop. Atmos. Res. Clarendon Laboratory Parks Road Oxford OX1 3PU England	/44/086557488
Prof. Robert B. Ellingson	Department of Meteorology University of Maryland College Park, MD 20742	(301)454-5088
Dr. Mark Esplin	Stewart Radiance Laboratory 139 The Great Road Bedford, MA 01730	(617)275-8273
Mr. Vincent Falcone	AFGL/LYS Hanscom AFB, MA 01731-5000	(617)377-4029
Dr. Jean-Marie Flaud	Laboratoire de Physique Moléculaire et Atmosphérique Université Pierre et Marie Curie Tour 13, 4 Place Jussieu 75252 Paris Cedex 05 France	/33/146337924
Mr. William Gallery	OptiMetrics, Inc. 50 Mall Road Burlington, MA 01803	(617)273-5808
Dr. Robert R. Gamache	Center for Atmospheric Research Univ. of Lowell Research Foundation 450 Aiken Street Lowell, MA 01854	(508)458-2504

Name	Affiliation	Phone Number
Dr. James R. Gillis	Boeing Aerospace Company M/S 87-08 P.O. Box 3999 Boeing Aerospace Company Seattle, WA 98124	(206)773-2277
Prof. Aaron Goldman	Physics Department University of Denver Denver, CO 80208	(303)871-2897
Dr. R. Earl Good	AFGL/OP Hanscom AFB, MA 01731-5000	(617)377-2952
Dr. Georges Graner	Laboratoire d'Infrarouge Université de Paris-Sud Bât.350 – Campus d'Orsay 91405 Orsay cedex France	/33/169417527
Dr. Phil Hanna	ITT Research Institute 185 Admiral Cochrane Dr. Annapolis MD 21401	(301)267-2413
Dr. Dieter Hausamann	DFVLR Institut für Optoelektronik 8031 Oberpfaffenhofen West Germany	/49/8153-28770
Dr. R.L. Hawkins	AFGL/OPI Hanscom AFB, MA 01731-5000	(617)377-3614
Mr. Andreas Hayden	Optical Group Perkin Elmer Corp. M/S 803 100 Wooster Heights Road Danbury, CT 06810	(203)797-5624
Dr. Mike Hoke	AFGL/OPI Hanscom AFB, MA 01731-5000	(617)377-3614
Dr. John R. Hummel	SPARTA, Inc. 24 Hartwell Avenue Lexington, MA 02173	(617)863-1060
Dr. Nicole Husson	Laboratoire de Météorologie Dynamique Ecole Polytechnique Route Départementale 36 91128 Palaiseau cedex France	/33/16941 8200 x2385

Name	Affiliation	Phone Number
Dr. John W. Johns	Herzberg Institute for Astrophysics NRC 100 Sussex Drive Ottawa, Ontario K1A OR6 Canada	(613)990-0735
Mr. Frank Kantrowitz	US Army Atmospheric Sciences Laboratory ATTN: SLCAS-AR-A White Sands Missile Range NM 88002-5501	(505)678-4313 AV 258-4313
Dr. Michael G. Kerr	MIT Lincoln Laboratory P.O. Box 73 Lexington, MA 02173	(617)981-3876
Col. John Kidd	Commander AFGL/CC Hanscom AFB, MA 01731-5000	(617)377-3601
Mr. Frank X. Kneizys	AFGL/OPI Hanscom AFB, MA 01731-5000	(617)377-3654
Dr. Anton Kohnle	Forschungsinstitut für Optik Schloss Kressbach D-7400 Tubingen West Germany	/49/416736-2100 Ext 7712
Mr. Joseph Kristl	ONTAR Corp. 129 University Road Brookline, MA 02146	(617)739-6607
Dr. Robert Kurucz	Smithsonian Astrophysical Observ. 60 Garden Street Cambridge, MA 02138	(617)495-7429
Dr. Walter Lafferty	Molecular Spectroscopy Division National Institute of Standards & Technology Gaithersburg, MD 20899	(603)924-6982
Dr. Paul Levan	AFGL/OPC Hanscom AFB, MA 01731-5000	(617)377-4550
Dr. Irving Lipschitz	Chemistry Dept. University of Lowell One University Ave. Lowell, MA 01854	(508)452-5000

Name	Affiliation	Phone Number
Dr. Chung Wang Lui	Centre for Research in Experimental Space Science York University 4700 Keele Street Downsview, Ontario M3J 1P3 Canada	(416)736-2100
Mr. Joseph Manning	OptiMetrics, Inc. 2008 Hogback Road, Suite 6 Ann Arbor, MI 48105	(313)973-1177
Dr. Steve Massie	NCAR P.O. Box 3000 Boulder, CO 80307	(303)497-1404
Dr. Susan McKenzie	Atmospheric and Space Division Mission Research Corp. 1 Tara Blvd., Suite 302 Nashua, NH 03062	(603)891-0070
Dr. John Mergenthaler	Lockheed Research Laboratory Dept. 9790, Bldg. 201 3251 Hanover Street Palo Alto, CA 94305	(415)424-2483
Dr. Christian Muller	Institute d'Aeronomie de Belgique 3 Avenue Circulaire B 1180 Bruxelles Belgium	/32/2-3748121
Mr. Ed Murphy	AFGL/OPA Hanscom AFB, MA 01731-5000	(617)377-4403
Dr. Bertil Nilsson	National Defense Research Institute Division 81 P.O. Box 1165 S-58 111 Linkoping Sweden	/46/13118000
Dr. Ronald A. Parker	Physical Research, Inc. 2201 Buena Vista, S.E. Albuquerque, NM 87106	(505)764-9001

Name	Affiliation	Phone Number
William Peterson	US Army Atmospheric Sciences Laboratory ATTN: SLCAS-AS-D White Sands Missile Range, NM 88002	(505)678-1465
Ms. Angela Phillips	Hughes Aircraft Co. P.O. Box 902 El Segundo, CA	(213)336-5977
Dr. Richard H. Picard	AFGL/OPE Hanscom AFB, MA 01731-5000	(617)377-2222
Dr. Alan Plaut	MIT Lincoln Laboratory Mail Stop N259 244 Wood Street. Lexington, MA 02173	(617)981-5500 x855-4147
Mr. Charles Randall	The Aerospace Corp. P.O. Box 92957 Los Angeles, CA 90009	(213)366-5977
Mr. Peter J. Rayer	Dept. of Atmospheric, Oceanic and Planetary Physics Clarendon Laboratory Oxford University, Parks Road Oxford OX1 3PU England	
Hank Revercomb	Space Science & Engineering Center 1225 West Dayton St. University of Wisconsin Madison, WI 53706	(608)263-6758
Dr. Curtis P. Rinsland	NASA Langley Research Center Mail Stop 401A Hampton, VA 23665	(804)864-2699
Dr. Philip Rosenkranz	Research Laboratory for Electronics Mass. Institute of Technology Cambriuge, MA 02139	(617)253-3073
Dr. Laurence Rosenmann	Laboratoire E.M2.C du CNRS et de l'E.C.P. Ecole Centrale des Arts & Manufactures Grande voie des Vignes 92295 Chatenay Malabry cedex France	/33/147027056

Name	Affiliation	Phone Number
Dr. Laurence S. Rothman	AFGL/OPI Hanscom AFB, MA 01731-5000	(617)377-2336
David C. Sanborn	AFGL/Summer Fellow Hanscom AFB, MA 01731-5000	
Dr. John Schroeder	Ontar Corporation 129 University Road Brookline, MA 02146	(617)739-6607
Dr. Eric L. Schweitzer	O/97-10 B201 Lockheed Missiles and Space Co. Research and Development Division 3251 Hanover Street Palo Alto, CA 91304	(415)424-2785
Dr. John E.A. Selby	Grumman Corporate Research Center Mail Stop A08-35 Bethpage, NY 11714	(516)575-6608
Lt. Scott D. Shannon	AFGL/OPI Hanscom AFB, MA 01731-5000	(617)377-3960
Mr. Eric P. Shettle	AFGL/OPA Hanscom AFB, MA 01731-5000	(617)377-3665
Mr. Donald R. Smith	AFGL/OPB Hanscom AFB, MA 01731-5000	(617)377-3203
Dr. MaryAnn H. Smith	NASA Langley Research Center Mail Stop 401A Hampton, VA 23665	(804)864-2701
Prof. Jeff Steinfeld	Dept. of Chemistry Mass. Institute of Technology Cambridge, MA 02139	(617)253-4525
Dr. Larry Strow	Physics Department UMBC Catonsville, MD 21228	(301)455-2528
Dr. Makoto Suzuki	The National Institute for Environmental Studies 16-2 Onogawa, Yatabe-Machi Tsukuba-gun, Ibaraki 305 Japan	/81/0298-51-2594

Name	Affiliation	Phone Number
Dr. Shooichi Taguchi	National Research Institute for Pollution and Resources Atmospheric Environment Laboratory 16-3 Onogawa Tsukuba-gun, Ibaraki 305 Japan	/81/0298-54-3188
Dr. Richard Tipping	Department of Physics & Astronomy University of Alabama Tuscaloosa, AL 35487	(205)348-3799
Dr. Robert A. Toth	Jet Propulsion Laboratory Mail Stop T1166 4800 Oak Grove Drive Pasadena, CA 91109	(213)354-6860
Dr. George A. Vanasse	AFGL/OPI Hanscom AFB, MA 01731-5000	(617)377-3655
Mr. Marty Venner	AFAL/LSNT Edwards AFB, CA 93523	(805)275-5584
Dr. Richard Wattson	Visidyne, Inc. 10 Corporate Place South Bedford Street Burlington, MA 01803	(617)273-2820
Mr. Rod Whitaker	Los Alamos National Laboratory ESS-5 MS F665 Los Alamos, NM 87545	(505)667-7672
Dr. Peter Wintersteiner	ARCON Corp. 260 Bear Hill Road Waltham, MA 02154	(617)890-3330
Mr. Robert Worsham	Atmospheric & Environmental Research, Inc. 840 Memorial Drive Cambridge, MA 02139	(617)547-6207

AUTHOR INDEX

SECURITY CLASSIFICATION OF THIS PAGE

REPORT DOCUMENTATION PAGE

Form Approved OMB No. 0704-0188

1a. REPORT SECURITY CLASSIFICATION UNCLASSIFIED	1b. RESTRICTIVE MARKINGS
2a. SECURITY CLASSIFICATION AUTHORITY	3. DISTRIBUTION/AVAILABILITY OF REPORT APPROVAL FOR PUBLIC RELEASE; DISTRIBUTION UNLIMITED.
2b. DECLASSIFICATION/DOWNGRADING SCHEDULE	
4. PERFORMING ORGANIZATION REPORT NUMBER(S) PL-TR-92-2092	5. MONITORING ORGANIZATION REPORT NUMBER(S)
6a. NAME OF PERFORMING ORGANIZATION Phillips Laboratory 6b. OFFICE SYMBOL (If applicable) GPOS	7a. NAME OF MONITORING ORGANIZATION
6c. ADDRESS (City, State, and ZIP Code) HANSCOM AFB, MA 01731-5000	7b. ADDRESS (City, State, and ZIP Code)
8a. NAME OF FUNDING/SPONSORING ORGANIZATION 8b. OFFICE SYMBOL (If applicable)	9. PROCUREMENT INSTRUMENT IDENTIFICATION NUMBER
8c. ADDRESS (City, State, and ZIP Code)	10. SOURCE OF FUNDING NUMBERS PROGRAM ELEMENT NO. 61102F; PROJECT NO. 2310; TASK NO. G1; WORK UNIT ACCESSION NO. 14

11. TITLE (Include Security Classification)

PROCEEDINGS OF THE HITRAN DATABASE CONFERENCE 8-9 June 1989

12. PERSONAL AUTHOR(S)

EDITOR, LAURENCE S. ROTHMAN

13a. TYPE OF REPORT	13b. TIME COVERED	14. DATE OF REPORT (Year, Month, Day)	15. PAGE COUNT
REPRINT	FROM _____ TO _____	1989 OCTOBER 16	460

16. SUPPLEMENTARY NOTATION

17. COSATI CODES		
FIELD	GROUP	SUB-GROUP
20	06	
04	01	

18. SUBJECT TERMS (Continue on reverse if necessary and identify by block number)
MOLECULAR SPECTROSCOPY; INFRARED; ULTRAVIOLET; MOLECULAR ABSORPTION; ATMOSPHERIC TRANSMITTANCE; SUB-MILLIMETER SPECTROSCOPY; DATABASES

19. ABSTRACT (Continue on reverse if necessary and identify by block number)

CONTAINS VIEWGRAPHS AND OTHER MATERIALS FOR THE 21 PAPERS PRESENTED AT THE HITRAN DATABASE CONFERENCE HELD AT THE GEOPHYSICS LABORATORY (AFSC), HANSCOM AFB, MASSACHUSETTS, 8 - 9 JUNE 1989.

20 DISTRIBUTION/AVAILABILITY OF ABSTRACT	21 ABSTRACT SECURITY CLASSIFICATION
☒ UNCLASSIFIED/UNLIMITED ☐ SAME AS RPT ☐ DTIC USERS	UNCLASSIFIED
22a. NAME OF RESPONSIBLE INDIVIDUAL LAURENCE S. ROTHMAN	22b TELEPHONE (Include Area Code) 617/377-2336 22c OFFICE SYMBOL PL/GPOS

DD Form 1473, JUN 86 *Previous editions are obsolete* SECURITY CLASSIFICATION OF THIS PAGE